The influence of ageing on the salt-frost resistance of concrete

Utgenannt, Peter

2004

LUND INSTITUTE OF TECHNOLOGY
LUND UNIVERSITY

Division of Building Materials

The influence of ageing on the salt-frost resistance of concrete

Peter Utgenannt

LUND INSTITUTE
OF TECHNOLOGY
Lund University

SP Swedish National Testing
and Research Institute

Report TVBM-1021 Doctoral Thesis

ISRN LUTVDG/TVBM--04/1021--SE(1-346)
ISSN 0348-7911 TVBM
ISBN 91-628-6000-3

Lund Institute of Technology
Division of Building Materials
Box 118
SE-221 00 Lund, Sweden

Telephone: 46-46-2227415
Telefax: 46-46-2224427
www.byggnadsmaterial.lth.se

Abstract

In addition to reinforcement corrosion, damage due to salt-frost attack of concrete exposed to cold, moist and saline environments is the most serious and frequent damage mechanism. Concrete structures exposed to saline sea water or to moist environments where deicing salts are used during the winter are examples of applications where a salt-frost resistant concrete is required in order to prevent damage due to salt-frost attack.

The work described here investigates the influence of ageing - the processes that change the properties of a material with time - on the salt-frost resistance of cement-bound materials such as concrete and mortar. Here, the influence of hydration, drying and carbonation as ageing mechanisms are investigated.

In order to be able to distinguish between the effects of drying and carbonation, climate chambers were built in which the same climates, differing only in their carbon dioxide (CO_2) concentrations, could be maintained. The effect of hydration was evaluated by testing the salt-frost resistance on specimens at different ages. The effect of drying and carbonation was evaluated after conditioning specimens of different ages for seven days in climates with increased CO_2 (~1 vol-%) and without CO_2 (filtered air), both at a relative humidity of 65 % and +20 °C.

Investigating the effect of ageing on 'micro'-concrete with OPC alone, or with silica (5 or 10 %) or slag (20, 35 or 65 %) as part of the binder and with water/binder ratios between 0.35 and 0.55, show that:

- Ageing has a strong influence on the salt-frost resistance of concrete.
- Carbonation is the most dominant ageing effect. The effect of hydration and drying is almost insignificant in comparison with the effect of carbonation.
- The effect of carbonation on the salt-frost resistance is different for concrete with different binder types/combinations. For concrete with OPC alone, or with silica (up to 10 %) or slag (up to some 30 %), carbonation leads to a significantly *improved* salt-frost resistance. For concrete with high slag contents (over some 50 %) carbonation leads to a markedly *poorer* salt-frost resistance.

The effect of carbonation on material properties that are important with respect to salt-frost resistance was further investigated. Mortar specimens of different qualities were conditioned in climates with and without carbon dioxide at 65 % RH and +20 °C until drying stopped and carbonation was completed. The properties of the pore structure of carbonated and uncarbonated material were evaluated by capillary suction and by measuring the freezable water content using low-temperature calorimetry. The frost and salt-frost resistance were evaluated by estimating the time until a critical degree of saturation was reached and by a limited salt-frost test.

Results from evaluating the pore structural changes as a result of carbonation show that:

- For all investigated materials, carbonation leads to a decrease in total porosity.
- For mortar with only OPC as the binder, carbonation leads to a marked densification of the pore structure, leading to a substantial reduction of freezable water content.
- For mortar with additions of silica or small amounts of slag, carbonation leads to a decrease in both coarse and fine pores, and thus a reduction of freezable water content.
- For mortar with high contents of slag, carbonation leads to a marked coarsening of the pore structure, thus leading to a substantial increase in freezable water content.

It is here suggested that, although different for different materials, it is the substantial change in pore structural properties that is the primary cause of the observed influence of carbonation on the salt-frost resistance. For materials with OPC alone, and OPC with silica or small amounts of slag, carbonation leads to a significant *decrease* in freezable water content. For these materials, carbonation leads to an improved salt-frost resistance. However, for materials with high contents of slag as part of the binder, carbonation leads to a marked *increase* in freezable water content and a much poorer salt-frost resistance.

The possibility of a chemical explanation, as presented in the literature, was briefly investigated for cement pastes with and without slag as part of the binder, using X-ray diffraction. The results showed that carbonation results principally in the same carbonate phases, regardless of whether slag is part of the binder or not. The most dominant phase is calcite, although small amounts of vaterite and possibly aragonite are also present. This investigation shows that, for the materials and conditioning climates used here, a chemical explanation as described in the literature can be ruled out. However, it cannot be totally excluded that there could be a chemical effect for other materials and/or other conditioning climates.

As a complement to the laboratory investigations, field investigations on the frost and salt-frost resistance of concrete of different qualities have been carried out at three exposure sites. Two sites were situated in saline environments (marine and highway), and one in a salt-free environment. Results after exposure of up to seven years show that the saline highway climate is the most aggressive with regard to salt-frost damage. Comparing results after seven years' exposure at the highway with laboratory testing according to Swedish Standard SS 13 72 44 shows that the laboratory standard classifies most concrete qualities correctly.

The pore structural changes due to carbonation found in this investigation not only influence the salt-frost resistance, as demonstrated here, but all durability aspects where the pore structural properties are of importance. The effect of carbonation should thus be considered for other degradation mechanisms as well. In fact, the marked effect that carbonation has on the chemical and physical properties should always be considered when carrying out investigations on cement-bound materials.

Preface

Most of the work described here has been carried out at the Department of Building Technology and Mechanics at the Swedish National Testing and Research Institute (SP) in Borås, Sweden. The academic studies have been carried out at the Division of Building Materials at the Lund Institute of Technology in Lund, Sweden.

The financial support provided by SBUF (the Development Fund of the Swedish Construction Industry), BFR (the Swedish Council for Building Research), FORMAS (the Swedish Research Council for Environment, Agricultural Sciences and Spatial Planning), Cementa AB and SP is gratefully acknowledged.

The primary supervisor of this project has been Professor Per-Erik Petersson at SP. First of all, I would like to thank Professor Petersson for giving me the opportunity to work with this interesting project. I am also grateful to him for introducing me to the subject of salt-frost resistance of concrete, and for sharing the expert knowledge that he possesses in this, as in other, fields of concrete technology. Finally, I wish to express my sincere gratitude to Prof. Petersson for the invaluable guidance and encouragement throughout the course of this investigation, as well as for the great effort and endless time put into reviewing the manuscripts leading to the finalisation of this work.

The secondary supervisor and examiner of this project has been Professor Göran Fagerlund, at the Division of Building Materials at the Lund Institute of Technology. To Professor Fagerlund I would first of all like to express my thanks for introducing me to the fascinating world of concrete during my years as a student with the civil engineering program in the early 1990s, and more specifically during the work with the master thesis in his division during 1994/1995. My thanks are also due to him for his guidance during the course of this work, and for sharing his expert knowledge in the field of concrete technology and in particular in the field of frost resistance of concrete.

Laboratory work accounts for the major part of this investigation, and has mainly been carried out at SP. The help from all experienced and skilled colleagues working in the laboratory at the Section of Building Materials at the Department of Building Technology and Mechanics at SP, who in one or another way have assisted this investigation, is gratefully acknowledged.

The field investigations described here have been carried out as part of the national ‘Durability of concrete structures in marine and saline highway environments’ project. That part presented here was initiated and financed equally by the cement producer Cementa AB and by SP. All work was carried out at the three field exposure sites and at SP. During the course of this field investigation, since its beginning in 1996, a large number of colleagues have been involved in this project. The help from all those who have been engaged in the work at the test sites or in the tiresome work of collecting data in the laboratory over the years has been most valuable.

The determination of freezable water content using Low-Temperature Calorimetry was carried out at Aalborg Portland Research and Development Centre (RDC) in Denmark. The help from the personnel at RDC with carrying out these determinations is gratefully acknowledged. My special thanks go to Dr. Dirch Bager at RDC for introducing me to the actual measuring technique, for letting the materials from this investigation be tested at

RDC, for carrying out the calculations as part of the determinations of the freezable water content and for sharing the expert knowledge that Dr. Bager possesses in this field.

Determination of sorption isotherms using an advanced sorption balance was carried out at the Division of Building Materials at the Lund Institute of Technology. The large number of measurements was carried out by Dr. Lars Wadsö, to whom I am very grateful both for the effort and time put into carrying out the measurements and also for prioritising these measurements at times when the sorption balance was heavily used. The results from these determinations are not fully presented here but will be published elsewhere.

I wish to thank all the colleagues at the Department of Building Technology and Mechanics at SP, as well as at the Division of Building Materials at the Lund Institute of Technology, for their assistance and support. The friendly atmosphere at both working places is appreciated.

The help from the personnel at the Section for Technical Services at the Department of Administrative and Technical Services at SP with building the climate chambers used for conditioning specimens in the investigations is gratefully acknowledged. Without these climate chambers, the work could not have been carried out.

The contributions from the following persons/groups are gratefully recognised:

- Professor Lars-Olof Nilsson, the successor of Professor Fagerlund at the Division of Building Materials at the Lund Institute of Technology, for help and support during the later part of the doctoral studies and this work.
- Dr. Jan-Erik Lindqvist at SP for expert help with the various microscope-based analyses carried out in the investigation, and for help and expertise regarding measurements of X-ray diffraction.
- Zoltan Solyom at the Department of Geology - Lithosphere and Biosphere Science, at the University of Lund, for carrying out the X-ray diffraction analysis.
- Sten-Åke Johansson at the Section for Marketing at the Department of Administrative and Technical Services at SP, for invaluable help with most sketches and illustrations in this publication, and for skilfully making these illustrations, based in many cases on poor drafts.
- The group of primarily Nordic researchers, long working together to solve the different questions related to frost and salt-frost damage of concrete and to develop a reliable freeze/thaw test method. Thanks for letting me take part in this inter-Nordic collaboration.
- Neil Muir at Angloscan Manuscript Ltd. for the invaluable help with checking the language and making the thesis easier to read.

Finally, I would like to take the opportunity to thank my family and especially my life companion, Annika, for the love and invaluable support shown to me during the course of this work.

Borås, February 2004

Peter Utgenannt

Contents

Appendices

Summary

Good resistance of concrete to salt-frost damage is important for structures exposed to cold, moist and saline environments. Concrete structures in contact with sea water or close to roads where de-icing salts are used during the winter are a couple of examples for which good salt-frost resistance is required. If a concrete structure with low salt-frost resistance is exposed to an aggressive environment, its surface may be severely damaged. In addition to aesthetic degradation, damage can result in loss of strength and can open the way for other damage mechanisms such as reinforcement corrosion, possibly leading to high repair or replacement costs. Knowledge of the mechanisms influencing salt-frost resistance is thus of great importance in order to know how to produce a salt-frost resistant concrete and how to test it.

The salt-frost resistance of concrete in a defined exposure environment is determined by the material properties, which to a large part are determined by the material composition, such as the water/cement-ratio and the amount of entrained air. However, ageing - the processes that change the properties of a material with time - may also influence the salt-frost resistance.

The work described in this thesis investigates the influence of ageing, and in particular the influence of carbonation on the salt-frost resistance of cement-bound materials such as concrete and mortar. Three ageing effects have been investigated:

- hydration (i.e. the continuing reaction between binder and water)
- drying
- carbonation (i.e. the reaction between carbon dioxide in the air and the paste in the concrete/mortar)

The work described in this thesis is briefly summarised below.

Laboratory investigation of the influence of ageing on the salt-frost resistance of concrete (Chapter 2-3)

Chapter 2 described verification of the influence of ageing on the salt-frost resistance of concrete, and Chapter 3 evaluated the influence of the different ageing effects.

The investigations described in Chapter 3 were carried out on ‘micro’-concrete qualities, made with OPC alone as the binder and also with OPC and different amounts of slag (20, 35 and 65 %) or silica (5 and 10 %) as part of the binder. Water/binder ratios between 0.35 and 0.55 were used. The salt-frost resistance was evaluated at different ages (between 17 and over 250 days at the start of testing) using a freeze/thaw test that cycled the temperature between +20 °C and –20 °C in a 24 hour cycle. The test surface was in contact with a 3 % NaCl solution freezing medium during freezing and thawing.

Before the freeze/thaw test started, the specimens were conditioned in three different climates:

1 Water storage until testing i.e. so that the test surface never dried.

2 Seven days in a climate chamber at 65 % RH / +20 °C, and without carbon dioxide content, followed by a three-day-long resaturation period.

3 Seven days in a climate chamber at 65 % RH / +20 °C and with elevated carbon dioxide content of ~1 vol-%, followed by a three-day-long resaturation period.

To be able to distinguish between the effects of drying and carbonation, two climate chambers were built, in which the same climates could be maintained, but with and without carbon dioxide.

The results from the freeze/thaw test showed that, for all concrete qualities, the effect of hydration and drying on the salt-frost resistance was significant at early ages, up to an age of about 30 days at the start of testing. However, the most dominant ageing effect on the salt-frost resistance was found to be carbonation. Although this was true at all ages, the effect was found to be different for materials with different binder types/combinations, but was so strong that the other ageing effects were more or less unimportant in comparison, at least for older concrete (over 30 days of age).

As an example, see the scaling during a freeze/thaw test for concrete with OPC alone and OPC + 65 % slag as part of the binder, conditioned in three different climates before testing, as shown in Figure S.1. The results are from tests that were started at an age of 31 days.

From the figure, it can be seen that there is a marked effect of carbonation on the amount of scaling for both the concrete quality with OPC alone as binder and for the quality with OPC + 65 % slag as part of the binder. However, the effect of carbonation is totally different, depending on the binder type. For concrete with only OPC as the binder, carbonation leads to a strong reduction of scaled-off material, i.e. to an *improved* salt-frost resistance. The opposite applies for concrete with high slag contents, with a strong increase in the amount of scaled-off material as a result of carbonation. Carbonation of concrete with high slag contents thus leads to *poorer* salt-frost resistance. It can be noted that, for concrete with slag, the scaling is very severe during the first 14 cycles, after which the rate of scaling becomes about the same as for uncarbonated material. The higher initial scaling is a result of the fact that the carbonated layer is scaled off during the initial part of the test.

For both materials, it can be seen from Figure S.1 that the effect of drying is very small compared to the effect of carbonation, i.e. the specimens dried in air without carbon dioxide show about the same amount of scaling as the water-cured, never-dried specimens.

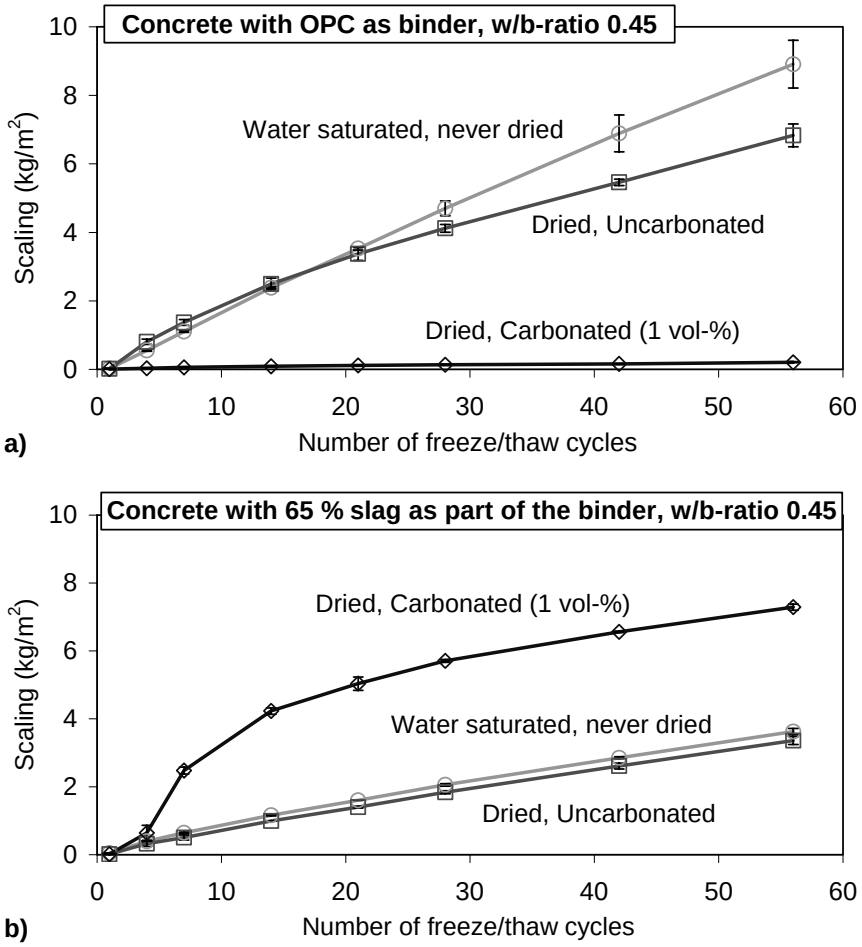

Figure S.1 *Scaling as a function of the number of freeze/thaw cycles for concrete with a w/b-ratio of 0.45, with different binders and conditioned in three different ways. a) OPC, b) OPC + 65 % slag*

For concrete with small amounts of silica as part of the binder, the effect of carbonation is similar, but somewhat less pronounced than for concrete with only OPC as the binder. That is, carbonation leads to improved salt-frost resistance for concrete with some silica as part of the binder, too.

Since the most dominant ageing effect with regard to the salt-frost resistance was found to be carbonation, the aim for the continued work was focused on explaining the effect of carbonation.

Literature review (Chapter 4)

The influence of ageing on the salt-frost resistance of cement-bound materials has been previously investigated to some extent. However, it was found from the literature review that results from previous investigations on the effect of ageing, and in particular of carbonation, differed in many cases.

The differences between the various investigations made it difficult to compare the results. However, some tendencies and discrepancies could be identified:

- Most investigations produced results showing that carbonation or ageing as such of concrete containing high slag contents leads to a poorer salt-frost resistance. The explanation for the effect of carbonation, however, differs in different investigations. Most investigations point toward a physical explanation, but some point toward a chemical explanation.
- For concrete with OPC as the binder, some discrepancies were found in the literature. Most investigations indicate a favourable effect of carbonation on the salt-frost resistance, explained by a densification of the pore structure. However, some investigations indicate a slight adverse effect, explained by a slight coarsening of the pore structure.
- Few investigations of material with silica as part of the binder were found in the literature. These investigations report a negative effect of ageing and carbonation on the salt-frost resistance for concrete with silica, explained by a coarsening of the pore structure as a result of carbonation. This is quite the opposite of what was found in this investigation.

Based on the literature review, some questions to be addressed were identified:

1. What influence has carbonation itself on the salt-frost resistance? In most investigations found in the literature, it was the combined effects of ageing that were studied, and not just those of carbonation alone.
2. How does carbonation influence the salt-frost resistance of materials with different binder combinations? Primarily the effect on material with OPC alone, and OPC with some silica as part of the binder, but also for concrete with high slag contents.
3. How do the material properties affecting the salt-frost resistance change as a result of carbonation?
4. What effect is the most dominant; the physical or the chemical, with respect to the effect of carbonation on the salt-frost resistance for materials containing high slag contents?

The first two questions were answered in Chapter 2 and 3 of this thesis, where the separate effect of carbonation was shown to have a marked influence on the salt-frost resistance, although differing for concrete with different binder types/combinations.

The last two questions were addressed in Chapters 5 to 10 of this thesis.

Laboratory studies on the influence of carbonation on factors influencing the salt-frost resistance (Chapter 5-10)

Investigations were carried out in order to study, and if possible to explain, the strong effect of carbonation on the salt-frost resistance. Specimens of mortar with OPC alone or with additions of slag (35 and 65 %) or silica (5 and 10 %) as part of the binder, and with different w/b-ratios, were conditioned in three different climates with different carbon dioxide contents. All climates had a relative humidity of 65 % and a temperature of +20 °C, but differed in respect of carbon dioxide concentrations, which were: increased (1 vol-%), natural (0.03-0.04 vol-%) and free from carbon dioxide (filtered air).

The effect of carbonation on the physical properties of the pore structure was investigated by means of capillary suction and determination of the freezable water content using low-temperature calorimetry. From the measurements, it was found that:

- Carbonation markedly changes the physical properties of the pore structure.
- Carbonation leads to a reduction of total porosity for all materials. However, the change in the pore structure is markedly different, depending on binder type/-combination.
- Carbonation of mortar with OPC alone as the binder leads to a relatively finer pore structure than for the uncarbonated material.
- For material with some silica as part of the binder, the reduction in porosity do not lead to any relative changes between the coarse and fine parts of the pore system, but to a marked reduction of both.
- For mortar with high contents of slag as part of the binder, carbonation leads to a marked coarsening of the pore system.

The effect of carbonation on the pore structure thus showed to be totally different for materials with different binder types/combinations.

The observed changes in pore structure lead to a marked change in the amount of freezable and non-freezable water content. For mortar with OPC or OPC and some silica as part of the binder, carbonation leads to a substantial reduction in freezable water content, but relatively more so for mortar with only OPC as the binder. The opposite applies for mortar with high contents of slag as part of the binder, i.e. carbonation leads to a considerable increase in the freezable water content.

Figure S.2 shows an example of the change in freezable water content as a result of carbonation for carbonated and uncarbonated mortar with OPC alone as the binder and with OPC + 65 % slag as part of the binder. The freezable water content was measured on capillary-saturated specimens during freezing, using low temperature calorimetry.

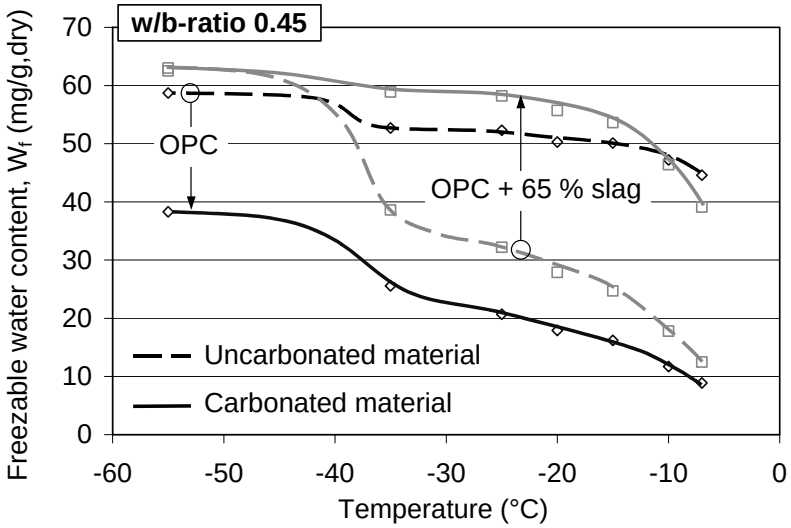

Figure S.2 *Freezable water content during freezing for uncarbonated (dashed lines) and carbonated (full lines) material of mortar with only OPC, and with OPC + 65 % slag as part of the binder, both with a w/b-ratio of 0.45.*

From the figure, it can be seen that for mortar with only OPC as the binder, carbonation leads to a substantial reduction in freezable water content. This reduction in freezable water content presumably leads to a higher frost and salt-frost resistance for this material with OPC alone as the binder.

For mortar with high slag contents in the binder, the effect of carbonation is the opposite, i.e. carbonation leads to a substantial increase in freezable water content, at least in the temperature range down to about –40 °C. This increase in freezable water content presumably leads to a lower frost and salt-frost resistance.

Another example, from the same type of measurement of freezable water content but for uncarbonated and carbonated mortar with 5 % silica as part of the binder, and with a w/b-ratio of 0.45, is shown in Figure S.3. The figure also shows the results for mortar with OPC alone as the binder.

From the figure it can be seen that, for uncarbonated material, there is a marked difference in freezable water content, depending on whether silica is part of the binder or not. Uncarbonated mortar with 5 % silica in the binder has a markedly lower freezable water content than has uncarbonated mortar with OPC alone as the binder.

The effect of carbonation, however, results in both mortars showing about the same freezable water content. The effect on the freezable water content, and thus presumably on the frost and salt-frost resistance, is stronger for mortar without silica, at least for the mortar qualities used here.

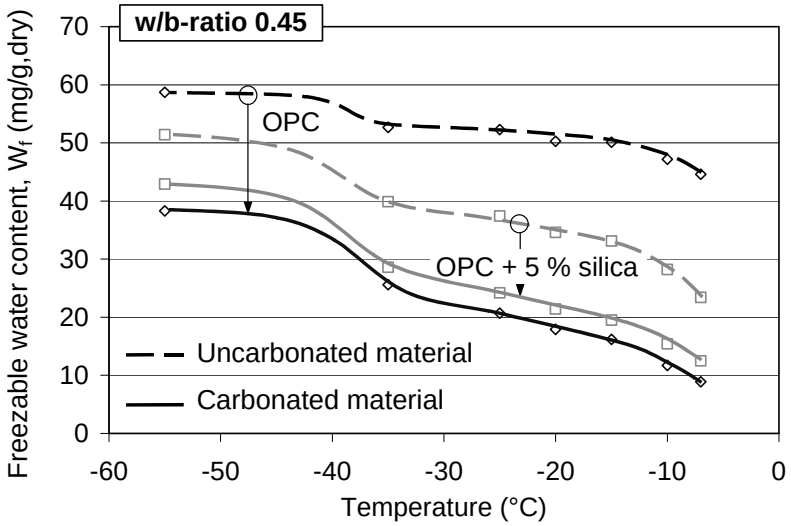

Figure S.3 *Freezable water content during freezing for uncarbonated (dashed lines) and carbonated (full lines) material of mortar with OPC alone and with OPC + 5 % silica as part of the binder, both with a w/b-ratio of 0.45.*

The possible chemical explanation, proposed in the literature, for the observed adverse effect of carbonation on concrete with a high slag content in the binder was examined by investigating the carbonate phases of pastes with only OPC as the binder, and with OPC + 65 % slag in the binder. The possible chemical explanation is based on the fact that carbonation of materials with high contents of slag as part of the binder should lead to the formation of the metastable carbonate phases vaterite and aragonite, whereas carbonation of materials with only OPC as the binder should, in principle, lead only to the formation of stable calcite. According to the chemical explanation, the metastable carbonates are dissolved during salt-frost attack, leading to a more rapid scaling of the carbonated layer.

Here, the carbonate phases formed during carbonation were analysed using X-ray diffraction. The pastes were conditioned in two climates with different carbon dioxide contents (natural air and air with 1 vol-% CO_2). The analysis showed that:

- There were no marked differences in carbonate phases between the pastes, i.e. carbonation of paste with only OPC resulted in the same carbonate phases as paste with OPC + 65 % slag. For both pastes, carbonation resulted in high amounts of calcium carbonate in the form of calcite but also some small amounts of vaterite and aragonite.
- Prolonged conditioning did not lead to any changes in carbonate phases.
- Conditioning in increased carbon dioxide content resulted in principle in the same carbonate phases as when conditioned in normal air.

From the results found in the present investigation, there are no indications of a chemical explanation as proposed in the literature for the effect of carbonation on the salt-frost

resistance; at least, not for the materials and conditioning climates used in this investigation. However, the clear difference between the results from this investigation and the results described in the literature shows that the processes of carbonation are complex and would need a more comprehensive study to be fully understood.

Based on the findings from this investigation, it is here presumed that the effect of carbonation on the pore structure, is the main reason for the influence on the salt-frost resistance.

Field exposure studies of the frost/salt-frost resistance of concrete (Chapter 11)

The laboratory investigations were complemented by investigations at three field exposure sites, all situated in the south-western part of Sweden. Two of these sites were situated in saline environments: one being a marine environment (Träslövsläge harbour), and one being a highway environment (Highway 40). The third exposure site was situated in a salt-free environment at SP's premises in Borås.

Since 1996 a large number of specimens of varying concrete qualities, including different binder types/combinations, different w/b-ratios and with varying air void contents, have been exposed at the test sites. The external and internal damage has been regularly evaluated by measuring the volumes of the specimens and by using ultrasonic pulse transmission time measurements.

The results after five years' exposure at the field exposure sites in a marine and a salt-free environment, and after seven years' exposure in a highway environment, show that:

- There are substantial differences in external frost damage (scaling), depending on the exposure climate. The most extensive external frost damage is observed on concrete specimens exposed in the highway environment. At the salt-free environment at SP's premises, no significant scaling can be found in any of the concrete specimens after five years' exposure. External damage is thus found only for concrete exposed to environments with salt.
- Internal damage is observed on a few concrete qualities at all three test sites, even when no salt is present.
- Internal damage is, with a few exceptions, observed only for concrete qualities without entrained air and for qualities with high w/b-ratios. However, for concrete qualities with OPC + 5 % silica as the binder, internal damage is found at lower w/b-ratios, down to a w/b-ratio of 0.40. This is indicated both by an increase in volume and by an increase in ultrasonic pulse transmission time.
- Both from the present investigation and from a Canadian field investigation in a marine environment (CANMET project), it has been shown that the salt-frost resistance decreases with increasing slag content as part of the binder. In the Canadian project, the specimens had been exposed to a marine climate for up to 25 years. This behaviour corresponds well with the findings from the laboratory investigations described in Chapter 3. The negative effect of slag as part of the binder on the scaling resistance is primarily an effect of carbonation.

- Comparing results from laboratory testing in accordance with Swedish Standard SS 13 72 44 with results after seven years' exposure at the highway exposure site (the most aggressive with regard to salt-frost damage), shows that the laboratory standard classifies most concrete qualities correctly.

It should be stressed that the seemingly higher susceptibility to internal damage for concrete with silica is valid only for concrete without entrained air. If using a sufficient amount of, and properly distributed, entrained air, there are no signs of any adverse effects on the frost resistance of incorporating silica as part of the binder.

Conclusions (Chapter 12)

The following main conclusions can be drawn from the investigations presented in this thesis:

- Ageing effects such as hydration, drying and carbonation have a marked influence on the salt-frost resistance of concrete.
- Carbonation is the most dominant ageing effect with regard to salt-frost resistance. The influence of hydration and drying is small and almost unimportant in comparison with the effect of carbonation, at least at an age of 30 days or older.
- Carbonation has a positive influence on the salt-frost resistance for concrete with only OPC as the binder and OPC with silica (up to 10 %) or slag (up to ~30 %) as part of the binder.
- Carbonation has a negative influence on the salt-frost resistance for concrete with high contents of slag as part of the binder (over some 50 %).
- According to results from this investigation, the influence of carbonation on the salt-frost resistance can be explained by the physical changes of the pore structure taking place as a result of carbonation. Carbonation leads to a marked change in evaporable and freezable water content as well as to changes in the behaviour during capillary suction and to a change in critical degree of saturation.

Finally, it must be noted that the strong effect that carbonation has on the physical and chemical properties of cement-bound materials not only influences the salt-frost resistance, but also most parameters that are important with regard to different durability aspects. It is therefore important that the effect of carbonation is taken thoroughly into account. This is especially true in laboratory investigations where the climate is normally ideal for a high rate of carbonation, and specimens with a large area to volume ratio are used.

Investigating the material properties of partially carbonated materials, which has often been done, and still is the case, is of limited use. The results are valid only for materials with that particular degree of carbonation. In order to obtain a more general knowledge, both carbonated and uncarbonated materials ought to be investigated, thus making it possible to calculate the properties of a material with any degree of carbonation.

1 Introduction

1.1 Background

Concrete can be regarded as a living material in the sense that many material properties change with time, through a process that may be called ageing. This is true both at the concrete surface and in the core, where the outside environment does not affect the material.

The effects of different ageing mechanisms are not constant with time. For young concrete, it is the reaction between cement and water that may be the most dominant ageing effect. Later, the effect of drying and carbonation becomes more dominating. For very old concrete, yet other mechanisms may be the most dominant. For example, for concrete exposed in a moist environment or in direct contact with water, leaching may be an important ageing mechanism. For concrete exposed to exceptional environments, such as highly chemically aggressive, the reaction between the concrete and the chemicals may be the most dominant ageing mechanism.

Ageing will affect the durability of concrete by changing the conditions for different types of attack: chemical or physical. One of the most frequent and serious damage mechanisms, in addition to reinforcement corrosion, is damage due to frost action. This is because concrete is a porous building material, able to hold high quantities of water. When exposed to low temperature, this water may freeze, which in turn may lead to damage if the concrete is not of a high enough quality.

Salt-frost resistance of concrete

In many parts of the world, the air temperature may go far below 0 °C and stay at freezing temperatures for long periods: days, weeks or even months. In many regions with freezing temperatures, de-icing agents are used on road surfaces and pavements for safety reasons. However, by using de-icing agents on or near concrete surfaces, a special type of frost action is created. This frost action may lead to salt-frost damage or what is known as scaling of the concrete surface.

Scaling due to salt-frost action leads initially to an aesthetic degradation of the concrete structure. However, the most serious effect of scaling is that it also opens up a path for other degradation mechanisms, such as reinforcement corrosion. This is because scaling leads to a reduction in the thickness of the protective layer above the reinforcement, and to possible micro-cracking of the surface layer. Micro-cracks in the surface layer lead to more rapid ingress of water and salt, as well as to higher rates of carbonation. Reduced cover over the reinforcement shortens the time until critical concentrations of salt and/or the carbonation front reach the reinforcement. When this occurs, corrosion of the reinforcement may be initiated leading to high repair costs or, if no repair is undertaken, to substantial damage threatening the integrity of the structure.

As an example, in Sweden there are over 10 000 concrete bridges of varying ages in the road network administrated by the Swedish National Road Administration (SNRA). These bridges represent a replacement value of over 6000 million Euros, and the yearly cost for service and maintenance is about 100 million Euros, according to data from SNRA. This illustrates the huge value represented by these types of structures. Damage leading to increased maintenance costs, or a shorter service life than planned leads to high costs for repair and/or reconstruction. Besides the actual costs for repair and reconstruction, there will also be substantial community costs generated by traffic delays caused by restrictions in the availability of the structure.

Historically, in Sweden in the end of the 1960s, a large number of concrete bridges and structures close to roads started to become damaged by salt-frost scaling. This was a result of the introduction of de-icing agents at that time for safety reasons on many road surfaces during the winter. This led to a change in the aggressiveness of the environment surrounding the concrete structures, resulting in severe surface scaling of older structures after only a couple of years' exposure. These older structures were built without air entrainment. Air entrainment in concrete started to be used in Sweden at the beginning of the 1960s, and little or no surface damage or inner frost damage has been detected for structures built of air-entrained concrete produced with pure air-entraining agents. This shows the great importance of air entrainment as protection against frost damage.

However, at the beginning of the 1970s, the use of plasticisers in concrete production rapidly increased, and a few years later there were again a large number of, in this case, newly-built concrete structures showing salt-frost damage. The reason for this was primarily a problem of compatibility between the types of cement, air entraining agent and plasticiser used, leading to a poor air-void structure unable to protect the concrete from salt-frost attack. This illustrates that if changes are made - changes of which we do not have any experience, whether in terms of material composition (leading to changes of material properties in terms of scaling resistance), or of the surrounding environment (thus changing the environmental 'load') - the effect of these changes on the salt-frost resistance is often hard to predict.

Even though much research on the mechanisms of frost and salt-frost damage has been carried out during the last 60 years, most knowledge of how to produce a salt-frost-resistant concrete and how to test the salt-frost resistance is based on experience. Experience from using ordinary Portland cement for over 100 years, and air-entraining agents for over 40 years, has resulted in experience on how 'common' concrete functions under normal conditions in the Nordic climate. To evaluate the frost resistance, test methods such as the Swedish freeze/thaw method, SS 13 72 44, have been developed. For conventional concrete with OPC as the binder, and with entrained air, this method has proven able to distinguish between concrete having good or poor scaling resistance. However, if using new types of materials, e.g. new types of cements, superplasticisers, secondary cementitious materials or fillers, we often do not have sufficient experience and knowledge either of how a frost-resistant concrete should be composed or how it should be tested. Better knowledge and more experience must be acquired.

Influence of ageing on the salt-frost resistance

The work described here is aimed at increasing knowledge about the effect of ageing on the salt-frost resistance of concrete. When investigating the effect of ageing, it is often the combined effects of different mechanisms that are studied: the sum of continued hydration, drying and carbonation. The literature describes investigations into the combined effects of ageing on the salt-frost resistance; see Chapter 4. However, there are only few investigations into the relative effects of the different ageing mechanisms, i.e. where different ageing effects have been investigated separately. In some cases, too, the results described in the literature are contradictory, and so more knowledge about the effect of ageing is needed, and especially knowledge about the relative influence of different ageing effects.

As an example of the effect of ageing, Petersson (1996) describes a field investigation carried out in a marine environment, in which the combined effects of ageing on the salt-frost resistance were studied. Concrete specimens of different qualities, all with OPC and in some cases with small additions of silica fume as part of the binder, and with different w/b-ratios, were produced and tested in accordance with the Swedish freeze/thaw standard, SS 13 72 44, at a concrete age of 31 days. Specimens of the same qualities were placed at a field exposure site on the Swedish west coast, where they were exposed to the aggressive marine climate (above sea level). After three years of exposure, the specimens were taken to the laboratory and their exposed surfaces were freeze/thaw-tested using the same method as before. Figure 1.1 shows the accumulated scaling after 14 freeze/thaw cycles for aged (three years at the exposure site) specimens and non-aged (tested at the normal test time) specimens.

From Figure 1.1, it can be seen that, for almost all concrete qualities, the scaling for the aged specimens was smaller than for the specimens tested at the normal test time. The effect of ageing during three years at the marine exposure site on the Swedish west coast was thus found to be positive with respect to scaling for these concrete qualities.

For concrete with other binder types, for example with large contents of slag, the effect of ageing has been shown to be the opposite, i.e. ageing leads to reduced scaling resistance. This was, for example, shown by Vesikari (1988), who investigated the effect of ageing on concrete qualities with different binder types/combinations; see Figure 1.2. Specimens were conditioned in two different ways before freeze/thaw testing. The conditioning procedures were, ‘Reference’: 7 days in water, followed by 21 days in air with 70 % relative humidity (RH), and ‘Aged’: 7 days in water, followed by 200 days in air with 70 % RH.

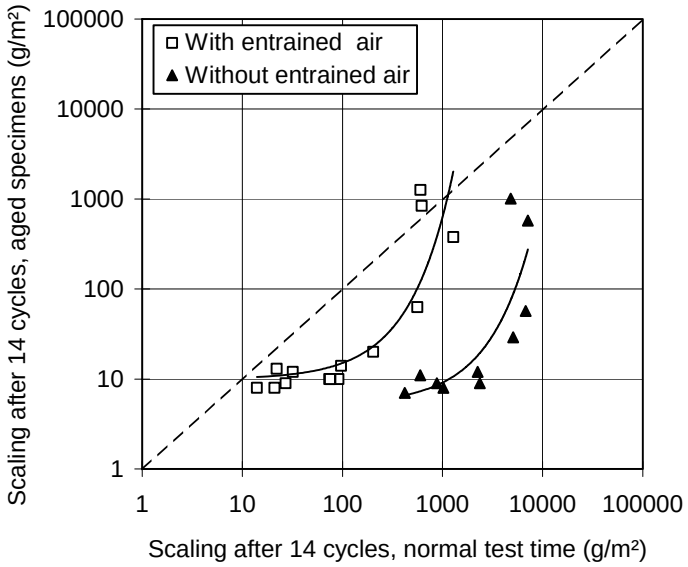

Figure 1.1 *Relation between the accumulated scaling after 14 freeze/thaw cycles for aged concrete (three years in a marine climate) and for concrete tested at an age of 31 days (normal test time). From Petersson (1996).*

From Figure 1.2, it can be seen that, for concrete containing high amounts of slag as part of the binder, the amount of damage after 75 freeze/thaw cycles is much higher for 'Aged' specimens than for the 'Reference' specimens. From the figure, it can also be seen that the same tendencies can be found for concrete containing silica as part of the binder. These results thus indicate that, for concrete with these binder types/combinations, ageing has a negative effect on the salt-frost resistance.

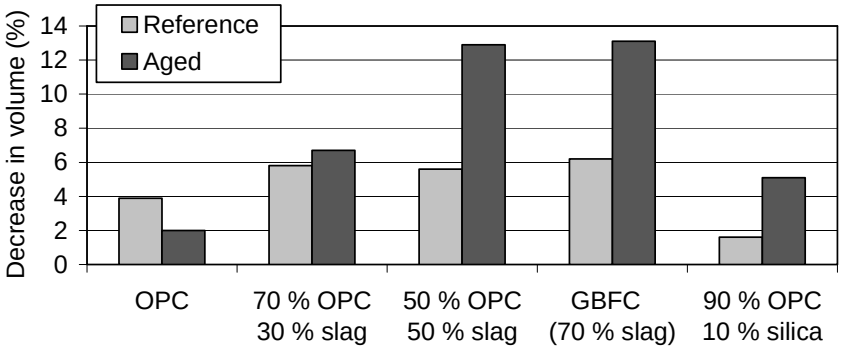

Figure 1.2 *Volume change after 75 freeze/thaw cycles for concrete with a w/b-ratio of 0.48 and entrained air and different binder types/combinations, conditioned in two different ways. Deduced from results presented in Vesikari (1988).*

In both examples above, the effect of ageing was investigated on concrete of different ages. However, there may also be differences in the salt-frost resistance of concretes with

the same age but conditioned in different ways. For example, Jacobsen et al. (1997) describe how different concrete qualities were conditioned in different climates before freeze/thaw testing at the same age. The conditioning climates had different relative humidities and ventilation, resulting in different evaporation rates from a free water surface. Figure 1.3 shows the scaling after seven freeze/thaw cycles for specimens conditioned for 14 days in different climates with different evaporation rates (followed by a 14 days resaturation period) before freeze/thaw testing started.

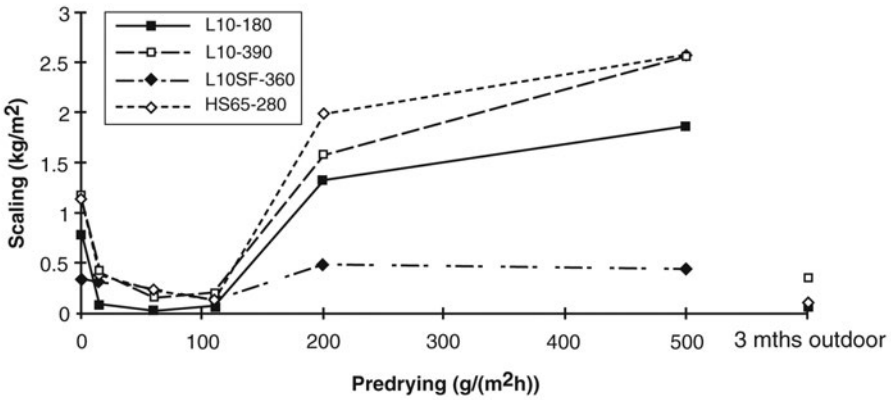

Figure 1.3 *Scaling after seven freeze/thaw cycles as a function of evaporation rate (from a free water surface) of the climate during conditioning for different concrete qualities: three with OPC alone as the binder, and one with OPC + 5 % silica (L10SF-360), all with a w/b-ratio of 0.45. Redrawn from Jacobsen et al. (1997).*

From the figure, it can be seen that there is a marked difference in damage, i.e. in the quantity of scaled-off material, depending on in what climate the specimens were conditioned prior to freeze/thaw testing. Never-dried specimens and specimens that had been conditioned in climates with high evaporation rates show markedly higher scaling than do specimens conditioned in climates with intermediate evaporation rates. The reason for this strong effect on the salt-frost resistance of only 14 days' conditioning is not clarified. Jacobsen et al. explain the influence of the drying regime on the amount of scaling by a change in the 'protective effect of the air-voids'. However, there are other possible explanations; for example, the effect of carbonation.

These are only a few examples of investigations showing that ageing has a substantial effect on the salt-frost resistance, both for concrete of different ages and for concretes of the same age but conditioned in different climates. However, the effect of ageing seems to differ for concrete with different binder types/combinations. The literature describes several more investigations into the effect of ageing on the salt-frost resistance. Some of them are discussed in Chapter 4. From the review of the investigations found in the literature, it could be concluded that there are contradictory results that need to be further investigated.

1.2 The aim of this investigation

The aim of this investigation was to:

1. Verify the effect of ageing and how it influences the salt-frost resistance of concrete
2. Identify the main mechanisms responsible for the ageing process
3. Quantify the influence of the different ageing effects on the salt-frost resistance.
4. Explain the mechanisms behind the ageing effects
5. Discuss how ageing effects influence the evaluation of freeze/thaw properties and the practical use of concrete

It was the aim not only to investigate the effect of ageing on the salt-frost resistance for concrete made with Ordinary Portland Cement (OPC), but also for concrete with blends of OPC and different amounts of secondary cementitious materials. The secondary cementitious materials used in this investigation were ground granulated blast furnace slag and silica fume respectively.

1.3 Limitations

The work described here is primarily aimed at investigating the possible physical explanations to the effect of ageing on the salt-frost resistance. As a result of ageing, there may also be chemical effects leading to the observed effects on the salt-frost resistance. In this investigation only very limited experiments are carried out in order to study possible chemical effects as a result of ageing.

The results presented in this investigation are valid only for the concrete and mortar compositions with the actual cement types, secondary cementitious materials, aggregates and admixtures used. It must also be noted that the results presented in this investigation are valid only for the conditioning climates used, i.e. climates with 65 % relative humidity and +20 °C and with a carbon dioxide content up to 1 vol-%. Using other materials, other relative humidities, other temperatures and other carbon dioxide concentrations may lead to other results.

The investigations describe here is limited to the influence on the salt-frost resistance of the ageing effects: hydration, drying (65 % RH / +20 °C) and carbonation. However, after investigating the relative influence of the different ageing effects, it was concluded that carbonation is by far the most important ageing effect with respect to salt-frost resistance. Because of this, most work in this thesis is focused on the effect of carbonation on the salt-frost resistance.

1.4 General remarks

The following are some general remarks referring to the work described in this thesis.

Materials

The same types of cement, slag and silica have been used in most investigations described in this thesis.

The cement type is a low-alkali, sulphate-resistant, Ordinary Portland Cement (Degerhamn Standard), produced by Cementa AB (Degerhamn, Sweden). The cement is CE-marked, and complies with EN 197-1, CEM I 42.5. The abbreviation OPC is used in this thesis when referring to the cement in the text and in the figures.

The slag used is a ground granulated blast furnace slag (Merit 5000) from Merox AB (Oxelösund, Sweden). It is type-approved in accordance with the requirements of the Swedish building regulations. It is referred to in this thesis simply as *slag*, often abbreviated to *sl* in the figures.

The silica used is a silica fume (Microsilica) from Elkem ASA (Kristiansand, Norway). It was used in the form of slurry, and was taken from a tank in Århus, Denmark. It is type-approved in accordance with the requirements of the Swedish building regulations. It is referred to in the text as *silica*, often abbreviated in the figures to *si*.

The field investigation described in Chapter 11 used a Dutch slag cement (~75 % slag) as a complement. The cement complies with EN 197-1, CEM III/B 42.5.

See Appendix 4 for chemical analyses of the OPC, slag, silica and slag cement.

In all cases, the amount of secondary cementitious materials in this investigation is expressed as a percentage of the binder weight. For example, if a concrete mix contains 400 kg of binder, and the binder is a mix of OPC and 65 % slag, the respective weights are 140 kg of OPC and 260 kg of slag.

Vocabulary

The terms ‘salt-frost resistance’ and ‘scaling resistance’ are intended to refer to the same property, i.e. the resistance to damage caused by frost attack in a saline environment. In this thesis, the two terms have been used ‘randomly’, and without any intended distinction in the meaning of the words. By using both, however, the text may be somewhat easier to read.

As was mentioned above, the cement type used in this investigation is an OPC of CEM I type, as classified in EN 197-1. The abbreviation OPC has been used when referring to this cement in the text and in the figures. However, in the literature review in Chapter 4, the cement types given in each reference are specified. Although the abbreviation OPC is

used in many of the references, this does not necessarily mean that the cement is a CEM I type material. References to more recent work in Chapter 4 use the EN 197-1 classifications where they have been given.

When referring to concrete or mortar mixes with blends of OPC and secondary cementitious materials, only the amount of cement replaced by the secondary cementitious material is given. For example, if a mix contains 35 % OPC and 65 % slag, this is referred to as OPC + 65 % slag, or if it contains 95 % OPC and 5 % silica this is referred to as OPC + 5 % silica.

The term, 'water/binder-ratio' (w/b-ratio), as used here, means the content of water in relation to binder (cement + secondary cementitious materials) in a concrete or mortar mix. No 'efficiency' factors for the secondary cementitious materials are used. In most cases, the term 'w/b-ratio' is also used when the mixes contains only OPC as the 'binder'.

Unless otherwise stated, the term 'age at test start' is the age of the concrete specimens at the start of the freeze/thaw test, i.e. their age when they are placed in the freezer.

Test procedures

In most cases when concrete or mortar have been freeze/thaw tested according to the Swedish freeze/thaw standard SS 13 72 44, or the other methods used (except for the S_{cr}-method), a 3 % sodium chloride solution has been used. However, for the S_{cr}-method, specimens were saturated to different degrees using pure tap water and then tested in the absence of any source of moisture during freezing and thawing, i.e. 'moisture-isolated'.

Unless otherwise stated, the climates in the climate chambers and in the other climate controlled areas within the laboratory were continuously registered and controlled to be within ± 5 % of the intended relative humidity and ± 2 °C of the intended temperature. When referring to different climates in the text, for example during conditioning of specimens, only the intended relative humidity and temperature are given, e.g. 65 % RH and +20 °C. However, the accuracy is always within ± 5 % for the relative humidity and ± 2 °C for the temperature.

Presentation of results

In most cases, each point in the figures presenting results from the investigations described in this thesis is a mean of two test specimens. In other cases, the number of specimens is mentioned in the text or in the figure text.

When presenting results from measurements of more than one specimen, the scatter of the results is shown as one standard deviation.

1.5 Organisation of the thesis

The following are some comments on the organisation of this thesis.

Chapter 1
Gives the background, aim and limitations, as well as some general remarks on the investigations.

Chapter 2
Presents the results from an initial investigation in which the effect of ageing on the salt-frost resistance was confirmed. These results were originally presented at the International RILEM workshop on *Frost resistance of concrete* in Essen, Germany, 1997, and were published in a paper in the Proceedings from the workshop. This paper is reproduced here as Appendix 1.

Chapter 3
Presents results from an investigation where the relative influence of different ageing effects on the salt-frost resistance of 'micro'-concrete is investigated. Most of these results have never been published before, although some were published in a paper in the Proceedings from the International RILEM workshop on *Frost damage in concrete* in Minneapolis, USA, 1999. This paper is reproduced here as Appendix 2.

Chapter 3 also describes the design and function of the climate chambers used for conditioning specimens in climates with and without carbon dioxide. These climate chambers were used for conditioning specimens tested in the investigations presented in Chapter 3 and Chapter 5 - 10.

Chapter 4
Gives a brief description of the most well known freeze/thaw mechanisms as well as a literature review of previous work on the effect of ageing and carbonation on the salt-frost resistance of concrete, mortars and cement pastes.

Chapter 5
Gives the material data and a description of the specimen production for the specimens used in the investigations presented in Chapter 6 - 9.

Chapter 6
Presents results from capillary suction and long-time water absorption tests on carbonated and uncarbonated mortars.

Chapter 7
Presents results from measurements of the critical degree of saturation as well as results from a limited investigation of the salt-frost resistance of carbonated and uncarbonated mortars.

Chapter 8
Presents results from measurements of the freezable water content on carbonated and uncarbonated mortars.

Chapter 9
Presents a comparison of some physical properties between results for carbonated specimens conditioned in normal air and in air with increased carbon dioxide content. This comparison is carried out in order to show the relevance of the results for specimens conditioned in a climate with somewhat elevated carbon dioxide content.

Chapter 10
Presents a comparison of the carbonate phases that formed in carbonated materials (hydrated pastes) conditioned in normal air and in air with elevated carbon dioxide content. The analysis of carbonate phases formed during carbonation gives an indication of whether the chemical explanation for the effect of carbonation on the salt-frost resistance described in the literature may be part of the explanation for the effects of carbonation found in the investigations described in this thesis.

The results presented in Chapter 5 - 10 have not been published before.

Chapter 11
Presents results from investigations carried out at three field exposure sites representing different environments: marine, highway, and a salt-free environment. Parts of the results were previously published in a paper in the proceedings from the Nordic workshop on *Durability of exposed concrete containing secondary cementitious materials* in Hirtshals, Denmark, 2001. This paper is reproduced here as Appendix 3.

Chapter 12
Presents the concluding discussion from the investigations presented in this thesis. Some consequences of the effect of carbonation on the use and testing of concrete are outlined, as are some suggestions for future research.

2 Studies of the influence of ageing on the salt-frost resistance of concrete - Initial investigation

2.1 Introduction

As was described in Chapter 1, ageing as such has been shown to have a substantial effect on the salt-frost resistance of concrete. It was further illustrated that for concrete specimens of the same age, exposed to different preconditioning climates before being freeze/-thaw tested, the salt-frost resistance was markedly different; see Figure 1.3. Different explanations for the effect of preconditioning have been found in the literature, but there is no clear consensus as to what effect is the most dominant. In order to investigate this, a laboratory investigation was carried out, studying the effect of different preconditioning climates. The results from this investigation have been presented in Utgenannt & Petersson (1997), which forms Appendix 1. The following is a summary of the investigation and of the most important observations.

2.2 Materials, specimens and preconditioning climates

Two concrete qualities were used: one quality with expected poor scaling resistance, with a water/binder-ratio of 0.40 and no entrained air (natural air content of 1.2 %), and one quality with expected good scaling resistance with a water/binder-ratio of 0.50 and with some entrained air (a total air content of 2.9 %). Details of the concrete composition are shown in Appendix 1. The OPC used was a low-alkali, sulphate-resistant cement. For chemical analysis, see Appendix 4.

A number of 150 mm cubes were cast for each concrete quality. After demoulding, 24 hours after casting, the cubes were placed in a water bath for six days. They were then randomly distributed and placed in two different climate-controlled areas. The preconditioning climates were:

Climate 1: 65 % RH / +20 °C with an evaporation rate from a free water surface of about 33 g/(m^2·h)

Climate 2: 50 % RH / +20 °C with an evaporation rate from a free water surface of about 45 g/(m^2·h).

Specimens, in the form of slabs 150·150·50 mm, were sawn from the cubes at 7 days and 21 days after casting. After cutting, the specimens were preconditioned in the two different climates until 28 days after casting.

2.3 The freeze/thaw test

After preconditioning, the specimens were freeze/thaw tested in accordance with Swedish Standard SS 13 72 44 (1995), which in most parts is equivalent to the draft RILEM recommendation Test Methods for the Freeze/Thaw Resistance of Concrete - Slab test and Cube test, RILEM TC 117-FDC (1995). The principle of the freeze/thaw test is that specimens with one side in contact with a freezing medium are exposed to 24-hour long freeze/thaw cycles, cycling the temperature between about +20 °C and –18 °C. The scaling resistance of the tested concrete is evaluated from the mass of material scaled off from the test surface of the specimen. The scaled-off material resulting from the freeze/-thaw exposure, is regularly collected after 7, 14, 21 (not required by the standard), 28, 42 and 56 freeze/thaw cycles.

Before the specimen is subjected to the freeze/thaw cycles, a 3 mm thick rubber sheet is glued to all surfaces but the test surface. This is carried out during the preconditioning period in the climate-controlled area. After preconditioning for seven days (some specimens were preconditioned for 21 days, which differs from the standardised procedure) in the climate-controlled area, the test surface is resaturated by applying a 3 mm deep layer of demineralised water to the test surface. This resaturation is continued for three days, after which the water is removed and replaced by a freezing medium; in this case, 3 % NaCl. Before freeze/thaw testing is started, the specimens are thermally insulated on all surfaces but the test surface, ensuring a one-dimensional heat flow. To prevent the freezing medium from evaporating, the test surface is covered by a flat polyethylene sheet. See the test set-up in Figure 2.1.

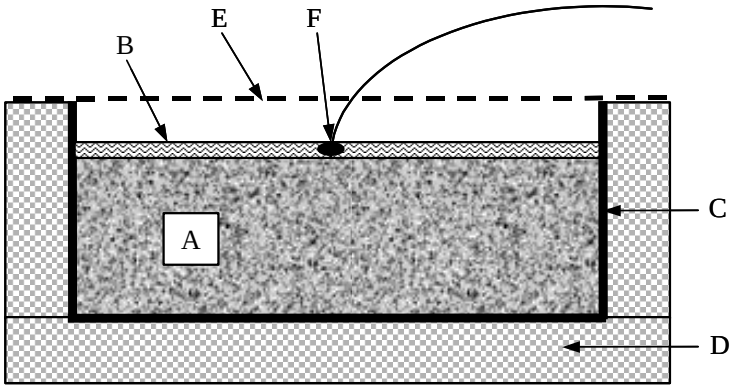

Figure 2.1 *Test set-up used for freeze/thaw test. A - Concrete specimen (150·150·50 mm), B - Freezing medium (3 mm, 3 % NaCl solution), C - rubber sheet for moisture insulation (3 mm), D - Polystyrene cellular plastic for thermal insulation (20 mm, density 18 kg/m^3), E - Polyethylene sheet to prevent the freezing medium from evaporating (0.1 - 0.2 mm thick), F - Temperature measuring device*

The temperature is measured in the freezing medium in the centre of the test surface. An example of a temperature cycle is shown in Figure 2.2, together with the maximum and minimum temperature limits as specified in Swedish Standard SS 13 72 44.

The scaled material is, as mentioned above, regularly collected. This material is dried at +105 °C, and the accumulated amount of scaled material is calculated. The results are expressed as scaled material in kg per square meter test surface (kg/m^2), as a function of the number of freeze/thaw cycles.

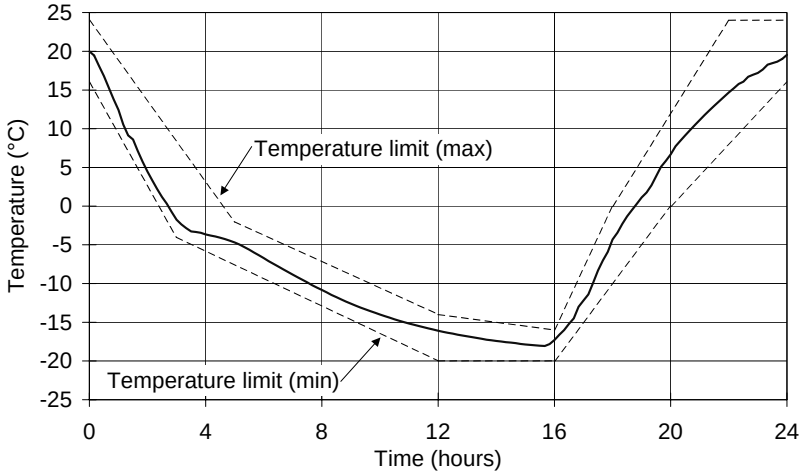

Figure 2.2 *Temperature cycle used. Limits for minimum and maximum temperatures in accordance with Swedish Standard SS 13 72 44 are shown.*

2.4 Results and discussion

Figure 2.3 shows the scaling results from freeze/thaw testing of the two concrete qualities after preconditioning for seven days in the two different climates, i.e. at 50 % RH and 65 % RH respectively.

It can be seen from the figure that for concrete with poor scaling resistance, i.e. the concrete quality with w/b-ratio 0.40 and with no entrained air, there is initially a relatively large difference in amount of scaling, depending on the preconditioning climate. After 7 freeze/thaw cycles, specimens conditioned at 50 % RH have nearly six times greater scaling than specimens conditioned at 65 % RH. However, the difference in scaling gradually declines during the course of the test, so that it is within the scatter of the results after 56 freeze/thaw cycles.

For concrete with good scaling resistance, i.e. the concrete quality with w/b-ratio 0.50 and with entrained air, the difference in scaling due to the different preconditioning climates is substantial throughout the test. The scaling is much greater for specimens conditioned at

50 % RH than for specimens conditioned at 65 % RH. The relation between the scaling depending on the preconditioning climate is almost constant during the test, with 15 to 20 times higher scaling for specimens preconditioned at 50 % RH than at 65 % RH.

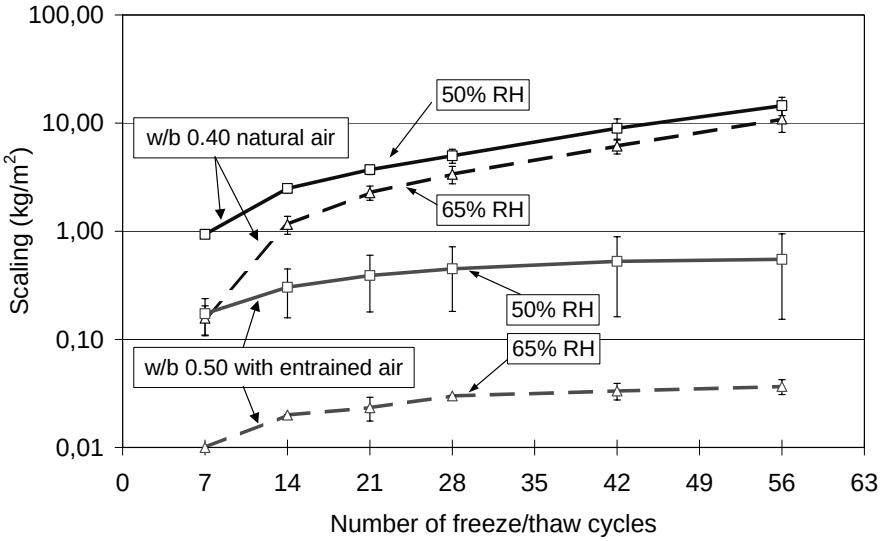

Figure 2.3 *Scaling as a function of the number of freeze/thaw cycles for specimens from two concrete qualities preconditioned for seven days in two different climates prior to freeze/thaw testing. Each point represents a mean value of three specimens. Redrawn from Appendix 1.*

These observations show that specimens preconditioned at 65 % RH have a higher scaling resistance than specimens conditioned at 50 % RH. For concrete with poor scaling resistance, this difference can be seen only at the beginning of the test; at the end of the test, the scaling is approximately the same regardless of the preconditioning climate. This implies that the scaling resistance of the outermost test surface is strongly dependent on the climate in which the specimens have been preconditioned.

For specimens with poor scaling resistance, the resistance of the surface is too low to withstand scaling during the entire freeze/thaw test, irrespective of the preconditioning climate. After 7 cycles, when the difference in scaling depending on the preconditioning climate is still evident, the properties of the test surface are still influencing the results. However, after only 14 cycles, the outermost surface seems to be entirely scaled off, which leads to the rate of scaling becoming less and less dependent on the surface properties and thus on the preconditioning climate. On the other hand, on specimens with good scaling resistance, the resistance of the outermost surface is high enough to influence the result throughout the test. The surface is only locally damaged, and the initial difference in scaling resistance due to the preconditioning climate is maintained during the test.

The results from this part of the investigation thus indicate that the properties of the outermost part of the concrete surface have a great influence on the scaling resistance. It also indicates that the properties of the surface seem to be markedly different, depending on the preconditioning climate. Preconditioning at 65 % RH for seven days leads to a surface with much higher scaling resistance than does preconditioning in 50 % RH during the same time.

Additional tests were carried out in order to verify and study the importance of the properties of the concrete surface on the scaling resistance. A number of specimens from the concrete quality with good scaling resistance, i.e. with a w/b-ratio of 0.50 and with entrained air, were produced as described above and preconditioned for seven days in the two different climates, i.e. 50 % RH and 65 % RH respectively. Directly before resaturation, a thin layer of the test surface, approximately 0.6 mm thick, was removed by grinding some of the specimens. The other specimens were left unground.

Figure 2.4 shows the scaling results from freeze/thaw testing specimens preconditioned in two different climates and with ground and unground test surfaces respectively.

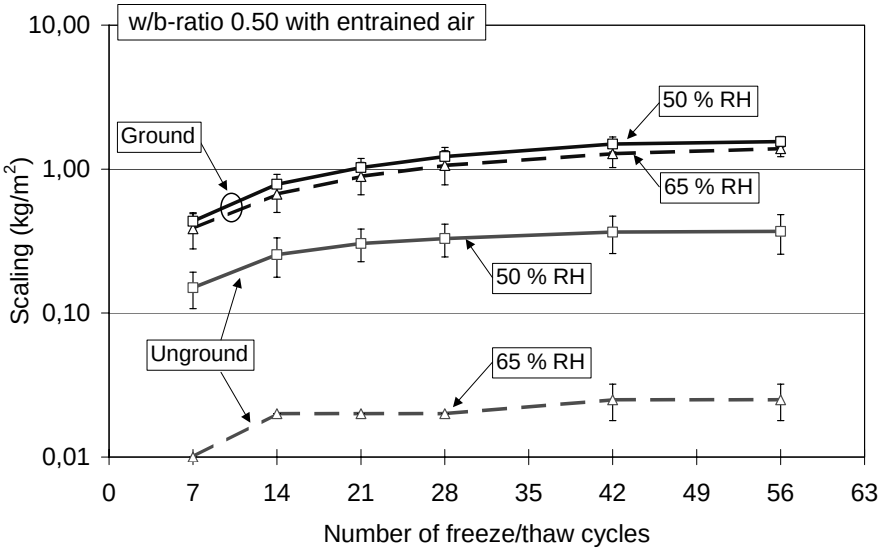

Figure 2.4 *Scaling as a function of the number of freeze/thaw cycles for specimens from one concrete quality preconditioned for seven days in two different climates. A thin layer was ground from the test surface of some specimens prior to resaturation and freeze/thaw testing. Redrawn from Appendix 1.*

As can be seen in the figure, the results for the unground specimens show a marked effect on the scaling resistance depending on the preconditioning climate, with preconditioning at 50 % RH leading to a poorer scaling resistance than preconditioning at 65 % RH. These results are, as expected, consistent with the results presented in Figure 2.3 for the same concrete quality, i.e. concrete with w/b-ratio 0.50 and with entrained air.

Removing a thin layer, less than 1 mm thick, of the test surface before resaturation and freeze/thaw testing, markedly changes the results. As can be seen in Figure 2.4, the scaling becomes almost identical for the specimens with ground surfaces, regardless of the preconditioning climate. The following conclusions can be drawn:

- The scaling resistance of concrete is strongly influenced by a very thin surface layer.
- The properties of the surface layer are strongly influenced by the preconditioning climate.
- The surface layer improves the scaling resistance of concrete, i.e. there seems to be a positive ageing effect, at least for the concrete and binder type used in this investigation.

Since the scaling resistance seems to be determined by the properties of a very thin surface layer, and since it has been shown that the properties of this layer are strongly dependent on the climate to which it is exposed, it can be assumed that the properties determining the scaling resistance are influenced by drying and/or carbonation.

Assuming that drying and/or carbonation is the cause of the significant effect of the preconditioning climate on the scaling resistance, scaling ought to be dependent on the length of the preconditioning period. This is confirmed by the results shown in Figure 2.5, which compares the scaling results for specimens with different preconditioning periods: 7 and 21 days respectively. This comparison involved specimens from both concrete qualities described in Section 2.2. Conditioning was carried out in both climates described in Section 2.2. The age of the specimens was the same at the start of the freeze/thaw test, regardless of preconditioning duration.

It can be seen from the figure that a longer preconditioning period leads to a higher scaling resistance (i.e. less scaling) in the interval 0.1 - 1.0 kg/m^2. Below 0.1 kg/m^2, the surface 'skin' always remains unbroken, and the scaling is therefore independent of preconditioning time. Above about 1 kg/m^2, the protective surface skin is always totally broken, and the rate of scaling is therefore also independent of the preconditioning time. The scatter of the scaling results is relatively low below 0.1 kg/m^2 and above 1.0 kg/m^2. This can be explained by the fact that below 0.1 kg/m^2 the surface skin is undamaged, leading to little scatter, while above 1.0 kg/m^2 the surface skin is totally scaled off, which also leads to little scatter between the scaling results. However, the scatter seems to be high in the 0.1 - 1.0 kg/m^2 interval. This is to be expected, since in this range the test surface consists of both damaged and undamaged material, leading to considerable scatter between the scaling results.

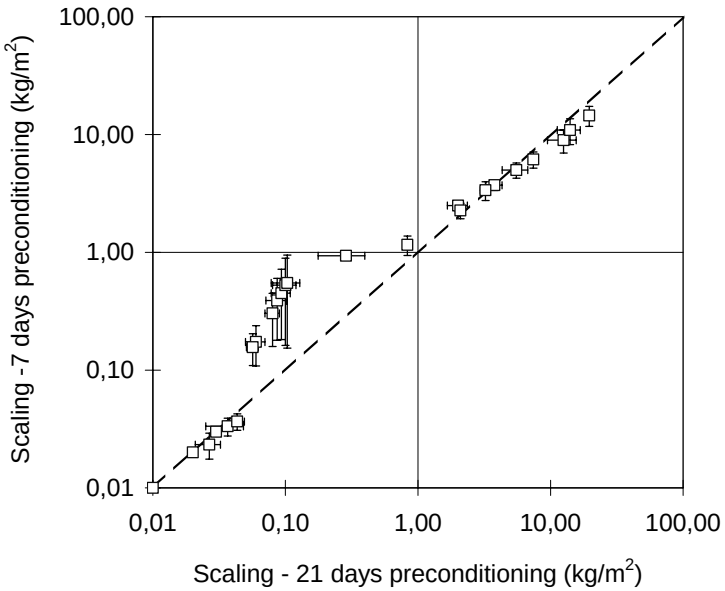

Figure 2.5 *Comparison between scaling results for specimens preconditioned for 7 and 21 days respectively. Each point represents the mean scaling for three specimens of the same concrete quality after the same number of freeze/-thaw cycles, preconditioned for 7 and 21 days respectively in a specific climate. Redrawn from Appendix 1.*

It can be noted that, in the Swedish SS 13 72 44 freeze/thaw standard, the acceptance criteria for 'Excellent' scaling resistance is < 0.1 kg/m^2, and the acceptance criteria for 'Acceptable' scaling resistance is < 1.0 kg/m^2. The scatter above and below these limits has been shown to be relatively small, which is highly desirable at the acceptance criteria limits.

The results presented in Figure 2.5 thus show that the scaling resistance of the surface 'skin' is improved as a result of a longer preconditioning time. A probable explanation for this might be a higher degree of carbonation and/or a higher degree of drying as a result of the longer preconditioning time. However, a higher degree of drying was previously shown to lead to a poorer scaling resistance (see Figure 2.3), where specimens conditioned at 50 % RH showed poorer scaling resistance than did specimens conditioned at 65 % RH (a lower relative humidity ought to lead to a higher degree of drying). This indicates that the positive effect on the scaling resistance as a result of a longer preconditioning time is a result of a higher degree of carbonation rather than an effect of drying.

2.5 Conclusions

The conclusions from this investigation are that:

- The scaling resistance seems to be strongly dependent on the properties of a thin surface layer, or surface 'skin'.
- The properties of the surface 'skin' are strongly influenced by the climate to which the surface is exposed. As an example, concrete exposed to a climate with 50 % RH (evaporation rate ~33 g/(m^2·h)) for only seven days results in a much poorer scaling resistance than that of concrete exposed to 65 % RH (evaporation rate ~45 g/(m^2·h)) for the same time.
- Since the surface 'skin' determining the scaling resistance is thin, it is suggested that the properties determining the scaling resistance might be affected by carbonation.
- Examples of the practical implications of what has been found in this investigation are:
  In the field: a sufficient degree of carbonation is preferred and should be specified before a newly-cast structure is exposed to salt-frost exposure.
- **In the laboratory**: it is very important to control the preconditioning climate within relatively narrow limits when preconditioning concrete specimens before freeze/thaw testing. Not only should the relative humidity, temperature and evaporation rate be controlled, as is the case today, but perhaps also the carbon dioxide content of the air in the climate-controlled areas where preconditioning is taking place.
- When freeze/thaw testing concrete, the scatter between scaling results is small as long as the surface 'skin' is undamaged (below 0.1 kg/m^2). The scatter is also small when the surface 'skin' is totally scaled off (above 1.0 kg/m^2). When only parts of the test surfaces are damaged, the scatter is high. When evaluating the results of a freeze/thaw test, an acceptance criterion should be chosen so that the scatter is minimised. This is the case for Swedish Standard SS 13 72 44, for which < 0.1 kg/m^2 is the limit for 'Excellent' scaling resistance, and < 1.0 kg/m^2 is the limit for 'Acceptable' scaling resistance.

3 Laboratory studies of the influence of ageing, and in particular of carbonation, on the salt-frost resistance of concrete

3.1 Introduction

This investigation has studied the influence of different ageing effects on the salt-frost resistance of concrete. The effects of hydration, drying and carbonation are investigated separately.

As was concluded from the investigation presented in Chapter 2, the scaling resistance seems to be influenced by carbonation of the concrete surface. Two special climate chambers were built in order further to investigate the possible effect of carbonation. These made it possible to store specimens in different climates; for example, with an elevated carbon dioxide content or without carbon dioxide. The chambers are described below in Section 3.2.

This part of the investigation further varied the number of concrete qualities used. In addition to the ordinary Portland cement used in the investigation presented in Chapter 2 some secondary cementitious materials were used as part of the binder in some of the concrete qualities in this investigation. The secondary cementitious materials used were silica and ground granulated blast furnace slag. The mix proportions of the resulting 'micro' concrete qualities, mixing procedures and preconditioning methods are described in Section 3.3.

The freeze/thaw test method used to investigate the influence of carbonation on the scaling resistance is described in Section 3.4.

The results are presented and discussed in Section 3.5. Some of the results were earlier presented in Utgenannt (1999), which forms Appendix 2, and are thus only briefly discussed here. The main conclusions are given in Section 3.6.

3.2 Climate chambers

3.2.1 Introduction

In order to investigate the effect of carbonation on the scaling resistance, specimens were conditioned before freezing in environments with elevated carbon dioxide content and in carbon dioxide-free environments. Two identical climate chambers were manufactured in order to make it possible to simultaneously study materials exposed to different climates. The chambers provided a means of varying the relative humidity, air flow speed (evaporation rate) and carbon dioxide content. The air temperature in the chambers was controlled by the temperature in the climate-controlled area where the chambers were placed.

In this investigation, both climate chambers were installed in a climate-controlled area with a controlled temperature of +20 ± 1 °C.

When making the climate chambers, it was important to be able to create and maintain a stable climate with and without any carbon dioxide. The following is a short description of the chamber design, followed by a description of the climates created in the chambers.

3.2.2 Design of the climate chambers

Each climate chamber consisted of a chamber and a tube system leading the air out from the chamber, through filters, into vessels with salt solutions and back into the chamber. The climate chambers therefore formed closed systems in which the air was recirculated. The chamber and the tube system are described separately below.

3.2.2.1 The chamber

A sketch of the climate chamber is shown in Figure 3.1.

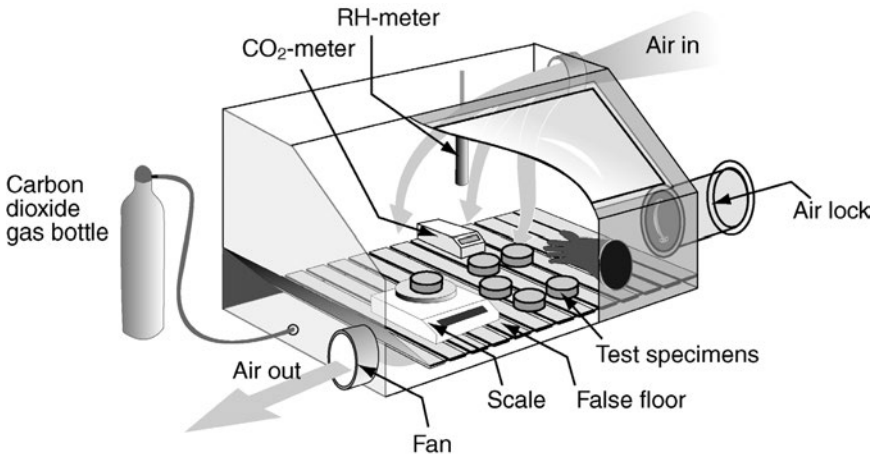

Figure 3.1 *Climate chamber.*

The chamber was made of 1.5 mm stainless steel, with a window of acrylic plastic (plexi-glass). The volume of the chamber was about 0.4 m^3. At the front there were three holes for rubber gloves, which made it possible to work inside the chamber without opening it. On one side, there was an air lock enabling specimens to be put into the chamber with a minimum effect on the climate in the chamber. The bottom of the chamber was covered by a false floor, providing an air gap of about 50 mm between the bottom of the chamber and the floor. The false floor was permeable, which enabled air to flow through. A fan powered the air flow through the false floor and out of the chamber, through the tube system and back into the chamber again. The inlet was placed near the ceiling of the chamber, forcing the air to flow down through the chamber, passing the specimens, out through the false floor and out of the chamber.

3.2.2.2 The tube system

A sketch of the tube system is shown in Figure 3.2.

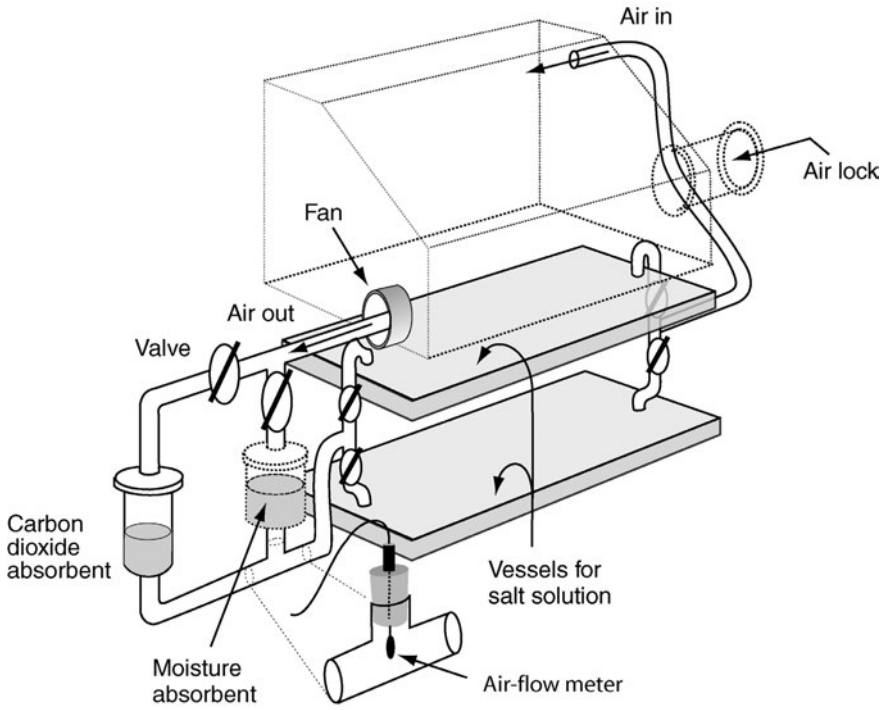

Figure 3.2 *Tube system.*

The tube system led the air out of the chamber, through carbon dioxide filters (optional) and moisture absorbents (optional), into the two vessels containing the saturated salt solution used for conditioning air to a given relative humidity and back into the chamber. The system was constructed of 50 mm diameter plexiglass tubes with PVC fittings (elbows, T-pieces, valves etc.). The filters containing carbon dioxide and moisture absorbents, together with the vessels containing the salt solution, were constructed of plexiglass. Ball valves were mounted at strategic positions in the tube system to enable the air flow to be directed as desired. The air flow velocity was measured by an air flow meter placed in the T-piece where the moisture absorbent was mounted when used. The air flow meter measured the velocity as m/s.

The moisture absorbent used was granulated silica gel (2-6 mm) with indicator ('MERCK' brand), and the carbon dioxide absorbent was soda lime pellets (2-5 mm) with indicator and with a CO_2 absorption capacity of 28 % by weight ('MERCK' brand).

As shown in Figure 3.2, two vessels of salt solution were connected to the tube system to increase the moisturising/drying capacity. The size of each vessel gave a salt solution surface of about 0.28 m^2, i.e. a total surface of about 0.56 m^2 if using both vessels.

3.2.3 Climate in the chambers

The climate in the chambers could be varied by:

- changing the saturated salt solution in the vessels, which changed the relative humidity
- changing the speed of the fan, i.e. the air flow, which changed the moisturising/drying capacity
- increasing or reducing the carbon dioxide concentration by adding carbon dioxide or by using carbon dioxide absorbents
- using a moisture absorbent thus rapidly reducing the moisture content of the air
- changing the temperature in the climate-controlled area where the chambers were placed, which also changed the temperature in the chamber

The following is a description of how the climates were recorded and what measuring devices were used in the climate chambers. A short description of the climates in the two chambers is also given.

3.2.3.1 Climate recording, and calibration of the measuring devices

The climate, i.e. relative humidity, temperature, air flow and carbon dioxide concentration, was continuously recorded by a computer. A logging program, where the time between the measurements can be set as 0.5, 1, 2, 5, 10, 20, 30 or 60 minutes, was developed. Normally, the climate was recorded every five minutes during the investigations described in this thesis. Table 3.1 lists the different measuring devices. Tables 3.2 and 3.3 show the results of calibration of the devices measuring relative humidity, temperature and carbon dioxide content. The device for measuring the air flow was calibrated by the manufacturer before delivery.

Table 3.1 *Measuring devices used in the climate chambers.*

Measurement	**Description**
Relative humidity and temperature	Testo®, Transducer for fixed humidity (0 to 100 % RH) and temperature measurement (–20 to +70 °C). Output signal is 0-10 V. The humidity signal is temperature-compensated. Accuracy: ± 2 % RH, ± 0.4 °C. (According to the manufacturer.)
Carbon dioxide	Telaire Europe AB, Type 2001VT. Infrared CO_2 sensor. Measuring range: 0 - 30000 ppm (0 - 3 vol-%) (Model 1), 0-3000 ppm (0 - 0.3 vol-%) (Model 2). Accuracy: ± 2 % relative. (According to the manufacturer.)
Air flow	Testo®, Heated ball probe for velocities between 0 and 10 m/s. Accuracy: ± 0.03 m/s +5 % of the measured value. (According to the manufacturer.)

Table 3.2 *Calibration of devices measuring relative humidity and temperature. Calibration performed in a climate chamber (Thunder 2500) at Lund Institute of Technology, Division of Building Materials.*

Calibration climate	**Device 1**	**Device 2**
RH (%)/Temp (°C)	**Registered RH (%)/Temp (°C)**	
30.0/20.0	29.6/20.1	29.5/20.1
52.0/20.0	52.2/20.1	51.9/20.1
66.0/20.0	67.3/20.1	66.9/20.1
90.0/20.0	91.8/20.1	91.5/20.1

Table 3.3 *Calibration of devices measuring the carbon dioxide content. Calibration performed by the manufacturer before delivery.*

Calibration climate	**Device 1**	**Device 2**
CO_2 vol-%	**Registered CO_2 vol-%**	
0	0	0
0.0390	-	0.040
0.0400	0.040	-
0.1571	-	0.157
1.51	1.51	-

3.2.3.2 Relative humidity and temperature

Various salts can be used in order to establish climates with specific relative humidities, as shown in Table 3.4. Only the salt solution creating a relative humidity of around 66 % was used, i.e. $NaNO_2$, in the investigations described in this thesis.

Table 3.4 *Salts that can be used to establish different levels of relative humidity.*

Temperature	**$MgCl_2 \cdot 6H_2O$**	**$NaHSO_4 \cdot H_2O$**	**$NaNO_2$**	**NaCl**	**KCl**	**K_2SO_4**
+20 °C	33 % RH	52 % RH	66 % RH	76 % RH	86 % RH	97 % RH

The climate in the climate-controlled area where the climate chambers were placed normally maintains a relative humidity of 50 % RH and a temperature of +20 °C. The humidity in the climate-controlled area is controlled within ± 3 %, and the temperature within ± 1 °C.

Since the climate chamber is a closed system, the effect of the lower relative humidity in the climate-controlled area on the relative humidity in the chamber is unimportant. The temperature in the climate-controlled area, however, affects the temperature in the climate chamber. If the temperature changes rapidly, the relative humidity changes in the chamber. Because of the ‘slowness’ of the salt solution, equilibrium in relative humidity is not restored immediately. This results in small changes in relative humidity in the chamber

when the temperature changes. Figure 3.3 shows the temperature in the two chambers over a period of one week, while Figure 3.4 shows the relative humidity over the same period. It can be seen from the diagrams that the temperature during the week was about + 20.8 ± 0.2 °C, and the relative humidity was 64.5 ± 0.5 % in both chambers. In other words, with this limited change in temperature, the relative humidity was quite stable. During the periods when the climate chambers were used in the investigations described in this thesis, there were only small fluctuations in the temperature and thus also relatively small fluctuations in the relative humidity.

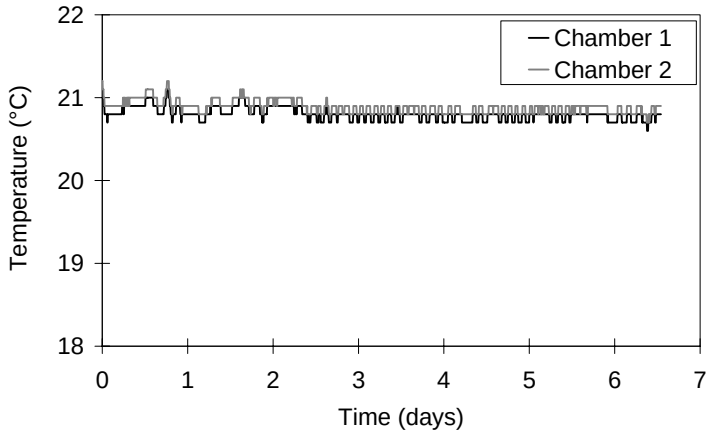

Figure 3.3 *Temperature during one week in the two climate chambers.*

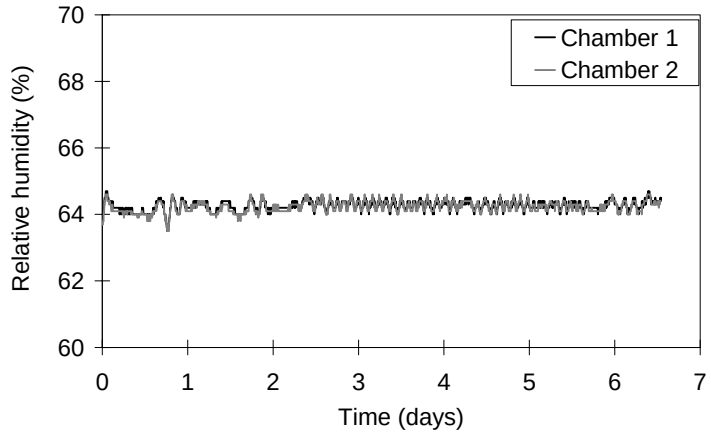

Figure 3.4 *Relative humidity during one week in the two climate chambers. Same time period as in Figure 3.3.*

As can be seen in Figures 3.3 and 3.4, the difference in temperature and relative humidity between the climate chambers is small and unimportant. This is an important feature when using the climate chambers for preconditioning, as has been done in much of the work described in this thesis.

When wet specimens were placed in the chambers, the relative humidity immediately increased. The reason for this is the high evaporation of water from the wet specimens and the slowness of the salt solution in restoring the relative humidity. A moisture absorbent was therefore used in order to restore the humidity more quickly. The air flow through the filter can be controlled by valves in the tube system. Figure 3.5 shows the relative humidity during a test to evaluate the efficiency of the moisture filter. Before the moisture filter was fitted, the relative humidity was raised to about 69 % by placing a bowl of water in the climate chamber for a couple of hours. The bowl of water was removed and the air was directed through the moisture filter. As can be seen from the diagram, the relative humidity decreased rapidly and the 'normal' relative humidity was reached within less than one hour. The same procedure was carried out without a moisture filter, and the relative humidity decreased much more slowly, reaching the 'normal' relative humidity after about three hours. An air flow velocity of about 0.26 m/s in the tube system was used in this comparative test.

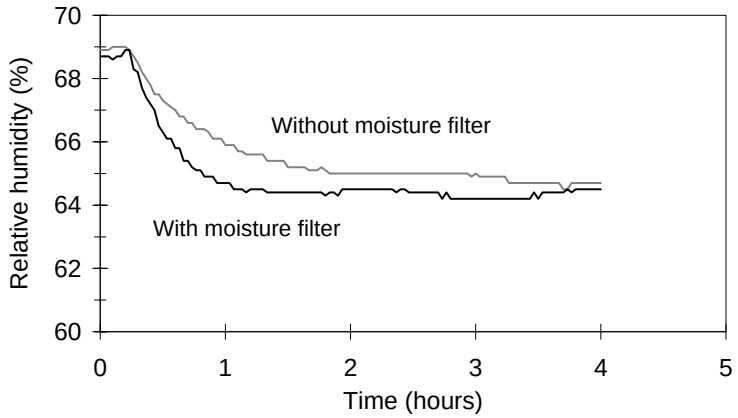

Figure 3.5 *Relative humidity with and without the moisture filter.*

When placing wet specimens in the climate chambers, the humidity rapidly increased during the first half hour after exposing the wet test surfaces to the air in the chamber; See Figure 3.6. The figure shows the increase in relative humidity resulting from exposure of six wet specimens used in this investigation. See Section 3.3.4 for a description of the specimens. The moisture filter was used to minimise the initial increase in relative humidity. The filter was fitted to the tube system, as shown in Figure 3.2, before the wet surfaces were exposed to the air in the chamber. After the initial increase in relative humidity, the humidity slowly decreased, reaching the desired relative humidity after about three to four hours. The moisture filter was then removed, and the air flow device was fitted to the tube system. The fan was adjusted to give the desired air flow.

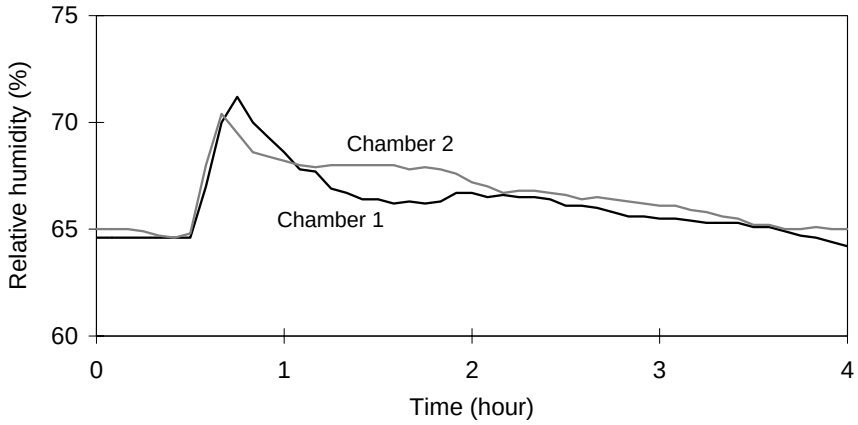

Figure 3.6 *Relative humidity in the two climate chambers during the first hours after exposure of six wet specimens to the air in the chambers.*

As can bee seen from Figure 3.6, the relative humidity during the first couple of hours in the climate chambers was higher than the desired ~65 % RH. However, this period of increased humidity is quite short, and seems to be about the same for both climate chambers, i.e. the specimens were exposed to the same climates during preconditioning irrespective of in which chamber they were preconditioned.

It should be noted that both climate chambers were equipped with electric scales. These scales were continuously turned on and thus generated a small amount of heat, resulting in a small temperature raise relative to the temperature in the climate-controlled area where the chambers were installed. Since the scales were continuously turned on, the temperature rise was more or less constant over time. Based on comparisons between the temperature in the climate-controlled area and in the climate chamber, the temperature raise was estimated as not exceeding +0.5 °C. It is probable that this small increase in temperature was primarily confined to the chambers where the scales were placed, and that the temperature of the air was slowly adjusted, i.e. cooled off, when passing through the tube system. The temperature of the air above the salt solution was thus likely to be somewhat lower than in the chamber, resulting in a somewhat lower relative humidity in the chamber than above the salt solution. For example, it can be assumed that the temperature in the chamber was +20.5 °C, while above the salt solution (66 % RH) it was +20.0 °C. This would lead to a relative humidity of about 64 % in the air of the chamber. This can be one explanation why, in most cases, the measured steady-state relative humidity in the chamber was around 64 - 65 %.

3.2.3.3 Air flow velocity

The air flow velocity could be varied by adjusting the speed of the fan that circulated the air in the system. The velocity could be varied between 0-0.40 m/s. When the chambers were in use, an air velocity of 0.25-0.30 m/s was normally used. The air flow velocity affects the rate of evaporation from wet surfaces in the chamber. Figures 3.7-3.8 show the

evaporation from a free water surface at different air flow velocities in the tube system. The evaporation from a water bowl (height 55 mm, diameter 92 mm) containing about 350 ml and placed on a scale, was continuously measured for about 24 hours. In order to prevent the water from taking up heat from the scale, a 20 mm thick piece of polystyrene cellular plastic was placed between the scale and the bottom of the bowl.

The figures also show the relative humidity in the chambers during the measurements. Evaporation at other air flow rates was also measured. The results from all measurements are shown as the calculated evaporation rate in Figure 3.9.

Figure 3.9 shows the evaporation rate from a free water surface as a function of air flow velocity in the tube system for the two chambers. The evaporation results indicate that, for both chambers, the rate of evaporation is more or less linear over the air flow velocity range studied (0.14-0.34 m/s). It can also be seen that the evaporation rates in the two chambers are more or less identical, which is an important feature for the climate chambers when used in the comparative investigations described in this thesis.

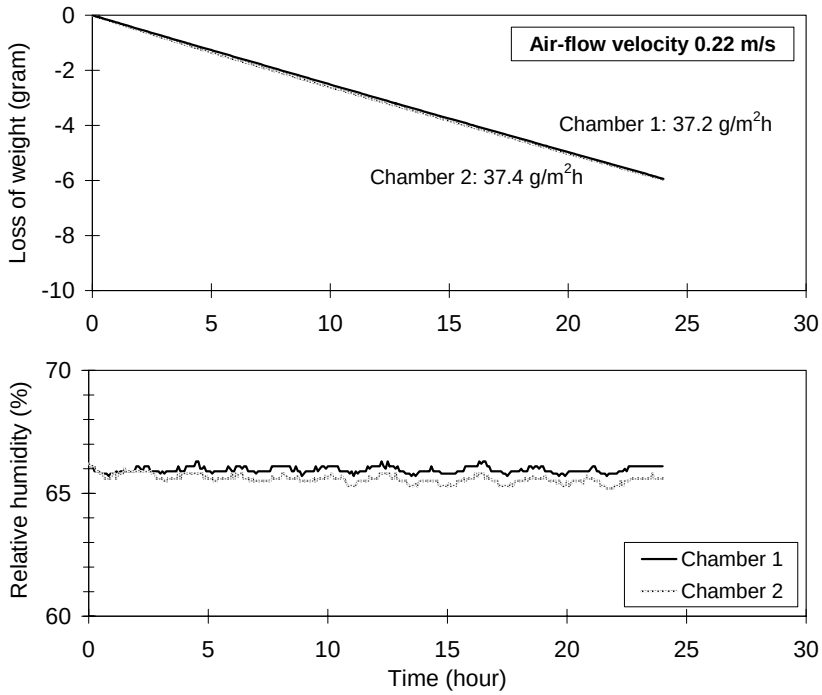

Figure 3.7 *Evaporation from a free water surface in the chambers at an air flow velocity of 0.22 m/s in the tube system (above), and the corresponding relative humidity during the measurement (below).*

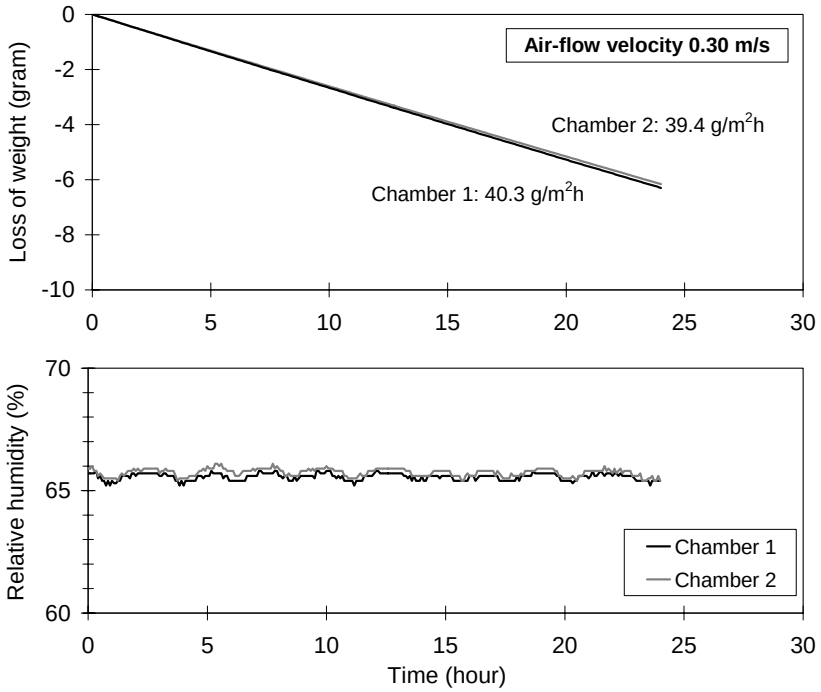

Figure 3.8 *Evaporation from a free water surface in the chambers at an air flow velocity of 0.30 m/s in the tube system (above), and the corresponding relative humidity during the measurement (below).*

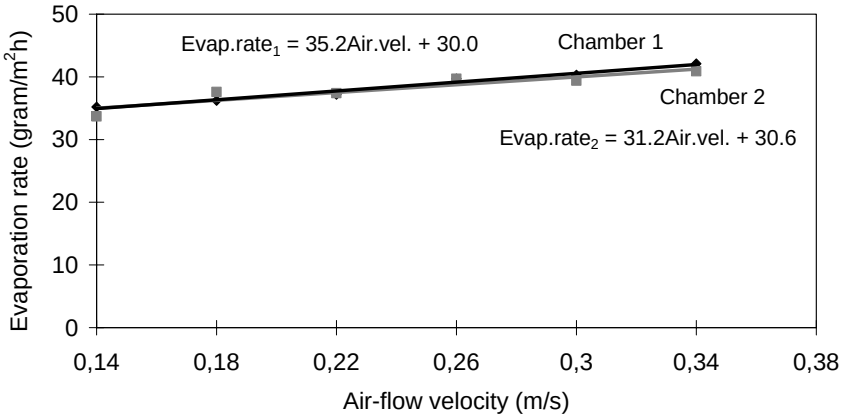

Figure 3.9 *Evaporation rate as function of air flow velocity for chambers 1 and 2 for an air flow velocity interval of 0.14 to 0.34 m/s. Each point represents one measurement.*

3.2.3.4 Influence on evaporation of position in the chamber

The influence on evaporation of where in the chamber the specimens are placed has been investigated. Six small plastic cups (height 43 mm, diameter 39 mm) with a volume of 50 ml were filled with water and placed in the two chambers; see the test set up in Figure 3.10. The cups were placed in the area where it was intended later to place the specimens during preconditioning. An air flow velocity of 0.26 m/s in the tube system was used for both chambers. The weights of the water-filled cups were measured at different time intervals. The weight changes for each cup as a function of time during the measurement is shown in Figure 3.11 for Chamber 1, and in Figure 3.12 for Chamber 2.

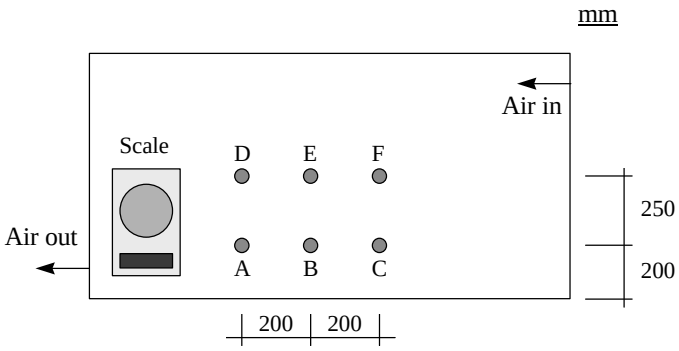

Figure 3.10 *Test set-up for investigating the influence on evaporation of position in the chamber. The climate chamber is seen from above with six water-filled cups placed at different positions.*

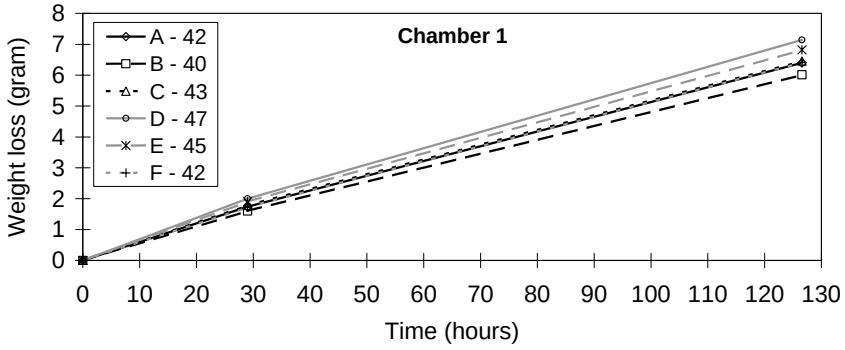

Figure 3.11 *Weight loss as function of time for water-filled cups in Chamber 1. The inset shows the results in terms of the calculated rate of evaporation during the measuring time in g/m^{2}h. Each point represents one measurement.*

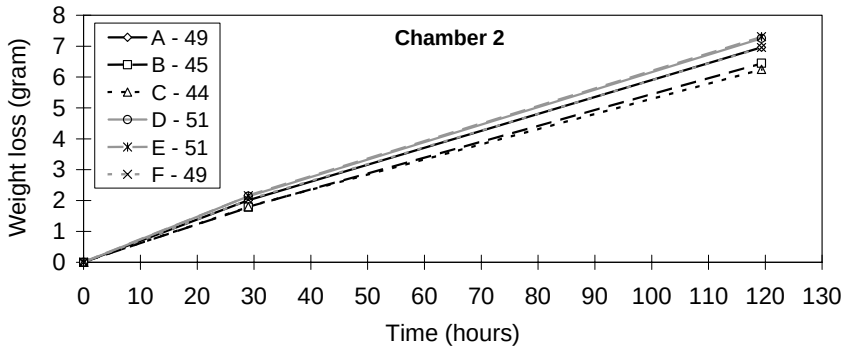

Figure 3.12 *Weight loss as function of time for water-filled cups in Chamber 2. The inset shows the results in terms of the calculated rate of evaporation during the measuring time in g/m^{2}h. Each point represents one measurement.*

The cups that were used for this test were relatively small, so that only small surface areas were exposed to the air. This was necessary in order to avoid an increase in the relative humidity in the air during the test period. However, because of the small exposed surfaces, edge effects occurred, which may have resulted in a significant natural scatter.

With reservation for the possible natural scatter caused by the edge effects, the results shown in Figures 3.11 and 3.12 indicate a relatively small spread in evaporation rate depending on location in the climate chambers. The results from both chambers are consistent and indicate a somewhat lower evaporation rate close to the chamber walls than in the middle of the chamber. This showed the importance of not placing specimens too close to the chamber walls, which was observed when preconditioning specimens during the investigations described in this thesis.

3.2.3.5 Carbon dioxide concentration

The carbon dioxide concentration in the air could be varied by using a carbon dioxide absorbent in a 'carbon dioxide filter', or by manually adding carbon dioxide from a gas tube. After adding carbon dioxide to the air in the chambers there was a steady natural decrease in the carbon dioxide content unless further carbon dioxide was added at intervals from the tube. This can partially be explained by a small leakage of air between the climate chamber and the climate laboratory, and by consumption of carbon dioxide by plastic and rubber details in the chamber construction. Figure 3.13 shows the fall in carbon dioxide concentration in the chamber over one week when no additional carbon dioxide was added. Figure 3.14 shows the carbon dioxide concentration when using a 'carbon dioxide filter'. From the diagram, the carbon dioxide content seems to be negative, which of course is not possible. The negative values are due to the fact that when the device measuring the carbon dioxide content cannot detect any CO_2 molecules, it generates a negative value.

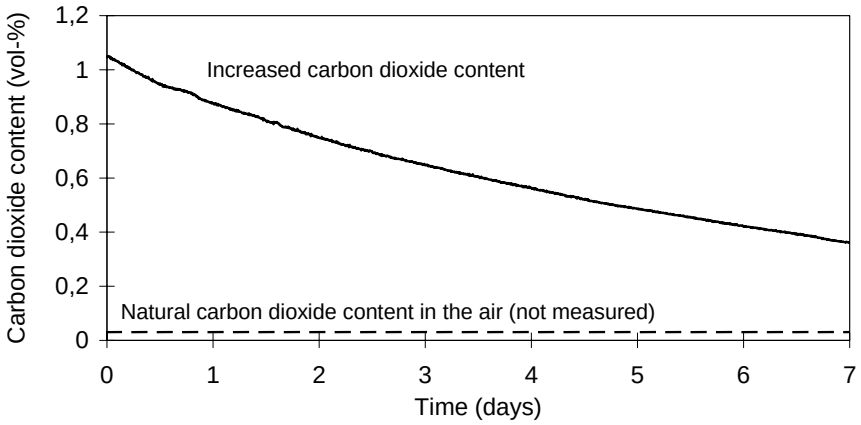

Figure 3.13 *Natural decrease in carbon dioxide concentration as a function of time for a climate with initially increased carbon dioxide content.*

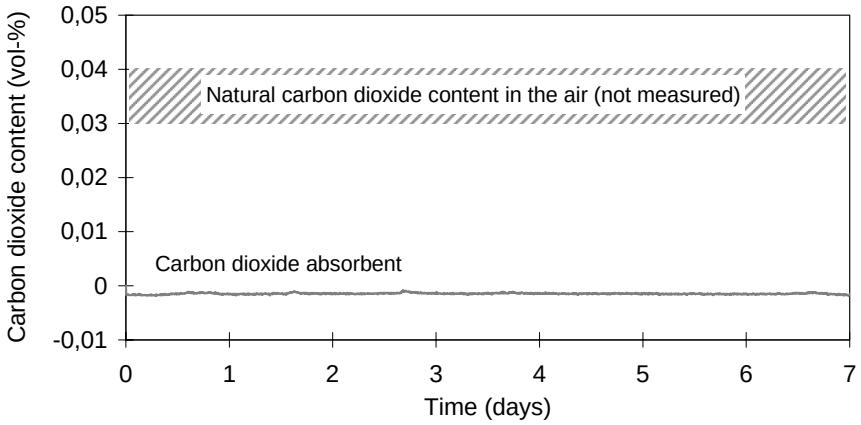

Figure 3.14 *Carbon dioxide concentration as a function of time for a chamber with carbon dioxide absorbent.*

As can be seen from Figure 3.13, the carbon dioxide content gradually decreased if no additional carbon dioxide was added. After one week, the carbon dioxide content had fallen to about 40 % of the initial value. The decrease was even more rapid when the chamber was used for preconditioning concrete specimens, which of course is explained by the fact that concrete reacts with carbon dioxide. In order to establish a relatively constant carbon dioxide content over time in the chamber, carbon dioxide had to be added on a regular basis. Figure 3.15 shows an example of the carbon dioxide concentration over seven days of conditioning of six concrete specimens used in the investigation, and described in Section 3.3.5. As can be seen, carbon dioxide was added several times per day during the first days, and later about once per day, to maintain the carbon dioxide level between 0.7 and 1.1 vol-%. As can be seen from the diagram, the carbon dioxide content was briefly raised to concentrations up to about 1.3 vol-% during the addition of

carbon dioxide from the gas tube. This high concentration normally levelled out within five minutes. The example shown in Figure 3.15 is representative of all preconditioning periods in climates with increased carbon dioxide content in the investigations described in this thesis.

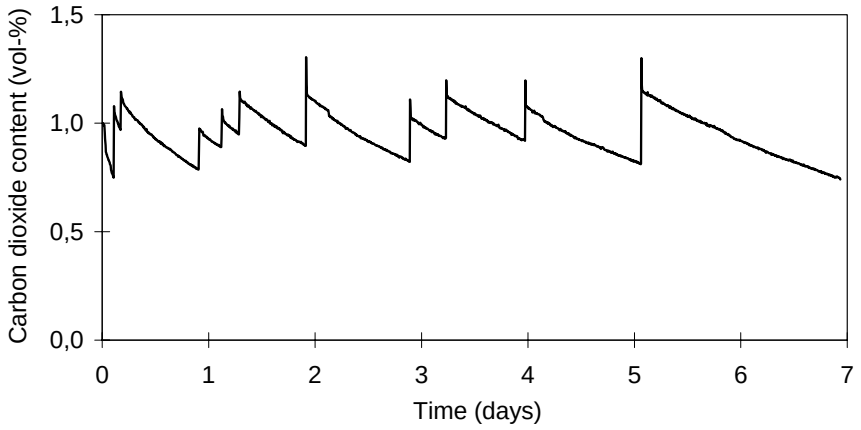

Figure 3.15 *Carbon dioxide content as a function of time during a seven-day-long preconditioning of six concrete specimens used in the investigation, as described in Section 3.3.5.*

When preconditioning specimens in the climate chamber without carbon dioxide, i.e. with the carbon dioxide filter fitted, care had to be taken not to let any carbon dioxide into the chamber while the specimens were being loaded into the chamber.

When the specimens were placed in the chamber, they were introduced through an air lock in order to minimise the amount of ambient air (i.e. with carbon dioxide) leaking into the chamber. Even so, the air lock allowed a small amount of air containing carbon dioxide to find its way into the climate chamber. In the case of the chamber with no carbon dioxide, this effect slightly increased the carbon dioxide concentration. Figure 3.16 shows an example of the increase in carbon dioxide concentration resulting from loading six specimens into the chamber. The figure also shows the reduction in carbon dioxide due to the absorption of carbon dioxide by the absorbent during the first one and a half hours after loading.

For the chamber with an elevated carbon dioxide content, the leakage of air into the chamber as a result of introducing specimens through the air lock did not have any effect on the carbon dioxide concentration in the chamber.

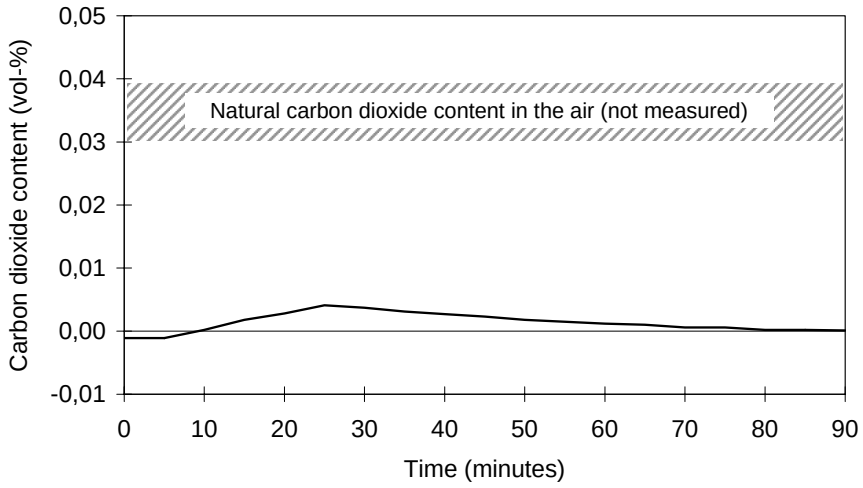

Figure 3.16 *Increase and decrease of carbon dioxide content during loading of six specimens in the chamber with a carbon dioxide-free atmosphere.*

It can be seen from the diagram that most of the carbon dioxide introduced into the system during the loading of specimens was consumed by the carbon dioxide absorbent during the first one and a half hours. To minimise the exposure of the specimens to carbon dioxide, the test surfaces were protected from evaporation and exposure to carbon dioxide by a plastic film, see Section 3.3.4. The protection was removed when the carbon dioxide content had fallen to zero, i.e. in this case, after one and a half hours. The data logging program recording climate data every five minutes indicated when the carbon dioxide had fallen to zero, so that the plastic film could be removed and the test surfaces exposed to the chamber atmosphere. During the preconditioning carried out in this investigation, care was always taken to check that the carbon dioxide content was close to zero (in the carbon dioxide-free chamber) before the test surfaces were exposed to the climate. This normally took between one and two hours after placing the specimens in the chamber.

3.2.4 Summary - Climate chambers

Two identical climate chambers were manufactured, to provide a means of varying relative humidity, air flow speed (evaporation rate) and carbon dioxide content. The carbon dioxide content could either be increased by adding carbon dioxide from a gas tube or be removed by using a carbon dioxide absorbent.

The two climate chambers were compared in order to investigate their ability to maintain stable and equal climates. These investigations showed that the climate, i.e. the temperature, relative humidity and evaporation rate, was the same for both climate chambers.

The effect on the relative humidity and carbon dioxide content of the introduction of wet specimens was also investigated. This showed the necessity of using a ‘moisture’ filter

during the first couple of hours after introducing wet specimens in to the chambers. It was also shown that specimens loaded into a chamber without carbon dioxide, i.e. with filtered air, should not immediately be exposed to the air in the chamber because of a temporarily increased carbon dioxide content. With the help of a data-logging program registering climate data every five minutes, it was carefully checked that the test surfaces were not exposed to the preconditioning climate until the carbon dioxide content had fallen close to zero. Waiting between one and two hours until exposing the test surfaces to the air in the chamber was sufficient to avoid unwanted carbonation.

3.3 Materials, specimens and preconditioning climates

3.3.1 Material composition

The investigation described in this chapter used ‘micro’ concrete qualities. By this is meant concrete with a maximum aggregate size of 8 mm, but with about the normal proportions between the different constituents. The reason to choose ‘micro’ concrete instead of normal concrete was the relatively small specimen size, giving a test surface of $78.5 \cdot 10^{-4}$ m^2. With this test surface size, concrete with large aggregates would possibly result in higher scatter between the scaling results. Since in most cases only two specimens of the same concrete quality were used, it was desired to minimise any scatter due to the material as much as possible. The specimen sizes and the number of specimens tested were determined by the capacity of the climate chambers, see Section 3.2.

Nine ‘micro’ concrete qualities were used in this investigation; compositions are shown in Table 3.5. The aggregate used was composed of naturally graded granitic material of different gradings. The gradings used were: 0/0.5 mm, 0.5/1 mm, 1/2 mm, 2/4 mm and 4/8 mm. The grain size curve used was proportioned in the same way as a grain size curve normally used in concrete with ‘normal’ aggregate size, i.e. for aggregate up to 32 mm. The air entraining agent used, ‘88L’ (produced by Cementa AB), is a vinsol/resin type. No other admixtures were used.

The OPC used was a low-alkali, sulphate-resistant cement and the secondary cementitious materials used were ground blast furnace slag and silica slurry; for chemical analysis, see Appendix 4.

Table 3.5 *'Micro' concrete compositions.*

Concrete quality	SCM[1)]	w/b-ratio	Eqv. w/c-ratio[2)]	Binder (kg/m^3)		Aggregate (kg/m^3) Gradings (mm)					Air entraining agent
				Cement	SCM	0/0.5	0.5/1	1/2	2/4	4/8	
OPC-35 air	-	0.35	0.35	625	-	394	239	267	310	197	Yes[3)]
OPC-45 air	-	0.45	0.45	448	-	455	276	309	357	227	Yes[3)]
OPC-55 air	-	0.55	0.55	364	-	478	290	324	376	239	Yes[3)]
20%slag-45	20 % slag	0.45	0.49	356	88.5	452	274	307	355	226	No
35%slag-45	35 % slag	0.45	0.52	294	158	459	279	311	360	229	No
65%slag-45	65 % slag	0.45	0.61	155	289	450	273	305	354	225	No
OPC2-45 air	-	0.45	0.45	449	-	455	276	309	358	228	Yes[3)]
5%sil-45 air	5 % silica	0.45	0.43	426	22.5	455	276	309	357	228	Yes[3)]
10%sil-45 air	10 % silica	0.45	0.41	404	44.8	456	277	309	358	228	Yes[3)]

[1)] SCM= Secondary Cementitious Materials, e.g. slag or silica, given as % by binder weight

[2)] Eqv. w/c-ratio= water/(cement + 2·silica + 0.6·slag)

[3)] The air entraining agent used was a vinsol/resin type, '88L', produced by Cementa AB

An initial investigation of the effect of air entrainment used micro concrete qualities with the same mix proportions as the three qualities with ordinary Portland cement shown in Table 3.5, with and without air entrainment, i.e. a total of six concrete qualities. The results from this investigation were presented in Utgenannt (1999), which is forming Appendix 2. The results presented in Appendix 2 are briefly discussed here. It should be noted that another type of air-entraining agent was used in the initial investigation presented in Appendix 2. It should also be noted that Table 1 in Appendix 2 is incorrect with respect to the proportion of the aggregates. The correct proportions are given in Table 3.5.

In order to make the mixes workable and to have about the same consistency, the binder content was increased in comparison with that of ordinary concrete qualities with the same w/b-ratio. For the quality with a w/b-ratio of 0.35, the increase in binder content was about 40 %, while for the qualities with w/b-ratios 0.45 and 0.55 the increase was about 10-15 % in comparison with ordinary concrete. This results in larger paste volumes and thus probably higher scaling when freeze/thaw-tested compared to ordinary concrete.

When producing the micro concrete qualities, one aim was to produce frost-resistant qualities with similar air void structures, i.e. similar spacing factor and specific surface. A spacing factor of about 0.2 mm was aimed at. After some trial mixes, it was found that an air content of about 13-14 % in the paste gave the desired air void structure. This led to different target values for the air content depending on the amount of paste (binder + water) in the mixes; see Table 3.6. For the qualities with slag as part of the binder, it was found that air entrainment was unnecessary in order to obtain the desired air void structure. Use of air entrainment in these mixes would result in too high air contents and lower spacing factors than required.

3.3.2 Mixing, casting and curing procedures

For each quality, one single mix of about 40 litres was produced using a forced action pan mixer (ROJO 60). Mixing was carried out according to the following procedure:

- All dry materials were mixed for 60 seconds.
- Water was added, mixed with the air entraining agent (if any).
- Mixed for 120 seconds.
- Stop for 30 seconds. Any unmixed material from the edge and bottom of the bowl was scraped into the rest of the material.
- Finally mixed for 60 seconds.

Directly after mixing, the concrete was cast in cylindrical moulds (PVC pipes) of two different dimensions (diameter · height): 100 · 105 mm and 40 · 45 mm. About 30 cylinders of each size were cast from each concrete quality. During casting, the moulds were filled in two stages, with 15 seconds' compaction between the fillings. A vibrating table (frequency 50-60 Hz, amplitude ± 0.5 mm) was used for compaction. After 24 hours in the moulds, the specimens were stripped and placed in lime-saturated water at +20 °C, where they remained until they were used for production of specimens for the freeze/test, see Section 3.3.4.

For qualities with entrained air, the air content in the fresh concrete was measured as prescribed in a Swedish standard similar to EN 12350-7 (2000) (the pressure method), except that a steel vessel of 1 litre was used instead of over 5 litres. The fresh air contents shown in Table 3.6 are mean values of measurements directly after mixing and after the casting was finished, approximately 30 minutes after mixing. In all cases, the difference in air content, before and after casting, was less than 0.3 %.

The air content, spacing factor and specific surface of the air void structure of the hardened concrete were measured on face-ground samples using an optical microscope, essentially in accordance with ASTM C 457 (1998). Results from microscopy measurements are shown in Table 3.6. It can be noted that the spacing factors for concrete with slag as part of the binder and without entrained air are relatively small. This is explained by the high natural air content of this type of micro concrete.

Table 3.6 *Air content in fresh concrete and results from measurements using an optical microscope on face-ground samples of hardened concrete.*

Concrete quality	Air content: fresh (vol-%) Actual (target)	Air content: hardened (vol-%) Total	Voids<2	<0.35 mm	Specific surface (mm^{-1})	Spacing factor (mm)
OPC-35 air	6.2 (6.5)	6.3	5.2	3.5	32	0.19
OPC-45 air	5.4 (5.3)	7.8	6.4	3.3	30	0.17
OPC-55 air	5.2 (4.9)	6.1	5.5	2.7	26	0.19
20%slag-45	Not measured	6.0	4.8	2.6	29	0.20
35%slag-45	Not measured	4.2	3.9	2.0	32	0.20
65%slag-45	Not measured	5.9	5.2	2.2	28	0.20
OPC2-45 air	5.4 (5.3)	5.6	4.8	2.1	23	0.23
5%sil-45 air	5.2 (5.3)	5.9	5.1	2.1	22	0.23
10%sil-45 air	4.6 (5.3)	4.8	3.6	1.8	25	0.24

3.3.3 Classification of the concrete qualities

In this investigation, freeze/thaw testing was started at different ages, from 7 to over 270 days after casting. At each testing age, the compressive strength was measured for each concrete quality. For the concrete qualities with OPC alone as the binder, the degree of hydration at each testing age was also measured. The two following sections describe the measured compressive strength and degree of hydration separately.

3.3.3.1 Compressive strength

Three wet-stored cylindrical specimens (diameter 40 mm · height 45 mm) were used for each measurement of the compressive strength. Before measuring the compressive strength, the end surfaces of the cylinders were ground to produce parallel pressure areas and to make the length/diameter-ratio approximately 1. The compressive strength was measured in a testing machine with a maximum load of 300 kN (Toni Comp III from Toni Technik). Table 3.7 shows the compressive strengths and standard deviations. In some cases, the standard deviation may seem high; this was due essentially to difficulties when grinding the relatively small test specimens, resulting in pressure areas not sufficiently parallel to ensure only small scatter.

Table 3.7 *Compressive strength at different ages. Each value is a mean of three measurements.*

Concrete quality	**Compressive strength and *(standard deviation)* in MPa at the age of *X* days**									
	***X*=7**	**17**	**24**	**31**	**38**	**66**	**73**	**122**	**136**	**276**
OPC-35 air	57 *(1.8)*	63 *(2.1)*	68 *(3.0)*	72 *(5.3)*	79 *(2.6)*	80 *(4.0)*	-	85 *(3.0)*	-	92 *(3.7)*
OPC-45 air	40 *(1.0)*	48 *(1.1)*	53 *(3.0)*	57 *(4.4)*	60 *(4.4)*	67 *(4.1)*	-	73 *(1.2)*	-	79 *(1.6)*
OPC-55 air	27 *(1.6)*	34 *(1.8)*	38 *(4.7)*	46 *(1.9)*	46 *(1.9)*	51 *(4.2)*	-	55 *(2.6)*	-	59 *(2.7)*
20%slag-45	-	50 *(3.3)*	-	65 *(0.2)*	-	-	75 *(2.7)*	79 *(2.6)*	-	-
35%slag-45	-	42 *(1.1)*	-	54 *(3.0)*	-	-	67 *(0.5)*	75 *(1.2)*	-	-
65%slag-45	-	29 *(1.4)*	-	39 *(0.5)*	-	-	53 *(2.7)*	61 *(1.1)*	-	-
OPC2-45 air	-	52 (2.9)	-	56 (2.1)	-	64 (0.6)	-	-	73 (1.7)	-
5%sil-45 air	-	57 (0.6)	-	64 (1.4)	-	77 (2.2)	-	-	78 (3.1)	-
10%sil-45 air	-	58 (2.6)	-	66 (4.8)	-	76 (2.5)	-	-	80 (4.8)	-

3.3.3.2 Degree of hydration

For concrete with OPC alone as the binder, the degree of hydration was calculated from measurements of non-evaporable water content (heating to +1050 °C). Materials from specimens used for compressive strength determination were used for these measurements. After the compressive strength was measured, one specimen was immediately crushed, saturated in alcohol and put into a ventilated oven at +105 °C. After one day, the material was ground and again placed in the ventilated oven at +105 °C. After seven days at +105 °C, the material was placed in a desiccator with silica gel to cool before being weighed. After weighing, the material was placed in an oven at +1050 °C for 24 hours. The weight was subsequently measured after the material had cooled down to room temperature in a desiccator.

The non-evaporable water content, W_n, was calculated from Equation 1 and the cement content, C, from Equation 2:

$$W_n = W_{105} - \frac{W_{1050}}{\left(1 - \frac{\mu_c + \mu_a \cdot g}{1+g}\right)} \qquad \text{[Eq. 1]}$$

$$C = \frac{1}{1+g}(1-\mu_c)\cdot(W_{105} - W_n) \qquad \text{[Eq. 2]}$$

where:

W_n	is the non-evaporable water content	[kg]
W_{105}	is the weight after drying at +105 °C	[kg]
W_{1050}	is the weight after ignition at +1050 °C	[kg]
μ_c	is the ignition loss of the dry cement	[kg/kg]
μ_a	is the ignition loss of the aggregate	[kg/kg]
g	is the aggregate: cement ratio	[-]

The derivation of these equations is discussed in Appendix 5. In Appendix 5 also some comments are given to calculations of the term W_n/C using an alternative equation, frequently used in other investigations.

Studies by Powers and Brownyard (1948) showed that during hydration cement chemically binds about 25 % by weight of water. This leads to the following expression for the degree of hydration (α), Equation 3:

$$\alpha \approx 4 \cdot \frac{W_n}{C} \qquad \text{[Eq. 3]}$$

The total porosity and the capillary porosity can be calculated assuming a structure of the cement paste in accordance with Powers and co-workers, i.e. a gel porosity of about 28 %, and by assuming that the volume of non-evaporable water is about 75 % of the volume of bulk water. The following expressions for the total porosity $(P_{tot})_{paste}$, Equation 4, and capillary porosity $(P_{cap})_{paste}$, Equation 5, of the cement paste are given in Fagerlund (2000). (It is assumed that the specific gravity of dry cement is 3.1 kg/litre and that of water is 1.0 kg/litre.)

$$\left(P_{tot}\right)_{Paste} = \frac{vct - 0.19 \cdot \alpha}{0.32 + vct} \qquad \text{[Eq. 4]}$$

$$\left(P_{cap}\right)_{Paste} = \frac{vct - 0.39 \cdot \alpha}{0.32 + vct} \qquad \text{[Eq. 5]}$$

Table 3.8 shows the calculated values for degree of hydration (Equation 3) and capillary porosity (Equation 5). For 'OPC-35 air', 'OPC-45 air' and 'OPC-55 air', each value is calculated from one single measurement of the non-evaporable water content. For 'OPC2-45 air', the given values for degree of hydration and capillary porosity are mean values of two measurements.

Table 3.8 *Degree of hydration calculated from Equations 1, 2 and 3, capillary porosity (in parenthesis) calculated from Equation 5.*

Concrete quality	**Degree of hydration and capillary porosity *(calculated)* at the age of *X* days**									
	***X*=7**	**17**	**24**	**31**	**38**	**66**	**73**	**122**	**136**	**276**
OPC-35 air	0.41 *(28)*	0.45 *(26)*	0.47 *(25)*	0.51 *(23)*	0.53 *(22)*	0.53 *(21)*	-	0.58 *(18)*	-	0.62 *(16)*
OPC-45 air	0.41 *(38)*	0.47 *(35)*	0.51 *(32)*	0.55 *(31)*	0.56 *(30)*	0.63 *(27)*	-	0.66 *(25)*	-	0.71 *(22)*
OPC-55 air	0.44 *(43)*	0.52 *(40)*	0.56 *(38)*	0.62 *(36)*	0.59 *(37)*	0.64 *(34)*	-	0.70 *(32)*	-	0.78 *(28)*
OPC2-45 air	-	0.50 *(33)*	-	0.54 *(31)*	-	0.64 *(26)*	-	-	0.64 *(26)*	-

3.3.4 Specimens for freeze/thaw testing

Specimens for freeze/thaw testing were produced from the large concrete cylinders (100 mm diameter · 105 mm height). Each cylinder was cut in half, to give two freeze/-thaw specimens (100 mm diameter · 50 mm height). One day before cutting, the concrete cylinders were removed from the water bath where they had been stored since demoulding. The surfaces of the cylinders were dried in air at room temperature for a couple of hours (this was necessary for the contact adhesive later used to bond to the concrete surface). The cylinders were then insulated by applying moisture-insulating PVC caps to the top and bottom of the cylinder, as shown in Figure 3.17. The caps consisted of a 50 mm PVC pipe part (100 mm diameter) with a lid, glued at one end of the pipe to form a cap. The inside dimensions of the caps were 100 mm diameter · 48 mm depth, which thus left only a small section of the middle of the cylinder exposed. The joint between the plastic cap and the concrete was sealed with contact adhesive, see Figure 3.17.

The insulated cylinders were stored in air for about 20 hours to allow the adhesive to dry before cutting the cylinders into freeze/thaw specimens.

The insulated cylinders were cut in the middle with a stone saw, producing two specimens. The cut surfaces were immediately brushed clean under water and then placed with the cut surface on a wet cloth. This was done to prevent the surfaces from drying and from being exposed to carbon dioxide.

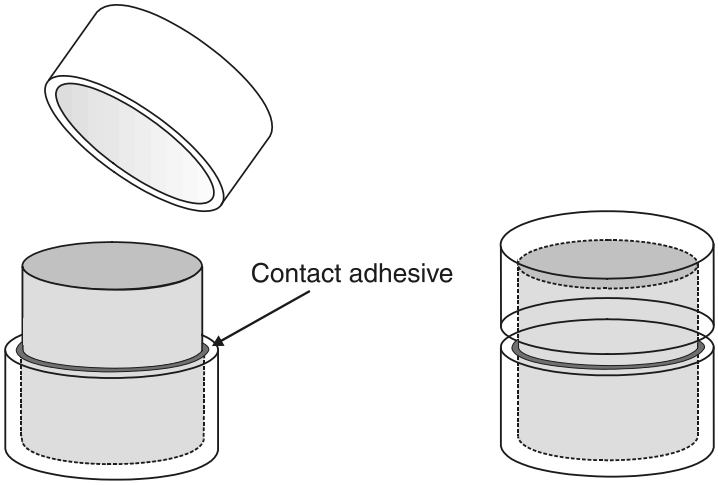

Figure 3.17 *Cylinder with insulated top and bottom*

Before the specimens were placed in the climate chambers, the cut surface was protected from air by a plastic film which was placed directly on the wet, cut surface and fastened with a rubber band, as shown in Figure 3.18. The plastic film protected the test surface of the specimens both from carbon dioxide in the air and from drying. In order further to prevent the possibility of carbonation, each specimen was individually placed in a plastic bag before being inserted into the climate chambers.

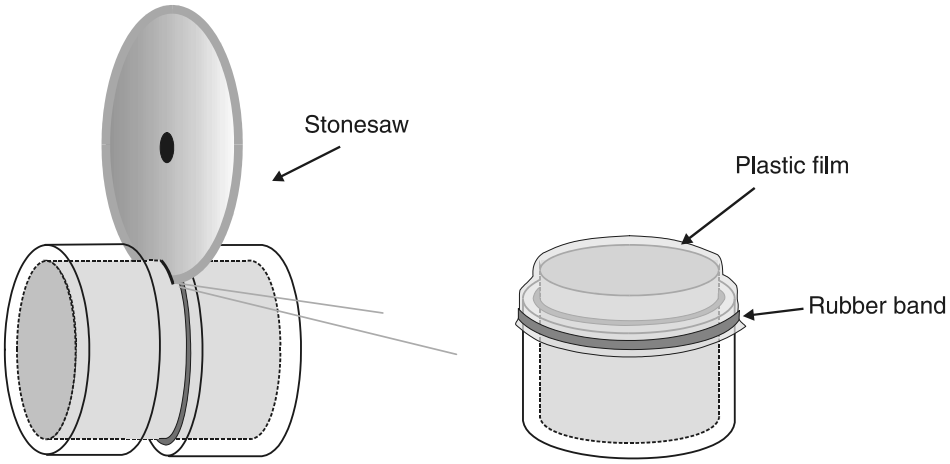

Figure 3.18 *Cutting a cylinder into two specimens and protection of the concrete surface from air by a plastic film.*

3.3.5 Preconditioning before freeze/thaw testing

Three different preconditioning regimes were used in this investigation:

1. Water storage until freeze/thaw testing i.e. so that the test surface never dried. (The concrete cylinder was removed from the water bath one day before the start of freeze/thaw testing to produce freeze/thaw specimens as described in Section 3.3.4. The cylinders were cut into freeze/thaw specimens just before the freeze/thaw test started. After cutting, the cut surfaces were immediately brushed clean under water and then placed with the cut surface on a wet cloth, ensuring that the test surfaces never dried out. The freeze/thaw test started within half an hour after cutting.)

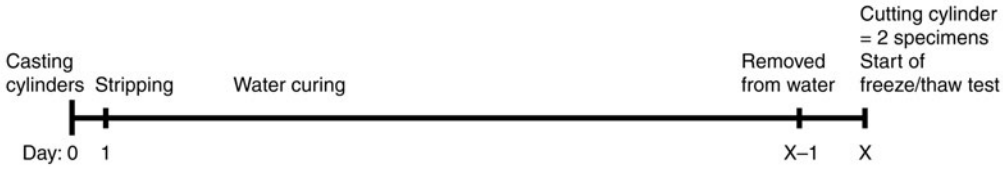

2. Seven days in a climate chamber at 65 % RH / +20 °C and without carbon dioxide content, followed by a three-day-long resaturation period before freeze/thaw testing. (The cylinders were stored in a water bath until one day before preconditioning in the climate chamber started. The specimens were produced as described in Section 3.3.4.)

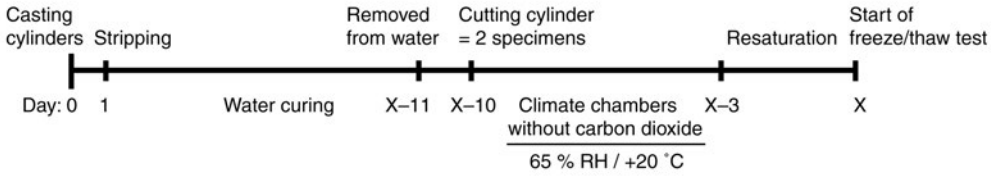

3. Seven days in a climate chamber at 65 % RH / +20 °C and with increased carbon dioxide content of ~1 vol-%, followed by a three-day-long resaturation period before freeze/thaw testing. (The cylinders were stored in a water bath until one day before preconditioning in the climate chamber started. The specimens were produced as described in Section 3.3.4.)

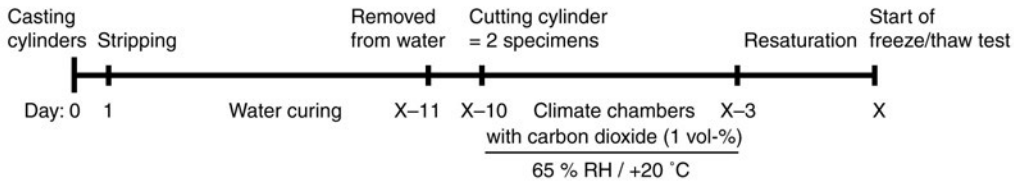

To be able to evaluate the effect of increasing age of the concrete on the salt-frost resistance, freeze/thaw testing was started at different ages after casting. In the illustrations above **x** is the age of the concrete in days after casting when the freeze/thaw test starts.

- For concrete with OPC alone as the binder, the freeze/thaw testing was started at seven different ages (**x**): 17, 24, 31, 38, 66, 122, 276 days after casting (for OPC concrete conditioned according to conditioning Regime 1, an additional freeze/-thaw testing was started at an age of 7 days).
- For concrete with slag as part of the binder, the freeze/thaw testing was started at four different ages (**x**): 17, 31, 73, 122 days after casting.
- For concrete with silica as part of the binder, the freeze/thaw testing was started at four different ages (**x**): 17, 31, 66, 136 days after casting.

The following is a brief description of the handling of the climate chambers and the specimens conditioned in the chambers. It should be noted that the climate chambers were used only for preconditioning specimens according to Regimes 2 and 3 as described above.

A full description of the climate chambers where the specimens were preconditioned is given in Section 3.2.

Preparing the climate chambers

A couple of days before a preconditioning period was about to start the climate chambers were prepared by adding carbon dioxide to the air in the chamber that was to have increased carbon dioxide content. The other chamber, with a carbon dioxide-free climate, was prepared by ensuring that the carbon dioxide filter was filled with an active absorbent.

Before the newly cut, wet specimens were loaded into the climate chambers, a 'moisture filter' with moisture absorbents was fitted to the tube system of each climate chamber. This was done to be able quickly to absorb the excess water on the specimens and to restore the relative humidity of the air in the chamber. The effect of the moisture filter is described in Section 3.2.

Loading the climate chambers

A maximum of six specimens (100 mm diameter) were placed in each climate chamber at a time. Specimens were inserted through the air lock in order to minimise the amount of ambient air leaking into the chambers when specimens were loaded.

Handling of specimens in the climate chambers

When the desired carbon dioxide concentration was reached, the plastic film covering the test surface was removed. Before doing this, the valves letting the air in the system circulate through the moisture filter were opened. The plastic film, and the rubber band holding it in place, were removed and placed in a plastic bag. The wet test surface was wiped off with a wet cloth. The specimens were then weighed. The weight of each specimen was registered again three times during the first four hours and about three times

during the next four days of exposure and finally before the specimens were removed from the climate chamber. It should be noted that all work, such as weighing the specimens, is carried out by using the rubber gloves attached to the climate chambers. This enables the specimens to be handled inside the climate chambers without any leakage of carbon dioxide into the chambers.

Resaturation of specimens

After seven days in the climate chamber, the specimens were removed from the chamber to be resaturated for three days before starting the freeze/thaw test. Before the specimens were removed, their weight was noted and they were put in plastic bags. The air lock was used to remove the specimens from the chamber. The specimens were weighed again on a scale outside the chamber before they were placed with the test surface downwards in a vessel containing de-ionised water at a temperature of +20 °C. To reduce the air and carbon dioxide concentration in the de-ionised water, the water was boiled before use. The specimens were again weighed five times during the first four hours and twice more during the next two days. The specimens were wiped with a wet cloth before being weighed. Resaturation was ended after three days, and the specimens were finally weighed once more before the freeze/thaw test started.

3.4 Freeze/thaw testing

After preconditioning and resaturation of the specimens as described in Section 3.3.5, the specimens were placed with the test surface downwards in a cylindrical glass cup with a diameter of 135 mm. The cup was filled with 170 ml (a 12 mm deep layer) 3 % NaCl solution. A plastic ring on the bottom of the cup maintained a 10 mm space between the test surface and the bottom of the cup. The temperature was measured in the salt solution under the test surface. The glass cup was thermally insulated on all sides except the bottom of the cup. The test set-up is shown in Figure 3.19.

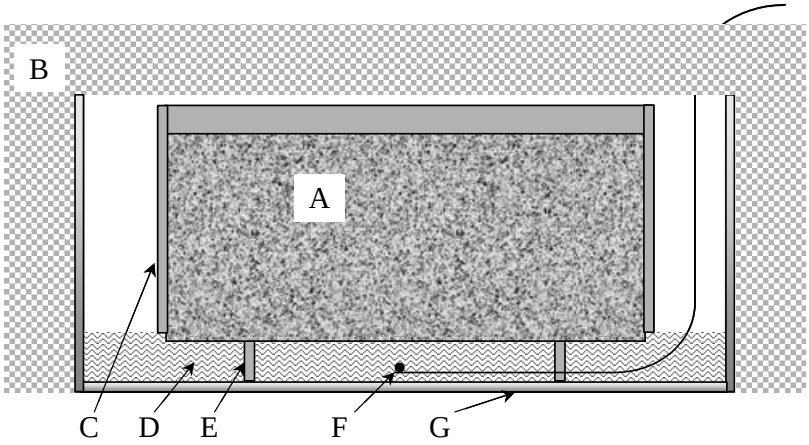

Figure 3.19 *Test set-up used for freeze/thaw test. A - Concrete specimen (diameter - 100 mm, height - 50 mm), B - Polystyrene cellular plastic for thermal insulation (20 mm, density 18 kg/m^3), C - Moisture insulating PVC cap, D - Freezing medium (12 mm, 3 % NaCl solution), E - Plastic spacer, F - Temperature measuring device, G - Glass cup*

The insulated cups with specimens were placed in temperature-controlled freezers. The freeze/thaw cycle used was similar to the freeze/thaw cycle used in Swedish Standard SS 13 72 44, i.e. a 24-hour cycle with temperatures between +20 °C and –18 °C, as shown in Figure 3.20.

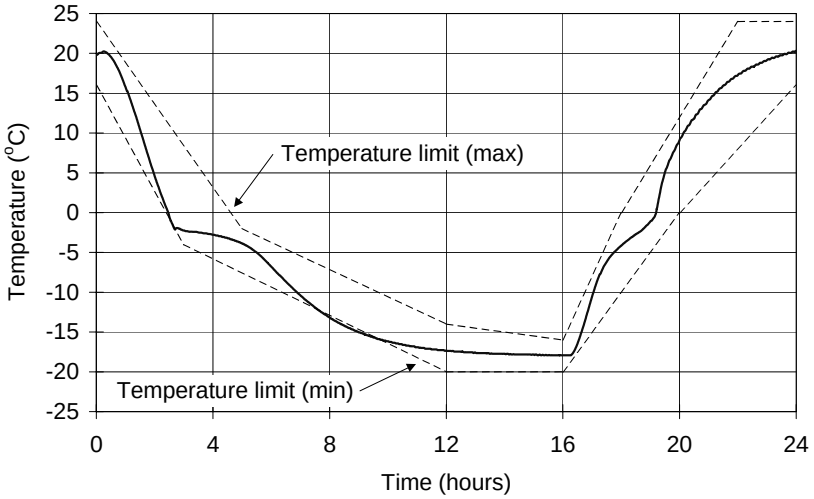

Figure 3.20 *Freeze/thaw cycle used in this investigation and temperature limits according to SS 13 72 44*

After 1, 4, 7, 14, 21, 28, 42 and 56 freeze/thaw cycles, the scaled material was brushed off, collected and dried at +105 °C until the material was completely dry, after which its

weight was measured. The results are given as the accumulated dry weight of the scaled material in kg per square meter test surface (kg/m²) as a function of the number of freeze/-thaw cycles.

The reason not to follow the method prescribed in Swedish Standard SS 13 72 44 was solely for practical reasons. When the specimens were conditioned in the climate chamber there was no possibility of gluing the moisture-insulating rubber sheet prescribed by the standard to the sides of the specimens. This was also found difficult to do before the specimens were placed in the chamber, and so an alternative freeze/thaw test set-up was used. The method used is similar to the earlier version of SS 13 72 44, called SS 13 72 36, which was a type of cup method similar to the one used here. However, the temperature curve used is the same as is used in SS 13 72 44. Although the absolute amount of scaling may differ somewhat between the standard method and the cup method used in this investigation, they both result in the same classification of salt-frost resistance of concrete.

During the course of freeze/thaw testing the large number of specimens (around 270 specimens in total) that were tested in this part of the investigation, it was found that there were some unwanted edge effects that to some degree influenced the scaling results.

While testing, it was seen that for some specimens the scaling was more pronounced at the edges of the specimen than at the inner parts of the test surface. This is probably a result of the difference in moisture access (from two sides) and of the two-dimensional heat flow at the edges of the specimens. At the inner parts of the test surface, the heat flow is one-dimensional, and moisture is accessible only from one side. These differences lead to the frost attack being more severe at the edges than at the inner parts of the test surface.

The investigation did not distinguish between scaling from the edges and scaling from the inner parts of the test surface. For concrete with low scaling resistance this is of no importance, since the possible extra scaling from the edges is small compared with the total scaling. However, for concrete with high scaling resistance, the extra scaling from the edges may be a large proportion of the total scaling, and thus the scaling resistance for these qualities may be somewhat underestimated. This should be born in mind when examining the results from testing according to this freeze/thaw method. However, as can be seen from the results described in Section 3.5, there is a substantial difference in scaling between the specimens showing high scaling resistance and those showing low scaling resistance. In the light of this, the possible effect of scaling at the edges depending on concrete quality is of no importance.

3.5 Results and discussion

3.5.1 Introduction

Utgenannt (1999) discusses the possible effects of carbonation on the scaling resistance for 'micro' concrete with ordinary Portland cement and with different w/b-ratio; see Appendix 2. In the investigation concrete qualities both with and without entrained air were studied. Specimens preconditioned for seven days in two different climates, with (~1 vol-%) and without carbon dioxide and with 65 % RH / +20 °C, were freeze/thaw tested at an age of 31 days in accordance with the freeze/thaw test method described in Section 3.4. The climate chambers described in Section 3.2 were used for preconditioning.

Figure 3.21 shows the scaling results for the concrete qualities with entrained air and with different w/b-ratios.

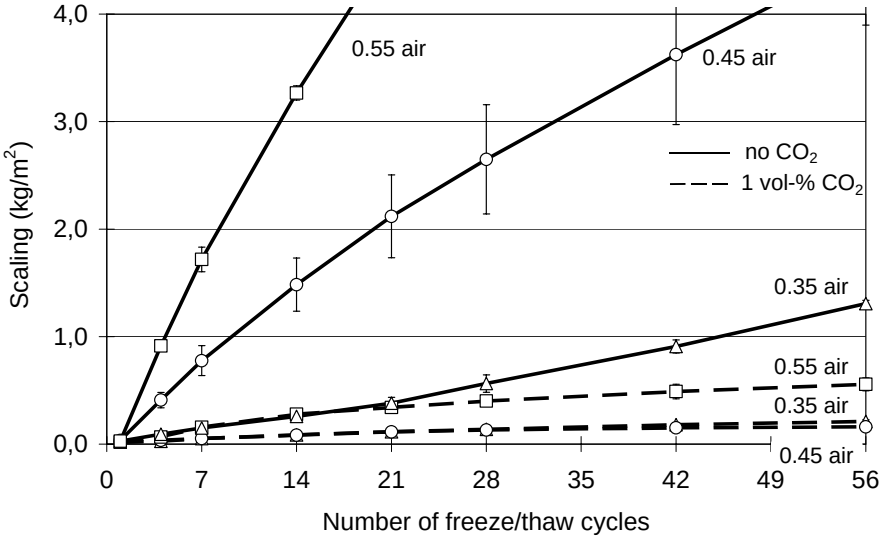

Figure 3.21 *Scaling as a function of the number of freeze/thaw cycles for concrete with OPC as the binder and different w/c-ratios and with entrained air, conditioned in two climate chambers, with (~1 vol-%) and without carbon dioxide respectively. From Appendix 2.*

The figure shows that the specimens preconditioned in an environment with increased carbon dioxide content (~1 vol-%) show much lower scaling than do specimens conditioned in the same climate but without carbon dioxide. In other words, carbonation of these concrete qualities improves the scaling resistance markedly. The results for specimens without entrained air show the same tendency, i.e. concrete with a carbonated test surface shows a significantly higher scaling resistance than does concrete with an uncarbonated test surface, see Appendix 2.

The results presented here indicate that the hypothesis in Chapter 2 is correct, i.e. that a protective layer exists, consisting of a carbonated skin. There are, however, also other ageing effects than carbonation that may influence the salt-frost resistance, e.g. hydration and drying. An additional investigation was carried out to investigate the influence of these ageing effects on the salt-frost resistance and also further to investigate the effect of carbonation. The results from this 'main' investigation are presented below.

3.5.2 The effect of carbon dioxide concentration

An increased carbon dioxide content of 1 vol-% was used in the investigation presented in Appendix 2, as well as in the 'main' investigation presented below. In order to verify the validity of the scaling results using preconditioning climates with increased carbon dioxide content, a complementary test was carried out where specimens were conditioned in normal air (0.03-0.04 vol-% carbon dioxide). The result from this test is shown in Figure 3.22. The concrete tested was produced with the same OPC and with the same air entraining agent as were used for the tests presented in Figure 3.21. The w/c-ratio was 0.45, and the fresh air content was 4.5 %. The aggregate used was composed of naturally graded granitic material of different gradings. The gradings used were: 0/8 mm, 4/8 mm and 8/16 mm. The freeze/thaw method used was SS 13 72 44, except that the concrete was 60 days old, instead of 21 days, before it was conditioned for seven days in two different climates: 65 % RH / +20 °C in normal air and in air without carbon dioxide. The freeze/-thaw test was carried out as was described in Chapter 2.

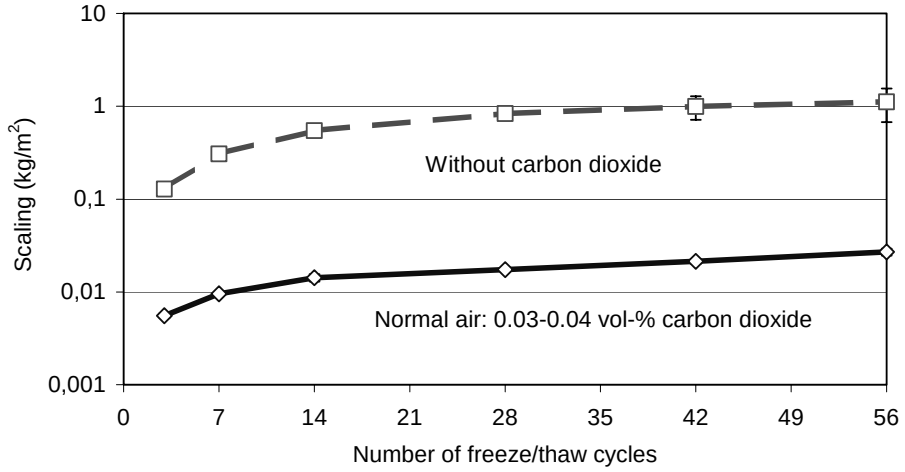

Figure 3.22 *Scaling as a function of the number of freeze/thaw cycles for specimens with entrained air preconditioned in two different climates, both with 65 % RH / +20 °C, one in normal air (0.03-0.04 vol-% carbon dioxide) and one in air without carbon dioxide. From Appendix 2.*

From the figure it can be seen that preconditioning in normal air also leads to a markedly improved scaling resistance. A seven days' long exposure to normal air thus results in a protective concrete 'skin' with properties similar to those found for concrete exposed to a climate with increased carbon dioxide content (~1 vol-%). These results verify the validity of using increased carbon dioxide content during preconditioning, at least as far as the effect of carbonation on the scaling resistance is concerned.

The reason for using increased carbon dioxide content during preconditioning before freeze/thaw testing in the investigations presented here is twofold. The primary reason is to simulate a longer exposure to 'normal' air than just for seven days as is the case before freeze/thaw testing. In reality, concrete is normally allowed to carbonate for longer than seven days before being exposed to a severe cold climate with de-icing salts. The chosen climate with around 1 vol-% carbon dioxide thus gives results more in accordance with what can be expected in reality.

A second reason for choosing increased carbon dioxide content has a more practical aspect. That is, when using the climate chambers described in Section 3.2 for preconditioning, it is easier to establish a stable climate with an increased carbon dioxide content than with a carbon dioxide content in line with what is found in normal air. Preconditioning in normal air in a large climate room was also not an option, since it was desired to precondition parallel specimens in 'exactly' the same climates, but with different carbon dioxide contents. The two identical climate chambers used were thus the best solution, and so an increased carbon dioxide content was preferred.

The reason for choosing a carbon dioxide concentration of 1 vol-% and not higher was because of results from an investigation presented in Knöfel & Eßer (1992). There, it was shown that carbonation in an environment with increased carbon dioxide content could lead to changes in the material properties not found when carbonated in normal air. However, Knöfel & Eßer (1992) conclude that an increased carbon dioxide content of around 1 vol-% gives about the same results as carbonation in normal air. This is further discussed in Chapter 4.

3.5.3 The effect of ageing on the salt-frost resistance - Main investigation

3.5.3.1 Introduction

In this part of the investigation the influence of different ageing effects on the salt-frost resistance was studied. The effects of hydration, drying and carbonation on the salt-frost resistance were investigated separately. In the investigation not only concrete with plain OPC as the binder was studied, but also blends of OPC with different amounts of ground granulated blast furnace slag and silica fume respectively.

Nine 'micro'-concrete qualities were freeze/thaw tested at different ages after casting. Concrete compositions are given in Section 3.3.1, and production of the specimens is described in Section 3.3.4. Freeze/thaw testing was carried out according to the method

described in Section 3.4. Depending on concrete quality, the freeze/thaw testing was started at different ages after casting, with the 'youngest' tested 17 days after casting and the 'oldest' at an age of 276 days after casting. For comparison, it can be noted that when freeze/thaw testing concrete according to the Swedish Standard SS 13 72 44, the specimens normally have an age of 31 days at the start of the freeze/thaw test.

Three different preconditioning climates were used for all concrete qualities and for all ages, as described in Section 3.3.5:

1. water-cured all the time until the start of the freeze/thaw test.
2. water-cured until ten days before the start of the freeze/thaw test. Before testing started, the specimens were dried for seven days in 65 % RH / +20 °C without carbon dioxide, followed by a three-day-long resaturation period.
3. water-cured until ten days before the start of the freeze/thaw test. Before testing started, the specimens were dried for seven days in 65 % RH / +20 °C with increased carbon dioxide concentration (~1 vol-%), followed by a three-day-long resaturation period.

Testing concrete conditioned in the three different climates at different ages after casting made it possible to investigate the relative effects of drying and carbonation at different ages, and also to study the combined effect of the development of hydration and degree of saturation on the salt-frost resistance.

This chapter presents a selection and discussion of the results, divided in sections dealing with the effect of hydration, drying, and carbonation separately. The results are presented based on the accumulated scaling after 14 freeze/thaw cycles for specimens preconditioned according to the three preconditioning regimes. The accumulated scaling after 14 freeze/thaw cycles was chosen because, at this relatively early stage of the freeze/thaw test, the scaling resistance of the test surface is still noticeable in the scaling results. Later in the freeze/thaw test, the scaling is in many cases so severe that differences in scaling resistance of the surface, because of (for example) drying, are not as apparent as earlier during the freeze/thaw test. Comparisons with the accumulated scaling after other numbers of freeze/thaw cycles have been made, and show that the conclusions are the same regardless of after how many freeze/thaw cycles the evaluation is carried out. Some comparisons with results from the accumulated scaling after 56 freeze/thaw cycles are shown. A complete presentation of the scaling results is given in Appendix 6.

3.5.3.2 The effect of hydration + degree of saturation

Testing water-cured specimens (that have not been allowed to dry out at any time) at different ages after casting makes it possible to evaluate the combined effect of increased hydration and increased degree of saturation on the salt-frost resistance. In this context, the effect of degree of hydration on the scaling resistance means the combined effects of the change in the different material properties as a result of hydration. For example, with increasing degree of hydration the capillary porosity decreases, the compressive and

tensile strengths increase, the amount of freezable water decreases and the degree of saturation might decrease as a result of self-desiccation. On the other hand, since the concrete was water-cured, the degree of saturation may increase as a result of ageing. The net effect of the decrease in degree of saturation as a result of hydration, and the possible increase as a result of water uptake, depends on material properties such as pore structure and permeability. Here, it is the combined effect of increase in degree of hydration and the change in degree of saturation with time that has been investigated. No attempt has been made to separate the effects. The degree of hydration was measured for concrete with OPC at different ages, see Section 3.3.3.2. For concrete with slag or silica as part of the binder, as well as for plain OPC concrete, the compressive strength at different ages was also measured. No measurement of the degree of saturation was carried out.

The freeze/thaw test for the concrete qualities with plain OPC as binder was started at seven different ages between 17 days and 276 days after casting. (For specimens water-cured until testing, an additional test was carried out, starting at an age of seven days.) For concrete with slag or silica as part of the binder, the freeze/thaw test was started at four different ages between 17 days and 136 days after casting.

Figure 3.23 shows the accumulated scaling after 14 freeze/thaw cycles for water-cured (never dried) specimens of different binder types/combinations, tested at different ages.

OPC

Figure 3.23a shows the results for concrete with plain OPC and with different w/b-ratios. From the figure it can be seen that there is, as expected, a significant effect on the scaling resistance depending on w/b-ratio, with an increase in scaling resistance with decreasing w/b-ratio. It can also be seen that there seems to be a small positive effect of ageing for the concrete qualities with w/b-ratios of 0.35 and 0.45, at least up to an age of 30 days at test start, after which the scaling becomes independent of age. For these concrete qualities, this can be interpreted as if the effect of the increase in the degree of hydration on the scaling resistance during the first 30 days outweighs the negative effect of the possible increase in the degree of saturation due to the water-curing. At later ages, the scaling resistance is the same regardless of age, implying that the positive effect of the slow increase in degree of hydration, as can be seen in Figure 3.24a (which also shows the compressive strength), is offset by the possibly increasing degree of saturation as a result of water curing. For the quality with a w/b-ratio of 0.55, there is no positive effect of ageing when water-cured.

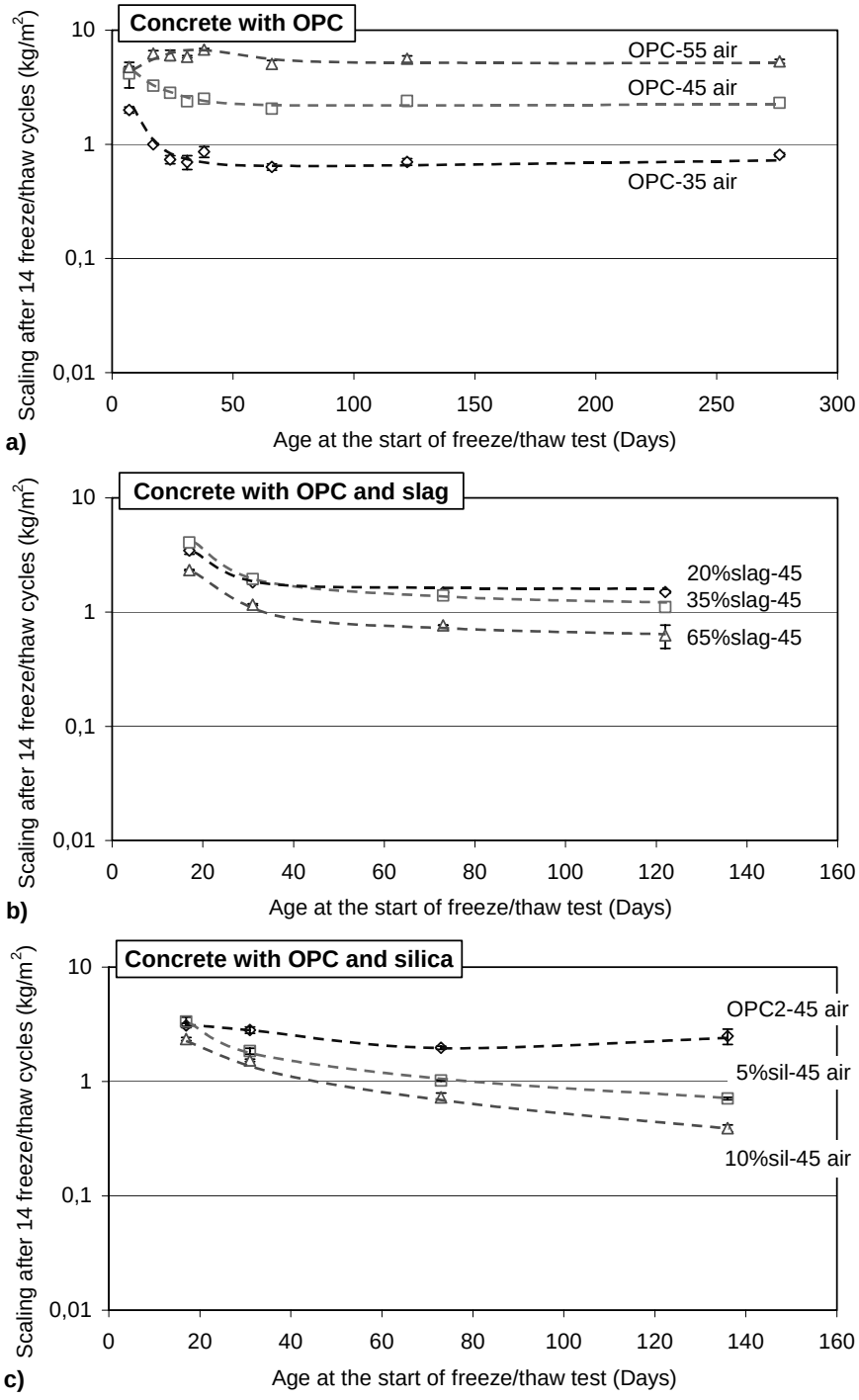

Figure 3.23 *Scaling after 14 freeze/thaw cycles for water-cured (never-dried) specimens as a function of age at the start of the freeze/thaw test. Note the scale on the x-axes. a) OPC, b) OPC + slag, c) OPC + silica*

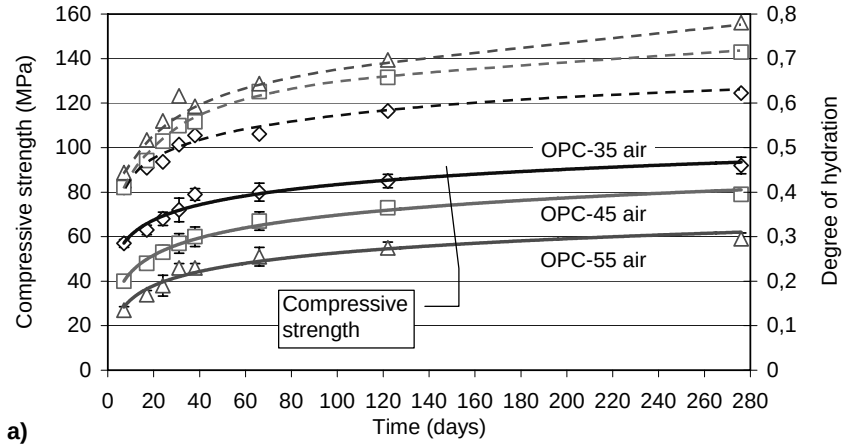

a)

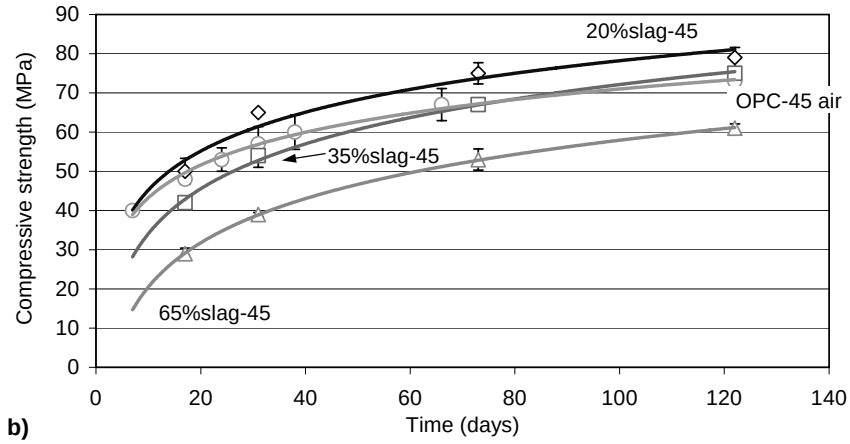

b)

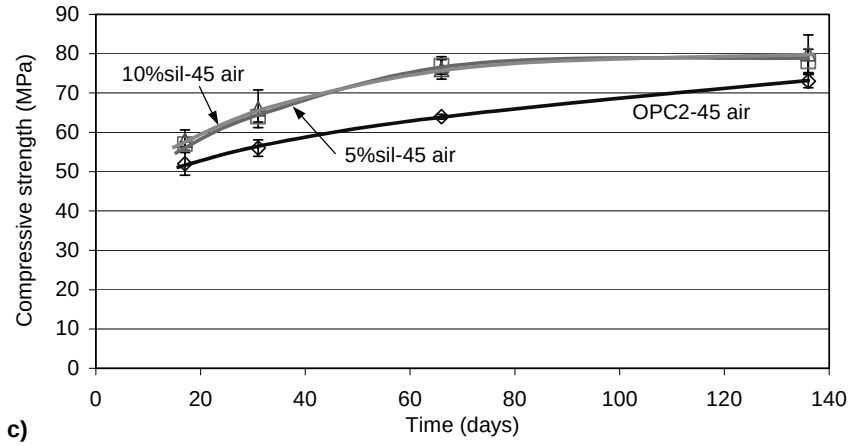

c)

Figure 3.24 *Compressive strength/degree of hydration (for OPC concrete) as a function of age. For compressive strength, each point is a mean of three specimens. For degree of hydration, each point is one measurement. Note scales on the x- and y-axes. a) OPC, b) OPC + slag, c) OPC + silica*

OPC + slag

Figure 3.23b shows the results for concrete with different amounts of slag as part of the binder, all with a w/b-ratio of 0.45. From the figure it can be seen that for water-cured, never-dried specimens the scaling resistance is somewhat improved with increasing slag content. It can also be seen that, for all concrete qualities, there is a marked positive effect of ageing. This positive effect is most pronounced at early ages, and for concrete with only 20 % slag as part of the binder the scaling is about the same when tested at an age of 30 days and older. For this concrete quality, the positive effects of increased hydration at ages over 30 days seem to be cancelled out by a continuing increase in the degree of saturation. For concrete with 35 % and 65 % of slag as part of the binder, there is also a small increase in scaling resistance with increasing age at test ages over 30 days. This can probably be explained by the relatively slow hydration process for these concrete qualities, indicated in this investigation by the slow development of compressive strength (see Figure 3.24b). For these concrete qualities, the positive effect of increased hydration on the scaling resistance is more pronounced than the possible negative effect of increased degree of saturation as a result of water curing.

OPC + silica

Figure 3.23c shows results for concrete with different amounts of silica as part of the binder, all with a w/b-ratio of 0.45. These concrete qualities were produced a couple of months after the concrete qualities with only OPC and with OPC + slag as binder. A ‘reference’ concrete with OPC and a w/b-ratio of 0.45 was therefore produced and tested as well. From the figure it can be seen that, for water-cured never-dried specimens, there seems to be an increase in scaling resistance with increasing silica content. For concrete with silica as part of the binder, there is a marked effect of ageing on the scaling resistance, with increased scaling resistance with increasing age at the start of testing. For concrete containing silica as part of the binder, it therefore seems as if the positive effect of hydration is greater than the negative effect of a possible gradual increase in the degree of saturation as a result of water curing.

The explanation for the higher improvement in scaling resistance during the first 60-70 days for concrete with silica as part of the binder, compared with concrete with only OPC as the binder, might be the more rapid development of hydration during this period. This can be seen from the more rapid increase in compressive strength during the first 70 days for concrete containing silica, compared with the concrete with only OPC as the binder (see Figure 3.24c).

Discussion

From the results presented in Figure 3.23 it can be seen that, for concrete with only OPC as the binder, the positive effect of ageing on the salt-frost resistance increases with decreasing w/b-ratio, at least at early ages. For concrete with slag as part of the binder, the positive effect of ageing increases with increasing slag content. The same is observed for concrete with silica as part of the binder, i.e. the positive effect of ageing is more pronounced the higher the silica content, at least up to 10 % as part of the binder. These

results indicate that the denser and less permeable the material, the more significant is the positive effect of ageing on the salt-frost resistance for water-cured never-dried material. This can probably be explained by the fact that the increase in the degree of hydration causes a reduction in the freezable water content. In addition, self-desiccation might occur in a denser cement paste, despite the fact that the surface is exposed to moisture. The degree of saturation might therefore become lower with time in dense concrete.

3.5.3.3 The effect of drying

The effect of drying and the effect of carbonation on the scaling resistance have been investigated separately. As has been previously mentioned, this was carried out by conditioning specimens in two climates that differed only in respect of carbon dioxide content, using the climate chambers described in Section 3.2. This section compares the scaling results for the specimens conditioned (dried) in the carbon dioxide-free climate with the results for the water-cured, never-dried, specimens discussed above. This gives a way of evaluating the relative effect of drying. In this context, 'drying' refers to the seven-day-long conditioning in 65 % RH and +20 °C without carbon dioxide. After this preconditioning, the specimens were resaturated for three days before the start of the freeze/thaw test. Comparisons are made for specimens with the same age at the start of freeze/thaw testing.

Figure 3.25 shows the accumulated scaling after 14 freeze/thaw cycles for the dried uncarbonated specimens of different binder types/combinations, tested at different ages.

In order to evaluate the effect of drying, the accumulated scaling after 14 cycles for the dried uncarbonated specimens ($SC_{0\%}$) has been divided by the accumulated scaling after 14 cycles for the water-cured specimens (SC_w). The quotient of these amounts of scaling is the relative effect of drying. A value below 1 indicates a positive effect of drying.

Figure 3.26 shows the relative effect of drying for specimens of different binder types/-combinations as a function of the age at the start of the freeze/thaw test.

OPC

Figure 3.26a shows the results for concrete with OPC and with different w/b-ratios. From the figure, it can be seen that there is a positive effect of drying at early ages, at least for the concrete qualities with w/b-ratios of 0.45 and 0.55. At later ages, above 31 days at the start of testing, the positive effect of drying is small and the effect of drying is further decreased and even shows a small increase in scaling at later ages. However, this negative effect of drying at later ages can be regarded as insignificant. The effect is less apparent at early ages for concrete with a w/b-ratio of 0.35. However, for this concrete quality, there seems to be a small positive effect of drying irrespective of at what age the freeze/thaw test is started.

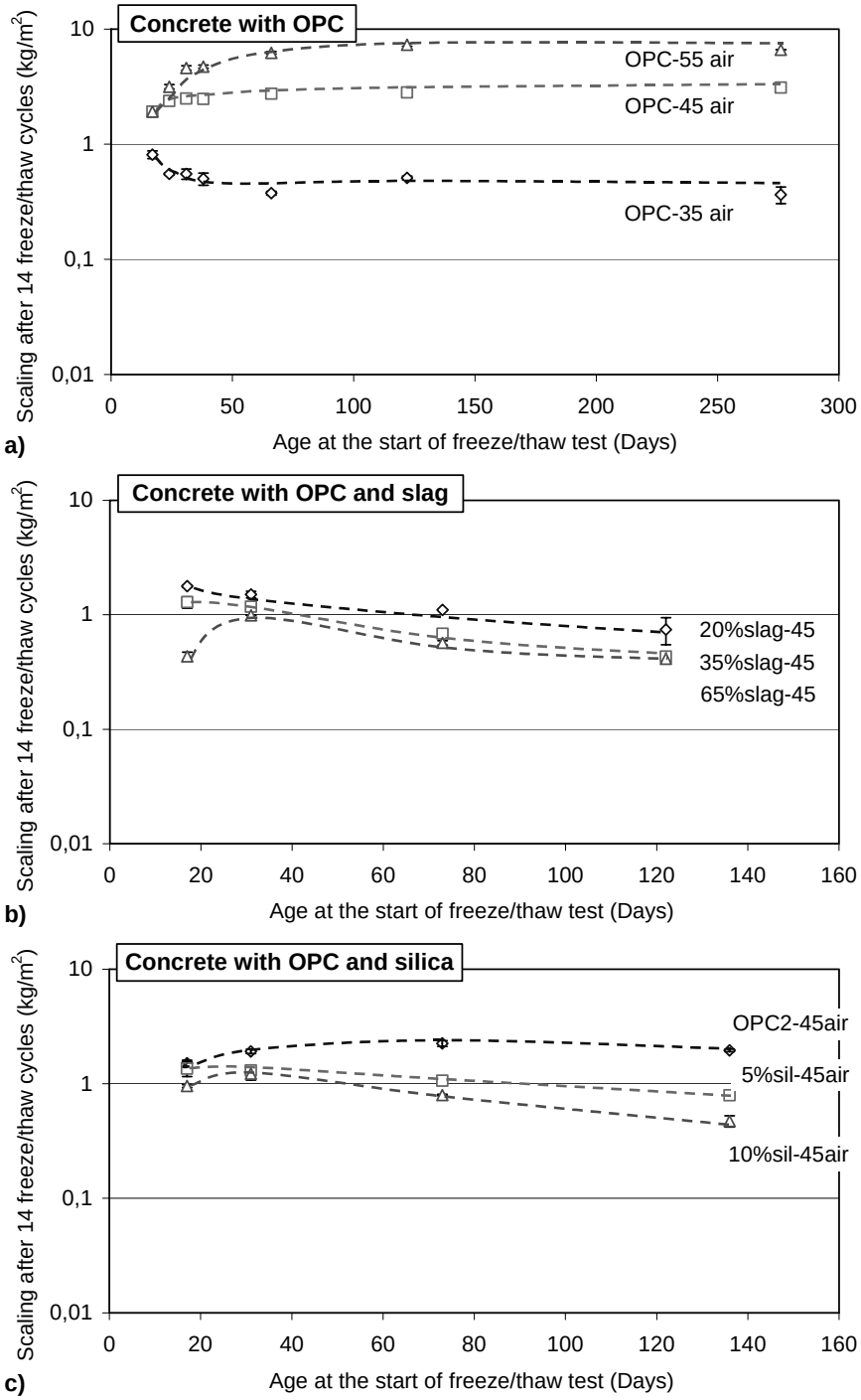

Figure 3.25 *Scaling after 14 freeze/thaw cycles for dried, uncarbonated specimens as a function of age at the start of the freeze/thaw test. Note scale on x-axes. a) OPC, b) OPC + slag, c) OPC + silica*

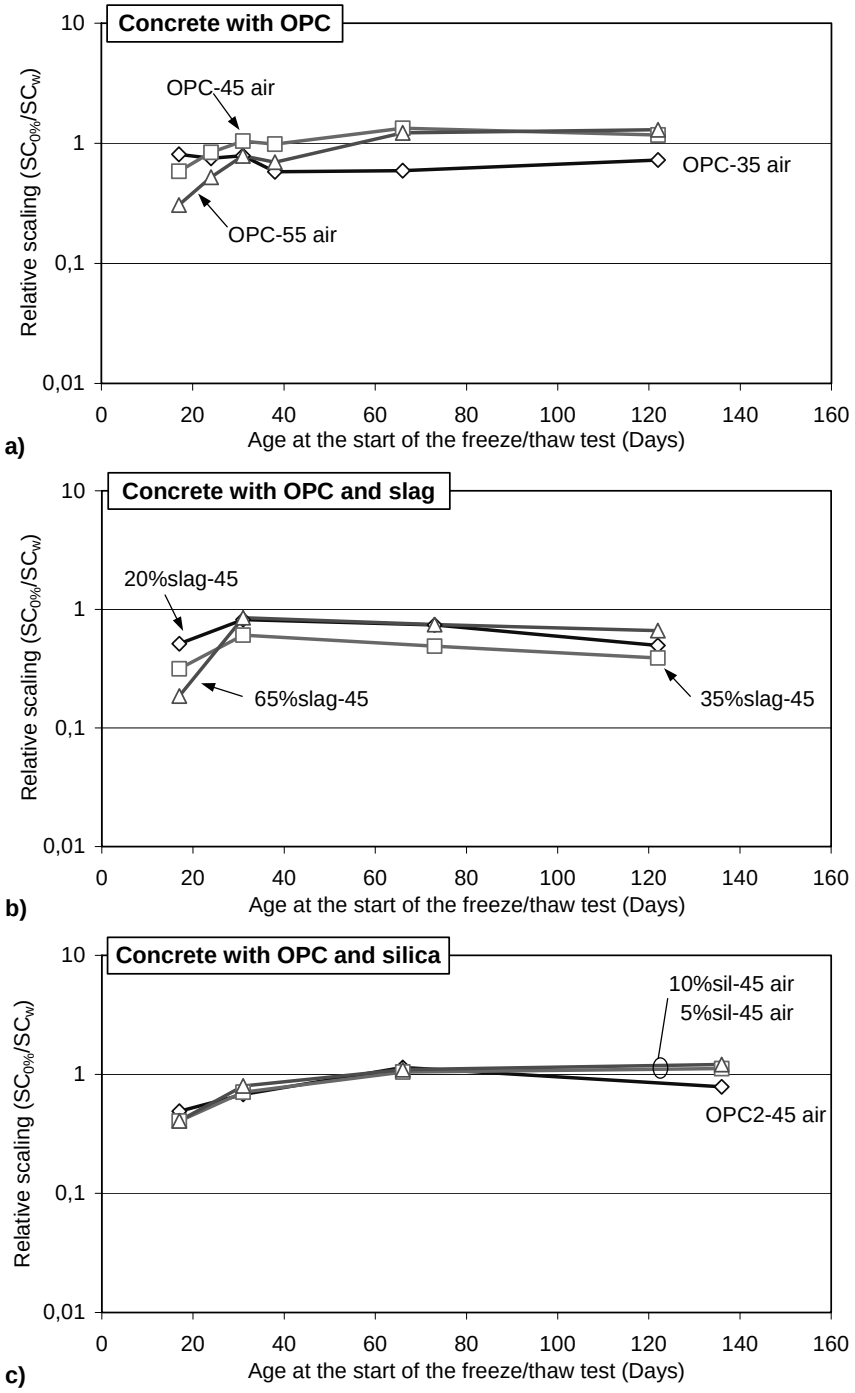

Figure 3.26 *Relative scaling after 14 freeze/thaw cycles as a function of age at the start of the freeze/thaw test. Effect of drying = scaling (dried uncarbonated) / scaling (water cured): ($SC_{0\%}/SC_w$).*
a) OPC, b) OPC + slag, c) OPC + silica

OPC + slag

Figure 3.26b shows the relative scaling for concrete with different amounts of slag as part of the binder, all with a w/b-ratio of 0.45. From the figure, it can be seen that there is a marked positive effect of drying at early ages, especially for concrete with high slag contents. However, the positive effect of drying decreases rapidly and, for concrete tested at an age of 31 days or more, there is a small and almost constant positive effect of drying independent of age at the start of testing.

OPC + silica

Figure 3.26c shows the relative scaling for concrete with different amounts of silica as part of the binder, all with a w/b-ratio of 0.45. From the figure, it can be seen that there is a positive effect of drying at early ages. This can be seen for all qualities, regardless of silica content. After 31 days, the effect of drying on the scaling resistance becomes gradually less pronounced, with no significant effect at an age of 60 days or more.

Discussion

For most concrete qualities tested in this investigation, drying seems to have a relatively small, but in most cases positive, effect on the scaling resistance. However, at early ages (before 31 days of age at the start of testing), the positive effect of drying is more pronounced. This indicates that at early ages, when the concrete is relatively permeable, a seven day-long drying time in a climate with 65 % RH and +20 °C leads to a relatively greater positive effect than does drying at later ages. The reason for this is unclear. However, one explanation may be that seven days of drying reduce the moisture content in the outer layers of a young permeable concrete more than it reduces the moisture content in the outer layers of an older, denser concrete.

For all specimens tested in this investigation, the weight loss during the seven day-long conditioning in 65 % RH and +20 °C, and the increase in weight during the three day-long resaturation, were regularly measured. Figure 3.27 shows an example for concrete specimens with OPC and different w/b-ratios conditioned in a climate without carbon dioxide. The specimens were tested at an age of 31 days.

From the figure, it can be seen that during drying the weight loss of the specimens, as expected, increases with increasing w/b-ratio. During the three-day-long resaturation, the weight increase is almost as great as the decrease during drying. There is, however, a small residual weight loss, indicating a somewhat lower degree of saturation than before drying.

It must be noted that some measurements of the weight increase during resaturation suffer from significant scatter. In Figure 3.27, this can be seen for the concrete quality with a w/b-ratio of 0.55. This high scatter is a result of an unwanted water uptake resulting from water being drawn up by capillary attraction between the specimen surface and the inner walls of the PVC cap fitted to the specimen as moisture insulation; see Figure 3.17. This unwanted moisture uptake led to an overestimation of the weight increase during resatura-

tion, which can be seen for concrete with a w/b-ratio of 0.55 in Figure 3.27. Because of this, the effect of drying cannot accurately be evaluated from these measurements. However, the measurement of the weight decrease during the seven day-long drying does not suffer from any significant scatter. Figure 3.28 shows the weight decrease after seven days' conditioning at 65 % RH and +20 °C for all tested concrete qualities as a function of age at the start of the freeze/thaw test.

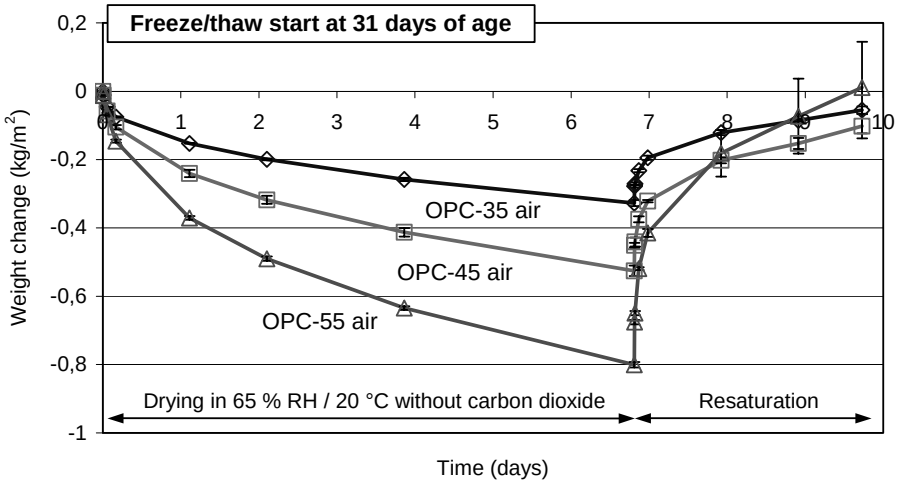

Figure 3.27 *Weight changes for concrete specimens with OPC during drying (seven days) and resaturation (three days). During drying, the specimens were conditioned in a carbon dioxide-free climate with 65 % RH and +20 °C.*

From Figure 3.28, it can be seen that for all concrete qualities there is a considerable weight loss at early ages when subjected to seven days of drying. However, the weight loss during drying is rapidly reduced and, for concrete with an age of 31 days or more at test start, the weight loss decreases only slowly with increasing age.

This considerable weight loss during drying at early ages corresponds well with the observed positive effect of drying on the scaling resistance discussed above and shown in Figure 3.26.

Comparing different concrete qualities shows, for example, that concrete with slag as part of the binder shows the highest weight loss during drying at early ages (Figure 3.28b), and also the most positive effect of drying on the scaling resistance (Figure 3.26b). The higher the slag content, the greater the weight loss during drying and the greater the positive effect on the scaling resistance. The same can be seen for concrete with only OPC as the binder and with different w/b-ratios; the higher the w/b-ratio, the greater the weight loss during drying (Figure 3.28a), and the more significant is the positive effect of drying on the scaling resistance (Figure 3.26a). For concrete with silica as part of the binder, the weight loss is about the same, regardless of the silica content, after seven days of drying (Figure 3.28c), and so also is the effect of drying on the scaling resistance (Figure 3.26c).

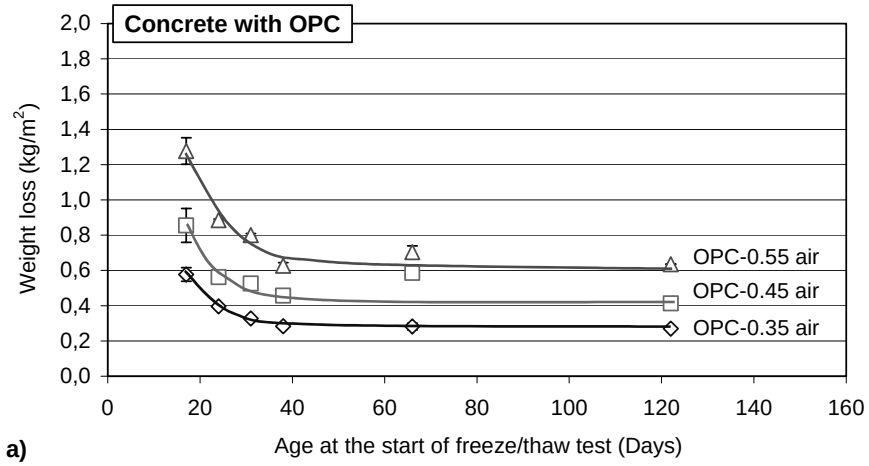

a)

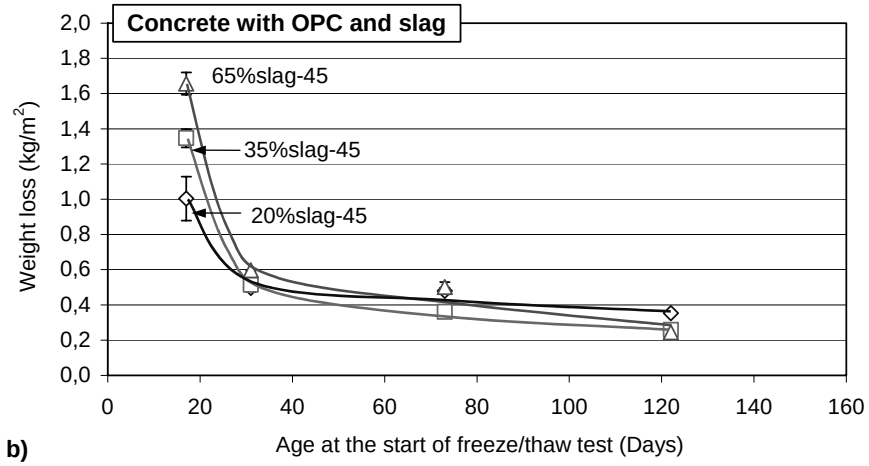

b)

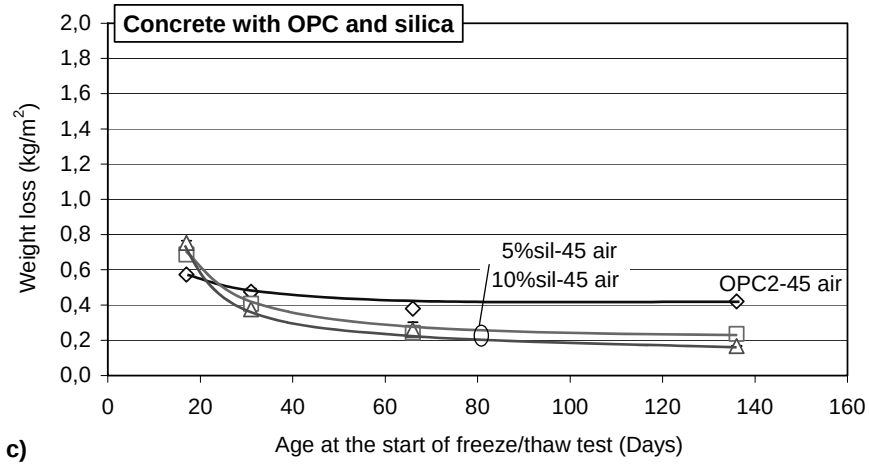

c)

Figure 3.28 *Weight loss after seven days of conditioning in 65 % RH and +20 °C as a function of age at the start of the freeze/thaw test.*
a) OPC, b) OPC + slag, c) OPC + silica

It can thus be concluded that the effect of drying on the scaling resistance is coupled to the amount of drying during conditioning. This is most evident at early ages. With increasing age at the start of drying, there is less change in weight loss during drying. Similarly, the effect of drying on the scaling resistance becomes less with increasing age.

However, from the results from this investigation it is not possible to explain the causes of the positive effect of drying. Drying leads to a decrease in the degree of saturation but may also lead to changes of the pore structure and the continuity of the pore structure in the outer surface layer. In other studies, it has been found that drying causes an increase in freezable water content (after being resaturated). The negative effect of this seems to be more than offset by the positive effect of reduced saturation. No further attempts have been made here to investigate which effects are the most important. However, it can be concluded that the effect of drying is positive and most significant at early ages, and that the effect of drying for concrete tested at an age of 31 days and more is small, at least for the drying climate used here, i.e. 65 % RH / +20 °C.

3.5.3.4 The effect of carbonation

As was mentioned above, the effect of carbonation on the scaling resistance was divorced from the effect of drying by conditioning specimens in two identical climates, but with and without carbon dioxide. Conditioning was carried out in the climate chambers described in Section 3.2. This section compares the scaling results for the specimens dried in the climate with carbon dioxide (1 vol-%) with the results for the specimens dried in a carbon dioxide-free environment.

Scaling results at a test age of 31 days

Figure 3.29 shows the scaling results for concrete with different binder types/combinations, conditioned both with and without carbon dioxide. The age of the specimens was 31 days at the start of testing.

OPC

Figure 3.29a shows the results for air-entrained concrete with plain OPC and with different w/b-ratios. As can be seen, the results are, as expected, very similar to those obtained with about the same concrete qualities in the initial investigation (see Figure 3.21). That is, concrete specimens made with plain OPC and preconditioned in an environment with carbon dioxide show much lower scaling than do specimens conditioned in an environment without carbon dioxide. For uncarbonated concrete, there is a marked difference in scaling resistance depending on the w/b-ratio, but this is less evident for carbonated concrete. Carbonated qualities with w/b-ratios of 0.35 and 0.45 show almost identical scaling, whereas concrete with a w/b-ratio of 0.55 still shows a somewhat higher amount of scaling.

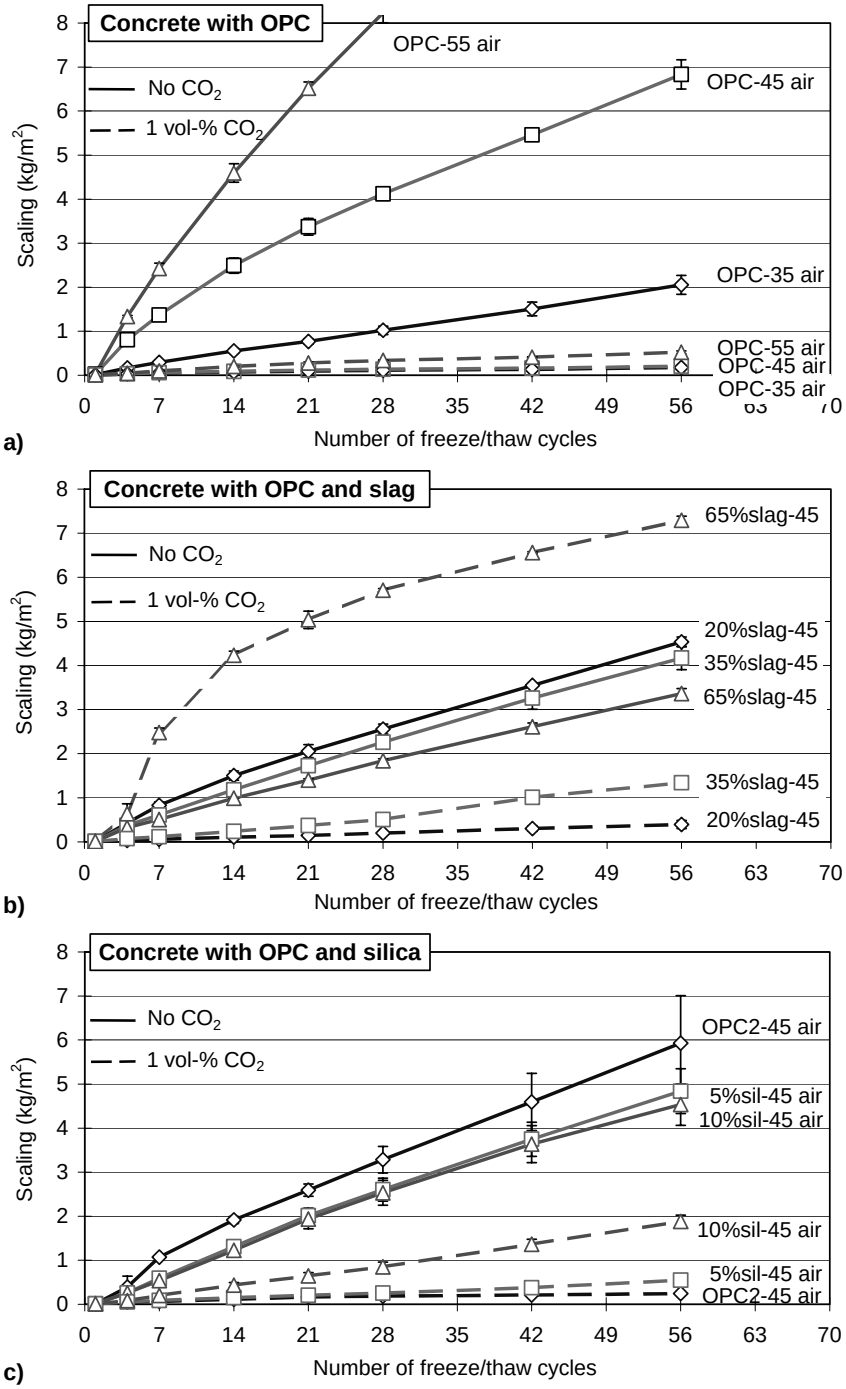

Figure 3.29 *Scaling as a function of the number of freeze/thaw cycles for concrete with different binder types/combinations, conditioned in climate chambers with and without carbon dioxide. The age at the start of the freeze/thaw test was 31 days. a) OPC, b) OPC + slag, c) OPC + silica*

OPC + slag

Figure 3.29b shows the scaling for non air-entrained concrete with different amounts of slag as part of the binder, all with a w/b-ratio of 0.45. From the figure, it can be seen that the scaling resistance of uncarbonated concrete containing slag as part of the binder increases somewhat with increasing slag content. However, in the case of carbonated concrete, the effect of slag on the scaling resistance is the opposite. For concrete with small amounts of slag, carbonation leads to an improved scaling resistance. But as the proportion of slag increases, the scaling resistance is reduced, so that for concrete with 65 % slag as part of the binder, carbonation leads to a marked decrease in scaling resistance.

From the appearance of the scaling curve for the carbonated concrete with 65 % slag as part of the binder, it is evident that severe scaling takes place during the first 14 freeze/-thaw cycles, after which the rate of scaling slows down and becomes about the same as for uncarbonated concrete. This indicates that a layer, probably the carbonated skin, is scaled off during the initial part of the freeze/thaw test. When the carbonated layer is scaled off, the rate of scaling becomes the same as for uncarbonated concrete. This negative effect of carbonation on the scaling resistance for concrete containing large amounts of slag has previously been reported by, for example, Stark & Ludwig (1997:1). They presented results that show that the initial very large scaling of carbonated concrete containing large amounts of slag as part of the binder corresponds very well with the thickness of the carbonated layer. This was confirmed by comparing the depth of the scaling with the depth of carbonation for different concrete qualities containing more than 60 % slag, and with and without entrained air. This is further discussed in Chapter 4.

OPC + silica

Figure 3.29c shows the scaling for air-entrained concrete with different amounts of silica as part of the binder, all with a w/b-ratio of 0.45. From the figure it can be seen that, for uncarbonated specimens, there seems to be a slight increase in scaling resistance as a result of incorporation of silica as part of the binder. There is, however, no significant difference between the qualities containing 5 % or 10 % silica. At freeze/thaw testing at later ages, the positive effect of silica is more pronounced, with a reduction of scaling as the silica content increases. See Appendix 6.

As can be seen in Figure 3.29c, carbonation leads to markedly improved scaling resistance for concretes both with and without silica as part of the binder in comparison with uncarbonated concrete. However, the improvement in scaling resistance is more pronounced the lower the silica content. At this test age, the difference in scaling between concrete made with only OPC and concrete made with OPC + 5 % silica is relatively small. However, for concrete with 10 % silica, the scaling of the carbonated concrete is considerably higher, indicating that the positive effect of carbonation is less apparent for this concrete quality.

From the complete presentation of scaling results in Appendix 6, it can be seen that the scaling is about the same for all qualities, regardless of silica content, during the first four to seven freeze/thaw cycles. After this, scaling increases at a higher rate for the concrete

with 10 % silica as part of the binder. After seven to 14 cycles, the rate of scaling for concrete with 5 % silica increases as well. This is true for all test ages in this investigation; see, for example the scaling for concrete where the freeze/thaw test started at an age of 136 days, Figure 3.30.

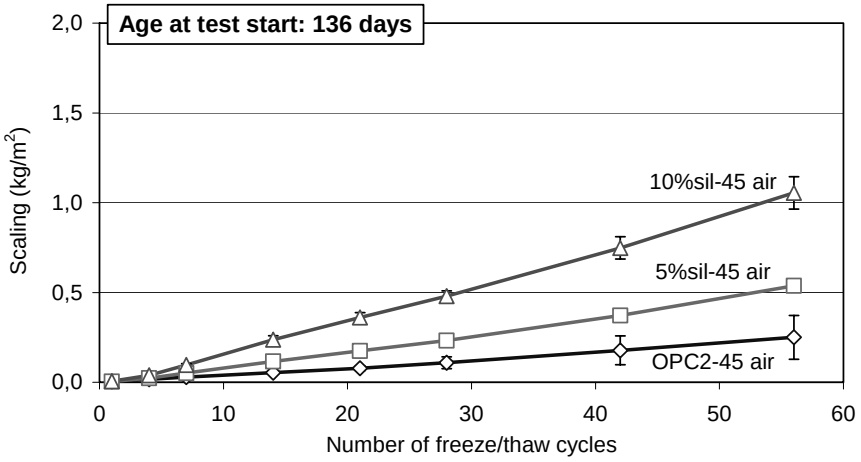

Figure 3.30 *Scaling as a function of number of freeze/thaw cycles for air-entrained carbonated concrete with different silica contents, all with a w/b-ratio of 0.45. Test start at an age of 136 days.*

The results presented in the figure indicate that the higher the silica content, the more rapidly is the protective carbonated skin scaled off. This indicates that the properties of the carbonated skin with respect to scaling resistance differ, depending on the amount of silica as part of the binder. The higher the silica content, the lower the scaling resistance of the carbonated layer seems to be.

These results are somewhat contradictory to results found in the literature, where the incorporation of silica is usually reported to lead to an increase in scaling resistance. The analysis of the air void structure (see Table 3.6 in Section 3.3.2) shows no marked differences that could perhaps explain the observed difference in scaling resistance for the carbonated material containing silica. The fact that the uncarbonated materials exhibit an increased scaling resistance when containing silica as part of the binder is a further indication that the air void systems do not markedly differ between the different concrete qualities.

Since it could be wondered whether preconditioning in a climate with increased carbon dioxide content (1 vol-%) and/or the applied freeze/thaw method in some way resulted in results different from those obtained using the standard SS 13 72 44 procedure, a limited complementary test was carried out. Spare concrete cylinders, more than three years old, of the same qualities as were used in the tests presented above were tested in accordance with the procedure in the Swedish freeze/thaw standard SS 13 72 44, as described in

Section 2.3. The concrete cylinders were water-cured for most of the time after casting. The sawn surfaces were conditioned for seven days in a climate-controlled area with 65 % RH and +20 °C and with air containing normal carbon dioxide content (0.03-0.04 vol-%). Figure 3.31 shows the scaling as a function of the number of freeze/thaw cycles.

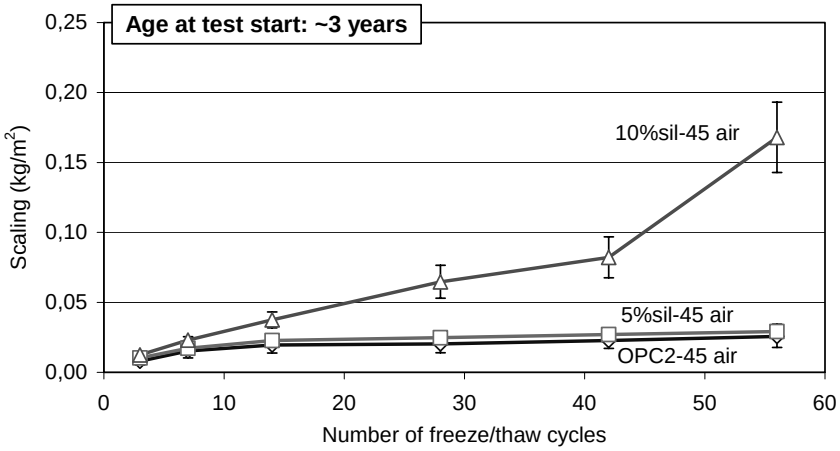

Figure 3.31 *Scaling as a function of number of freeze/thaw cycles for air-entrained carbonated concrete with different silica contents, all with a w/b-ratio of 0.45. Test start at an age of over three years.*

From the figure, it can be seen that when conditioning the specimens in normal air and testing in accordance with she Swedish freeze/thaw standard, the same tendency is again seen, i.e. concrete containing high silica contents shows higher scaling than does concrete with no or only 5 % silica. This limited test thus indicated that the applied conditioning climate with increased carbon dioxide content and the applied test method could not be the cause of any 'unnatural' results.

In order to investigate the homogeneity of the different materials and to see how well the silica (in the form of slurry) was dispersed, thin sections with a size of 80 · 50 mm were analysed. A Danish test method DS 423.36 (1995) was used to estimate the dispersion, counting clusters of undispersed silica using a microscope. The results showed that not a single cluster of undispersed silica could be found in any of the qualities. The reason for the observed lesser effect of carbonation on these concrete qualities could therefore not be due to problems with dispersion of the silica.

It cannot be explained why the results for concrete containing silica, especially the quality containing 10 %, show a less positive effect of carbonation than was found for material with OPC alone as the binder. The material composition used for these 'micro' concrete qualities, and the fact that no plasticiser was used, which is common when using silica as part of the binder, may be the reason for the discrepancy with the conventional idea that silica leads to an improved scaling resistance.

One possible explanation for the observed lower scaling resistance for carbonated concrete containing silica as part of the binder might be the consumption of calcium hydroxide during hydration of concrete containing silica; see Taylor (1997). In concrete with only OPC as the binder, there is a large amount of calcium hydroxide available for transformation to calcium carbonate. For concrete with silica as part of the binder, much of this calcium hydroxide is consumed by the reaction with the silica particles and is thus not available for carbonation. As is discussed in Chapter 4, a larger amount of C-S-H gel will be carbonated in a material with a low calcium hydroxide content. This leads to formation of other products as a result of carbonation and possibly to a different scaling resistance of the carbonated layer than would have been the case if only calcium hydroxide was carbonated. However, this explanation does not account for the often-reported positive effects on scaling resistance of incorporation of silica as part of the binder. This needs to be investigated further, although not as part of the present investigation.

Influence of carbonation on the scaling results - testing at different ages

In the same way as for water-cured and dried uncarbonated specimens, carbonated specimens were also freeze/thaw tested at different ages. The accumulated scaling results after 14 freeze/thaw cycles for the dried carbonated specimens of different binder types/-combinations and tested at different ages is shown in Figure 3.32.

Section 3.5.3.3 discussed the relative effect of drying on the scaling resistance. Here the relative effect of carbonation at different ages at the start of testing is evaluated by comparing scaling results for carbonated and uncarbonated specimens.

In order to evaluate the effect of carbonation, the accumulated scaling of the dried carbonated specimens ($SC_{1\%}$) after 14 cycles has been divided by the accumulated scaling of the dried uncarbonated specimens ($SC_{0\%}$) after 14 cycles. The quotient between these amounts of scaling is the relative effect of carbonation. A value below 1 indicates a positive effect of carbonation.

Figure 3.33 shows the relative effect of carbonation for specimens of different binder types/combinations as a function of age at the start of the freeze/thaw test. For comparison, the relative effect of drying is also shown in the figure (dashed lines, taken from Figure 3.26).

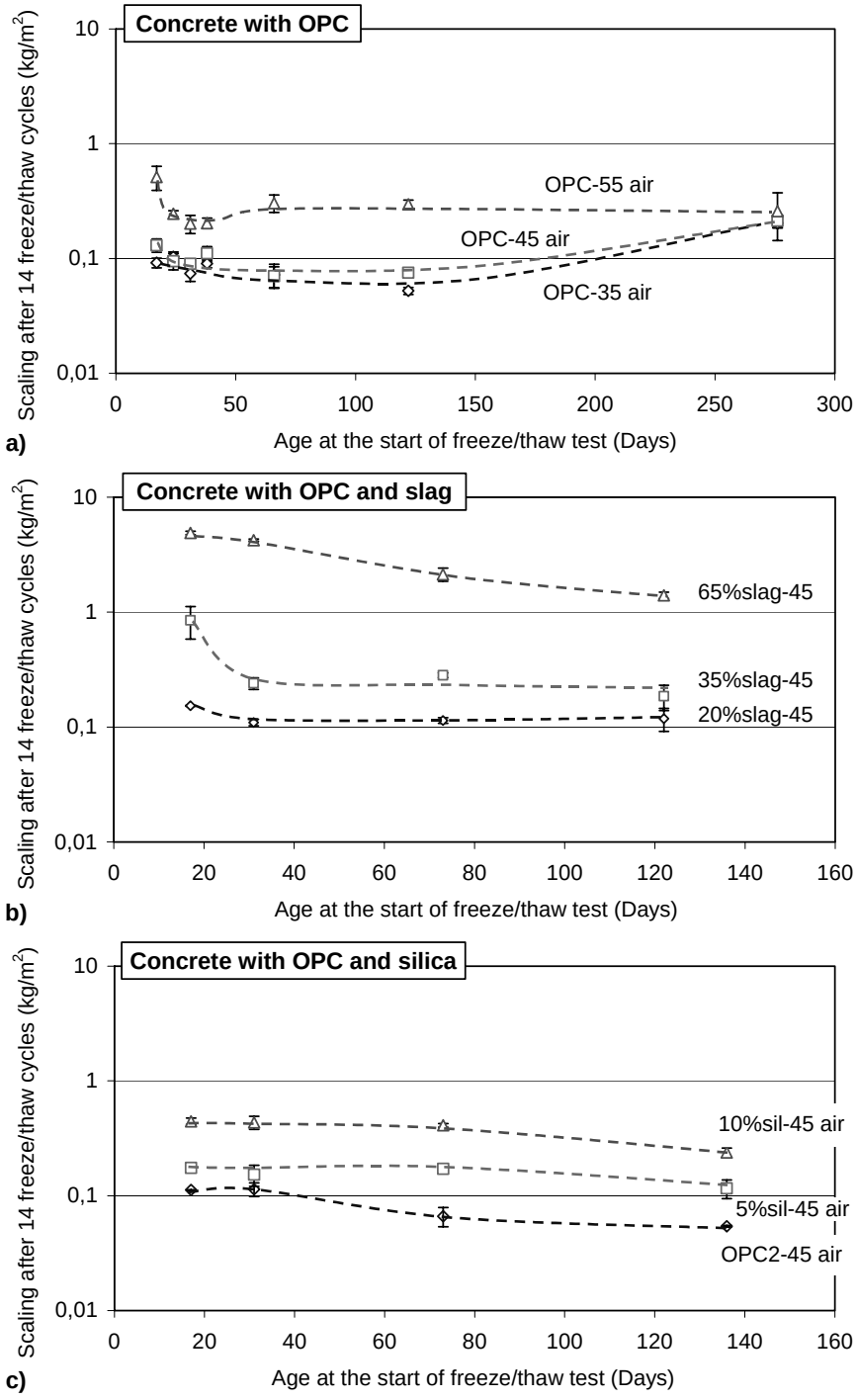

Figure 3.32 *Scaling after 14 freeze/thaw cycles for dried, carbonated specimens as a function of age at the start of the freeze/thaw test. Note the scale on the x-axis. a) OPC, b) OPC + slag, c) OPC + silica*

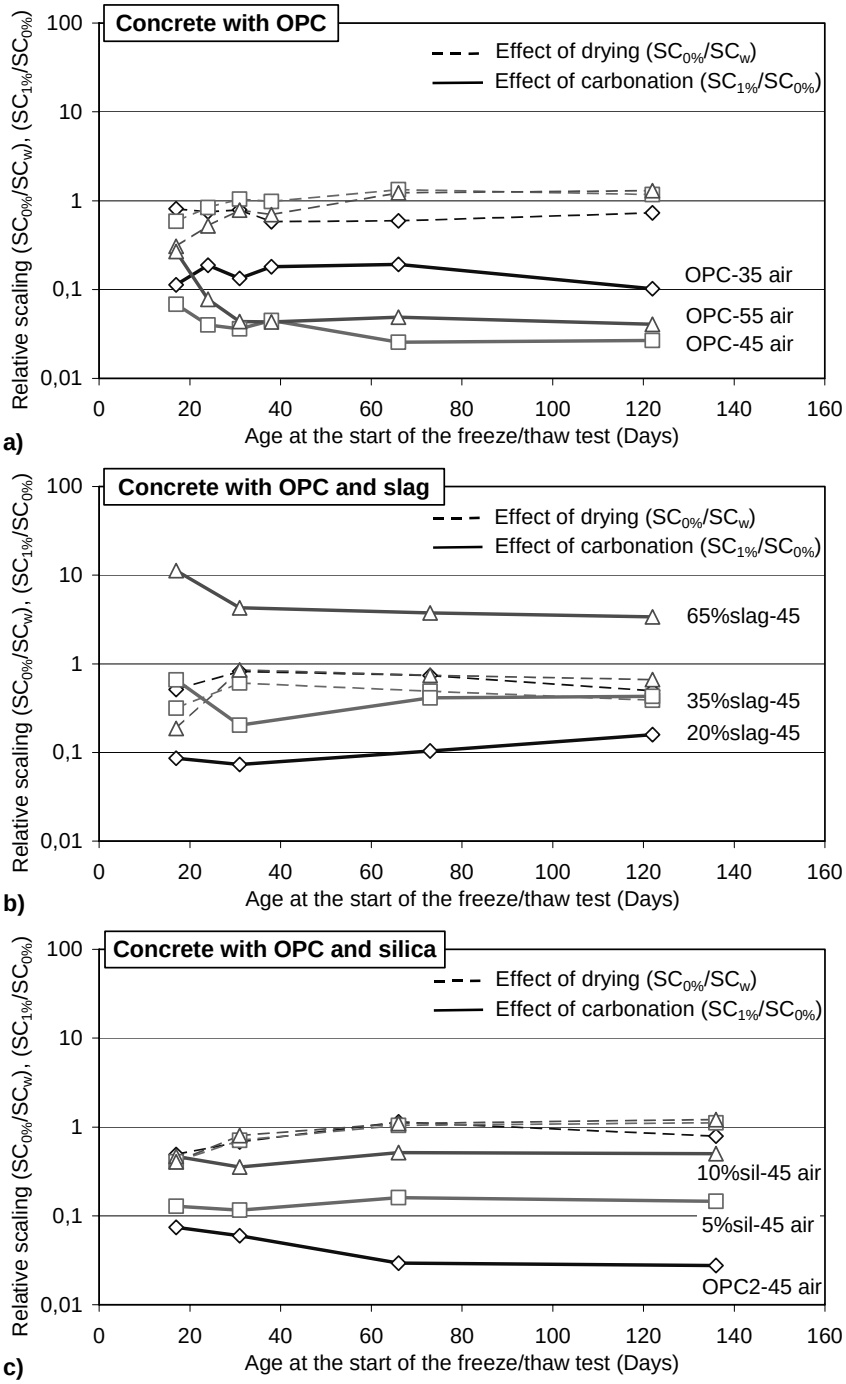

Figure 3.33 *Relative scaling after 14 freeze/thaw cycles as a function of age at start of the freeze-/thaw test. Effect of carbonation = scaling (carbonated) / scaling (uncarbonated):($SC_{1\%}/SC_{0\%}$). Effect of drying = scaling (uncarbonated) / scaling (water cured):($SC_{0\%}/SC_w$). a) OPC, b) OPC + slag, c) OPC + silica*

OPC

Figure 3.33a shows the relative effect of carbonation for concrete with OPC and different w/b-ratios. It can be seen that the effect of carbonation, regardless of the w/b-ratio, is markedly positive with respect to the scaling resistance. This is true at all test ages, although the positive effect is less pronounced at very young test ages, at least for concrete with w/b-ratios of 0.45 and 0.55. However, at an age of 31 days or more, the effect of carbonation for these concrete qualities is substantial, with around 30 times less scaling than for uncarbonated concrete.

The relative effect of carbonation for the quality with a w/b-ratio of 0.35 is less pronounced although the amount of scaling is reduced by five to ten times as a result of carbonation. The smaller relative effect of carbonation for this concrete quality is primarily a result of the relatively high scaling resistance of the uncarbonated material. For example, comparing the scaling of the uncarbonated specimens with w/b-ratios of 0.35 and 0.45 (Figure 3.25a) shows that the quality with a w/b-ratio of 0.35 has less than one-third of the amount of scaling than has the concrete quality with a w/b-ratio of 0.45. However, for the carbonated specimens (Figure 3.32a), the scaling is about the same.

It must be noted that with the freeze/thaw test method used, which is described in Section 3.4, the amount of scaling for concrete with high scaling resistance is somewhat overestimated because of edge effects. These edge effects result in a relatively high scaling on the edges of the specimen, whereas the inner parts of the test surface show reduced scaling. This leads to an underestimation of the scaling resistance for specimens with high scaling resistance. The positive effect of carbonation for the quality with a w/b-ratio of 0.35 is thus probably somewhat more significant than can be seen from Figure 3.33a. The influence of edge effects is further discussed in Section 3.4.

Compared to the effect of carbonation, the effect of drying (dashed lines in Figure 3.33a) on the scaling resistance is very small. This is true regardless of the w/b-ratio, at least for material tested at an age of 31 days or over.

OPC + slag

The relative effect of carbonation on the scaling resistance for concrete qualities containing slag as part of the binder, all with a w/b-ratio of 0.45, is shown in Figure 3.33b. As can be seen, there is a considerable difference depending on the amount of slag as part of the binder. For concrete with 20 % slag as part of the binder, the effect of carbonation is markedly positive at all ages, with about ten times lower scaling as a result of carbonation. For concrete with 35 % slag as part of the binder, there is only a small positive effect of carbonation at early ages. At an age of 31 days or more, however, this quality also shows a marked positive effect of carbonation, with less than half the scaling of uncarbonated concrete.

The relative effect of carbonation for concrete with 65 % slag as part of the binder is the opposite. The effect of carbonation for this concrete quality is negative at all test ages. The

negative effect of carbonation is most marked at early ages, with almost ten times higher scaling as a result of carbonation. At an age of 31 days or more, the negative effect is smaller, but the scaling is still over three times as high as for the uncarbonated material. For samples older than 31 days of age at the start of testing, the relative effect of carbonation is almost the same regardless of the age at the start of testing.

Compared to the effect of carbonation, the effect of drying (dashed lines in Figure 3.33b) on the scaling resistance for concrete with low (20 %) and high (65 %) slag contents is very small. However, since the effect of carbonation differs very considerably, depending on the slag content, there is an intermediate slag content where the effect of carbonation is about the same as the effect of drying. From the figure it can be seen that this is somewhere between 35 % and 65 % slag as part of the binder.

For concrete with slag as part of the binder, the results have shown that the effect of carbonation changes from positive for concrete with low slag contents to negative for concrete with high slag contents. It should be noted that these are the effects of only seven days' carbonation in a climate with a somewhat increased carbon dioxide content. A longer time for carbonation would probably show an even more pronounced effect of carbonation for these concrete qualities.

OPC + silica

Figure 3.33c shows the relative effect of carbonation on the scaling resistance for concrete qualities with different silica contents as part of the binder, all with a w/b-ratio of 0.45. The results show a marked difference in the effect of carbonation on the scaling resistance, depending on the content of silica as part of the binder. As was discussed above, the effect of carbonation for concrete without silica is strong, with about 30 times lower scaling for carbonated concrete tested at an age of 31 days or more. For concrete with 5 % silica as part of the binder, there is a marked positive effect of carbonation on the scaling resistance, although not as apparent as for concrete without silica. The effect of carbonation is about the same, regardless of age at the start of testing, with almost 10 times lower scaling as a result of carbonation.

For concrete with 10 % silica as part of the binder, the positive effect of carbonation is less pronounced than for concrete without silica or with only 5 %. However, as can be seen from Figure 3.33c, the effect is positive, with about half the amount of scaling as for uncarbonated concrete. The positive effect is almost the same, regardless of age at the start of testing.

Compared to the effect of carbonation, the effect of drying (dashed lines in Figure 3.33c) on the scaling resistance of concrete with silica as part of the binder is very small, at least for concrete with up to 5 % silica. The effect of carbonation is less pronounced for concrete with 10 % silica, but since the effect of drying is small the effect of carbonation is comparably very large.

3.5.4 Summary - the effect of ageing

This section provides a brief summary of the results of this investigation, studying the influence of different ageing effects on the salt-frost resistance of concrete.

A number of 'micro'-concrete qualities made with OPC alone and with incorporation of secondary cementitious materials were studied. The ageing effects investigated were hydration, drying and carbonation.

The effect of hydration was studied on water-cured never-dried specimens, stored in water until the start of the freeze/thaw test. The test was started at different ages, depending on the concrete quality, with a maximum age of 276 days. Since the specimens were water-cured until the start of testing, it was not only the effect of hydration but also the possible effect of the water curing, e.g. increased degree of saturation with time, that was investigated.

The effect of drying and of carbonation on the scaling resistance was investigated by conditioning specimens in climates that differed only in respect of the carbon dioxide content. Preconditioning was carried out for seven days in climates with 65 % relative humidity and +20 °C, with and without (1 vol-%) carbon dioxide.

From the studies of the effect of hydration (and possible effects of water curing), drying and carbonation, it can be concluded that, for all concrete qualities, the most significant effects on the scaling resistance occurred at early ages. For most concrete qualities with an age of 31 days or more at the time of testing, there were only small differences in scaling resistance, depending on the age of the samples at the time of testing. From the results presented here, an age of around 30 days could thus be recommended for a standard freeze/thaw test. In this respect, the prescribed age for testing, as specified in the Swedish freeze/thaw standard SS 13 72 44, i.e. 31 days at the time of testing, is in line with what could be recommended based on the results from this investigation.

The effects of drying and carbonation are illustrated below by the results from testing (at an age of 31 days) concrete with OPC alone and concrete with slag or silica as part of the binder. In order to illustrate the effect of ageing on the scaling results after different numbers of freeze/thaw cycles, both the accumulated scaling after 14 cycles and that after 56 freeze/thaw cycles are evaluated.

OPC

Figure 3.34 shows the accumulated scaling after 14 and 56 freeze/thaw cycles for concrete with OPC alone as the binder, and with different w/b-ratios, preconditioned in three different climates. For all specimens, the freeze/thaw test started at an age of 31 days.

From the figure, it can be seen that the amount of scaling for water-cured never-dried and for the dried, uncarbonated specimens is about the same and, as expected, increases markedly with increasing w/b-ratio. The figure clearly shows that there is a large positive effect

of carbonation on the scaling resistance for OPC concrete, regardless of the w/b-ratio. From the figure, it can also be seen that the effect of drying on the scaling resistance is small in comparison with the strong effect of carbonation. This applies both for scaling at 14 freeze/thaw cycles and for scaling at 56 freeze/thaw cycles.

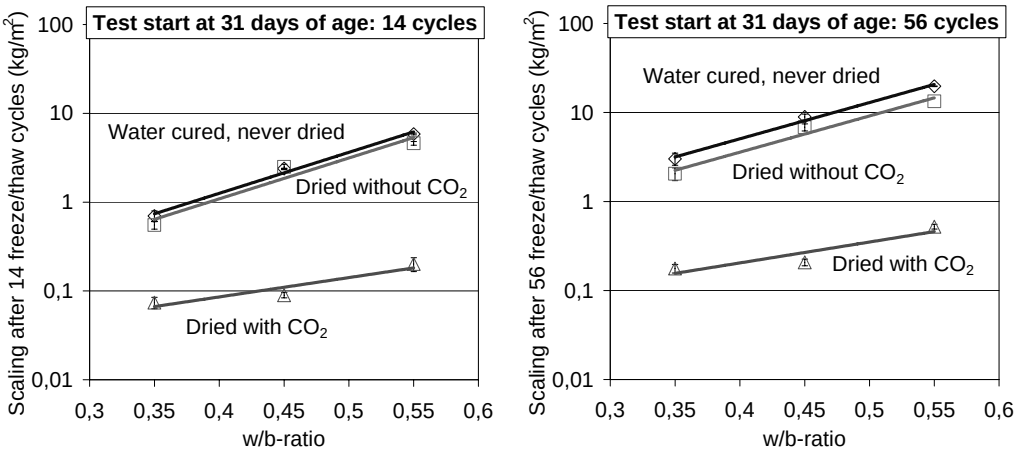

Figure 3.34 *Scaling after 14 (left) and 56 (right) freeze/thaw cycles as a function of w/b-ratio for concrete with OPC, conditioned in three different climates.*

OPC + slag

Figure 3.35 shows the accumulated scaling after 14 and 56 freeze/thaw cycles for concrete with OPC and different amounts of slag as part of the binder, preconditioned in three different climates. For all specimens, the freeze/thaw test started at an age of 31 days.

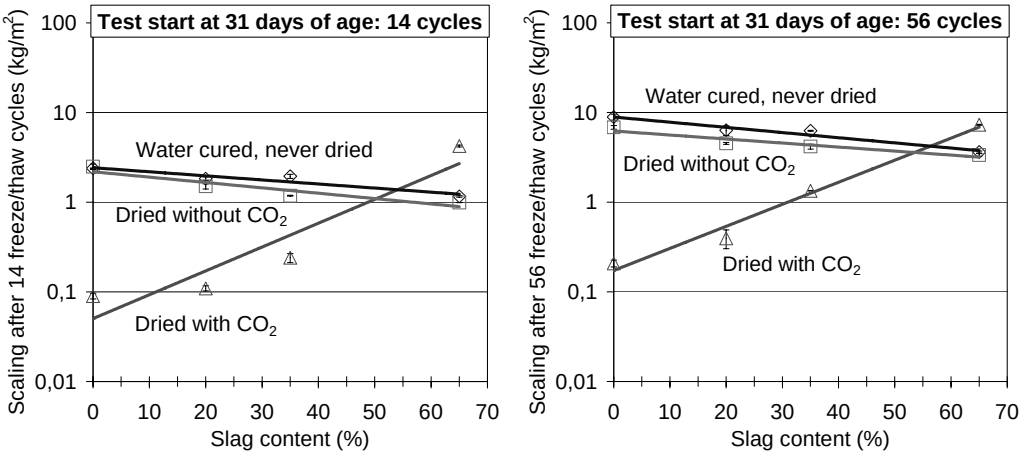

Figure 3.35 *Scaling after 14 (left) and 56 (right) freeze/thaw cycles as a function of slag content for specimens with a w/b-ratio of 0.45, conditioned in three different climates.*

From the figure, it can be seen that the amount of scaling for the water-cured and for the dried, uncarbonated specimens is about the same, and decreases somewhat with increasing slag content. The reverse applies for the carbonated specimens, with a marked increase in scaling with increasing slag content. From the figure, it can clearly be seen that the effect of drying on the scaling resistance is small in comparison with the strong effect of carbonation. However, the effect of carbonation differs, depending on the slag content.

For concrete with low contents of slag as part of the binder, the effect of carbonation is positive with respect to scaling resistance, but for concrete with high contents of slag the effect is negative. From the results it can be seen that, at a slag content around 50-55 % by binder weight, the effect of carbonation becomes negative with respect to the scaling resistance. This applies both for scaling at 14 freeze/thaw cycles and for scaling at 56 freeze/thaw cycles.

OPC + silica

Figure 3.36 shows the accumulated scaling after 14 and 56 freeze/thaw cycles for concrete with OPC and different amounts of silica as part of the binder, preconditioned in three different climates. For all specimens, the freeze/thaw test started at an age of 31 days.

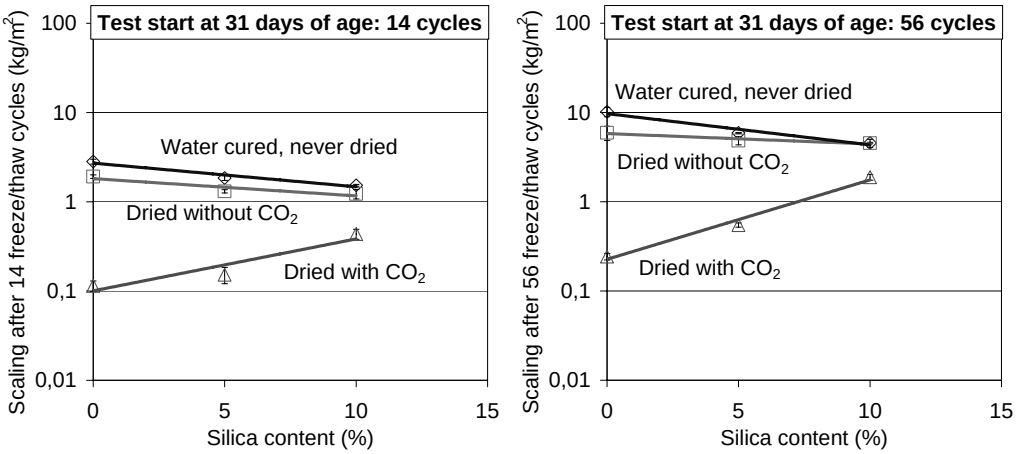

Figure 3.36 *Scaling after 14 (left) and 56 (right) freeze/thaw cycles as a function of silica content for specimens with a w/b-ratio of 0.45, conditioned in three different climates.*

From the figure, it can be seen that the amount of scaling for the water-cured and for the dried, uncarbonated specimens is about the same, and decreases somewhat with increasing silica content. The reverse applies for the carbonated specimens, with an increasing amount of scaling with increasing silica content. It can clearly be seen that the effect of drying on the scaling resistance is small in comparison with the strong effect of carbonation. For all qualities, carbonation leads to a marked positive effect on the scaling resistance, although this decreases with increasing silica content.

3.6 Conclusions

The following conclusions can be drawn from the investigations presented in Chapter 3:

- Ageing effects such as hydration, drying and carbonation have a marked influence on the salt-frost resistance of concrete.
- Carbonation is the most dominant ageing effect with regard to salt-frost resistance. The influence of hydration and drying is small compared to the effect of carbonation, at least at an age of 30 days or older.
- For ‘micro’ concrete with Ordinary Portland Cement (OPC) as binder, carbonation strongly improves the scaling resistance. The carbonated layer creates a protective skin, and the properties of this skin determine the scaling resistance.
- For ‘micro’ concrete with ground granulated blast furnace slag as part of the binder, carbonation improves the scaling resistance for concrete with low to medium amounts of slag as part of the binder. However, the positive effect of carbonation is not as high as for concrete with OPC alone as the binder, and is considerably reduced with increasing slag content. For concrete with high slag contents (65 % of binder weight), the effect of carbonation on the scaling resistance is even markedly negative. Carbonation of concrete with high slag contents thus leads to a carbonated skin, where the properties of the material are altered in a way that leads to a considerable reduction of the scaling resistance.
- For ‘micro’ concrete with silica as part of the binder, the tendency is the same as for concrete made with only OPC as binder, i.e. carbonation leads to a marked improvement of the scaling resistance. However, the improvement is reduced with increasing silica content.
- If comparing the scaling resistance for water-cured, never-dried, specimens with specimens dried for seven days and resaturated for three days, the scaling resistance for all concrete qualities is somewhat improved by the short drying, at least at early ages. At test ages of 31 days and more, the effect of drying on the scaling resistance of uncarbonated specimens is low.
- For all concrete qualities, the most significant effects of ageing take place during about the first 30 days. The Swedish test method, SS 13 72 44, the ‘slab test’, specifies that freeze/thaw testing should start at an age of 31 days. In this respect, the test start age as specified in the standard is in line with what could be recommended based on the results from this investigation.
- The effect of drying (without carbonation), as well as the effect of increasing hydration and increasing degree of saturation with time, has only a slight effect on the scaling resistance compared with the strong effect of carbonation.

4 Literature review

4.1 Introduction

In principle, the fundamental degradation mechanisms behind freeze/thaw attack on concrete are well understood; see Section 4.2. Nevertheless, it is often difficult to design concrete for good frost resistance and also to develop reliable test methods. In fact, most knowledge today is still based on experience. The reasons for this probably include: the very complicated structure and chemical composition of concrete, not least where newly developed types are concerned, the difficulty of predicting the moisture content and temperature variations in concrete subjected to real exposure conditions, the effects of chlorides and de-icing agents, the combined effects of different degradation mechanisms, and other reasons.

Another parameter which complicates the situation is the ageing of concrete, and its influence on the frost and salt-frost resistance. Some work on this subject is presented in the literature, see Section 4.3, but the effect is far from fully understood. The ageing effect is studied in this thesis, with particular attention paid to the influence of carbonation.

According to the degradation mechanisms presented by Powers (1949, 1953, 1965, 1975), pore structure parameters play an important role for the understanding of the freeze/thaw process. Pore structure influences important parameters such as:

- *capillary suction*, which is important for the degree of saturation and the amount of ice formed during freezing.
- *freezable and non-freezable water contents* as functions of temperature, which influence the ice-forming ratio and the amount of ice formed during freezing. Hysteresis effects between freezing and melting may also give information on the pore structure.
- *critical degree of saturation*, which gives information about how much of the pore system that has to be filled with air in order to eliminate the risk of frost damage.

Chapters 5 - 10 in this thesis present results from work carried out in order to explain the effect of carbonation on the frost and salt-frost resistance of concrete. The three parameters presented above, i.e. capillary suction, freezable water content and critical degree of saturation, have been determined for a number of carbonated and uncarbonated mortar mixtures with different binder types/combinations.

4.2 Freeze/thaw mechanisms

4.2.1 Introduction

Frost damage is normally grouped into two categories:

- Internal cracking - Micro-cracks and macro-cracks develop throughout the entire volume of the concrete material. The micro-cracking is a result of a combination of freezing and a high degree of water saturation in the concrete. Internal cracking leads to higher permeability, lower Young´s modulus, lower strength, etc. It also opens up paths for other types of damage, such as reinforcement corrosion, alkali-silica reactions and others.
- Surface scaling - This type of damage is caused by a combination of freezing and local high moisture saturation at the concrete surface. Experience from research and practice shows that the attack becomes much more severe when various types of de-icing agents are used: see for example Arnfelt (1943) and Verbeck & Klieger (1957). Scaling is primarily an aesthetic problem. If the scaling becomes extensive, however, it can lead to reduced load-carrying capacity and also to various types of durability problems, such as reinforcement corrosion.

The mechanisms behind frost damage are normally assumed to be the same for both internal cracking and surface scaling. In both cases, the damage takes place at freezing when the degree of saturation exceeds a critical value. However, the mechanisms behind the strong influence of de-icing agents on the scaling are not fully understood. One possible explanation may be found in the fact that pure water fully transforms to ice when the temperature falls below zero degrees. A salt solution, on the other hand, contains unfrozen solution down to the eutectic temperature. This is, for example, –21 °C for sodium chloride solutions. This means that the concrete can absorb water for longer periods when the freezing medium is a salt solution than when it is pure water. This leads to a higher degree of saturation and, consequently, to a higher risk of frost damage.

Other explanations are given by Powers (1975), Lindmark (1998) and others.

4.2.2 Mechanisms

Over 50 years ago, Powers presented his theories about the mechanisms behind freeze/-thaw damage of concrete. According to the hydraulic pressure mechanism theory (Powers (1949)), water is squeezed through the pores in the cement paste due to the volume change taking place when water is transformed to ice. This produces a hydraulic pressure which may be high enough to fracture the concrete.

Another mechanism, the microscopic ice crystal growth theory (Powers and Helmuth (1953), Powers (1965)), implies that ice in the pores attracts unfrozen water, the driving

force being the energy difference between ice and unfrozen water. This makes the ice crystals grow, causing pressure on the pore walls, which may induce frost damage.

Powers also found that air-entrainment is an excellent way of protecting concrete from freeze/thaw damage (Powers (1949)). He also formulated the theories about the influence of the pore size distribution and introduced the spacing factor concept.

The theories presented in Powers & Helmuth (1953) did not account for the chemicals dissolved in the water in the pores of cement paste. Such chemicals change the energy state of water and lead to osmotic phenomena taking place during freezing and thawing. To take these effects into account, the microscopic ice body growth mechanism was complemented with the osmotic effects in Powers (1975). According to this theory, the differences in concentration of dissolved chemicals in different parts of the pore system during freezing lead to a redistribution of water causing pressure of osmotic nature.

Much other valuable research has been carried out and reported during the last 50-60 years: see, for example, Arnfelt (1943), Verbeck & Klieger (1957), Everett (1961), Warris (1963), Vuorinen (1969), Fagerlund (1971), Litvan (1972), Fagerlund (1973), Setzer (1976), Sellevold & Bager (1980), Pigeon (1989), Matala (1995), Jacobsen (1995), Stark & Ludwig (1997:1), Auberg (1998), Lindmark (1998), Kaufmann (2000), Rönning (2001), Hasholt (2002). However, in fact, no better theories about the mechanisms causing freeze/thaw damage have been developed so far. Power's fundamental work on freeze/-thaw and concrete is still relevant. Sections 4.2.3 - 4.2.4 present the three main mechanisms according to Powers in more detail.

4.2.3 Hydraulic pressure

Figure 4.1 shows a water-filled pore connected to a partly air-filled pore by a thin, tube-shaped pore. When the temperature is lowered, and becomes sufficiently low, the water starts freezing and ice crystals form in the water. The temperature at which freezing is initiated depends on the size of the pore, the concentration of and type of dissolved chemicals in the pore water and on possible supercooling effects. When ice crystals start to form, water is squeezed, due to the increase in volume when water transforms to ice, from the water-filled pore, through the tube-shaped pore to the air-filled pore. The squeezing of water through the fine pore initiates a hydraulic pressure which may be high enough to fracture the concrete. The hydraulic pressure becomes higher the thinner and the longer the tube-shaped pore is and the higher the ice formation rate.

The protective effect of air pores in the cement paste is, according to the hydraulic pressure theory, explained by the fact that well distributed air pores shorten the distance the water has to be squeezed through the fine pore system before it reaches an air-filled pore. For each pore system, a critical spacing factor exists. This factor defines the largest acceptable mean distance between the air pores for a frost-resistant concrete. The theories about the positive effect of entrained air, the influence of the air void distribution and the introduction of the spacing factor concept are given in Powers (1949).

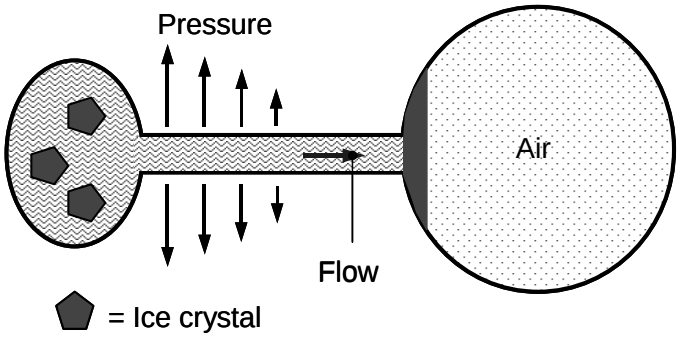

Figure 4.1 *Illustration of the hydraulic pressure mechanism.*

According to the theory behind the hydraulic pressure mechanism, the internal pressures causing damage increase with increasing ice formation rate. The ice formation rate in turn increases with increased cooling rate and, consequently, for zero cooling rate the internal pressure should be zero. This has been observed and is reported in Powers & Helmuth (1953), see Figure 4.2. The figure shows the temperature and the dilation curves for a cement paste with w/c-ratio 0.60 without entrained air.

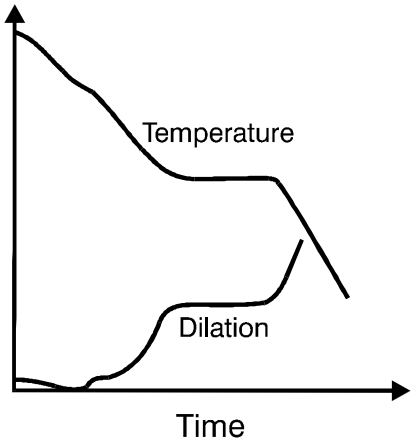

Figure 4.2 *Dilation and temperature curves (sketch) illustrating the hydraulic pressure mechanism for a cement paste without entrained air and with w/c-ratio 0.60. Redrawn from Powers & Helmuth (1953).*

From the figure, it can be seen that when the decrease in temperature is stopped, i.e. the cooling rate is zero, the expansion stops (in the experiment the temperature was held at ~ – 8 °C for 22 minutes). When the cooling is resumed, expansion starts again. This illustrates that the frost attack caused by hydraulic pressure can be stated to be cooling rate-dependent.

According to Powers, the hydraulic pressure mechanism is probably applicable to most concrete qualities but particularly to concrete qualities where the amount of non-freezable water is low, i.e. for concrete qualities with relatively high w/b-ratios.

4.2.4 Microscopic ice body growth and osmotic pressure

Assume a water-filled capillary pore and a partly air-filled pore connected to a pore system of finer pores (small capillaries and gel pores), as in Figure 4.3. No connection to an outer water source (isolated freezing).

In the figure, the pore system between the water-filled pore and the air-filled pore represents a system of small water filled gel pores and small capillary pores. When the temperature of the water in the pore system falls below 0 °C the water in the larger capillary pore will start to freeze to ice. As was mentioned above, the temperature at which freezing is initiated is dependent on the size of the pore, the amount of dissolved chemicals in the pore water and on possible supercooling effects. As long as there is no ice in the pore system, the water in the capillaries and the water in the finer parts of the pore system, i.e. the small capillaries and the gel pores, may be regarded as being in thermodynamic equilibrium. As soon as the temperature falls to a point where ice is starting to form in the coarse capillaries, this equilibrium is broken. The equilibrium is broken since, at a given temperature and a given pressure, the free energy of ice is lower than that of water. To regenerate the equilibrium, water is transported from the water-saturated small capillaries and gel pores towards the ice. This transport of water in a water insulated material results in drying causing shrinkage of the cement paste and a decrease in the free energy of the still unfrozen water in the finer pore system.

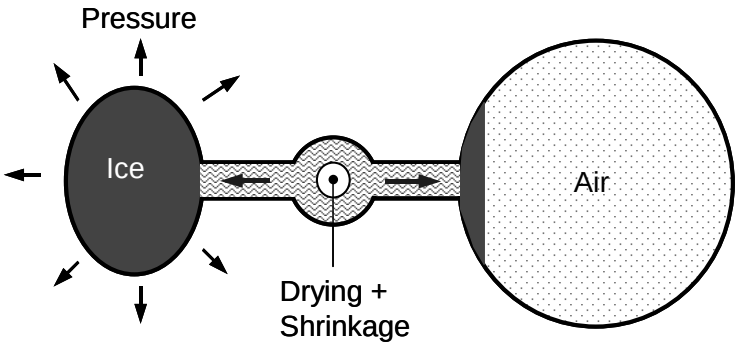

Figure 4.3 *Illustration of microscopic ice body growth.*

More ice can be formed when the water transported from the small capillaries and gel pores reaches the ice-filled coarse capillaries. As a result of this, pressure acting on the pore walls is built up. This pressure leads to an increase in free energy of the ice and thus a lower potential for transport of water from the finer pore system towards the ice. Water will, however, continue to be transported towards the ice until equilibrium is reached. If

equilibrium is not reached before the pressure built up by the growing ice exceeds the tensile strength of the material, the ice will cause permanent damage.

As in the hydraulic pressure theory, the protective effect of air pores is explained by the fact that the air pores provide space for water to be transformed to ice without exerting any pressure. According to the microscopic ice body growth theory, ice formed in the air pores will compete with the ice in the coarse capillaries for water from the fine pore system. Since ice is growing in a stress-less state in the air pores (assuming that the air pores are at least partly filled with air), the free energy of the ice growing in the air pore is lower than the free energy of ice growing under pressure in a capillary pore. The driving potential, i.e. the difference in free energy, will thus be higher between the water in the fine pore system and the ice in the air pores than between the water in the fine pore system and the ice in the coarse capillaries. The water therefore 'prefers' to move towards the ice in the air pore. This leads to less water being transported to the coarse capillaries containing ice, resulting in a slower and lower build-up of pressure. However, for air pores to be protective, they have to be closely spaced so that there are enough sites where ice can grow in a stress-less state. Depending on the pore structure of the material, the temperature and the time at this temperature, there exists a maximum allowable distance between the air pores if the pressure built up by the ice in the capillaries is not to exceed the tensile strength of the material. This distance between the air-filled pores is given by a critical spacing factor, analogous with the theories behind the hydraulic pressure theory.

The theory, presented in Powers & Helmuth (1953), did not account for the fact that the water in the pores of cement paste is not pure water but contains dissolved chemicals. However, in Powers (1975) the effect of dissolved chemicals on the energy state of water, which leads to osmotic phenomena taking place during freezing and thawing, was taken into account. This theory complemented the original theories about microscopic ice body growth.

Assume a water-filled capillary pore and a partly air-filled pore connected to a pore system of finer pores (small capillaries and gel pores), as in Figure 4.4.

As long as all pore water is in the form of fluid, the concentration of dissolved chemicals, C_1, is the same in the whole pore system. Because of the dissolved chemicals, ice will start to form at a lower temperature than if the pore solution was pure water. The dissolved chemicals thus lower the freezing temperature. However, if the temperature is lowered far enough, ice will start forming in the coarse water-filled capillary pores. The concentration of the dissolved chemicals in the unfrozen water will thus increase in the pores where the ice is formed, C_2. The increase in dissolved chemical content leads to a lower freezing point in the unfrozen water. The ice will stop growing when the concentration of chemicals in the surrounding pore water is such that the melting point is equal to the actual temperature.

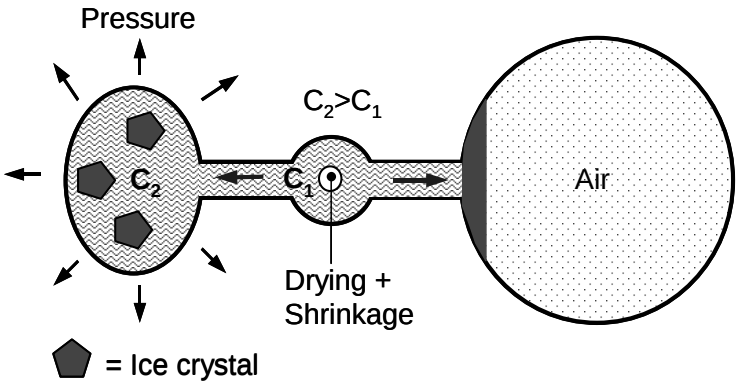

Figure 4.4 *Illustration of osmotic pressure.*

The difference in concentration of dissolved chemicals between the two pores initiates an osmotic effect, causing water in solutions with low concentration to move towards solutions with higher concentration. That is, water will move from the fine pores towards the coarser capillaries, which are partly filled with ice crystals. This redistribution of water towards the coarser capillaries results in the concentration in the pore water in these coarse capillaries being lowered. This in turn leads to an increased freezing point in the pore water, so that ice can again start forming, resulting in an increasing pressure acting on the pore walls. The redistribution of water, the growth of ice bodies and the increase in pressure acting on the pore walls will continue until equilibrium is reached. A change in temperature will again lead to a changed equilibrium and a further redistribution of pore water, ice formation or melting etc.

As in the 'pure' microscopic ice body growth theory, the role of air voids is to compete with the ice formed in the capillary pores for the water in the finer pore system. The air voids thus provide sites for water to freeze without exerting pressure on the pore walls. Since there probably exists a small amount of water in the air pores, this will freeze as soon as the freezing point is reached. The concentration of the solution thus increases, which results in the same type of osmotic effect as is acting between the finer pore system and the coarse capillaries where ice bodies are formed. If the air-filled pores are sufficiently closely spaced, the air pores will provide enough sites for ice to grow without damaging the cement paste, i.e. there will be no damage as long as the critical spacing factor is not exceeded.

According to the theories behind the microscopic ice body growth, and the later complementing theory about osmotic pressures, the internal pressures causing damage increase in principal with decreasing temperature and the time the concrete is kept at freezing temperatures. According to the theories, water transport from the small capillaries and gel pores towards the coarse capillaries in which there is ice continues as long as the energy equilibrium is broken, i.e. also when the temperature is held constant at a temperature below 0 °C. This implies that also during constant freezing temperatures there could be an

expansion because of a continuing growth of ice, thus increasing the pressure on the pore walls. This has been observed, and is reported in Powers & Helmuth (1953); see Figure 4.5, which shows the temperature and the dilation curves for a cement paste with w/b-ratio 0.45 without entrained air.

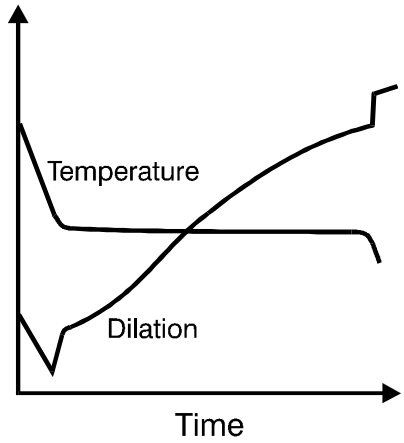

Figure 4.5 *Dilation and temperature curves (sketch) illustrating the microscopic ice body growth mechanism for a cement paste without entrained air with w/c-ratio 0.45. Redrawn from Powers & Helmuth (1953).*

From the figure, it can be seen that when the decrease in temperature is stopped, i.e. the cooling rate is zero, the expansion continues (in the experiment the temperature was stopped at ~ –19 °C for 6 hours). The expansion continues during the whole time the temperature is constant, meaning that equilibrium is not reached during this time. This shows that the frost attack caused by microscopic ice body growth (and osmotic pressure) is not sensitive to the cooling rate, but it is on the other hand dependent on the time during which the concrete is kept in an environment with a temperature below zero.

As for the hydraulic pressure mechanism, the microscopic ice body growth mechanism is probably also applicable to most concrete qualities. However, according to Powers, the microscopic ice body growth mechanism is probably somewhat more applicable to concrete qualities in which the content of non-freezable water is high, i.e. concrete qualities with relatively low w/b-ratios.

4.2.5 Critical degree of saturation

Although different theories have been developed to try to explain the mechanisms acting during freezing and thawing, there is probably no single theory that alone explains the frost problem. In reality, it is most likely a combination of different mechanisms acting, and these may be different for different concrete qualities and in different climatic conditions.

Independent of what mechanism or mechanisms that are acting, damage due to frost is a moisture problem. If the moisture content in a material, i.e. degree of saturation, is too high there is a risk of frost damage. When a critical moisture content has been reached, the material has reached a 'critical degree of saturation'. Exposing a material, which has reached a critical degree of saturation to freezing and thawing, leads to damage. The critical degree of saturation of a material can be regarded as a material property and can be estimated by a method described in Fagerlund (1977). The concept of critical degree of saturation is briefly presented below.

The degree of saturation, *S*, of a material is given by:

$$S = \frac{W_e}{P_{tot}}$$

where:

W_e	is the total evaporable water content	[m^3/m^3]
P_{tot}	is the total porosity	[m^3/m^3]

For a completely dry material with an empty pore system, the degree of saturation is 0 and for a totally water-filled pore system, including the air pores, the degree of saturation is 1.

If we suppose that there is a critical spacing factor, as is proposed according to the fundamental degradation mechanisms: *hydraulic pressure* by Powers (1949) and *microscopic ice body growth (and osmotic pressure)* by Powers & Helmuth (1953) and Powers (1975), then there must also be a critical degree of saturation. This can be illustrated as in Figure 4.6, which shows concrete containing air voids which are filled with water to different degrees.

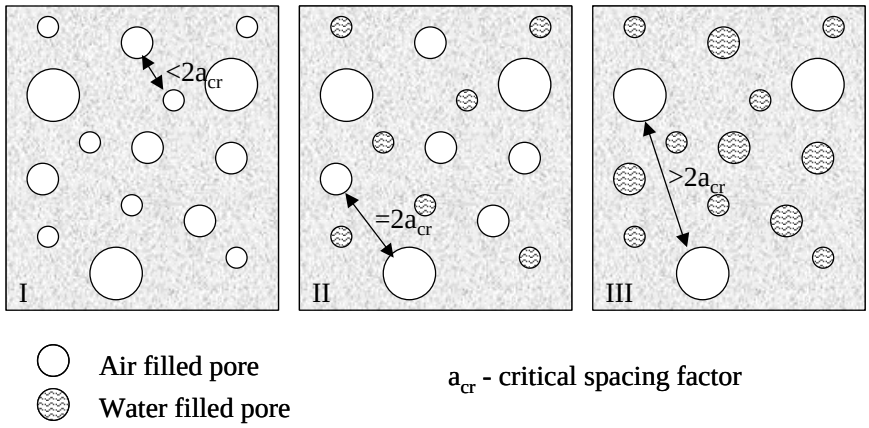

Figure 4.6 *Illustration of concrete with air voids, which are filled with water to different degrees.*

In illustration I in the figure, the degree of saturation is low and most pores are air-filled. The longest distance between two air pores is less than twice the critical spacing factor. In illustration II, the degree of saturation has increased as has the longest distance between two empty air voids. The distance is twice the critical spacing factor and thus the degree of saturation has reached a critical level. If the degree of saturation is further increased, there will be only some large pores still air-filled, illustration III. The longest distance between two air voids has now increased to exceed twice the critical spacing factor, which means that the degree of saturation has exceeded the critical limit. The material will at this stage be damaged if exposed to frost action.

The estimation of the critical degree of saturation according to the method described in Fagerlund (1977) is carried out by:

1. preconditioning specimens to various degrees of saturation
2. measuring the fundamental frequency or dynamic E-modulus
3. exposing the specimens to freezing and thawing in moisture sealed condition
4. measuring the fundamental frequency or dynamic E-modulus after freezing

An alternative of measuring the fundamental frequency or dynamic E-modulus is to measure the length change during freeze/thaw.

Damage is detected by measuring the reduction in E-modulus or the dilation during freezing. The results are plotted in a diagram and the critical degree of saturation can be estimated by the nick-point, as in Figure 4.7.

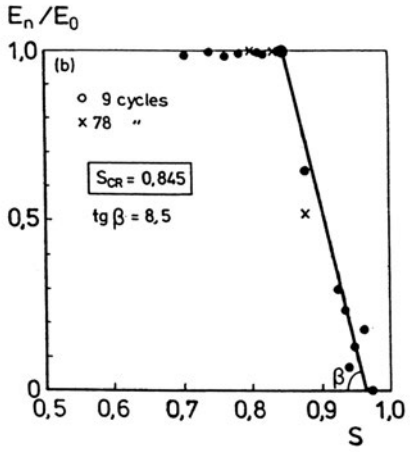

Figure 4.7 *Change in E-modulus as a function of degree of saturation. E_n= dynamic E-modulus after n freeze/thaw cycles, E_0= dynamic E-modulus before freezing. From Fagerlund (1982).*

From the figure it can be seen that as long as the specimens have a degree of saturation below ~0.845, the specimens do not show any decrease in E-modulus, i.e. damage.

However, if this value is exceeded, the specimens show significant drops in E-modulus, indicating extensive damage. The critical degree of saturation is estimated from the nick point at the degree of saturation when the specimens start to show damage.

When the critical degree of saturation of a material is determined, the question to answer is how long time it takes for the material to reach the critical value. This is, of course, dependent on the climate in which the concrete is exposed. In a dry climate the critical value may never be reached, whereas in a moist climate the critical value may be rapidly reached. In order to estimate the time to reach the critical degree of saturation in a wet environment, the material can be exposed to long-time water absorption according to a procedure described in Fagerlund (1977). During water absorption it is assumed that all small pores (gel pores and capillary pores) become rapidly water-filled. The larger air-filled pores are filled with water much more slowly. However, since air is soluble in water and the air in pores surrounded by water is under pressure, the air will slowly dissolve in the water, resulting in the air-filled pores slowly becoming water-filled. The air pressure in the pores increases with decreasing pore sizes, and so the air in the smallest pores is dissolved first. The theories behind water-filling of air voids in porous materials are first presented in Fagerlund (1979). The theories are further developed and presented in Fagerlund (1993). According to the theory, water-filling of the air voids is controlled by the rate of diffusion of the air and the size distribution of the air voids; that is, the higher the permeability of the material and the smaller the air voids, the faster is the water absorption and thus the increase in degree of saturation.

4.3 Literature review of carbonation and its effect on the salt-frost resistance of concrete

4.3.1 Introduction

The effect of carbonation on different material properties of concrete and other cement-bound materials has been studied for a long time. Also the effect of carbonation on the pore structure has been investigated to some extent, and it has been shown that carbonation leads to structural changes influencing, for example, the compressive strength and the permeability of concrete. Investigations of the effect of carbonation on the frost and salt-frost resistance of concrete are few, and in some cases contradictory. In the literature there are also two different explanations for the reported effects of carbonation on the salt-frost resistance: one physical and one chemical.

The following is a brief description of the carbonation process, followed by a review of knowledge of the effect of carbonation on the pore structure as well as its effect on frost and salt-frost resistance.

4.3.2 The carbonation process

Carbonation of cement-bound materials, such as concrete, is a spontaneous process in normal air. Carbon dioxide in the air reacts primarily with the hydrated phases of the cement paste to form new carbonated phases. Carbonation starts at the exposed surfaces and proceeds inwards. The rate of carbonation is affected by material properties, e.g. permeability and exposure conditions, e.g. carbon dioxide concentration and relative humidity of the air. Because carbon dioxide has to diffuse through the pore system, including the carbonated zone, carbonation proceeds into a material at a decreasing rate. In general, under constant conditions, the depth of carbonation increases in proportion to the square root of time.

Carbonation of concrete is often regarded as negative with respect to durability. This is primarily because of the effect carbonation has on the pH-value of the pore solution. Carbonation decreases the pH-value significantly from above 12.5 in an uncarbonated concrete to below 9 in a carbonated. This reduces the corrosion-inhibiting effect on the embedded rebar in the concrete. When the carbonated zone reaches the rebar, there will be risk of corrosion. Carbonation, however, may also lead to positive effects with regard to durability, e.g. increased compressive strength, decreased permeability etc. Carbonation also has a significant effect on the frost and salt-frost resistance, although this can differ for different binder types/combinations, as will be discussed below.

The carbonation process in its simplest form can be divided in three steps (Stark & Wicht (1995)):

1. Diffusion of CO_2 through the capillary pore system and dissolution of calcium hydroxide $Ca(OH)_2$ in the pore water:

$$Ca(OH)_2 \rightarrow Ca^{2+} + 2OH^-$$

2. Dissolution of CO_2 in the pore water:

$$CO_2 + H_2O \rightarrow H_2CO_3 \rightarrow 2H^+ + CO_3^{2-}$$

   H_2CO_3 will be in equilibrium with the carbonate CO_3^{2-}.

3. Neutralisation of $Ca(OH)_2$ through reaction with H_2CO_3

$$Ca(OH)_2 + H_2CO_3 \rightarrow CaCO_3 + 2H_2O$$

or

$$Ca^{2+} + 2OH^- + 2H^+ + CO_3^{2-} \rightarrow CaCO_3 + 2H_2O$$

In addition, the calcium-silicate-hydrate (C-S-H) gel reacts with carbon dioxide. In general, this reaction can be expressed as (Matala (1995)):

$$CaO_x SiO_{2\,y} H_2 O_z + xCO_2 \rightarrow xCaCO_3 + ySiO_2 \cdot (z - w) H_2 O + wH_2 O$$

Other hydration phases, such as the aluminate phases, as well as unhydrated phases, might also react with carbon dioxide. However, the reaction of the calcium hydroxide and the C-S-H gel is responsible for the majority of the produced calcium carbonates. The carbonation process is not as simple as might appear from the above. The neutralisation takes place in many steps with intermediate reactions. For further information about the carbonation process and the effect of carbonation, see for example Parrott (1987) and Richardson (1988). Carbonation models are further discussed for example in Bier (1988), Atlassi (1993) and Matala (1995).

The literature contains somewhat different opinions about at what stage of carbonation calcium hydroxide and the C-S-H gel carbonate. Most investigations, however, report a more or less simultaneous carbonation. Hunt & Tomes (1962) report that, for hydrated cement pastes of OPC conditioned in pure carbon dioxide, carbonation of phases other than calcium hydroxide can occur while calcium hydroxide is still present. That is, calcium hydroxide does not first have to be consumed, which has often been stated, before carbonation of the C-S-H gel can begin. Slegers & Rouxhet (1976) report that carbonation of hydrated C_3S stored for 2.5 years in a normal atmosphere leads to a complete disappearance of the C-S-H gel, whereas calcium hydroxide could still be found. The same tendency is found for cement mortar with OPC alone and with blends of up to 30 % fly ash carbonated in normal air; see Fagerlund (1988). Dunster (1989) reports an investigation of carbonation of hydrated cement pastes of OPC in normal air. It is reported that carbonation of calcium hydroxide and C-S-H gel occurs simultaneously, but that the rate of carbonation decreases with time for the remaining calcium hydroxide crystals when these are coated with calcium carbonates. The same tendencies are reported in Groves et al. (1991) for hydrated C_3S cement pastes carbonated in pure CO_2 and normal air respectively. From the investigations reported in the literature, it thus seems that carbonation of the calcium hydroxide and C-S-H gel take place more or less simultaneously.

The products produced by carbonation of calcium hydroxide and C-S-H gel are not, however, entirely the same. There are in principal three mineralogical forms of calcium carbonate: calcite, aragonite and vaterite. According to the literature review presented in Matala (1995), solubility is highest for vaterite and lowest for calcite. It is also reported that the ‘metastable’ phases of vaterite and aragonite are formed first, followed by a transformation into the more stable form calcite. The transformation of calcium hydroxide to calcium carbonate causes a volume increase depending on crystal form: 3 % for aragonite, 12 % for calcite and 19 % for vaterite, see Houst (1993). According to Richardson (1988), the major mineralogical form of calcium carbonate in concrete is calcite.

When calcium hydroxide reacts with carbon dioxide, only calcium carbonate and water is produced. When the C-S-H gel reacts an amorphous porous silica gel is also produced, in

addition to the calcium carbonate and water (Bier (1988)). Depending on the amounts of calcium hydroxide and C-S-H gel that carbonate, the effects on the pore structure of the carbonated material will be different. Concrete with high contents of secondary cementitious materials with low calcium oxide (CaO) contents (e.g. blast furnace slag, fly ash, and silica) leads to a lower content of calcium hydroxide in the hydrated cement paste compared to a concrete using only OPC as binder. The secondary cementitious materials mentioned above also react with the calcium hydroxide produced by the cement reaction, resulting in more C-S-H gel and thus a further lowering of the calcium hydroxide content. This leads to a relatively small amount of carbonation of calcium hydroxide and a relatively larger amount of carbonation of the C-S-H gel for concrete containing high contents of secondary cementitious materials with low CaO contents.

The phases of calcium carbonate formed during carbonation may differ depending on the cement type and binder combination. For example, Stark & Ludwig (1997:1) report that carbonated cement paste of OPC contained only calcium carbonate in the form of calcite, whereas carbonated cement paste of a slag cement with high contents of slag as part of the binder showed considerable amounts of aragonite and vaterite in addition to calcite. According to Stark & Ludwig (1997:1) this could be due to the fact that, for a hydrated paste with slag cement, the C-S-H gel carbonates to a higher degree than is the case for a hydrated paste with OPC. The reason for this would be the lower calcium hydroxide content in the slag cement paste than in the OPC paste. When C-S-H gel carbonates the product should, according to Stark & Ludwig (1997:1), to a high degree result in formation of the carbonated phases of aragonite and vaterite, whereas calcium hydroxide should result only in calcite. There are, however, other investigations that report high contents of especially vaterite, even for materials made with OPC. For example, Cole & Kroone (1960) show that carbonation of mortars made with OPC and conditioned in 100 vol-% carbon dioxide as well as in normal air, leads to "*poorly crystallized vaterite, aragonite and calcite*".

According to Atlassi (1993), who describes concrete with silica as part of the binder, the amount of calcium hydroxide available for carbonation is much less than in concrete with OPC alone as the binder. This leads to the amount of calcite formed during carbonation decreasing, whereas the amount of vaterite or C-S-H-$CaCO_3$ (CO_2 reacting with the bound CaO in the C-S-H gel) increases. According to Atlassi this "*is an indication that calcite is primarily formed when $Ca(OH)_2$ is carbonated and vaterite and/or C-S-H-$CaCO_3$ when the C-S-H is attacked by carbon dioxide.*"

In order for carbonation to take place, there has to be a sufficient amount of pore water in the pore system in which the carbon dioxide can dissolve. This means that in a completely dry material there will be no significant carbonation. On the other hand, if the pore system is fully saturated, diffusion of carbon dioxide into the material is slow and so the rate of carbonation is also slow. Atlassi (1993) describes a carbonation model, divided into four different stages depending on the moisture state of the material. In the first stage, where the material is saturated or nearly water saturated, the carbonation is very slow. At this stage, according to the model, calcium hydroxide will be consumed first and thereafter the

CaO will be dissolved from the C-S-H gel. The calcium carbonate phase produced at this stage is calcite. In the second stage, where the relative humidity is between 40 % and 95 % RH, both calcium hydroxide and C-S-H gel carbonate simultaneously. Calcium hydroxide, which liberates water as a result of carbonation, forms calcite down to relatively dry conditions. The carbonation of the C-S-H gel will, however, result in the formation of vaterite or C-S-H-$CaCO_3$. In the third stage, where the relative humidity is between 11 % and 40 %, water in the pore system is not present as liquid but as a layer of molecules adsorbed to the pore surfaces. At this stage, calcium hydroxide may still be carbonated. Carbonation of the C-S-H gel is limited and, if any, carbonation will create a C-S-H-$CaCO_3$ type of material. In the fourth stage where the relative humidity is around 11 %, carbonation of C-S-H is minimal and if any carbonation takes place it is calcium hydroxide that carbonates.

Influence of relative humidity on the rate of carbonation

The highest rate of carbonation is often reported to take place at intermediate relative humidities. Verbeck (1958) investigated the shrinkage caused by carbonation and by drying of mortars and cement pastes stored in climates with different relative humidities. From the investigation, it can be concluded that the shrinkage caused by carbonation is most significant when carbonation took place in a climate with a relative humidity between 50 % and 75 %.

Wierig (1984) investigated the depth of carbonation for concrete stored in climates with different relative humidities and temperatures for up to 16 years. It was shown in this investigation that the greatest carbonation depth was found for concrete stored in climates with a relative humidity around 65 %. This was found for concretes made with Portland cement and slag cement respectively. It was also shown that the influence of temperature on the carbonation rate is of little importance (+5 °C to +20 °C).

Parrott (1991/92) investigated the amount of carbonated material of cement pastes conditioned in climates with normal air and with different relative humidities. The results show that the influence of the relative humidity on the amount of carbonated material is different for concrete with different w/b-ratios and also with different binder combinations, see Figure 4.8.

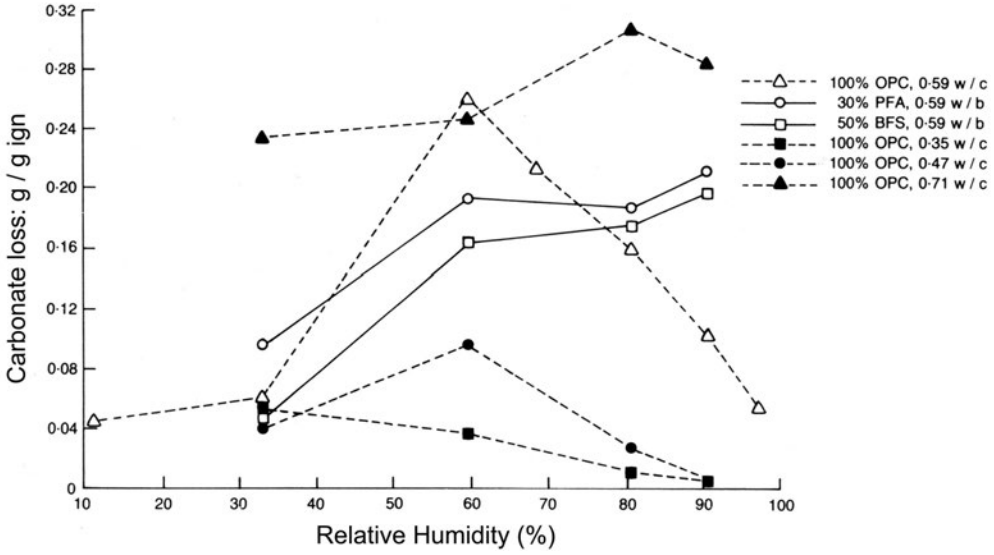

Figure 4.8 *Thermogravimetric carbonate loss versus relative humidity for carbonation. From Parrott (1991/92).*

From the figure it can be seen that for OPC paste with a w/c-ratio of 0.59, the highest amount of carbonation is found in conditions with around 60 % RH, with a significant decrease in carbonation with increasing relative humidity. However, for pastes with the same w/b-ratio but with large contents of slag or fly ash, the amount of carbonated material increases with increasing relative humidity up to 90 % RH. The same tendency is found for OPC pastes with higher w/c-ratios. The opposite tendency is found for OPC pastes with lower w/c-ratios, with increasing amount of carbonates as the relative humidity falls to 33 % RH. According to Parrott (2003), the differences between the various materials in their response to the relative humidity is explained by the differences in porosity and pore structure between the materials and to the extent to which pore water blocks diffusion of carbon dioxide.

Houst (1993) presents an investigation, where cement paste prisms with different w/c-ratios were stored in climates with increased carbon dioxide content (~2 vol-%) and with different relative humidities. From this investigation, the results show that the rate of carbonation is highest in the region of 50 to 80 % relative humidity. This is valid for all w/c-ratios that were tested, see Figure 4.9. However, from the results it can be seen that there is a tendency for qualities with lower w/c-ratios to carbonate somewhat more rapidly at a lower relative humidity than do qualities with higher w/c-ratios. For example, the quality with a w/c-ratio of 0.30 shows the highest carbonation at a relative humidity around 50 %, whereas the quality with a w/c-ratio of 0.80 shows the highest carbonation at a relative humidity around 75 %. The tendency is that the higher the w/c-ratio, the higher is the relative humidity at which the rate of carbonation is the highest. This correspond with the results presented in Parrott (1991/92).

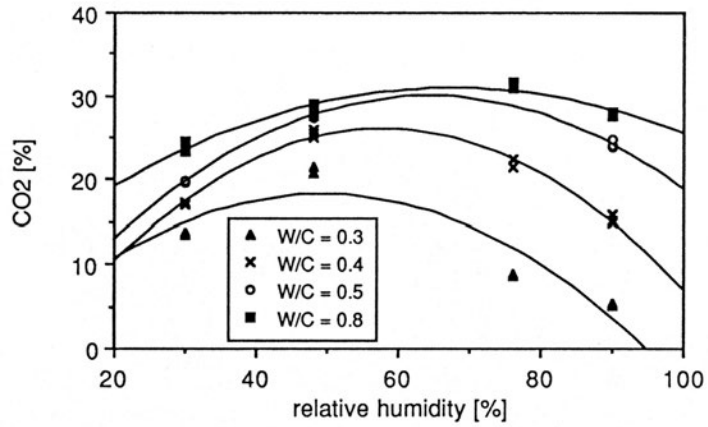

Figure 4.9 *Carbonate content of hardened cement paste determined after exposing to ~2 vol-% CO_2. From Houst (1993).*

Consequently, from most investigations found in the literature, the rate of carbonation is found to be highest at intermediate relative humidities, i.e. between 50 % and 80 % RH. However, there seems to be a dependency between the w/b-ratio of the material, or rather the properties of the pore structure of the material, and the relative humidity at which the rate of carbonation is the highest. The higher the w/b-ratio, the higher the relative humidity at which the rate of carbonation is the highest, and vice versa. However, at very high and very low relative humidities, carbonation is slow and independent of the w/b-ratio.

4.3.3 Carbonation shrinkage

During carbonation in an environment with an intermediate relative humidity, concrete will shrink more than can be explained by shrinkage due to drying alone. The excess shrinkage is due to carbonation, i.e. carbonation shrinkage. This occurs despite the fact that the carbonate products lead to a volume increase relative to the original uncarbonated products. As was mentioned above, Verbeck (1958) investigated the shrinkage caused by carbonation and by drying of mortars and cement pastes stored in climates with different relative humidities. Figure 4.10 shows the length change due to drying and due to carbonation for mortars conditioned in climates with different relative humidities, with (probably 100 vol-% CO_2) and without carbon dioxide. From the figure, it can be seen that the carbonation shrinkage is negligible at 100 % RH and below 25 % RH, but that between 50 % RH and 75 % RH carbonation shrinkage is as high as or even higher than the drying shrinkage.

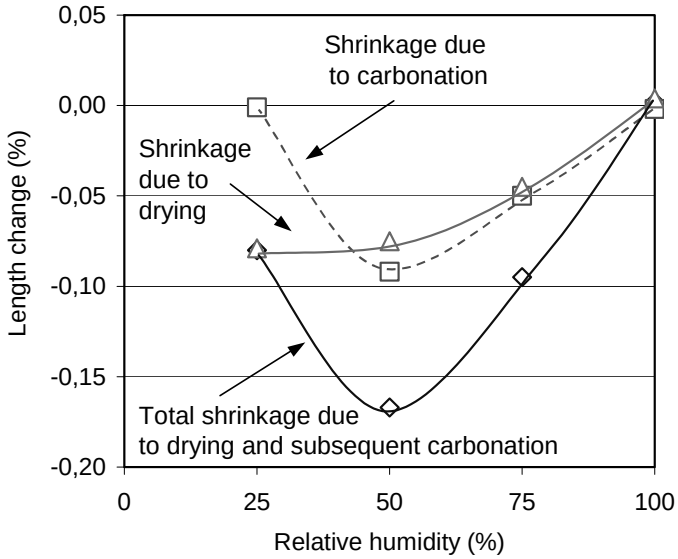

Figure 4.10 *Drying shrinkage and carbonation shrinkage of mortar at different relative humidities. Redrawn from Verbeck (1958).*

There are a couple of different theories explaining carbonation shrinkage. Powers (1962) explains carbonation shrinkage by dissolution of calcium hydroxide crystals while the crystals are under pressure. The calcium hydroxide crystals are under pressure because of shrinkage caused by drying. The calcium carbonates are then deposited in places where the carbonate is not under pressure. The stress relief caused by this results in a shrinkage which, according to calculations in Powers (1962), agrees "*reasonably well*" with experimental data. Another explanation is that, as a result of carbonation of calcium hydroxide, non-evaporable water is released. The released water could then evaporate, which would result in shrinkage. The review of carbonation shrinkage presented in Richardson (1988), gives several references explaining carbonation shrinkage by a loss of non-evaporable water, Swenson & Sereda (1968) being one of these.

In what respect carbonation shrinkage leads to a change of the durability, caused for example by micro-cracks in the carbonated layer or between the carbonated and uncarbonated layer, is not known by the present author. However, the increase in compressive strength, together with observed increase in tensile strength, in the carbonated zone, as is reported by numerous investigations (see literature review in Bier (1988)) is an indication that carbonation shrinkage does not lead to any significant micro-cracking leading to decreased durability. This is valid at least for material made with OPC as binder. For concrete with high slag contents, however, carbonation has been reported to have no effect, or even a small negative effect on the compressive strength, see Meyer (1968). However, this effect does not need to be a result of carbonation shrinkage but can be a result of the significant pore structural changes caused by carbonation. See below in Section 4.3.5.

4.3.4 The effect of carbon dioxide concentration

The concentration of carbon dioxide in normal air is around 0.03 - 0.04 vol-%, although it can vary between different regional areas. For example, the concentration is probably considerably higher in urban areas, where carbon dioxide from traffic and industries leads to a local increase in carbon dioxide significantly higher than in rural areas. Tuutti (1982) states that the carbon dioxide content varies between 0.03 vol-% in rural areas and 0.1 vol-% in urban areas. However, according to Tuutti (1982), the concentration may locally be even higher, for example close to traffic facilities. An example given in Tuutti (1982) shows that the carbon dioxide content measured in a silo containing grains was 1 vol-%. Neville (1995) reports average carbon dioxide values in urban areas of 0.3 vol-% and, in exceptional cases, as high as 1.0 vol-%. An example of a structure exposed to very high concentrations of carbon dioxide is traffic tunnels.

When investigating the effect of carbonation on different material properties, an increased carbon dioxide content has often been used to speed up the rate of carbonation. Normally, a carbon dioxide content of between 2 and 10 vol-% has been used. In some investigations, higher concentrations and even up to 100 vol-% carbon dioxide have been used. However, carbonation at elevated carbon dioxide contents has been shown to result in exaggerated or even unnatural effects, leading to results and conclusions not applicable to natural carbonation. For example, Knöfel & Eßer (1992) describe an investigation into the effect of carbonation on different material properties for materials conditioned in climates with different carbon dioxide contents. In the investigation, mortars made with different cements including OPC and slag cement were exposed to climates with normal air (0.03 vol-%) and air with 1 vol-%, 3 vol-% and 100 vol-% of carbon dioxide. The work investigated material properties such as compressive strength, pore size distribution measured by mercury intrusion porosimetry, open porosity measured by water absorption and phase analysis using X-ray diffraction. According to the investigations presented in Knöfel & Eßer (1992), carbonation in normal air and in 1 vol-% of carbon dioxide gave about the same material properties. However, for material conditioned in climates with 3 vol-% and 100 vol-% carbon dioxide, the material properties differed significantly from the properties obtained when conditioned in normal air. It is thus concluded in Knöfel & Eßer (1992) that conditioning in climates with increased carbon dioxide content should not be carried out at a CO_2 concentration above 1 vol-%. Since the limit according to Knöfel & Eßer (1992) is as low as 1 vol-% carbon dioxide, many of the investigations in which increased carbon dioxide contents have been used have led to results of which the relevance might be questioned. It can also be noted that, as was found in the literature, that a carbon dioxide concentration around 1 vol-% is the highest observed natural concentration.

The present investigation has performed carbonation in a climate with an elevated carbon dioxide concentration of ~1 vol-%. In order to investigate the relevance of the results from the specimens conditioned in elevated carbon dioxide content, some additional tests have been carried out on specimens conditioned in normal air; see Chapter 9 and 10.

4.3.5 The effect of ageing, and in particular of carbonation, on the pore structure

The effect of carbonation on the pore structure of concrete has been investigated primarily on concrete with OPC alone as the binder. In recent years, concrete containing different amounts of slag as part of the binder has also been investigated. However, few investigations of the effect of carbonation on the pore structure of concrete containing silica as part of the binder have been carried out.

Pihlajavaara (OPC)

For cement paste of OPC with different w/c-ratios (0.3 - 0.5), Pihlajavaara (1968) presented results from sorption isotherm measurements in addition to Mercury Intrusion Porosimetry (MIP) measurements on uncarbonated and carbonated material. Specimens were carbonated in air with a carbon dioxide content of 0.05 vol-% at +20 °C and 40 % and 70 % RH. Results from the measurements showed a reduction of total pore volume for carbonated material compared to uncarbonated. The reduction in total pore volume was primarily found to be because of a reduction in the coarse pores. The absorption and desorption isotherm measurements showed that the water content at a given relative humidity, both during absorption and desorption, was significantly lower for the carbonated material than for the uncarbonated. Calculations of the specific surface area using the BET theory showed that carbonation led to a significant reduction of the specific surface area. Even though the effect of carbonation on the pore structure seems clear from the results presented in Pihlajavaara (1968), there are some questions regarding the testing procedure that probably also may have a significant effect on the pore structure. For example, the age of the uncarbonated and carbonated specimens at the time of testing differed significantly. The age of the uncarbonated material was about three months, whereas the age of the carbonated material was over 27 months. It is also not quite clear on what specimens the carbonation was carried out, i.e. if it was on previously dried specimens (+105 °C) or not. The severe drying at +105 °C, carried out before MIP measurement and measuring the absorption isotherm, probably also led to pore structural changes.

Hilsdorf et al. (OPC, Slag)

After the results reported by Pihlajavaara, these findings have been confirmed in other investigations, primarily by investigations carried out by researchers at the University of Karlsruhe, Germany, at 'Institut für Massivbau und Baustofftechnologie'. The effect of carbonation on the pore structure of cement paste, mortars and concrete is reported in several publications from the 1980s. For example, Hilsdorf et al. (1984) present results from MIP measurements for carbonated (~2 % CO_2) and uncarbonated specimens of cement pastes made of OPC and with a w/c-ratio of 0.50. (Many of the results presented in Hilsdorf et al. (1984) were probably originally presented in Kropp (1983)). Details of the possible drying procedure before MIP measurement are not given. The results show a marked reduction of the total porosity, with a major part of the reduction attributed to capillary pores. This paper also presents results for mortar with a w/b-ratio of 0.50 with

Portland blast furnace slag cement (~75 % slag). The presented results, which are deduced from data originally reported by Smolczyk & Romberg (1976), show that also for cement with high slag contents (in this case mixed in a mortar) there is a reduction in total porosity as a result of carbonation. However, even though the total porosity is reduced, the capillary porosity for this cement type with high slag contents as part of the binder is reported to increase as a result of carbonation.

Bier (OPC, Slag, Fly ash)

In another publication from the University of Karlsruhe, Bier (1987) presents results from MIP measurements and thermal analysis of cement pastes with different w/b-ratios and with OPC as well as with blended cement types containing different amounts of slag (30 % - 75 %) and fly ash (10 % - 50 %) as part of the binder. From measurements of the carbonation depth after 28 days of carbonation in an environment with 65 % RH, +20 °C and ~2 % CO_2, it is shown that the carbonation depth is significantly higher for the pastes containing cement with slag or fly ash than for the OPC paste. This is explained by the lower calcium hydroxide contents in the blended cements. Further results presented in Bier (1987) show that:

- Carbonation leads to a reduction of the total porosity for all cement types and binder combinations investigated. However, the results from the MIP measurements show that the reduction in porosity is attributed to different categories of pore sizes, depending on the cement type. For OPC pastes, the capillary pore volume is reduced and carbonation leads to a shift towards finer capillary pores, whereas for pastes with 75 % slag as part of the binder there is a significant coarsening of the pore structure. For pastes containing high amounts of fly ash (50 %), too, carbonation leads to a coarsening of the pore structure, although the results for pastes with fly ash show some discrepancy depending on the curing time.
- The explanation for the different effects of carbonation is that for OPC pastes it is primarily the calcium hydroxide that is transformed to calcium carbonate during carbonation, whereas the lower calcium hydroxide content in the cement pastes with high slag or fly ash contents leads to a decomposition of the Calcium-Silicate-Hydrate (C-S-H) gel. The higher the content of slag or fly ash in the paste, the lower is the calcium hydroxide content in the uncarbonated material and the more C-S-H is decomposed during carbonation. It is reported that the decomposition of C-S-H leads to calcium carbonate and silica gel. The formation of silica gel, which has a coarser pore structure than the original C-S-H gel, provides the explanation for the increase in coarse porosity for cement pastes with high contents of slag or fly ash.

Litvan (OPC, Slag)

Other researchers report similar results. For example, Litvan (1987) describes results from a field investigation of 20-year-old concrete from two houses: one made of concrete with OPC with a w/c-ratio of 0.61, and one made of concrete with Granulated Blast Furnace Slag Cement (GBFSC) with a w/b-ratio of 0.58. The houses were built only for test

purposes, had no windows and were not heated. The GBFS cement is probably a type CEM III/B cement, i.e. with a minimum of 66 % slag by weight. Specimens were taken from drilled cores. From measurements of the carbonation depths it is concluded that, in the field, the GBFSC concrete shows a significantly higher rate of carbonation than does OPC concrete. Carbonation measurements from the inside and outside of the house show that carbonation progresses faster from the inside of the house than from the outside. Pore structure analysis was performed using MIP measurements on specimens preconditioned in vacuum. The results showed that for OPC concrete the total porosity decreased, whereas for GBFSC concrete the total porosity was more or less unchanged as a result of carbonation. The results also showed that, for GBFSC concrete, carbonation leads to a significant coarsening of the pore structure, whereas for OPC concrete carbonation results in a reduction of both coarse and fine pores.

Matala (OPC, Slag, Silica, Fly ash)

Matala (1988) describes an investigation of the pore structural changes caused by carbonation on mortars made with OPC and with OPC blended with secondary cementitious materials (silica, fly ash and slag). Mortars were produced with OPC alone as the binder and with replacements of 10 % and 20 % of silica, 20 % fly ash and 30 % slag. The w/b-ratio was 0.45 for all mortars, and no air entrainment was used. Mortar prisms were cast and stored immersed in water for 28 days. The specimens were subsequently stored for 14 days in air (probably laboratory air, i.e. with carbon dioxide) at 70 % RH and 20 °C. After this, the specimens were divided in two groups: 'non-carbonated' and 'carbonated'. The 'non-carbonated' specimens were "*covered airtightly by plastic sheet*" and the 'carbonated' specimens were exposed to an atmosphere with 3 vol-% carbon dioxide. Other parameters of the conditioning climate are not described. It must be noted that not only the degree of carbonation, but also the drying history, differed between the 'carbonated' and 'non-carbonated' materials. Carbonation continued until the carbonation depth was 8 mm (conditioning time is not given). Samples from the 'carbonated' and 'uncarbonated' mortar prisms were then cut off, and the pore size distribution was measured by MIP. Drying method prior to MIP measurement is not described.

Results from the MIP measurements show that, for all mortar qualities, the total porosity decreases as a result of carbonation, except for mortar with silica as part of the binder. For these qualities, the total porosity is about the same for both carbonated and noncarbonated material. For all mortar qualities, the MIP results show that carbonation leads to a coarsening of the pore structure, with the coarsening being most significant for the concrete qualities containing silica and slag as part of the binder. A slight coarsening of the pore structure is also observed for the mortar with OPC alone as the binder. This is contradictory to results presented by others. Bier (1987), for example, presents results showing a significant reduction of the coarse porosity as a result of carbonation for cement pastes with OPC as binder. It must, however, be noted that the 'non-carbonated' materials used in Matala (1988) were probably somewhat carbonated as a result of the 14 days' conditioning in normal laboratory air. Another difference between carbonated and noncarbonated material is the difference in drying regimes that may have caused changes of the pore structure. The non-carbonated material was dried only for 14 days in 70 % RH,

whereas the carbonated material was dried in an unknown climate for an unknown time of carbonation in 3 vol-% CO_2.

In one of the most recent and most comprehensive investigations, Matala (1995), studied the effect of carbonation on the pore structure of cement pastes, mortars and concretes, made with OPC or with blends of OPC with different slag contents (50 % or 70 %) and with different w/b-ratios (0.35 - 0.75). The pore structural changes were measured by MIP, Low Temperature Calorimetry (LTC) and water suction test. Changes in the chemical composition of carbonated mortars and pastes were analysed by thermogravimetry (+ gas analysis), infrared spectroscopy and X-ray diffractometry.

Results from the investigations carried out and presented in Matala (1995) show that:

- Carbonation leads to a decrease in total porosity for all binder combinations.
- Carbonation leads to a coarsening of the pore structure, even for material with only OPC as binder. The coarsening, however, was greater the higher the slag content. For materials with OPC alone as the binder, the decrease in total porosity and the coarsening of the pore structure as a result of carbonation is caused by a change of porosity in the 'micropore' range (<1.5 nm). In material containing slag as part of the binder, the pore structural changes are due to a change in porosity in the 'microcapillary' range (1.5 - 4 nm).
- The cause of the more significant coarsening of the pore structure for material with high slag contents as part of the binder, in comparison with material with only OPC as binder, is the lower content of calcium hydroxide. A more pronounced carbonation of the C-S-H gel for material with slag as part of the binder is also part of the explanation.

The results regarding the effect of carbonation on materials with OPC alone as the binder presented in Matala (1995) differ somewhat from results from other investigations referred to above. In most other investigations, carbonation of material containing only OPC as binder leads to a lower total porosity and a decrease in capillary porosity. The results presented in Matala (1995) also indicate a lower total porosity but a higher capillary porosity as a result of carbonation. The reason for this is unclear, and might be because of differences in the composition of the OPC used in the different investigations. There are, however, other reasons coupled to the test procedures used in Matala (1995) that may cause pore structural changes. One is the obvious differences in the preconditioning procedures before testing, between the carbonated and the uncarbonated material, possibly leading to marked changes of the pore structure. The preconditioning procedures used before testing differed in respect of:

- **age:** 28 days for 'uncarbonated' material, and 13 months for 'carbonated' material.
- **degree of drying:** drying at 45 % RH for 21 days for 'uncarbonated' material, and for over twelve months for the 'carbonated' material.
- **degree of carbonation:** 'uncarbonated' material was exposed to laboratory air with carbon dioxide for 21 days, 'carbonated' material for almost 13 months.

It is thus not only the degree of carbonation that differs, but also a significant difference in age and degree of drying. This probably has a significant effect on the pore structure of the different materials. The fact that even the 'uncarbonated' material was somewhat carbonated, which was confirmed in Matala (1995) by measurements of the calcium carbonate content in the materials, probably influences the results.

With these differences between 'uncarbonated' and 'carbonated' materials, the reported results of carbonation on the pore structure of materials with OPC alone as the binder seem even stranger, i.e. that the carbonated material had a higher capillary porosity. Since the 'carbonated' specimens were significantly older than the 'uncarbonated' specimens when measurements were carried out, the capillary porosity ought to be significantly reduced as a result of prolonged hydration of the carbonated material. Matala (1995) reports the opposite.

According to Matala (2003), the difference in the reported results regarding the effect of capillary porosity for material with OPC may be because of differences in measuring techniques. The conclusions in Matala (1995) concerning the effect of carbonation on the capillary porosity of OPC were based on Low Temperature Calorimetry (LTC) measurements and not, as is usually the case in many other investigations, on Mercury Intrusion Porosimetry (MIP) measurements. According to Matala (2003), the results from the MIP measurements presented in Matala (1995) actually show that with this measuring technique the capillary porosity decreases as a result of carbonation for material with OPC. However, according to Matala (2003), the results obtained by the MIP method are less reliable than the somewhat different results obtained by LTC measurements. According to the author, the MIP measurement is less reliable because the specimens were subjected to a severe pre-drying in vacuum before measurement. This technique results in a measurement of the distribution of the 'pore openings' instead of the pore size distribution. This view of the shortcomings of the MIP method is shared by other researchers, such as Diamond (2000). The LTC method requires a conditioning of the specimens that is significantly milder than the preconditioning of the MIP samples (the specimens used in Matala (1995) were, however, 'vacuum-treated' for two days before saturation and the LTC measurement was carried out). From the thawing curve, the pore size distribution can be calculated for the 'real' pore structure, and not for the sizes of the 'pore openings', at least if assuming that the material has not been damaged during freezing.

Matala (1998) presents an investigation of the effect of carbonation on mortars and cement pastes with OPC alone as the binder as well as with OPC with replacements of 5 % and 10 % silica. This investigation was carried out in parallel with the investigations presented in Matala (1995). Low Temperature Calorimetry measurements (LTC) were used to investigate the non-freezable and freezable water content and thus the pore structure. The results indicate that, for mortar with OPC alone as the binder as well as with some silica as part of the binder, carbonation leads to a coarsening of the pore structure and an increase in freezable water content. This coarsening of the pore structure is reported to lead to a significant reduction of the scaling resistance when freeze/thaw tested. This is further commented in Section 4.3.6.

The investigation presented in Matala (1998) uses the same curing procedures as in the investigations described in Matala (1995). This leads to the same uncertainties about other possible effects than carbonation that may influence the pore structure. The results presented in Matala (1998) as well as in Matala (1995) must be evaluated with these uncertainties in mind.

Parrott (OPC, Slag, Fly ash)

Parrott (1992) describes results from an investigation where cement paste prisms (w/b-ratio 0.59) made of three different cements were stored in different environments, both in the laboratory and in the field, and investigated after four years of exposure. The cement types were OPC, cement with 30 % fly ash and cement with 50 % ground granulated blast furnace slag respectively. The effect of carbonation was investigated by analysing the water absorption rate, capillary porosity and gel porosity at different depths of the prisms. The capillary and gel porosity were evaluated by sorption isotherms, which seem to have been a mix of absorption and desorption isotherms. The investigation concludes that for cement paste prisms with OPC, carbonated material shows a reduced capillary porosity, a reduced continuity of the pore system and also reduced water absorption rates compared with uncarbonated material. For cement paste prisms with 30 % fly ash or with 50 % ground granulated blast furnace slag, carbonated material showed an increase in capillary porosity as well as in water absorption rate.

Houst (OPC)

Houst (1995) presents results from investigations of microstructural changes of hydrated cement paste due to carbonation. The investigations carried out include MIP measurements and sorption measurements. Prisms of cement paste with OPC and with different w/c-ratios (0.30 - 0.80) were cured in lime-saturated water for six months. From the prisms, 3 mm thick slices were cut and stored in an environment with 80 % - 90 % CO_2 and 76 % relative humidity. How the uncarbonated material was conditioned is not described. Water absorption isotherms were measured on carbonated and uncarbonated material dried at +105 °C before being conditioned in environments with different relative humidities. MIP measurements were also carried out on carbonated and uncarbonated material. The preconditioning is not described. The presented results show that total porosity is reduced for all investigated cement pastes (w/c-ratios) as a result of carbonation. It is also shown that the reduction in porosity increases as the w/c-ratio falls, and that all pore sizes are reduced as a result of carbonation. The water vapour sorption measurements show that the absorption isotherms were always lower for carbonated material than for uncarbonated, i.e. the evaporable water content at a given relative humidity was lower for carbonated material than for uncarbonated material. Calculating the specific surface area by using BET from the sorption isotherms showed a marked reduction in specific surface area as a result of carbonation.

Auberg (OPC, Slag)

Auberg (1998) presents an investigation of precision data for the German CIF- and CDF-test for evaluation of the frost and salt-frost resistance. The influence of material and test

parameters on the results from the freeze/thaw tests was also investigated, including the effect of carbonation. The effect of carbonation on the pore structure measured by MIP and on the freezable water content measured by LTC was investigated. Concrete qualities with only OPC as binder were investigated, as were qualities with cements with different slag contents (36 %, 58 %, and 78 %). The concrete composition, w/b-ratio, air entrainment etc. was not described. Concrete specimens were stored for seven days in water after production. They were thereafter conditioned in two different climates: normal laboratory air and nitrogen gas, for 21 days. Both climates were at 65 % RH and +20 °C. After conditioning, cores (diameter 20 mm) were drilled from the specimens. The cores were subsequently cut, to give a 1 mm thick carbonated sample (the outermost 1 mm of the surface) and a 2 mm thick uncarbonated sample from the inner part of the core. The materials were therefore of the same age, but with different drying histories and possibly also with somewhat different material compositions due to differences between the composition in the surface and core materials. The pore size distribution was measured by MIP. The drying method was not described. Figure 4.11 shows the amount of capillary porosity in the surface layer and in the core material of the different concrete qualities for both conditioning climates.

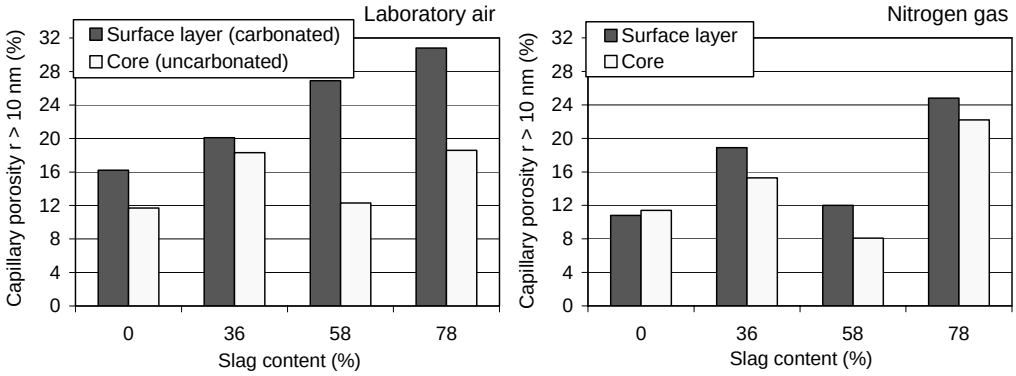

Figure 4.11 *Capillary porosity (r > 10 nm) in the surface layer and in the core material for concrete with different slag contents and conditioned in two different climates. Left: laboratory air (with carbon dioxide). Right: nitrogen gas (without carbon dioxide). Redrawn from Auberg (1998).*

From the figure, it can be seen that for the materials conditioned in laboratory air, i.e. where the surface layer is carbonated, the capillary porosity increases as a result of carbonation for all concrete qualities. However, the increase in capillary porosity is more significant for the concretes containing 58 % slag or more. The increase in capillary porosity can partly be explained by the difference in material properties between the material in the surface layer and the core material. As can be seen in Figure 4.11, the capillary porosity for the materials conditioned in nitrogen gas is somewhat higher in the surface layer than in the core material, at least for the concretes containing slag as part of the binder. The results presented in Auberg (1998) thus show that for concretes with OPC as binder, and concrete with 58 % and 78 % slag as part of the binder, carbonation leads to

a significant increase in capillary porosity. However, for concrete with 36 % slag as part of the binder, the higher capillary porosity in the surface layer may be because of differences in material properties between the material in the surface layer and in the core material.

The amount of freezable water in the surface layer and in the core material was measured using LTC for the concrete with OPC as binder, and for the concrete qualities with 58 % and 78 % slag as part of the binder. The test samples were comparable to the ones used by the MIP measurement, i.e. a 1 mm thick carbonated sample (the outermost 1 mm of the surface) and a 2 mm thick uncarbonated sample from the inner part of the core. Before LTC measurement, the samples were placed in a 3 % sodium chloride solution for seven days. The heat flow was then measured during cooling and heating from +20 °C to –60 °C. According to Auberg (1998), two freezing peaks could be seen during cooling. The primary freezing peak was seen between –10 °C and –20 °C, and the secondary at temperatures below –40 °C. Figure 4.12 shows the heat of ice formation in the temperature interval –10 °C to –20 °C during freezing, i.e. a measure of how much water that freezes in this temperature interval, for the carbonated and uncarbonated materials.

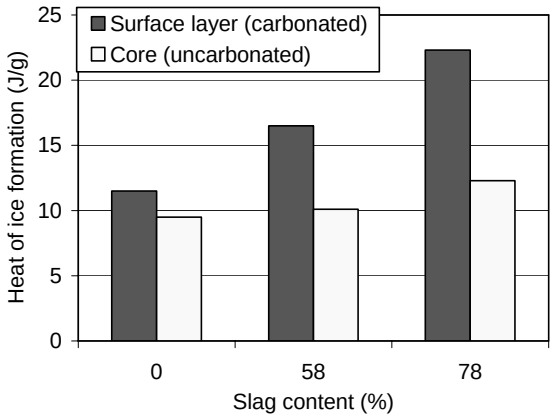

Figure 4.12 *Heat of ice formation (over the temperature interval –10 °C to –20 °C) for carbonated and uncarbonated concrete, with different amounts of slag as part of the binder. Redrawn from Auberg (1998).*

From the figure, it can be seen that the amount of freezable water down to –20 °C increases for all tested concretes as a result of carbonation. However, the increase in the amount of freezable water as a result of carbonation is more significant the higher the slag content. According to Auberg (1998), the increase in freezable water is explained by the increase in capillary porosity caused by carbonation. See Figure 4.11.

4.3.6 The effect of ageing, and in particular of carbonation, on the frost and salt-frost resistance

To some extent, the effect of carbonation on the frost and salt-frost resistance has been investigated for materials with OPC or OPC blended with slag as part of the binder. The results from these investigations are, however, somewhat contradictory, as will be discussed below. Differences in preconditioning and testing procedures as well as in investigated materials also make it sometimes difficult to evaluate the results. Investigations about the effect of carbonation on the salt-frost resistance for material with silica as part of the binder are few.

Bonzel & Siebel (OPC)

Bonzel & Siebel (1977) describe an investigation where two different freeze/thaw test methods were evaluated. The investigation did not evaluate the effect of carbonation as such on the salt-frost resistance but, by conditioning specimens for different times in laboratory air at a constant temperature and relative humidity, the combined effect of ageing factors such as carbonation, drying and age (degree of hydration) can be evaluated.

Concrete of different Ordinary Portland Cements, with and without entrained air and with w/c-ratios between 0.40 and 0.60, was tested. Cement types 'PZ 350 F' and 'PZ 450 F' were used for most concrete qualities. For composition of the clinker phase, see Bonzel & Siebel (1977). The results were about the same regardless of what freeze/thaw method was used. Here only the method called 'Eintauchverfahren' (Immersing procedure) is described.

A number of 100 mm cubes were cast from each concrete quality. One day after casting they were demoulded and placed in water for seven days, and were then conditioned in normal laboratory air at 65 % RH and 20 °C for 48 days. Some extra specimens were conditioned in the laboratory air for one and a half years before freeze/thaw testing started. One day before the freeze/thaw test was started, the specimens were resaturated (immersed) in 3 % sodium chloride solution in containers, each holding two 100 mm cubes. After resaturation, the freezing procedure was started by freezing the containers for 15.5 hours at –15 °C. Thawing was carried out by placing the containers in a water bath at +20 °C for 8.5 hours. Normally 100 freeze/thaw cycles were carried out, and the scaled material was weighed at regular intervals.

The results show that for all concrete qualities, irrespective of w/c-ratio or if the concrete was air-entrained or not, the specimens conditioned for a longer period (1.5 years) showed greater amount of damage than those specimens conditioned for a shorter period (48 days). According to this investigation, the higher degree of carbonation, the more the specimen surface was dried and the older the specimen were at the start of the freeze/thaw test, the poorer was the scaling resistance - at least for the cement types, concrete compositions and freeze/thaw test procedure used in the investigation.

Gunter et al. (OPC, Slag)

Gunter et al. (1987) investigated the effect of curing and type of cement on the salt-frost resistance. Concretes made with OPC and with blast furnace slag cements with different w/b-ratios (0.40 - 0.50) and different air contents were investigated. Concrete specimens were conditioned in climates at +20 °C and 65 % RH and with different carbon dioxide contents (0, 0.03 and 2 vol-% CO_2). Specimens conditioned for 49 days after an initial six days long water curing were freeze/thaw tested using a test method where specimens (100 mm cubes) were stored in saturated NaCl-solution (–15 °C) for eight hours followed by storage in tap water (+20 °C) for 16 hours. The presented results show that, after 70 freeze/thaw cycles, concrete with a w/b-ratio of 0.50 and entrained air (~4.5 %) with OPC as binder shows less damage for the carbonated specimens than for the uncarbonated. The loss in volume (damage) for the carbonated specimens was 7 - 9 vol-%, regardless of carbon dioxide content in the air during conditioning (0.03 or 2 vol-%). The loss in volume for the uncarbonated material was about twice as high, i.e. 16 vol-%. The results were the opposite for concrete with blast furnace slag cement (75 % slag). Uncarbonated concrete showed the least loss in volume (~7 vol-%), whereas the volume loss increased with increasing carbon dioxide content in the air during conditioning, with a volume loss of 15 % if conditioned in 0.03 vol-% CO_2 and a volume loss of almost 30 % if conditioned in 2 vol-% CO_2.

In order to explain this behaviour, the pore structure of cement pastes produced with the two different cement types and with a w/b-ratio of 0.50 was investigated by MIP measurements. The pastes were conditioned in climates with different carbon dioxide concentrations (0.03 vol-% and 2 vol-%). After some time for carbonation, samples were taken from the outer carbonated zone as well as from the inner uncarbonated zone (which means that the uncarbonated and carbonated material does not have the same drying history or the same composition). The samples were dried at +105 °C before MIP measurement was carried out. The results from MIP measurement showed that carbonation of the paste with OPC resulted in a significant reduction of the total porosity as well as a reduction of the coarse porosity. The result was the opposite for cement paste with a high slag content, with a slight increase in total porosity and a significant increase in coarse pores as a result of carbonation. The change in salt-frost resistance as a result of carbonation is explained by the pore structural changes.

Vesikari (OPC, Slag, Silica)

Vesikari (1988) investigated the effect of ageing on the durability of concrete with OPC as well as with slag (30 % - 70 %) and silica (10 %) as part of the binder. The work included determining the salt-frost resistance using a test procedure similar to that used in the investigation presented in Gunter et al. (1987), i.e. specimens (100 mm cubes) were stored in saturated NaCl-solution (–15 °C) for eight hours, followed by storage in tap water (+20 °C) for 16 hours. After seven days in water, concrete with a w/b-ratio of 0.48 and entrained air (~5 %) was conditioned in two different climates:

- ‘reference’ climate - 21 days in normal laboratory air with 70 % RH
- ‘carbonation’ climate - 200 days in normal laboratory air with 70 % RH

An additional conditioning procedure, with repeated wetting and drying, was investigated. These results are, however, not commented on here. It must be noted that, because of the 21 day long conditioning in laboratory air, the 'reference' concrete is not uncarbonated concrete. It must also be noted that there was a significant difference in age at the start of testing: 28 days for the 'reference' concrete, and over 200 days for the 'carbonated' concrete, leading to different drying histories and degrees of hydration at the start of the freeze/thaw test. This means that it is the total effect of ageing that was investigated, and not only the effect of carbonation.

Figure 4.13 shows the volume change after 75 freeze/thaw cycles deduced from the results presented in Vesikari (1988).

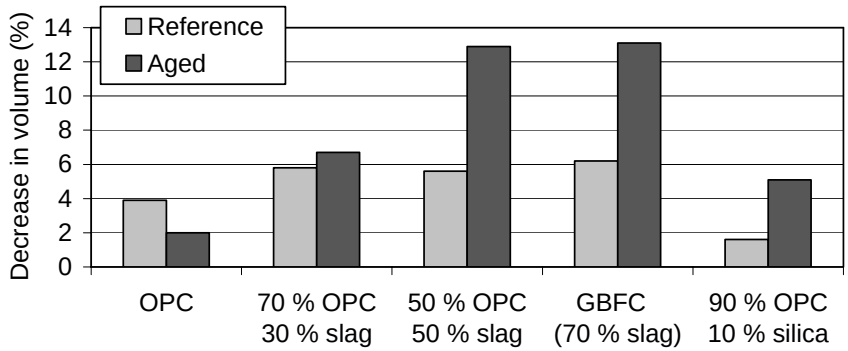

Figure 4.13 *Volume change after 75 freeze/thaw cycles for concrete with a w/b-ratio of 0.48 and entrained air and different binder combinations, conditioned in two ways. Deduced from results presented in Vesikari (1988).*

From the figure it can be seen that for concrete with OPC alone as the binder, the 'carbonated' concrete has a significantly lower amount of damage than the 'reference' concrete. The opposite is found for concrete with slag as part of the binder, i.e. the 'carbonated' concrete shows a markedly greater amount of damage than does the 'reference' concrete. The negative effect of ageing on concrete with slag as part of the binder seems to increase with increasing slag content, at least up to a content of 50 % slag. For concrete with 10 % silica as part of the binder, the effect of ageing is the same as for concrete with high slag content, i.e. ageing leads to increased amount of damage.

Vesikari (1988) explains the seemingly positive effect of ageing for OPC concrete and the negative effect of carbonation for concrete with high slag contents by referring to the pore structural effects of carbonation reported in Gunter et al. (1987). It must, however, be born in mind that the carbonated and uncarbonated materials investigated in Gunter et al. (1987) were of the same age at testing. The age of the materials investigated in Vesikari (1988), on the other hand, were significantly different: 'uncarbonated' tested at an age of 28 days, and 'carbonated' tested at an age of over 200 days. The 'carbonated' materials thus had a higher degree of hydration (higher compressive strength, reduced amount of capillary porosity etc.) at the test start than did the 'uncarbonated' specimens.

For concrete with high slag contents, the results indicate that the amount of damage increases with increased ageing. The higher degree of hydration for the 'carbonated' specimens thus does not seem to improve the scaling resistance, and so the negative effect of ageing can be attributed to carbonation and drying. For concrete with OPC, however, the reduced scaling for the 'carbonated' specimens could be because of the greater degree of hydration as well as an effect of carbonation or drying. The testing procedure used in Vesikari (1988), i.e. testing at significantly different ages and with both materials carbonated (although to different degrees), thus makes it difficult to distinguish and evaluate the relative effects of carbonation, drying and increased degree of hydration on the salt-frost resistance.

Matala (OPC, Slag, Silica, Fly ash)

Matala (1988) reported an investigation of the salt-frost resistance of concrete with OPC as well as with OPC blended with 10 % or 20 % silica, 20 % fly ash respectively 30 % slag as part of the binder. All concrete qualities were produced with entrained air (6 - 7 %) and a w/b-ratio of 0.45. After production, cubes (100 mm) were stored in 95 % RH and +20 °C for seven or 28 days. After this, the specimens were divided in two groups and stored in normal laboratory air with 70 % RH and +20 °C for three weeks (referred to as 'non-carbonated' samples), and for eleven months (referred to as 'carbonated' samples). It must be noted that the 'non-carbonated' material was also subjected to normal laboratory air for three weeks, which probably led to a significant carbonation of the concrete surface. After conditioning, the cubes were immersed in water for seven days. The salt-frost resistance was subsequently determined using a test procedure similar to that used in the investigation described in Gunter et al. (1987) and in Vesikari (1988), i.e. cubes were subjected to freeze/thaw cycles immersed in saturated NaCl-solution (–15 °C) for eight hours, followed by storage in tap water (+20 °C) for 16 hours. The cubes were subjected to over 100 freeze/thaw cycles. It must be noted that the 'non-carbonated' and 'carbonated' specimens were of different ages at the start of the freeze/thaw test. The freeze/thaw test of the 'non-carbonated' specimens was started at an age of between one and one and a half months, whereas the age of the 'carbonated' specimens at the start of testing was about twelve months. It was thus not only the effect of carbonation on the salt-frost resistance that was investigated, but also of other ageing effects, i.e. drying and age (degree of hydration).

The results from the salt-frost resistance test showed that, for concrete with fly ash as part of the binder, ageing led to a slight increase in salt-frost resistance. For concrete with OPC alone as the binder, ageing did not lead to any significant change in salt-frost resistance. However, for the concrete qualities with silica and with slag as part of the binder, the effect of ageing led to a significant decrease in salt-frost resistance.

According to Matala (1988), the cause of the effect of ageing on the salt-frost resistance is the change in total porosity and the change in pore size distribution as a result of carbonation. The pore structural changes due to carbonation on mortar qualities were also investigated and presented in Matala (1988). This is discussed above in Section 4.3.2. For material with fly ash, the significant decrease in total porosity as a result of carbonation is

stated to be the reason for the increase in salt-frost resistance. For material with silica and slag as part of the binder, the decrease in salt-frost resistance as a result of carbonation is stated to be because of the significant coarsening of the pore structure taking place due to carbonation.

In the comprehensive investigation about the effect of carbonation on the pore structure of concrete containing granulated blast furnace slag presented in Matala (1995) and discussed in Section 4.3.2, the effect on the salt-frost resistance was also investigated. Concrete qualities with OPC, and with 50 % or 70 % slag as part of the binder, and with w/b-ratios between 0.35 and 0.75, with and without entrained air, were investigated. The specimens (100 mm cubes) were stored for seven days in 95 % RH and were then divided in two groups: 'non-aged' and 'carbonated'. The non-aged specimens were conditioned for 21 days in normal laboratory air at +20 °C and 45 % RH, whereas the 'carbonated' specimens were conditioned in the same climate for one year before the freeze/thaw test was started. It must be noted that at the start of the freeze/thaw test the drying time and age (degree of hydration) of the specimens varied significantly between the 'non-aged' and the 'carbonated' materials. It must also be noted that the 'non-aged' specimens were able to carbonate during the 21-day conditioning period.

The freeze/thaw test was performed according to a Finnish standard (SFS 5449), which specifies freeze/thaw cycles with freezing in saturated NaCl solution at –15 °C for eight hours and thawing in tap water at +20 °C for 16 hours. Before the freeze/thaw test was started, the specimens were saturated for 21 days in tap water (seven days according to the standard). The scaling results after between 50 and 500 freeze/thaw cycles, depending on concrete quality, showed that for all concrete qualities, including different air contents, w/b-ratios, type of binder and strength, the amount of scaling increased as a result of carbonation and the other ageing effects. This is true both for concrete with OPC alone as the binder and for blends with high contents of slag as part of the binder. A rapid deterioration, i.e. a high rate of scaling, can be seen early during the freeze/thaw test for 'carbonated' concrete with high slag contents as part of the binder. After this rapid scaling, the rate of scaling becomes almost the same as for the 'non-aged' materials. According to Matala (1995), there is a significant correlation between the carbonated volume and the volume of scaling during the rapid deterioration. For concrete with high slag contents it is thus the carbonated material that is scaled off during the initial rapid scaling. After this layer is scaled off, the rate of scaling becomes comparable with the rate of scaling for the 'non-aged' material. This leads to the conclusion that the properties of the material below the carbonated layer are about the same as for the 'non-aged' material which, according to Matala (1995), means that the drying cannot be the primary reason for the increase in deterioration for the aged/carbonated material. According to Matala (1995), the negative effect of ageing on the salt-frost resistance of concrete is the result of the pore structural changes caused by carbonation. These pore structural changes are further discussed in Section 4.3.2.

Besides the explanation that it is the pore structural changes due to carbonation that lead to the decrease in salt-frost resistance, Matala (1995) does not exclude the possibility of a

chemical degradation process working in parallel with the physical. It is, for example, reported in Matala (1995) that there is a clear difference in the morphologies of calcium carbonates formed in OPC and those formed in slag concretes. Carbonation of slag concrete was found to lead to higher amounts of poorly crystallized vaterite than did carbonation of OPC concrete. The possibility of a chemical cause for the rapid deterioration of the carbonated layer of concrete with high slag contents was further discussed in Matala (1997). The changes in composition of carbonates were investigated using different techniques TG + EGA (Thermogravimetry + Evolved Gas Analysis), IR (Infra-red spectroscopy) and XRD (X-ray diffractometry). These analyses showed a clear difference between the calcium carbonates formed in OPC concretes and concretes containing large contents of slag as part of the binder. Concrete with high slag contents produced higher amounts of 'poorly' crystallized vaterite and aragonite. According to Matala (1997) this "*may be one reason for the rapid frost-salt scaling in carbonated GBFS* (Granulated Blast Furnace Slag) *concretes, since these polyforms are observed to be quite soluble in chlorine solutions*".

Matala (1998) describes an investigation into the effect of ageing on the salt-frost resistance of concrete containing silica as part of the binder. Concrete with and without air entrainment, with w/b-ratios of between 0.35 and 0.75, made with OPC and with additions of 5 and 10 % silica in the binder content, was tested. For each concrete quality, a number of 100 mm cubes were produced. The cubes were stored for seven days in 95 % RH and were thereafter divided in two groups: 'non-aged' and 'carbonated'. The 'non-aged' specimens were subsequently stored in laboratory air with 45 % RH for 21 days, and the 'carbonated' specimens in the same climate for about twelve months before the test was started. It must be noted that the 'non-aged' specimens were exposed to normal laboratory air for 21 days and thus were probably significantly carbonated on the surfaces.

The freeze/thaw test was performed according to the same Finnish freeze/thaw method as was used in Matala (1995), i.e. freeze/thaw cycles with freezing in saturated NaCl solution at –15 °C for eight hours and thawing in tap water at +20 °C for 16 hours. Before the freeze/thaw test was started, the specimens were saturated for seven days in tap water. The results after 200 - 400 freeze/thaw cycles showed that for all concrete qualities, i.e. with different air contents, w/b-ratios, silica fume addition and strength, the amount of scaling was higher for the 'carbonated' materials than for the 'non-aged'. That is, ageing leads to a decrease of the scaling resistance for the tested concrete qualities, whether made with OPC alone or with 5 % or 10 % silica as part of the binder. According to Matala (1998), the explanation for the negative effect of ageing on the salt-frost resistance is the observed coarsening of the pore structure and the increase in freezable water content above –20 °C in the carbonated zone.

The effect on the pore structure was further investigated on mortars and is discussed in Section 4.3.2. It must be noted that, as has been mentioned above, there were significant differences in the preconditioning procedures between the 'carbonated' and the 'non-aged' materials. This led to marked differences in age, degree of drying and degree of carbonation between the materials at the time of testing. These differences may have led to pore

structural changes other than those caused by carbonation, changes that might have affected the salt-frost resistance.

A negative effect of drying has previously been reported for cement paste by Sellevold & Bager (1985) and Bager & Sellevold (1986:2). These authors showed by low-temperature calorimeter measurements that, for cement paste with OPC and with w/b-ratios between 0.40 and 0.60, even a mild drying followed by a resaturation period results in a significant increase in freezable water content. According to them, the explanation for the increase in freezable water content as a result of drying and resaturation is that the drying increases the continuity of the pore system. An increased continuity as result of an opening of pore 'necks' would lead to the ice front passing through the opened pores at higher temperatures, i.e. a greater amount of the pore water would freeze at higher temperatures than would be the case for a never-dried paste. These effects of drying may be one explanation for the negative effect on the salt-frost resistance found for material with OPC as the binder, and with and without small amounts of silica as part of the binder, conditioned for long times in an environment with 45 % RH, reported in Matala (1998).

Virtanen (OPC, Slag, Silica)

Virtanen (1989) reports a field investigation of the effect of ageing on the salt-frost resistance of concrete. At an age of seven years, cores were drilled out of two concrete roads: one road made of concrete with OPC as binder and one road made of concrete with OPC and 60 % slag as the binder. Both concrete qualities were air-entrained (3.2 - 3.4 %) and with a w/b-ratio of 0.42. Three drilled cores with a diameter of 100 mm, per concrete quality were freeze/thaw tested using a test procedure similar to that used in the investigation described in Gunter et al. (1987) and Vesikari (1988), i.e. specimens were stored in saturated NaCl-solution at –15 °C for eight hours, followed by storage in tap water at +20 °C for 16 hours. The length of the cores used for freeze/thaw testing was not given. Measurement of the depth of carbonation showed a significantly smaller depth of carbonation for the slag concrete (max. 5 mm) than for OPC concrete (max. 15 mm). The results from the freeze/thaw test showed that the concrete with OPC alone as the binder showed a significantly greater amount of damage than the concrete containing 60 % slag as binder. After 100 freeze/thaw cycles, the volume loss for the slag concrete was less than 5 vol-%, whereas for the OPC concrete the volume loss was almost 40 vol-%. The damage was reported to be most intense on the cut surfaces of the cylinders, whereas the upper surfaces (the carbonated surfaces) were less damaged. Virtanen (1989) explained this by the fact that drilling out the cores led to micro-cracking on the cut surfaces, which in turn led to higher scaling.

Virtanen (1989) also describes a field investigation of concrete containing about 7 % of silica as part of the binder. Results from freeze/thaw testing of drilled cores after five years of exposure showed about the same damage as when the same concrete was freeze/thaw tested in an unaged condition a short time after production. For the aged concrete with silica as part of the binder, the amount of damage was also reported to be highest at the cut surfaces, which Virtanen (1989) explained by induced micro-cracking during drilling.

The conclusion drawn in Virtanen (1989) is that 'ageing' of concrete containing silica or high contents of slag does not influence the concrete's salt-frost resistance. It must, however, be noted that the drilled out and freeze/thaw tested cores were carbonated only on one surface. (Assuming a core length of 100 mm, the carbonated part constituted less than 20 % of the total test surface.) It is thus primarily the salt-frost resistance of well-hydrated but uncarbonated materials that was tested. As was mentioned above, it was reported that there were significant differences in the amount of damage on the different surfaces. The carbonated top surface was significantly less damaged than the uncarbonated cut (drilled) surfaces. If we disregard the hypothesis in Virtanen (1989) that the possible micro-cracks caused during drilling were the explanation for the higher scaling for the cut surfaces, it can instead be concluded that carbonation significantly improves the scaling resistance.

The results for concrete containing large contents of slag as part of the binder are somewhat contradictory to those that have been observed in other investigations. Here, the carbonated layer was reported to be less damaged than the cut surfaces. On the other hand, other investigations of carbonation of concrete containing high slag contents have been reported to lead to a significant reduction of scaling resistance. It must, however, be noted that the in Virtanen (1989) reported carbonated layer for the slag concrete is very thin. Normally, the rate of carbonation of concrete containing high slag contents is reported to be higher than that of a comparable concrete quality with only OPC as binder. This would, after seven years' exposure, lead to a significantly greater carbonation depth for the slag concrete than for OPC concrete. This is, however, not the case. The reported carbonation depth of the drilled-out cores was significantly smaller for the slag concrete than for the OPC concrete. A possible explanation for the reported relatively small amount of damage on the carbonated surface of the slag concrete can thus be that, for the slag concrete, a large part of the carbonated layer was already scaled off when the cores were drilled out from the road surface. This could, for example, be due to a slow gradual scaling during repeated freezing and thawing and/or abrasion by traffic or by snow clearance during the winter time during the seven years of exposure. This would leave only a thin carbonated layer, which was also the case. Because of the small carbonation depth for the slag concrete, it was in principal only uncarbonated surfaces that were freeze/thaw tested. The effect of carbonation on the salt-frost resistance of concrete containing high slag contents can thus not be evaluated from the investigations presented in Virtanen (1989).

Soers & Meyskens (OPC, Slag)

Soers & Meyskens (1991) briefly report both field investigations and laboratory investigations of the salt-frost resistance of concrete with OPC and with slag cements as binder. The effect of carbonation on the pore structure was evaluated by means of fluorescence microscopy and the salt-frost resistance was evaluated according to a method, ISO/DIS 4846, which was a draft standard for a freeze/thaw test. The specimen was tested with the test surface facing upwards. A 3 % sodium chloride solution was used as the freezing medium, and the surface was exposed to repeated freezing and thawing cycles.

A concrete road (Highway A17 between Brugge - Kortrijk), with the major part of the road surface made with concrete containing a slag cement with between 35 and 65 % granulated blast furnace slag, was visually inspected. From the visual inspection at an age of eight years it is reported that the concrete surface was damaged and showed "*..different grades of roughness, ...*". A small part of the road was made with concrete with Portland cement as binder. After eight years' exposure, the surface of this concrete was " .. *nearly intact*.", i.e. it showed significantly less damage than the part of the concrete road with slag concrete.

In order to investigate the effect of carbonation on the salt-frost resistance, Soers & Meyskens (1991) reported that cores were produced from a 'road concrete' with slag cement (35 - 65 % slag as part of the binder). Material composition is not described, but a compressive strength of 72 MPa at an age of 28 days indicates a relatively low w/b-ratio. Cores were stored in a saturated CO_2 atmosphere (!) with a relative humidity of between 65 % and 80 % for 9, 16 and 25 days, resulting in different carbonation depths. These cores were subsequently freeze/thaw tested (using $CaCl_2$ as de-icing agent), together with 'uncarbonated' cores. The results showed clearly that the scaling resistance decreased with increased carbonation depth, i.e. the higher the carbonation depth, the more significant was the scaling.

The effect of carbonation was further investigated on 'laboratory concrete' with various cement types, but with the same w/b-ratio. The material composition is unfortunately not described, and nor is the conditioning procedure/climate or what kind of specimens were used. Testing the salt-frost resistance of these concrete qualities shows, according to Soers & Meyskens (1991), among other things that:

- The rate of carbonation increases with the slag content in the binder.
- For all types of concrete with slag cements as binder, carbonation leads to an increase in scaling.
- Concrete with OPC as binder carbonates at a lower rate than does concrete containing slag cement
- For concrete with OPC as binder, the scaling resistance '*...does not seem to be affected by carbonation.*'

The negative effect of carbonation on the scaling resistance for concrete with slag cements containing high contents of slag as part of the binder is, according to Soers & Meyskens (1991), caused by an observed increase in permeability for the carbonated zone.

Hartmann (OPC, Slag)

Hartmann (1993) analyses the German freeze/thaw test CDF-test method, which is described in Setzer (2001), with respect to the effect of material properties and the test procedure on the scaling results. Briefly, testing the scaling resistance of concrete by the CDF procedure is carried out as follows. Specimens with cast test surfaces (against Teflon), are stored in water until an age of seven days and subsequently in laboratory air at

+20 °C and 65 % RH for 21 days. The specimens are then subjected to resaturation by capillary suction for seven days before the freeze/thaw test is started. After capillary suction, the specimens are subjected to 28 freeze/thaw cycles (12 hours per cycle) between +20 °C and –20 °C. During freezing and thawing, the specimens are placed with the test surface downwards in a container with a 3 % NaCl solution as the freezing medium. After a specified number of freeze/thaw cycles, the scaled-off material is collected, dried and weighed. The result after 28 freeze/thaw cycles is expressed as the accumulated scaled material.

The investigation presented in Hartmann (1993) included the effect of the curing time on the amount of scaling. In the investigation a large number of different concrete qualities were tested, most with a w/b-ratio around 0.50, but with different cement types: two different ordinary Portland cements and two different slag cements. However, most concrete qualities were produced with the ordinary Portland cements. A double set of specimens were produced for some concrete qualities (eleven qualities). Most of these concrete qualities were produced with OPC. The first set was tested at an age of around 35 days, which is as specified in the test method. The second set of specimens was treated in the same way, but was conditioned for a longer time before being freeze/thaw tested. Conditioning was carried out in laboratory air at +20 °C and 65 % RH. Depending on concrete quality, the second set of specimens was tested at 86 to 497 days after the first set of specimens was tested, and thus had a higher degree of hydration, a significantly longer drying time and a higher degree of carbonation. According to the results presented in Hartmann (1993), the second set of specimens, i.e. the specimens that had been conditioned for the longest time, showed a significantly higher scaling than the specimens tested at an earlier age. See Figure 4.14.

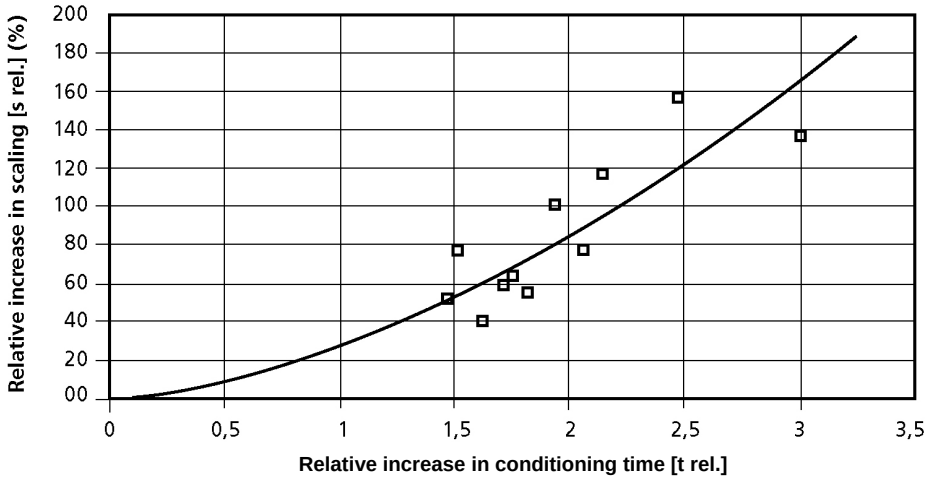

Figure 4.14 *Relative increase in scaling as a function of the age of testing expressed as the relative increase in conditioning time. Specimens were conditioned in laboratory air at +20 °C and 65 % RH.* $t_{rel.}=(t-t_0)/t_0$, $s_{rel.}=100x(s-s_0)/s_0$. *Redrawn from Hartmann (1993).*

From the figure it can be seen that, with an increased conditioning time, there is a tendency for increased scaling. The conclusion presented in Hartmann (1993) is that the ageing effects and primarily carbonation leads to a reduction of the scaling resistance. These results are somewhat contradictory to the results presented in Gunter et al. (1987), where it was shown that carbonation of concrete with OPC leads to a somewhat increased scaling resistance.

Stark & Ludwig (OPC, Slag)

Researchers at the F. A. Finger Institute for Building Materials Science at the University of Architecture and Building in Weimar (Bauhaus-Universität), Germany, have extensively investigated the frost and salt-frost resistance of concrete, primarily with high slag contents as part of the binder. In the following review, it is mainly results presented in Stark & Ludwig (1997:1) that will be discussed. It must, however, be noted that the some of the results presented in Stark & Ludwig (1997:1) were published earlier. For example, some results can be found in Stark & Wicht (1995), and probably also in earlier papers. Here, it is the work presented in Stark & Ludwig (1997:1) that is referred to, since this publication includes the most complete presentation of results.

Stark & Ludwig (1997:1) present results from an investigation of the frost and salt-frost resistance of concrete with slag cements with high binder slag contents. The scaling resistance of a concrete made with slag cement with 60 % slag as part of the binder was tested using the CDF-test, see Setzer (2001). The appearance of the scaling curve showed that the curve could be divided in two phases; an initial scaling phase, where the rate of scaling was high, followed by a phase with a significantly lower rate of scaling. This was the case both for concrete with and without entrained air. It was suspected that the initial rapid scaling was influenced by the carbonation of the concrete surface. This was tested by measuring the depth of carbonation of different blast furnace cement concrete qualities prior to freeze/thaw testing in accordance with the CDF-test. A significant correlation was found by comparing the depth of carbonation with the amount of scaling (expressed as depth of scaling) at the point where the rapid initial scaling phase was ended, i.e. at the 'nick point' in the scaling curve; see Figure 4.15. This shows that for these concrete qualities with high contents of slag as part of the binder, the resistance towards salt-frost scaling was significantly lower in the carbonated surface layer than in the uncarbonated material below this layer.

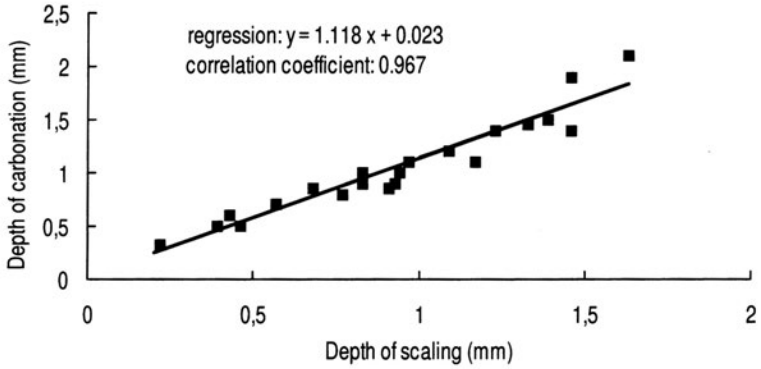

Figure 4.15 *Depth of carbonation as a function of the depth of scaling at the nick point for concrete qualities with various blast furnace slag cements. From Stark (1997), redrawn from Stark & Ludwig (1997:1).*

The influence of carbonation on the salt-frost resistance was further investigated by freeze/thaw testing concrete specimens that had been stored in climates with different carbon dioxide contents prior to test start, (Stark & Ludwig (1997:1)). The concrete used was made with slag cement containing 65 % slag as part of the binder. The w/b-ratio was 0.50 and no air entrainment was used. After seven days of water storage, the specimens were conditioned in three different climates, all with +20 °C and 65 % RH but with different carbon dioxide concentrations. The carbon dioxide concentrations were: 0 (nitrogen gas), ~0,03 vol-% (normal laboratory air) and 3 vol-% (increased). After conditioning in the different climates for 21 days, the specimens were treated and freeze/thaw tested in accordance with the CDF-method. The scaling results showed a significant influence of the conditioning climate, i.e. carbon dioxide concentration in the air, see Figure 4.16.

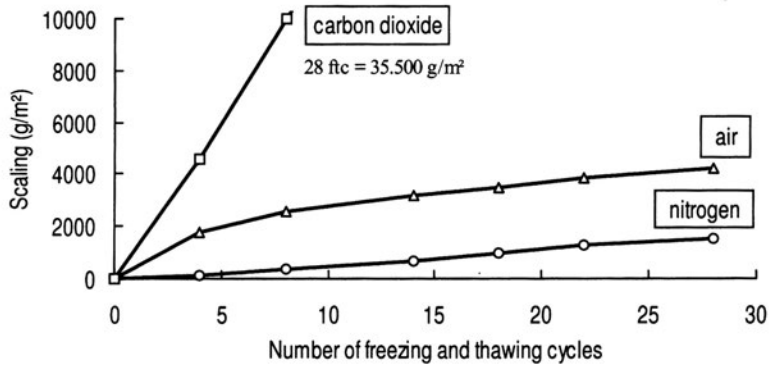

Figure 4.16 *Scaling as a function of the number of freeze/thaw cycles for concrete qualities made with slag cement conditioned in different climates with different carbon dioxide contents. From Stark (1997), redrawn from Stark & Ludwig (1997:1).*

From the figure, it can be seen that the specimens conditioned in the climate with increased carbon dioxide content show the highest scaling, whereas the specimens conditioned in an environment without carbon dioxide (nitrogen gas) show the smallest amount of scaling. The specimens conditioned in normal air show a scaling in between, where two scaling phases can be noticed; a high rate of scaling during the first four to eight freeze/-thaw cycles, followed by a slower scaling rate. The rate of scaling during the second scaling phase is about the same as for the uncarbonated specimens.

The cause of the influence of carbonation on the scaling resistance of concrete made with slag cements was investigated. Some results of microstructural investigations on carbonated and non-carbonated material of mortar qualities made with both OPC and with slag cement as binder are shown in Stark & Ludwig (1997:1). The material properties, the conditioning procedures and the test procedures used are not given. For mortar with slag as part of the binder, the results show a significant decrease in total porosity, although with a redistribution of pore sizes leading to an increase in capillary pores for the carbonated material. For mortar with OPC as the binder, no significant effect of the total porosity could be found, although carbonation led to a small increase in the capillary porosity compared with the uncarbonated material. (It is stated in the paper that carbonation of the mortar with OPC alone as the binder leads to a '*slight reduction of capillary pores*'. The results presented graphically in their Figure 12, however, show the opposite).

The conclusion drawn in Stark & Ludwig (1997:1) about the cause of the increased degradation during salt-frost testing of the carbonated material, compared with the uncarbonated material with high slag contents, was that the increase in capillary porosity caused by carbonation could not be the main cause. This conclusion was based on the finding that, during frost attack without salt, there was no sign of higher scaling in the carbonated zone. This would have been expected according to Stark & Ludwig (1997:1) if the increase in capillary porosity was the main cause of the lower salt-frost resistance of the carbonated layer. It was therefore suggested that the negative effect of carbonation on the salt-frost resistance of concrete containing high contents of slag was because of a chemical effect.

In order to investigate possible chemical effects, phase analyses using X-ray diffraction was carried out on materials made with OPC and on slag cement containing high contents of slag as part of the binder. The results showed that only calcium carbonate in the form of calcite was found in the carbonated OPC material. In the material containing high contents of slag, however, calcium carbonates in the form of aragonite and vaterite were found in addition to calcite. It is suggested that the explanation for this is that when calcium hydroxide carbonates, calcite is formed and when the C-S-H gel carbonates, aragonite and vaterite are formed. Since the calcium hydroxide content is significantly lower in a material containing slag than it is in a material with OPC as the binder, it is suggested that the C-S-H gel in the slag material carbonates to a higher degree than does the C-S-H gel in an OPC material. This would thus lead to more carbonated phases in the form of aragonite and vaterite in the slag material.

Based on the findings of aragonite and vaterite in carbonated material with slag as part of the binder, the hypothesis put forward in Stark & Ludwig (1997:1) was:

> *"The metastable modifications of $CaCO_3$, vaterite and aragonite are dissolved by the combined attack of frost and chloride. This leads to an extensive erosion of the concrete surface. In the deeper carbonated layers, the dissolution of vaterite/aragonite may lead to the new formation of calcite in the microstructure. The change in volume implied may further aggravate the damage initiated by the dissolution process."*

To try to confirm the hypothesis, phase analysis using Scanning Electron Microscope (SEM) and Electron Probe Microanalysis (EPMA) were carried out on carbonated material before and after being subjected to salt-frost cycles. From this investigation it was shown that, before the exposure to salt-frost attack, aragonite and vaterite could be detected in the material containing high slag contents. However, after the salt-frost attack, calcite still was visible but the calcium carbonate modifications, aragonite and vaterite, were almost completely decomposed. This, according to Stark & Ludwig (1997:1), supports the hypothesis of the chemical explanation for the negative effect of carbonation on the salt-frost resistance of concrete containing high contents of slag as part of the binder.

Stark & Ludwig (1997:2) present an investigation of the effect of carbonation on the microstructure of concrete containing different amounts of slag as part of the binder. Carbonated and uncarbonated material of six concrete qualities made with different cement types with different slag contents (0 - 75 %), without air entraining agents and with a w/b-ratio of 0.50 were investigated. The way in which the concrete specimens were carbonated is not described. The carbonated material to be analysed was taken from the 0-2 mm surface layer, and the uncarbonated material was taken from a zone 3 - 20 mm below the surface. This may have resulted in significant differences in material compositions and so also in the material properties, as the material composition in the surface layer (if cast and not cut) may differ significantly from the composition of the 'bulk' material. The capillary porosity of the carbonated and uncarbonated materials was measured, although the method was not described. It is, however, probable that MIP was used. See Figure 4.17.

From the figure, it can be seen that the capillary porosity is somewhat reduced as a result of carbonation for concrete with OPC alone as the binder, or concrete with OPC and a small amount of slag as part of the binder. For concrete with higher slag content, carbonation leads to a significant increase in capillary porosity, with the increase in capillary porosity being higher the higher the slag content.

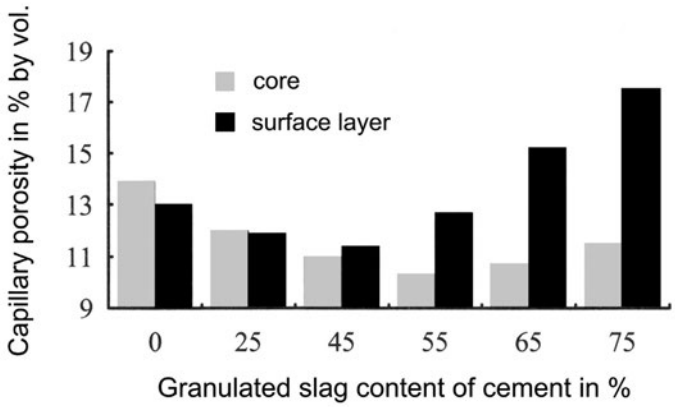

Figure 4.17 *Capillary porosity of the carbonated surface layer and the uncarbonated core material for concrete qualities with different amounts of slag as part of the binder. Note the scale on the y-axis. From Stark & Ludwig (1997:2).*

The increase in capillary porosity for the concrete with high slag contents cannot, according to Stark & Ludwig (1997:2), totally explain the decrease in scaling resistance caused by carbonation. This is based on the findings that the concrete quality with 55 % slag as part of the binder and the OPC concrete have about the same capillary porosity, Figure 4.17, but show totally different scaling behaviours when tested with the CDF method. The slag concrete has about twice the rate of scaling in the surface layer as has the OPC concrete.

Stark & Ludwig (1997:2) present results from freeze/thaw testing of concrete qualities with the same composition as those described above but with entrained air (~5 vol-%). The air void structure was analysed and showed about the same spacing factor regardless of concrete quality. The concrete qualities with high slag contents even showed 'better' air void parameters than for the OPC concrete. The scaling results, however, showed that the higher the slag content, the less positive was the effect of air on the scaling resistance. For concrete with OPC and with entrained air, the scaling was about one-tenth of the scaling for the same concrete quality without air. For concrete with 75 % slag as part of the binder, the scaling of the air-entrained concrete was only about 10 % lower for concrete with entrained air than for concrete with no air entrainment. According to Stark & Ludwig (1997:2), this further indicates that the negative effect of carbonation on the salt-frost resistance for concrete containing high slag contents cannot only be because of a physical effect.

In order further to investigate the possibility of chemical causes for the negative effect of carbonation on the salt frost-resistance, the types of carbonate phases formed during carbonation were analysed for different cement types with different slag contents; see Stark & Ludwig (1997:2). The same cement types as were used in the concretes investigated above were used for producing hydrated cement prisms. All cement pastes had a w/b-ratio of 0.35. After production, the specimens were stored for seven days in water,

followed by conditioning for 21 days in an atmosphere with increased carbon dioxide content (~1 vol-%) and a temperature of +20 °C and RH of 65 %. After conditioning, the carbonated layers of the different pastes were examined by 'radiography' (a method unknown to the present author). Figure 4.18 shows the type of carbonated phases found in the different hydrated cements.

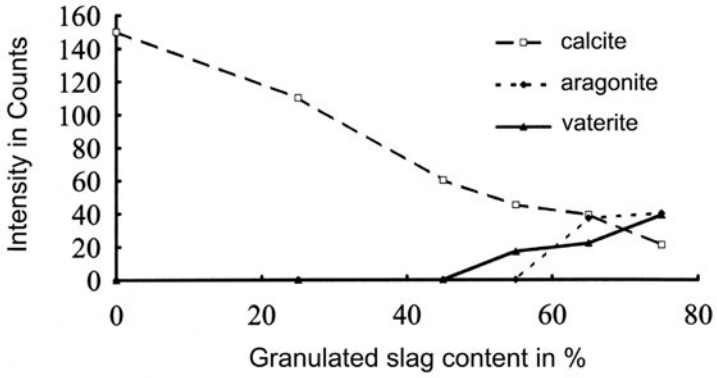

Figure 4.18 *Type and 'amount' of different carbonated phases depending on the slag content of the hydrated cements. From Stark & Ludwig (1997:2).*

From the figure, it can be seen that, for hydrated cements with up to 45 % slag as part of the binder, the only carbonated phase found is calcite. For pastes with higher slag contents, an increasing amount of aragonite and vaterite and a lower content of calcite may be observed.

The hydrated cement prisms were subsequently subjected to salt-frost testing by the CDF test method. After only a few freeze/thaw cycles, the carbonated phases of the surface layer of the hydrated cements with high slag contents were analysed by using X-ray diffraction. The results show that after only a couple of cycles the large proportion of 'metastable' calcium carbonates (vaterite/aragonite) that existed before the freeze/thaw test had transformed into calcite. According to Stark & Ludwig (1997:2) this transformation of the 'metastable' carbonates during salt frost attack to 'badly crystalline' calcite is the reason for the negative effect of carbonation on the salt-frost resistance.

Stark & Ludwig (1997:2) describe how parallel measurements were made using freezing medias (e.g. distilled water, alcohol solutions and urea solutions) other than the normally used 3 % NaCl solution as specified in the CDF-test. It is reported that these measurements confirm that it is the effect of metastable carbonates that leads to the negative effect of carbonation on the salt-frost resistance for concrete containing high slag contents.

Stark (1997) briefly describes an investigation in which the chemical causes of differences in frost and salt-frost resistance of concrete made with OPC were investigated. From investigating the scaling resistance of concrete without air-entrainment by the CDF-

method, it was found that the C_3A content of the cement could not be correlated with the amount of scaling during testing. Other factors, such as the compressive strength, degree of hydration, portion of gel porosity, capillary porosity, total porosity and air void content, were investigated with respect to possible correlation with frost or salt-frost resistance. According to Stark (1997), no significant correlation was found for any of these factors. Stark does not give a description of the procedure in which the correlation between these factors and the frost and salt-frost resistance was investigated. The question of whether phase transformations of carbonate phases take place during frost and salt-frost attack and whether these transformations influence the durability of the material, was raised. Analyses of the formation of ettringite during salt-frost attack using x-ray diffraction found a correlation between ettringite formed during salt-frost attack and the amount of scaling. These findings show, according to Stark (1997), that both frost and salt-frost resistance of concrete made with OPC are influenced by phase transformations taking place during frost attack. It was, however, also concluded that "*In contrast to the processes observed for blast furnace cement concrete, in the case of Portland cement concretes with artificial air voids these phase transformations are of minor importance*"

Jacobsen et al. (OPC, Silica)

Jacobsen et al. (1997) described investigation of the effect of different drying regimes prior to testing the salt-frost resistance according to SS 13 72 44. Specimens of different concrete qualities, either with OPC alone or of OPC with small amounts of silica, and all with a w/b-ratio of 0.45, were conditioned for 14 days in different climates. Climates with different relative humidity and temperatures were used to obtain different rates of evaporation (from a free water surface). The evaporation rates ranged from 0 $g/m^2 \cdot h$ (never-dried, 'virgin') to 500 $g/m^2 \cdot h$ (ventilated oven at +40 °C). Additional specimens were conditioned for a period of three months in the field. After conditioning, the specimens were resaturated for 14 days with tap water, after which the water was replaced by 3 % NaCl solution and the freeze/thaw test were started.

Figure 4.19 shows the scaling after seven freeze/thaw cycles as a function of the evaporation rate during conditioning. From the figure, it can be seen that the scaling is high for the never-dried specimens and for those conditioned in climates with high evaporation rates. The scaling is significantly lower for specimens conditioned in climates with intermediate evaporation rates. Jacobsen et al. (1997) explain this positive effect on the scaling resistance of a 'mild' drying by "*... the protective effect of the air voids is activated at mild drying, whereas they seem to be less effective for the virgin specimen, and have practically no effect after tough drying.*".

From the presented results, it can be seen that the adverse effect of high evaporation rate drying on the salt-frost resistance is less pronounced for concrete containing silica than it is for concretes with only OPC as the binder. It can also be seen that the specimens conditioned in the field for three months show about the same scaling as do specimens subjected to a mild drying during conditioning.

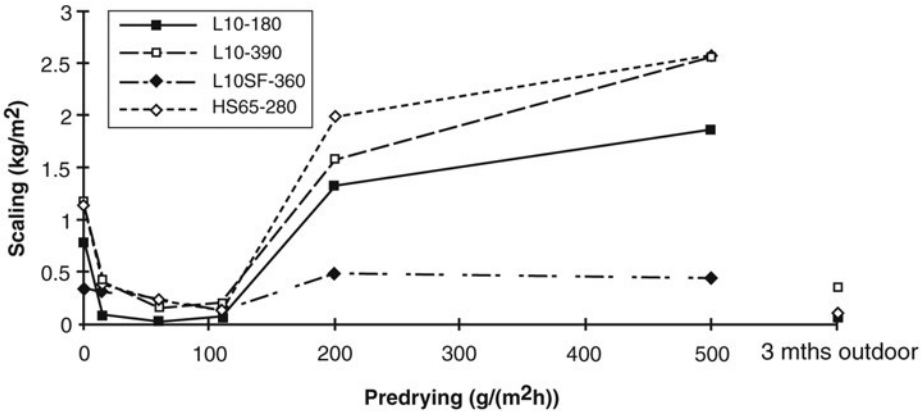

Figure 4.19 *Scaling after seven freeze/thaw cycles as a function of evaporation rate (from a free water surface) of the climate during conditioning for different concrete qualities: three with OPC alone as the binder, and one with OPC + 5 % silica (L10SF-360), all with a w/b-ratio of 0.45. Redrawn from Jacobsen et al. (1997).*

From the experience from the present investigation, the effect of drying described in Jacobsen et al. (1997) can be explained by the effect of carbonation rather than by a change in the protective effect of the air-voids, at least for the 'virgin' concretes and those conditioned in climates with 'mild' drying. This is further discussed in Chapter 12.

Utgenannt & Petersson (OPC, Slag)

Utgenannt & Petersson (1997) present an investigation of the influence of preconditioning on the scaling resistance. The results from this investigation show that, for OPC concrete, a thin carbonated layer that strongly affects the scaling resistance is produced during preconditioning. This carbonated layer strongly increases the scaling resistance of OPC concrete. This investigation is described in full in Chapter 2.

Utgenannt (1999) describes the influence of carbonation on the scaling resistance for OPC concrete. It was shown by testing carbonated and uncarbonated surfaces, conditioned in exactly the same way except for the carbon dioxide in the air, that the thin carbonated surface layer has a significantly higher scaling resistance than the uncarbonated. It was also shown that, for concrete containing high slag contents, the effect of carbonation was the opposite, i.e. carbonation led to a decrease of the scaling resistance. This investigation is described in full in Chapter 3.

Auberg (OPC, Slag)

Auberg (1998) investigated the influence of carbonation on the salt-frost resistance by freeze/thaw testing specimens with cast, carbonated surfaces and specimens with cut, uncarbonated surfaces. The investigation covered two concrete qualities, made with OPC (CEM I) and with a blast furnace slag cement (CEM III/B) respectively. Both concretes

were made with a w/b-ratio of 0.50 and without entrained air. Preconditioning of the specimens was not described. However, the specimens used were probably produced and conditioned in accordance with the CDF procedure, Setzer (2001). The procedure is briefly described above. Here, the carbonated surface layer of some specimens were cut off just before the seven day long resaturation was started, i.e. after the 21 day long conditioning in laboratory air. All specimens, i.e. both with cut and uncut surfaces, were subjected to resaturation before the freeze/thaw test was started. Figure 4.20 shows the accumulated scaling for the tested concrete qualities with cast carbonated surfaces and cut uncarbonated surfaces.

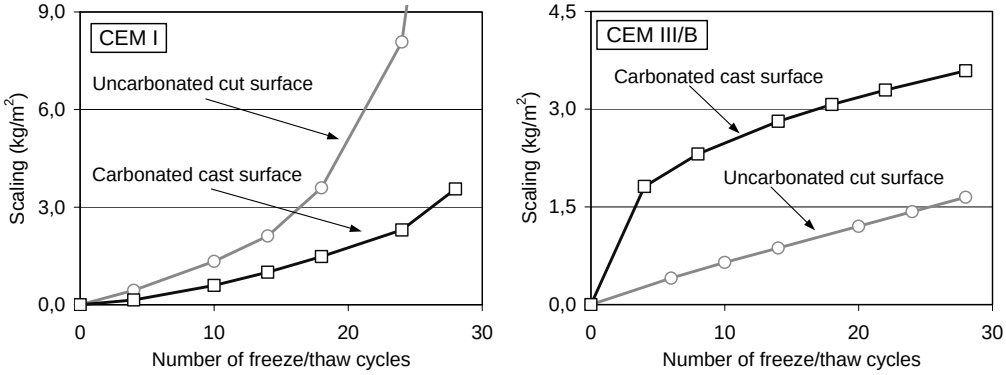

Figure 4.20 *Scaling as a function of the number of freeze/thaw cycles for carbonated (cast) surfaces and uncarbonated (cut) surfaces of two concrete qualities. Left: concrete with CEM I. Right: concrete with CEM III/B. Redrawn from Auberg (1998).*

From the figure it can be seen that, for concrete with CEM I, carbonation leads to an improved scaling resistance or, for this specific concrete quality, to delayed degradation. For concrete with CEM III/B as binder, the effect of carbonation on the scaling resistance is the opposite, with a significant decrease in salt-frost resistance in the carbonated layer.

The test procedure applied in Auberg (1998) for investigating the influence of carbonation on the salt-frost resistance is similar to the procedure used in Utgenannt & Petersson (1997) described in Chapter 2: see Appendix 1. In principle, only the freeze/thaw test methods differ between the investigations. The results found in Auberg (1998) confirm the results presented in Utgenannt & Petersson (1997).

According to Auberg (1998), the primary explanation for the decrease in scaling resistance for the carbonated CEM III/B concrete is the increase in capillary porosity and increase in freezable water as a result of carbonation. The explanation for the increase in scaling resistance in the carbonated layer for CEM I concrete is that the carbonated surface layer is denser and is further strengthened by the formation of stable calcite. It is further explained that the increased scaling rate after the carbonated layer is scaled off is because the uncarbonated material has a higher capillary porosity, which leads to a more rapid

uptake of freezing medium. This conclusion, i.e. that the uncarbonated material of CEM I concrete has a higher capillary porosity than carbonated material, seems somewhat strange since this was not found in the same reference, i.e. in Auberg (1998). On the contrary, the results presented in Auberg (1998) showed a significant increase in capillary porosity for CEM I concrete as well, as a result of carbonation; see Figure 4.11. This also makes the conclusion about the denser carbonated surface somewhat questionable, especially since it was reported that the freezable water content increased as a result of carbonation for CEM I concrete as well. See Figure 4.12.

Auberg (1998) further investigated the ageing effect by freeze thaw/testing of different concrete qualities conditioned until different ages. Concrete made of four different cements, one CEM I, two different CEM III/A and one CEM III/B, were produced. Qualities both with and without entrained air, but all with a w/b-ratio of 0.5, were produced. The concrete specimens for freeze/thaw testing were conditioned as described in the CDF procedure, but the time of conditioning in laboratory air at +20 °C and 65 % RH varied. Some specimens were conditioned as described in the CDF procedure, meaning a test age of 35 days, while others were conditioned for a longer time, to an age of 180 days at start of the freeze/thaw test. This method tests the combined effect of carbonation, drying and age (degree of hydration) on the salt-frost resistance of concrete.

Auberg (1998) states that the results show that, for most tested concrete qualities, the amount of scaling at the end of the freeze/thaw test (28 days) was higher the longer the conditioning time in the laboratory. This was especially evident for the concrete qualities made with CEM III. For concrete with a slag content of over 66 %, the initial high scaling during the first freeze/thaw cycles corresponded to the depth of carbonation, which resulted in a significant increase in initial scaling with conditioning age. For concrete with CEM I, the negative effect of ageing is less apparent, with some qualities even showing an increase in scaling resistance. However, from the about 24 concrete qualities with CEM I that were tested, only five qualities showed signs of an increased scaling resistance. It must be noted that almost all qualities showed a scaling after 28 freeze/thaw cycles of over 1 kg/m^2 and a majority of qualities a scaling of over 2 kg/m^2. Most concrete qualities thus showed relatively poor scaling resistance, and it is therefore difficult from this investigation to evaluate the influence of ageing on the scaling resistance, at least for the concrete qualities with CEM I as binder.

Rönning (OPC, Silica)

Rönning (2001) described investigations of the effect of different curing conditions and the effect of ageing on concrete made from CEM I with (9 %) and without silica as part of the binder, and with and without air entrainment. The w/b ratio for all the concrete qualities was 0.45. Concrete cylinders were subjected to three different curing conditions, and tested at different ages. The curing procedures were (age at test start): *water curing* (56 days), *dry curing*, 50 % RH / +20 °C (56 days) and *cyclic wet and dry curing* (112 days). The effect of ageing was evaluated from testing specimens from concrete cylinders conditioned for a further year in each climate after the initial age at testing.

Ten days prior to the start of testing, specimens were cut from the concrete cylinders for freeze/thaw testing in accordance with Swedish Standard 13 72 44. The specimens were then conditioned as described in the standard, i.e. seven days in 65 % RH / +20 °C, followed by three days' resaturation. It must be noted that the test surfaces of all specimens were conditioned in the same way for the same time, regardless of the curing regime prior to cutting the specimens. It is thus the response of the core material to the boundary conditions for the 100 mm diameter cylinders that was investigated.

To investigate the effect of ageing, specimens were also conditioned for a further year after the initial test. These concrete specimens, too, were cut ten days before the start of the freeze/thaw testing and conditioned as prescribed in SS 13 72 44. The difference in ageing between the initially tested specimens and those produced from the cores after the further year in each climate are: age (degree of hydration) and possible changes in moisture state and other effects on material properties due to the different curing climates. It must be noted that the effect of carbonation was not taken into account in any other way than that the age of the specimens differed significantly (twelve months) when exposed to the seven day-long conditioning prior to freeze/thaw testing.

According to the author, the results presented in Rönning (2001) show that the ageing effect was negative with respect to the salt-frost resistance for concrete without entrained air, but not for concrete with a proper air void system. It was further concluded that the influence of silica fume on the ageing effects were positive in the 'majority' of cases for all curing conditions. Finally, however, Rönning states:

> '*No clear systematic effects of curing conditions and ageing were found. The reasons for the observed, very mixed behaviour between different curing regimes and ageing remain to large extent unexplained.*'

Brandes (OPC, Slag)

A number of investigations into the influence of ageing on frost and salt-frost resistance of concrete are at present in progress. One example is a PhD project, briefly presented in Brandes (2002). In one part of the investigation, concrete is conditioned for different periods before being freeze/thaw tested in accordance with the CDF-procedure, i.e. in a similar way to that in Auberg (1998). Concrete qualities with CEM I and CEM II/B-S, with w/b-ratios of 0.40 and 0.50, and with entrained air, were tested. Specimens were conditioned in laboratory air at +20 °C and 65 % RH until ages of 28 days, three months, six months and twelve months, before being subjected to resaturation and freeze/thaw testing. According to Brandes (2002), all the results show the same trends for all concrete qualities, i.e. the amount of scaling decreases with increasing conditioning time. This is especially apparent during the initial part of the freeze/thaw test, when there is a significant difference in scaling depending on the conditioning time. The scaling during the initial part shows that the scaling resistance of the carbonated layer increases with increasing conditioning time. After the carbonated layer is scaled off, the rate of scaling is about the same irrespective of conditioning time. This corresponds well with the results presented in Utgenannt & Petersson (1997).

4.3.7 Conclusions based on the literature review

The following conclusions can be drawn from the review of the investigations concerning the effect of ageing, and particularly of carbonation, on the pore structure of materials with different types of binder:

- Carbonation of calcium hydroxide and C-S-H gel produces three mineralogical forms of calcium carbonate: calcite, aragonite and vaterite. Aragonite and vaterite are less chemical stable than calcite.
- In principle, carbonation of calcium hydroxide results only in the calcite form of calcium carbonate. Carbonation of C-S-H gel results in the formation of aragonite and vaterite as well as in a porous silica gel and calcite. Calcite is thus the main carbonate phase for OPC concrete. For concrete with additions of secondary cementitious materials, the calcium hydroxide content decreases with increasing amounts of additions. For such concrete qualities, the formation of the other carbonate types, i.e. aragonite and vaterite, increases with increasing amount of addition.
- The reported effects of carbonation on the pore structure for materials with OPC are somewhat contradictory. However, most results indicate that carbonation of materials with OPC leads to a densification of the pore structure with a decrease in total porosity, and that this decrease is due to a reduction of primarily capillary pores.
- The reported effects of carbonation on the pore structure for materials with high slag contents seem to be more consistent. The results found in the literature show that for material with high slag contents, carbonation leads to a decrease in total porosity. However, as opposed to material with OPC alone as the binder, carbonation of material with high contents of slag leads to a coarsening of the pore structure.
- The effect of carbonation on the pore structure of materials containing silica as part of the binder is unclear. The few investigations carried out on materials containing silica indicates a coarsening of the pore structure as a result of carbonation. However, results from these investigations also showed an increase in coarse porosity for material with OPC as the binder as a result of carbonation. This result is contradictory to results presented in several other investigations.

The following conclusions can be drawn from the review of the investigations concerning the effect of ageing, and particularly of carbonation, on the frost and salt-frost resistance of materials with different types of binder:

- In most investigations it is the influence of the <u>combined</u> ageing effects on the salt-frost resistance that are investigated, i.e. the effect of carbonation, drying and age (degree of hydration). The effect of carbonation alone, with all other parameters kept constant, is studied in only a few investigations. In some investigations there are, apart from differences in ageing, significant differences in material composition/properties between aged and non-aged specimens. This is because, in some

cases, aged specimens have been taken from a cast concrete surface, whereas the non-aged specimens have been cut from the core material.

- For concrete with OPC as binder, the effect of ageing on the salt-frost resistance is unclear. Reports of both positive and negative effect of ageing on the salt-frost resistance can be found in the literature.
- For concrete with high slag contents as part of the binder, most investigations show a significant decrease in salt-frost resistance as a result of ageing. This decrease in salt-frost resistance is attributed to the carbonated surface layer.
- The well-documented negative effect of ageing on the salt-frost resistance of concrete containing high slag contents is explained by either a physical or a chemical effect, or a combination of both. The physical explanation is a coarsening of the pore structure resulting in an increase in capillary porosity and an increase in freezable water content as a result of carbonation. The chemical explanation is that the products formed by carbonation in a concrete containing high slag contents consists to a large degree of metastable carbonates, i.e. aragonite and vaterite. During salt-frost attack, these metastable carbonates decompose, which leads to the observed decrease in salt-frost resistance.
- For concrete containing silica as part of the binder, only few investigations into the effects of ageing on the salt-frost resistance have been carried out. Most of these investigations indicate that ageing has a negative effect on the salt-frost resistance for the tested concrete qualities.

From the literature review, it can be seen that there are some significant differences and contradictory results that need to be investigated. The questions to be answered are:

1. What influence has *carbonation* on the salt-frost resistance? In most investigations discussed above, it is the combined effect of many ageing effects that are studied, and not just those of carbonation alone.
2. How does carbonation influence the salt-frost resistance of materials with different binder combinations? Primarily the effect on material with OPC and OPC with some silica as part of the binder, but also for concrete with high slag contents.
3. How do the material properties affecting the salt-frost resistance change as a result of carbonation?
4. What effect is the most dominant; the physical or the chemical, with respect to the effect of carbonation on the salt-frost resistance for materials containing high slag contents?

An attempt has been made in this thesis to answer the three first questions. Questions 1 and 2 are addressed In Chapters 2 and 3 of this thesis, and Question 3 is addressed in Chapters 5 to 9. The chemical effects of carbonation on the salt-frost resistance are only briefly investigated; see Chapter 10. A more comprehensive investigation into the possible chemical effects of carbonation on durability aspects such as the salt-frost resistance is required in order to be able to answer the fourth question. However, it is not an aim of the present investigation further to investigate the possible chemical effects.

5 Laboratory studies of the influence of carbonation on factors influencing salt-frost resistance - General structure of the test programme

5.1 Introduction

Previous investigations, and the experimental work presented in Chapters 2 and 3 of this thesis, have shown carbonation of the concrete surface to have a marked effect on the salt-frost resistance of materials containing OPC alone or OPC blended with secondary cementitious materials. Some explanations for this effect of carbonation have been discussed in Chapter 4. However, there is still a lack of knowledge of a more complete explanation for the effect of carbonation. This investigation studies the effect of carbonation on some factors influencing the salt-frost resistance of concrete.

5.2 Overview of the studies

The effect of carbonation on the following factors is investigated:

- capillary suction and long-time water absorption (Chapter 6)
- critical degree of saturation and salt-frost resistance (Chapter 7)
- freezable water content (Chapter 8).

This chapter describes the materials, specimens and preconditioning of the specimens for the materials used. All investigations studied mortar qualities with OPC and with different amounts of slag and silica.

The effect of carbonation was investigated by conditioning specimens of the different mortar qualities in two climates that differed only in respect of their carbon dioxide content. Both climates had a relative humidity of 65 % RH and a temperature of +20 °C: one with an elevated carbon dioxide content of ~1 vol-%, and one without carbon dioxide, i.e. filtered air. Specimens were stored in these climates until their weights changed only slightly over time, indicating that the materials were in equilibrium with 65 % RH and, for the carbonated material, that carbonation was more or less complete. All specimens were conditioned for at least twelve months before specimens were used in the above investigations. Conditioning was carried out in the climate chambers descried in Chapter 3.

To check the validity of using an elevated carbon dioxide concentration of 1 vol-% for carbonation, some measurements were also carried out on specimens conditioned in normal laboratory air, i.e. 65 % RH / +20 °C with 0.03-0.04 vol-% carbon dioxide. Results from these complementary investigations are given in Chapter 9.

5.3 Materials, specimens and conditioning

Material composition

Eleven mortar qualities were used, with compositions as shown in Table 5.1. The aggregate was naturally graded granitic material of different gradings. The gradings used were: 0.125/0.25 mm, 0.25/0.5 mm and 0.5/1.0 mm. All mortar qualities were produced without any addition of admixtures, such as plasticisers or air-entraining agents. The OPC used was a low-alkali, sulphate-resistant cement and the secondary cementitious materials used were ground blast furnace slag and silica slurry; for chemical analysis, see Appendix 4.

Table 5.1 *Mix composition of mortar qualities used in the investigations described in Chapters 6 to 9.*

Mortar quality	SCM[1)]	w/b-ratio	Eqv. w/c-ratio[2)]	Binder (kg/m^3) Cement	SCM	Aggregate (kg/m^3) size in mm 0.125/0.25	0.25/0.50	0.50/1.00
OPC-35	-	0.35	0.35	994.8	-	298.3	298,3	298.3
OPC-45	-	0.45	0.45	699.9	-	413.4	413.4	413.4
OPC-55	-	0.55	0.55	576.9	-	447.0	447.0	447.0
OPC + 35 % sl-45	35 % slag	0.45	0.52	452.6	243.6	411.2	411.2	411.2
OPC + 65 % sl-35	65 % slag	0.35	0.47	343.1	637.3	294.2	294.2	294.2
OPC + 65 % sl-45	65 % slag	0.45	0.61	242.5	450.4	409.3	409.3	409.3
OPC + 65 % sl-55	65 % slag	0.55	0.74	200.2	371.8	443.3	443.3	443.3
OPC + 5 % si-35	5 % silica	0.35	0.33	939.2	49.4	296.6	296.6	296.6
OPC + 5 % si-45	5 % silica	0.45	0.43	662.2	34.9	411.8	411.8	411.8
OPC + 5 % si-55	5 % silica	0.55	0.52	546.2	28.7	445.5	445.5	445.5
OPC + 10 % si-45	10 % silica	0.45	0.41	624.9	69.4	410.2	410.2	410.2

[1)] SCM= Secondary Cementitious Materials, i.e. slag or silica, given as % dry material by binder weight.

[2)] Eqv. w/c-ratio= water/(cement + 2·silica + 0.6·slag).

Other investigations have often used plain cement paste for studying different material properties. Plain pastes can be an acceptable alternative if they are correctly mixed and cast in such a way as to produce a homogenous paste without cracks and without separation. However, the difficulty in producing homogeneous non-separating pastes, especially pastes with high water/binder-ratios, resulted in using mortar in this investigation. Another reason for using mortar was because the aggregate, particularly the fine fractions, influences the properties of the paste to a great extent; see, for example, the investigation by Winslow & Cohen et al. (1994) showing that concrete and mortar have a pore size distribution different than that of pastes without aggregate.

The aim with the chosen mortar mixes was to produce materials similar to the paste-sand matrix found in normal concrete. When producing the mortars, it was also important to obtain consistencies that were workable and yet not of too low a viscosity that might have resulted in separation during setting. The reason for not using aggregate larger than 1 mm

was primarily to be able to produce thin specimens (minimum thickness ~3 times the largest aggregate size).

A useful parameter describing the paste-sand matrix is the ratio between the surface area of the aggregate and the volume of binder paste. This ratio is a measure of how large a volume of interfacial transition zones (ITZ) there might exist in a material. The ITZ is important because of the differences in material properties such as porosity, reaction products etc. found in the binder paste close to the aggregate surface in comparison with the properties in the 'bulk' binder paste (Scrivener & Gartner (1987)). As an example, assuming a thickness of about 10 μm for the transition zone, and a perfectly even distribution of the aggregate in the binder paste, a ratio between the aggregate surface area and the binder paste volume of 20 mm^2/mm^3 (aggregate surface area/binder paste volume) would result in 20 % of the volume of binder paste being in the ITZ. Of course, in a real concrete the distribution of particles is not perfect, reducing the volume of ITZ in the paste. However, the above example indicates the potentially great influence the properties of ITZ might have on the global material properties.

Table 5.2 show the ratios of the aggregate surface area to the volume of the binder-paste (cement + SCM + water), i.e. A_{agg}/V_{paste}-ratio, for the materials used in this investigation, in the freeze/thaw investigation described in Chapter 3, and for representative normal concretes. When the specific surface is calculated, approximate mean values for different aggregate fractions are assumed on the basis of measurements presented in Shacklock & Walker (1958). Appendix 7 gives an example calculating the A_{agg}/V_{paste}-ratio for mortar, micro-concrete and normal concrete with w/b-ratio of 0.45.

Table 5.2 *Ratio of the surface area of the aggregate to the binder-paste volume, A_{agg}/V_{paste}-ratio (mm^2/mm^3)*

w/b-ratio	Mortar	Micro-concrete	Normal concrete
0.35	9.0	12.1	14.0
0.45	15.4	16.9	14.2
0.55	18.0	19.2	15.2

It can be seen from the ratio between aggregate surface area and binder-paste volume in Table 5.2 that, for mixes with w/b-ratio of 0.45 and 0.55, the A_{agg}/V_{paste} ratio for mortar and for micro-concrete correspond fairly well with the ratio obtained for normal concrete. This is also true for micro-concrete versus normal concrete with a w/b-ratio of 0.35. However, for mortar with a w/b-ratio of 0.35, the A_{agg}/V_{paste} ratio is significantly lower than for normal concrete. This implies that mortar with a w/b-ratio of 0.35 has a proportionally larger volume of binder paste than has concrete with the same w/b-ratio and thus a lower ITZ volume. The reason for choosing the actual mix composition for the mortar with a w/b-ratio of 0.35 was because of the consistency. With a lower amount of binder paste, the mix was not sufficiently workable, which would probably have led to a less homogeneous mortar. Since, in this investigation, a material property such as permeability is of great importance, a homogeneous mortar was preferred to a mix identical to normal

concrete. It must be noted that it is primarily the relative change caused by carbonation that is of interest, and not a comparison of different mortar qualities, i.e. even though the composition of the mortar does not fully match that of concrete, the effect of carbonation on each individual mortar can still be evaluated.

Air void analysis

An air void analysis has been carried out for all mortar qualities studied in this investigation; see Table 5.3. The analysis determined the total air void content and the content of air voids below 2 mm and 0.35 mm. From this, the specific surface and spacing factor were calculated. The air void analysis was carried out by image analysis of thin sections in accordance with NT BUILD 381 (1991). In no case was the size of the thin sections smaller than $30 \cdot 60$ mm^2, giving an area of 1800 mm^2. The analysis, using an optical microscope, was carried out automatically, analysing about 180 images (4 mm^2) evenly distributed across the whole thin section area.

Table 5.3 *Air void analysis. Each value is the result from one measurement.*

Mortar quality	Air content (vol-%)			Specific surface (mm^{-1})	Spacing factor (mm)
	Total	Voids < 2 mm	<0.35 mm		
OPC-35	0.6	0.6	0.1	14	1.3
OPC-45	1.0	1.0	0.2	14	0.97
OPC-55	1.7	1.7	0.6	18	0.61
OPC + 35 % sl-45	1.9	1.9	1.3	33	0.31
OPC + 65 % sl-35	1.6	1.6	1.3	35	0.35
OPC + 65 % sl-45	1.9	1.9	1.5	36	0.29
OPC + 65 % sl-55	2.6	2.2	1.5	34	0.28
OPC + 5 % si-35	0.9	0.9	0.3	17	0.90
OPC + 5 % si-45	1.3	1.3	0.5	17	0.70
OPC + 5 % si-55	0.8	0.8	0.8	34	0.43
OPC + 10 % si-45	1.7	1.7	0.9	21	0.53

Mixing and specimen production

Two mix batches of about 1.2 litres were produced for each mortar quality in this investigation, using a 5-litre mortar mixer from Toni Technik (as specified in EN 196). Mixing was carried out as follows:

- All dry materials were mixed for 30 seconds.
- Water was added for 30 seconds.
- Slow mixing (140 rpm) for 60 seconds.
- Stop for 45 seconds. Any unmixed material from the edge and bottom of the bowl was scraped into the rest of the material by hand.
- Slow mixing (140 rpm) for 60 seconds.
- Rapid mixing (285 rpm) for 30 seconds.
- Finally slow mixing (140 rpm) for 30 seconds.

Directly after mixing, the mortar was cast in moulds made of cylindrical plastic bottles, with inner diameter of 74 mm, and with a volume of 0.5 litre. During casting, the bottles were filled at three intervals with ten seconds compaction between the fillings. A vibrating table (frequency 50-60 Hz, amplitude ± 0.5 mm) was used for compaction. After the last compaction, the bottle was checked to make sure that it was totally filled before the lid was screwed on to the bottle. After casting was finished, the bottles were mounted on a rotating wheel where they were rotated at 3-4 rpm during the first 24 hours. This slow rotation was carried out to prevent separation.

The homogeneity of the mortar, as a result of the above casting procedure, was checked by cutting some hardened test mixes in pieces and thereafter measuring the densities. The measured densities showed very little spread, which indicates a homogeneous material.

After 14 days in the moulds, the 'mortar bottles' were stripped and immediately cut into thin discs, of thicknesses 3, 5 and 10 mm, by using a diamond saw (Logitech CS 10). About 45 discs, each of thickness 3 and 5 mm, and three 10 mm thick discs, were produced from each mortar quality. Four drilled specimens, 14 mm diameter and 100 mm long, were also produced from each quality. Directly after sawing, each disc was quickly cleaned with a brush under water, after which they were separately placed in plastic bags. To minimise the exposure of the specimens to air, and thus preventing them from carbonating, this procedure was carried out as quickly as possible. To keep carbonation to a minimum, the specimens were also kept wet at all times during the short air exposures. An estimation of the longest time a wet specimen was exposed to air is 1-2 minutes.

Conditioning

After all specimens had been cut and put in plastic bags, they were randomly divided into three groups and placed in three different conditioning climates:

1. A climate chamber with a relative humidity of 65 %, a temperature of +20 °C and an increased carbon dioxide content of ~1 volume-%.
2. A climate chamber with a relative humidity of 65 %, a temperature of +20 °C and no carbon dioxide. Air filtered with CO_2 absorbent.
3. A climate-controlled area with normal air and with a relative humidity of 65 % and a temperature of +20 °C. Carbon dioxide content of 0.03-0.04 volume-%.

For a description of the climate chambers used for conditioning the specimens in climates with an elevated carbon dioxide concentration or without carbon dioxide, see Chapter 3.

Once inside the chambers, the specimens were removed from the plastic bags and wiped with a wet cloth, after which the initial weight was measured. Each specimen was thereafter weighed at regular intervals, about six times during the first six months. The specimens were stored standing in racks with about 15 mm between the specimens, enabling all sides of the specimens to dry evenly.

The specimens were stored in their respective climates as long as the weight of the specimens continued to change significantly. When the weight change 'stopped', it indicated that carbonation of the specimens stored in a CO_2-rich climate was completed and that the specimens were in equilibrium with the relative humidity in the air (~65 %). As proof of completed carbonation, the depth of carbonation was checked with phenolphthalein and microscopy. The first measurements on the specimens were started after more than twelve months' conditioning.

Weight change during conditioning

Figure 5.1 shows examples of the weight changes during conditioning in the climate without carbon dioxide and that with increased carbon dioxide. The weight changes are related to the initial specimen weights, i.e. at the first weighing inside the climate chambers. The figure shows the weight change during conditioning for the specimens used in the capillary suction test described in Chapter 6. The example shown in Figure 5.1 is representative of all specimens of the same mortar qualities conditioned in the two climates. Figure 5.2, for comparison, shows the weight change for the specimens used for determination of the critical degree of saturation (Chapter 7). As can be seen, the weight change for these specimens is almost identical with that of the specimens used in the capillary suction test, Figure 5.1. This low scatter between specimens indicates homogenous materials and an 'evenness' of the climate in the climate chambers.

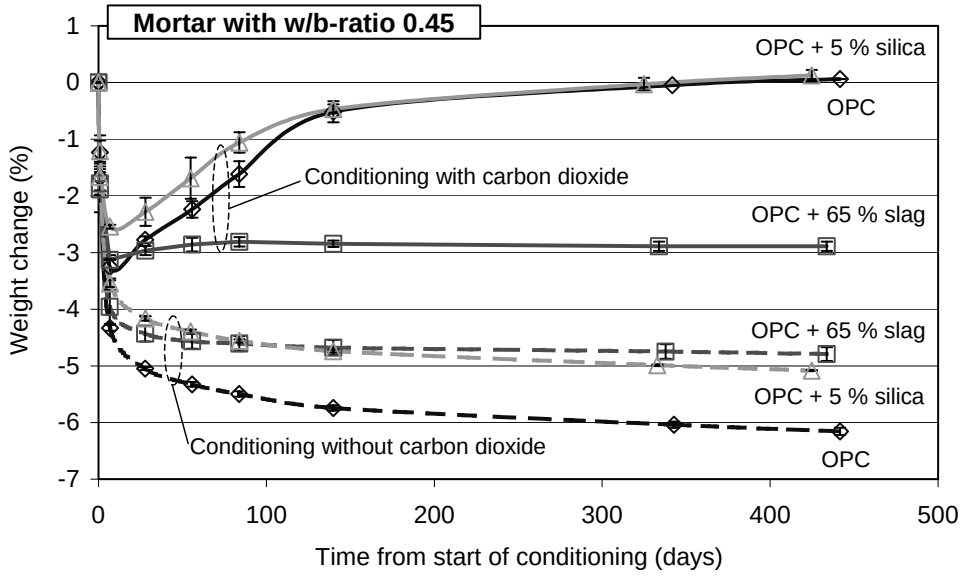

Figure 5.1 *Weight change as a function of time during conditioning in 65 % RH and +20 °C in climates with and without carbon dioxide. Mortar specimens with different binder types/combinations, all with a w/b-ratio of 0.45. Each point is a mean of three specimens. Specimens used in the capillary suction test, Chapter 6.*

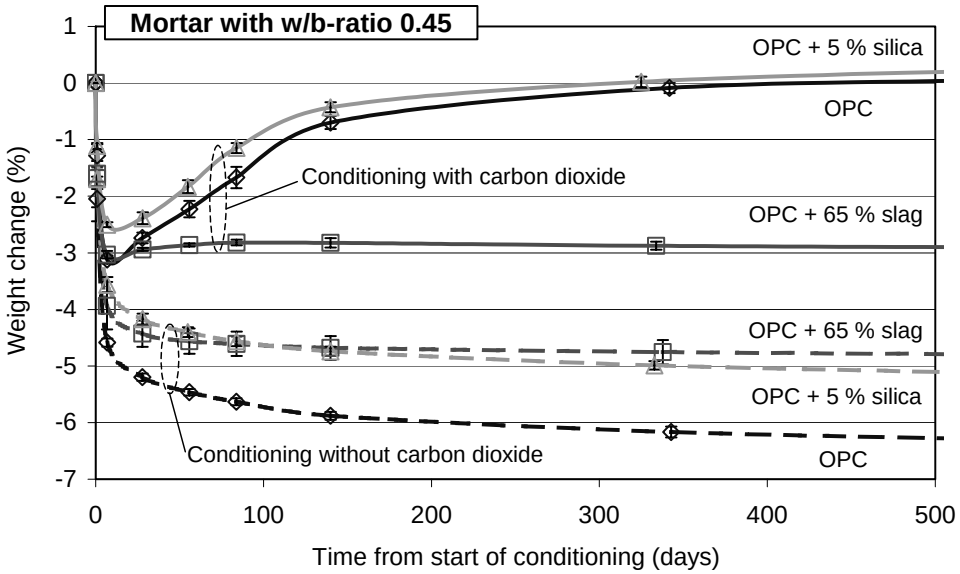

Figure 5.2 *Weight change as a function of time during conditioning at 65 % RH and +20 °C in climates with and without carbon dioxide. Mortar specimens with different binder types/combinations, all with a w/b-ratio of 0.45. Each point is a mean of three specimens. Specimens used for determination of the critical degree of saturation, Chapter 7.*

From both figures, it can be seen that the specimens conditioned in the climate without carbon dioxide lost weight due to drying during the whole preconditioning time; initially very rapidly during the first week, and thereafter at a slower rate. The weight loss is greatest for mortar with only OPC as the binder, and somewhat less for mortar containing slag and silica as part of the binder. For mortar containing slag as part of the binder, the weight loss has almost stopped within the first couple of months, whereas for concrete with only OPC, or with OPC and some silica, the weight loss continues during the whole conditioning time, although at a very slow rate.

For the specimens conditioned in the climate with an increased carbon dioxide content, there is a significant weight loss caused by drying during the first week in the climate chambers. However, the decrease in weight stops, and a significant increase in weight occurs as a result of carbonation, during the continued conditioning. For mortar with plain OPC, and OPC with some silica, there is a significant weight increase during about the first four months, after which the weight increase slows and has almost stopped after about one year's conditioning.

After the rapid initial drying, the weight increase as a result of carbonation for mortars with high slag contents is small, and occurs only for a couple of months. From the figure it can also be seen that the weight of the carbonated specimens containing high contents of slag as part of the binder decreases somewhat during conditioning after the first three

months. This indicates that the material containing slag carbonates much more quickly than do the materials with only OPC, or OPC with some silica as part of the binder. For the latter materials, the weight increase due to carbonation exceeds the weight loss due to drying throughout the conditioning period of more than a year.

6 Studies of the effects of carbonation on capillary suction

6.1 Introduction

One basic and straightforward way of making a rough characterisation of the pore structure of a material is to carry out a capillary suction test. When exposing a material to capillary suction, there will first be an initial period of very rapid water uptake, followed by a period with slow water uptake. Information about the pore structure and resistance to water penetration is provided by the period of rapid water uptake. The period of slow water uptake provides information about the long-time water absorption and at what rate the degree of saturation is increasing.

In principle, the water uptake during the first, rapid part of the capillary suction has no influence on the salt-frost resistance. This is because the period of rapid water uptake in the surface layer will be very short, resulting in the nick point in the water absorption curve - where the initial rapid water uptake changes to the stage of slow water uptake - being reached almost immediately. What is of importance with regard to the frost and salt-frost resistance, however, is the degree of saturation at the nick point and the rate at which the degree of saturation increases during the stage of slow water uptake. Together with information on the total porosity and critical degree of saturation, the results from a capillary suction test give an indication of the length of time for which a material exposed to capillary suction may be frost-resistant if exposed to freezing temperatures, i.e. the time until a critical degree of saturation is reached.

6.2 Test procedure

Carbonated and uncarbonated mortar specimens of eleven mortar qualities with different binder types/combinations were tested. Production and preconditioning of the specimens are described in Chapter 5. The specimens preconditioned in the climates without carbon dioxide and with an increased carbon dioxide content (~1 vol-%) were used for the capillary suction tests. In all cases, the ages of the specimens were over twelve months at the start of the test. Three specimens, all with a thickness of 5 mm, were used for each mortar quality. To protect uncarbonated specimens from unwanted carbonation, the specimens were placed in plastic bags inside the climate chambers (at the end of preconditioning) before they were moved to the climate-controlled area where the capillary suction test was carried out. The capillary suction test was started within ten minutes of removal of the specimens from the climate chambers. Before the start of the tests, the initial weight of the specimens was measured, i.e. at equilibrium with 65 % relative humidity. The reason for not drying the specimens in an oven before the capillary suction test, which is often prescribed in standardised test methods, was because of the possibility that high temperatures might lead to damage in the paste, resulting in absorption results not valid for undried paste.

After measuring the initial weight, each specimen was placed with one side in water in individual plastic Petri dishes. Some grains of sand (fraction 0.5 mm) were placed on the bottom of each dish in order to create a space between the bottom of the dish and the bottom surface of the specimens. Each dish was filled with an amount of pre-boiled tap water (+20 °C) to bring the water 1-2 mm up the sides of the mortar specimens. See Figure 6.1.

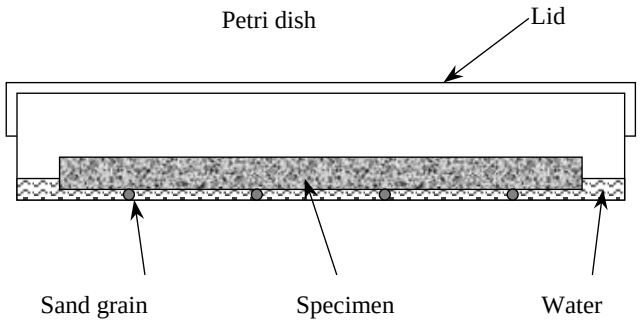

Figure 6.1 *Test set-up for the capillary suction test.*

After the specimens were placed in the dishes, lids were placed on top of the dishes, resulting in a stable climate and a minimum of air exchange between the air inside the dishes and the surrounding air. Besides, evaporation from the top surface of the specimen was avoided.

The weight change of each specimen, i.e. the water uptake, was measured at regular intervals. Initially, measurements were made after short intervals: 4, 9, 16, 25, 49 … etc. minutes, and then less frequently: one measurement per day - one measurement per month. Before each weighing, the specimen was surface-dried with a wet cloth. After weighing, the specimen was immediately put back into the Petri dish. The water level in the dishes was adjusted if necessary by adding water to keep the water level 1-2 mm above the bottom surface of the specimen.

The water absorption test was carried out in a climate-controlled area with 65 % RH and +20 °C. At all times, except during weighing, the dishes containing the specimens were stored in a closed container with a relative humidity close to 100 %.

During the initial stage with rapid water uptake, see Figure 6.2, the absorption was found often to increase almost linearly with the square root of time, which has been shown by Fagerlund (1982), Hall (1989) and others. During the second stage, with slower water uptake, the absorption also increased almost linearly with the square root of time, at least during the first week. The point defined by the intersection of the two lines describing rapid and slow water absorption respectively, is called the nick point of the absorption curve.

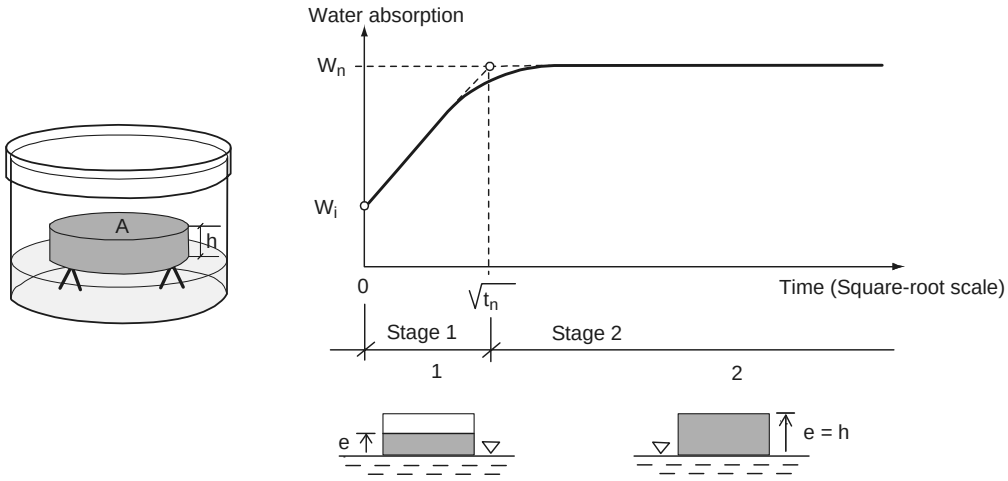

Figure 6.2 *Schematic test set up and example of an absorption curve.*

After 10-12 months' testing, the specimens were used for determining the total porosity. This was done in two alternative ways, using the same specimens:

1. Drying the specimens under vacuum in a desiccator with silica gel and, after reaching an almost steady weight (after two weeks), vacuum-saturating the specimens to give the weight when all open pores were fully saturated.
2. Drying the specimens in a ventilated oven at +105 °C until no more weight loss was registered, giving the dry weight. After cooling in a desiccator, the specimens were vacuum-saturated, to give the weight when all open pores were fully saturated

In both cases, vacuum saturation was carried out in accordance with the test procedure recommendations in RILEM CDC 3 (1994).

With the first procedure, the specimens were dried under vacuum (1-15 mbar, depending on the humidity in the desiccator) for about two weeks in a desiccator with silica gel. During this time, the vacuum treatment was interrupted four times for weighing the specimens and changing the silica gel. Weighing the specimens was carried out in order to register when the weight loss was decreasing and the drying could be stopped. During each of these interruptions, pure nitrogen was used to raise the pressure in the desiccator to atmospheric pressure. Pure nitrogen was chosen instead of normal air to avoid carbonation of the uncarbonated specimens. After drying in the desiccator, the specimens were vacuum-saturated in accordance with the procedure described in RILEM CDC 3, i.e. vacuum treatment (1-3 mbar) for three hours, followed by water saturation for one hour while the vacuum pump was still running, followed by allowing the pressure in the desiccator to rise to atmospheric pressure. The specimens were finally weighed twice, over 24 hours apart, and no significant change in weight were found.

The second procedure was carried out by drying at +105 °C until no further weight loss was registered, followed by vacuum saturation as described above. The specimens used were the same as was used during the first drying procedure described above. The first procedure was supposed not to change the pore structure significantly. However, as the second procedure was likely to cause changes in the pore structure, it was carried out after the first procedure.

Comparing the results from these two procedures showed that, for all materials, the first procedure, i.e. vacuum drying, resulted in the highest weights for the vacuum-saturated specimens, i.e. the greatest total porosity. The increase in weight (%) for vacuum-saturated specimens dried with vacuum *vs*. specimens dried at +105 °C is shown in Table 6.1. The weight increase is related to the evaporable water content when saturated after drying at +105 °C, and calculated according to Equation 6.1:

$$Difference = \frac{Q_{sat:vacuum} - Q_{sat:105}}{Q_{sat:105} - Q_{dry:105}} \cdot 100 \ (\%) \qquad \text{[Eq. 6.1]}$$

where:

$Q_{sat:vacuum}$	is the saturated weight after vacuum-drying	[kg]
$Q_{sat:105}$	is the saturated weight after drying at +105 °C	[kg]
$Q_{dry:105}$	is the dry weight after drying at +105 °C	[kg]

From the calculated difference in saturation presented in Table 6.1, it can be seen that, for all materials, saturation after drying in vacuum results in the highest saturation. For some materials, vacuum-drying leads to more than 10 % higher saturation than does drying at +105 °C. Determining the total porosity after drying at +105 °C thus seems significantly to underestimate the total porosity. One reason for vacuum-drying leading to a higher saturation than does drying at +105 °C is that vacuum-drying is a 'milder' drying technique. When vacuum-drying a material, the water in the smallest pores is not dried out. Drying at +105 °C, on the other hand, results in complete drying of all evaporable water, even in the smallest pores. The difference in saturation after vacuum saturation depending on drying method might be because, if the smallest pores are emptied by drying, they are not again filled using the vacuum saturation method used in this investigation. This results in drying at +105 °C leading to lower saturation than does vacuum-drying. Another reason for the difference in saturation depending on the drying procedure might be because of irreversible changes in the pore structure caused by drying at +105 °C. This has, for example, been reported by Gallé (2001).

Table 6.1 *Increase in saturation (%) when using vacuum-drying compared to drying at +105 °C before vacuum saturation.*

Mortar quality		Increase in saturation (%)
OPC-35	**Uncarbo.**	4.1
	Carbo.	2.4
OPC-45	**Uncarbo.**	4.2
	Carbo.	8.7
OPC-55	**Uncarbo.**	2.4
	Carbo.	2.3
OPC + 35 % sl-45	**Uncarbo.**	5.1
	Carbo.	2.5
OPC + 65 % sl-35	**Uncarbo.**	8.2
	Carbo.	2.8
OPC + 65 % sl-45	**Uncarbo.**	6.9
	Carbo.	1.8
OPC + 65 % sl-55	**Uncarbo.**	5.4
	Carbo.	1.2
OPC + 5 % si-35	**Uncarbo.**	3.7
	Carbo.	4.9
OPC + 5 % si-45	**Uncarbo.**	4.4
	Carbo.	10.9
OPC + 5 % si-55	**Uncarbo.**	4.3
	Carbo.	2.2
OPC + 10 % si-45	**Uncarbo.**	6.7
	Carbo.	10.9

In this investigation, the saturated weights obtained after vacuum-drying have been used for calculations of the total porosity.

The total porosity is calculated according to Equation 6.2:

$$P_{tot} = \frac{V_{p,open}}{V_{tot}} = \frac{\left(Q_{sat:a} - Q_{dry:105}\right)/\rho_w}{\left(Q_{sat:a} - Q_{sat:w}\right)/\rho_w} \cdot 100 \ (\%) \qquad \text{[Eq. 6.2]}$$

where:

$V_{p,open}$	is the pore volume open to water	[m^3]
V_{tot}	is the total volume of the specimen	[m^3]
$Q_{sat:a}$	is the weight in air of a vacuum-saturated specimen	[kg]
$Q_{sat:w}$	is the weight in water of a vacuum-saturated specimen	[kg]
$Q_{dry:105}$	is the weight of a completely dry specimen (+105 °C)	[kg]
ρ_w	is the density of water	[kg/m^3]

The water-filled porosity at the nick point is calculated from Equation 6.2 by substituting the numerator by $Q_n - Q_{dry:105}$, where Q_n is the specimen weight at the nick point.

When presenting the results from the capillary suction test, the absorbed water is expressed as absorbed water in kg/m^2 during the initial stage of the test and as degree of saturation during the long-time water absorption stage. For the initial part, the water absorption at time t is calculated from Equation 6.3:

$$W = \frac{Q_t - Q_{dry:105}}{A_{spec}} \text{ (kg/m}^2\text{)} \qquad \text{[Eq. 6.3]}$$

where:

Q_t	is the weight in air of a capillary suction specimen at time t	[kg]
A_{spec}	is the specimen area	[m^2]

For the long-time water absorption stage, the degree of saturation at time *t*, S_t, is calculated from Equation 6.4:

$$S_t = \frac{Q_t - Q_{dry:105}}{Q_{sat:a} - Q_{dry:105}} \qquad \text{[Eq. 6.4]}$$

6.3 Results

The capillary suction curves for the eleven mortar qualities during the initial part of the capillary suction (from start up to a maximum of ten days) are shown in Figures 6.3 - 6.7. During this stage, the results are presented as water absorption in kg/m^2 as a function of the square root of time (seconds^{½}). In the figures each point is a mean of three specimens.

The capillary suction curves during the long-time water absorption (from about ten days to a maximum of 350 days) are shown in Figures 6.8 - 6.12. During this stage, the results are presented as degree of saturation as a function of time in days. In the figures each point is a mean of three specimens.

Table 6.2 shows the results from measurements of the total open porosity, as well as the calculated amount of porosity that is water-filled at the nick point. The table also shows the dry density calculated from the dry weight (+105 °C) divided by the specimen volume measured after the capillary suction test was concluded. Total porosity and dry density are calculated from measurements on two specimens per material, except those marked in the table, for which results from three specimens have been used.

Appendix 8 provides a complete presentation of the results from capillary suction, presented as water absorption in kg/m^2.

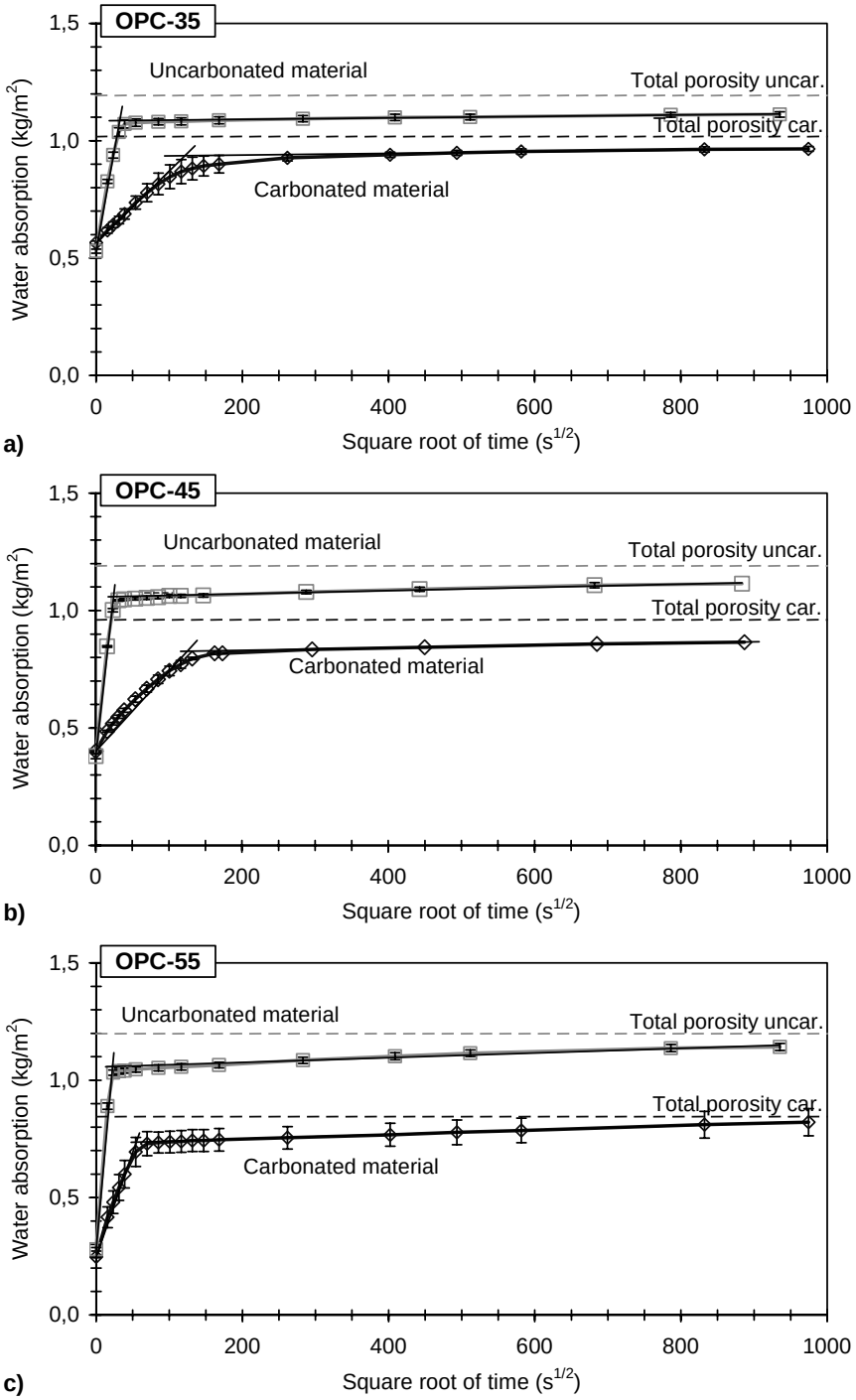

Figure 6.3 *Water absorption as a function of time for mortar with OPC as binder. a) w/b-ratio 0.35, b) w/b-ratio 0.45, c) w/b-ratio 0.55*

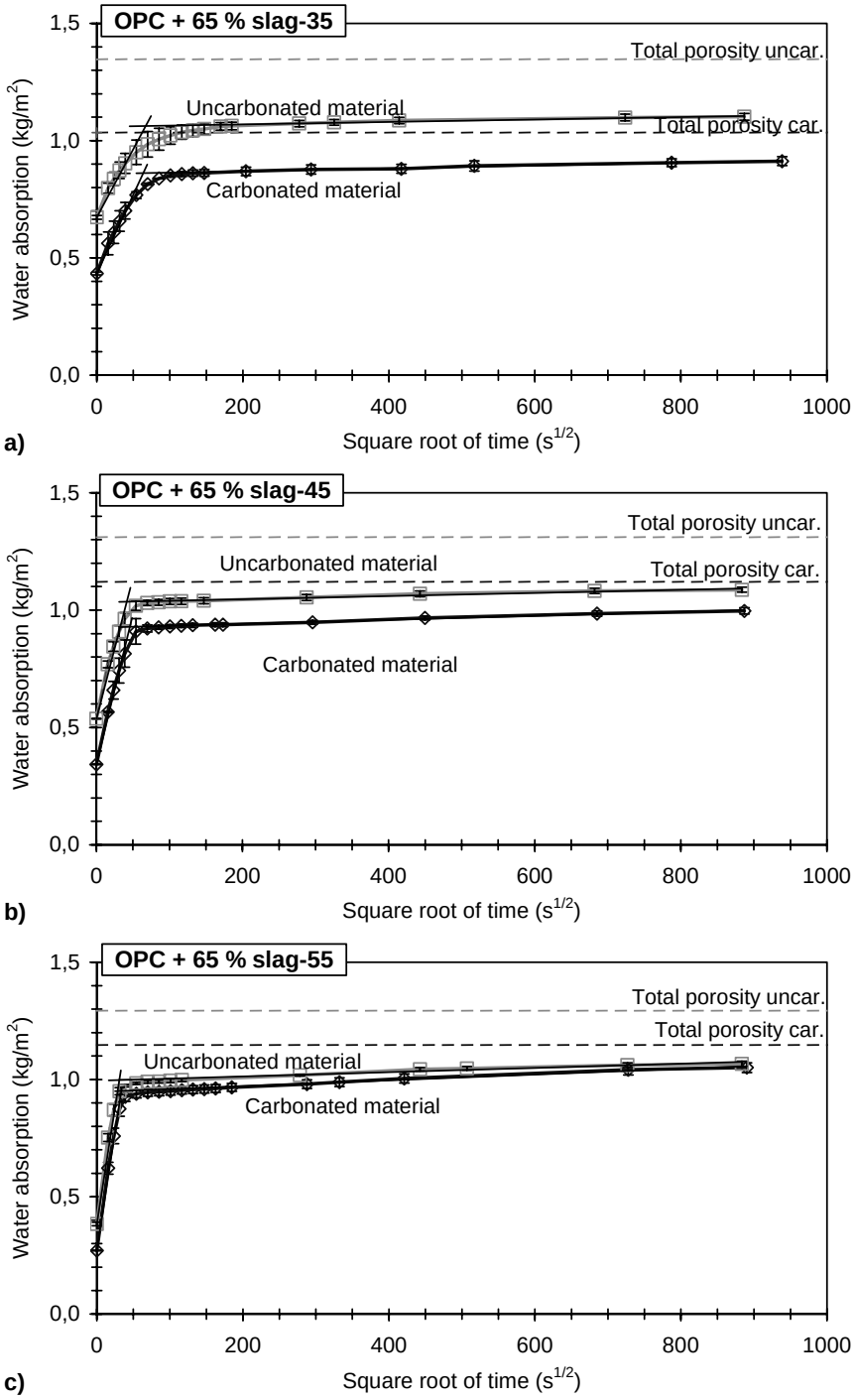

Figure 6.4 *Water absorption as a function of time for mortar with OPC and 65 % slag as part of the binder.*
a) w/b-ratio 0.35, b) w/b-ratio 0.45, c) w/b-ratio 0.55

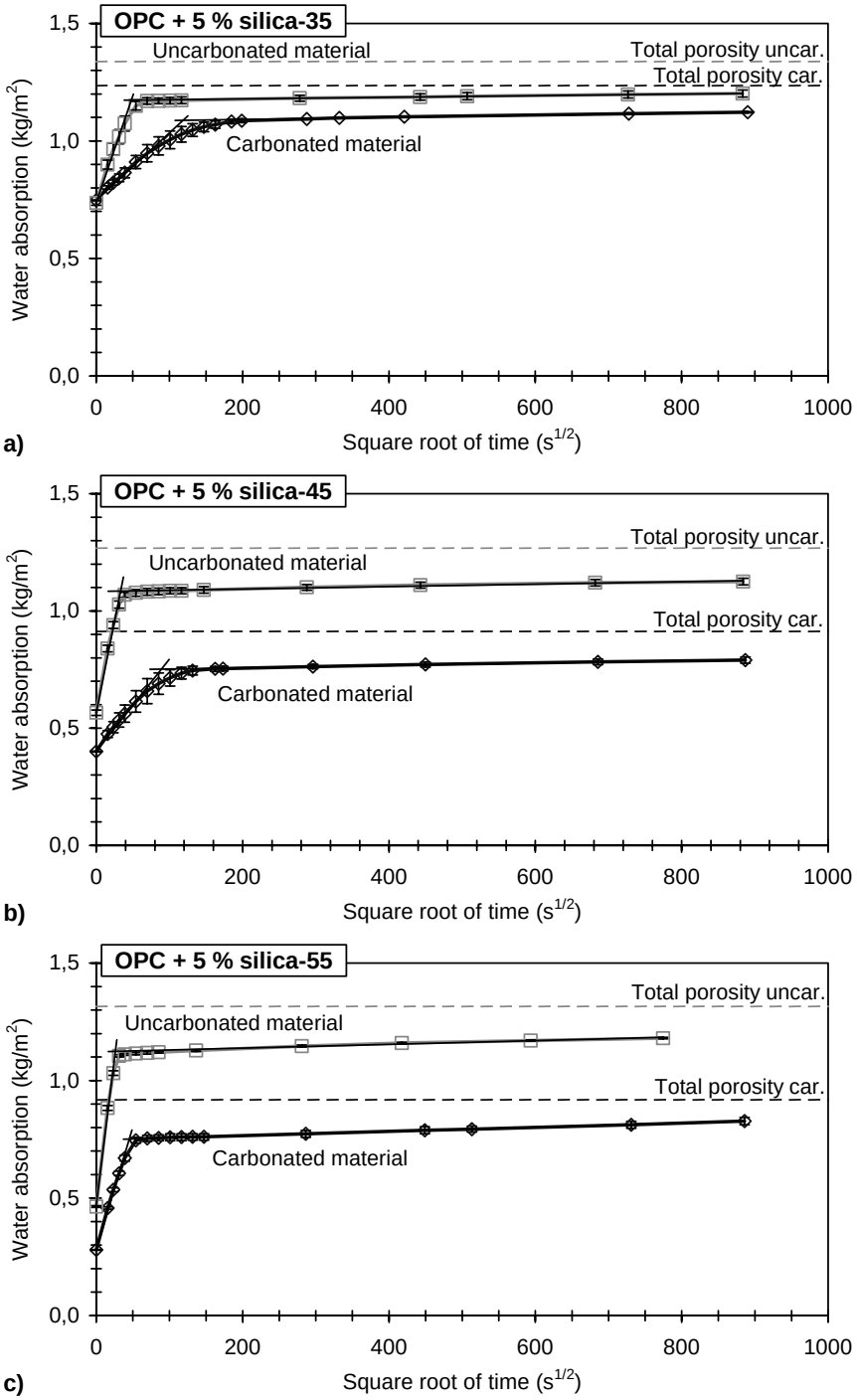

Figure 6.5 *Water absorption as a function of time for mortar with OPC and 5 % silica as part of the binder.*
a) w/b-ratio 0.35, b) w/b-ratio 0.45, c) w/b-ratio 0.55

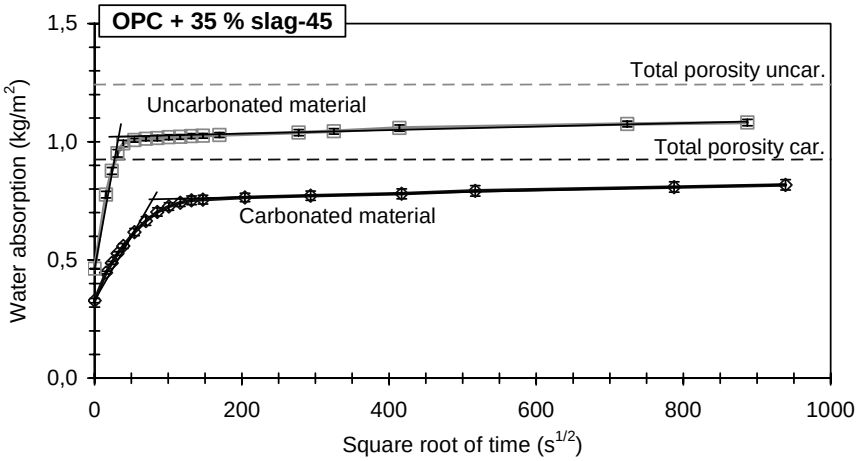

Figure 6.6 *Water absorption as a function of time for mortar with OPC and 35 % slag as part of the binder and with a w/b-ratio of 0.45.*

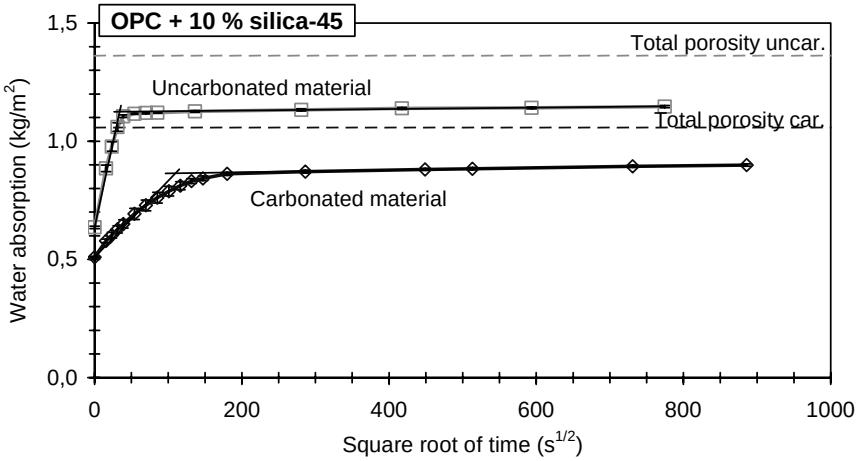

Figure 6.7 *Water absorption as a function of time for mortar with OPC and 10 % silica as part of the binder and with a w/b-ratio of 0.45.*

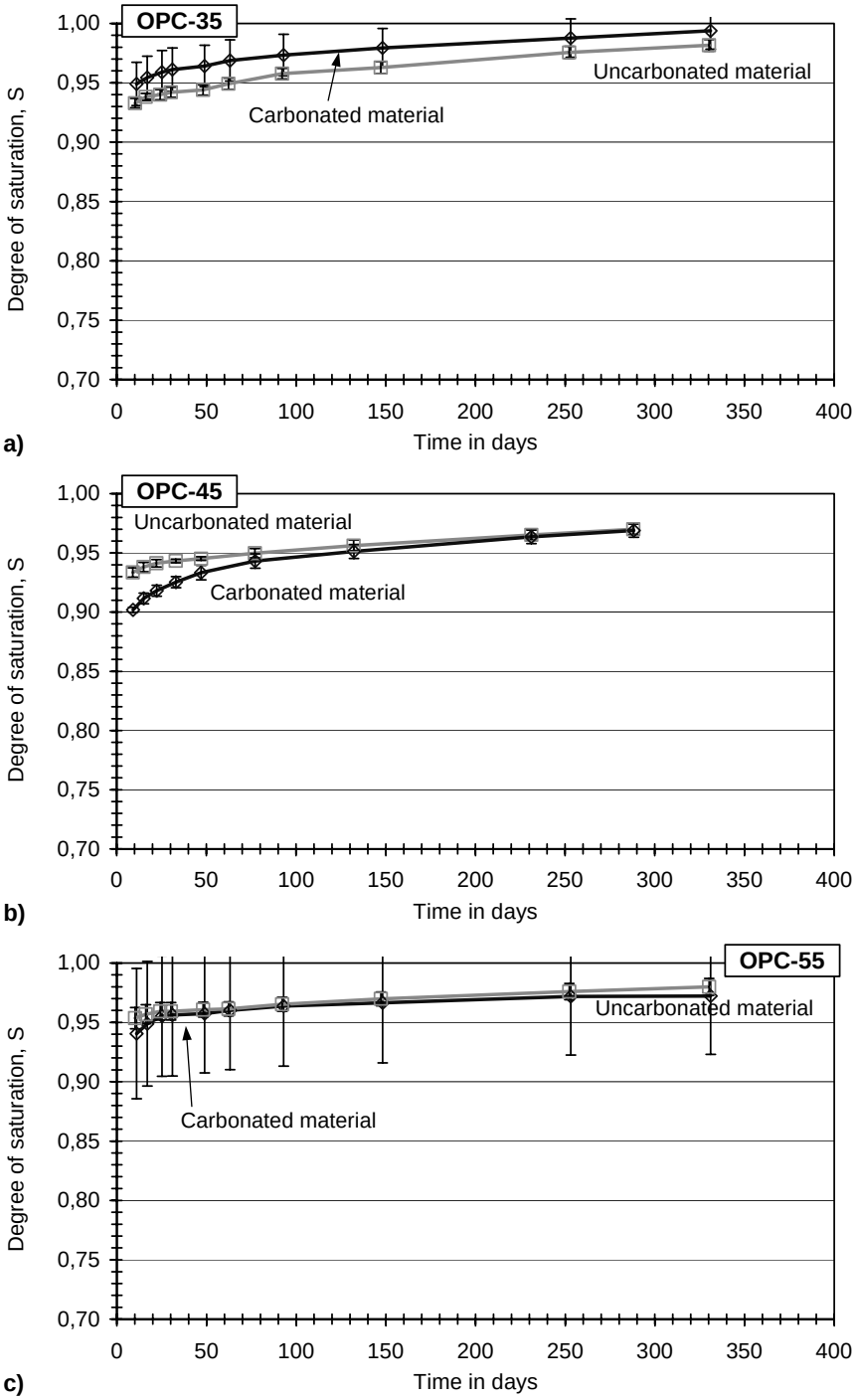

Figure 6.8 *Degree of saturation during long-time water absorption as a function of time for mortar with OPC as binder.*
a) w/b-ratio 0.35, b) w/b-ratio 0.45, c) w/b-ratio 0.55

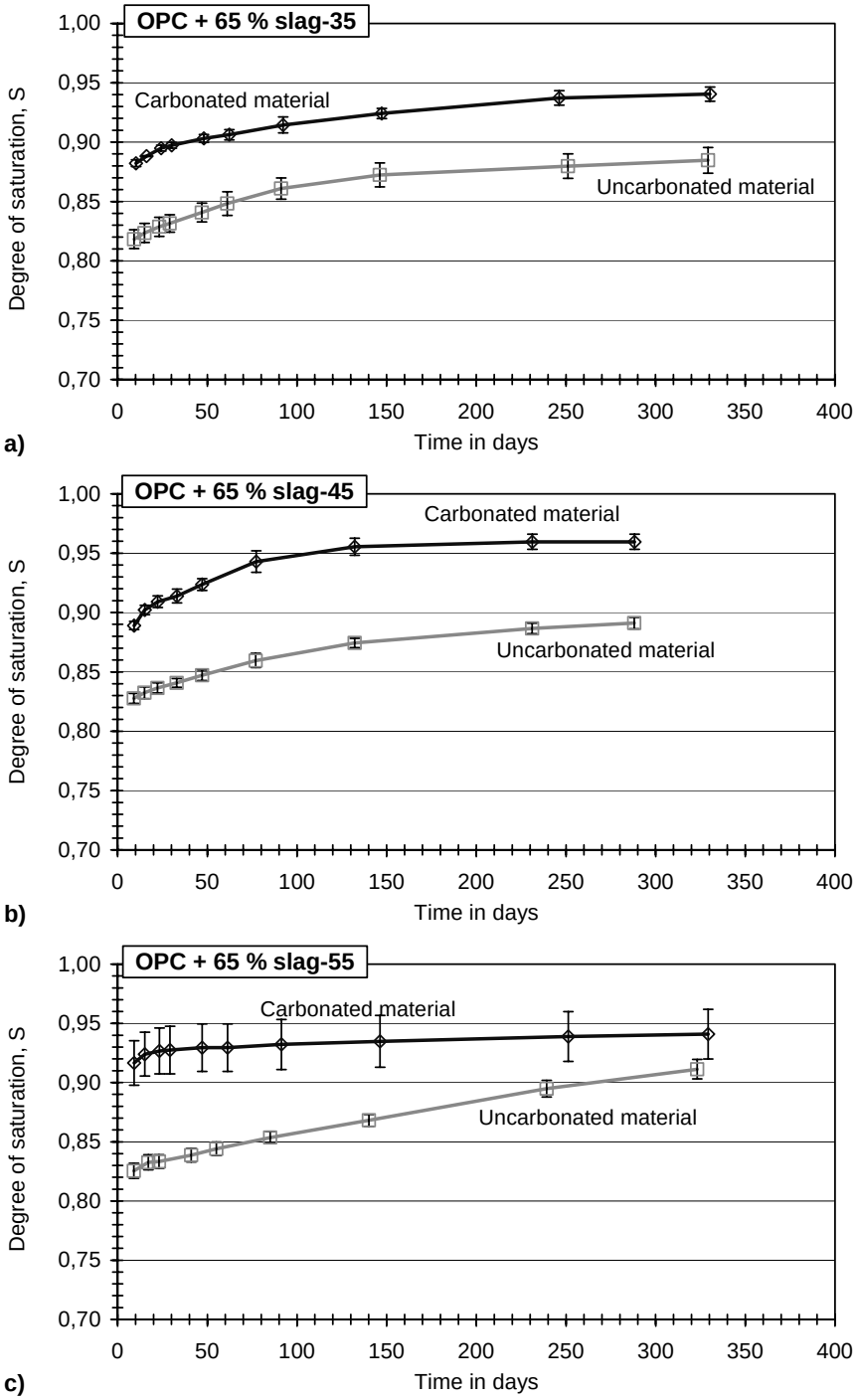

Figure 6.9 *Degree of saturation during long-time water absorption as a function of time for mortar with OPC and 65 % slag as part of the binder. a) w/b-ratio 0.35, b) w/b-ratio 0.45, c) w/b-ratio 0.55*

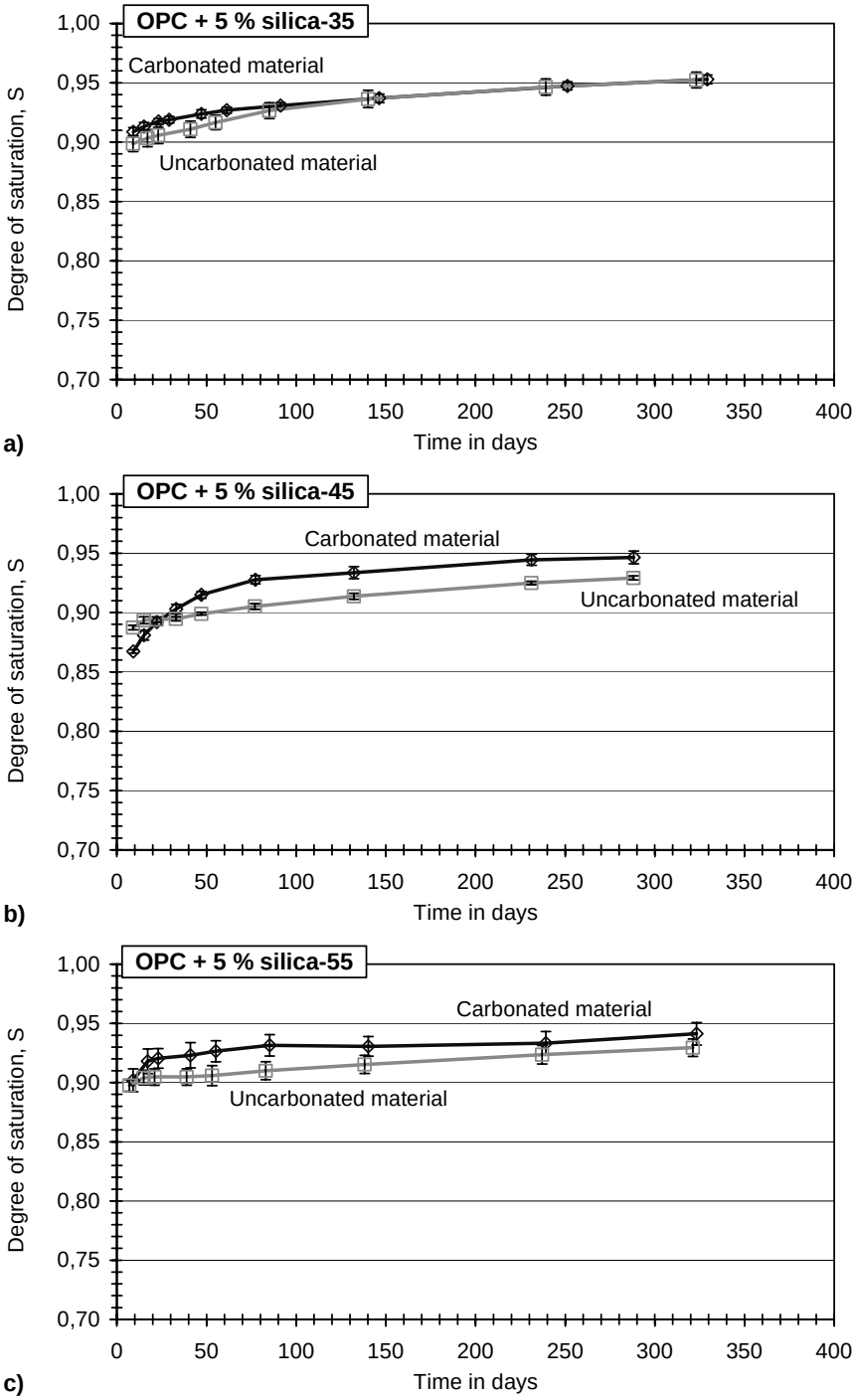

Figure 6.10 *Degree of saturation during long-time water absorption as a function of time for mortar with OPC and 5 % silica as part of the binder. a) w/b-ratio 0.35, b) w/b-ratio 0.45, c) w/b-ratio 0.55*

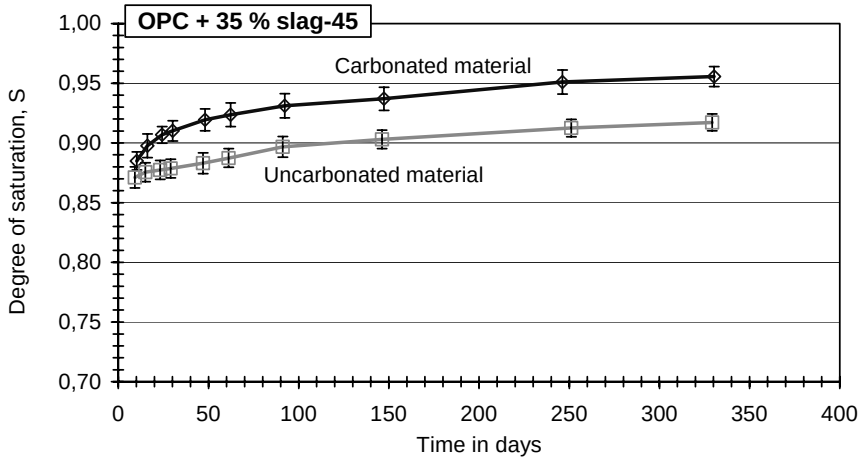

Figure 6.11 *Degree of saturation during long-time water absorption as a function of time for mortar with OPC and 35 % slag as part of the binder and with a w/b-ratio of 0.45.*

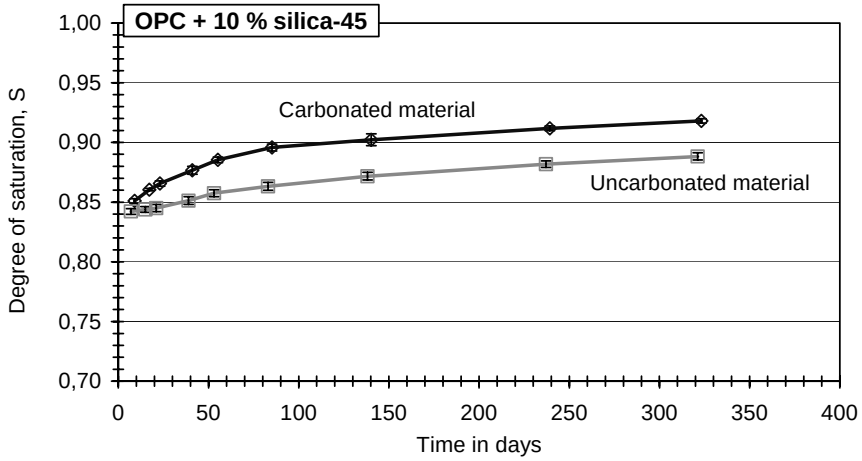

Figure 6.12 *Degree of saturation during long-time water absorption as a function of time for mortar with OPC and 10 % silica as part of the binder and with a w/b-ratio of 0.45.*

Table 6.2 *Total porosity, porosity filled at the nick point and dry density for the tested materials. All values, except those marked are means and standard deviation from two specimens.*

Mortar quality		Total porosity, P_{tot} (%)		Porosity filled at the nick point (%)	Dry density (kg/m^3)	
		Mean	Std.dev.		Mean	Std.dev.
OPC-35	**Uncarbo.**	24.0	0.09	21.6	2065	1
	Carbo.	21.6[1)]	0.77	19.8	2160	5
OPC-45[2)]	**Uncarbo.**	23.1	0.25	20.3	2065	5
	Carbo.	18.7	0.01	16.1	2208	1
OPC-55	**Uncarbo.**	24.0	0.36	21.2	2036	10
	Carbo.	17.2	0.47	14.5	2206	11
OPC + 35 % sl-45	**Uncarbo.**	24.4	0.10	20.1	2029	2
	Carbo.	18.3	0.71	15.0	2176	21
OPC + 65 % sl-35	**Uncarbo.**	27.2	0.16	21.5	1963	3
	Carbo.	21.2	0.19	17.6	2101	2
OPC + 65 % sl-45[2)]	**Uncarbo.**	26.3	0.33	20.7	1978	9
	Carbo.	22.3	0.21	18.4	2078	6
OPC + 65 % sl-55	**Uncarbo.**	25.7	0.02	19.8	1982	1
	Carbo.	23.3	0.20	19.3	2047	7
OPC + 5 % si-35	**Uncarbo.**	26.3	0.31	23.1	2023	3
	Carbo.	24.6[1)]	0.23	21.7	2086	1
OPC + 5 % si-45[2)]	**Uncarbo.**	25.4	0.12	21.7	2025	3
	Carbo.	19.5	0.21	16.0	2181	6
OPC + 5 % si-55	**Uncarbo.**	25.7	0.12	21.9	1999	0
	Carbo.	18.5	0.29	15.2	2162	8
OPC + 10 % si-45	**Uncarbo.**	26.4	0.14	21.8	1995	4
	Carbo.	21.5	0.22	17.7	2122	7

[1)] These carbonated qualities are very dense and it is difficult to fill all the pores with water with the method based on vacuum saturation. These values of total porosity are, therefore, probably underestimated.

[2)] Calculated means and standard deviations based on measurements on three specimens.

6.4 Discussion - Capillary suction before the nick point

6.4.1 Introduction

During the initial stage of capillary suction, i.e. during the rapid water absorption before the nick point, it is primarily the empty capillary pores that are filled with water.

From the initial absorption stage, two coefficients can be derived: *m*, which primarily depends on the material properties such as the constitution of the pore structure, and which can be described as the *resistance to water penetration*, and the second coefficient, *c*, the *coefficient of capillarity*, which is dependent on the properties of the material, such as the

constitution of the pore structure, as well as on the total porosity. The coefficient of capillarity is also dependent on the moisture content at the start of the test, i.e. by the conditioning prior to testing and the moisture history of the material. The coefficients can be derived from the following equations:

$$m = \frac{t_n}{h^2} \qquad (\mathrm{s/m^2}) \qquad \text{[Eq. 6.5]}$$

$$c = \frac{W_n - W_i}{\sqrt{t_n}} \qquad (\mathrm{kg/(m^2 \cdot s^{1/2})}) \qquad \text{[Eq. 6.6]}$$

where:

t_n	is the time when the nick point between the two absorption stages is reached	[s]
h	is the specimen thickness	[m]
W_n	is the content of water absorbed per unit area at the nick point	[kg/m^2]
W_i	is the initial content of water per unit area at the start of the test	[kg/m^2]

In this investigation, W_i corresponds to the water content in the material at equilibrium with a relative humidity of 65 % at +20 °C. Since the coefficient of capillarity is strongly dependent on the preconditioning, the suffix 65 is used to illustrate preconditioning at 65 % RH; thus, c_{65} is used in this investigation.

A high value of c_{65} signifies a rapid water filling of the pores that were empty at the start of the test, and indicates a coarse continuous pore structure and/or a large volume of unfilled pores at the start of the test. A low value of c_{65} signifies a slow water filling of the pores that were empty at the start of the test, and indicates a fine pore structure, perhaps combined with limited connectivity of the capillary pores and/or a small volume of unfilled pores at the start of the test.

The coefficient *m* describes the velocity at which the water front penetrates the specimen, and is determined primarily by the pore structure, and not by the total porosity. A high value of *m* indicates a dense material with fine capillary pores, resulting in slow water absorption. A low value of *m* indicates a coarse pore structure with large and continuous capillaries, resulting in rapid water absorption.

The values of *m* and c_{65} for the eleven mortars tested are shown in Table 6.3.

Table 6.3 *Calculated data based on the initial rapid water absorption stage of capillary suction.*

Mortar quality		t_n (s)	W_n (kg/m^2)	m ·10^6 (s/m^2)	c_{65} (kg/(m^2·s$^{1/2}$))
OPC-35	**Uncarbo.**	1038	1.081	41.5	0.0171
	Carbo.	13843	0.925	554	0.00306
OPC-45	**Uncarbo.**	580	1.052	23.4	0.0278
	Carbo.	14170	0.826	567	0.00358
OPC-55	**Uncarbo.**	514	1.062	20.6	0.0345
	Carbo.	3289	0.711	132	0.00809
OPC + 35 % sl-45	**Uncarbo.**	1083	1.022	43.3	0.0170
	Carbo.	6276	0.757	251	0.00540
OPC + 65 % sl-35	**Uncarbo.**	4518	1.064	181	0.00582
	Carbo.	4077	0.862	163	0.00671
OPC + 65 % sl-45	**Uncarbo.**	1686	1.033	67.4	0.0120
	Carbo.	2081	0.924	83.2	0.0128
OPC + 65 % sl-55	**Uncarbo.**	961	0.998	38.4	0.0198
	Carbo.	1111	0.951	44.4	0.0204
OPC + 5 % si-35	**Uncarbo.**	2266	1.172	90.6	0.00913
	Carbo.	13916	1.085	557	0.00286
OPC + 5 % si-45	**Uncarbo.**	1110	1.086	44.4	0.0156
	Carbo.	7955	0.752	318	0.00393
OPC + 5 % si-55	**Uncarbo.**	685	1.122	27.4	0.0248
	Carbo.	2012	0.751	80.5	0.0105
OPC + 10 % si-45	**Uncarbo.**	1150	1.121	46.0	0.0143
	Carbo.	12086	0.864	483	0.00323

Plotting *m* against c_{65}, Figure 6.13, shows good correlation between the coefficients regardless of material. Since there seems to be a strong correlation between the coefficients *m* and c_{65}, the emphasis will be on the resistance to water penetration, *m*, in the following.

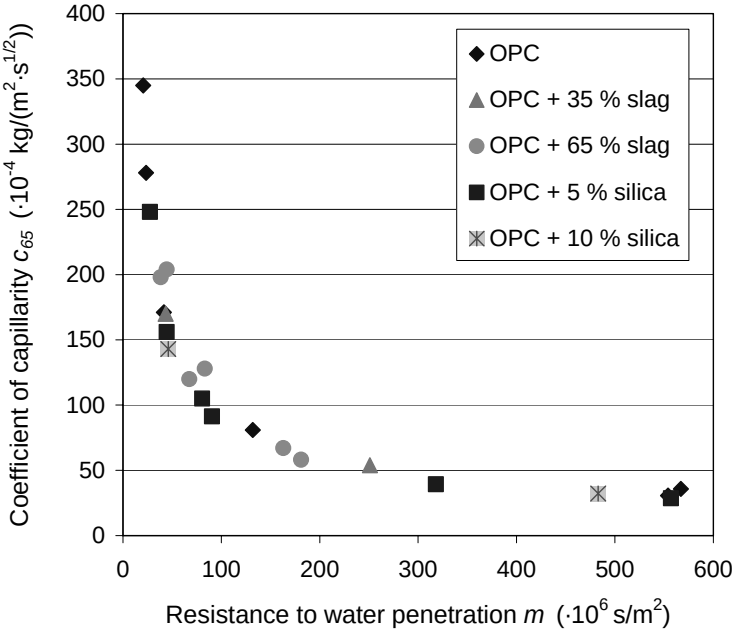

Figure 6.13 *Coefficient of capillarity, c_{65}, as a function of the resistance to water penetration, m, for carbonated and uncarbonated material.*

6.4.2 Mortar with OPC alone as the binder

For mortar with only OPC as the binder, Figure 6.14, the resistance to water penetration for uncarbonated mortar is relatively low, indicating a coarse, open, continuous, pore structure. The higher the w/c-ratio for the uncarbonated mortar, the lower the resistance to water penetration.

Carbonated mortar has a significantly higher resistance to water penetration than has uncarbonated material. This marked increase in resistance to water penetration due to carbonation indicates a denser, less continuous pore structure with finer capillary pores for the carbonated material. This is true for all w/c-ratios investigated, although less marked for a w/c-ratio of 0.55 than for w/c-ratios of 0.35 or 0.45. For the two latter mortar qualities, the carbonated material has 10-20 times higher resistance to water penetration than has uncarbonated material.

As can be seen in Figure 6.14, the resistance to water penetration for carbonated mortar with a w/c-ratio of 0.55 is significantly lower than that of carbonated mortar with a w/b-ratio of 0.35 or 0.45. This indicates that the pore structure of mortar with a w/b-ratio of or above 0.55 is so coarse that the carbonation products do not fill the pore system to the same degree as for materials with lower w/b-ratios.

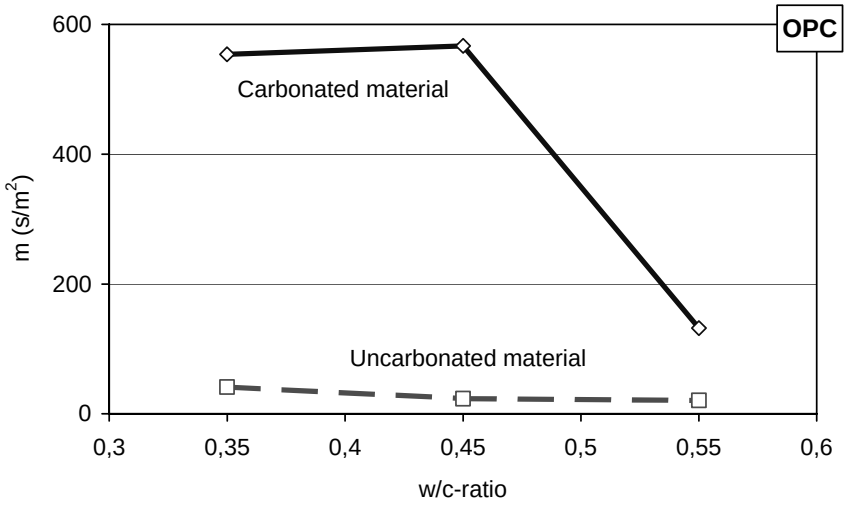

Figure 6.14 *Resistance to water penetration for carbonated and uncarbonated mortar with OPC as binder.*

6.4.3 Mortar with silica as part of the binder

For mortar with OPC and 5 % silica as the binder (Figure 6.15a), the tendency is the same as for mortar with only OPC. That is, the uncarbonated mortar has a relatively low resistance to water penetration and the resistance decreases with increasing w/b-ratio. Also for carbonated material the tendency is the same, i.e. for all mortars with silica as part of the binder, carbonation leads to a significant increase in the resistance to water penetration.

Compared to mortar with OPC alone as the binder, uncarbonated mortar with silica shows somewhat higher values for resistance to water penetration. However, the resistance to water penetration of carbonated mortars with OPC as the binder and a w/b-ratio of 0.45 or 0.55 is significantly higher than for mortar with the same w/b-ratio but with some silica as part of the binder. This indicates that carbonation of mortar with only OPC as the binder leads to a relatively greater change in pore structure than when the mortar includes silica as part of the binder.

As for mortar without silica, the mortar with 5 % silica and with a w/b-ratio of 0.55 carbonation has a less significant effect on the resistance to water penetration than for mortars with lower w/b-ratios. As was mentioned above, this is an indication that the pore structure of mortar with a w/b-ratio of 0.55 is too coarse to be as affected by carbonation as mortars with lower w/b-ratios have proven to be.

Figure 6.15b shows the resistance to water penetration of mortar qualities containing 0 %, 5 % and 10 % silica as part of the binder, all with a w/b-ratio of 0.45. For all the qualities, the resistance to water penetration increases markedly as a result of carbonation. The

influence of silica content is unclear, but it seems as if increased content increases the resistance to water penetration somewhat for uncarbonated concrete but reduces it for carbonated concrete.

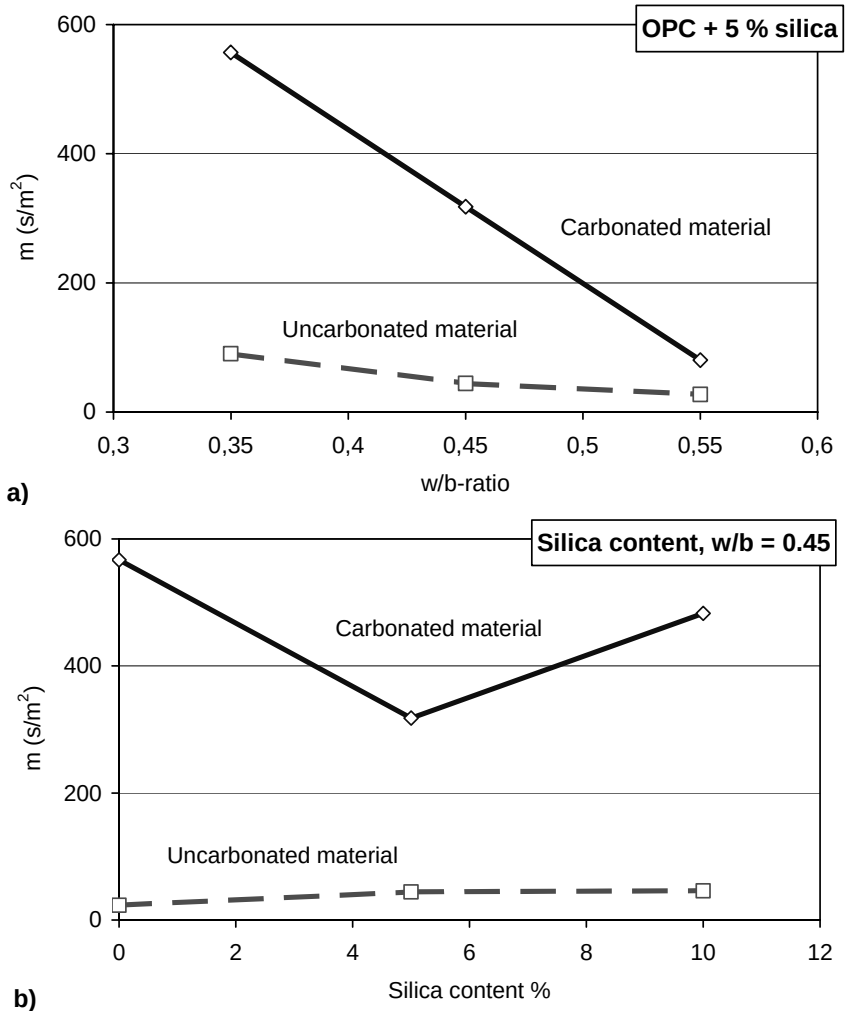

Figure 6.15 *Resistance to water penetration for carbonated and uncarbonated mortar with OPC and OPC + 5 or 10 % silica as binder. a) mortar with 5 % silica and different w/b-ratios, b) mortar with different silica content and a w/b-ratio of 0.45.*

6.4.4 Mortar with slag as part of the binder

For mortar with high amount of slag (65 %) as part of the binder, there is hardly any difference between the resistance to water penetration of carbonated or uncarbonated material (Figure 6.16a). This is relevant for all the water/binder-ratios studied.

Compared to mortar with only OPC as the binder, uncarbonated mortars containing slag show a significantly higher resistance to water penetration; see Figure 6.16b.

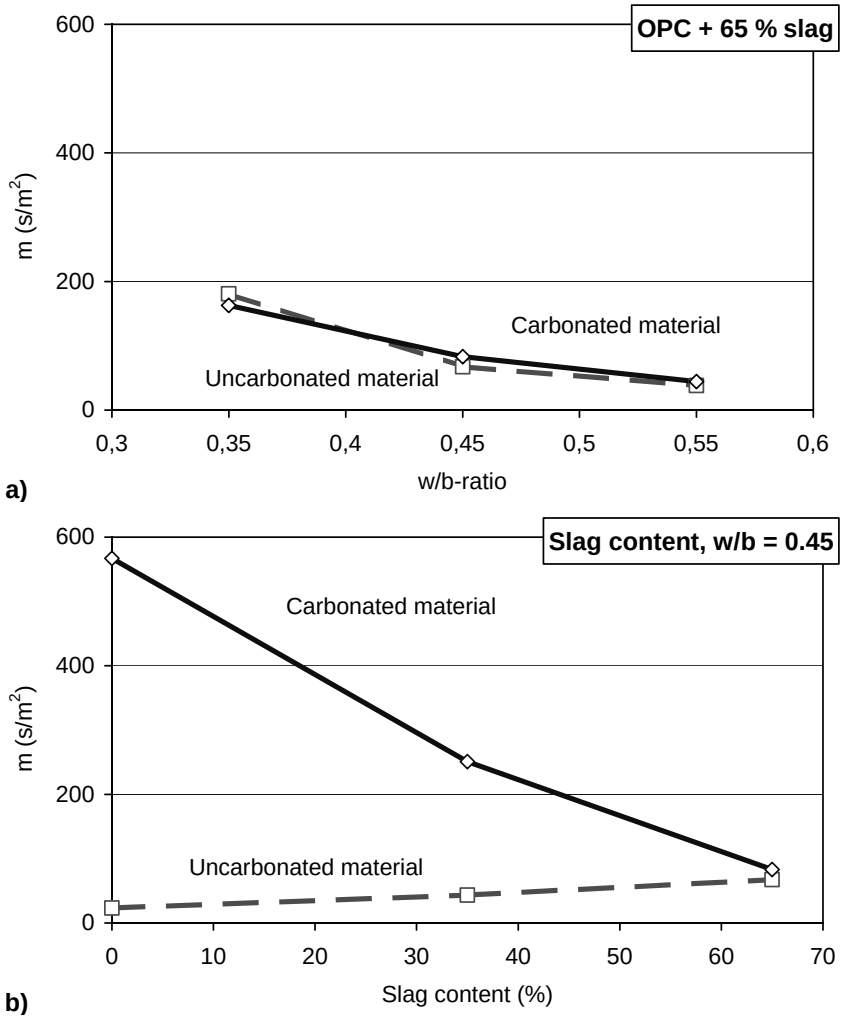

Figure 6.16 *Resistance to water penetration for carbonated and uncarbonated mortar with OPC and OPC + 35 or 65 % slag as binder. a) mortar with 65 % slag and different w/b-ratios, b) mortar with different slag content and a w/b-ratio of 0.45.*

The uncarbonated mortars containing slag thus seems to have a denser pore structure than uncarbonated mortar with only OPC as binder. However, the resistance to water penetration is considerably increased as a result of carbonation for mortar with OPC or with only small amounts of slag as part of the binder. The effect of carbonation on the resistance to water penetration is lower the higher the slag content. The marked effect of carbonation found for mortars with OPC or OPC with some silica as part of the binder is thus not

found in mortars with high amounts of slag as part of the binder. For mortar with OPC or OPC with some silica as the binder, it seems as if the coarse pore structure of the uncarbonated mortar becomes densified as a result of carbonation. For mortar with large amounts of slag as part of the binder, no densification of the pore structure can be seen from the water absorption measurements, even though the total porosity is lowered as a result of carbonation.

6.4.5 The degree of saturation at the nick point

The degree of saturation at the nick point changes as a result of carbonation, although the position of the point differs for different mortar qualities (Figure 6.17). The degree of saturation at the nick point is calculated from the water-filled porosity at the nick point divided by the total porosity; see Table 6.2. For the mortar qualities with OPC and OPC with 5 % silica and with a w/b-ratio of 0.35, the values of the total porosity for the carbonated materials are probably underestimated; see Table 6.2. These results, therefore, have not been included when evaluating the results.

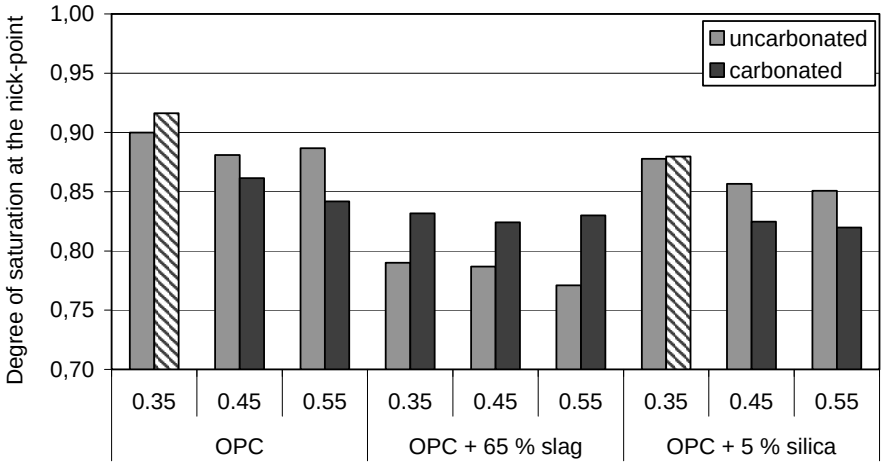

Figure 6.17 *Degree of saturation at the nick point for carbonated and uncarbonated mortars of different qualities. Striped bars represent uncertain values.*

From the figure, it can be seen that, both for the mortar with only OPC and for mortar with 5 % silica as part of the binder, the degree of saturation at the nick point is somewhat reduced as a result of carbonation. The observed decrease in the degree of saturation of the carbonated materials at the nick point is an indication that carbonation leads to a pore structure being more difficult to rapidly fill at capillary suction, i.e. that a greater part of the porosity is empty at the nick point than is the case for uncarbonated material.

For mortar with 65 % slag as part of the binder, the effect of carbonation is quite the opposite of that of mortar with OPC alone or OPC with some silica as part of the binder. For all materials with 65 % slag as part of the binder, the carbonated material has a markedly

higher degree of saturation at the nick point than has uncarbonated material. For the materials containing slag, carbonation thus leads to a pore structure where less of the porosity is empty at the nick point than is the case for uncarbonated material.

Assuming that the air void structure is not changed by carbonation, the observed changes in the degree of saturation at the nick point must be because of pore structural changes. For mortar with OPC alone, and OPC with some silica as part of the binder, the pore structural changes as a result of carbonation seem to lead to a finer pore system, which takes longer time to fill, and/or to a pore structure where air is more easily trapped and has to be slowly dissolved in the pore water and transported out of the material. The opposite applies for mortar with high contents of slag as part of the binder; for them, carbonation seems to lead to a coarser pore structure, which is more rapidly filled with water, and/or to a pore structure where less air is trapped.

The change in the degree of saturation at the nick point as a result of carbonation may be one of many reasons for the change in salt-frost resistance caused by carbonation. This, together with the change in critical degree of saturation and freezable water content discussed in Chapters 7 and 8 respectively, may be part of the explanation for the changes in salt-frost resistance that have been found as a result of carbonation.

6.5 Discussion - Long-time water absorption

After the rapid water filling of primarily the capillary porosity, i.e. up to the nick point, a stage of slower water uptake takes place.

The amount of porosity that is air-filled at the nick point, and which can therefore be filled with water during the long-time water absorption stage, can be calculated from Table 6.2. This water uptake is assumed to take place in air pores that may be filled with water because of a slow dissolution of the air in the surrounding pore water, according to the mechanism described in Fagerlund (1993). However, if we compare the measured air void contents using an optical microscope, the results of which are shown in Table 5.3 in Chapter 5, with the calculated contents of empty pores at the nick point, $P_{nick\ point}$, it can be seen that there is a lack of correlation (see Table 6.4). It must be noted that carbonation is assumed not to change the air void content.

It can be seen from Table 6.4 that the amount of empty porosity at the nick point exceeds the measured air void content for all materials, indicating that the empty porosity at the nick point does not consist only of air voids. Part of the difference can probably be explained by the uncertainty of the air void measurements at these low natural air void contents. Even though uncertainties in the air void determinations may be part of the explanation, they are probably not the only reason. The fact that the difference in the amount of empty porosity at the nick point and the measured air void content differs markedly between the different materials points towards another explanation. Mortars with only OPC as the binder show the smallest difference between the air void content and

the empty porosity at the nick point, $P_{nick\ point}$, whereas mortar with 65 % slag shows the highest difference. It can also be seen that, for most mortar qualities, the uncarbonated mortars show a higher difference than the carbonated. This is especially true for mortars with 65 % slag as part of the binder. If a systematic underestimation of the air void content was the only reason for the discrepancy between the measured air void content and the empty porosity at the nick point, there is no reason why there should be such a marked difference between the different mortars and for carbonated and uncarbonated material of the same mortar quality.

Table 6.4 *Measured air void content, P_{air}, compared to the empty air-filled porosity at the nick point, $P_{nick\ point}$.*

Mortar quality		**Air void content, P_{air} (%)**	**Air filled porosity at nick point, $P_{nick\ point}$ (%)**	**$P_{nick\ point}$ - P_{air} (%)**
OPC-35	**Uncarbo.**	0.6	2.4	1.8
	Carbo.	0.6	1.8	1.2
OPC-45	**Uncarbo.**	1.0	2.8	1.8
	Carbo.	1.0	2.6	1.6
OPC-55	**Uncarbo.**	1.7	2.8	1.1
	Carbo.	1.7	2.7	1.0
OPC + 35 % sl-45	**Uncarbo.**	1.9	4.3	2.4
	Carbo.	1.9	3.3	1.4
OPC + 65 % sl-35	**Uncarbo.**	1.6	5.7	4.1
	Carbo.	1.6	3.6	2.0
OPC + 65 % sl-45	**Uncarbo.**	1.9	5.6	3.7
	Carbo.	1.9	3.9	2.0
OPC + 65 % sl-55	**Uncarbo.**	2.6	5.9	3.3
	Carbo.	2.6	4.0	1.4
OPC + 5 % si-35	**Uncarbo.**	0.9	3.2	2.3
	Carbo.	0.9	2,9	2.0
OPC + 5 % si-45	**Uncarbo.**	1.3	3.7	2.4
	Carbo.	1.3	3.5	2.2
OPC + 5 % si-55	**Uncarbo.**	0.8	3.8	3.0
	Carbo.	0.8	3.3	2.5
OPC + 10 % si-45	**Uncarbo.**	1.7	4.6	2.9
	Carbo.	1.7	3.8	2.1

Because of the difference between the amounts of empty air pores at the nick point and the content of air in air voids, air must be present in the pore system in other pores than the air voids. Air might, for example, be trapped in other parts of the pore system during the rapid initial water absorption. In order for trapped air to be stable and not immediately dissolved in the pore solution, the size of the trapped air pores must be relatively large, leading to only air trapped in the coarse capillary pore system possibly being of significance. This is

because, according to the theory about water-filling of air-filled pores given in Fagerlund (1993), the smaller the air pores the more rapidly the air is dissolved in the pore solution. Another possibility is that part of the water absorption taking place after the nick point is the result of a slow filling of very small capillary pores.

It is not the aim of this investigation to explain the mechanisms and processes of the slow water filling after the nick point has been reached. It can, however, be concluded that air seems to exist in pores other than the air voids, e.g. as entrapped air in the pore system or as unfilled small capillaries. The filling of the air-filled spaces beyond the nick point may take place at different rates, depending on what mechanisms are acting.

In the literature, the long-time water absorption after the nick point is often modelled by fitting logarithmic regression lines to the water absorption measurements; see, for example, Fagerlund (1982). When this is done for limited time intervals, the logarithmic model may be a good approximation. However, when a logarithmic model is fitted to measurements over longer time periods, as is the case in the present investigation, the logarithmic model does not apply. This is also shown in Fagerlund (1993). Figure 6.18 shows an example in which a logarithmic regression line is fitted to the water absorption measurement from day 10 to day 288. It also shows a logarithmic regression line fitted to the water absorption measurements at a later stage, from day 77 to day 288 (the dashed line).

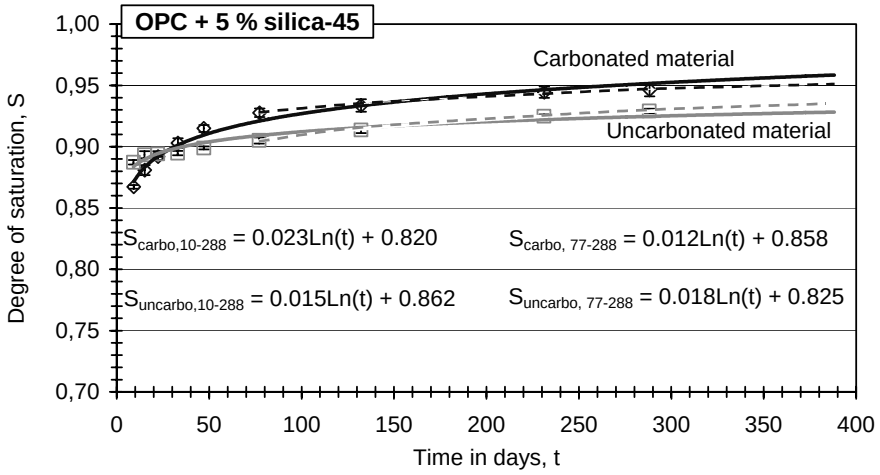

Figure 6.18 *Degree of saturation as a function of time for carbonated and uncarbonated mortar of quality OPC + 5 % silica - 45. Logarithmic regression lines are fitted to different parts of the degree of saturation results.*

From the figure it can be seen that, depending on within what interval the regression is made, markedly different inclination coefficients are found, thus leading to different interpretations of the results depending on the interval within which the regression is made. This shows that fitting a logarithmic regression line to the water absorption measurement over long periods may be misleading. It must be further noted that, if using logarithmic

regression lines for extrapolation over a longer time period, this will lead to the degree of saturation exceeding unity. Since a degree of saturation value exceeding unity is not possible, this further illustrates the shortcomings of using logarithmic regression lines. However, for shorter periods, a logarithmic regression line may be a good approximation.

No regression lines have been fitted to the water absorption measurements in the present investigation.

When determining the total porosity, which is needed to calculate the degree of saturation, there is an uncertainty about the absolute value of the total porosity, which also makes calculation of the degree of saturation somewhat uncertain. The uncertainty is based on the fact that not all the pores are filled when vacuum-saturating the specimens. Therefore, the total porosity will be underestimated and the degree of saturation consequently overestimated. Possible difficulties with filling all empty pores with water during vacuum saturation are probably most probable for dense impermeable materials, i.e. for materials with low w/b-ratios and for materials, which are densified by carbonation.

Figure 6.8-12 shows the long-time water absorption as the degree of saturation as a function of time. From the figures it can be seen that, for mortar with OPC or OPC with some silica as part of the binder, there are relatively small differences in the long-time water absorption caused by carbonation. In cases were there are marked differences at an early age, these differences level out during the long-time water absorption, and at later ages the rate of water uptake is about the same regardless of whether the mortar is carbonated or not.

For mortar with high slag contents, the effect of carbonation on the long-time water absorption is more evident. As can be seen in Figure 6.9, the carbonated materials have a much higher degree of saturation throughout the long-time water absorption in this investigation. This is true for all w/b-ratios tested in this investigation. For these mortars containing high contents of slag as part of the binder, the markedly increased degree of saturation as a result of carbonation may be one reason for the observed decrease in scaling resistance.

It can be noted that, in most cases, mortar containing high slag contents has a lower degree of saturation than has mortar with OPC or OPC with some silica as part of the binder. This can partly be explained by the higher natural air void content for those materials containing slag as part of the binder; see Table 5.3 in Chapter 5. However, a lower degree of saturation does not mean a higher salt-frost resistance. In order to evaluate the salt-frost resistance, the critical degree of saturation must be known.

6.6 Conclusions

The following conclusions can be drawn from the capillary suction test:

- Carbonation significantly changes the capillary suction behaviour, although to different extents for different mortar qualities. For mortar with OPC or OPC with small amounts of silica as part of the binder, carbonation leads to a significantly higher resistance to water penetration, indicating a finer and probably also less continuous pore structure compared with uncarbonated material. For mortar with high contents of slag, carbonation does not significantly change the resistance to water penetration.
- Carbonation leads to a reduced total porosity for all mortars tested.
- The degree of saturation at the nick point, i.e. where the initial rapid water absorption changes to the stage of slow water absorption, is decreased as a result of carbonation for mortar with OPC or OPC with some silica as part of the binder. The reverse applies for mortar with high contents of slag as part of the binder, i.e. carbonation leads to an increase in the degree of saturation at the nick point.
- During long-time water absorption, the degree of saturation for mortar with OPC and OPC with some silica as part of the binder is about the same for both carbonated and uncarbonated material. However, for mortar with high slag contents, the degree of saturation is significantly increased as a result of carbonation.

7 Studies of the effects of carbonation on critical degree of saturation

7.1 Introduction

In order to evaluate the frost resistance from long-time water absorption measurements, it is necessary to know the critical degree of saturation (S_{cr}) of the materials. S_{cr} is the maximum degree of saturation that can be allowed for a material, at a defined temperature below zero, if frost damage is not to occur, and can be experimentally determined by a method described in Fagerlund (1977). This method has subsequently been presented as a RILEM recommendation in RILEM CDC 3 (1994). This investigation has performed the test procedures essentially in accordance with this recommendation.

As a complement to evaluation of the frost resistance with the S_{cr}-test, a limited study of the salt-frost resistance of the same mortar qualities was carried out. The results from this study are presented in Section 7.6.

7.2 Test procedure

A comprehensive description of the method used for determining the critical degree of saturation is found in RILEM CDC 3. Briefly, a test is carried out as follows:

Specimens were saturated to different degrees of saturation. Normally, this is done by drying at +50 °C for one week, followed by vacuum saturation to the desired degree of saturation. However, in this investigation, the specimens were saturated as follows:

- **1st saturation** - No drying. Water absorption for ~24 hours. Specimens in equilibrium with 65 % RH at the start of water absorption.
- **2nd saturation** - Drying at +50 °C for one week, followed by water absorption for ~24 hours.
- **3d saturation and thereafter** - According to the procedure in RILEM CDC 3, i.e. drying at +50 °C for one week, followed by vacuum saturation and short drying at +50 °C to the desired degree of saturation.

The reason for not saturating the specimens in accordance with the procedure in RILEM CDC 3 during the two first rounds of saturation was to be able to start the freeze/thaw testing of the specimens with a presumably low degree of saturation and so be able to reuse the specimens by gradually increasing the degree of saturation. Another reason was to find out if water absorption for as short a time as 24 hours would result in a degree of saturation higher than the critical degree of saturation, and also to find the effect of drying, if any, at +50 °C on the water absorption. Water absorption was carried out according to the procedure described in Chapter 6.

After saturation either by water absorption or by vacuum saturation, the specimens were weighed in water and in air to give the initial volume. After vacuum saturation, the specimens were rapidly dried to a selected degree of saturation in an oven at +50 °C (in no case for more than five minutes). When the selected degree of saturation was reached, the specimens were individually wrapped in plastic film and put into plastic bags to prevent evaporation. To ensure an evenly distributed moisture state in the specimens before the freeze/thaw exposure started, the specimens were stored for about one day in a climate-controlled area at +20 °C.

Before the specimens were placed in a freeze/thaw cabinet for the first time, the initial dynamic E-modulus was determined indirectly by measuring the fundamental frequency (instrument from GrindoSonic, type MK 5 'industrial'). The fundamental frequency was determined by holding the transducer from the instrument on one side of a specimen, which was placed flat on a soft plastic foam bed, and tapping with a nail on the other side of the specimen, Figure 7.1. This procedure proved repeatedly to give the same values of fundamental frequency.

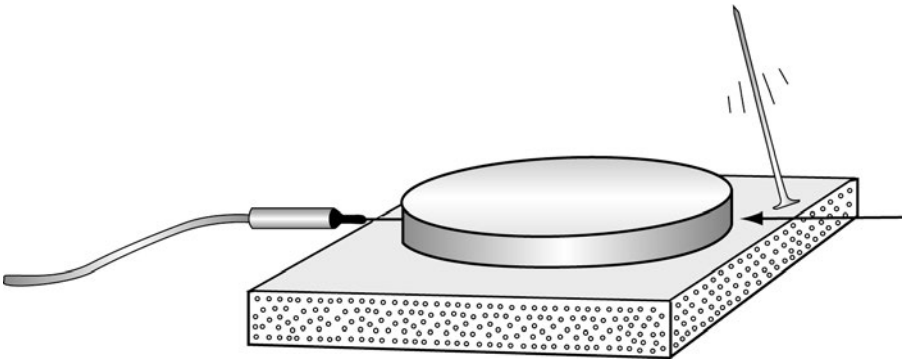

Figure 7.1 *Schematic sketch of the determination of the fundamental frequency of specimens used in the S_{cr}-test.*

In the freeze/thaw cabinet, the specimens were exposed to 24 hour freeze/thaw cycles, cycling the temperature between +5 °C and –20 °C, Figure 7.2. After six freeze/thaw cycles, the specimens were removed from the freeze/thaw cabinet. The temperature was increased to +20 °C over a period of one hour, after which the fundamental frequency and the volume were measured again. The measured fundamental frequency after exposure to freeze/thaw cycles was compared with the initial fundamental frequency. If the specimens were deemed as undamaged (see criteria below), they were reused by drying and resaturation to higher degrees of saturation. After completion of the S_{cr}-test, the specimens were dried at +105 °C for one week, then weighed after cooling in a desiccator, followed by vacuum saturation and weighing in water and air to give the final specimen volume.

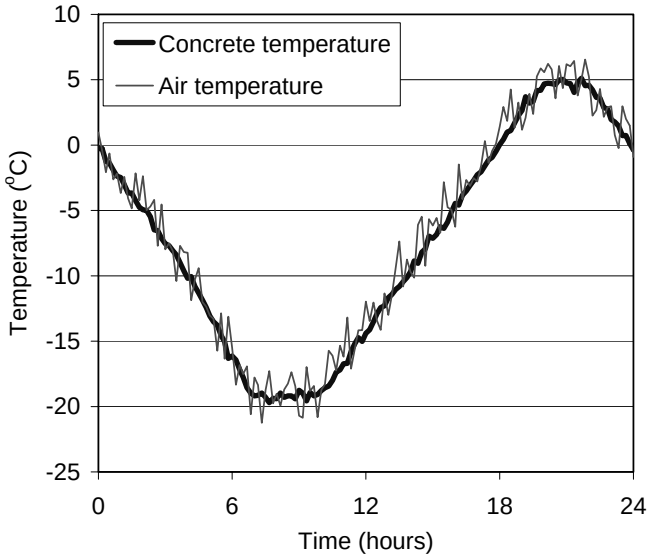

Figure 7.2 *Temperature in concrete and in air during one freeze/thaw cycle used in the S_{cr}-test.*

From the measurements of the weight and volume of the specimens it is possible to calculate the degree of saturation and change in volume caused by the frost action. From the measurement of the fundamental frequency, initially before the test started and after every exposure to the freeze/thaw procedure, the change in dynamic E-modulus (fundamental frequency) as a result of the frost action can be calculated. The degree of saturation (S) is calculated according to Equation 7.1 (for a complete set of equations, see RILEM CDC 3):

$$S_n = \frac{Q_n - Q_{dry:105}}{Q_{(sat:a)end} - Q_{dry:105} - (V_{end} - V_n) \cdot \rho_w} \qquad \text{[Eq. 7.1]}$$

where:

S_n	is the degree of saturation during the n:th freeze/thaw procedure	[-]
Q_n	is the weight of a specimen before the n:th freeze/thaw procedure	[kg]
$Q_{(sat:a)end}$	is the weight in air of a vacuum-saturated specimen after the test is ended. Before vacuum saturation, the specimen is dried at +105 °C.	[kg]
$Q_{dry:105}$	is the weight of a completely dry specimen, dried in an oven at +105 °C after the test is ended	[kg]
V_n	is the volume of a specimen before the n:th freeze/thaw procedure	[m^3]
V_{end}	is the volume of a specimen after the test is ended	[m^3]
ρ_w	is the density of water (1000 kg/m^3)	[kg/m^3]

The term $V_{end} - V_n$ adjusts the open pore volume of a specimen to possible volume changes caused by newly created cracks during the course of the S_{cr}-test. It is also assumed that no air-filled pores are opened or water filled during freezing.

Since the specimens are reused as long as they are not deemed as damaged, Q_n and V_n have to be determined before each repeated freeze/thaw procedure.

The residual dynamic E-modulus was calculated in accordance with RILEM CDC 3 from Equation 7.2:

$$\frac{E_n}{E_0} = \left(\frac{f_n}{f_0} \right)^2 \qquad \text{[Eq. 7.2]}$$

where

$\frac{E_n}{E_0}$	is the residual dynamic E-modulus	[-]
f_n	is the fundamental frequency after the n:th freeze/thaw procedure	[Hz]
f_0	is the fundamental frequency before the first freeze/thaw procedure	[Hz]

The critical degree of saturation was evaluated by plotting the residual dynamic E-modulus against the degree of saturation. The critical degree of saturation is often indicated by a well-defined nick-point, found analytically by linear regression. However, this was not the case for most of the results found in this investigation. The critical degree of saturation was therefore determined graphically as the degree of saturation for specimens with a loss in E-modulus of 10 %, i.e. when $E_n/E_0=0.90$.

7.3 Specimens

This investigation used mortar specimens of the same type and size as were used for the capillary suction test described in Chapter 6, i.e. 5 mm thick mortar discs with a diameter of 74 mm.

The focus has been on the three main mortar qualities ‘OPC-45’, ‘OPC + 65 % slag-45’ and ‘OPC + 5 % silica-45’. See Table 5.1 in Chapter 5 for information on the mortar composition.

Three carbonated and three uncarbonated specimens from each of the tested qualities were used to determine the critical degree of saturation. By starting with low degrees of saturation, the specimens were in most cases not immediately destroyed, and could therefore be used again with a higher degree of saturation until the critical degree of saturation was reached. The specimens were regarded as undamaged and reused as long as $E_n/E_0>0.90$.

The specimens were produced and conditioned as described in Chapter 5. This investigation used specimens conditioned for about 19 months in climate chambers with (1 vol-%) and without carbon dioxide.

7.4 Results

Results from measurements of the fundamental frequency on specimens conditioned to different degrees of saturation and subjected to six freeze/thaw cycles (+5 °C to –20 °C) are presented in Appendix 10. All calculations were carried out in accordance with the procedures in RILEM CDC 3. Figure 7.3 is a plot of the residual dynamic E-modulus against the degree of saturation, and shows estimates of the critical degree of saturation.

The results presented in Figure 7.3 were calculated strictly in accordance with the procedure in RILEM CDC 3. This involves measuring the fully saturated weight of specimens dried at +105 °C and then vacuum-saturated. It was found, as described in Chapter 6, that this procedure to determine the vacuum-saturated weight did not give the highest value for the saturated weight. Instead, it was shown that the highest value for the saturated weight was given by vacuum drying rather than by drying at +105 °C before vacuum saturation. Given this, the values for the saturated weights using vacuum drying were used when evaluating the results from the capillary suction test.

Since different procedures to determine the saturated weights have been used here in the S_{cr}-test and in the capillary suction test the results cannot be compared without a correction. To be able to use the calculated degree of saturation from the long-time water absorption in the capillary suction test in Chapter 6 for estimating the time until a critical degree of saturation is reached, the values for the saturated weights for the specimens used here in the S_{cr}-test therefore have to be corrected.

From the present investigation it has further been shown that using the S_{cr}-test procedure in accordance with the RILEM CDC 3 recommendation leads to significant uncertainties in the results for the types of specimens and materials used here; see discussion in Appendix 9. The most important factor causing uncertainties is the gradual weight change of the specimens during the test procedure. This weight change can be due to carbonation (for the initially uncarbonated specimens), leaching during the vacuum saturation process or other undesired effects as a result of for example drying, influencing the weight and/or the porosity and pore structure during repeated drying at elevated temperatures during the course of the test.

The uncertainties found when using the S_{cr}-test procedure in accordance with 'RILEM CDC 3' is further discussed in Appendix 9, which also includes a description of a procedure to calculate corrected values for the degree of saturation. This correction is based on the following assumptions:

- All specimens of the same mortar quality have the same total open porosity.
- All specimens of the same mortar quality have the same degree of saturation after the same time of capillary suction.

Based on the above assumptions and the results from specimens used in the capillary suction test (Chapter 6), corrected values for the degree of saturation for the specimens used in this S_{cr}-test could be calculated. These calculations are made and discussed in Appendix 9. The corrected values of the degree of saturation are presented in Figure 7.4 and in Appendix 10.

The critical degree of saturation can be estimated from the calculated corrected degrees of saturation, together with the measured residual dynamic E-modulus after freezing. From this estimated critical degree of saturation, and the long-time-water absorption from the capillary suction test, the time until a critical degree of saturation is reached may be estimated for all tested materials.

It must, however, be noted that the corrections of the degrees of saturation leads to possible uncertainties. Because of this the results found from this investigation should be regarded as indications rather than facts. In order to obtain more accurate estimations of the critical degree of saturation, an alternative test procedure, should be used. However, it has not been the aim of this investigation to develop a new method for determining the critical degree of saturation, which is why testing has been carried out in accordance with the procedure recommended by RILEM in CDC 3.

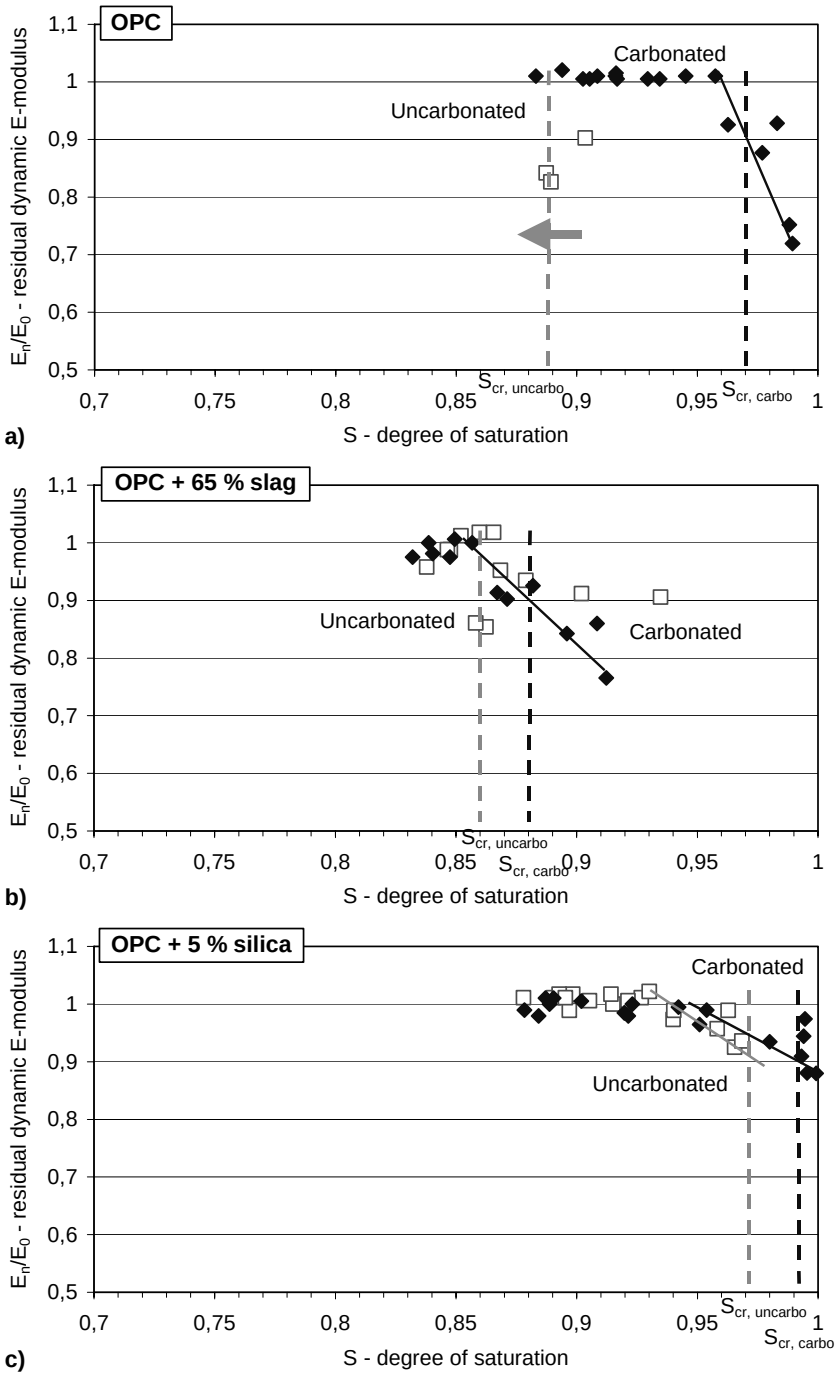

Figure 7.3 *Residual dynamic E-modulus as a function of the degree of saturation for carbonated and uncarbonated materials of different mortar qualities, all with a w/b-ratio of 0.45. Each point is one measurement.*
a) OPC, b) OPC + 65 % slag, c) OPC + 5 % silica

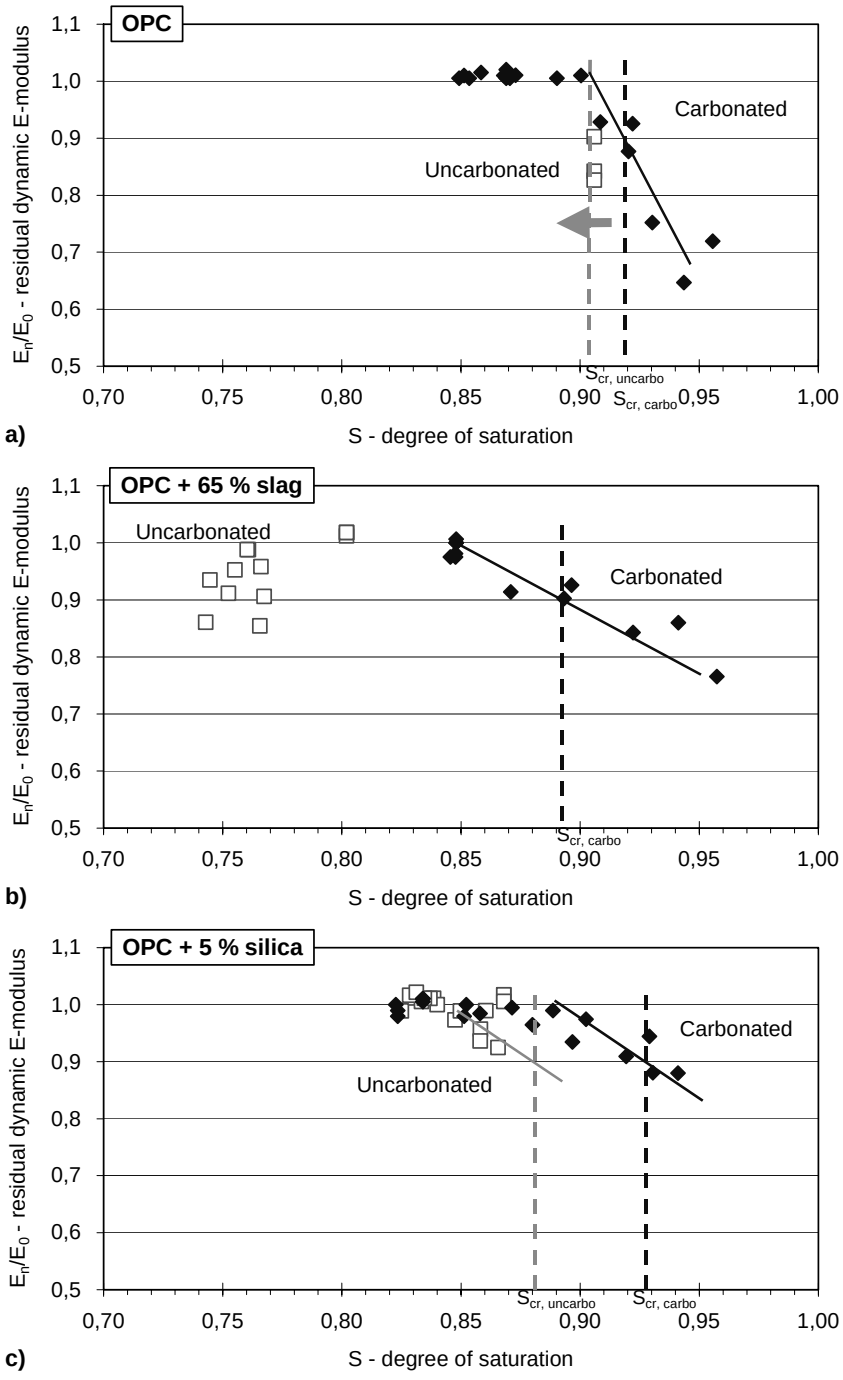

Figure 7.4 *Residual dynamic E-modulus as a function of the corrected degree of saturation for carbonated and uncarbonated materials of different mortar qualities, all with a w/b-ratio of 0.45. Each point is one measurement. a) OPC, b) OPC + 65 % slag, c) OPC + 5 % silica*

7.5 Discussion - critical degree of saturation

7.5.1 Results

The following discussion of the results considers the results from the corrected calculation of the degree of saturation; see Figure 7.4 and Appendix 10.

From the results presented in Figure 7.4, it can be seen that, for the tested mortar qualities, there are generally no well-defined nick-points to indicate the critical degree of saturation. Probable reasons for this are:

- **Specimen size:** a thin circular specimen might not be ideal for determination of fundamental frequency.
- **Mortar quality:** some of the mortar qualities might be too dense, making it difficult with the vacuum saturation method that was used to reach a degree of saturation resulting in frost damage.
- **Test procedure:** the procedure, involving drying at +50 °C for one week prior to vacuum resaturation, leads as shown in Appendix 9 to weight changes during the course of the test. These weight changes are the results of carbonation, leaching during vacuum saturation and other possible undesired effects of drying in elevated temperatures. The weight changes indicate that material properties such as porosity, pore structure etc. are altered during the course of the test, leading to uncertainties when determining the critical degree of saturation.
- **Number of specimens:** the small number of specimens used (3) might be too small for obtaining reliable results.

Although in most cases there is a lack of well-defined nick-points giving the critical degree of saturation, it is still possible to estimate the critical degree of saturation graphically. The critical degree of saturation is assumed to be reached when the loss in E-modulus is 10 %, i.e. E_n/E_0=0.90. From these estimates, and the degree of saturation during the long-time water absorption as described in Chapter 6, the time until a critical degree of saturation for the tested materials can be estimated. Below, the results for each mortar quality are discussed individually.

7.5.1.1 ‘OPC - 45’ mortar quality

From the results shown in Figure 7.4a and in Appendix 10, it can be found that the critical degree of saturation for the uncarbonated mortar is reached already within 24 hours of capillary suction, resulting in a loss of 10 % or more in E-modulus. Since the uncarbonated specimens were already damaged during the first freeze/thaw test, it is not possible to estimate the critical degree of saturation. However, it can be noted that less than 24 hours of capillary suction results in frost damage to this uncarbonated mortar, when tested with the actual freeze/thaw procedure.

Since all three uncarbonated specimens were already damaged after the first freeze/thaw test and therefore not affected by the corrections made in the calculation of the degree of saturation, the conclusion that less than 24 hours of capillary suction result in a critical degree of saturation is quite safe.

For the carbonated specimens, the change in weight during the course of the S_{cr}-test is small; see discussion in Appendix 9. This indicates that the errors in connection with the correction of specimen weights during the course of the test for these specimens are probably small. Since the correction of specimen weights during the course of the test has been shown to be the largest source of errors, the uncertainty of the estimated S_{cr}-value for the carbonated specimens is limited. From the results for the degree of saturation (Appendix 10), it can also be seen that the spread between the specimens seems to be small, which gives an indication of the validity of the estimated S_{cr}-values.

Table 7.1 shows the estimated values for the critical degree of saturation according to the 'corrected' calculations.

By comparing the S_{cr}-value with the long-time water absorption, Figure 6.8b in Chapter 6, the time needed for the degree of saturation to reach a critical level can be estimated, i.e. $S_t > S_{cr}$. With a S_{cr}-value of 0.92, S_t will reach a critical level after about 20 days of capillary suction for carbonated specimens.

Table 7.1 *Estimated S_{cr}-values for 'OPC - 45' mortar.*

Mortar quality	**S_{cr} corrected[1)] Figure 7.4a**
OPC-45 uncarbonated	<0.90
OPC-45 carbonated	0.92

[1)] see Appendix 9.

For this type of mortar, with only Portland cement as the binder, carbonation leads to a significantly higher frost resistance if comparing the time of capillary suction required before frost damage occurs: less than 1 day for uncarbonated material, and around 20 days for carbonated material.

7.5.1.2 'OPC + 65 % slag - 45' mortar quality

For the mortar quality with OPC and 65 % slag as part of the binder and with a water/binder-ratio of 0.45, there are significant uncertainties in the estimations of a critical degree of saturation. This is true especially for uncarbonated, but also to some extent for carbonated, specimens.

From the corrected calculations of the degree of saturation for the uncarbonated material, Appendix 10, it can be seen that the degree of saturation does not increase during the

course of the test, even though attempts gradually to increase the saturation were made. This is probably an effect of the weight correction discussed in Appendix 9 and leads to many uncertainties in the calculations, uncertainties that it is not possible to estimate, and for which it is not therefore possible to correct. For this uncarbonated mortar with 65 % slag as part of the binder, there thus seem to be too many uncertainties to be able to give a credible estimate of the critical degree of saturation.

For the carbonated specimens, a significant decrease in weight during the course of the S_{cr}-test was found, see Appendix 9. The reason for this decrease in weight might be due to leaching during vacuum saturation or other undesired effects, for example during drying at elevated temperatures. In this case, the corrections of the specimen weights made during the course of the S_{cr}-test might lead to overestimates of the degree of saturation and so also of the critical degree of saturation.

For the carbonated material, all three specimens are clearly damaged, and the results in Figure 7.4b indicate smaller scatter between the carbonated specimens compared to the uncarbonated.

Table 7.2 shows the estimated values for critical degree of saturation according to the corrected calculations.

If assuming a critical degree of saturation of 0.89 for the carbonated material, and compare this with the long-time water absorption (Figure 6.9b in Chapter 6), a critical degree of saturation level will be reached within 10 days of capillary suction for the carbonated specimens.

Table 7.2 *Estimated S_{cr}-values for 'OPC + 65 % slag - 45' mortar.*

Mortar quality	**S_{cr} corrected[1)] Figure 7.4b**
OPC + 65 % slag - 45 uncarbonated	-
OPC + 65 % slag - 45 carbonated	0.89

[1)] see Appendix 9.

The results indicate that, for carbonated material, quite a short period of capillary suction (less than ten days) is needed before a critical degree of saturation is reached for this mortar quality. For the uncarbonated mortar, the spread in results between the specimens, and the gradual weight increase during the course of the test, results in considerable uncertainties. Because of this, no estimate of how long a period of capillary suction is needed to reach a critical degree of saturation can be made. It can, however, be concluded that for this uncarbonated mortar quality with a high slag content it was difficult, with the used method, to reach a critical degree of saturation, even after repeated drying and vacuum saturation procedures. This indicates that the time until a critical degree of

saturation is reached probably is relatively long, at least significantly longer than for the carbonated material of the same mortar quality.

One possible reason for the considerable difficulties in finding critical degrees of saturation for this material containing large contents of slag as part of the binder may be the relatively large content of natural air void content and air trapped in the pore system, as discussed in Chapter 6. It was shown there that both the natural air void content and the amount of air-filled spaces (e.g. air trapped in the pore system) at the nick-point during capillary suction was significantly higher for mortar with high slag contents than for mortar with OPC alone or OPC with some silica as part of the binder.

7.5.1.3 'OPC + 5 % silica - 45' mortar quality

No well-defined nick-point giving a clear critical degree of saturation can be found for mortar with OPC and 5 % silica as part of the binder and with water/binder-ratio of 0.45. The results in Figure 7.4c and Appendix 10 indicate that it is difficult to obtain a saturation high enough to find a critical degree of saturation with the applied S_{cr}-test procedure. Even when freeze/thaw tested after the last full vacuum saturation, only limited damage could be detected. However, in some cases, the damage was large enough to qualify as damage according to the 10 % criterion.

Assuming an S_{cr}-value for the uncarbonated material of 0.88, results in a required time of capillary suction of around 10 days before a critical degree of saturation is reached (estimated from the long-time water absorption, Figure 6.10b in Chapter 6).

It must be noted that the uncarbonated specimens gained weight during the course of the S_{cr}-test, see Appendix 9. If we assume that this increase in weight during the repeated drying and resaturation procedures was a result of carbonation, then the specimens must be significantly carbonated. The estimated critical degree of saturation is thus not applicable to a completely uncarbonated material. This partial carbonation may be one reason for the difficulty in obtaining high enough degrees of saturation for damage to occur. As can be seen below, this was also a problem when saturating the fully carbonated material of the same mortar quality. The gradual carbonation may thus influence the determination of a critical degree of saturation for the uncarbonated material, leading to a seemingly higher frost resistance than would otherwise be the case if the material was completely uncarbonated.

Only small changes in weight during the course of the S_{cr}-test can be observed for the carbonated specimens, see Appendix 9. This is in agreement with what was found for the carbonated 'OPC - 45' specimens, and indicates that the errors resulting from correcting the specimen weights during the course of the test are probably small. From Appendix 10, it can be seen that these specimens also show a relatively small scatter in the degree of saturation at the onset of damage.

Table 7.3 shows the estimated values for critical degree of saturation according to the corrected calculations.

Assuming an S_{cr}-value of 0.93 results in a required time of capillary suction of around 90 days before a critical degree of saturation is reached for carbonated specimens (estimated from the long-time water absorption, Figure 6.10b in Chapter 6).

Table 7.3 *Estimated S_{cr}-values for mortar 'OPC + 5 % silica - 45'.*

Mortar quality	**S_{cr} corrected[1)] Figure 7.4c**
OPC + 5 % silica - 45 Uncarbonated	0.88
OPC + 5 % silica - 45 Carbonated	0.93

[1)] see Appendix 9.

For mortar with OPC and 5 % silica as part of the binder, it can be concluded that carbonation seems to increase the frost resistance. The carbonated mortar does not reach the critical degree of saturation before 90 days of capillary suction, whereas the uncarbonated mortar reaches a critical degree of saturation within the first 10 days of water absorption.

As for mortar with a high slag content as part of the binder, it was difficult to estimate the critical degree of saturation for mortar with some silica as part of the binder. The reason for this might be the same, i.e. that the natural air void content and also the air-filled porosity at the nick-point were relatively higher for this material than for mortar with only OPC as the binder, see Table 6.4. A higher air content results in better protection against frost damage. This assumes that the drying and resaturation procedure applied does not result in a filling of air voids, but that the air voids are more or less intact throughout the course of the S_{cr}- test. If this is the case, it may lead to difficulties in obtaining high enough degrees of saturation for damaging the material, i.e. not reaching a critical degree of saturation.

7.5.2 Possible improvements in the S_{cr}-test

In order to increase the reliability of the results when estimating the critical degree of saturation by the RILEM CDC 3 method, the following measures and modifications are suggested:

- **If possible, use specimens only once:** This requires a large number of specimens, but minimises the errors from the possible weight change occurring during the S_{cr}-test.
- **Change the drying procedure:** The drying procedure used in RILEM CDC 3, i.e. drying in an oven at +50 °C for several days, has resulted in significant weight changes for some of the material qualities. For example, all uncarbonated materials

showed a significant increase in weight between subsequent dryings, indicating an undesired carbonation. The undesired effect of carbonation and other possible effects due to drying at an elevated temperature might be eliminated if another drying technique was used. It is suggested that the drying technique used in the water absorption test (Chapter 6) could be tested, i.e. drying in a desiccator with a drying agent and applied vacuum. This would lead to a somewhat more time-consuming drying procedure, but without the undesired carbonation and the possible negative effects of the elevated temperatures. It might also make it possible to create higher degrees of saturation in the specimens. When using the prescribed drying technique, i.e. +50 °C, it was noted that it was difficult, for some mortar qualities, to reach a saturation high enough to create damage. With the suggested drying technique, i.e. drying in vacuum, it was shown in Chapter 6 that vacuum saturation after drying in vacuum resulted in higher specimen weights than did vacuum saturation after drying at +105 °C. This implies that vacuum drying before vacuum saturation would lead to higher possible degrees of saturation than produced by drying at +50 °C.

7.6 Study of the salt-frost resistance

7.6.1 Introduction

A limited investigation of the salt-frost resistance was carried out as a complement to the S_{cr} determinations. Specimens of the same mortar qualities as were used in the S_{cr}-test were exposed to repeated freeze/thaw cycles while stored in a freezing medium of 3 % NaCl solution. Measuring the fundamental frequency and quantity of scaled material after each freeze/thaw cycle provided information about the salt-frost resistance.

Because of the significant differences in the amount of natural air voids for the tested mortar qualities, it must be emphasised that the results must not be used for comparing salt-frost resistance between different mortar qualities. The results must merely be seen as indications of the effect of carbonation on the salt-frost resistance for each individual mortar quality.

In this limited investigation, only one specimen per mortar quality was used. This should be born in mind when evaluating the results from this study.

7.6.2 Specimens

This investigation used mortar specimens of the same type and size as used in the capillary suction test (Chapter 6) and in the S_{cr}-test, i.e. 5 mm thick mortar discs with a diameter of 74 mm. Here, as in the S_{cr}-test, the emphasis has been on the three main mortar qualities 'OPC - 45', 'OPC + 65 % slag - 45' and 'OPC + 5 % silica - 45'. For information about the mortar composition, see Table 5.1 in Chapter 5. Both carbonated and uncarbonated specimens of these qualities were tested.

The specimens were conditioned in climate chambers with (1 vol-%) and without carbon dioxide (65 % RH and +20 °C). The specimens used here were conditioned for about 22 months in the climate chambers prior to the salt-frost test. See Chapter 5 for a description of specimen production and conditioning procedure.

7.6.3 Test procedure

The test procedure used in this investigation is not a standardised or published method, but an in-laboratory method developed for this investigation. The following is a brief description of the test procedure.

Before the salt-frost test was started, the specimens were subjected to capillary suction for three days. The capillary suction test was carried out essentially in accordance with the procedure described in Chapter 6. This was done in order for the specimen to be capillary-saturated at the start of the freeze/thaw test. One difference from the capillary suction procedure described in Chapter 6 was that the specimens in this investigation were completely immersed in water during the capillary suction test, and not as is described in Chapter 6 with only one side in water.

After about three days in water, the capillary suction was stopped and the specimens were dried with a wet cloth and weighed, giving the initial specimen weight at the start of the salt-frost test. Before the test started, the initial fundamental frequency for the specimens were measured, as described in Section 7.2. Each specimen was then individually placed in a Petri dish (the same as was used during capillary suction) with a thin 1 mm diameter copper ring as a spacer between the specimen and the bottom of the dish. Each dish was filled with 30 ml of freezing media, ensuring that the specimen was fully immersed in liquid. One specimen was tested for each carbonated and uncarbonated mortar quality.

The dishes with the specimens were placed in a freeze/thaw cabinet and subjected to the same freeze/thaw cycle as in the S_{cr}-test, i.e. a 24 hour freeze/thaw cycle, cycling the temperature between +5 °C and –20 °C, see Figure 7.2.

After each freeze/thaw cycle, the Petri dishes and specimens were removed from the freezer and placed in a climate-controlled area in the laboratory (+20 °C) for the freezing medium and the pore solution in the specimens to melt. After about one hour in the laboratory, the fundamental frequency and the weight of each specimen were measured.

The scaled-off material was also collected, dried (+105 °C) and weighed. During thawing, the specimens were always placed in the same Petri dish and in the same water as during freezing. As a consequence of this procedure the freeze/thaw cycle did not follow the cycle shown in Figure 7.2 during the last hours of thawing. It is primarily about 2 to 3 hours during the late thawing phase that differ, with a maximum temperature of some + 15 to + 20 °C instead of + 5 °C.

After the fundamental frequency was measured, and the scaled material was collected, the specimens were again placed in the Petri dishes, filled with freezing media, and placed in the freeze/thaw cabinet for the next freeze/thaw cycle. This procedure was carried out until the specimens were significantly damaged, either by scaling or by internal damage, indicated by a reduction of the fundamental frequency.

It should be noted that the applied salt-frost method is very severe, with cooling taking place in all directions and with the longest distance from any part of the interior of the specimen to the outer freezing medium of only 2.5 mm. This means that all parts of the specimens have close access to the outer liquid, leading to possible rapid increase of the degree of saturation during the salt-frost test.

7.6.4 Results

The measured fundamental frequency was used for calculating the residual dynamic E-modulus as was described in Section 7.2.

Figure 7.5 shows the residual dynamic modulus as a function of the number of freeze/thaw cycles for specimens tested with 3 % NaCl solution as freezing medium. The figure also shows the accumulated amount of scaling in gram.

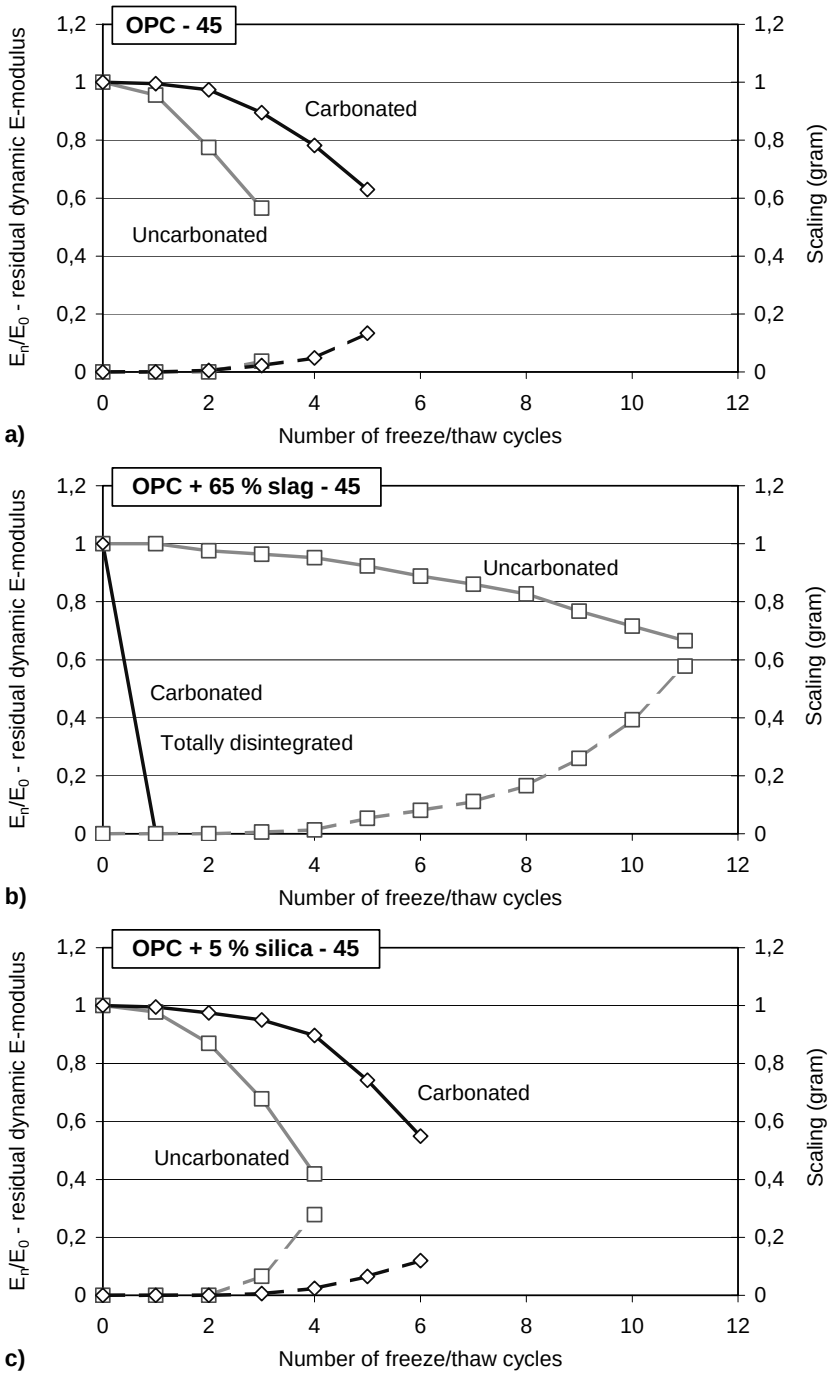

Figure 7.5 *Residual dynamic E-modulus and scaling versus number of freeze/thaw cycles for carbonated and uncarbonated mortars of different qualities, all with a w/b-ratio of 0.45. A scaling of 1 gram corresponds to approx. 0.12 kg/m^2. a) OPC, b) OPC + 65 % slag, c) OPC + 5 % silica.*

7.6.5 Discussion

OPC

For the 'OPC - 45' mortar quality, the results presented in Figure 7.5a show rapid development of damage. After only one freeze/thaw cycle, the uncarbonated mortar already shows significant changes in the fundamental frequency, indicating damage. For this uncarbonated mortar, a very short exposure to water absorption leads to a degree of saturation exceeding a critical value. This is in agreement with what was found in the S_{cr}-test (see Section 7.4), where it was shown that less than one day of capillary suction (one-sided) led to a degree of saturation exceeding a critical value.

For the carbonated material of the same mortar quality, a gradual decrease in residual dynamic E-modulus can be seen after a couple of freeze/thaw cycles. Compared to the uncarbonated material, carbonation of this mortar quality leads to an improved salt-frost resistance. However, both the uncarbonated and carbonated materials show relatively rapid damage development. This can probably be explained by the low natural air-void content for this mortar quality (see Table 5.3), and the severity of the applied salt-frost method.

The scaling of both the carbonated and uncarbonated specimens was limited during the short testing period needed before significant internal damage was detected.

OPC +65 % slag

For the 'OPC + 65 % slag - 45' mortar quality, the results presented in Figure 7.5b show that the carbonated material is completely disintegrated after only one freeze/thaw cycle. The fundamental frequency and the weight cannot be measured because of the extensive damage. This indicates a low salt-frost resistance, leading to just a couple of days' exposure to capillary suction resulting in frost damage if the material is exposed to frost attack in combination with a salt solution as freezing media.

The uncarbonated specimen of the same mortar quality shows a significantly higher salt-frost resistance, with a slow gradual decrease in residual dynamic E-modulus with increasing freeze/thaw cycles, indicating internal damage. Comparing the results for the carbonated and uncarbonated materials, shows that carbonation of this mortar quality leads to a strong reduction in salt-frost resistance.

It was shown in the S_{cr}-test presented above that, with the drying and vacuum saturation procedure used, it was difficult to saturate the uncarbonated material to or above a critical state. The results found here for the uncarbonated material show that during this severe salt-frost test, too, the uncarbonated material seems to be relatively more difficult to saturate to a critical state than the other tested materials. One explanation for this may be the relatively high natural air void content for this mortar quality, see Table 5.3.

Because of the total disintegration of the carbonated material, no scaling could be discerned. For the uncarbonated material, which was much more slowly damaged, a clear increase in scaling with increasing number of freeze/thaw cycles could be found.

OPC + 5 % silica

For the 'OPC + 5 % silica - 45' mortar quality, the results presented in Figure 7.5c show about the same appearance as for the 'OPC - 45' mortar quality. The uncarbonated quality shows damage within the first two freeze/thaw cycles, indicating a low salt-frost resistance, while damage to the carbonated material develops more slowly, indicating that carbonation increases the salt-frost resistance for this mortar quality. The relatively rapid damage development can be explained (as for the mortar quality with only OPC as binder) by the low natural air void content, see Table 5.3.

It may be questioned why materials, which according to the S_{cr} test would need weeks of water storage in order to reach a critical degree of saturation, can be damaged within just a couple of freeze/thaw cycles when frozen in contact with a freezing medium. This can be explained by the fact that, during freezing in a 3 % NaCl solution, the specimen is surrounded by a liquid solution during the whole freeze/thaw cycle. This leads to different effects, e.g. micro ice-lens growth, thermally induced contraction of entrapped air etc., leading to a more rapid increase in the degree of saturation than compared with water storage at +20 °C. See discussion about water uptake during freezing in Lindmark (1998).

This way of rapidly increasing the degree of saturation without forcing in water may be an alternative to the procedure of drying and vacuum-saturating specimens as in the S_{cr}-test, Section 7.2.

Photos of salt-frost damage

Figure 7.6 shows photos of three carbonated specimens damaged during the salt-frost test. The photos have been taken through an optical microscope, and show damaged specimens of three mortar qualities: 'OPC - 55', 'OPC + 65 % slag - 55' and 'OPC + 5 % silica - 55'. These mortar qualities were freeze/thaw tested in contact with 3 % NaCl solution in exactly the same way as was described for the mortar qualities with a w/b-ratio of 0.45 above. For these qualities, all specimens, carbonated and uncarbonated, were totally damaged after the first freeze/thaw cycle when tested with a 3 % NaCl solution. There were no obvious differences in salt-frost resistance for them when tested with this very severe salt-frost method.

The reason for presenting photos of specimens of mortar qualities with a w/b-ratio of 0.55 instead of pictures of the qualities with a w/b-ratio of 0.45 is that the 0.55 w/b-ratio qualities were subjected to only one freeze/thaw cycle, whereas the other specimens were subjected to repeated freeze/thaw cycles until the specimens were totally damaged. At this stage, it was not possible to produce thin sections because the damage was too extensive.

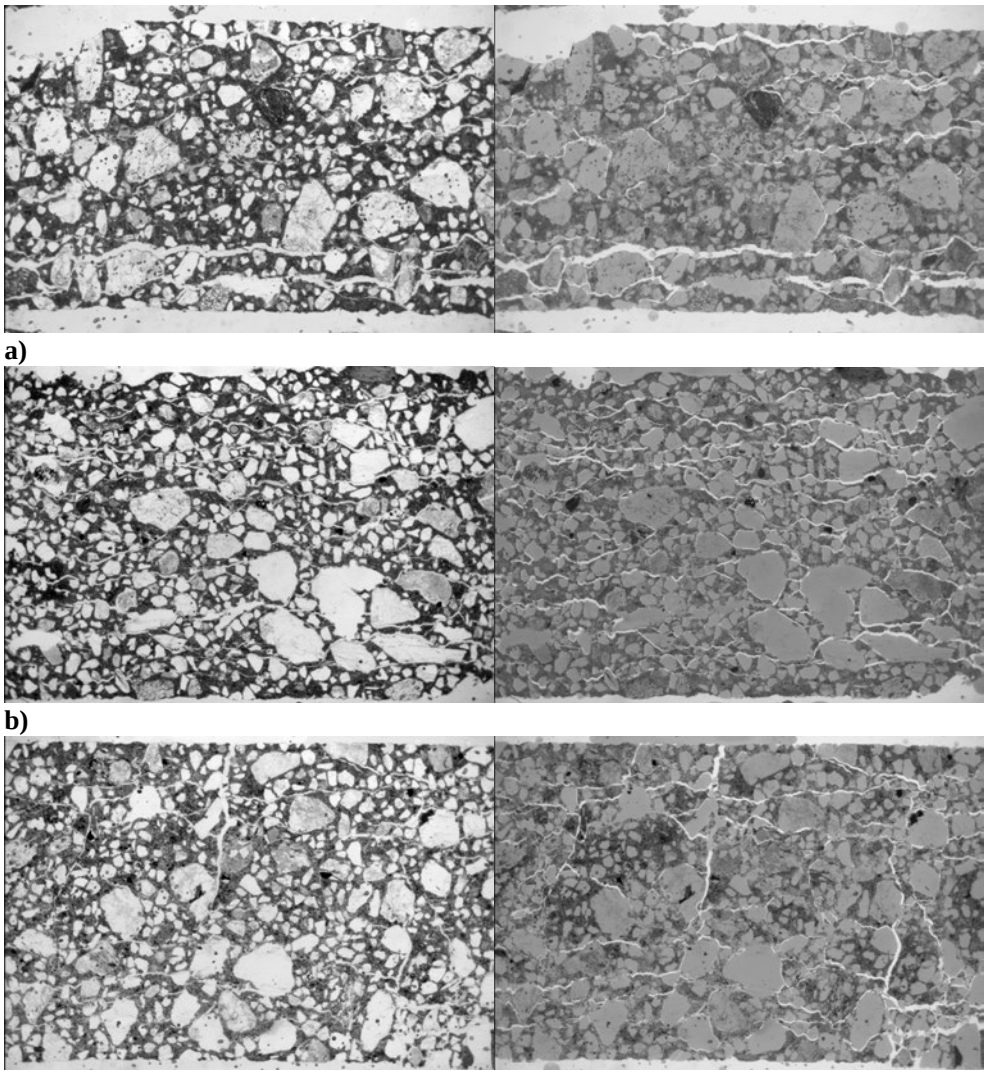

a)

b)

c)

Figure 7.6 *Photos of damaged carbonated specimens of different mortar qualities, all with a w/b-ratio of 0.55. Cross-sections of 5 mm thick specimens. To the left: photo in plain light, to the right: fluorescence microscopy-image covering the same area. a) OPC, b) OPC + 65 % slag, c) OPC + 5 % silica*

The figure shows cross-sections of 5 mm thick specimens. It can be seen that the damage pattern is about the same for all three mortar qualities, with cracks parallel to the surface at different distances below the surface. The distance between the cracks is less than 1 mm. This pattern of cracks parallel to the surface at different depths below the surface is in accordance with what could be expected if assuming microscopic ice body growth to be the dominating damage mechanism, see Lindmark (1998). However, also the hydraulic pressure theory predicts this type of cracking.

7.7 Conclusions

From the estimation of the critical degree of saturation for carbonated and uncarbonated mortars of quality 'OPC - 45', 'OPC + 65 % slag - 45' and 'OPC + 5 % silica - 45', in accordance with the RILEM CDC 3 test procedure, the following conclusions can be drawn:

- For the type of specimens and materials used in this investigation, the RILEM CDC 3 test procedure resulted in many sources of errors, leading to significant uncertainties in the results. The most significant source of error was an observed weight change of the specimens during the course of the test. The weight changes, which are probably the effects of undesired carbonation or leaching, lead to changes in primarily the dry (+105 °C) and vacuum-saturated specimen weights, but also to changes in the specimen weights during the course of the S_{cr}-test. The weight changes, and therefore the uncertainties in the calculations of the degree of saturation, are different for different materials. However, assuming that the total open porosity is the same for all specimens of the same materials, and assuming that all specimens of the same quality have the same degree of saturation after the same time of capillary suction, it is possible to apply corrections to the degree of saturation calculations, see Appendix 9. This correction, together with a gradual correction of the specimen weights because of the gradual weight change during the course of the test, results in corrected degrees of saturations where the errors are assumed to be minimised. It should be noted that the greater the weight change during the S_{cr}-test, the more uncertain are the results.
- Even though there are some uncertainties in the measurements, the estimated values for critical degree of saturation, S_{cr}, based on the corrected weights are assumed to be relevant. Comparing these S_{cr}-values with the long-time absorption from the capillary suction test in Chapter 6 results in the following times in contact with water until a critical degree of saturation is reached:

Mortar quality	Uncarbonated	Carbonated
OPC - 45	Less than 1 day	~20 days
OPC + 65 % slag - 45	Not able to be estimated	~10 days
OPC + 5 % silica - 45	~10 days	~90 days

- The results found here indicate that carbonation of mortar with only OPC as the binder, or with OPC and some silica as part of the binder, leads to an increase in frost resistance, i.e. a longer time of capillary suction is needed to reach a critical degree of saturation. For uncarbonated mortar with OPC and 65 % slag as part of the binder, large uncertainties and large scatter in the results make the measurements unreliable, which means that a critical degree of saturation not could be estimated. For the carbonated mortar, on the other hand, a time of capillary suction of less than ten days results in a critical degree of saturation, implying a relatively poor frost resistance.

In the limited investigation into the salt-frost resistance, the following conclusions can be drawn:

- For mortar with OPC, or OPC and some silica as part of the binder, carbonation leads to an improved scaling resistance. The low natural air void content for these mortar qualities and the severity of the applied freeze/thaw method lead, however, to a rapid development of damage for all materials.
- For mortar with OPC and high contents of slag as part of the binder, carbonation leads to a strong reduction of the salt-frost resistance. The uncarbonated material shows a substantially better salt-frost resistance, which can be explained by the relatively high natural air-void content for this mortar quality.
- The crack pattern for material freeze/thaw tested in contact with a 3 % NaCl solution as the freezing medium shows cracks parallel to the specimen surface at different depths below the surface, this is true for all tested materials.

8 Studies of the effects of carbonation on freezable water content

8.1 Introduction

When evaluating the effect of carbonation on the freeze/thaw resistance, the amount of freezable water at different temperatures is of great interest; normally the higher the amount of freezable water, the higher the risk of frost damage. The freezable and non-freezable water contents also give information on the pore structure of the materials, i.e. what proportions of the pore system that contain ice and water respectively at a certain freezing temperature. This knowledge is of importance when evaluating the effect of carbonation on the pore structure and on its possible effects on the freeze/thaw durability.

The freezable water content of uncarbonated and carbonated material of different mortar qualities was measured using Low-Temperature Calorimetry (LTC). All LTC measurements were carried out at the Aalborg Portland Research and Development Centre (RDC) in Aalborg, Denmark.

8.2 Materials and specimens

This investigation includes all mortar qualities described in Chapter 5 and used in the capillary suction investigation (Chapter 6), except those with a water/binder-ratio of 0.35. The reason for not including these qualities was primarily because the mortar specimens were not fully carbonated, and because the testing resources were limited. For each quality, both carbonated and uncarbonated material was investigated. For material specifications, see Chapter 5.

The specimens should be water-saturated to a point where all capillary and gel pores, but not the air voids, were filled with water. It was chosen to use relatively old specimens and let them absorb water for about one week, to ensure a well-hydrated material with a water-filled pore system with a minimum of water-filled air pores. Great care was taken during handling of the specimens, throughout preconditioning as well as during the preparation of the test material, to avoid unwanted carbonation and to avoid drying the material after water absorption.

The specimens used for the low-temperature calorimetry measurements were produced from cores that were drilled from mortar cast in plastic bottles (see the description in Chapter 5). The drilled cores had a length of approximately 100 mm and a diameter of ~14 mm. They were conditioned in the same way as the specimens used in the capillary suction test in Chapter 6 and in the S_{cr} and salt-frost investigations described in Chapter 7, i.e. in the climate chambers as described in Chapter 5. The climates in the chambers were 65 % relative humidity and +20 °C, with one of two atmospheres: either carbon dioxide-free, or with about 1 % by volume of carbon dioxide.

After conditioning in the respective climates for over 20 months, the cores were used to produce specimens for the low-temperature calorimetry measurements. Each core was cut at both ends, resulting in specimens about 60 mm long. From the cut ends, the carbonation was estimated by spraying phenolphthalein on the cut surface. The simple phenolphthalein test showed that all specimens conditioned in the atmosphere with elevated carbon dioxide content were 'fully' carbonated. A further indication of the degree of carbonation is the weight change during the over 20 months-long conditioning in the climate chambers, as shown in Figure 8.1. The figure shows the weight change for cores of the three main mortar qualities during conditioning, expressed as a percentage of the weight at the start of conditioning, i.e. in a saturated 'virgin' state at an age of 14 days. The figure shows the weight change of cores conditioned in climates with and without carbon dioxide.

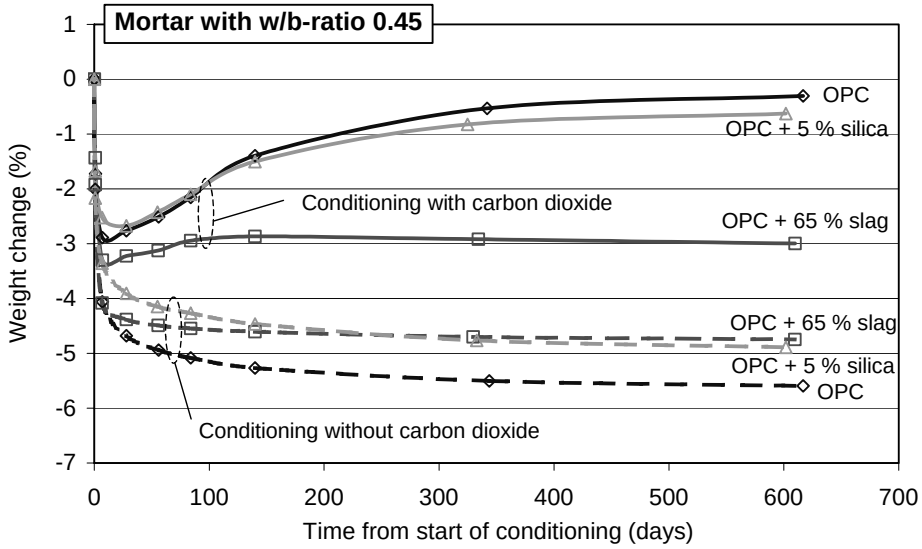

Figure 8.l *Weight change as a function of time during conditioning in 65 % RH and +20 °C in climates with (~1 vol-%) and without carbon dioxide. Drilled cores of different mortar qualities, all with a w/b-ratio of 0.45, used for specimen production for the measurement of the freezable water content. Each point is one measurement.*

From the figure it can be seen that the mortar cores conditioned in the climate without carbon dioxide lost weight because of drying during the whole preconditioning time. The weight loss is very rapid during the first week, and thereafter drying proceeds at a slower rate. The weight loss is greatest for mortar with OPC alone as the binder, and somewhat less for mortar containing slag and silica as part of the binder. For mortar containing slag as part of the binder, the weight loss has almost stopped within the first couple of months' conditioning, whereas for concrete with OPC only, and OPC with some silica as part of the binder, the weight loss continues during the whole conditioning time, although at a very slow rate.

The fact that the cores conditioned in the climate without carbon dioxide lose weight during the whole conditioning time is an indication that no unwanted carbonation takes place.

For the cores conditioned in the climate with an increased carbon dioxide content, there is a significant weight loss caused by drying during the first week of conditioning. However, the decrease in weight stops after only a short time, after which an increase in weight can be seen during the continued conditioning. This increase in weight is a result of carbonation. For mortar with OPC and OPC with some silica as part of the binder, there is a significant weight increase during about the first half year of conditioning, after which the weight increase slows down. After about a year of conditioning, the weight change has almost stopped, indicating a high degree of carbonation. For mortar containing high amounts of slag as part of the binder there is, after the rapid initial drying, only a small increase in weight as a result of carbonation. This weight increase takes place for only a couple of months, after which the weight increase stops. From the figure it can be seen that the weight of this mortar even decreases during the continued conditioning after the first half year. This indicates that the material containing slag carbonates much more quickly than do the materials with only OPC or OPC with some silica as part of the binder. For the latter materials, the weight increase due to carbonation exceeds the weight loss due to drying throughout the over 20-month-long conditioning period. However, for material containing slag, carbonation is ended within the first half year of conditioning, after which the weight loss due to drying becomes comparable with the weight loss for the uncarbonated material of the same mortar quality.

The weight change for the 14 mm cores in Figure 8.1 can be compared with the weight change for specimens of the same mortar qualities but with a different specimen size (5 mm thick discs with diameter of 74 mm) used in the capillary suction and S_{cr}-test, see Chapter 5. It can be seen that the appearances of the weight change curves are very similar, although with an expected somewhat slower carbonation weight increase for the 14 mm cores than for the 5 mm thick discs.

As was mentioned above, after the conditioning was ended, specimens were cut from the conditioned cores. These specimens were subsequently subjected to capillary suction for seven days in principle according to the procedure described in Chapter 6.

When capillary suction was ended, the surface of the specimens was ground on a rotating Streuer polishing machine, ensuring that any surface effect, e.g. unwanted carbonation, was removed. Grinding was also necessary because the diameter of the specimens could not exceed 14 mm in order to fit into the measuring cell in the calorimeter that was used. Because of this, the diameter was reduced somewhat by grinding, to ensure that the diameter of the specimens was about 13.5 mm. This grinding was more than sufficient to eliminate the possible small, unwanted carbonation on some of the uncarbonated materials. After grinding, the specimens were individually placed in airtight test tubes and immediately sent by mail to the laboratory where the measurements of freezable water were carried out.

8.3 Test method

Ice formation during freezing, and melting during thawing, were measured using a low-temperature micro-calorimeter. The tests were carried out using a Calvet micro-calorimeter (brand SETARAM) at the Aalborg Portland Research and Development Centre (RDC) in Aalborg, Denmark. The apparatus and the principal of the test method is described in le Sage de Fontenay & Sellevold (1980).

Before measurement was started, the surface dry weight was measured by weighing a capillary-saturated specimen that had been wiped off with a wet cloth. After sprinkling a few milligrams of AgI powder on the surface of the specimen, it was placed in the calorimeter, see Figure 8.2. The specimens were sprinkled with AgI to minimise the effect of supercooling, i.e. when water does not freeze until a temperature below the normal freezing point. The effect of AgI in minimising the effect of supercooling has, for example been reported by Sellevold & Bager (1980). In their paper, they report a possible super-cooling of more than –10 °C if not using the AgI powder. Kaufmann (2000) reports a less severe supercooling of about –6 °C in experiments carried out without any nucleating agent. The effect of the AgI powder is that it provides nucleation points for the ice, thus minimising the supercooling.

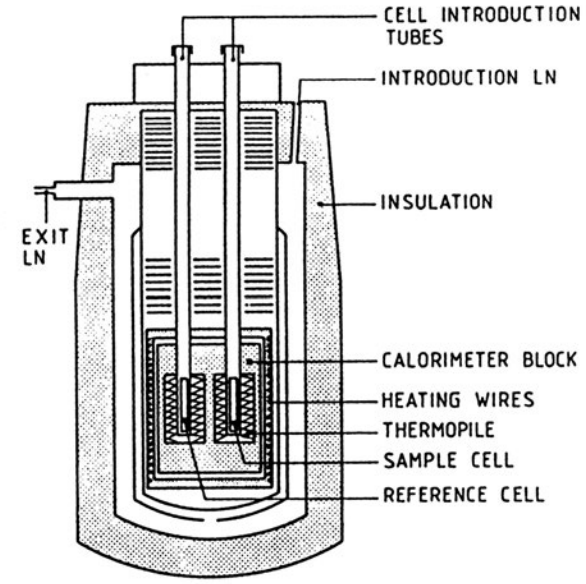

Figure 8.2 *Schematic diagram of the low-temperature Calvet micro-calorimeter. From le Sage de Fontenay & Sellevold (1980).*

With the specimen well inside the calorimeter, the measurement was started. The temperature was first lowered to about –60 °C at a cooling rate of 3.3 °C/hour, and then heated to temperatures above 0 °C at a heating rate of 4.1 °C/hour. The heat flow was

continuously measured during cooling and heating. From the heat flow, the apparent heat capacity, given as Joule/(gram surface dry material and degree Celsius) of the specimen was calculated. From this, the amount of ice formed as a function of temperature was calculated in accordance with the procedures described in le Sage de Fontenay & Sellevold (1980). The calculations allow for the temperature dependence of the heat of fusion as well as the temperature dependence of the heat capacity of the specimen; see le Sage de Fontenay & Sellevold (1980).

All calculations have been carried out by personnel at Aalborg Portland RDC in accordance with the increment method described in le Sage de Fontenay & Sellevold (1980). This method is based on some more or less incorrect assumptions, e.g. that both ice and water are at atmospheric pressure (which is not true after freezing has started). The method has, however, been used in numerous investigations using the low-temperature calorimeter technique since the mid 1970s; see the comprehensive work of Bager D. H., Sellevold E. J. and le Sage de Fontenay C. It was used here without any changes, in what was primarily a comparative test.

After the measurement was finished, the dry weight of the specimen was determined by drying at +105 °C.

8.4 Results

The results in the form of apparent heat capacity as a function of the calorimeter block temperature during cooling and heating are shown in Figures 8.3 to 8.7. According to Sellevold & Bager (1980), the calorimeter block temperature differs from the specimen temperature by some 0.4 - 0.8 °C during periods of small freeze/thaw activity. During periods of high freeze/thaw activity, the temperature lag could, according to them, reach several degrees. This can be confirmed in this investigation by studying the heating curves in Figure 8.3 to 8.7, which show melting until about +2 °C, which of course is an effect of the temperature lag between the specimen and the calorimeter block temperature.

The results presented are given as a function of the calorimeter block temperature and not as a function of the specimen temperature. This is a possible source of error since, as stated above, the temperature might differ somewhat between the calorimeter block and the specimen, especially at temperatures with high freeze/thaw activity. However, these possible errors are minimised by the fact that the freezable water content is not calculated at temperatures where there is high freeze/thaw activity. The large ice formation and melting peaks are at temperatures around and above –5 °C. Calculating freezable water contents at this temperature would probably bring large errors. However, since in this investigation the freezable water content is calculated at a lower temperature (–7 °C), when the freeze/thaw activity is relatively low, the possible errors are assumed to be minimised. The fact that this is primarily a comparative test, comparing the properties of carbonated and uncarbonated material, and not a search for absolute values, makes the

possible errors less important since the same assumptions are made for both uncarbonated and carbonated materials.

From the apparent heat capacity results, the freezable water contents at –7 °C, –10 °C, –15 °C, –20 °C, –25 °C, –35 °C and –55 °C have been calculated both during freezing and thawing (Table 8.1 and Table 8.2).

The freezable water content as a function of temperature during freezing (cooling) and thawing (heating) is shown in Figures 8.8 - 8.12 for all the tested uncarbonated and carbonated mortar qualities.

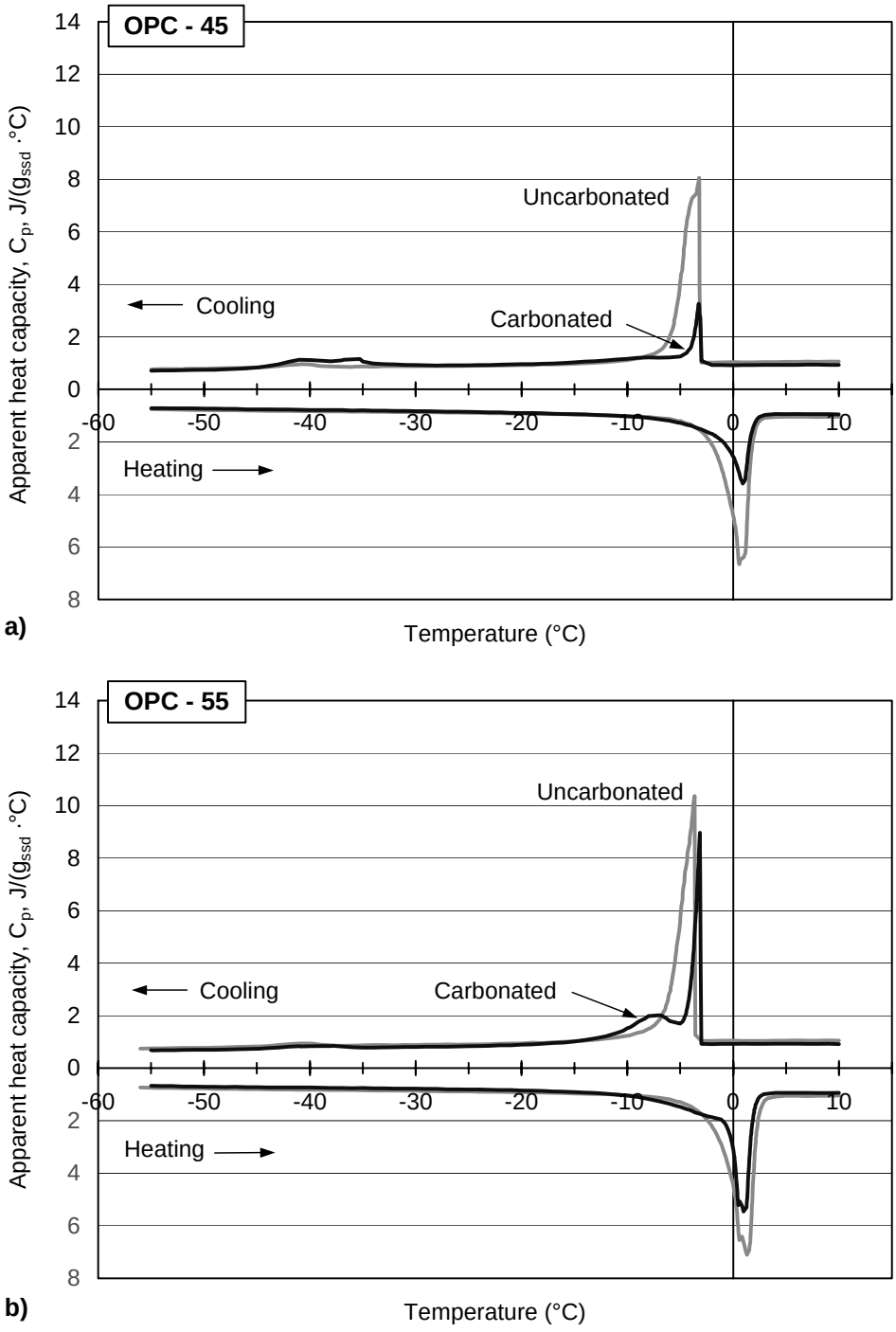

Figure 8.3 *Apparent heat capacity as a function of calorimeter block temperature during cooling (←) and heating (→) for mortar with only OPC as the binder and with different w/b-ratios. a) w/b-ratio 0.45, b) w/b-ratio 0.55*

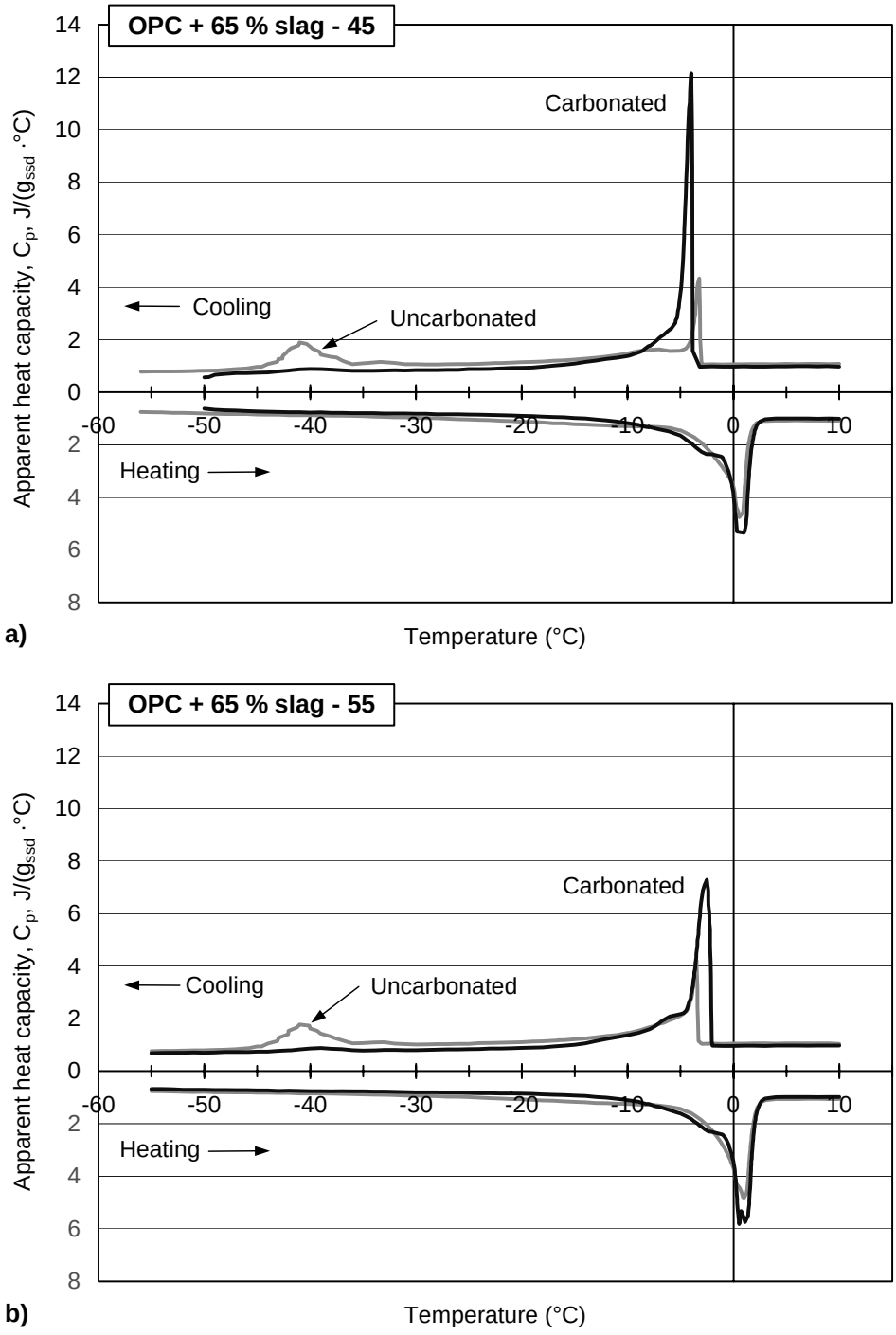

Figure 8.4 *Apparent heat capacity as a function of calorimeter block temperature during cooling (←) and heating (→) for mortar with 65 % slag as part of the binder and with different w/b-ratios. a) w/b-ratio 0.45, b) w/b-ratio 0.55*

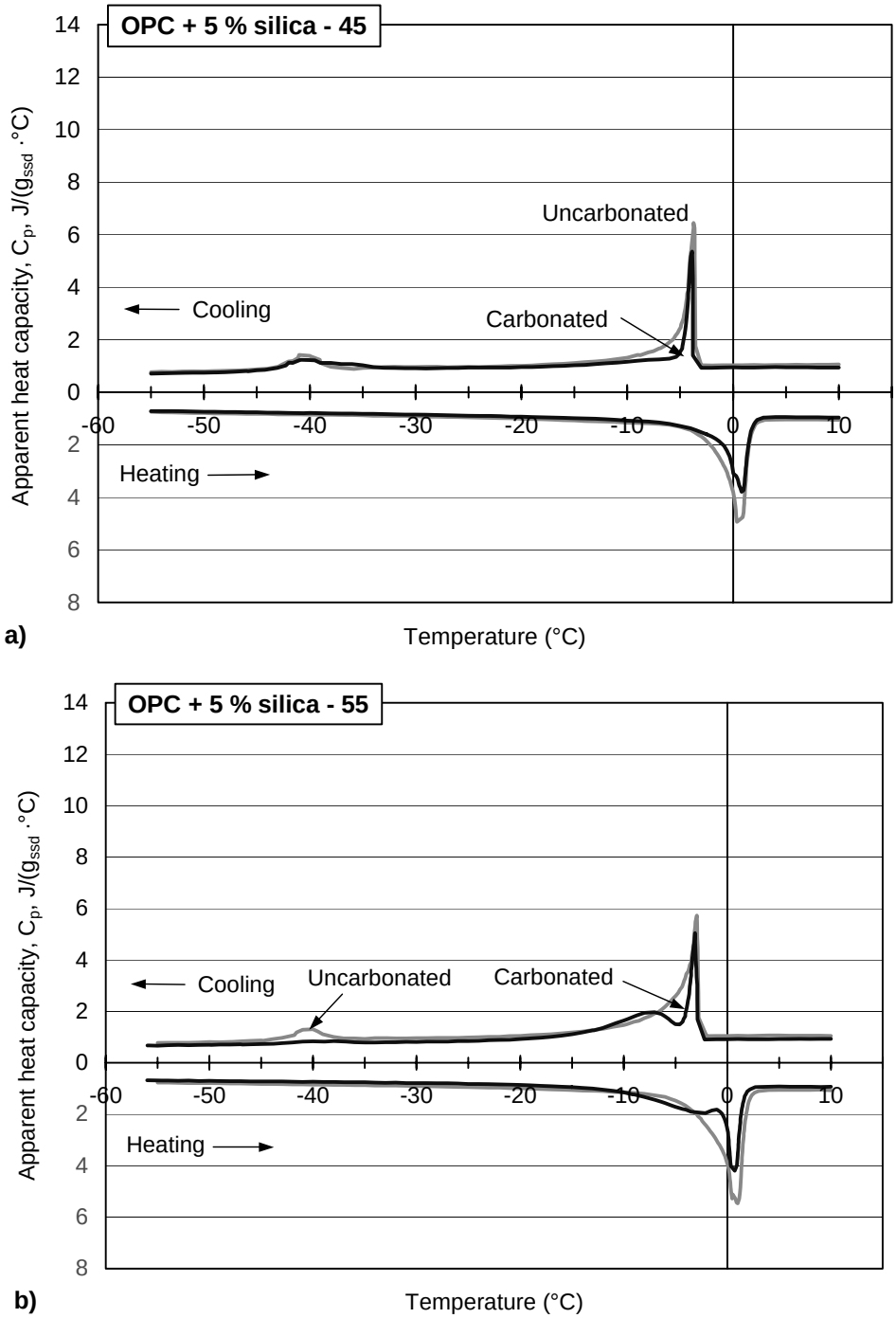

Figure 8.5 *Apparent heat capacity as a function of calorimeter block temperature during cooling (←) and heating (→) for mortar with 5 % silica as part of the binder and with different w/b-ratios. a) w/b-ratio 0.45, b) w/b-ratio 0.55*

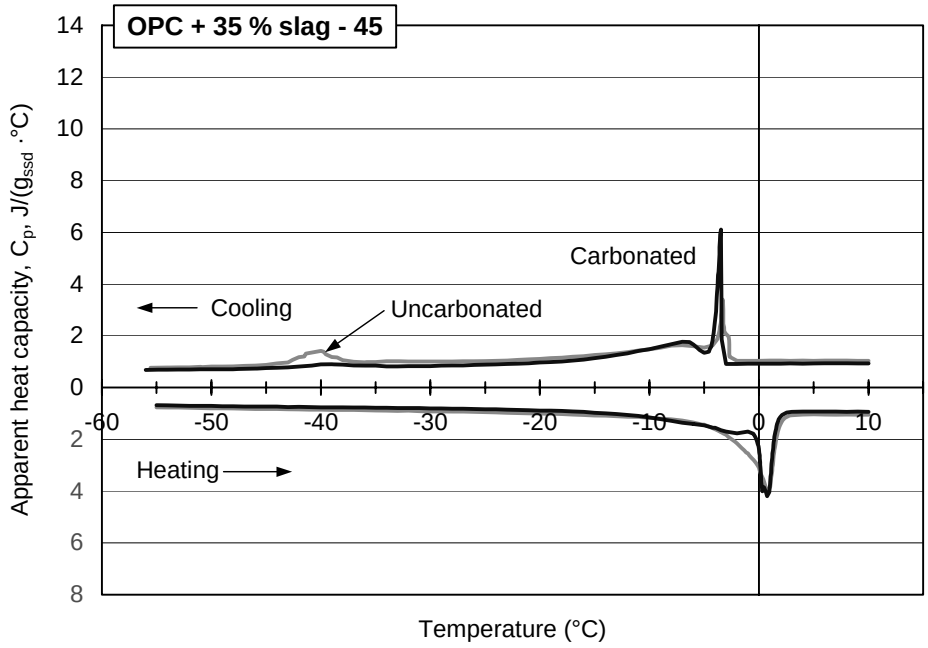

Figure 8.6 *Apparent heat capacity as a function of calorimeter block temperature during cooling (←) and heating (→) for mortar with 35 % slag as part of the binder, w/b-ratio of 0.45.*

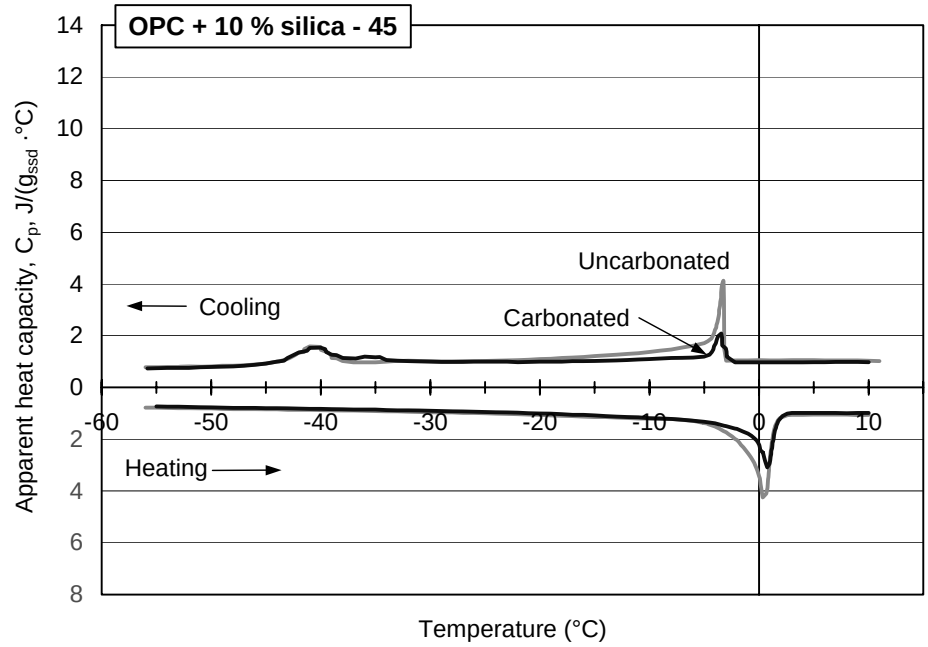

Figure 8.7 *Apparent heat capacity as a function of calorimeter block temperature during cooling (←) and heating (→) for mortar with 10 % silica as part of the binder, w/b-ratio of 0.45.*

Table 8.1 *Measured evaporable water content (W_e) and calculated freezable (W_f) water content during cooling.*

Mortar quality		W_e	W_f (mg_{ice}/g_{dry}) cooling						
		mg/g_{dry}	-7	-10	-15	-20	-25	-35	-55°C
OPC-45	**Uncarbo.**	96	44.6	47.2	50.1	50.3	52.3	52.7	58.7
	Carbo.	70	8.9	11.7	16.2	17.9	20.7	25.6	38.3
OPC-55	**Uncarbo.**	107	50.6	54.8	59.5	60.1	62.7	63.3	68.1
	Carbo.	72	26.7	36.1	42.9	44.6	46.8	47.6	52.3
OPC + 65 % sl-45	**Uncarbo.**	108	12.5	17.8	24.7	27.9	32.2	38.6	63.0
	Carbo.	88	39.1	46.4	53.6	55.7	58.2	58.9	62.5
OPC + 65 % sl-55	**Uncarbo.**	105	16.2	21.9	28.8	31.9	36.3	41.9	65.4
	Carbo.	85	41.7	48.0	54.8	56.4	59.0	60.0	66.4
OPC + 5 % si-45	**Uncarbo.**	105	23.4	28.2	33.1	34.6	37.4	39.9	51.4
	Carbo.	78	12.5	15.4	19.5	21.4	24.2	28.6	42.9
OPC + 5 % si-55	**Uncarbo.**	111	30.1	37.2	44.0	46.6	50.0	52.6	62.8
	Carbo.	69	19.9	30.1	38.8	41.5	44.4	45.7	49.7
OPC + 35 % sl-45	**Uncarbo.**	99	12.0	17.5	25.1	28.6	32.6	36.9	51.6
	Carbo.	68	15.7	22.4	30.7	33.3	36.5	37.9	42.9
OPC + 10 % si-45	**Uncarbo.**	112	13.1	17.3	23.5	26.4	30.0	34.0	49.6
	Carbo.	91	6.3	8.1	11.5	12.7	16.0	22.4	42.5

Table 8.2 *Measured evaporable water content (W_e) and calculated freezable (W_f) water content during heating.*

Mortar quality		W_e	W_f (mg_{ice}/g_{dry}) heating						
		mg/g_{dry}	-7	-10	-15	-20	-25	-35	-55°C
OPC-45	**Uncarbo.**	96	50.6	51.7	55.0	55.7	58.3	59.5	60.7
	Carbo.	70	28.5	30.5	33.9	35.6	38.2	39.5	40.5
OPC-55	**Uncarbo.**	107	61.7	63.0	66.7	67.5	70.3	71.3	70.1
	Carbo.	72	42.8	45.9	50.1	51.6	54.2	55.2	57.0
OPC + 65 % sl-45	**Uncarbo.**	108	40.2	43.4	50.9	55.1	60.5	64.6	68.5
	Carbo.	88	51.1	55.3	61.3	62.8	65.8	66.7	67.5
OPC + 65 % sl-55	**Uncarbo.**	105	45.0	47.8	55.3	59.1	64.0	67.2	69.3
	Carbo.	85	53.7	57.0	62.6	63.8	66.8	67.9	69.9
OPC + 5 % si-45	**Uncarbo.**	105	38.5	40.8	45.9	48.2	51.7	53.8	55.1
	Carbo.	78	29.0	31.0	35.8	38.0	41.1	43.4	44.6
OPC + 5 % si-55	**Uncarbo.**	111	49.7	52.3	57.5	59.6	63.2	65.3	65.7
	Carbo.	69	35.0	39.5	45.1	46.6	49.2	49.8	48.9
OPC + 35 % sl-45	**Uncarbo.**	99	36.5	39.2	44.5	46.6	50.2	52.4	54.3
	Carbo.	68	30.7	34.7	40.4	42.2	45.1	46.4	48.3
OPC + 10 % si-45	**Uncarbo.**	112	32.5	34.6	40.7	43.8	48.0	51.1	53.4
	Carbo.	91	23.1	26.0	31.8	34.7	38.6	41.7	44.6

The non freezable water content, W_{nf}, can be calculated by subtracting the freezable water content W_f from the evaporable water content W_e.

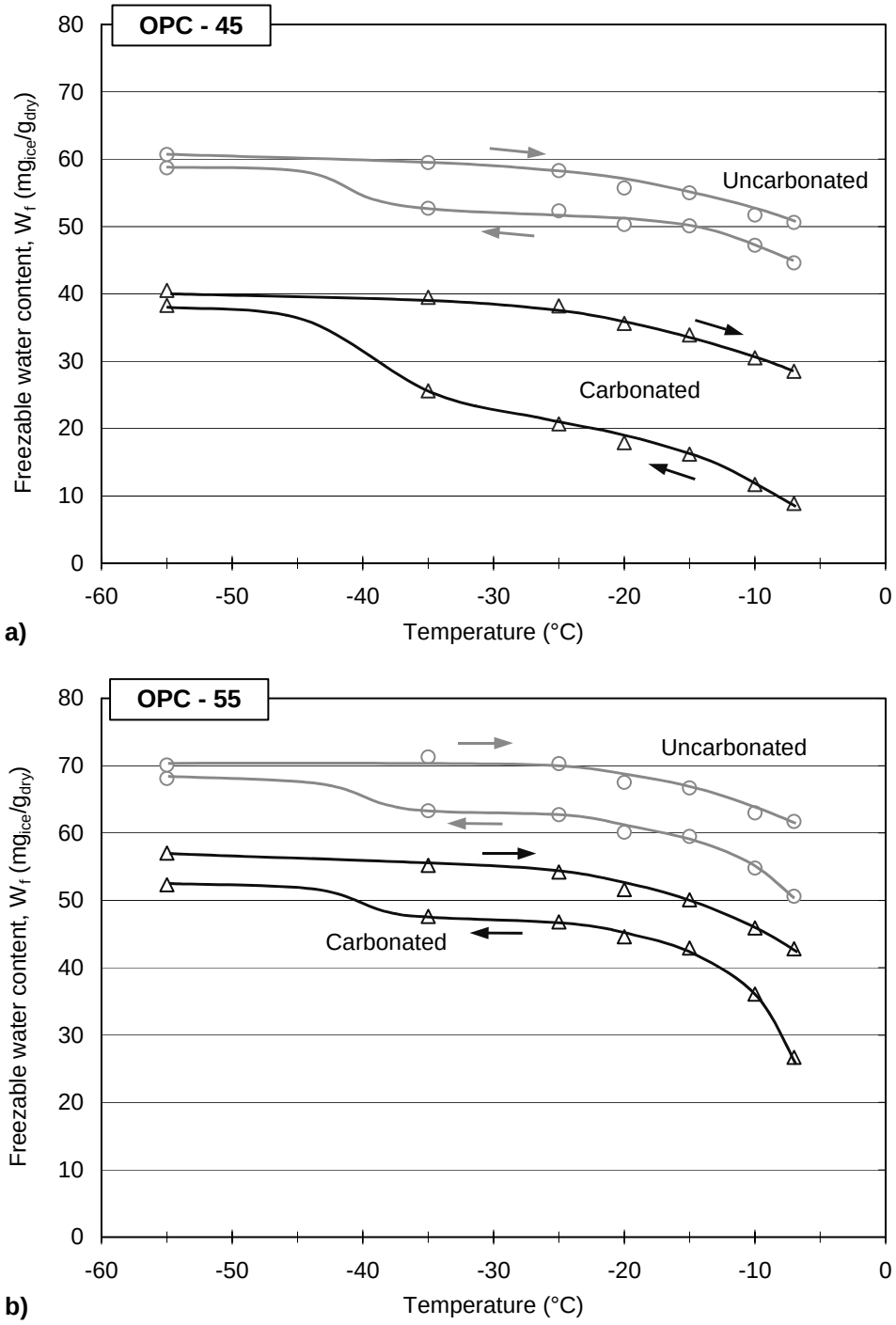

Figure 8.8 *Freezable water content as a function of temperature during cooling (←) and heating (→) for mortar with OPC alone as the binder and with different w/b-ratios. a) w/b-ratio 0.45, b) w/b-ratio 0.55*

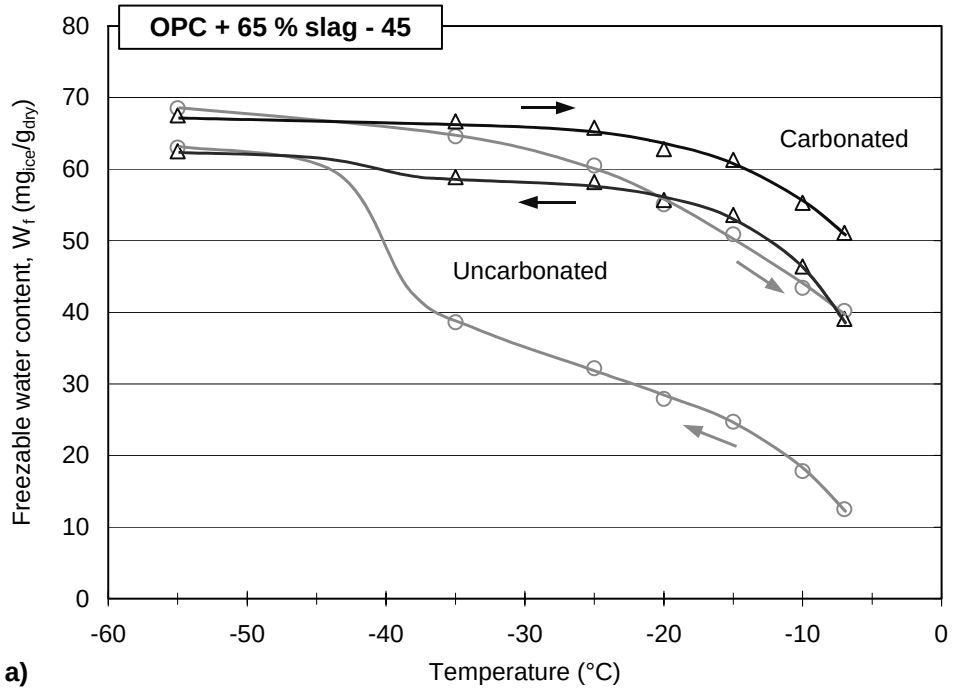

a)

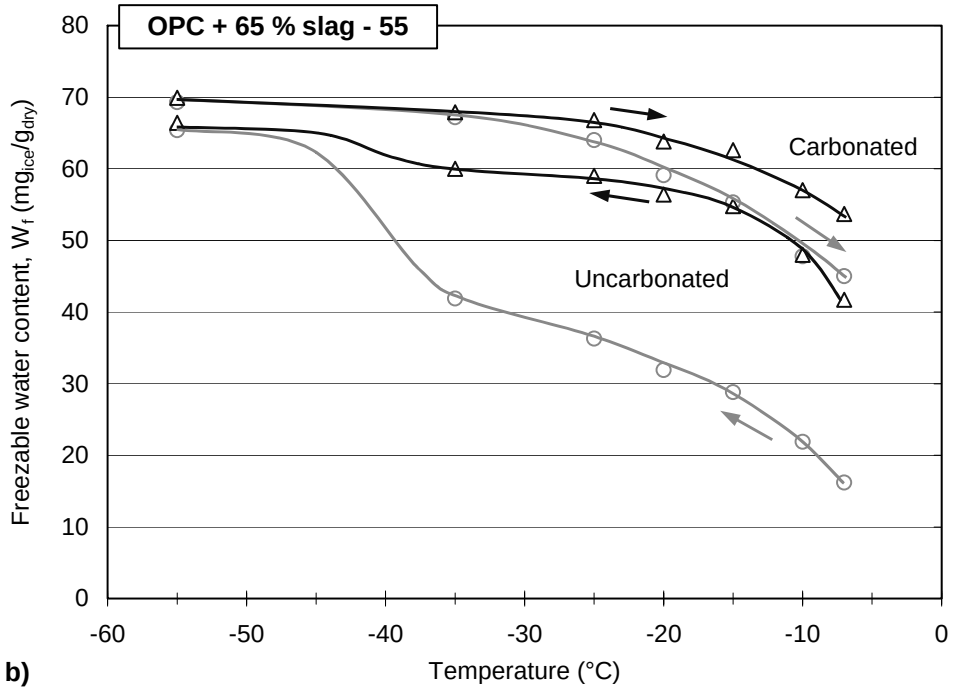

b)

Figure 8.9 *Freezable water content as a function of temperature during cooling (←) and heating (→) for mortar with 65 % slag as part of the binder and with different w/b-ratios. a) w/b-ratio 0.45, b) w/b-ratio 0.55*

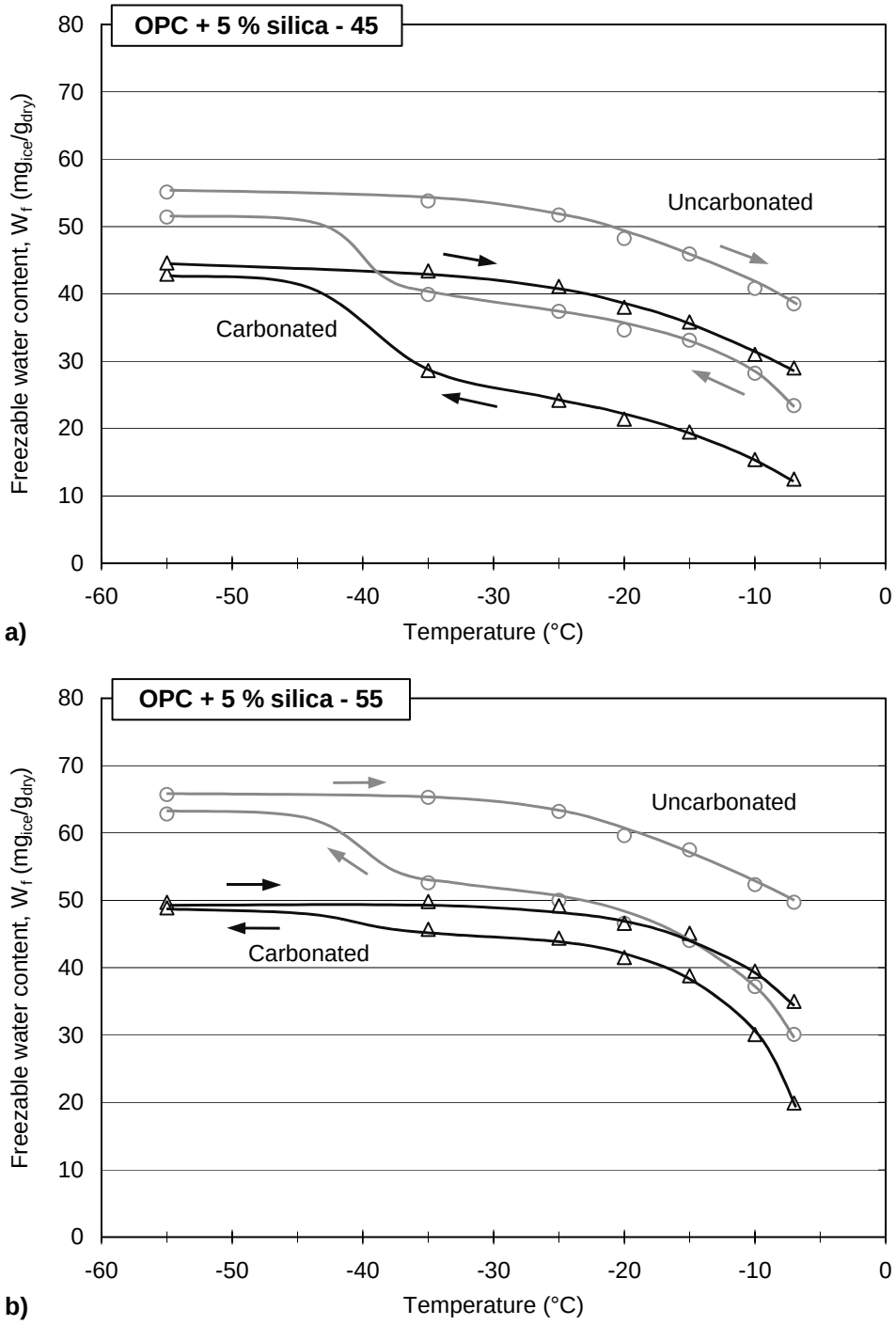

Figure 8.10 *Freezable water content as a function of temperature during cooling (←) and heating (→) for mortar with 5 % silica as part of the binder and with different w/b-ratios. a) w/b-ratio 0.45, b) w/b-ratio 0.55*

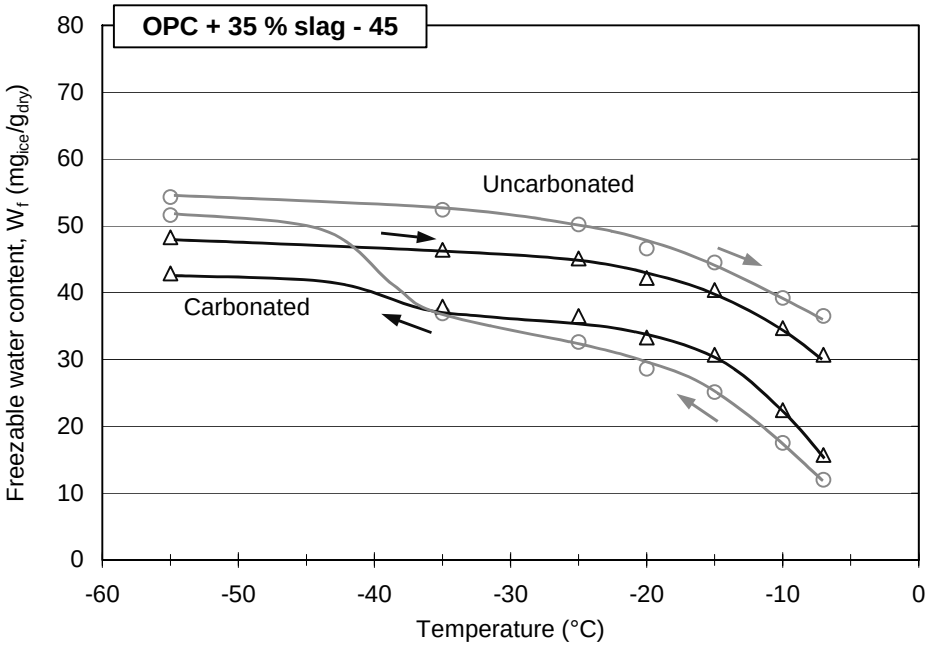

Figure 8.11 *Freezable water content as a function of temperature during cooling (←) and heating (→) for mortar with 35 % slag as part of the binder, w/b-ratio of 0.45.*

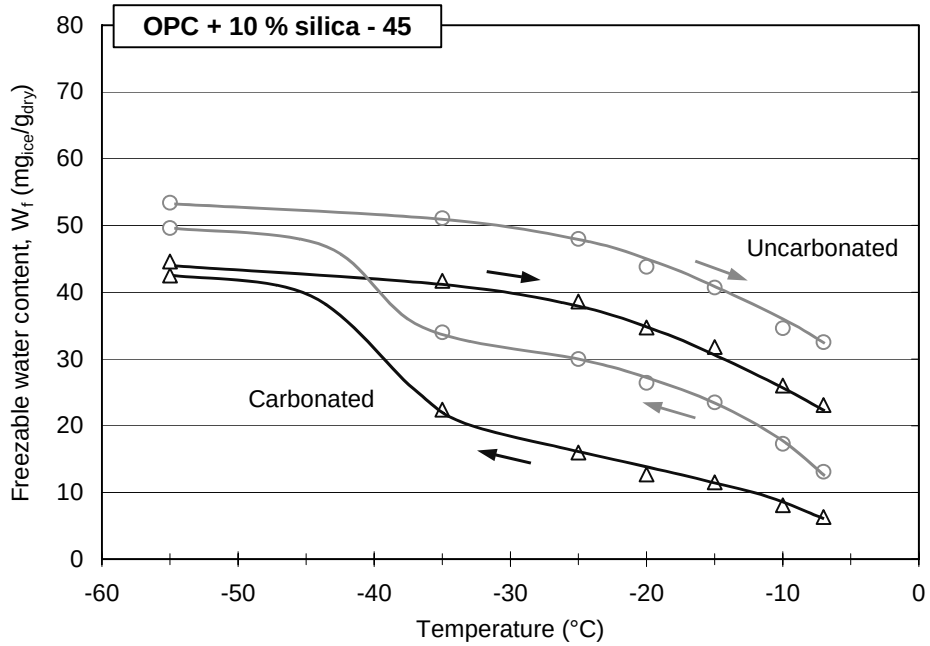

Figure 8.12 *Freezable water content as a function of temperature during cooling (←) and heating (→) for mortar with 10 % silica as part of the binder, w/b-ratio of 0.45.*

8.5 Discussion

8.5.1 General discussion of interpretation of the results

The low-temperature calorimeter (LTC) measurements carried out in this investigation provide information about the freezable and non-freezable water content at different temperatures during freezing and thawing. However, the amount of freezable and non-freezable water at different temperatures varies, depending on the constitution of the pore structure of the material. The LTC measurements therefore also provided information on the pore structure. From these measurements, it is possible to calculate a full pore size distribution; see e.g. Sellevold & Bager (1980). However, this requires a large number of assumptions, e.g. a certain pore geometry (often a circular cylindrical model is chosen) and some assumptions about the thermodynamics acting during freezing and thawing. These assumptions lead probably to very coarse approximations, and in turn to a more or less incorrect pore size distribution. Since, in the present author's view, it is possible to elucidate much valuable information from the LTC measurements without too advanced calculations, no such calculation of pore size distributions is made here. Instead, it is the comparisons between carbonated and uncarbonated materials that are of primary interest, and not the absolute values of pore size distribution.

The following is a brief discussion of the information about the pore structure that can be found from the measurements carried out in this investigation, and how the results are interpreted.

Hysteresis between ice formation during cooling and ice melting during heating

From Figures 8.3 - 8.7 showing the apparent heat capacity as a function of temperature, it can be seen that there is a clear hysteresis between the freezing (cooling) curve and the thawing (heating) curve. The cause of this hysteresis is not fully understood, although it is generally assumed to be an effect of pore geometry. For example, Fagerlund (1974) presents an explanation for the freezing/thawing hysteresis. Fagerlund's explanation is similar to the 'ink-bottle' theory explaining hysteresis for vapour absorption and desorption.

The hysteresis during freezing and thawing is assumed to be a result of the geometry of the pore structure; see Figure 8.13, redrawn from Fagerlund (1974). The figure shows a hypothetical pore structure with different pore sizes, and the corresponding non-freezable water content during freezing and thawing.

Consider the pore structure in Figure 8.13. When the temperature is lowered, ice is first formed, after some supercooling, in the largest pore 'A'. As the temperature is further lowered, ice is subsequently formed in pore 'B'. Since pore 'D' is of the same size as pore 'B', this water would also freeze if it had been in contact with ice. This is, however, not the case, since the water in pore 'D' is isolated from the ice in pore 'B' by the water in the smaller pore 'C'. The water in pore 'D' will be supercooled and not be able to freeze until the temperature has been lowered sufficiently for the water in pore 'C' to freeze, when the

water in pore ‘D’ will freeze simultaneously with the water in pore ‘C’. This freezing behaviour presumes supercooling of water, and that water has to be in contact with ice, or other nucleating agent, to be able to form to ice. If pore ‘C’ is very narrow so that ice cannot be formed, supercooled water will freeze by homogenous nucleation at about –40 °C; see Langham & Mason (1958). The freezing curve as a result of the stepwise freezing in the pores can be seen in the right-hand part of Figure 8.13.

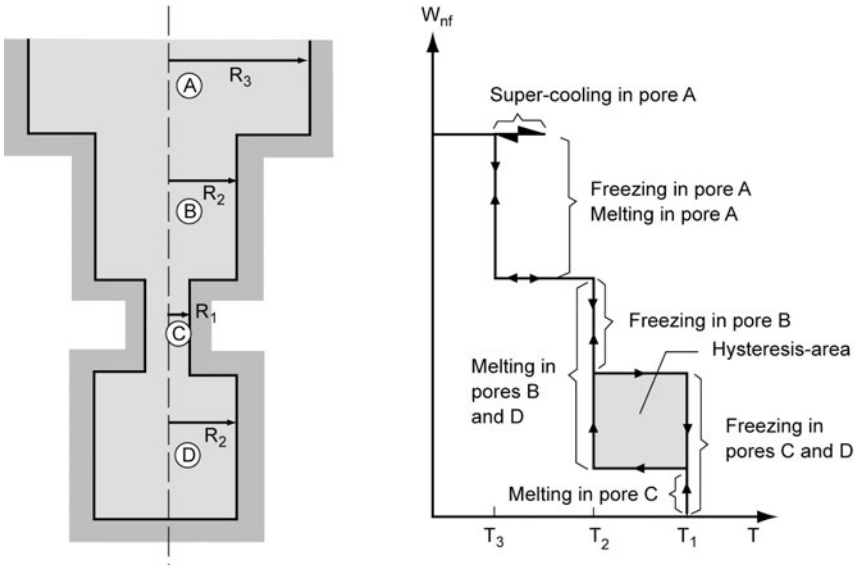

Figure 8.13 *Hypothetical freezing and thawing hysteresis in an ink-bottle pore. Redrawn from Fagerlund (1974).*

During thawing, it is assumed that ice melts at a temperature corresponding to each individual pore size, regardless of the pore sizes of the neighbouring pores. Since the ice first melts in the smallest pores, the ice in pore ‘C’ will melt first, followed by simultaneous melting in pores ‘B’ and ‘D’, after which the ice in pore ‘A’ will melt as the temperature is further raised. As can be seen in the right-hand part of Figure 8,13 the water in pore ‘D’ melts at a higher temperature, T_2, than that at which it was frozen, T_1, which thereby explains the hysteresis between the freezing and thawing curves.

A mechanism similar to the one presented in Fagerlund (1974) was proposed by Sellevold & Bager (1980) and Sellevold & Bager (1985), in which a hypothesis was presented where the spreading of ice is thought of as a moving front from the specimen surface and inwards. According to their hypothesis, the spreading of the ice front in a pore system with variable cross-sections is controlled by the pore necks, while the melting is controlled by the actual sizes of the pores. This hypothesis is in principle the same as the explanation put forward in Fagerlund (1974) and the ‘ink bottle’ theory explaining the hysteresis between desorption and absorption isotherms.

In reality, the pore structure of cement-based materials is of course not as simple as is shown in Figure 8.13. The real pore structure of a cement-based material is more likely to be a chaotic mix of different pore shapes and sizes caused by the different hydration products. In recent years, the use of Environmental Scanning Electron Microscopy (ESEM) has made it possible to study the structure of the hydration products at a nano-level without first subjecting the material to detrimental preconditioning procedures, e.g. drying. For example, Stark & Möser (2002) present an investigation of the microstructure of Portland cement paste using ESEM; see Figure 8.14. The ESEM results that they show indicate a various and complex structure far from the normal convenience-based assumptions about circular cylindrical pores.

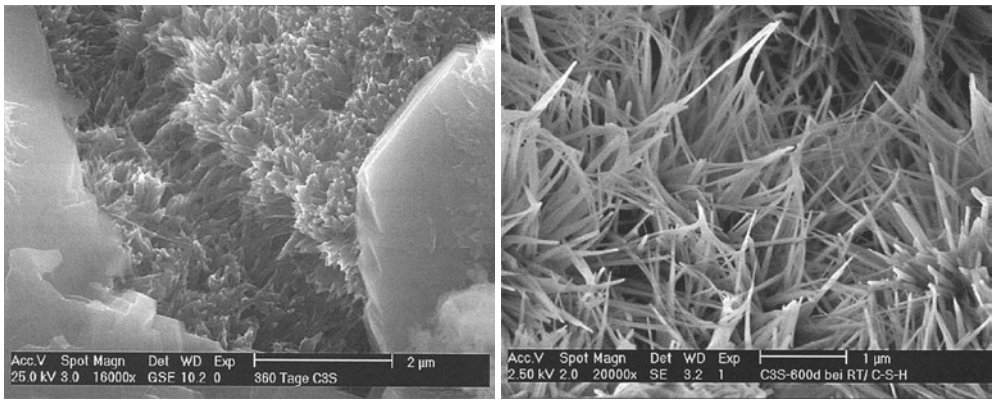

Figure 8.14 *Photos of hydrated C_3S. To the left: C_3S hydrated for 360 days - CSH phases (needles) and calcium hydroxide (crystals). To the right: C_3S hydrated for 600 days - needle-like CSH phases. From Stark & Möser (2002).*

Even though the real pore structure is certainly not made up of cylindrical pores of different sizes, it may be assumed that the real pore structure, although much more complex, consists of pore spaces of different sizes, and that there might be restrictions and 'dead ends' as in the hypothetical pore structure shown in Figure 8.13. If this is the case, the above possible causes of the hysteresis might also be valid for pore structures of real cement-based materials.

An example of the hysteresis between ice formation during freezing, and melting during thawing, is shown in Figure 8.15. The figure shows the non-freezable water content as a function of temperature during freezing and thawing for carbonated and uncarbonated mortar with 65 % slag as part of the binder and with a w/b-ratio of 0.45.

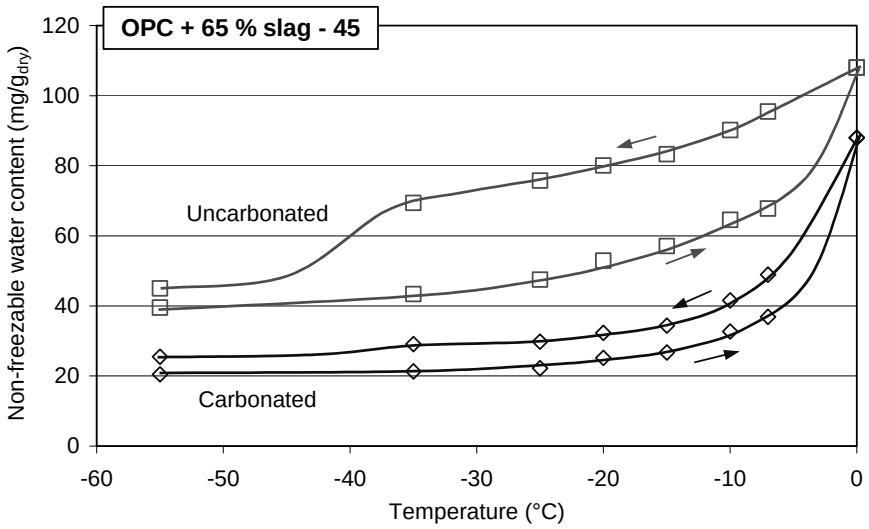

Figure 8.15 *Non-freezable water content as a function of temperature during cooling (←) and heating (→) for carbonated and uncarbonated mortar with 65 % slag as part of the binder, w/b-ratio of 0.45.*

From the figure, it can be seen that the hysteresis between cooling and heating is much more significant for the uncarbonated material than for the carbonated. This implies that carbonation of this material with high contents of slag as part of the binder leads to a more 'open' pore structure, with few restrictions in the pore system.

Another technique used for evaluating the pore structure of a material is to measure sorption isotherms, i.e. the water content of a material in equilibrium with different relative humidities. Sorption isotherms are divided into *Desorption* (stepwise drying from a wet state) and *Absorption* (stepwise wetting from a dry state). From these measurements, information about the constitution of the pore structure of the material can be obtained. Normally, this technique too leads to significant hysteresis. In the literature, there are several different theories explaining the hysteresis between the desorption and absorption isotherms. Some of these theories are discussed in Ahlgren (1972). One of the theories, the 'ink-bottle' theory, is similar to the theory discussed above about restrictions in the pore system leading to the observed hysteresis between non-freezable water content during freezing and thawing.

According to the 'ink-bottle' theory, the pore structure may contain large pores that are connected to the rest of the pore structure through smaller pores, see Figure 8.16. Assuming that both the large and the small pores are water filled at the start of desorption, the large pores will not be emptied until the relative humidity is low enough for the small pores to be emptied. During absorption, on the other hand, the small pores will be filled first at a lower relative humidity and the larger pores later at a higher humidity. This gives isotherms as in the illustration in Figure 8.16.

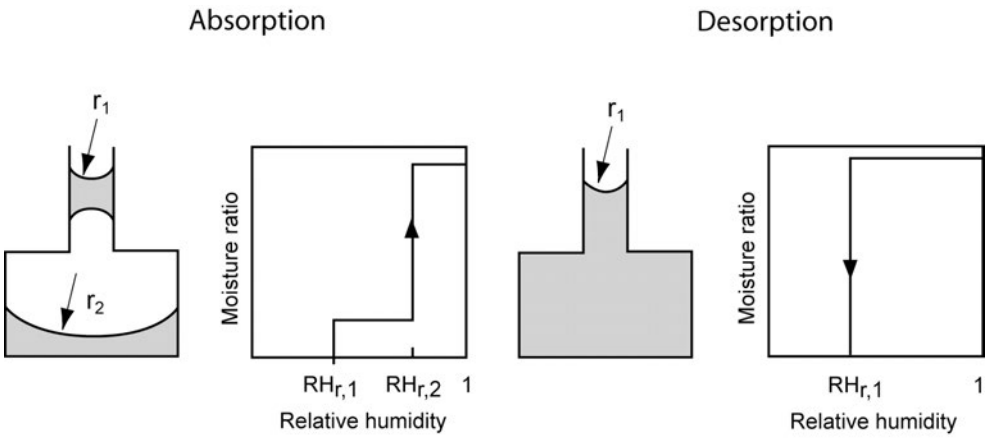

Figure 8.16 *'Ink-bottle' pore, and its absorption (left) and desorption (right) isotherms.*

The 'ink-bottle' theory and the theory of restrictions in the pore system discussed above are similar. During freezing of a saturated material, water in a pore isolated by a smaller pore may not freeze until the temperature is low enough for the water in the smaller pore to freeze. During thawing, however, ice will melt first in the small pores, but the ice in the larger pore will not melt until a higher temperature. Likewise for the sorption isotherm, during desorption water may not evaporate in the larger pore until the relative humidity is low enough for the water in the smaller pore to evaporate. During absorption, however, the smaller pore will first be filled at a low relative humidity, followed by filling of the larger pore at a high relative humidity.

As can be seen, there are great similarities between the mechanisms explaining the hysteresis during cooling-heating and during desorption-absorption. This implies that the results from measurements (on the same material) of the freezable water content at different temperatures and of the water content at different relative humidities would give comparable results, not in absolute terms, but with respect to the appearance of the cooling-heating and desorption-absorption curves.

For comparison, sorption isotherms were measured for the same carbonated and uncarbonated materials for which the non-freezable water content during cooling and heating was shown in Figure 8.15. The sorption isotherms for the carbonated and uncarbonated materials are shown in Figure 8.17. The measurements were carried out using an advanced sorption balance (DVS-1000) at the Division of Building Materials at Lund Institute of Technology. The apparatus and the procedure used is described in Johannesson & Utgenannt (2001). The sorption isotherms shown in Figure 8.17 were measured on crushed samples from initially saturated specimens conditioned in the climate chambers as described in Chapter 5. After 14 months of conditioning, the specimens were capillary-saturated for about 15 months, as described in Chapter 6, before the measurements were started. Three measurements were made for carbonated material, starting at RH = '1' going down to RH = '0' and up to RH = '0.4', followed by two measurements starting at

RH = ‘1’ going down to RH = ‘0’ and up to RH = ‘1’ again. For uncarbonated material, two measurements according to the first interrupted ‘loop’ and one measurement according to the full ‘loop’, were made.

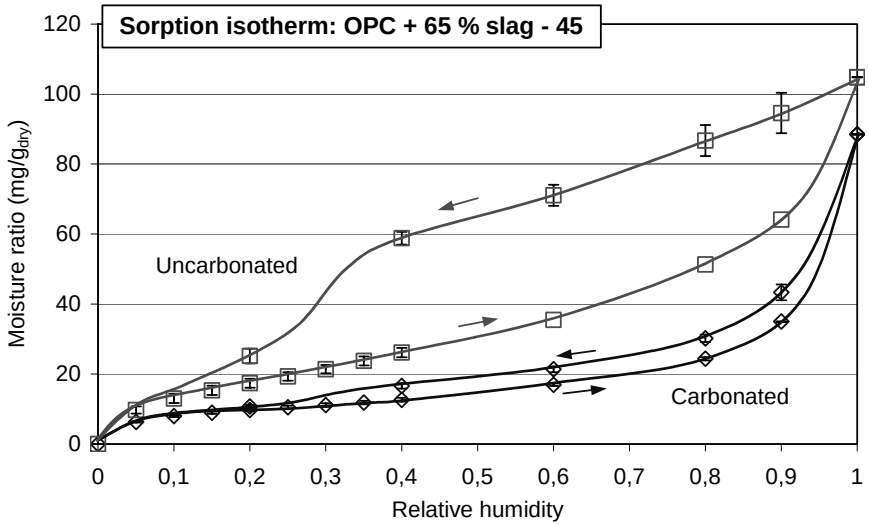

Figure 8.17 *Moisture ratio as a function of relative humidity during desorption (←) and absorption (→) for carbonated and uncarbonated mortar with 65 % slag as part of the binder, w/b-ratio of 0.45.*

There is a similarity between the sorption isotherms in Figure 8.17 and the non-freezable water content from the same materials shown in Figure 8.15. Both methods show substantial hysteresis for the uncarbonated material. For the carbonated material, on the other hand, the hysteresis between the desorption-absorption and cooling-heating curve is less apparent. The great similarity between the desorption-absorption isotherms and the non-freezable water content during cooling and heating implies similar mechanisms causing the hysteresis in the two methods. A more thorough comparison between results from sorption measurements and LTC measurements would be of great interest, since both techniques provide a means of investigating the constitution of the pore structure. It was, however, not an aim of the present investigation to compare different techniques for evaluation of the pore structure.

The similarity in results strengthens the interpretation that the hysteresis between the cooling and heating curves is a result of restrictions in the pore system, as suggested by Fagerlund (1974) and Sellevold & Bager (1980). Consequently, when interpreting the results from this investigation, the existence of hysteresis or changes in hysteresis due to carbonation is explained by the existence of restrictions in the pore system and by alterations of the ‘restrictivity’ of the pore structure due to carbonation. This means that hysteresis is interpreted here as an indication of a pore system with a considerable amount of restricting pore necks, hindering a continuous spread of the ice front. Small hysteresis,

on the other hand, is interpreted as an indication of a pore system with few pore necks, resulting in a continuous spread of the ice front. This is valuable information when evaluating the properties of the pore structures of the different materials.

Appearance of the apparent heat capacity curve

For most materials there is, during cooling, an initial ice formation at temperatures around –5 °C, during which the water in the large pores is frozen. The initial ice formation 'peak' is a result of supercooling of water, i.e. all water in pores large enough for ice to form is formed simultaneously as soon as the first ice formation takes place, normally above or around –5 °C if a nucleation agent, such as AgI, is used.

After the initial ice formation, there are normally one or two more ice formation peaks during cooling. These peaks are, according to Sellevold & Bager (1980), indications of the existence of restricting pore necks hindering the spread of the ice front; see discussion about the hysteresis between ice formation and melting above. Restrictions in the pore system may lead to water being 'trapped' in relatively large pores in which the water would be frozen if the restricting pore necks did not exist. At some temperature below the freezing point of the water trapped by the restricting pore necks, the temperature is low enough for ice formation to take place in pores with the size of the restricting pore necks. At this temperature, the unfrozen trapped water will immediately freeze, resulting in an ice formation peak. In this investigation, a second ice formation peak around –40 °C can be observed for several materials. Furthermore, as was mentioned above, supercooled water cannot exist below about –40 °C, and so it freezes by homogeneous nucleation; see Langham & Mason (1958).

Evaluation of the pore structure

During thawing, ice is assumed to melt as determined by the size of the pores, and not as determined by the size of the pore necks, which is assumed to be the case during freezing. The constitution of the pore structure is therefore evaluated from the thawing curve. As the temperature increases from a frozen state, ice melts first in the smallest pores and as the temperature increases the melting continues in larger and larger pores. When evaluating the pore system, it is the non-freezable water content, W_{nf}, that is of primary interest, as the non-freezable water content provides information about the amount of water that is held in pores small enough for the water to remain unfrozen at a certain temperature. However, when evaluating the changes in material properties that are important with respect to freeze/thaw durability, it is the freezable water content that is of primary interest. This is because it is the freezable water that may cause damage due to frost attack. When evaluating the freezable water content, it is important that all studied materials have reached the same moisture state. Here, all materials were subjected to seven days of capillary suction, ensuring that 'all' gel and capillary pores were water-filled at test start.

As was mentioned above, no pore size distribution calculations dividing the pore structure into a large number of pore sizes were carried out here. Instead, the porosity was divided into two categories; coarse and fine pores, which should correspond to capillary and gel

porosity. It is here assumed that, depending on whether the water is frozen or unfrozen at –10 °C, the pore structure can be divided into fine and coarse pores. This means that, during thawing, the unfrozen water at –10 °C is held in pores belonging to the fine pore system, mainly consisting of what might be called gel pores, while the frozen water at –10 °C is held in larger pores, mainly capillary pores. The temperature –10 °C has been chosen on the basis of a corresponding pore water meniscus of ~13 nm calculated pore size, assuming circular cylindrical pores, a liquid/vapour interface and assuming ice being under normal atmospheric pressure and pore water being under reduced pressure as described by the Kelvin equation. According to the Kelvin equation, 13 nm corresponds to a relative humidity of ~92%. Assuming a pore radius of around 13 nm as the dividing line between 'fine' and 'coarse' pores corresponds with what is found in the literature as the dividing line between small gel pores and larger capillary pores; see Table 8.3.

Table 8.3 *Classification of pore sizes, assuming circular cylindrical pores (radii).*

Pore class	**Romberg (1978)**	**Setzer (1997)**[1)]		**Oberholster (1987)**	
Capillaries	10^5 – 10 nm	**Macro**	$2 \cdot 10^6 – 60 \cdot 10^3$ nm	**Large**	$7.5 \cdot 10^3$ – 25 nm
		Meso	$60 \cdot 10^3 – 2 \cdot 10^3$ nm	**Medium**	25 – 5 nm
		Micro	$2 \cdot 10^3$ – 60 nm		
Gel pores	10 – 1 nm	**Meso**	60 – 2 nm	**Small gel capillaries**	5 – 1.2 nm
		Micro	<2 nm	**Micropores**	1.2 – 0.2 nm

[1)] Setzer (1997) expresses the pore radius as hydraulic radius. These values are here multiplied with 2 to represent pores with a circular cylindrical shape.

From the table, it can be seen that there are some differences in classification of pore sizes, depending on the author. However, since all models of the pore structure of cement-based materials are simplifications of a very complex structure, and since the pore size distribution in cement paste ranges from gel pores with a radius of less than 1 nm (10^{-9} m) to air pores with radius over 1 mm (10^{-3} m), the differences may be regarded as unimportant. Depending on author, the dividing zone between capillary pores and gel pores ranges from 5 nm to 60 nm. Assuming a dividing pore radii between small gel pores and larger capillary pores to be around 13 nm thus seems to be reasonable.

The validity of the division into fine and coarse pores based on the freezable and non-freezable water content at –10 °C during heating can further be validated by comparing the results found from these measurements with what could theoretically be expected. Powers formulated relations between the degree of hydration and w/c-ratio for uncarbonated cement pastes leading to the following equations for calculating the gel (P_{gel}) and capillary (P_{cap}) porosity in %:

$$P_{gel} \approx \frac{0.20 \cdot \alpha}{0.32 + w/c} \cdot 100 \qquad \text{[Eq. 8.1]}$$

$$P_{cap} \approx \frac{w/c - 0.39 \cdot \alpha}{0.32 + w/c} \cdot 100 \qquad \text{[Eq. 8.2]}$$

where

α	is the degree of hydration (between 0 and 1)	[-]
w	is the water content	[kg]
c	is the cement content	[kg]

Let us consider the uncarbonated and carbonated mortars with OPC alone as the binder and with w/b-ratios of 0.45 and 0.55 as examples. From the measurement of the freezable water content, the division of the porosity into fine and coarse parts based on the results at –10 °C during heating can be compared to what could be theoretically expected from the equations above.

In order to be able to calculate the gel and capillary porosity from Equations 8.1 and 8.2, the degree of hydration must be known. This investigation did not measure the degree of hydration. However, in the investigation described in Chapter 3, the degree of hydration was measured at different ages for micro-concrete made with the same cement type and with w/b-ratios of 0.45 and 0.55; (see Table 3.8 and Figure 3.24a). From these measurements it may be assumed that, for a mortar older than 20 months and with a w/b-ratio of 0.45, the degree of hydration is about 0.75, and for mortar with a w/b-ratio of 0.55 it is about 0.85. Assuming these degrees of hydration, the gel and capillary porosity can be calculated, see Table 8.4.

Table 8.4 *Calculated gel and capillary porosity in % for uncarbonated OPC pastes from Equations 8.1 and 8.2.*

Paste quality	Total porosity %	Gel porosity %	Capillary porosity %
OPC-45	40.0	19.5	20.5
OPC-55	44.6	19.5	25.1

These calculated values of gel and capillary porosity for uncarbonated cement paste can be compared with the division of porosity into fine and coarse porosity based on the calculated amount of ice formation at –10 °C during melting. The coarse porosity can be

calculated by Equation 8.3, dividing the volume of ice at –10 °C during melting by the specimen volume. The total porosity is calculated from Equation 8.4, dividing the volume of the evaporable water by the specimen volume. The fine porosity is thus the total porosity less the coarse porosity.

To be able to calculate the specimen volumes, the density of the dry materials has to be known. The dry densities for the materials tested here are found from measurements carried out on specimens used in the capillary suction test in Chapter 6, see Table 8.5.

Table 8.5 *Dry densities for uncarbonated and carbonated mortar with OPC alone as the binder and with different w/b-ratios. From the capillary suction test in Chapter 6.*

Mortar quality		**Density, dry kg/liter**
OPC-45	**Uncarbo.**	2.065
	Carbo.	2.208
OPC-55	**Uncarbo.**	2.036
	Carbo.	2.206

Assuming that the density of ice, at all temperatures below 0 °C, is 0.92 kg/liter, and that the density of water in all pores and at all temperatures is 1.0 kg/liter, the porosities can be calculated. As an example, the following is calculation of the coarse and total porosity for the uncarbonated mortar with a w/b-ratio of 0.45.

$$P_{coarse} = \left(\frac{Q_{dry} \cdot W_f}{\rho_{ice}} \Big/ \frac{Q_{dry}}{\rho_{material,dry}} \right) \cdot 100 = \left(\frac{0.0517}{0.92} \Big/ \frac{1}{2.065} \right) \cdot 100 = 11.6\,\% \qquad \text{[Eq. 8.3]}$$

$$P_{total} = \left(\frac{Q_{dry} \cdot W_e}{\rho_{water}} \Big/ \frac{Q_{dry}}{\rho_{material,dry}} \right) \cdot 100 = \left(\frac{0.096}{1} \Big/ \frac{1}{2.065} \right) \cdot 100 = 19.8\,\% \qquad \text{[Eq. 8.4]}$$

where

P_{coarse}	is the coarse porosity	[%]
P_{total}	is the total porosity	[%]
Q_{dry}	is the dry weight of a specimen	[kg]
W_f	is the freezable water content per dry weight of the material, Table 8.2	[$kg_{ice}/kg_{dry,material}$]
$\rho_{material,\,dry}$	is the density of the dry material	[kg/m^3]
ρ_{ice}	is the density of ice	[kg/m^3]
ρ_{water}	is the density of water.	[kg/m^3]

The fine porosity is calculated as the difference between the total and the coarse porosity.

Table 8.6 shows the calculated total porosity divided into fine and coarse porosity.

Table 8.6 *Calculated total, coarse and fine porosity based on the amount of evaporable and freezable water content.*

Mortar quality		Total porosity %	Fine porosity %	Coarse porosity %
OPC-45	**Uncarbo.**	19.8	8.2	11.6
	Carbo.	15.5	8.2	7.3
OPC-55	**Uncarbo.**	21.8	7.9	13.9
	Carbo.	15.9	4.9	11.0

It must be noted that the total porosity calculated here is considerably lower than the calculated total porosity for the same materials in Chapter 6; compare Table 8.6 with Table 6.2. This is explained by the fact that the total porosity in Chapter 6 was calculated from measurements on fully vacuum-saturated specimens, whereas here the specimens were subjected to only seven days of capillary suction. The total porosity calculated here should instead be compared with the porosity filled at the nick-point in Chapter 6, Table 6.2. Bearing in mind that the total porosity calculated here is the value of only one specimen, the comparison with the porosity filled at the nick-point corresponds fairly well.

The porosities given in Table 8.6 are valid for mortar, whereas the calculated theoretical porosities in Table 8.4 is valid for cement paste. To be able to compare the porosities, the porosities found for the mortars must be related to the paste content of the mortars. The porosity of the cement paste can be calculated by dividing the mortar porosities by the paste content. The paste content is calculated from the water and cement content in the mortar mixes; see Table 5.1 in Chapter 5. The paste content can be calculated from Equation 8.5. The percentage paste content for mortar with OPC and a w/b-ratio of 0.45 is shown below as an example, assuming a water density of 1000 kg/m^3 and a cement density of 3100 kg/m^3:

$$\frac{V_{paste}}{V_{mortar}} = \left(\left(\frac{m_{cem}}{\rho_{cem}} + \frac{m_{cem} \cdot w/c}{\rho_{water}} \right) \Big/ V_{mortar} \right) \cdot 100 = \left(\left(\frac{699.9}{3100} + \frac{699.9 \cdot 0.45}{1000} \right) \Big/ 1 \right) \cdot 100 = 54\,\% \quad \text{[Eq. 8.5]}$$

where

V_{paste}	is the volume of cement paste in the mortar mix	[m^3]
V_{mortar}	is the volume of the mortar mix	[m^3]
m_{cem}	is the mass of cement in the mix	[kg]
w/c	is the water/cement-ratio	[-]
ρ_{cem}	is the density of the cement	[kg/m^3]
ρ_{water}	is the density of water	[kg/m^3]

The same calculations for mortar with a w/b-ratio of 0.55 give a paste content of 50 %.

Dividing the porosities in Table 8.6 by the calculated paste contents gives the porosities in Table 8.7.

Table 8.7 *Porosities of the paste in the OPC mortars with w/b-ratios of 0.45 and 0.55, based on values in Table 8.6 and calculated paste contents.*

Mortar quality		Total porosity %	Fine porosity %	Coarse porosity %
OPC-45	**Uncarbo.**	36.7	15.2	21.5
	Carbo.	28.7	15.2	13.5
OPC-55	**Uncarbo.**	43.6	15.8	27.8
	Carbo.	31.8	9.8	22.0

Comparing the calculated fine and coarse porosities (Table 8.7) with the calculated theoretical gel and capillary porosities (Table 8.4) shows good correlation for the uncarbonated mortars. However, for the carbonated mortars, the correlation is (as could be expected) poor, as Power's equations assume uncarbonated paste. From the results, it can be seen that the measured total porosity for uncarbonated mortar is somewhat lower than, but in the same range as, the calculated total porosity. This can be explained by the fact that the total porosity was measured on specimens that had been capillary-saturated for only seven days, and not on vacuum-saturated specimens, which would lead to higher total porosity as was discussed above. A higher total porosity would also lead to better agreement between the fine porosity and the gel porosity.

The example above shows that the fine and coarse porosities seem to be in the same range as the gel and capillary porosities. This is an indication that the chosen limit, i.e. pores in which water is unfrozen at –10 °C during thawing, seems to be relevant. In other words, the amount of unfrozen water at –10 °C gives the fine pores, and pores in which water is frozen at this temperature give the coarse pores.

When evaluating the results from the low-temperature calorimetry measurements, it must be born in mind that a large number of assumptions have been made, e.g. that ice always exists at atmospheric pressure, that the pore water can be looked upon as pure water and that unfrozen water in a saturated specimen is at atmospheric pressure; see Bager & Sellevold (1986:1).

This investigation has assumed a rough division into fine and coarse pores. With this rough division, it is assumed that the errors due to the assumptions are relatively small. As has been stated before, this is primarily a comparative test between carbonated and uncarbonated material of the same mortar, and not a search for absolute values, which makes the results relevant despite the possible uncertainties.

8.5.2 Discussion of the results

From the results of the apparent heat capacity in Figures 8.3 - 8.7 and the calculated freezable water content (Tables 8.1 and 8.2), it can be seen that there are significant differences both between different materials and between carbonated and uncarbonated

materials of the same mortar quality. Here, the discussion about the effect of carbonation is concentrated on pore structural effects and effects on the freezable water content.

8.5.2.1 The effect of carbonation on the pore structure

For all mortar qualities, carbonation leads to a reduction of the evaporable water content, i.e. a reduction in open porosity. Table 8.1 shows the evaporable water content after seven days of capillary suction, complemented by the illustration in Figure 8.18.

From the figure, it can be seen that the evaporable water content is markedly reduced for all mortars as a result of carbonation, although to different extents for different concrete qualities. The reduction is greatest for mortar with OPC alone as the binder, or with OPC and small amounts of silica or slag as part of the binder. For mortar containing high amounts of slag as part of the binder, the reduction in evaporable water content as a result of carbonation is less pronounced. Also for mortar with 10 % silica, the reduction in evaporable water content is somewhat smaller.

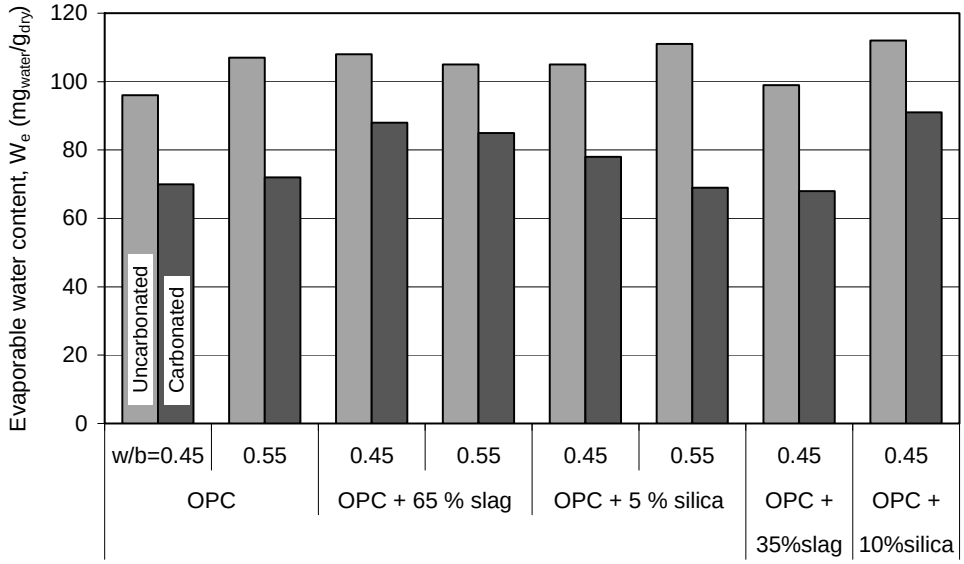

Figure 8.18 *Evaporable water content after seven days of capillary suction for carbonated and uncarbonated mortars with different binder combinations and w/b-ratios.*

The change in evaporable water content found for the specimens used for the LTC measurement corresponds well with the changes in total porosity measured on the specimens of the same material used in the capillary suction test in Chapter 6 (see Table 6.2). The total porosity was markedly reduced as a result of carbonation, although mostly for mortar with only OPC as the binder or OPC with small amounts of silica or slag as part of the binder. For mortar with high contents of slag as part of the binder, on the other hand, the reduction was smaller. That is, the porosity measurements in Chapter 6 and the evaporable water

content measured here correspond well. It must be noted that different procedures were used when measuring the total porosity and when measuring the evaporable water content. Total porosity was measured after drying in vacuum followed by vacuum saturation, whereas the evaporable water content was measured on specimens subjected to capillary suction for only seven days, and so a small difference is to be expected.

Although the evaporable water content, or more specifically the porosity, is reduced for all mortar qualities as a result of carbonation, the result is not the same. The effect of carbonation on the fine and coarse porosity is namely markedly different for different mortar qualities. The effect of carbonation on the pore structure is discussed below for each mortar quality separately.

Mortar with OPC alone as the binder

For the mortar qualities with only OPC as the binder, and with w/b-ratios of 0.45 and 0.55, the porosity is markedly reduced as a result of carbonation. The reduction in porosity seems to be greater the higher the w/b-ratio; at least for the mortar qualities used here.

Figure 8.19 shows the relative amount of fine and coarse pores, according to the division discussed above, i.e. freezable (coarse) and non-freezable (fine) water content at –10 °C during thawing.

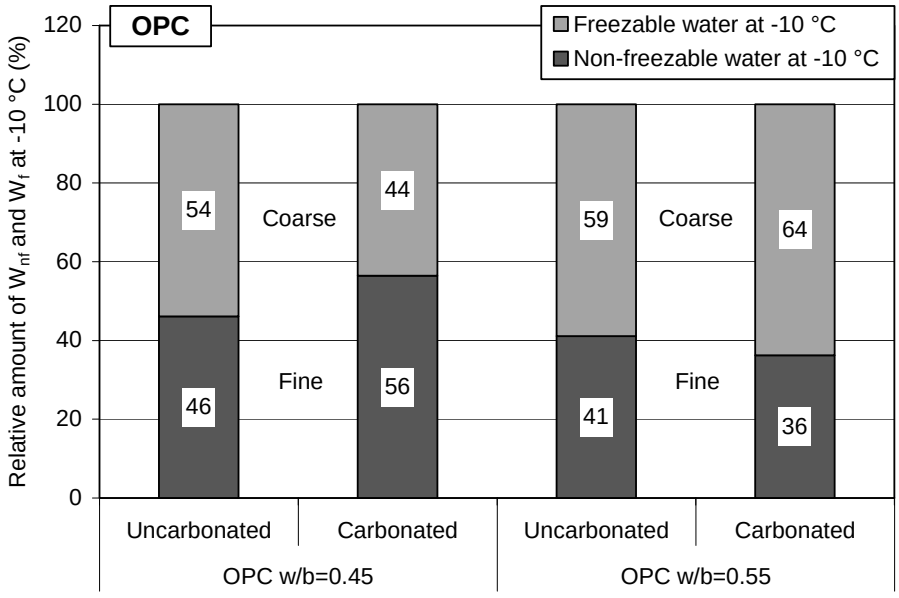

Figure 8.19 *Relative amount of fine and coarse pores for uncarbonated and carbonated mortar with OPC alone as the binder and with different w/b-ratios.*

From the figure, it can be seen that for the mortar quality with a w/b-ratio of 0.45, carbonation leads to a relatively finer pore structure, with a larger part of the porosity belonging to the fine porosity. For mortar with a w/b-ratio of 0.55, carbonation leads to a somewhat coarser pore structure. However, in absolute terms, the coarse porosity decreases markedly for both mortar qualities having only OPC as the binder; see Table 8.8.

From the table, it can be seen that the coarse porosity is markedly reduced as a result of carbonation for both mortar qualities. However, for mortar with a w/b-ratio of 0.55, the amount of fine porosity is reduced more, resulting in a relatively 'coarser' pore structure for the carbonated mortar with a w/b-ratio of 0.55 than for uncarbonated mortar.

Table 8.8 *Freezable and non-freezable water at –10 °C during thawing for uncarbonated and carbonated mortar with OPC as the binder and with different w/b-ratios.*

Mortar quality		**W_{nf} at –10 °C (fine pores) (mg/g_{dry})**	**W_f at –10 °C (coarse pores) (mg_{ice}/g_{dry})**
OPC-45	**Uncarbo.**	44.3	51.7
	Carbo.	39.5	30.5
OPC-55	**Uncarbo.**	44.0	63.0
	Carbo.	26.1	45.9

From the figures showing the apparent heat capacity during cooling and heating (Figure 8.3a), it can be seen that for mortar with a w/b-ratio of 0.45 there is a clear difference between uncarbonated and carbonated mortar. For the uncarbonated material, almost all ice formation takes place above –10 °C. After this initially large ice formation, there is only limited ice formation as the temperature decreases. Even at –40 °C, where normally a significant amount of ice is formed due to homogeneous nucleation of supercooled water, there seems to be only very limited ice formation. This is an indication of a coarse pore structure with few restricting pore necks.

For the carbonated material of same mortar quality, ice formation above –10 °C is markedly reduced, with only a small initial ice formation at around –5 °C. At around –40 °C, the carbonated material, on the other hand, shows a more marked increase in ice formation compared with the uncarbonated material. This indicates that carbonation leads to a finer pore structure and a pore system consisting of more restricting pore necks.

That carbonation of this mortar with a w/b-ratio of 0.45 leads to a finer pore system with restricting pore necks compared to uncarbonated material is evident from the hysteresis between the cooling and heating curves. This difference in hysteresis can be seen from the calculated amounts of freezable water content during cooling and heating in Tables 8.1 and 8.2 and in Figure 8.8a, where the freezable water content during cooling and heating at different temperatures is illustrated. From the figure, it can seen that carbonation leads to a marked change in the constitution of the pore system, leading to an increase in hysteresis, indicating formation of restrictions in the pore system as a result of carbonation.

For the mortar quality with a w/b-ratio of 0.55, there is apparently less difference between carbonated and uncarbonated material than for mortar with a w/b ratio of 0.45 (Figure 8.3b). From the apparent heat capacity, it can be seen that for both carbonated and uncarbonated material almost all ice formation take place above –10 °C, with no marked ice formation at –40 °C. In this respect, both the carbonated and uncarbonated mortars seem to have pore structures with few restrictions in the pore system. If, however, we look at the ice formation between 0 and –10 °C, there seems to be a change in the pore structure of the carbonated material resulting in ice formation at somewhat lower temperatures than for the uncarbonated material. For the carbonated material, this results in a second ice formation peak between –5 °C and –10 °C.

The similarity in the hysteresis behaviour for freezable water content during cooling and heating for carbonated and uncarbonated material with a w/b-ratio of 0.55 (Figure 8.8b), shows that carbonation does not lead to the same formation of restricting pore necks as it does for mortar with a w/b-ratio of 0.45. In this respect, carbonation of mortar with a w/b-ratio of 0.45 results in a more extensive alteration of the pore structure, at least with respect to the formation of restrictions in the pore system.

Mortar with OPC and slag as part of the binder

The total porosity of the mortar qualities with OPC and large amounts of slag as part of the binder is reduced as a result of carbonation, although not to the same degree as for mortar with OPC alone as the binder. The relative change in fine and coarse porosity as a result of carbonation is markedly different in comparison with the mortars with only OPC as the binder. Figure 8.20 shows the relative amount of fine and coarse pores for uncarbonated and carbonated mortars with OPC and 65 % slag as part of the binder and with w/b-ratios of 0.45 and 0.55. From the figure it can be seen that, for both mortar qualities, carbonation leads to a coarser pore structure.

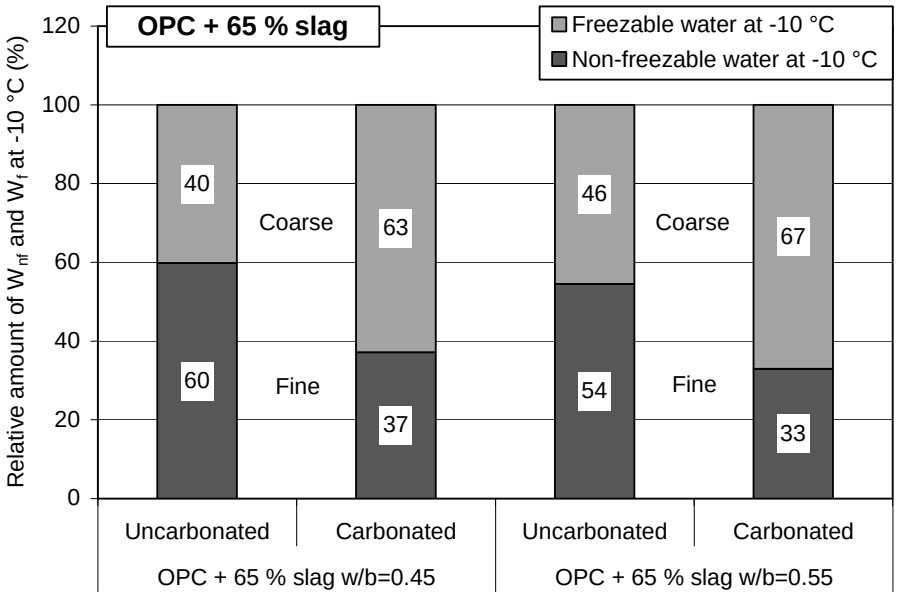

Figure 8.20 *Relative amount of fine and coarse pores for uncarbonated and carbonated mortar with OPC and 65 % slag as part of the binder and with different w/b-ratios.*

From the figure, it can also be seen that for both mortar qualities carbonation leads to a significant coarsening of the pore structure. In absolute terms, it is the fine porosity that is most reduced (Table 8.9). However, even though the total porosity is reduced as a result of carbonation, the coarse porosity is markedly increased, indicating a totally different behaviour than for mortar with only OPC as the binder.

Table 8.9 *Freezable and non-freezable water at –10 °C during thawing for uncarbonated and carbonated mortar with OPC and different amounts of slag as part of the binder and with different w/b-ratios.*

Mortar quality		**W_{nf} at –10 °C (fine pores) (mg/g_{dry})**	**W_f at –10 °C (coarse pores) (mg_{ice}/g_{dry})**
OPC + 65 % slag-45	**Uncarbo.**	64.6	43.4
	Carbo.	32.7	55.3
OPC + 65 % slag-55	**Uncarbo.**	57.2	47.8
	Carbo.	28.0	57.0
OPC + 35 % slag-45	**Uncarbo.**	59.8	39.2
	Carbo.	33.3	34.7

From the apparent heat capacity curves, it can be seen that for both mortar qualities with large amounts of slag as part of the binder there is a large difference between the ice formation during cooling for carbonated and uncarbonated material (Figures 8.4a-b). For the uncarbonated materials, there is some initial ice formation at a temperature around –5 °C,

followed by gradually decreasing ice formation with decreasing temperature down to about – 40 °C, where a second ice formation peak can be seen. This is an indication of a quite fine pore structure with restrictions in the pore system.

For the carbonated material, however, the majority of ice is formed during the initial freezing at temperatures above –10 °C. Below –10 °C, only small amounts of ice form, with the large ice formation found for the uncarbonated material around –40 °C being absent for carbonated material. This is an indication of a relatively coarse pore structure, with few restrictions in the pore system.

Carbonation of these mortar qualities leads to a pore structure with less restricting pore necks compared to uncarbonated material, which is evident from the hysteresis between the cooling and heating curves. The difference in hysteresis can be seen from the calculated amounts of freezable water content during cooling and heating in Tables 8.1 and 8.2 and in Figure 8.9a-b, where the freezable water content at different temperatures is illustrated. From the figure, it can be seen that the uncarbonated materials has a large hysteresis between the cooling and heating curves, whereas carbonation leads to the hysteresis being markedly reduced. Carbonation of these mortar qualities with 65 % slag as part of the binder thus leads to a major change of the pore structure, towards a more ‘open’ pore structure with less restricting pore necks. This is true both for mortars with a w/b-ratio of 0.45 and for those with a w/b-ratio of 0.55.

For mortar with OPC and 35 % slag as part of the binder, carbonation leads to a large reduction in the porosity, similar to that which was found for mortar with only OPC as the binder. However, the relative change in pore structure is more similar to that which was found for mortar with a higher slag content, i.e. a relative coarsening of the pore structure (Figure 8.21).

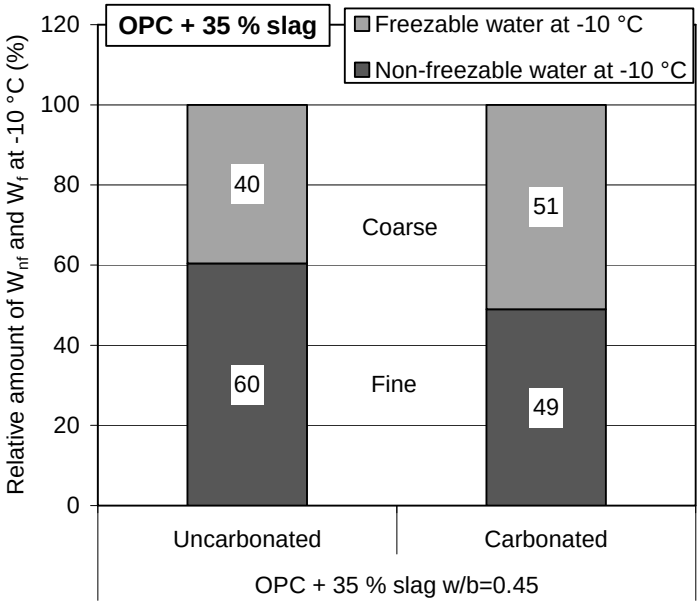

Figure 8.21 *Relative amount of fine and coarse pores for uncarbonated and carbonated mortar with OPC and 35 % slag as part of the binder and with a w/b-ratio of 0.45.*

From the figure, it can be seen that carbonation of this mortar containing 35 % slag as part of the binder leads to a coarsening of the pore structure, although not as apparent as for mortar with 65 % slag as part of the binder. In absolute terms, the coarse porosity decreases somewhat as a result of carbonation, but the major part of the reduction in porosity is within the fine porosity, Table 8.9.

A marked difference between carbonated and uncarbonated material can be seen in the apparent heat capacity curves, Figure 8.6. The uncarbonated material shows a relatively limited initial ice formation above –5 °C, after which the rate of ice formation is slowly reduced. The carbonated material shows an initial large ice formation above –5 °C, followed by a rapid reduction in the ice formation rate and then an increase to give a second peak between –5 °C and –10 °C. At around –40 °C, the uncarbonated material shows considerable ice formation, which indicates a pore structure with restricting pore necks. For the carbonated material, there is no marked ice formation at –40 °C, indicating that carbonation for this material results in a pore system with less restricting pore necks. This is further illustrated in Figure 8.11, which shows the freezable water content at different temperatures during cooling and heating. The figure shows that there is a more marked hysteresis for the uncarbonated material than for the carbonated material, indicating a pore structure with less restricting pore necks as a result of carbonation.

Mortar with OPC and silica as part of the binder

For mortar with OPC and 5 % silica as part of the binder, and with w/b-ratios of 0.45 and 0.55, the porosity is markedly reduced as a result of carbonation. The reduction is in the same region as for mortar with OPC alone as the binder and, in the same way as for OPC mortar, the reduction in porosity seems to be greater the higher the w/b-ratio, at least for the mortar qualities used here. The relative amount of fine and coarse pores in the uncarbonated and carbonated materials shows, however, that the effect of carbonation on the pore structure is somewhat different from mortar with OPC alone as the binder (Figure 8.22).

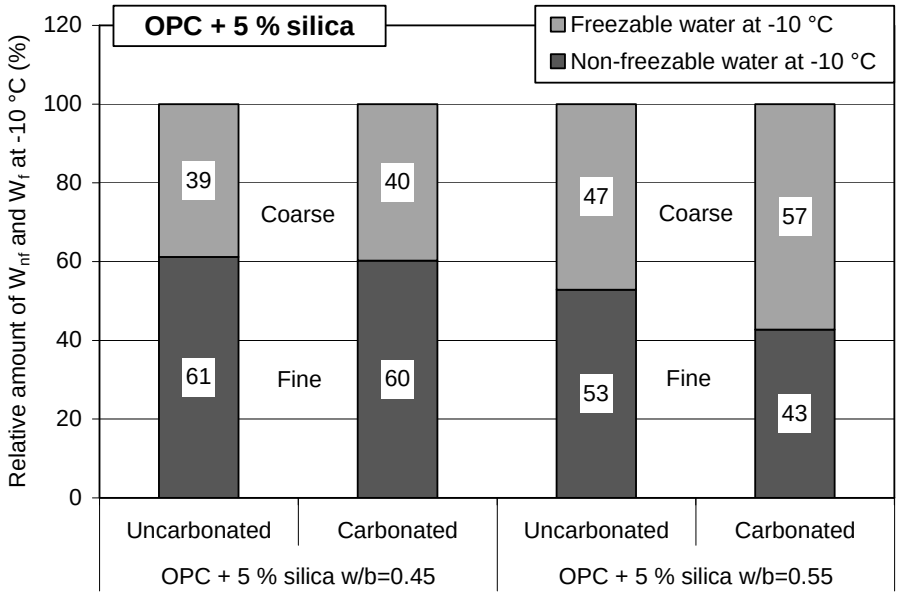

Figure 8.22 *Relative amount of fine and coarse pores for uncarbonated and carbonated mortars with OPC and 5 % silica as part of the binder and with different w/b-ratios.*

From the figure, it can be seen that for the mortar quality with a w/b-ratio of 0.45 carbonation does not lead to any obvious relative changes of the pore structure. For mortar with a w/b-ratio of 0.55, carbonation leads to a relatively coarser pore structure. However, in absolute terms, the coarse porosity decreases markedly for both mortar qualities, as shown in Table 8.10.

From the table, it can be seen that the coarse porosity is reduced as a result of carbonation for both mortar qualities with 5 % silica as part of the binder. However, for mortar with a w/b-ratio of 0.55, the amount of fine porosity is relatively more reduced resulting in a relatively coarser pore structure for the carbonated mortar with a w/b-ratio of 0.55 than for uncarbonated mortar.

Table 8.10 *Freezable and non-freezable water at –10 °C during thawing for uncarbonated and carbonated mortar with OPC and different amounts of silica as part of the binder and with different w/b-ratios.*

Mortar quality		W_{nf} at –10 °C (fine pores) (mg/g_{dry})	W_f at –10 °C (coarse pores) (mg_{ice}/g_{dry})
OPC + 5 % silica-45	**Uncarbo.**	64.2	40.8
	Carbo.	47.0	31.0
OPC + 5 % silica-55	**Uncarbo.**	58.7	52.3
	Carbo.	29.5	39.5
OPC+ 10 % silica-45	**Uncarbo.**	59.8	39.2
	Carbo.	33.3	34.7

Compared to mortar with OPC alone as the binder, carbonation of the mortar quality with silica and with a w/b-ratio of 0.45 leads to small relative changes between coarse and fine pores, whereas carbonation of mortar with OPC alone as the binder and with a w/b-ratio of 0.45 leads to a considerably finer pore system. However, for mortar with a w/b-ratio of 0.55, the tendency is the same regardless of whether silica is part of the binder or not, i.e. carbonation leads to a relatively coarser pore structure.

When comparing mortar with OPC alone and mortar with OPC and some silica as part of the binder, it must be noted that the uncarbonated mortars with silica as part of the binder have a markedly finer pore system. After carbonation, however, the relative amount of coarse and fine pores is about the same, regardless of whether silica is part of the binder or not. This is more so for mortar with a w/b-ratio of 0.45, whereas for carbonated mortar with a w/b-ratio of 0.55 incorporation of silica leads to a relatively finer pore structure.

For the mortar quality with OPC and 5 % silica as part of the binder, and with a w/b-ratio of 0.45, the differences in ice formation during cooling between the carbonated and uncarbonated material are relatively small (Figure 8.5a). From the apparent heat capacity curves, it can be seen that both uncarbonated and carbonated materials have a large initial ice formation at a temperature around –5 °C. However, ice formation for the carbonated material is somewhat less, and is more rapidly reduced than is the case for uncarbonated material.

At –40 °C, both carbonated and uncarbonated materials show a marked second ice formation peak, indicating a pore system with restrictions in the pore system. This is further illustrated by the calculated amount of freezable water during cooling and heating (Tables 8.1 and 8.2 and Figure 8.10a). From the figure, it can be seen that the hysteresis between the cooling and heating curves is about the same for both the carbonated and uncarbonated material. For this mortar with small amounts of silica and a w/b-ratio of 0.45, carbonation does not seem to change the pore structure in the same marked way as for mortar with only OPC or with OPC and large amounts of slag as part of the binder. For mortar with small contents of silica, both carbonated and uncarbonated materials show a marked

hysteresis between cooling and heating, indicating the existence of restricting pore necks for both materials.

For mortar with OPC and 5 % silica as part of the binder and a w/b-ratio of 0.55, there is a marked difference in apparent heat capacity between carbonated and uncarbonated material (Figure 8.5b). After an initial large ice formation at temperatures above –5 °C for both materials, the carbonated material shows a rapid decrease in ice formation rate, whereas the ice formation rate for the uncarbonated material is reduced more slowly. For the carbonated material, a second ice formation peak at around –8 °C can be seen, after which the ice formation rate is reduced.

At around –40 °C, there is a marked increase in ice formation for the uncarbonated material, but no sign of any ice formation for carbonated material. This is an indication of the existence of restricting pore necks in the uncarbonated material, while the carbonated material seems to be more ‘open’. This is further illustrated by the curves showing the freezable water content at different temperature during cooling and heating, Figure 8.10b. From the figure, it can be seen that the hysteresis is more marked for the uncarbonated material than for the carbonated material. The smaller hysteresis between the cooling and heating curves for the carbonated material compared with the uncarbonated indicates that carbonation of this material does not lead to any restrictions in the pore system but, on the contrary, reduces the existing pore restrictions found in the pore system of the uncarbonated material.

For mortar with 10 % silica as part of the binder, the reduction in porosity as a result of carbonation is somewhat less than for mortar with OPC alone or OPC and 5 % silica as part of the binder. The relative amount of fine and coarse pores in the uncarbonated and carbonated materials shown in Figure 8.23, however, shows that the effect of carbonation on the pore structure is about the same as for mortar with 5 % silica s part of the binder.

From the figure, it can be seen that carbonation does not lead to any relative changes in the constitution of the pore structure. The reduction in total porosity is divided between coarse and fine pores, resulting in the same relationship between coarse and fine pores before and after carbonation. In absolute terms, the coarse porosity decreases somewhat, but the most substantial reduction is in the fine porosity, Table 8.10.

One marked difference in relation to mortar with 5 % silica as part of the binder with the same w/b-ratio is that mortar with 10 % silica has a larger proportion of fine pores, with this being true for both uncarbonated and carbonated material.

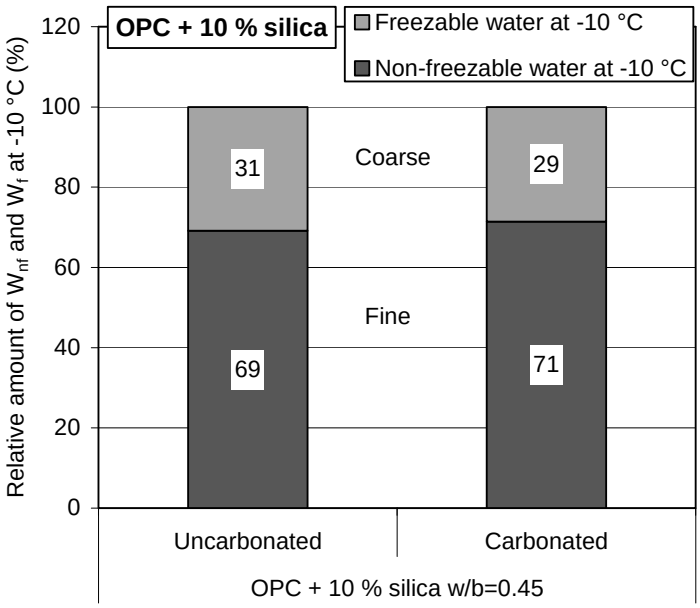

Figure 8.23 *Relative amount of fine and coarse pores for uncarbonated and carbonated mortars with OPC and 10 % silica as part of the binder and with a w/b-ratio of 0.45.*

For mortar with OPC and 10 % silica as part of the binder, there is a significant difference in ice formation between carbonated and uncarbonated mortar, as can be seen in Figure 8.7. From the apparent heat capacity curves, it can be seen that the uncarbonated material shows an initial large ice formation above –5 °C, after which the rate of ice formation slowly decreases. The carbonated material shows a relatively small initial ice formation above –5 °C, which very rapidly decreases. Both the uncarbonated and the carbonated material show a substantial ice formation around –40 °C, with a somewhat more pronounced ice formation for the carbonated material. This indicates, for both the uncarbonated and the carbonated material, the presence of pore structures with restrictions in the pore systems. This is, however, more evident for the carbonated material than for the uncarbonated. This is further illustrated by the curves showing the freezable water content at different temperatures during cooling and heating (Figure 8.12). From the figure, it can be seen that there is a marked hysteresis for both the uncarbonated and the carbonated material. The hysteresis is, however, somewhat more pronounced for the carbonated material. This indicates that carbonation of this mortar, which from the beginning had a pore system with significant restrictions, leads to a further formation of restrictions in the pore structure.

8.5.2.2 The effect of carbonation on the freezable water content during cooling

The pore structural changes caused as a result of carbonation and discussed above lead to changes in the temperature at which water in the material freezes. Since it is primarily the freezable part of the water in a material that is of importance with respect to the durability

against frost attack, the freezable water content at different temperatures is of great importance.

The effect of carbonation on the freezable water content is different for different mortar qualities. The following discusses the effect of carbonation on the freezable water content for each mortar quality separately. When discussing the change in freezable water content, it is primarily the freezable water content during cooling that is addressed here.

Mortar with OPC alone as the binder

For mortar with OPC alone as the binder, carbonation leads to a large change in freezable water content during cooling. This is true for both mortar qualities tested in this investigation (w/b-ratios of 0.45 and 0.55), for which carbonation leads to a marked reduction in freezable water content. The effect is, however, most marked for the quality with a w/b-ratio of 0.45; see Figure 8.8a-b.

For mortar with a w/b-ratio of 0.45, uncarbonated material has a freezable water content at –10 °C during cooling of 47 mg_{ice}/g_{dry} whereas carbonated material has a freezable water content of only 12 mg_{ice}/g_{dry}. Carbonation thus leads to a reduction of the freezable water content of some 75 % at –10 °C. At –20 °C, the freezable water content is 50 mg_{ice}/g_{dry} for uncarbonated and 18 mg_{ice}/g_{dry} for carbonated material, i.e. a reduction of some 65 % as a result of carbonation.

The same tendency is found for mortar with a w/b-ratio of 0.55 (Figure 8.8b), with a marked reduction of freezable water content as a result of carbonation. However, the relative change is somewhat less than for mortar with a w/b-ratio of 0.45. At –10 °C, the change in freezable water content is some 34 %, whereas at –20 °C the change is around 25 %.

Mortar with OPC and slag as part of the binder

For mortar with large contents of slag as part of the binder, the effect of carbonation on the freezable water content is totally different from that which was found for mortar with OPC alone as the binder. For mortar with 65 % slag as part of the binder, the freezable water content during cooling markedly increases as a result of carbonation. This is true for both mortar qualities with 65 % slag as part of the binder, independent of their w/b-ratios, investigated here.

For mortar with a w/b-ratio of 0.45 (Figure 8.9a), the uncarbonated material has a freezable water content of 18 mg_{ice}/g_{dry} at –10 °C during cooling, whereas the carbonated material has a freezable water content of 46 mg_{ice}/g_{dry} at the same temperature. Carbonation thus leads to an increase in freezable water content of over 150 %. At –20 °C, the freezable water content is 28 mg_{ice}/g_{dry} for uncarbonated material and 56 mg_{ice}/g_{dry} for carbonated material, i.e. an increase of some 100 % as a result of carbonation.

The same tendency is found for mortar with a w/b-ratio of 0.55 (Figure 8.9b), with a marked increase of freezable water content as a result of carbonation. The relative change is somewhat less than for mortar with a w/b-ratio of 0.45, but the effect of carbonation is still strong with over 100 % increase in freezable water content at –10 °C, and an increase of over 75 % at –20 °C.

It must be noted that there is a relatively limited difference in freezable water content depending on w/b-ratio for the mortars with 65 % slag as part of the binder. This is true both for uncarbonated and carbonated material. This indicates that the effect of the w/b-ratio on the freezable water content is less for mortars with high contents of slag as part of the binder than for mortar with OPC alone as the binder, at least for the mortar qualities investigated here.

The effect of carbonation becomes less apparent for mortar with less slag as part of the binder. For mortar with 35 % slag and a w/b-ratio of 0.45 (Figure 8.11), the effect of carbonation is relatively limited. For this mortar, the amount of freezable water content at –10 °C is increased by some 28 % as a result of carbonation, while at –20 °C the increase is only about 16 %. The negative effect of carbonation with regard to the freezable water content thus decreases with decreasing slag content.

Mortar with OPC and silica as part of the binder

For mortar with small contents of silica as part of the binder carbonation leads, as is the case for mortar with OPC alone as the binder, to a substantial reduction of freezable water content. The effect of carbonation is more pronounced for mortar with a w/b-ratio of 0.45 than for mortar with a w/b-ratio of 0.55, which was also the case for mortar with OPC alone as the binder.

For mortar with 5 % silica as part of the binder and with a w/b ratio 0.45 (Figure 8.10a), uncarbonated material has a freezable water content of 28 mg_{ice}/g_{dry} at –10 °C during cooling, whereas carbonated material has a freezable water content of only 15 mg_{ice}/g_{dry}. Carbonation thus leads to a reduction of the freezable water content of some 45 % at –10 °C. At –20 °C, the freezable water content is 35 mg_{ice}/g_{dry} for uncarbonated material and 21 mg_{ice}/g_{dry} for carbonated material, i.e. a reduction of some 40 % as a result of carbonation.

For mortar with 5 % silica as part of the binder and with a w/b-ratio of 0.55 (Figure 8.10b), the effect of carbonation on the freezable water content during cooling is smaller, although it still results in a decrease in the amount of freezable water. At –10 °C, the reduction in the amount of freezable water due to carbonation is about 20 %, whereas at –20 °C the reduction is about 10 %. In the same way as for mortar with OPC alone as the binder, the effect of carbonation on the freezable water content is most pronounced for mortars with a w/b-ratio of 0.45 in comparison with mortars with higher w/b-ratios, at least for the qualities investigated here.

For mortar with higher silica contents (up to 10 %), the effect of carbonation is the same as for mortar with no or only 5 % silica as part of the binder (Figure 8.12). For mortar with 10 % silica and with a w/b-ratio of 0.45, carbonation leads to a significant reduction in freezable water content. At –10 °C during cooling, carbonation reduces the freezable water content by over 50 %. The reduction is about the same at –20 °C, with over 50 % lower freezable water content for the carbonated material than for the uncarbonated.

It must be noted that the amount of freezable water content for uncarbonated material decreases with increasing silica content as part of the binder, at least at silica content up to some 10 %. For carbonated material, however, the differences between the mortars with and without silica as part of the binder are considerably reduced. Carbonated mortars without silica, and with 5 % silica, show about the same amount of freezable water during cooling, whereas mortar with 10 % silica shows somewhat lower amounts of freezable water content. However, the differences are much less than for uncarbonated material. Carbonation for these materials thus seems to result in materials with more 'similar' properties, at least for these investigated mortar qualities with a w/b-ratio of 0.45 and with respect to the amount of freezable water content during cooling.

8.5.2.3 The effect of secondary cementitious materials on the results from LTC measurements

From the discussion of the effect of carbonation on the pore structure and on the freezable water content for each individual mortar quality above, it can be seen that there are large differences depending on mortar quality. This is true for both uncarbonated and carbonated materials. In the above presentation, the primary focus was to compare the uncarbonated materials with carbonated materials of the same mortar quality. However, since there are considerable differences between the different mortar qualities, depending on binder type/combination, these differences are illustrated in this section. The following is a discussion of the effect of using secondary cementitious materials (slag and silica) as part of the binder for mortar with a w/b-ratio of 0.45. Mortars containing slag and silica respectively are evaluated separately, with the mortar quality with OPC alone as the binder as reference quality.

The same division of fine and coarse porosity as was discussed above in Section 8.5.1 is used here; that is, the unfrozen water at –10 °C from the melting curve is regarded as water held in pores belonging to the fine pore system, whereas the frozen water at this temperature is held in pores belonging to the coarse pore system.

Effect of slag as part of the binder

The results from the low-temperature calorimeter measurements show that the incorporation of slag has a major influence on the properties of both the uncarbonated and the carbonated materials.

Uncarbonated material

For the uncarbonated materials, it can be seen that the initial ice formation above and around –5 °C for mortar with 65 % slag (Figure 8.4a) and mortar with 35 % slag (Figure 8.6) is less than for mortar with OPC alone as the binder (Figure 8.3a). Uncarbonated mortar qualities from both qualities containing slag also show substantial ice formation at temperatures around –40 °C, which is not found for OPC mortar. This indicates that incorporation of slag as part of the binder results in pore structures with more restrictions in the pore systems than in mortar with OPC alone as the binder.

Figure 8.24 shows the evaporable water content as freezable and non-freezable water content at –10 °C from the melting curve for mortar with and without slag as part of the binder. It can be seen that the evaporable water content (open porosity) increases with increasing slag content.

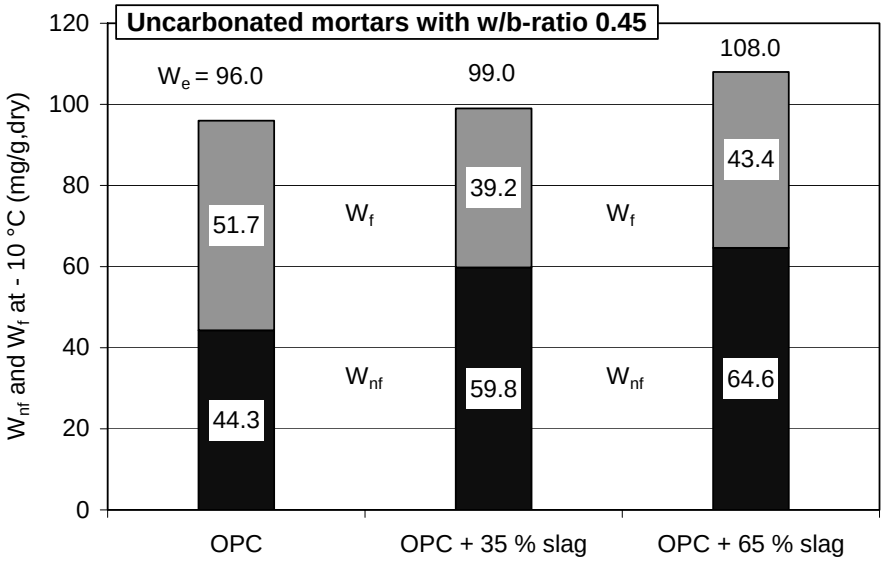

Figure 8.24 *Evaporable water content as freezable and non-freezable water contents at –10 °C from the melting curve for uncarbonated mortars with a w/b-ratio of 0.45 and with and without slag as part of the binder.*

It can also be seen that the amount of non-freezable water increases with increasing slag content, indicating a larger amount of fine pores for uncarbonated mortars containing slag as part of the binder. The amount of freezable water, on the other hand, is markedly reduced for the mortars containing slag, indicating that mortar with OPC alone as the binder has a coarser pore structure than have the mortars with slag as part of the binder. Incorporation of slag as part of the binder therefore seems, for uncarbonated material, to result in larger total porosity, although with larger amounts of fine pores and smaller amounts of coarse pores than in mortar with OPC alone as the binder.

Carbonated material

The effect of carbonation on the pore structure of materials with different amounts of slag as part of the binder is markedly different, depending on the slag content. Figure 8.25 shows the evaporable water content as freezable and non-freezable water content at –10 °C from the melting curve for carbonated mortars with slag as part of the binder. It can be seen that the mortar with 65 % slag has a much higher evaporable water content than have mortars with OPC alone or OPC + 35 % slag as part of the binder. It can also be seen that carbonation leads to a large change in the amount of freezable and non-freezable water contents, i.e. a change in the constitution of the pore structure. For the carbonated materials, the amount of fine porosity (non-freezable water) is smaller the higher the amount of slag as part of the binder, which is quite opposite to what was found for uncarbonated mortar. On the contrary, the amount of coarse porosity increases with increasing slag content, which is also opposite to what was found for the uncarbonated materials. Carbonation thus results in a densification of the pore structure for mortar with OPC alone as the binder, and a coarsening of the pore structure for mortar containing large amounts of slag as part of binder.

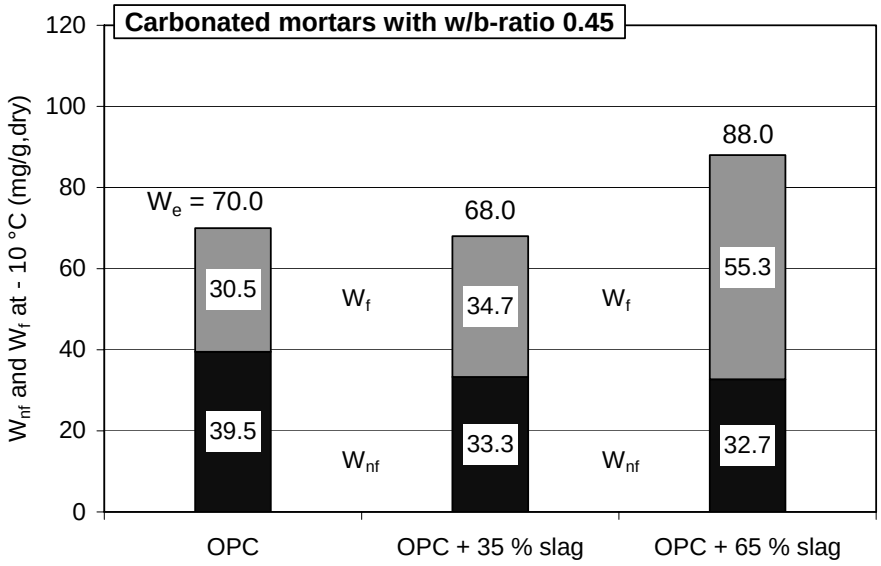

Figure 8.25 *Evaporable water content as freezable and non-freezable water contents at –10 °C from the melting curve for carbonated mortars with a w/b-ratio of 0.45 and slag as part of the binder.*

Discussion

The relative change as a result of carbonation in freezable and non-freezable water content at –10 °C (thawing) is illustrated in Figure 8.26. It can be seen that the change in freezable water (coarse porosity) is almost linear, from a substantial *reduction* of the coarse porosity for mortar with OPC alone as the binder to a marked *increase* in coarse porosity for

mortar containing large amounts of slag (65 %) as part of the binder. The change in the non-freezable water content (fine porosity) is in the opposite direction, with only some decrease in fine porosity for mortar with OPC alone as the binder and a large reduction in fine porosity for the mortars containing slag as part of the binder.

It must be noted that at a slag content of around 45 % the change in coarse porosity as a result of carbonation turns positive. That is, for mortar with a slag content exceeding about 45 % slag as part of the binder, carbonation leads to an *increase* in coarse porosity. This can be compared with the results from freeze/thaw testing 'micro'-concrete in Chapter 3, where it was shown that the effect of carbonation was positive with respect to the salt-frost resistance for concrete with OPC alone as the binder, and negative for concrete with high contents of slag as part of the binder. When evaluating the effect of carbonation on the salt-frost resistance for concretes with different slag contents, it was shown that for concrete with some 50 % slag as part of the binder the effect of carbonation on the salt-frost resistance turned negative; see Figure 3.35 in Chapter 3. In other words, for concrete containing over some 50 % slag as part of the binder, carbonation leads to higher salt-frost damage than is the case for uncarbonated concrete. This corresponds well with the change in coarse porosity as a result of carbonation found here, i.e. carbonation leads to an increased amount of coarse porosity at a slag content around some 45 %.

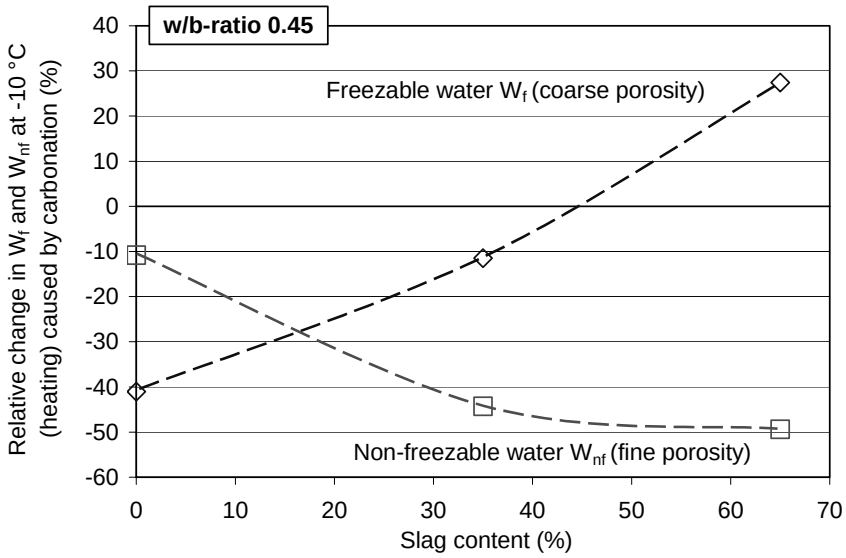

Figure 8.26 *Relative change in freezable and non-freezable water content at –10 °C from the heating curve as a result of carbonation, for mortars containing slag as part of the binder.*

The marked difference in the effect of carbonation on the pore structure, and thus also on the freezable water content depending on the binder type/combination, is illustrated in Figure 8.27 for mortar with OPC alone and OPC with 65 % slag as part of the binder, both

with a w/b-ratio of 0.45. The figure shows the freezable water content as a function of temperature during freezing for carbonated and uncarbonated materials.

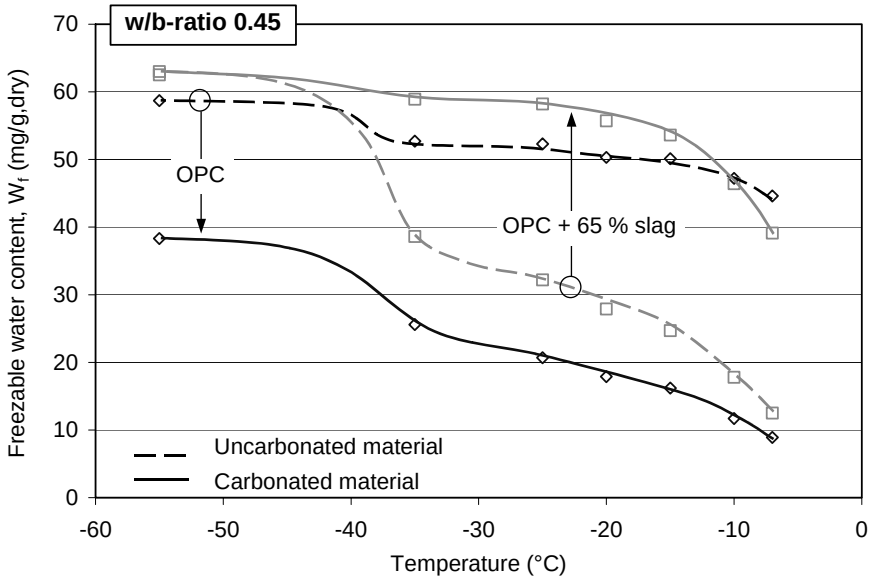

Figure 8.27 *Freezable water content during freezing for uncarbonated (dashed lines) and carbonated (full lines) material of mortar with OPC alone and with OPC + 65 % slag as part of the binder, both with a w/b-ratio of 0.45.*

From the figure, it can be seen that for mortar with OPC alone as the binder, carbonation leads to a strong *reduction* in freezable water content, which is true over the whole temperature range 0 to –55 °C. For mortar with OPC alone as the binder, which in an uncarbonated state has a high freezable water content, carbonation thus leads to a substantial reduction of freezable water and presumably also leads to a *higher* frost and salt-frost resistance.

The effect of carbonation is the opposite for mortar with high contents of slag as part of the binder, i.e. carbonation leads to a considerable *increase* in freezable water content, at least in the temperature range down to some –40 °C. The effect of carbonation thus leads to a markedly higher freezable water content and presumably also to a *lower* frost and salt-frost resistance

It must be noted that carbonation of the mortar quality tested here with high contents of slag as part of the binder leads to a freezable water content comparable with, and below –10 °C even higher than, the value for uncarbonated mortar with OPC alone as the binder.

Effect of silica as part of the binder

The incorporation of silica as part of the binder has a marked influence on the pore structure, although not as strong as when using large amounts of slag as part of the binder - at least, not with the amounts of silica used here.

Uncarbonated material

The most significant differences can be found for uncarbonated materials with different amounts of silica as part of the binder. Figure 8.28 shows the evaporable water content for uncarbonated mortars with silica as part of the binder and with a w/b-ratio of 0.45, as freezable and non-freezable water contents at –10 °C from the melting curve.

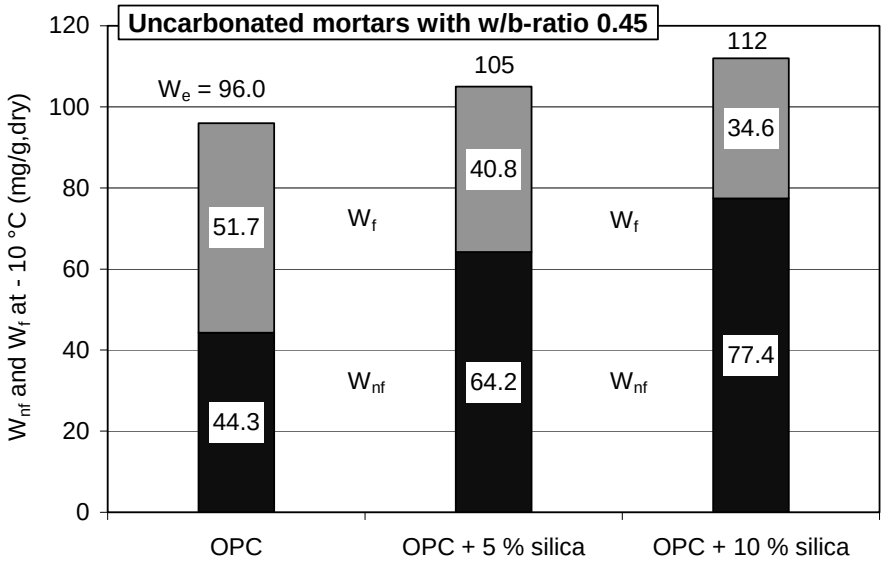

Figure 8.28 *Evaporable water content as freezable and non-freezable water contents at –10 °C from the melting curve for uncarbonated mortars with a w/b-ratio of 0.45 and different amounts of silica as part of the binder.*

From the figure, it can be seen that there are relatively large differences in the pore structures, depending on the silica content. The higher the silica content, the higher the amount of fine porosity (non-freezable water) and the lower the amount of coarse porosity (freezable water). For uncarbonated mortar, the incorporation of silica thus seems to result in considerably finer pore systems, although with an increasing amount of evaporable water with increasing silica content.

Carbonated material

For carbonated material, the effect of silica on the pore structure is somewhat different from the effect on uncarbonated material. Figure 8.29 shows the evaporable water content as freezable and non-freezable water at –10 °C from the melting curve. As for the uncar-

bonated materials (Figure 8.28), the evaporable water content is higher the higher the silica content for the carbonated materials. The relative amount of fine porosity is also in the same range, with increasing amount of fine porosity with increasing silica content. The coarse porosity is, however, markedly changed in comparison with the uncarbonated materials. When carbonated, the material has about the same amount of coarse porosity, regardless of silica content, whereas for uncarbonated mortar the amount of coarse porosity was substantially reduced with increasing silica content.

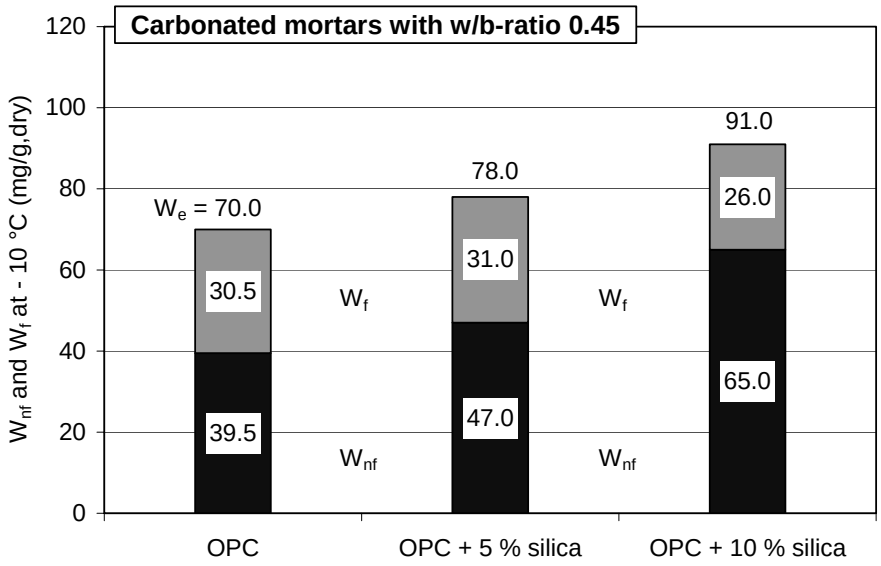

Figure 8.29 *Evaporable water content as freezable and non-freezable water contents at –10 °C from the heating curve for carbonated mortars with a w/b-ratio of 0.45 and different amounts of silica as part of the binder.*

Discussion

The relative change in freezable and non-freezable water content at –10 °C from the melting curve as a result of carbonation is illustrated in Figure 8.30. It can be seen that there is a significant reduction in freezable water content (coarse porosity) for all mortars due to carbonation. However, the largest relative reduction is found for mortar with OPC alone as the binder, whereas the two mortars containing silica show about the same relative reduction. The change of the non-freezable water content (fine porosity) is in the opposite direction, with only some decrease in fine porosity for mortar with OPC alone as the binder, and a more substantial reduction for the mortars containing silica as part of the binder, with the largest relative reduction for mortar containing 5 % silica. Though there seem to be large differences in the relative reduction of coarse and fine porosity, carbonation seems to result in changes making the pore structures of the carbonated materials more similar than when comparing uncarbonated materials. Carbonation thus levels out the differences found, especially in coarse porosity, between the uncarbonated materials with different silica contents.

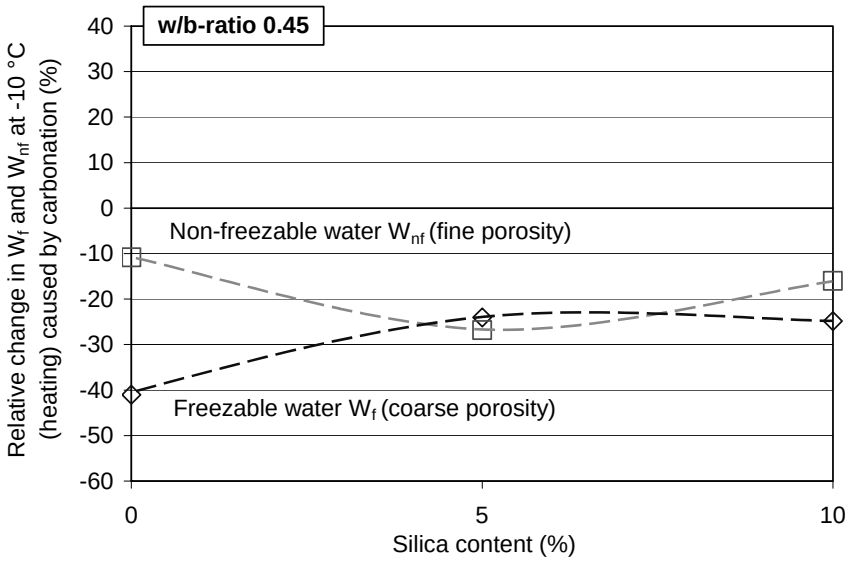

Figure 8.30 *Relative change in freezable and non-freezable water content at –10 °C from the melting curve as a result of carbonation for mortars containing silica as part of the binder.*

The difference in the effect of carbonation on the pore structure and thus on the freezable water content depending on whether silica is part of the binder or not, is illustrated in Figure 8.31 for mortar with OPC alone and OPC + 5 % silica as part of the binder, both with a w/b-ratio of 0.45. The figure shows the freezable water content as a function of temperature during freezing for carbonated and uncarbonated materials.

From the figure it can be seen that, for uncarbonated material, there is a significant difference in freezable water content, depending on whether silica is part of the binder or not. Uncarbonated mortar with 5 % silica as binder has a markedly lower freezable water content than has uncarbonated mortar with OPC alone as the binder. The effect of carbonation, however, results in the differences between the uncarbonated materials decreasing considerably. Carbonation of mortar with OPC alone as the binder results in a material with the same, or even somewhat lower, freezable water content than in carbonated mortar containing silica. The effect of carbonation thus is stronger for mortar without silica, at least for the mortar qualities used here.

It must be noted that the marked effect on the freezable water content of incorporating silica as part of the binder is attributed only to uncarbonated mortar. For carbonated mortar, the freezable water content is about the same, regardless of whether silica is part of the binder or not, at least for silica contents up to 5 %.

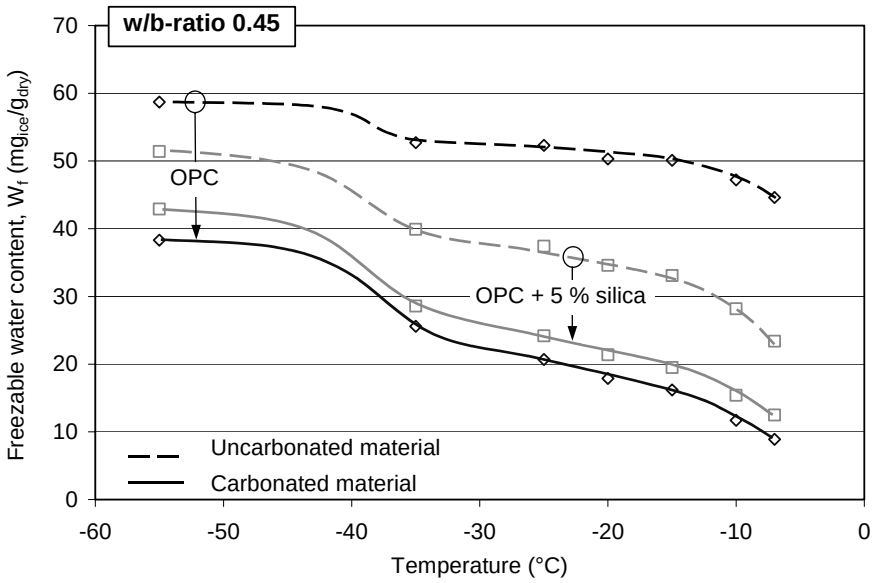

Figure 8.31 *Freezable water content during freezing for uncarbonated (dashed lines) and carbonated (full lines) material of mortar with OPC alone and with OPC + 5 % silica as part of the binder, both with a w/b-ratio of 0.45.*

8.6 Conclusions

The following conclusions may be drawn from the Low-Temperature Calorimetry measurements:

- Most tested materials show marked hysteresis between at what temperature ice is formed (freezing curve) and at what temperature ice is melted (thawing curve). High hysteresis indicates considerable restrictions in the pore system, caused by restricting pore necks. Low hysteresis, on the other hand, indicates a material with an 'open' pore system with few restricting pore necks.
- Carbonation significantly changes the properties of the pore structure, leading to changes in the evaporable water content as well as in the freezable and non-freezable water contents. However, the effect of carbonation is different for mortar qualities with different binder types/combinations tested in this investigation.
- For all mortars tested in this investigation, carbonation resulted in a reduction of evaporable water content (open porosity). The reduction was relatively greatest for mortar with OPC alone or with OPC and small amounts of slag or silica as part of the binder. The reduction is relatively less for mortars with large contents of slag (65 %) as part of the binder.
- For mortar with OPC alone as the binder, carbonation leads to large reduction of both fine and coarse pores, leading to a strong *decrease* in freezable water content. The results also indicate that carbonation of mortar with a w/b-ratio of 0.45 leads

to a marked formation of restrictions in the pore structure. For mortar with a w/b-ratio of 0.55, no such indication can be found.

- For mortar with large amounts of slag as part of the binder (65 %), carbonation leads, as opposed to mortar with OPC alone as the binder, to a significant coarsening of the pore structure, leading to a strong *increase* in freezable water content. The results also show that carbonation of mortar with high slag contents leads to a more ‘open’ pore structure, with few restricting pore necks.
- The results indicate that the higher the slag content, the greater is the increase in freezable water content (coarse porosity) as a result of carbonation.
- For mortar containing 5 % silica as part of the binder, the reduction in open porosity as a result of carbonation is attributed equally to the fine and coarse pores leading to a significant reduction of freezable water content. The results show that both uncarbonated and carbonated mortars have pore systems with considerable amounts of restrictions, caused by restricting pore necks.

9 The effect of carbon dioxide concentration on physical properties of the carbonated zone

9.1 Introduction

Most carbonated materials used in the investigations described in this publication have been carbonated in an environment with an elevated carbon dioxide content of ~1 vol-% CO_2. According to Knöfel & Eßer (1992), carbonation in an environment with elevated carbon dioxide content may lead to structural changes of the pore system that are not found in material carbonated in an environment with normal carbon dioxide content. However, according to their investigation, carbonation in an atmosphere with a carbon dioxide content of up to 1.0 vol-% CO_2 gives a pore structure with about the same properties as when carbonated in an environment with normal air. As was discussed in Chapter 4, this was the primary reason for choosing a carbon dioxide content of 1 vol-% in the investigations presented in this publication.

A limited comparison was carried out in order to verify that the results for the specimens subjected to accelerated carbonation are similar to the results from specimens carbonated in normal air. Results from Low-Temperature Calorimetry (LTC) measurements, and results from capillary suction carried out as a part of preconditioning specimens for LTC measurements, were compared for materials carbonated in normal air and in air with elevated carbon dioxide content.

The low-temperature calorimetry measurements were carried out at the Aalborg Portland Research and Development Centre in Aalborg, Denmark, as described in Chapter 8.

Here, it is the physical effect of carbonation, i.e. the effect of carbonation on the pore structure, that is investigated. Changes in the pore structure lead in turn to changes in the evaporable, freezable and non-freezable water content, as well as in the water absorption behaviour during capillary suction. Chapter 10 describes a limited chemical investigation, carried out to investigate what carbonate phases that are formed during carbonation in climates with different carbon dioxide contents.

9.2 Materials and specimens

This comparison investigated specimens of four mortar qualities with different binder types/combinations. Specimens of mortar with only OPC, OPC with 5 % silica and OPC with 65 % slag as part of the binder, all with w/b-ratios of 0.55, were compared. In addition, one mortar with OPC + 65 % slag and a w/b-ratio of 0.45 was included.

Material compositions are described in Chapter 5. Specimen conditioning and production of specimens for the LTC measurement are described in Chapter 8. The specimens carbonated in normal air were conditioned in the laboratory in a climate-controlled area

with 65 % RH and +20 °C. The specimens carbonated in a climate with increased carbon dioxide content were conditioned in a climate chamber as was described in Chapter 8.

For ‘OPC - 55’ and ‘OPC + 5 % silica - 55’ mortar qualities, carbonation was incomplete after the over 20 month-long conditioning in normal air at 65 % RH and +20 °C. When measuring the carbonation depth with the phenolphthalein method before the test, both materials showed an uncarbonated core of between 6 and 7 mm in diameter, with a somewhat larger uncarbonated core for the mortar containing silica. With a specimen diameter of ~13.5 mm, the part that was carbonated corresponded to about 80 % of the specimen volume for mortar with OPC alone as the binder, and about 70 % for mortar with some silica as part of the binder. For both mortar qualities with 65 % slag as part of the binder (w/b-ratios of 0.45 and 0.55), the specimens were fully carbonated.

One specimen was tested for each mortar quality and conditioning climate.

9.3 Results and discussion

9.3.1 Introduction

The results from the low-temperature calorimetry measurements are interpreted in the same way as in Chapter 8, see Section 8.5.1. Here, the emphasis was on the change in non-freezable water content. This was because, when evaluating the effect of carbonation in different environments, it is primarily the effect on the pore structure that is of interest, and the pore structure is best evaluated based on the non-freezable water content.

The following pages compare and discuss the results from the LTC measurements and the results from capillary suction for each mortar quality individually.

9.3.2 Mortar with OPC alone as the binder

Figure 9.1 shows the result of the low-temperature calorimetry measurement for the naturally carbonated mortar with only OPC as the binder and with a w/b-ratio of 0.55. The results are given as the apparent heat capacity as a function of the calorimeter block temperature during cooling and heating. The figure also shows the results for uncarbonated and carbonated (~1 vol-%) materials of the same mortar quality.

From the figure it, can be seen that there is a close resemblance between the results for the naturally carbonated specimen and the specimen carbonated in an environment with elevated carbon dioxide content. During cooling, both carbonated specimens show a significantly smaller initial ice formation than does the uncarbonated specimen. As for the carbonated (1 vol-%) specimen, the naturally carbonated specimen shows incipient formation of a small second ice formation peak between –5 and –10 °C, although this is not as apparent as for the specimen subjected to accelerated carbonation.

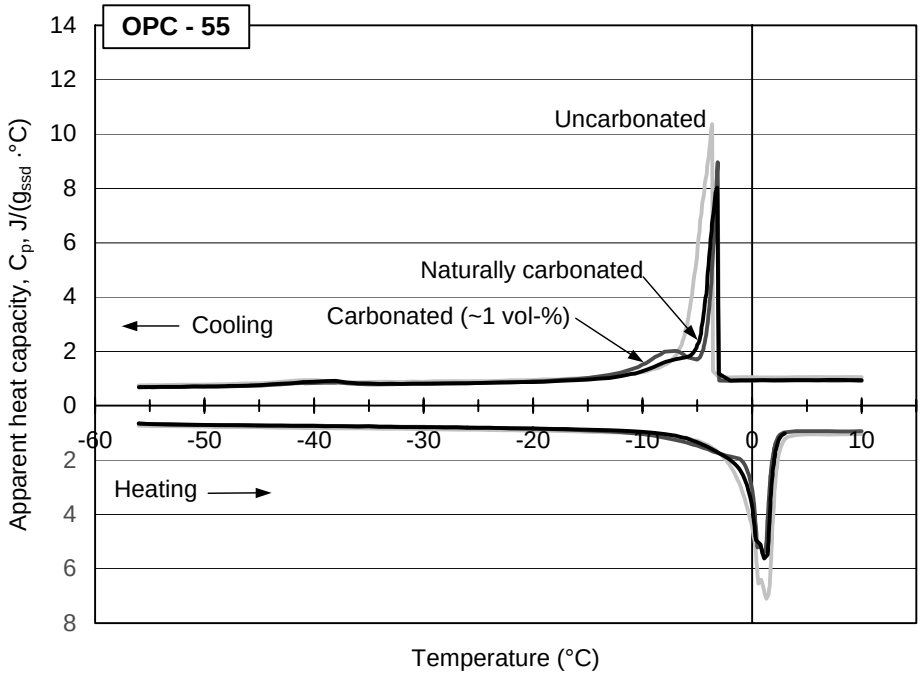

Figure 9.1 *Apparent heat capacity as a function of calorimeter block temperature during cooling (←) and heating (→) for uncarbonated and carbonated (naturally and in ~1 vol-%) mortar with only OPC as the binder and with a w/b-ratio of 0.55.*

In addition, during heating the apparent heat capacities of the two carbonated materials are very similar, with a significantly lower melting 'peak' around 0 °C than compared with the uncarbonated specimen.

Non-freezable water content

Table 9.1 shows the evaporable water and the non-freezable water content for mortar during cooling and heating. Because the naturally carbonated specimen was not fully carbonated, results were calculated for a 'fictitious' specimen (80 % carbonated) calculated from the results for the uncarbonated and carbonated (1 vol-%) specimens (0.2 · uncarbonated value + 0.8 · carbonated value).

Table 9.1 *Measured evaporable water content (W_e) and calculated non-freezable (W_{nf}) water content during cooling and heating for mortar with only OPC as the binder and with a w/b-ratio of 0.55.*

Mortar quality		W_e mg/g_{dry}	W_{nf} (mg_{ice}/g_{dry}) cooling -7	-10	-15	-20	-25	-35	-55°C
OPC - 55	**Uncarbonated**	107	56.4	52.2	47.5	46.9	44.3	43.7	38.9
	Carbonated (acc)	72	45.3	35.9	29.1	27.4	25.2	24.4	19.7
	Naturally carbo.	78	44.3	38.5	33.3	32.4	29.9	28.9	22.3
	Calculated 80 %	*79*	*47.5*	*39.2*	*32.8*	*31.3*	*29.0*	*28.3*	*23.5*
		W_e mg/g_{dry}	W_{nf} (mg_{ice}/g_{dry}) heating -7	-10	-15	-20	-25	-35	-55°C
OPC - 55	**Uncarbonated**	107	45.3	44.0	40.3	39.5	36.7	35.7	36.9
	Carbonated (acc)	72	29.2	26.1	21.9	20.4	17.8	16.8	15.0
	Naturally carbo.	78	29.0	27.0	23.3	22.3	19.5	18.0	15.8
	Calculated 80 %	*79*	*32.4*	*29.7*	*25.6*	*24.2*	*21.6*	*20.6*	*19.4*

From the results shown in Table 9.1, it can be seen that the non-freezable water contents for the naturally carbonated material and for the carbonated material correspond well. The small difference can probably be explained by incomplete carbonation for the naturally carbonated material. This is confirmed from the calculated results for a 'fictitious' specimen (80 % carbonated), which corresponds very well with the results for the naturally carbonated material.

Water absorption during capillary suction

Figure 9.2 shows the results from capillary suction for the three specimens conditioned in different climates from 'OPC - 55' mortar quality. The results are expressed as the moisture ratio in % as a function of the square root of time.

From the figure, it can be seen that the water absorption for the naturally carbonated specimen corresponds well with the water absorption for the carbonated (1 vol-%) specimen. During the first stage of capillary suction both carbonated materials show almost identical water absorption, indicating a close similarity between the constitutions of the pore structures. In this case, the pore structure of the carbonated materials is denser and the resistance to water penetration is higher than is the case for the uncarbonated material. In the second slow water absorption stage, the naturally carbonated specimen shows a somewhat higher moisture ratio, which could also be expected as about 20 % of the naturally carbonated specimen is uncarbonated. Calculating a 'fictitious' moisture ratio during the slow water absorption stage for a material carbonated to 80 % results in a close to identical moisture ratio with the ratio for the naturally carbonated material.

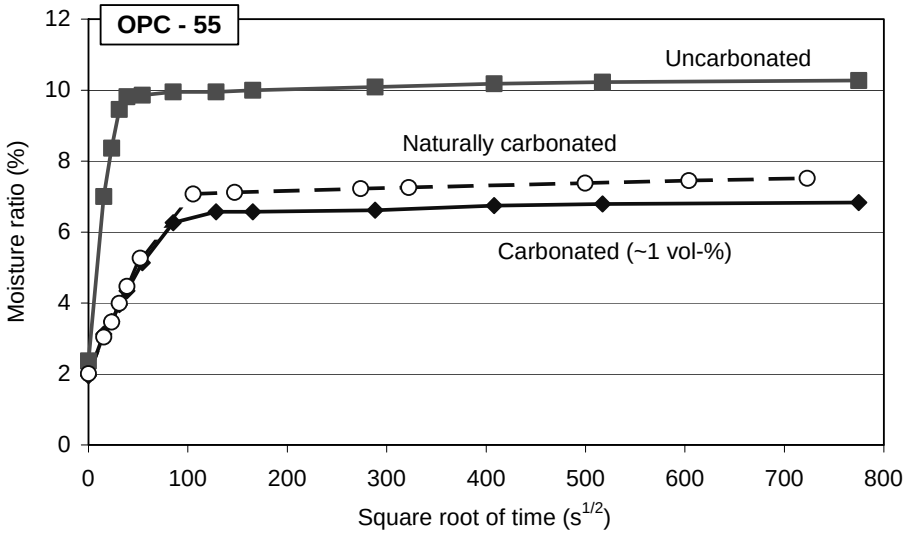

Figure 9.2 *Moisture ratio during capillary suction as a function of the square root of time for uncarbonated and carbonated (naturally and in ~1 vol-%) mortar with only OPC as the binder and with a w/b-ratio of 0.55.*

Conclusion

For the mortar quality with only OPC as the binder and with a w/b-ratio of 0.55, no significant differences were found in the results from capillary suction or the LTC measurements, regardless of in what climate the specimens were conditioned. This indicates that carbonation in an elevated carbon dioxide content leads to the same structural changes as carbonation in natural air, at least up to 1 vol-% carbon dioxide.

9.3.3 Mortar with OPC and 5 % silica as part of the binder

Figure 9.3 shows the result of the low-temperature calorimetry measurement for the naturally carbonated mortar with OPC + 5 % silica as part of the binder and with a w/b-ratio of 0.55. The results are expressed as apparent heat capacity as a function of temperature during cooling and heating. The figure also shows the results for uncarbonated and carbonated (1 vol-%) materials of the same mortar quality.

From the figure, it can be seen that the apparent heat capacities of the two carbonated specimens show a close resemblance. During cooling, both carbonated materials show relatively large initial ice formation, as do also the uncarbonated materials. However, for the two carbonated materials, ice formation rapidly decreases and a second ice formation peak can be seen for both materials between –5 °C and –10 °C.

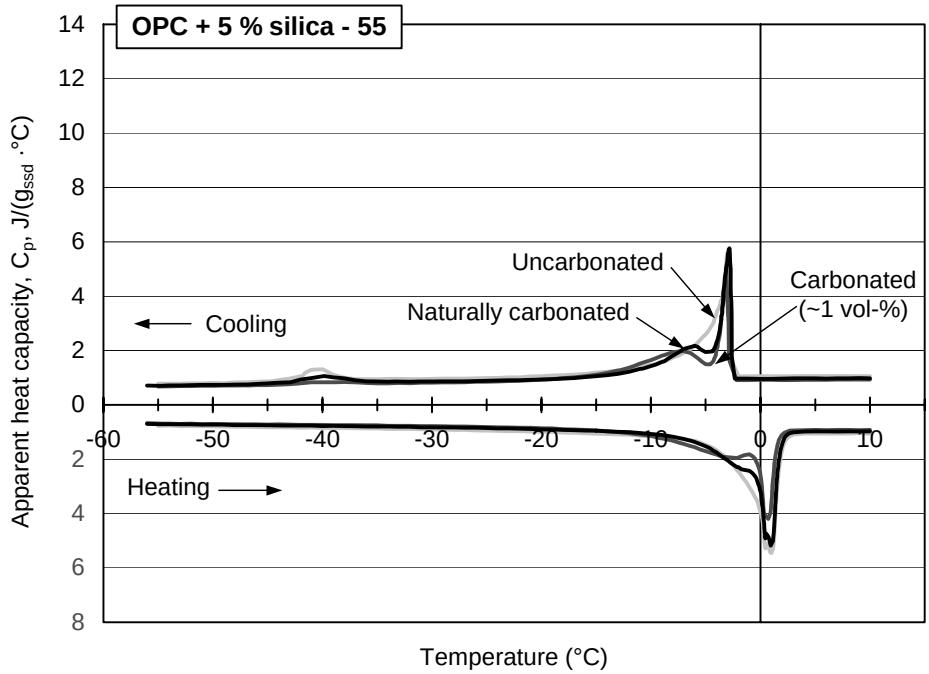

Figure 9.3 *Apparent heat capacity as a function of calorimeter block temperature during cooling (←) and heating (→) for uncarbonated and carbonated (naturally and in ~1 vol-%) mortar with OPC + 5 % silica as part of binder and with a w/b-ratio of 0.55.*

At –40 °C, the uncarbonated material show significant ice formation, while the carbonated (1 vol-%) material shows only slight ice formation. For the naturally carbonated material, the ice formation at –40 °C is similar to, but somewhat larger than, that for the fully carbonated (1 vol-%) material.

During thawing, there are some small differences between the materials at the thawing 'peak' around 0 °C. However, the differences are relatively small, and can be explained (as was mentioned above) by the fact that the naturally carbonated specimen was not completely carbonated, but had a core of uncarbonated material of about 30 % of the specimen volume.

Non-freezable water content

Table 9.2 shows the evaporable and calculated non-freezable water contents during cooling and heating. The table also shows results for a 'fictitious' specimen, carbonated to about 70 %, calculated from the results for the uncarbonated and carbonated (1 vol-%) specimens.

From the table, it can be seen that the results for the naturally carbonated specimen are closer to the results for the carbonated (1 vol-%) specimen than to the results for the

uncarbonated specimen. There is, however, a significant difference between the two carbonated specimens, which can be explained by the incomplete carbonation for this material. As can be seen, the results for the calculated 'fictitious' specimen (carbonated to 70 %) agree very well with the results for the naturally carbonated specimen.

Table 9.2 *Measured evaporable water content (W_e) and calculated non-freezable (W_{nf}) water content during cooling and heating for mortar with OPC + 5 % silica as part of the binder and with a w/b-ratio of 0.55.*

Mortar quality		W_e mg/g_{dry}	W_{nf} (mg_{ice}/g_{dry}) cooling -7	-10	-15	-20	-25	-35	-55°C
OPC + 5% silica - 55	**Uncarbonated**	111	80.9	73.8	67.0	64.4	61	58.4	48.2
	Carbonated (acc)	69	49.1	38.9	30.2	27.5	24.6	23.3	19.3
	Naturally carbo.	85	57.6	50	43.2	41.5	38.4	36.5	27.6
	Calculated 70 %	*82*	*58.6*	*49.4*	*41.2*	*38.6*	*35.5*	*33.8*	*28.0*
		W_e mg/g_{dry}	W_{nf} (mg_{ice}/g_{dry}) heating -7	-10	-15	-20	-25	-35	-55°C
OPC + 5% silica - 55	**Uncarbonated**	111	61.3	58.7	53.5	51.4	47.8	45.7	45.3
	Carbonated (acc)	69	34	29.5	23.9	22.4	19.8	19.2	20.1
	Naturally carbo.	85	40.2	37.5	32.9	31.5	28.6	28.8	26.5
	Calculated 70 %	*82*	*42.2*	*38.3*	*32.8*	*31.1*	*28.2*	*27.2*	*27.7*

Water absorption during capillary suction

Figure 9.4 shows the results from capillary suction for the three specimens conditioned in different climates, made from mortar with 5 % silica and a w/b-ratio of 0.55. The results show that the moisture ratio for the naturally carbonated specimen is somewhat higher than for the fully carbonated (1 vol-%) specimen, although the appearance of the capillary suction curves for the two carbonated materials are very similar. The water absorption rate during the first stage of capillary suction is about the same, and the time until the nick-point is reached is also the same, for both carbonated materials. This indicates similar pore structures; in this case more dense and with a higher resistance to water penetration than for the uncarbonated material.

The higher moisture ratio for the naturally carbonated material compared to the fully carbonated (1 vol-%) is to be expected, and is due to the incomplete carbonation of the naturally carbonated specimen. If we calculate a moisture ratio during the slow water absorption stage for a 'fictitious' specimen (carbonated to 70 %), the result will be very close to that for the naturally carbonated specimen.

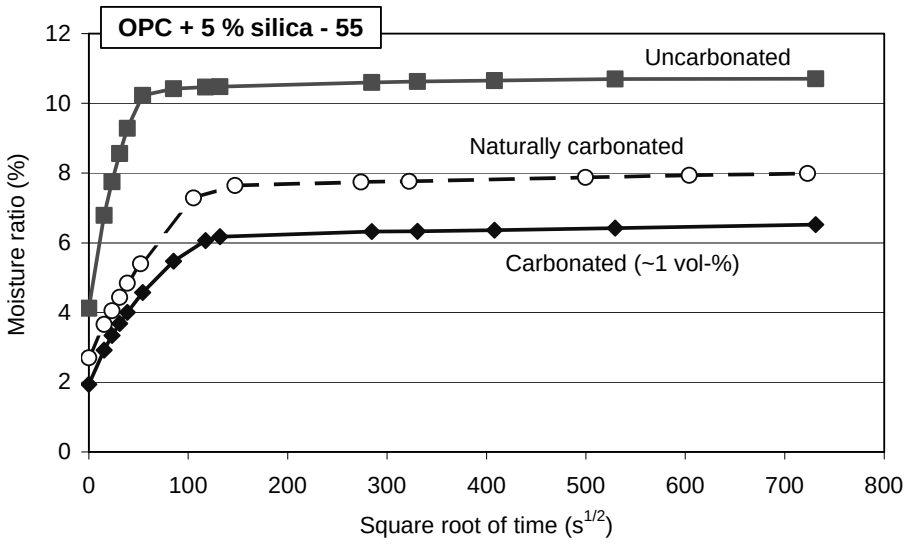

Figure 9.4 *Moisture ratio during capillary suction as a function of the square root of time for uncarbonated and carbonated (naturally and in ~1 vol-%) mortar with OPC + 5 % silica as part of the binder and with a w/b-ratio of 0.55.*

Conclusion

Even though the results from the naturally carbonated specimen might seem significantly different from the fully carbonated (1 vol-%) specimen, this difference can largely be explained by the incomplete carbonation of the naturally carbonated specimen. If this is taken into account, the results from both capillary suction and the LTC measurements show a good correlation between naturally carbonated and fully carbonated (1 vol-%) materials. This is an indication that for mortar containing small amounts of silica, and for mortar with only OPC as binder, accelerated carbonation in 1 vol-% carbon dioxide results in the same pore structural changes as does natural carbonation.

9.3.4 Mortar with OPC and 65 % slag as part of the binder

Mortar with w/b-ratio 0.55

The LTC measurement for mortar with OPC and 65 % slag as part of the binder, and with a w/b-ratio of 0.55, failed because of a power failure during the measurement. Even though no results from the calorimetric measurements are at hand, the results from capillary suction during preconditioning before the LTC measurement was carried out can be used for comparison, Figure 9.5.

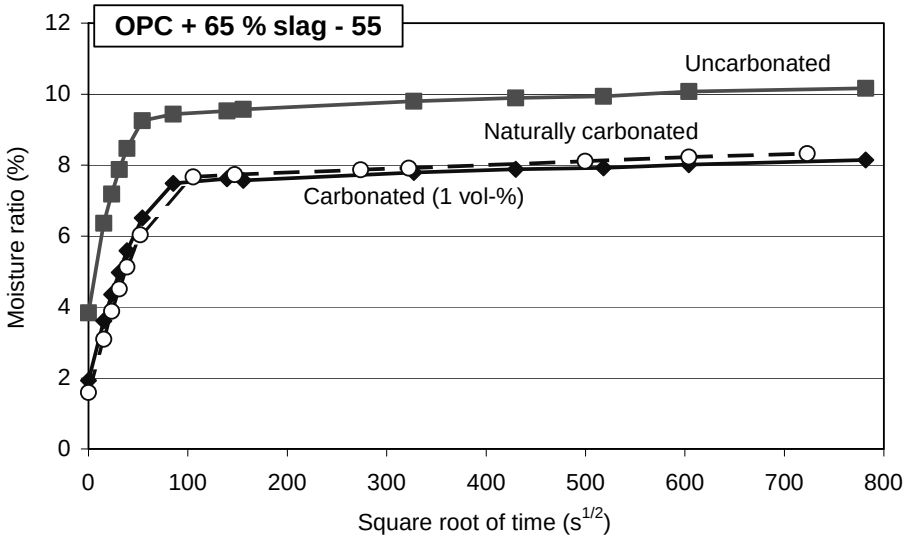

Figure 9.5 *Moisture ratio during capillary suction as a function of the square root of time for uncarbonated and carbonated (naturally and in ~1 vol-%) mortar with OPC + 65 % slag as part of the binder and with a w/b-ratio of 0.55.*

From the figure, it can be seen that capillary suction leads to almost identical water absorption for the naturally carbonated and the fully carbonated (1 vol-%) specimens. This is true for both the first rapid and the second slow stage of capillary suction. Since this material proved to be fully carbonated (using the phenolphthalein test), an identical moisture ratio was expected. The results from the capillary suction test thus indicate that carbonation of this material containing large amounts of slag as part of the binder results in the same pore structural changes, regardless of carbon dioxide content in the preconditioning climate, at least up to 1 vol-% carbon dioxide.

Mortar with w/b-ratio 0.45

The LTC measurements on mortar with 65 % slag as part of the binder and with a w/b-ratio of 0.45 were more successful. Figure 9.6 shows the result of the low-temperature calorimetry measurement for the naturally carbonated 'OPC + 65 % slag - 45' mortar as the apparent heat capacity as a function of temperature during cooling and heating. The figure also shows the results for uncarbonated and carbonated (1 vol-%) materials of the same mortar quality.

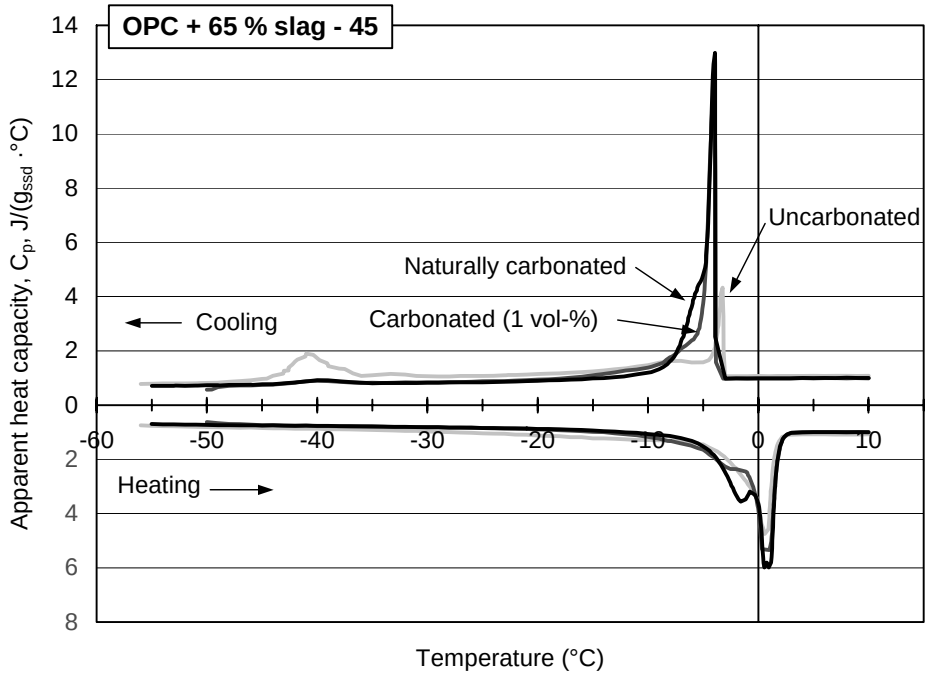

Figure 9.6 *Apparent heat capacity as a function of calorimeter block temperature during cooling (←) and heating (→) for uncarbonated and carbonated (naturally and in ~1 vol-%) mortar with OPC + 65 % slag as part of the binder and with a w/b-ratio of 0.55.*

From the figure, it can be seen that the results from the LTC measurements show very similar results for the two carbonated materials. Both materials show a large initial ice formation around –5 °C. After this initially large ice formation, formation decreases with no significant ice formation peaks for any of the carbonated materials at lower temperatures. For uncarbonated material, on the other hand, a small initial ice formation is followed by a significant ice formation at around –40 °C.

The appearance of the apparent heat capacity curve during thawing is about the same for both carbonated materials, with significant melting 'peaks' close to 0 °C. For the carbonated materials, a second melting 'peak' at a couple of degrees below 0 °C can be seen. The two peaks might be an indication of a pore structure with two different pore size intervals containing significant amount of pore space. The melting peak at a couple of degrees below zero is somewhat more apparent for the naturally carbonated material. The differences between the carbonated materials are small, but indicate that the naturally carbonated material may have a somewhat more significant division into two dominant pore size intervals.

Non-freezable water content

Table 9.3 shows the evaporable and calculated non-freezable water contents during cooling and heating.

Table 9.3 *Measured evaporable water content (W_e) and calculated non-freezable (W_{nf}) water content during cooling and heating for mortar with OPC + 65 % slag as part of the binder and with a w/b-ratio of 0.55.*

Mortar quality		**W_e**	**W_{nf} (mg_{ice}/g_{dry}) cooling**						
		mg/g_{dry}	-7	-10	-15	-20	-25	-35	-55°C
OPC + 65% slag - 45	**Uncarbonated**	108	95.5	90.2	83.3	80.1	75.8	69.4	45.0
	Carbonated (acc)	88	48.9	41.6	34.4	32.3	29.8	29.1	25.5
	Naturally carbo.	90	39.1	33.7	28.9	28.6	25.7	26.1	21.8
		W_e	**W_{nf} (mg_{ice}/g_{dry}) heating**						
		mg/g_{dry}	-7	-10	-15	-20	-25	-35	-55°C
OPC + 65% slag - 45	**Uncarbonated**	108	67.8	64.6	57.1	52.9	47.5	43.4	39.5
	Carbonated (acc)	88	36.9	32.7	26.7	25.2	22.2	21.3	20.5
	Naturally carbo.	90	32.3	29.7	24.9	23.9	20.9	19.7	17.8

From the results presented in the table, it can be seen that both the evaporable water content and the non-freezable water content during cooling and during heating are comparable for the carbonated materials. The naturally carbonated material, however, generally shows a somewhat lower amount of non-freezable water content than does the material exposed to accelerated carbonation. The difference is relatively small, considering that only one measurement on one specimen per material was carried out. However, the difference does indicate that carbonation in natural air possibly leads to a coarser pore structure, which is the interpretation of lower non-freezable water content (provided equal evaporable water content), than does carbonation in an atmosphere with elevated CO_2 content.

One objection to the use of accelerated carbonation was that this could possibly lead to unnatural pore structural changes compared to natural carbonation, especially for mortars containing large contents of slag as part of the binder. For this material, it was feared that accelerated carbonation might lead to changes resulting in too coarse a pore structure compared to natural carbonation. If this were the case, it would lead to an overestimation of the effect of carbonation on the pore structure for this type of material. The results found here, however, point in the opposite direction, i.e. that the naturally carbonated material has a somewhat coarser pore structure than does material exposed to accelerated carbonation. This implies that the results from the investigations carried out and presented in this thesis for mortar containing large amounts of slag as part of the binder, and using specimens carbonated in an atmosphere with elevated CO_2 content (1 vol-%), give relevant results or results that might even somewhat underestimate the effect of natural carbonation.

Water absorption during capillary suction

Figure 9.7 shows the results from capillary suction of the three specimens conditioned in different climates from mortar quality with 65 % slag as part of the binder and with a w/b-ratio of 0.45.

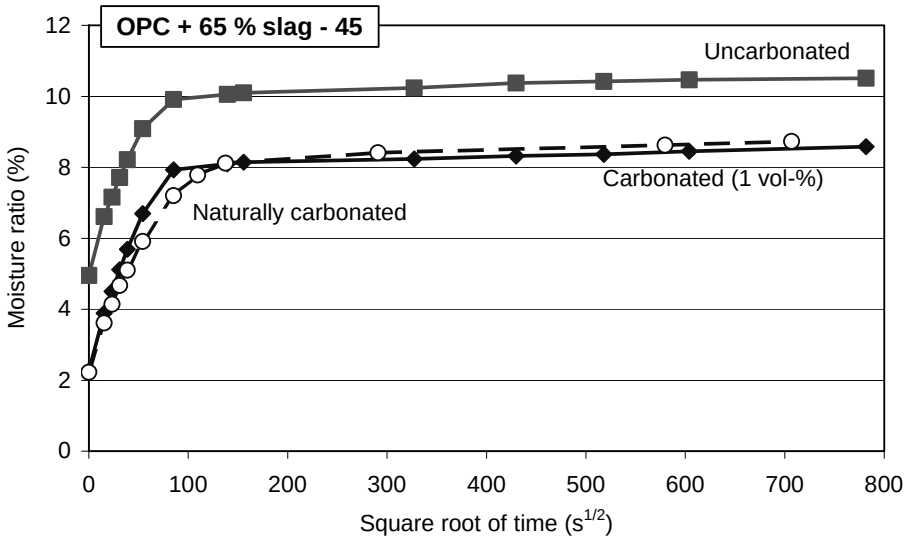

Figure 9.7 *Moisture ratio during capillary suction as a function of the square root of time for uncarbonated and carbonated (naturally and in ~1 vol-%) mortar with OPC + 65 % slag as part of the binder and with a w/b-ratio of 0.45.*

From the figure, it can be seen that water absorption during capillary suction is close to identical for the two carbonated materials. This is the same result as was found for mortar with the same binder combination but with a w/b-ratio of 0.55. The results from the capillary suction are thus a further indication that carbonation of this material containing large amounts of slag as part of the binder results in the same pore structural changes, regardless of carbon dioxide content in the environment during preconditioning, at least up to 1 vol-% carbon dioxide.

9.4 Conclusions

Carbonation of mortar with OPC alone, OPC with 5 % silica and OPC with 65 % slag as part of the binder in environments with different carbon dioxide contents (natural air and air with ~ 1.0 vol-% carbon dioxide) shows similar results regardless of carbon dioxide content. This shows that carbonation using an elevated carbon dioxide content of ~1 vol-% results in the same type of structural changes as were found for materials carbonated in normal air. The results found here thus strengthen the validity and relevance of the results from the investigations presented in this thesis using an elevated carbon dioxide content of ~1 vol-%.

10 The effect of carbon dioxide concentration on the mineralogical composition of the carbonated zone

10.1 Introduction

When using unnatural concentrations in order to accelerate a process, there is always a risk of effects that would not take place under normal circumstances. Chapter 9 described a limited investigation of the physical effects of carbonation as a result of conditioning in environments with different carbon dioxide contents. The results indicated that the pore structural effects of carbonation were the same for the tested materials, regardless of carbon dioxide content during carbonation, at least for carbon dioxide contents up to 1 vol-%. In order also to investigate the chemical effects of accelerated carbonation, a limited investigation using X-ray diffraction was carried out. The results from this investigation are presented in this chapter.

Another reason for carrying out this chemical investigation is that there are descriptions in the literature of chemical explanations for the effect of carbonation on the salt-frost resistance. For example, Stark & Ludwig (1997:1) explain the observed negative effect of carbonation on the scaling resistance of concrete containing high contents of slag as part of the binder as due to primarily chemical effects. According to them, carbonation of materials with different binder types/combinations leads to the formation of different carbonate phases. Carbonation of materials containing high amounts of slag, for example, leads to the formation of calcite and also significant amounts of the metastable carbonate forms, aragonite and vaterite. Carbonation of materials with only OPC as the binder leads primarily to the formation of calcite. These differences in formation of different carbonate phases would, according to Stark & Ludwig (1997:1), be the reason for the adverse effects of carbonation on the salt-frost resistance of these materials.

The limited chemical investigation carried out here thus also serves as an indication of whether the chemical explanations for the effect of carbonation presented in Stark & Ludwig (1997:1) may be part of the explanation for the findings from the investigations described in this thesis.

10.2 Materials, specimens and test method

In this investigation, two pastes were produced: one with only OPC as the binder, and one with OPC + 65 % slag as part of the binder, both with a w/b-ratio of 0.45. The OPC and slag used were the same as were used in all other investigations described in this thesis (for chemical analysis, see Appendix 4). The reason for producing new pastes instead of analysing the carbonated mortars used in the different investigations described above was that with the technique used (X-ray diffraction) the diffractions from the aggregate in the mortars interfere with those from the carbonate phases. Due to this effect, it is practically impossible to distinguish all possible crucial diffractions from the carbonate phases in the

paste of a mortar from aggregate diffractions, which in itself is very complex. It is here assumed that carbonation of concrete, mortar and pastes results in the same formation of carbonate phases.

The pastes were mixed using a 5-litre mortar mixer from Toni Technik. The pastes were cast in moulds consisting of cylindrical plastic bottles. After casting, the bottles were mounted on a rotating wheel and turned at 3-4 r/min for the first 24 hours in order to prevent separation. After seven days in the moulds, the 'paste bottles' were stripped and the paste cylinders immediately cut into thin discs, with a thickness of ~3 mm. Immediately after cutting, the discs were crushed (particles with a size less than 2 mm) and divided in two parts, which were immediately placed in two environments with different carbon dioxide concentrations. The time for cutting, crushing and placing in the different environments was kept at a minimum to prevent unwanted carbonation before being placed in the correct environment. The two environments used were the same as in the investigation described in Chapter 9, i.e. one with an elevated carbon dioxide content (~1 vol-%) and one with normal laboratory air, both with 65 % RH and +20 °C. Conditioning with increased carbon dioxide was carried out in the climate chamber described in Chapter 3. Conditioning in normal air was carried out in a climate-controlled area in the laboratory.

The crushed material was conditioned for eleven weeks in the respective climates before an analysis of the formed carbonate phases was carried out using X-ray diffraction analysis. A second analysis was made after conditioning for about two years. It must be noted that, due to the fact that no analysis after two years was planned, carbon dioxide was only sporadically let into the chamber with increased carbon dioxide content. As a result of this, the carbon dioxide concentration in this chamber was significantly below 1 vol-% for most of the time during the two years of conditioning. However, it was at all times higher than the CO_2 concentration in natural air.

The X-ray diffraction analysis was carried out at the Department of Geology - Lithosphere and Biosphere Science, at the University of Lund. One sample of each material conditioned in the two climates was analysed. The crushed samples were put in airtight test tubes prior to transportation to Lund. Before analysis, the material was further crushed in alcohol and pipetted on to a silicon plate and put in a sample-holder of siliceous material using a pipette. The analysis was carried out in a Philips PW 1710 X-ray diffractometer within the scanning range 20° to 60° ($2 \cdot \theta$), with steps of 0.020° ($2 \cdot \theta$) and a time constant of 0.5 second.

When evaluating measurements from X-ray diffraction, the term reflection is commonly used. However, the X-ray beam is not actually reflected, but diffracted, and so this term is used here.

10.3 Results and discussion

10.3.1 Comparison between carbonate phases for pastes carbonated in environments with different carbon dioxide concentrations

The results from the X-ray diffraction analysis after eleven weeks of conditioning in the two different climates for paste with OPC are shown in Figure 10.1. The corresponding results for paste with 65 % slag as part of the binder are shown in Figure 10.2.

Paste with OPC - 11 weeks

Figure 10.1a shows the X-ray diffractogram for the crushed material of OPC paste conditioned in a climate with natural carbon dioxide content for eleven weeks. The diffractogram shows strong diffractions demonstrating the existence of calcite. There are also some clear diffractions indicating the existence of vaterite and aragonite as well as unhydrated cement. These diffractions are, however, not as strong as those for calcite, indicating that most calcium carbonate is in the form of calcite. The diffraction at 16.9 ° (θ) shows that small amounts of uncarbonated calcium hydroxide also seem to be present.

Figure 10.1b shows the X-ray diffractogram for material of the same OPC paste but conditioned in a climate with increased carbon dioxide content (~1 vol-%). The results are essentially the same as when carbonated in normal air, i.e. clear strong diffractions demonstrating a significant amount of calcite and some smaller diffractions that reveal also the presence of vaterite, aragonite as well as small amounts of unhydrated cement and calcium hydroxide.

For materials with OPC alone as the binder, these results indicate that carbonation in a climate with increased carbon dioxide content results in the same carbonate phases as if carbonated in air with normal carbon dioxide, at least if the increased carbon dioxide content does not exceed 1 vol-% CO_2.

Paste with OPC and 65 % slag as part of the binder - 11 weeks

Figure 10.2a shows the X-ray diffractogram for crushed cement paste with high contents of slag as part of the binder, conditioned in air with normal carbon dioxide content for eleven weeks. From the results, it can be seen that there are some clear diffractions demonstrating the presence of calcite. There are also some diffractions revealing the presence of vaterite and aragonite as well as some unhydrated cement. The calcite diffractions, however, show the strongest intensity, indicating that most of the carbonation product is in the form of calcite. For this material, there are no detectable diffractions indicating the presence of calcium hydroxide.

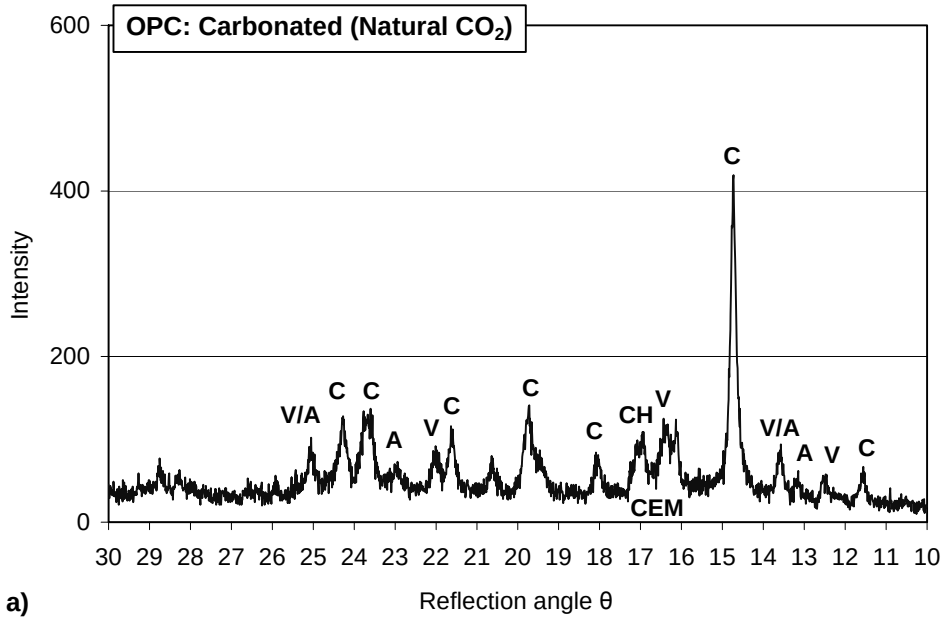

a)

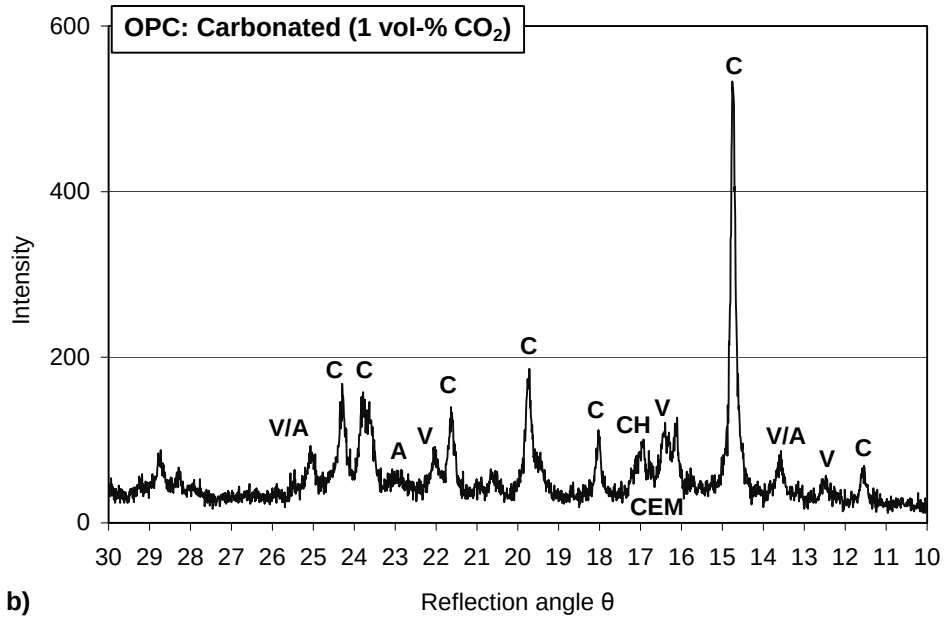

b)

Figure 10.1 *X-ray diffraction of cement pastes with only OPC as the binder, conditioned in climates with different carbon dioxide contents for eleven weeks. (CH - Calcium Hydroxide, C - Calcite, A - Aragonite, V - Vaterite, CEM - unhydrated cement). a) natural air, b) air with 1 vol-% carbon dioxide.*

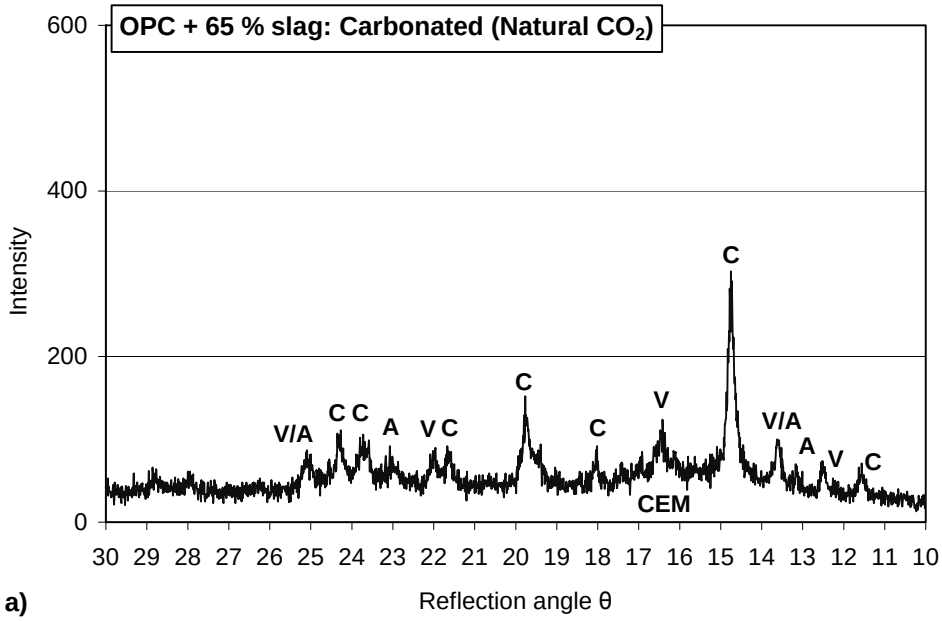

a)

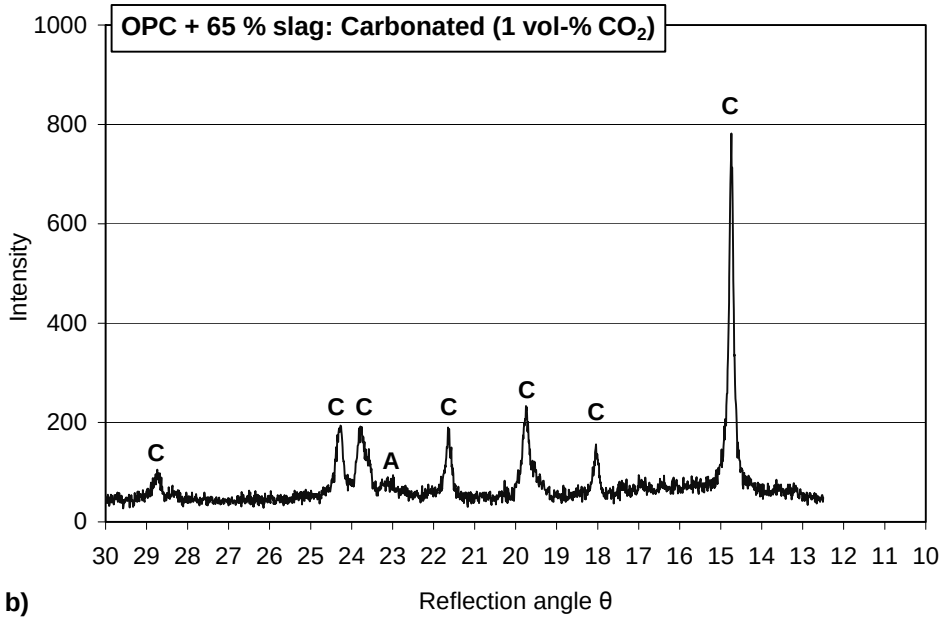

b)

Figure 10.2 *X-ray diffraction of cement pastes with OPC and 65 % slag as part of the binder, conditioned in climates with different carbon dioxide contents for eleven weeks. (CH - Calcium Hydroxide, C - Calcite, A - Aragonite, V - Vaterite, CEM - unhydrated cement). a) natural air, b) air with 1 vol-% carbon dioxide.*

The X-ray diffractogram for material of the same paste with slag and conditioned in a climate with increased carbon dioxide content is shown in Figure 10.2b. The results show clear diffractions with high intensity, demonstrating the presence of calcite. No other significant diffractions can be identified. This shows that for paste with slag as part of the binder there is a small difference in carbonation products formed depending on in what climate, i.e. at what carbon dioxide content, carbonation takes place.

The results show that in both climates the most dominant carbonate phase formed is calcite. However, when carbonated in natural air, there are also indications of small amounts of calcium carbonate in the form of vaterite and aragonite. When carbonated in an environment with an elevated carbon dioxide content, no such indications are found. The reason for this is not known. One possible explanation, however, is that carbonation in the climate with increased carbon dioxide content for eleven weeks results in more complete carbonation than does carbonation in natural air for the same period. According to Matala (1995), carbonation first leads to the formation of vaterite and aragonite, and as a result of further carbonation these products are transformed to calcite. To investigate if a longer time of conditioning would lead to other carbonate phases a second analysis was carried out after two years of conditioning.

The results from the X-ray diffraction analysis after two years' conditioning in the respective climates are shown in Figure 10.3 for the OPC paste, and in Figure 10.4 for the paste with OPC + 65 % slag as part of the binder. For comparison, the results from the analysis after eleven weeks are also shown.

Paste with OPC - 2 years

For materials with OPC alone as the binder, these results indicate that carbonation in a climate with increased carbon dioxide content (Figure 10.3b) results in the same carbonate phases as if carbonated in air with normal carbon dioxide (Figure 10.3a), at least if the increased carbon dioxide content does not exceed 1 vol-% CO_2. That is, the most dominating and strong diffractions are found for calcite, whereas some weaker diffractions reveal the presence of some vaterite and possibly also some small amounts of aragonite. The diffraction at 16.9 ° (θ) indicates that some uncarbonated calcium hydroxide is also present, even after two years of conditioning in climates with carbon dioxide.

For OPC paste, the results after two years' conditioning are about the same as after eleven weeks, indicating that prolonged carbonation does not lead to any significant changes in carbonate phases; at least, not with the materials, conditioning climates and conditioning times used here.

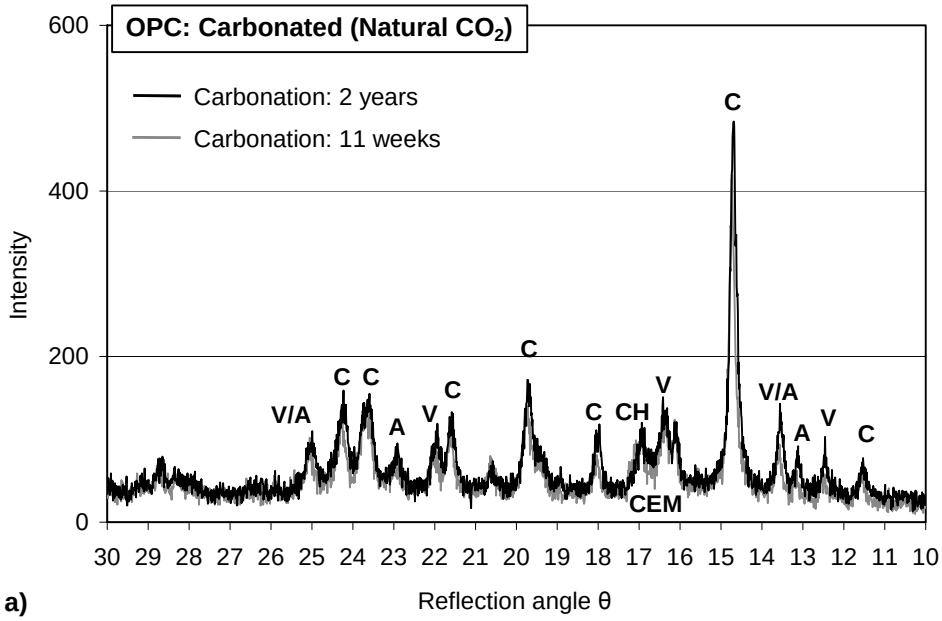

a)

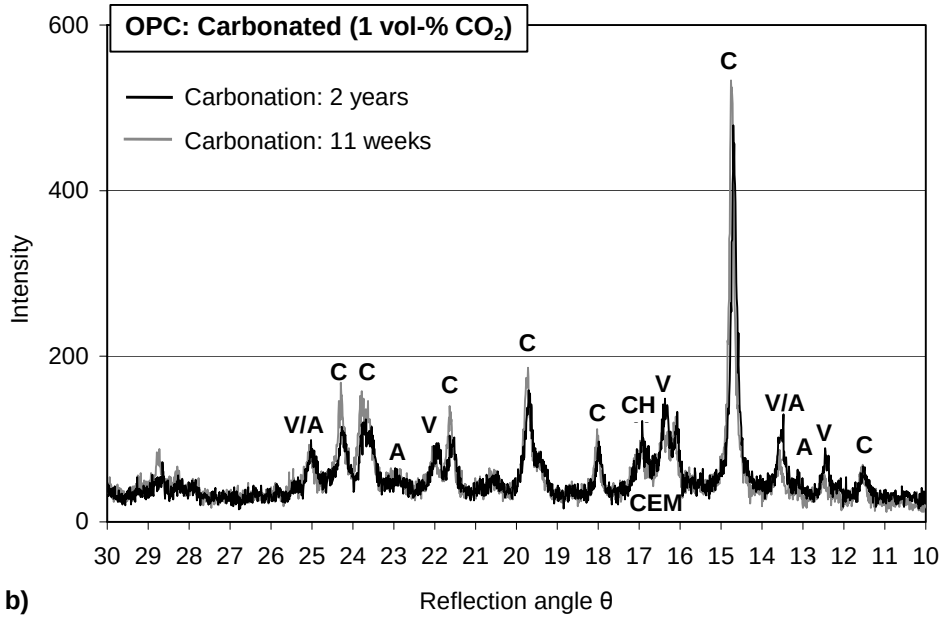

b)

Figure 10.3 *X-ray diffraction of cement pastes with only OPC as the binder and conditioned in two climates with different carbon dioxide contents for eleven weeks and two years respectively. (CH - Calcium Hydroxide, C - Calcite, A - Aragonite, V - Vaterite, CEM - unhydrated cement). a) natural air, b) air with 1 vol-% carbon dioxide.*

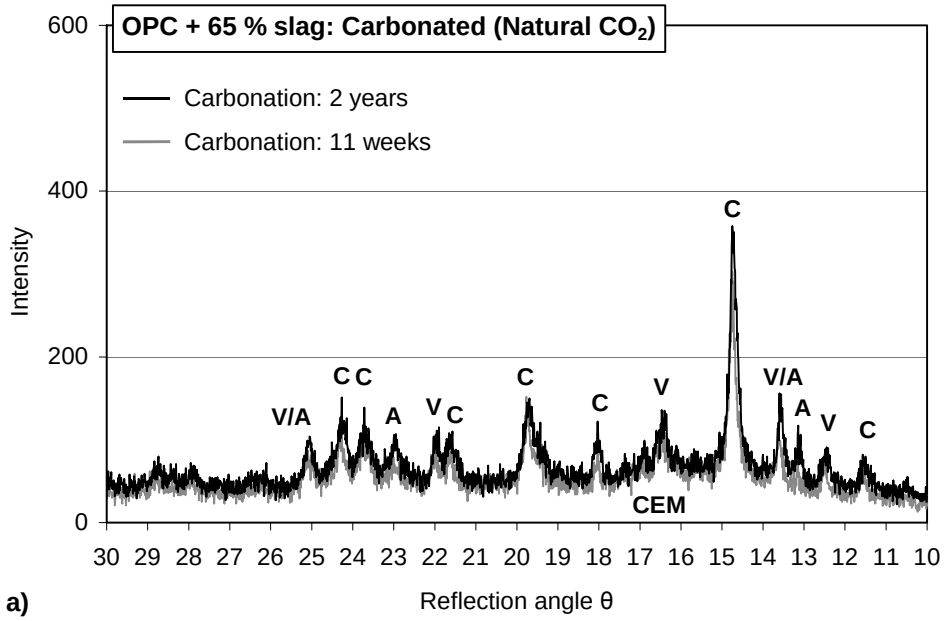

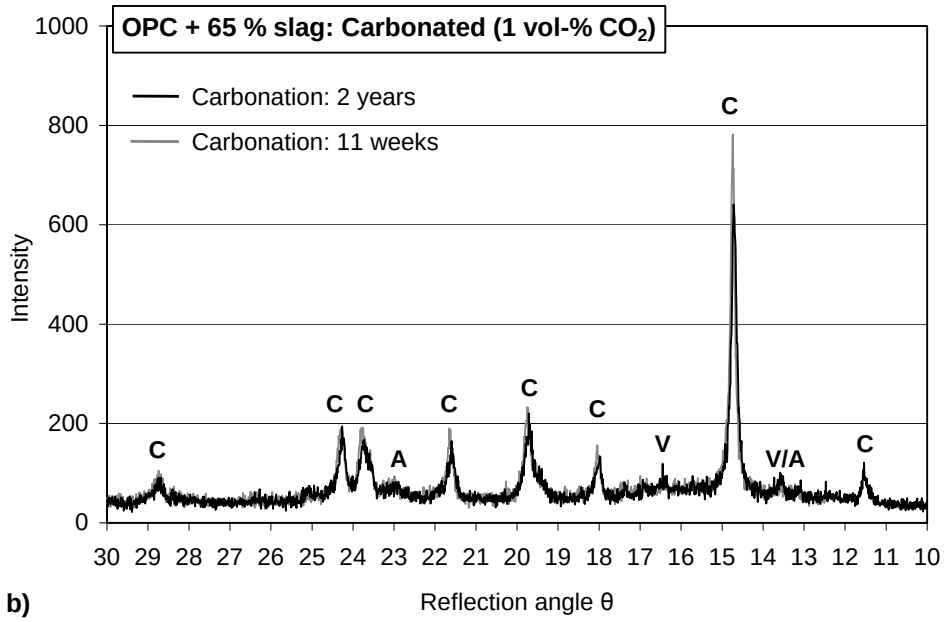

Figure 10.4 *X-ray diffraction of cement pastes with OPC and 65 % slag as part of the binder and conditioned in two climates with different carbon dioxide contents for eleven weeks and two years respectively. (CH - Calcium Hydroxide, C - Calcite, A - Aragonite, V - Vaterite, CEM - unhydrated cement). a) natural air, b) air with 1 vol-% carbon dioxide.*

Paste with OPC and 65 % slag as part of the binder - 2 years

For cement paste with high contents of slag as part of the binder the results are essentially the same after two years as after eleven weeks. The X-ray diffractogram for material conditioned in normal air (Figure 10.4a) shows strong calcite diffractions and some smaller diffractions of vaterite and aragonite. For material conditioned in an environment with increased carbon dioxide content (Figure 10.4b), the results show essentially only calcium carbonate in the form of calcite. There are also some indications of the presence of small amounts of calcium carbonate in the form of vaterite and aragonite. It can, however, be inferred from the diffractogram that the amounts of these two carbonate phases are small in comparison with the calcite phase. This shows that the same differences in carbonate phases due to carbon dioxide content in the conditioning climate found for this material after conditioning for eleven weeks, still exist after conditioning for two years. In other words, prolonged carbonation of this material, too, does not seem to lead to any significant changes in carbonate phases, at least not with the materials, conditioning climates and conditioning times used here.

Discussion

From the results for the OPC paste (Figure 10.3a) and the paste with OPC + 65 % slag as part of the binder (Figure 10.4a) carbonated in normal air, it can be seen that there are no marked differences between the carbonate phases that are formed; at least, not with the materials used in this investigation when conditioned in normal air for eleven weeks and two years respectively. The only difference, however small, between carbonated paste with and without slag as part of the binder is that the carbonated OPC paste shows indications of some small amounts of residual calcium hydroxide, even after two years' conditioning. This is not found for pastes with slag as part of the binder. One explanation for this might be the lower amount of calcium hydroxide present in uncarbonated materials with high contents of slag as part of the binder.

In the investigations described in this thesis, carbonation was carried out in an environment with 1 vol-% carbon dioxide. For material with OPC alone as the binder, it was shown that the same carbonate phases were formed in natural air as in an environment with 1 vol-% carbon dioxide. However, for material with high contents of slag as part of the binder, a slight difference in the formed carbonate phases was found, depending on the carbon dioxide content in the air during conditioning. It is not known how this small difference might affect the results for carbonated mortars and micro-concretes in the investigations described here.

However, it can be concluded that in both climates carbonation of materials with high contents of slag as part of the binder leads to calcite as the main form of calcium carbonate. It can also be concluded that since calcite is the stable form of the carbonate phases, the materials carbonated in environments with increased carbon dioxide content have more stable forms of carbonates than material carbonated in natural air, which have been shown also to include vaterite and aragonite. This implies that the effect of carbonation for the materials containing high contents of slag as part of the binder might be somewhat

underestimated when carbonated in an environment with increased carbon dioxide content. However, as was mentioned above, since the effects of carbonation on (for example) the salt-frost resistance of material containing high contents of slag are very clear, a slight underestimation does not significantly change the interpretation of the results for material carbonated in the elevated carbon dioxide concentration described in this thesis.

It must be noted that, in Chapter 9, results were presented that pointed towards the fact that carbonation in natural air of mortar with 65 % slag as part of the binder results in a somewhat coarser pore structure than occurs with accelerated carbonation in 1 vol-% CO_2. This is also an indication that the results for mortar carbonated in elevated carbon dioxide content may somewhat underestimate the 'true' effect of carbonation for these materials. However, since the effect of carbonation on the salt-frost resistance for materials with high slag contents is very clear, a slight underestimation does not significantly change the conclusions.

10.3.2 Chemical effects of carbonation as a cause of effects of carbonation on the salt-frost resistance

In the literature review presented in Chapter 4 it was found that, in addition to 'physical' explanations for the effect of carbonation on the salt-frost resistance, there are also explanations based on chemical processes. For example, Stark & Ludwig (1997:1) explain the observed negative effect of carbonation on the scaling resistance of concrete containing high contents of slag as part of the binder by primarily a chemical effect. According to them, carbonation of concrete with high slag contents led to formation of calcium carbonate in the form of aragonite, vaterite and calcite. The metastable carbonate forms, aragonite and vaterite, dissolve as the result of a combined attack of frost and chloride, which leads to an extensive erosion of the carbonated layer. Carbonation of concrete with only OPC as the binder, however, leads essentially to carbonates in the form of calcite. The paper presented a phase analysis of two carbonated cement pastes, one with OPC alone and one with 65 % slag as part of the binder; see Figure 10.5. However, it did not describe how the pastes had been conditioned, i.e. in what relative humidity and carbon dioxide content the pastes had been conditioned, or for how long.

From Figure 10.5, it can be seen that the carbonated sample with only OPC as the binder shows only two significant diffractions: one representing uncarbonated calcium hydroxide, and one representing calcium carbonate in the form of calcite. However, for the carbonated paste containing high contents of slag as part of the binder, there are five significant diffractions. Four of them represent aragonite and/or vaterite, and one represents calcite. It must be noted that some of the diffractions indicative of vaterite and aragonite show a higher intensity than the calcite diffraction. For these pastes, there therefore seems to be a significant difference in what phases are formed as a result of carbonation.

The results presented above from analysing the carbonate phases of carbonated pastes with only OPC as the binder, and with OPC + 65 % slag as part of the binder, using X-ray

diffraction, do not confirm the findings in Stark & Ludwig (1997:1). On the contrary, carbonation in a climate with increased carbon dioxide content resulted in the opposite effect. Paste with only OPC as the binder showed dominant calcite diffractions, with some clear diffractions indicating the existence of vaterite and possibly also aragonite. Paste with 65 % slag as part of the binder showed no, or only few, signs of vaterite and aragonite, but very dominant calcite diffractions. For pastes carbonated in normal air, there were no significant differences in the formation of carbonate phases between the two pastes. Both showed dominant calcite diffractions and some smaller but still significant diffractions revealing vaterite and aragonite.

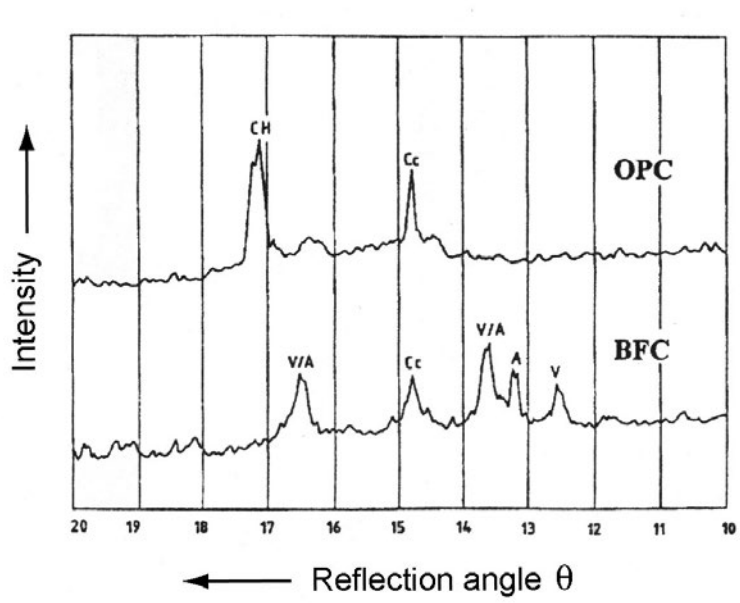

Figure 10.5 *X-ray diffraction of carbonated surface area of Ordinary Portland Cement pastes and Blast Furnace Cement pastes. (CH - Calcium Hydroxide, Cc - Calcite, A - Aragonite, V - Vaterite). From Stark & Ludwig (1997:1).*

The results found here for pastes with high slag contents carbonated in an elevated carbon dioxide atmosphere differ significantly from the results presented in Stark & Ludwig (1997:1). There is therefore no support from the present investigation for the idea that the effect of carbonation on the salt-frost resistance of materials with high slag contents (as used in the investigations described here) could be explained by a chemical process similar to that proposed by Stark & Ludwig. On the contrary, the results found here indicate that a chemical explanation as described by Stark & Ludwig is ruled out for the materials used in this investigation. In fact, in this investigation, pastes with OPC alone as the binder showed more marked diffractions revealing the existence of vaterite and aragonite in the carbonated paste than did pastes with high slag content. This means that if the chemical effects proposed by Stark & Ludwig had an effect on the samples in the present investigation, this could be expected to be more dominant for material with only OPC as

the binder than for material with 65 % slag as part of the binder. The results found in the investigations described here provide no such indications.

It must be noted that the results presented here are valid only for the climates, the cement type and type of granulated blast furnace slag used in this investigation. Other cement types and other secondary cementitious materials, as well as climates with other carbon dioxide contents and other relative humidities may lead to other results. The results presented here therefore do not exclude the possibility that there could be chemical effects for some materials conditioned in climates with some special characteristics that significantly influence the salt-frost resistance of cement-bound materials. However, the results presented above show that, for the materials used, nothing points toward chemical processes as a general explanation for the marked effects of carbonation on the salt-frost resistance.

The significant difference between the results from this study and those described by Stark and Ludwig implies that the processes controlling the relation between the type of binder and phase formation in connection with carbonation are complex and would need a more comprehensive study to be fully understood. Possible chemical explanations should not be excluded but instead further investigated. This would include investigation of the influence of material composition (cement type and type of secondary cementitious material) as well as that of conditioning climates (relative humidity and carbon dioxide content) on the formation of carbonate phases. This knowledge, together with examinations of the physical effects of carbonation, would make it possible to evaluate the physical and chemical effects of carbonation on different durability aspects, such as salt-frost resistance and resistance to chloride attack. Since carbonation is a spontaneous process, and can hardly be avoided in normal environments, the physical and chemical effects of carbonation on all durability aspects are of great importance.

10.4 Conclusions

The following conclusions can be drawn from comparing the carbonate phases formed as a result of conditioning pastes of OPC alone and OPC with 65 % slag as part of the binder in environments with different carbon dioxide contents, using X-ray diffraction analysis:

- Carbonation of cement paste of OPC with a w/b-ratio of 0.45 leads to the same phases of calcium carbonate, regardless of carbon dioxide concentration during conditioning, at least up to 1 vol-% carbon dioxide. For OPC paste, carbonation leads to the formation of primarily calcite, but also to small amounts of vaterite and aragonite.
- Carbonation of cement paste with 65 % slag as part of the binder in different environments leads to somewhat different results. Slag paste carbonated in normal air leads to the formation of primarily calcite, although vaterite and possibly also aragonite are formed as well. Carbonation in an environment with 1 vol-% CO_2, on the other hand, leads almost exclusively to calcite.

- The carbonate phases formed as a result of carbonation in normal air are the same for paste with only OPC as the binder and with OPC + 65 % slag as part of the binder, at least for the materials used in this investigation.
- X-ray diffraction analysis after conditioning in the different climates for two years gives the same results as after conditioning for eleven weeks. This is true both for the materials conditioned in normal air and in air with increased carbon dioxide content. This indicates that a prolonged conditioning time does not significantly change the formation of carbonate phases, at least not compared to the phases found after eleven weeks of conditioning.
- The results from this investigation do not confirm or support the chemical explanation for the effect of carbonation on the salt-frost resistance of concrete containing high contents of slag, as presented in Stark & Ludwig (1997:1). On the contrary, the results found here indicate that a chemical explanation as described by Stark & Ludwig is excluded for the materials and conditioning climates used in the investigations presented in this thesis. However, using other materials and/or other conditioning climates may lead to other results.
- Even though there are no indications of a significant chemical effect on the salt-frost resistance for the materials investigated here, a chemical effect as such cannot be excluded. The significant difference between the results from this study and that presented by Stark and Ludwig shows that the processes of carbonation are complex and would need a more comprehensive study to be fully understood.

11 Field exposure studies of the frost and salt-frost resistance of concrete

11.1 Introduction

The laboratory investigations were complemented by investigations at three field exposure sites. Two of these exposure sites were situated in saline environments: one being a marine environment and one a highway environment. The third exposure site was situated in a salt-free environment. The sites are described in Section 11.2.

The climates at the field exposure sites are described below in Section 11.2.2. For a more complete description of the climates, see Appendix 11, which shows meteorological data for the winter seasons (October - April) 1996/1997 to 2002/2003.

Over 100 mixtures of varying concrete qualities have been exposed at the sites since autumn 1996. This report describes the results for concrete qualities produced with four different binder types/combinations with different w/b-ratios and air contents. The material data and the test methods used are described in Section 11.3.

The results are presented and discussed in Section 11.4, with conclusions in Section 11.5. Some of the results were previously presented in Utgenannt & Petersson (2001), which is forming Appendix 3.

11.2 Field exposure sites

11.2.1 Description of the field exposure sites

The three field exposure sites are located in the south-western part of Sweden: one in a highway environment beside highway 40 (60 km east of Gothenburg), one in a marine environment at Träslövsläge harbour (80 km south of Gothenburg), and one in an environment without salt exposure on SP's premises in Borås (70 km east of Gothenburg). The following are descriptions of the sites.

Road environment - Highway 40

The field exposure site at highway 40 was established in the autumn of 1996. It consists of a 200 meter long and a couple of metres wide gravel area along the highway, with specimens mounted in steel frames at road level, Figure 11.1. A guard rail separates the exposure site from the traffic, and it is placed in such a way as to ensure that the specimens are fully exposed to the splash water from the traffic. The climate around the specimens is moist, and the specimens are exposed during the winter to low temperatures and de-icing salts, producing a climate corresponding to exposure class XD 3/XF 4 in EN 206-1 (2001).

Highway 40 leads from Gothenburg to the east, through Borås and towards Jönköping. Over the year, the daily average number of vehicles passing the field exposure site is around 12000, of which 1250 are heavy vehicles (data from measurements carried out by the Swedish National Road Administration in 2000).

Figure 11.1 *Field exposure site at Highway 40. Specimens placed in steel frames behind a guard rail (right).*

For safety reasons, de-icing salts are used during the winter in many parts of Sweden to keep road surfaces free from snow and ice. The de-icing agent used is sodium chloride, which is spread either in the form of a solution (about 24 % NaCl) as a preventive measure, or as crystals when spread on snow. In this region, de-icing salts are normally used between October and April. Table 11.1 shows an estimate of the total amount of salt spread on the highway per square metre and year. The figures are based on data from the Swedish National Road Administration. The table also shows the number of occasions de-icing salts were spread on the highway each winter season.

Table 11.1 *Estimated total annual amount of salt spread on Highway 40 per square metre and the number of occasions de-icing salts were spread on the road each winter season.*

Winter season	**96-97**	**97-98**	**98-99**	**99-00**	**00-01**	**01-02**	**02-03**
Amount of salt (kg/m^2)	1.9	2.4	2.3	2.1	1.1	1.2	1.2
Number of occasions	126	157	151	141	117	148	145

As can be seen in Table 11.1, the amount of salt spread on the road was markedly reduced around year 2000. This was due to the introduction of the new method of applying salt, as a solution, which uses a smaller amount of salt.

The exposure to de-icing salts at different locations at the field exposure site and at different locations on bridges and columns exposed to the climate along Highway 40 has been studied and reported. Wirje & Offrell (1996) present results from investigations of chloride ingress into mortar specimens placed at different locations along the road. They showed, for example, that the ingress of salt in the specimens used in the present investigation was the same, regardless of where along the field test site the specimens were placed. They also showed that the ingress of chlorides decreases with increasing height above the road level. Tang & Utgenannt (2000) present results from collecting splash water at different locations around the exposure site. The results confirm the findings in Wirje & Offrell (1996).

Marine environment - Träslövsläge harbour

The field exposure site in Träslövsläge harbour was established in 1991. Specimens at the site are mounted on top of a pontoon that is situated behind a pier, Figure 11.2. The specimens are not in direct contact with the sea water, but are frequently splashed with sea water in stormy weather. The climate is damp, and the specimens are exposed to low temperatures during the winter, giving a climate corresponding to exposure class XS3/ XF4 in EN 206-1. The sodium chloride content in the sea water varies somewhat, but ~1.5 % NaCl can be regarded as a mean value.

Figure 11.2 *Field exposure site in a marine climate at Träslövsläge harbour. Specimens are mounted on top of pontoons.*

Environment without salt exposure - SP's premises

A field exposure site was established at SP's premises in Borås in the autumn of 1996. Specimens are mounted on pallets, as shown in Figure 11.3. The specimens are exposed only to natural precipitation, without exposure to de-icing salts, resulting in a climate corresponding to exposure class XC4/XF 3 in EN 206-1.

The climate at the SP field exposure site was not measured. However, the site is only a few kilometers from the field exposure site beside Highway 40, and so it is assumed that the climates at the two test sites are about the same except for the salt exposure.

Figure 11.3 *Field exposure site in an environment without salt exposure at SP's premises. Specimens are placed on pallets.*

11.2.2 Climates at the exposure sites

The climates at the highway and the marine test sites were recorded at climate stations owned and administered by the Swedish National Road Administration. The climate at the exposure site at SP's premises is assumed to be the same as at the highway exposure site.

The climate station recording the highway climate (Viared, no. 1508) is situated only a couple of hundred meters from the field exposure site, while the station recording the climate at the marine exposure site (Nygård, no. 1307) is situated a couple of kilometres east of the test site. At both climate stations, data is recorded every half hour from the beginning of October to the end of April. The data registered is:

- Air and road surface temperature
- Relative humidity in the air
- Wind direction and wind speed
- Amount of precipitation, classified as three types: rain, snow or sleet.

The main emphasis in this report is on air temperature, relative humidity and the amount and type of precipitation. Appendix 11 shows a summary of the climate for each winter season at the highway and the marine exposure sites. It also includes a figure showing the temperature during each winter season; see the example in Figure 11.4.

It can be seen from Figure 11.4 that the air temperature during the 2002-2003 winter season fluctuated widely over relatively short periods of time. This is typical of the recorded temperatures at both exposure sites during the winter seasons since 1996. The temperature at the beginning and end of the winter seasons mostly fluctuates between several degrees above zero down to about –5 °C, while at mid-winter the fluctuation is often between temperatures below zero, with occasional peaks at a couple of degrees above zero. The minimum temperatures are normally between –15 °C and –25 °C.

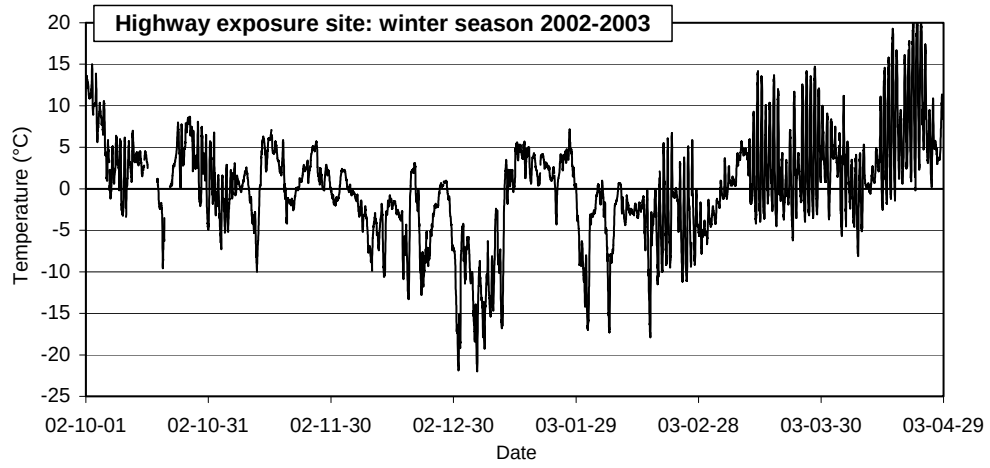

Figure 11.4 *Air temperature at the highway exposure site during the 2002-2003 winter season.*

Comparing the registered temperatures at the highway exposure site with the temperatures at the marine exposure site shows that the temperatures at the marine exposure site are in most cases somewhat milder than at the road site. However, the rate at which the temperature rises or falls is about the same at both sites. See example in Figure 11.5.

It should be noted that the climate representing the marine exposure site is actually recorded at a climate station a couple of kilometres to the east of the site, i.e. in the inland direction. The actual climate at the marine exposure site may therefore differ somewhat from the recorded climate. If there is a difference, it is most likely that the climate at the marine exposure site is somewhat milder than the climate at the climate station. However, any difference is probably small, and is assumed to be unimportant.

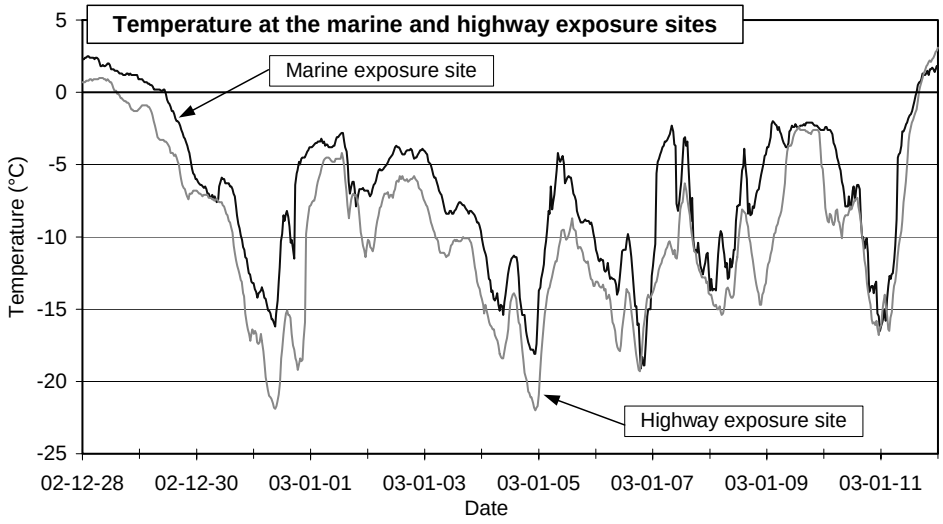

Figure 11.5 *Air temperatures at the marine and highway exposure sites over 15 days at the end of 2002 and the beginning of 2003.*

The number of temperature cycles, and the time below a certain temperature (t), has been calculated from the continuously recorded air temperatures; see example in Figure 11.6.

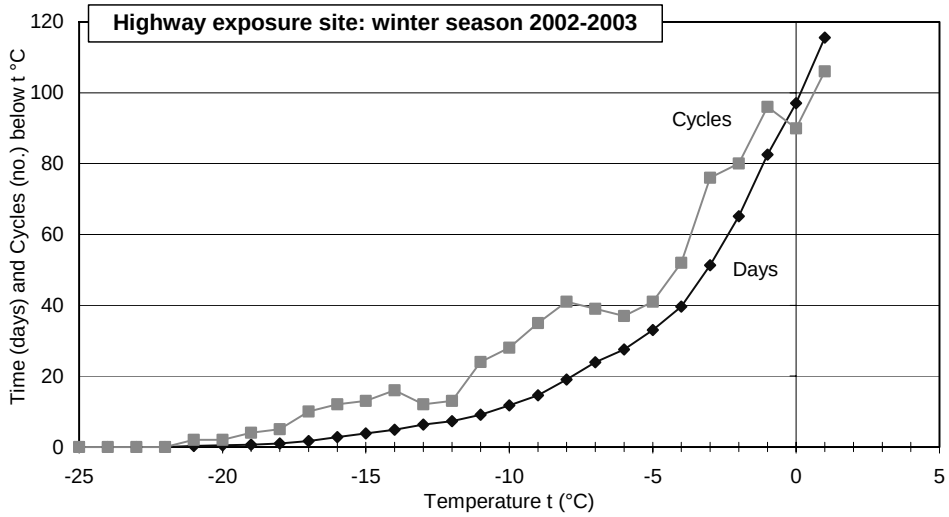

Figure 11.6 *Number of cycles and the time below a certain temperature, t °C, at the highway exposure site during the 2002-2003 winter season.*

From the figure, it can be seen that the temperature at the highway exposure site during the 2002/2003 winter season, was below 0 °C for almost 100 days. However, the appearance of the curve showing the time in days below a certain temperature indicates that most of the time below zero seems to be at temperatures just below 0 °C, with more than 60

days between 0 and –5 °C. The time below a certain temperature slowly decreases with decreasing temperature. The minimum temperature during the 2002/2003 winter season was around –21 °C, which was held for a total of about seven hours during two periods.

Figure 11.6 also shows the number of cycles at a certain temperature. For example, there were about 90 cycles at 0 °C, and about 30 cycles at –10 °C. During the 2002/2003 winter season, there were only two cycles at –20 °C.

Table 11.2 shows the number of cycles and the time below certain temperatures for the seven winter seasons during which the specimens have been exposed at the highway exposure site. Table 11.3 shows corresponding information for the marine exposure site.

Table 11.2 *Number of cycles and the time in days below a certain temperature t at a climate station close to the highway exposure site at Highway 40. (Number of cycles at temperature t/Days below temperature t)*

Winter season	**96-97**	**97-98**	**98-99**	**99-00**	**00-01**	**01-02**	**02-03**
t = 0 °C	81 / 72	95 / 59	90 / 71	89 / 52	59 / 62	88 / 47	90 / 97
-2 °C	75 / 52	61 / 34	49 / 44	69 / 29	58 / 40	55 / 28	80 / 65
-5 °C	42 / 31	39 / 17	38 / 18	35 / 10	43 / 22	26 / 12	41 / 33
-10 °C	32 / 13	15 / 3	19 / 5	3 / 1	9 / 5	8 / 4	28 / 12
-15 °C	25 / 5	1 / 0.2	1 / 0.3	1 / 0.2	3 / 0.4	5 / 2	13 / 4
-20 °C	6 / 1	-	-	-	-	2 / 0.3	2 / 0.5
-25 °C	-	-	-	-	-	-	-

Table 11.3 *Number of cycles and the time in days below a certain temperature t at a climate station close to the field exposure site at Träslövsläge harbour. (Number of cycles at temperature t/Days below temperature t)*

Winter season	**96-97**	**97-98**	**98-99**	**99-00**	**00-01**	**01-02**	**02-03**
t = 0 °C	72 / 50	78 / 33	66 / 46	79 / 26	76 / 42	61 / 29	99 / 79
-2 °C	55 / 29	48 / 19	57 / 29	31 / 13	51 / 27	53 / 18	94 / 49
-5 °C	37 / 16	34 / 9	40 / 12	16 / 4	33 / 12	21 / 7	62 / 23
-10 °C	22 / 5	1 / 0.2	13 / 3	5 / 0.8	9 / 4	4 / 2	22 / 6
-15 °C	5 / 0.6	-	3 / 0.5	3 / 0.2	3 / 0.4	5 / 1	7 / 0.8
-20 °C	-	-	-	-	-	2 / 0.1	-
-25 °C	-	-	-	-	-	-	-

From the calculated numbers of cycles and the time below a certain temperature given in Tables 11.2 and 11.3, it can be seen that the climate at the marine exposure site is somewhat milder than that at the highway site. In particular, the time below 0 °C is considerably higher at the highway exposure site than at the marine exposure site. The difference between the climates is not as apparent in terms of the number of cycles at a certain temperature. In most cases, however, there are a larger number of cycles at the highway exposure site than at the marine exposure site.

Appendix 11 shows monthly values for the temperature (mean, maximum and minimum temperatures), relative humidity in the air, and the precipitation.

From the precipitation data shown for each winter season since 1996/1997 in Appendix 11, it can be seen that there are some noticeable differences between the two exposure sites. It can, for example, be seen that during winter the precipitation at the marine exposure site falls mostly as rain, while that at the highway site falls mostly as snow or sleet. It can also be seen that the total amount of precipitation during the winter is somewhat higher at the marine exposure site than at the highway exposure site.

However, on an annual basis, the precipitation at the highway exposure site is significantly higher than at the marine exposure site. This can be seen in Table 11.4, which shows the annual precipitation since 1996 at climate stations situated within about 10 km from the two exposure sites. These climate stations are run by the Swedish Meteorological and Hydrological Institute, and work all year round, whereas the climate stations run by the Swedish National Road Administration work only during the winter. Since the latter show a somewhat higher precipitation during the winter at the marine exposure site than at the highway exposure site, the reverse must apply during the five 'summer' months, i.e. a considerably higher precipitation at the highway exposure site than at the marine exposure site.

Table 11.4 *Annual precipitations at two climate stations situated within about 10 km from the highway and marine exposure sites. Precipitation data from the Swedish Meteorological and Hydrological Institute.*

Precipitation	**1996**	**1997**	**1998**	**1999**	**2000**	**2001**	**2002**
Highway (Borås)	796	905	1256	1859	1323	904	1127
Marine (Varberg)	573	766	1076	1142	970	770	829

11.2.3 Comparison between temperatures at the field exposure sites and the temperature cycle during freeze/thaw testing in accordance with SS 13 72 44

Chapter 2 gave a short description of the Swedish standard for testing the scaling resistance of concrete, SS 13 72 44, known as the 'slab test'. During freeze/thaw testing, specimens are subjected to 24 hour-long freeze/thaw cycles, cycling the temperature between about +20 °C and –20 °C. As can be seen from Figure 2.2 in Chapter 2, the temperature in the freezing medium on the surface of the specimen should follow a certain cycle, with maximum and minimum temperature limits leading to relatively high cooling and heating rates. It can be questioned if this temperature cycle, both with regard to maximum and minimum temperatures and to the high cooling and heating rates, is too aggressive and unnatural to give relevant test results. This has been discussed in Petersson (1997), who points out that, for the natural damage mechanisms to be active, a freeze/thaw cycle resembling the natural temperature variations in the field should be used. With

unnatural freeze/thaw cycles, e.g. with too high cooling or heating rates, damage mechanisms not normally encountered under 'natural' conditions may occur, thus leading to misleading test results. According to Petersson (1997), a 24 hour freeze/thaw cycle with a minimum temperature of –20 °C can, as a compromise, be assumed to be representative for most parts of Europe. It is, however, pointed out that for regions with other temperature cycles, these can be used in stead. Of course, a full cycle between +20 °C and –20 °C within 24 hours is highly unnatural. However, that part of the temperature cycle above 0 °C is probably of little importance with respect to frost damage, in comparison with the importance of the minimum temperature and the cooling and heating rates at temperatures below 0 °C.

From the measured air temperatures at both climate stations close to the marine and highway exposure sites, it can be seen that there are a large number of rapid temperature fluctuations during a winter season; see Appendix 11. During these fluctuations, the temperature changes rapidly from several degrees below zero (often between –10 °C and –15 °C) to temperatures above zero within a short time span, often within a couple of hours. An example of the rapid temperature fluctuations (although not to above zero) can be seen in Figure 11.5, where the temperature changed rapidly through 10 to 15 degrees within a couple of hours. These rapid temperature changes mean that (at least during short periods) the cooling and heating rate in reality are at least as high as, and sometimes even higher than, in the laboratory test.

During the winter seasons since 1996/1997, there are examples of freeze/thaw cycles that are almost in full accordance with the temperature cycle used in the 'slab test' - at least as far as the part below 0 °C is concerned; see the example in Figure 11.7. The figure shows the air temperature at the highway exposure site during two days at the beginning of March 2001, together with the temperature limits specified in the 'slab test'.

From the figure it can be seen that the air temperature cycle is almost exactly the same as the prescribed temperature cycle in the 'slab test'. During cooling down to –17 °C, the air temperature matches the laboratory cycle, resulting in a high enough cooling rate and an almost low enough minimum temperature. During thawing, the heating rate is somewhat slower than in the laboratory cycle. It can, however, be seen that the heating rate during most parts of the thawing from –17 ° to + 0 °C corresponds to the requirements of the laboratory method.

The same correlation between the 'real' temperature cycle and the laboratory cycle can also be seen at the marine exposure site; see Figure 11.8, which shows the recorded air temperature at the marine exposure site during two days at the beginning of March 2001 (the same time period as at the highway exposure site in Figure 11.7). As can be seen from the figure, the real temperature cycle corresponds well with the standard cycle in the 'slab test'.

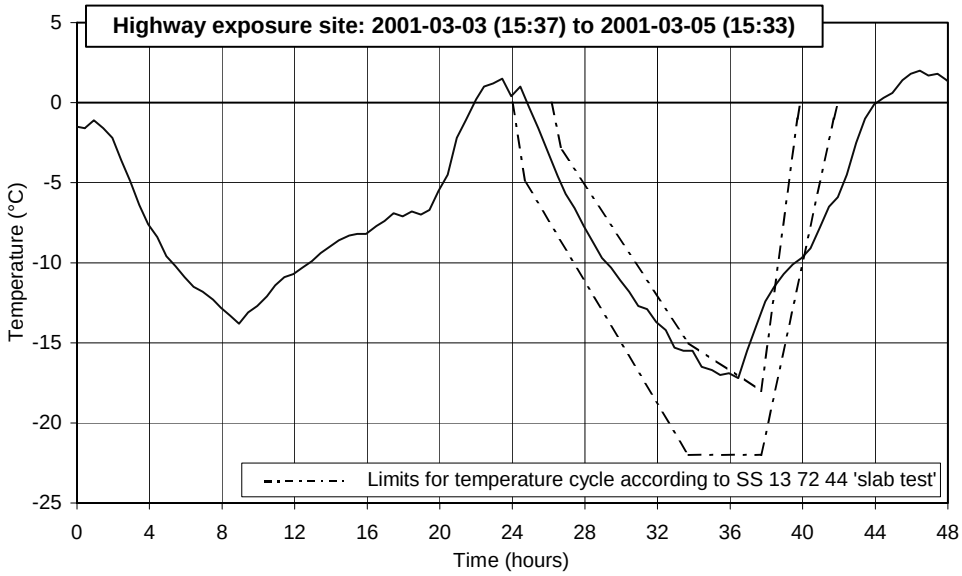

Figure 11.7 *Air temperatures at the highway exposure site during two days at the beginning of March 2001. The dotted lines represent the temperature limits specified in the laboratory test method SS 13 72 44.*

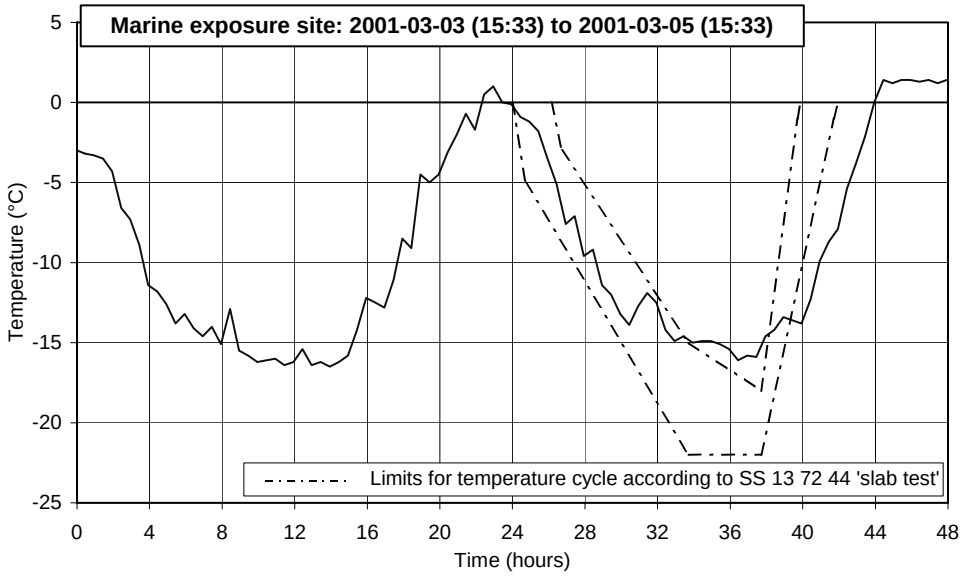

Figure 11.8 *Air temperatures at the marine exposure site during two days at the beginning of March 2001. The dotted lines represent the temperature limits according to the laboratory test method SS 13 72 44.*

From the examples above, it seems that cooling rates in accordance with what is prescribed in the laboratory test are relatively frequent in reality. This can be explained by the relatively low prescribed cooling rates of about 1.5 - 2.0 °C/hour during cooling below 0 °C in the laboratory test. However, heating rates in accordance with the laboratory test seem to be more uncommon in reality, at least in the region where the exposure sites are situated. This is due to the relatively high rates (~5.5 °C/hour) prescribed in the laboratory test. This is true at least if requiring the same heating rate from –20 °C up to over 0 °C. However, over shorter temperature ranges, it is not unusual for the temperature to increase at more than 5 °C/hour. Even if rapid temperature changes from –20 °C to over 0 °C are not common in reality, they do exist; see the example in Figure 11.9, which shows the temperature rise during the first day in January 2002 at the highway exposure site.

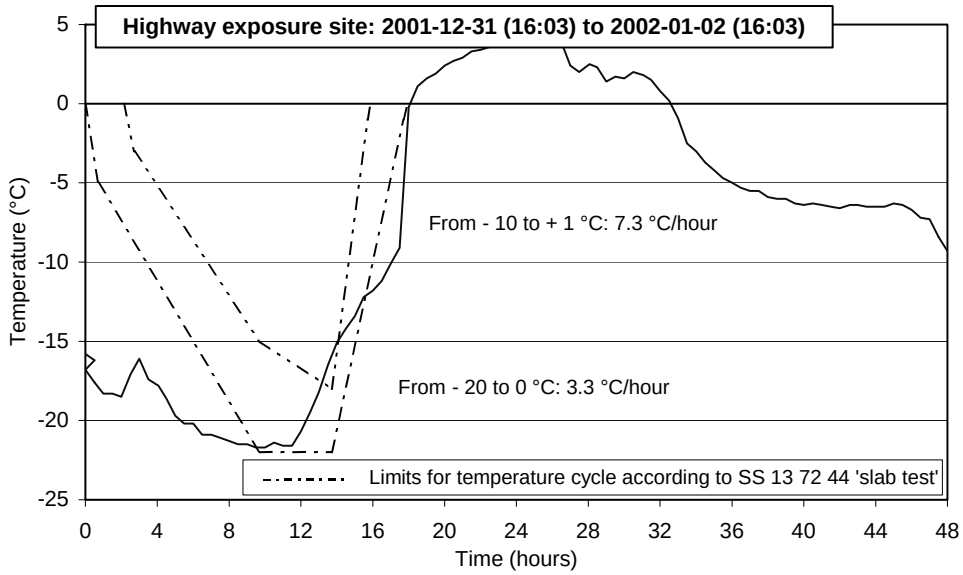

Figure 11.9 *Air temperatures at the highway exposure site during two days at the beginning of January 2002. The dotted lines represent the temperature limits according to the laboratory test method SS 13 72 44.*

It can be seen from Figure 11.9 that the air temperature rises rapidly from below –20 °C to above 0 °C within about six hours. This results in a relatively high mean heating rate over the six-hour period (3.3 °C/hour) and a very high heating rate of over 7 °C per hour during heating from –10 to +1 °C. This example shows that, in the actual climate at the highway exposure site, an increase in temperature of the same order as in the laboratory test not is unnatural.

It must be noted that, in the examples above, the registered air temperatures at the exposure sites are compared with the temperature cycle in the freezing media in the laboratory test. This comparison may be questioned, since the temperature of the concrete surface

probably responds more slowly to changes in air temperature. This would result in somewhat lower cooling and heating rates than is shown in the figures above. There are, however, other effects working in the opposite direction, that could result in higher heating and cooling rates at the concrete surface than is registered by the air temperature. These effects are cooling and heating due to radiation. The cooling effect of radiation during a cold night with a clear sky, and the heating effect of the sun on a sunny day, may be significant, and probably faster than the rate of change of surface temperature due to changes in the air temperature.

The examples described above show that the temperature cycle prescribed in laboratory test method SS 13 72 44 are not unnatural or too aggressive compared with reality, at least not in comparison with the actual climate in the south-western part of Sweden. In other parts of Europe where frost damage might be a problem, other types of freeze/thaw cycles in the laboratory test may be more appropriate to correlate with what is experienced in the field.

From the climate data presented in Appendix 11 and briefly discussed above, it can be concluded that:

- The mean temperature at the highway exposure site is lower than at the marine exposure site. This leads to a shorter time below certain temperatures below 0 °C, and also to some extent to fewer cycles at temperatures below 0 °C at the marine exposure site in comparison with the temperatures and number of cycles at the highway exposure site.
- The temperature fluctuation leads to rapid temperature changes within short time periods, which is true at both exposure sites.
- The minimum temperatures occurring a couple of times each winter season are about –15 to –25 °C at the highway exposure site and a couple of degrees milder at the marine exposure site.
- The precipitation during the winter is somewhat higher at the marine exposure site than at the highway exposure site. However, the wet road climate, as a result of the extensive use of de-icing salts at the highway exposure site, leads to a very moist microclimate around the specimens at the highway exposure site. This makes the microclimate at the highway exposure site at least as moist as at the marine exposure site.
- The temperature cycle used in the SS 13 72 44 laboratory test is relevant both with respect to minimum temperatures and cooling and heating rates. During the winter months, the temperature continuously fluctuates between temperatures around –10 to –15 °C to above 0 °C, with heating and cooling rates of the same order as in the laboratory test. Occasionally there are even temperature changes very much like those in the laboratory test. It must be noted that the freeze/thaw cycle in the laboratory test is relevant for the climate in the south-western part of Sweden. Other freeze/thaw cycles may be more appropriate in other climatic regions.

11.3 Materials, specimens and test methods

The binder types/combinations used in this investigation are shown in Table 11.5. For chemical composition, see Appendix 4.

Table 11.5 *Binder types/combinations used in this investigation*

Binder type/combination		**Comments**
1	OPC[1)] (CEM I)	Low alkali, sulphate-resistant
2	OPC[1)] + 5 % silica by binder weight	Silica in the form of slurry
3	OPC[1)] + 30 % slag by binder weight	Ground blast furnace slag added in the mixer
4	CEM III/B	Dutch slag cement, ~70 % slag

[1)] OPC = Ordinary Portland Cement (Degerhamn standard by Cementa AB)

Ten different concrete qualities were produced for each of the binder types/combinations. Concrete qualities with five different water/binder (w/b) ratios (0.30, 0.35, 0.40, 0.50, 0.75), and with and without entrained air, were produced for all binder combinations. As aggregate, 0/8 mm natural and 8/16 mm crushed graded granitic material was used for all mixes. A naphthalene-based plasticiser, Melcrete, was used for mixtures with w/b-ratio of 0.40 and lower. The air-entraining agent used, L16, is a tall-oil derivative. A summary of concrete constituents and properties is presented in Table 11.6. For a complete presentation, see Utgenannt (1997).

All concrete batches were produced in the autumn of 1996, and a number of 150 mm cubes were cast from each batch. The following laboratory tests were carried out on each concrete mix for characterisation of the concrete qualities:

Testing the fresh concrete:

- Air content
- Density
- Slump
- Remoulding test

Testing the hardened concrete:

- Compressive strength in accordance with Swedish Standard (SS) 13 72 10.
- Salt-frost resistance in accordance with SS 13 72 44 (‘the slab test’).
- Microscopic determination of the air void system, essentially in accordance with ASTM C 457.

Results from these tests are given partly in Table 11.6, and fully in Utgenannt (1997).

Table 11.6 *Concrete qualities used in this investigation.*

Binder type	w/b-ratio	Eqv. w/c-ratio[1]	Cement (kg/m^3)	SCM[2] (kg/m^3)	AEA[3]	Air con. fresh (%)	Slump (mm)	Compressive strength (MPa) Dry[4]	Wet[5]	Scaling (kg/m^2)[6] 28	56
OPC	0.30	0.30	500	-	Yes	4.8	240	95	87	0.024	0.035
	0.35	0.35	450	-	Yes	4.8	190	95	87	0.054	0.085
	0.40	0.40	420	-	Yes	4.6	125	67	62	0.014	0.023
	0.50	0.50	370	-	Yes	4.6	90	49	45	0.017	0.022
	0.75	0.75	260	-	Yes	4.7	100	21	19	0.127	0.141
	0.30	0.30	500	-	No	1.1	120	102	94	0.156	0.256
	0.35	0.35	450	-	No	1.2	140	91	84	1.94	4.39
	0.40	0.40	420	-	No	0.8	130	87	80	3.11	7.92
	0.50	0.50	385	-	No	0.8	70	56	52	5.09	14.5
	0.75	0.75	265	-	No	0.9	60	31	29	4.34	>15
OPC +5 % silica	0.30	0.29	475	25	Yes	4.6	100	103	95	0.041	0.119
	0.35	0.33	427.5	22.5	Yes	4.5	90	91	84	0.022	0.041
	0.40	0.38	399	21	Yes	4.8	105	72	66	0.023	0.035
	0.50	0.48	361	19	Yes	4.6	70	57	52	0.020	0.026
	0.75	0.71	237.5	12.5	Yes	4.3	70	25	23	0.190	0.200
	0.30	0.29	475	25	No	1.1	125	121	111	0.120	0.200
	0.35	0.33	427.5	22.5	No	1.1	90	105	97	0.360	0.890
	0.40	0.38	399	21	No	0.5	100	84	77	1.67	3.25
	0.50	0.48	370.5	19.5	No	1.2	60	67	62	1.86	4.61
	0.75	0.71	256.5	13.5	No	0.3	75	35	32	3.45	6.58
OPC +30 % slag	0.30	0.34	350	150	Yes	4.8	230	90	83	0.031	0.045
	0.35	0.40	315	135	Yes	4.8	130	86	79	0.086	0.139
	0.40	0.45	294	126	Yes	4.4	110	65	60	0.041	0.067
	0.50	0.57	259	111	Yes	4.8	80	49	45	0.021	0.033
	0.75	0.85	175	75	Yes	4.4	100	20	18	0.490	0.538
	0.30	0.34	350	150	No	0.7	220	101	93	0.097	0.128
	0.35	0.40	315	135	No	1.1	140	91	84	1.78	3.61
	0.40	0.45	294	126	No	0.9	120	78	72	1.78	3.83
	0.50	0.57	273	117	No	1.3	80	52	48	0.864	1.94
	0.75	0.85	185.5	79.5	No	0.5	80	25	23	1.58	4.37
CEM III/B ~70 % slag	0.30	0.30	520	-	Yes	4.8	200	78	72	0.245	0.356
	0.35	0.35	460	-	Yes	4.7	200	74	68	0.434	0.615
	0.40	0.40	420	-	Yes	4.3	120	61	56	0.568	0.845
	0.50	0.50	380	-	Yes	4.5	70	46	42	0.993	1.66
	0.75	0.75	255	-	Yes	4.4	90	26	24	2.05	3.16
	0.30	0.30	520	-	No	0.8	200	99	91	0.221	0.281
	0.35	0.35	470	-	No	0.7	200	80	74	0.490	0.653
	0.40	0.40	420	-	No	0.9	125	68	63	0.837	1.14
	0.50	0.50	400	-	No	1.0	65	54	50	1.21	1.61
	0.75	0.75	265	-	No	0.1	100	31	29	3.94	6.89

[1] Eqv. w/c-ratio= water/(cement + 2·silica + 0.6·slag). Not applicable for CEM III/B cement.

[2] SCM - Secondary Cementitious Materials

[3] AEA - Air Entraining Agent

[4] Dry stored cubes tested in accordance with SS 13 72 10 at the age of 28 days

[5] Recalculated to wet stored cubes according to SS 13 70 03; $f_{wet,cube} = 0.92 \cdot f_{dry,cube}$

[6] According to the 'Slab test', SS 13 72 44, freeze/thaw started at the age of 31 days

All cubes were demoulded 24 hours after casting, and stored in lime-saturated water for six days. The cubes for compressive strength and scaling test were treated as described in the respective standards. The cubes for analysing the air-void structure were stored in a climate-controlled area at 50 % RH and +20 °C until the analysis was carried out.

The cubes for production of specimens to be placed at the field exposure sites were, after water storage, stored in a climate-controlled area at 50 % relative humidity and +20 °C for a period of between one and a half and three months. Between eight and twelve days before the specimens were placed at the field exposure sites, the cubes were cut, resulting in two specimens with the shape of a half 150 mm cube with one cut surface and the rest mould surfaces. After cutting, the specimens were stored in a climate-controlled area at 50 % RH and +20 °C until they were placed at the test sites. During this second conditioning period, the volume of, and ultrasonic pulse transmission time through, each specimen were measured as described below. Two specimens of each quality were then placed at each test site.

In order to detect both internal and external frost damage, the change in volume and ultrasonic pulse transmission time was measured on a regular basis. The first measurement was carried out before placing the specimens at the test sites. The specimens at the highway site have subsequently been measured once a year, and the specimens at the other two sites after two, four and five years.

The volumes of the specimens are calculated from results obtained from measuring the weight of the specimens in water and surface-dry in air respectively. The ultrasonic pulse transmission time through the specimen is measured as a mean of three measurement positions, where possible, on each specimen, Figure 11.10.

Before measuring the volume of the specimens, they were placed in a water bath for at least two days. When weighing the specimens under water, they were placed in a holder with the whole specimen under water as in Figure 11.10. The weight stabilised normally within two minutes and was then registered. The wet specimen was immediately dried with a wet cloth and weighed again in a surface-dry state.

After the volume of the specimens had been measured, the specimens were stored in laboratory climate for at least one week before the ultrasonic pulse transmission time was measured. When measuring this, the specimen was placed in a holder with three holes on each side enabling measurements on the same place each time. Before transmission time measurements were carried out, the apparatus was calibrated against two calibration rods with specified transmission times of $51 \cdot 10^{-6}$ and $26.3 \cdot 10^{-6}$ seconds respectively. The transducers used produce a pulse with a frequency of $200 \cdot 10^{3}$ Hz. For normal undamaged concrete, a transmission time of between 30 and $35 \cdot 10^{-6}$ seconds was measured over the 150 mm wide specimens.

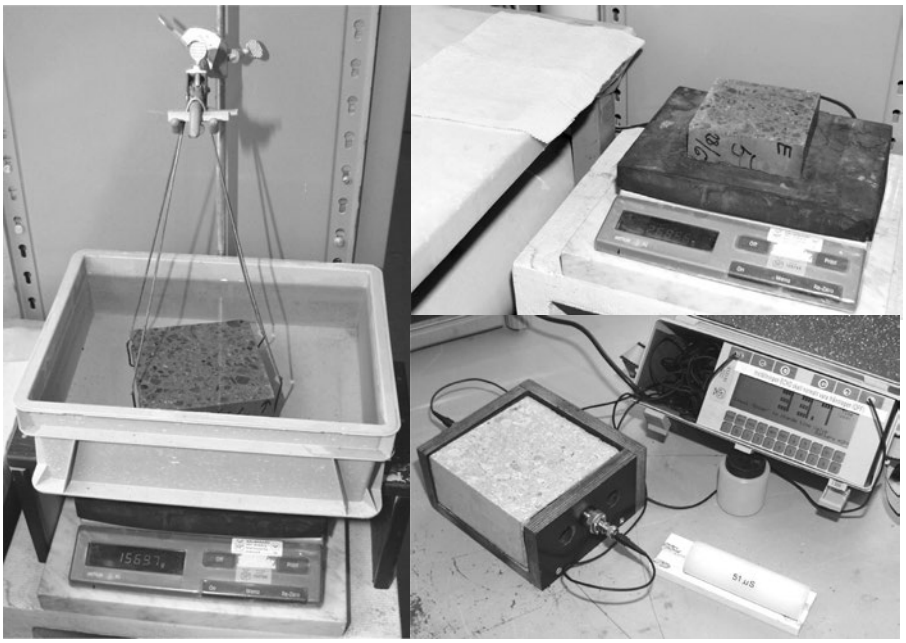

Figure 11.10 *Measurement of the specimen weight in water (left), surface-dry in air (above right) and measurement of the ultrasonic pulse transmission time (below right).*

11.4 Results and discussion

11.4.1 Introduction

This section presents and discusses the results from the volume and ultrasonic pulse transmission time (UPTT) measurements carried out on specimens exposed at the three field exposure sites. The results are also compared with results from laboratory tests as well as with results from other field investigations.

The results are divided into external and internal frost damage, depending on the method by which the damage is detected. A change in volume (if decreasing) is regarded as external damage, while a change in transmission time (if increasing) is regarded as internal damage. This is a coarse division, and in reality there is no clear distinction between external and internal frost damage. An increase in transmission time may be caused by cracks close to the specimen surface or, without cracking, by changes in the centre of the material. The UPTT technique does not give complete unambiguity in distinguishing this type of external damage from internal cracking. To make this distinction, the material has to be examined further, for example by microscopic analysis using thin sections or polished sections. These methods were used for some materials in this investigation.

11.4.2 External frost damage

Significant differences can be seen when comparing external damage (scaling) in the form of volume change after five winter seasons for specimens exposed at the three field exposure sites. The results for concrete with and without entrained air are presented separately below.

11.4.2.1 External frost damage - concrete without entrained air

Figure 11.11 shows the volume change for the different concrete qualities without entrained air, exposed for five years at the three exposure sites.

Highway environment

As can be seen from the Figure 11.11a, all qualities with a w/b-ratio of 0.75 show a marked volume reduction, i.e. surface damage. There is, however, a considerable difference depending on the binder type, with most damage occurring to concrete with CEM III/B and OPC + 30 % slag, and somewhat less damage for concrete with OPC + 5 % silica or with only OPC as binder. The amount of damage is not as extensive for qualities with lower w/b-ratios. However, for concrete with CEM III/B as binder, a substantial volume reduction can also be seen for concretes with w/b-ratios of 0.50 and 0.40. No significant volume reduction for qualities with 0.50 w/b-ratio or below can be seen for concretes with the other binder types. However, on the other hand, a marked increase in volume can be seen for concrete with OPC + 5 % silica as binder and with w/b-ratios of 0.50 and 0.40. This increase in volume indicates internal damage (micro-cracks) that increases the specimen volume. For these qualities, further indication of internal damage was provided by the measurements of ultrasonic pulse transmission time, see below.

Marine environment

As can be seen in Figure 11.11b, the amount of damage is less at the marine exposure site than at the highway exposure site. Only the qualities with CEM III/B and OPC+ 30 % slag show damage for qualities with high w/b-ratios. No significant volume reduction could be detected for any of the concrete qualities with w/b-ratio of 0.50 or below. However, as at the highway exposure site, the quality with OPC + 5 % silica as part of the binder, and with w/b-ratio of 0.50, shows a marked increase in volume, indicating internal damage. This is further confirmed by the ultrasonic pulse transmission time measurements presented below.

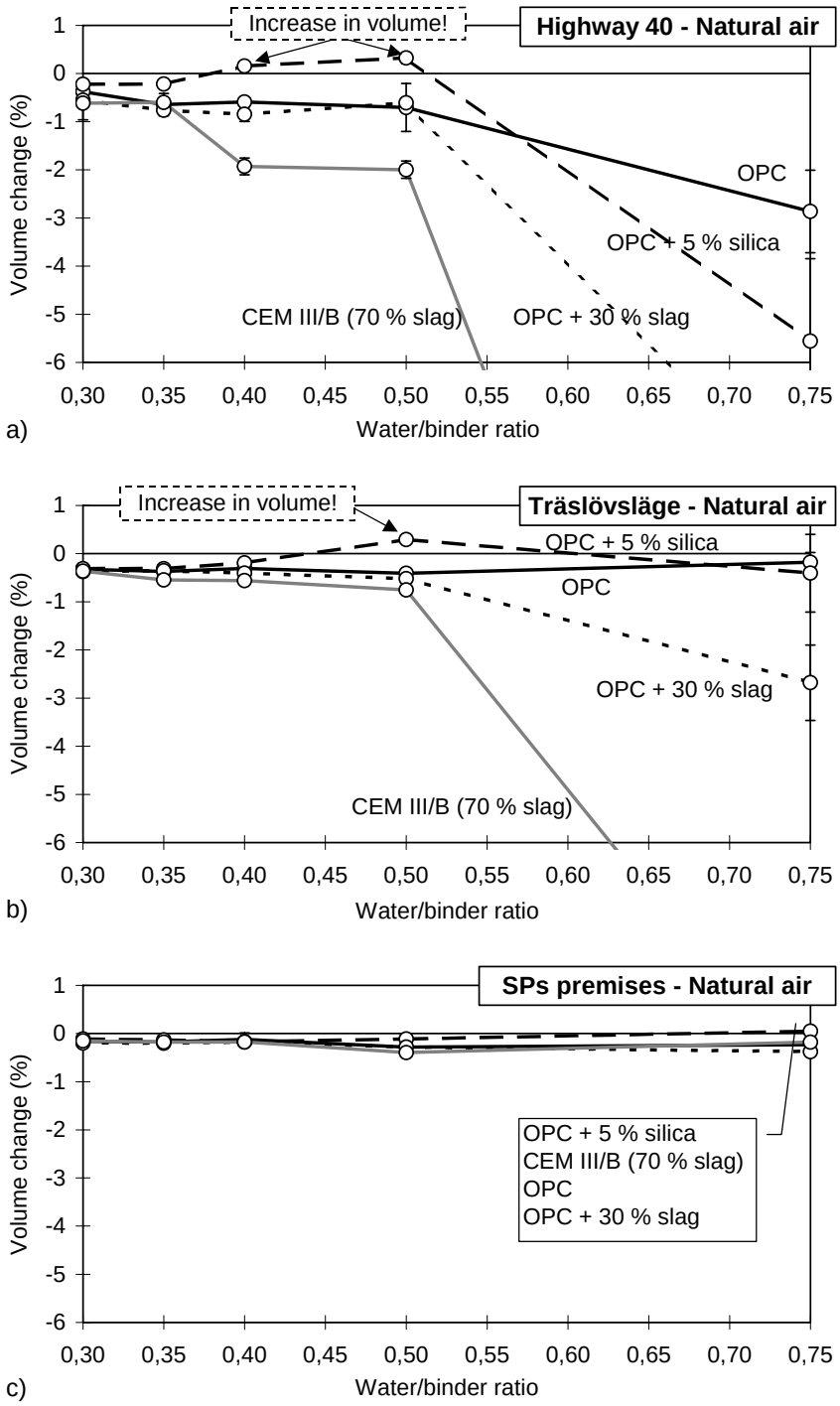

Figure 11.11 *Volume change after five winter seasons: concrete with different binder combinations and water/binder-ratios and without entrained air.*
a) Highway environment, b) Marine environment, c) Salt-free environment

Environment without salt exposure

For the specimens exposed at SP's premises, Figure 11.11c, no concrete quality, regardless of w/b-ratio, showed any noticable decrease in volume after five years' exposure. However, visual inspection after seven years' exposure showed extensive cracks on all specimen surfaces of concrete made with CEM III/B binder and a w/b ratio of 0,75; see Figure 11.12.

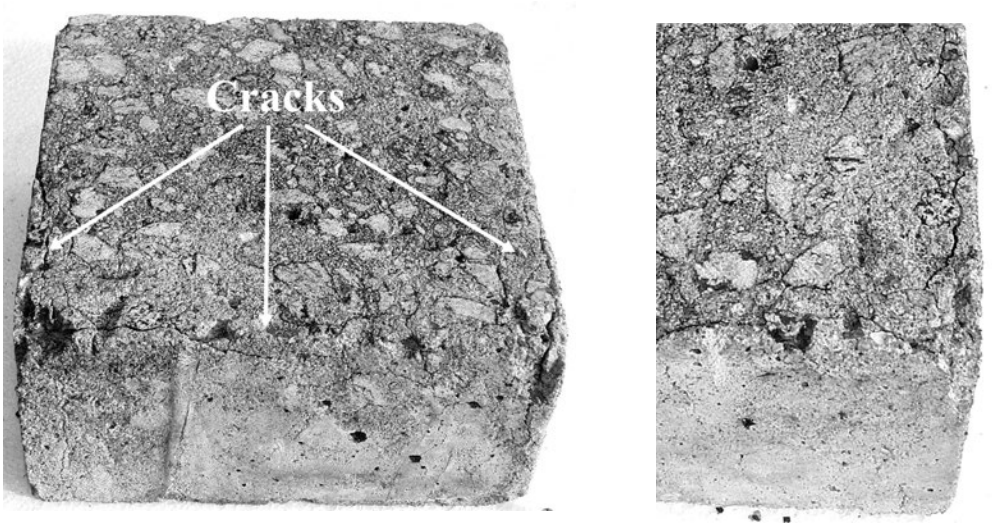

Figure 11.12 *Picture of a specimen (CEM III/B, w/b-ratio 0.75) exposed at the exposure site at SP's premises for seven years. To the right, a magnification of one of the corners.*

From the figure it can be seen that there is extensive cracking parallel to the surfaces of the specimen. A typical crack runs parallel to the side at a depth of a couple of mm and up to about 10 mm below the surface. From the visual inspection of the specimen, it seemed as if the cracks were within the carbonated zone of the specimen. External damage thus occurs to this concrete quality even though the environment is not saline.

The concrete quality with OPC + 5 % silica as binder and a w/b-ratio of 0.75 shows a slight increase in volume, which might be an indication of internal damage. The ultrasonic pulse transmission time measurements shown below also indicate internal damage for this concrete quality.

Discussion

As can be seen from the figures showing the volume changes after five winter seasons for concrete qualities without entrained air, the exposure climate seems to have a strong influence on the amount of frost damage (volume change). The most extensive damage is seen at the highway exposure site, and the least damage is found at the exposure site at SP's premises. Concrete exposed at the marine exposure site show some damage, although not

as apparent as for concrete exposed at the highway exposure site. The difference in damage depending on exposure climate can probably be explained by differences in:

- **Temperature**. The temperature in the marine environment is somewhat milder with higher mean and minimum temperatures than at the highway environment or the environment at SP's premises. The time during which the air temperature is below a certain temperature lower than 0 °C, and the number of passages below this temperature, is also lower at the marine exposure site than at the highway exposure site; see temperature data in Table 11.2 and Table 11.3 or in Appendix 11. The air temperature at the highway exposure site and the site at SP's premises is about the same.
- **Moisture conditions**. The amount of precipitation during the winter months is about the same at all three exposure sites, with somewhat more precipitation at the marine exposure site. However, the moisture conditions in the microclimate surrounding the specimens differ considerably. At the marine exposure site, the specimens are exposed primarily to natural precipitation and spraying with sea water during windy weather. At the highway exposure site, the specimens are exposed to natural precipitation and also to splashing from the traffic at times when the road surface is wet. Since de-icing salts are used, the road surface is wet for most of the winter months, and so these specimens are exposed to a very moist environment. At the exposure site at SP's premises, however, the specimens are exposed only to natural precipitation.
- **Salt concentration**. The exposure to salt varies considerably at the three test sites, with a (at least occasionally) much higher salt concentration in the water splashed over the samples at the highway site than in the sea water spray at the marine environment. For the specimens at the test site at SP's premises there is no exposure to salt.

An interesting observation is the increase in volume for some concrete qualities with OPC + 5 % silica as binder and with a w/b-ratio over 0.35. This increase is seen primarily at the highway and marine exposure sites. An increase in volume is probably caused by internal damage, i.e. micro-cracks; see further discussion below. A limitation of the volume measurements is that the measured volume is the resultant of both a possible negative and a possible positive element, in the respective forms of a volume loss due to surface scaling and a volume increase due to internal cracking. Concrete qualities with an apparent volume loss might, therefore, also have a small increase in volume caused by internal cracking without this being observed. It is therefore important to complement volume measurements with other techniques in order to detect possible internal damage, e.g. ultrasonic pulse transmission time measurements, as has been done here.

11.4.2.2 External frost damage - concrete with entrained air

The results for external frost damage for concrete with entrained air are presented in Figure 11.13 for all the exposure sites. The effect of air entrainment is positive at all exposure sites in respect of scaling resistance.

Highway environment

From Figure 11.13a it can be seen that, for the specimens at the highway exposure site, all concrete qualities with w/b-ratio of 0.75 show signs of damage. The damage is, however, relatively small for concrete with only OPC as the binder, whereas the damage is substantial for concrete with slag as part of the binder, with increasing damage with increasing slag content. Concrete with w/b-ratio of 0.75 and some silica as part of the binder also shows some damage. All concrete qualities with w/b-ratios of 0.50 or below, except for those containing large contents of slag as part of the binder, show only limited external damage after five years' exposure. For concretes with high slag contents, however, both those with a w/b-ratio of 0.50 and those with a w/b ratio of 0.40 show signs of damage. For these qualities, air entrainment does not seem to have a noticeable effect on the salt-frost resistance, at least not in the aggressive highway climate at Highway 40.

Marine environment

As can be seen from the results in Figure 11.13b, after five years' exposure at the marine test site there is only relatively little damage to concrete with entrained air. Only the concrete with CEM III/B cement as binder and a w/b-ratio of 0.75 shows significant damage. For the other concrete qualities with a w/b-ratio of 0.75, the amount of damage is relatively small, although with some small differences depending on binder type used. For concrete with w/b-ratio of 0.50 or below, no damage can be seen for any of the different concrete qualities.

Environment without salt exposure

As can be seen in Figure 11.13c, after five years' exposure there is no visible damage for any of the concrete qualities with entrained air, even at as high w/b-ratios as 0.75.

Discussion

At none of the exposure sites did concrete qualities containing air show signs of visible evidence in the form of a volume increase, indicating internal damage. Air entrainment thus seems to reduce the risk of internal damage, at least up until five years' exposure.

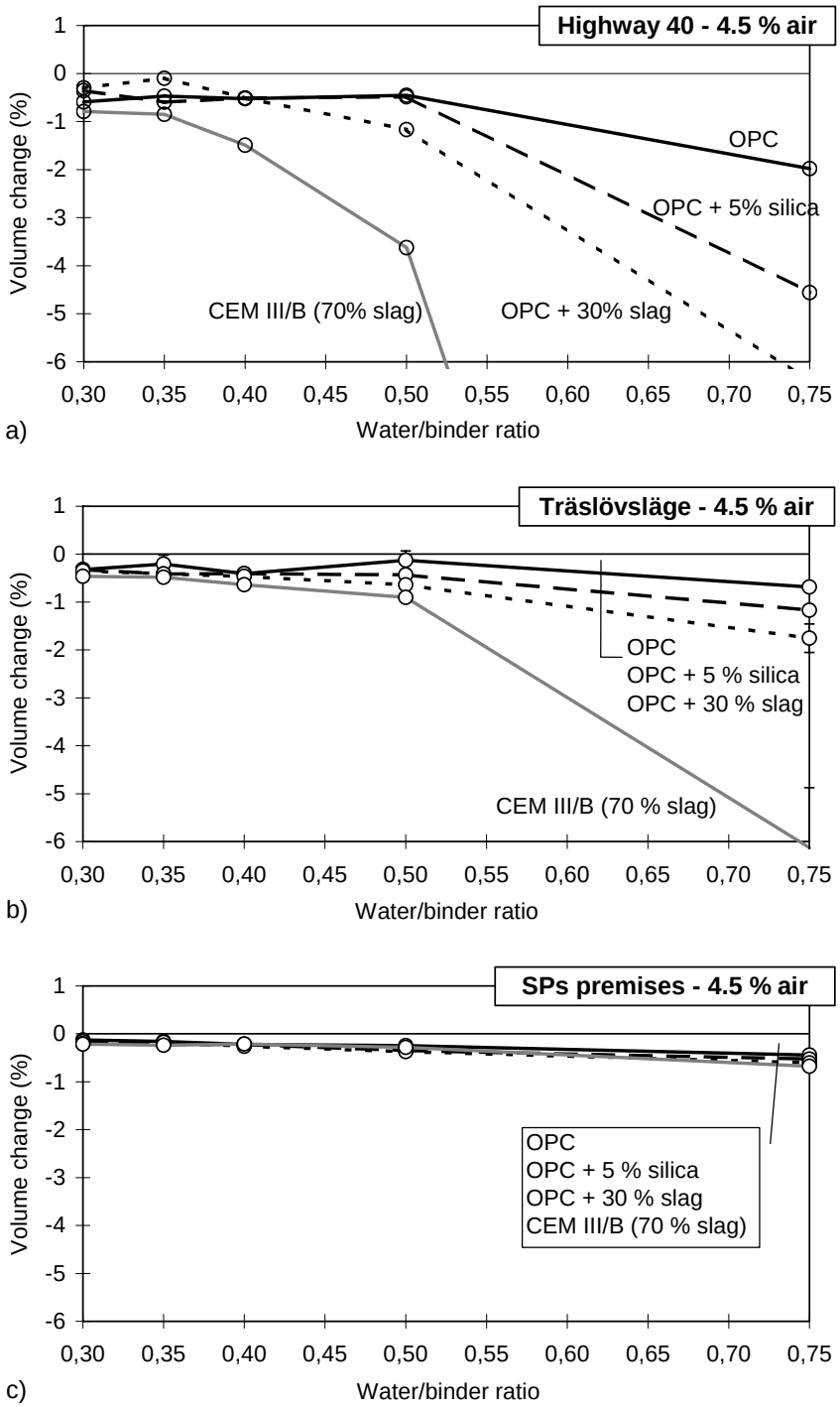

Figure 11.13 *Volume change after five winter seasons: concrete with different binder combinations and water/binder-ratios and with entrained air (~4.5 %). a) Highway environment, b) Marine environment, c) Salt-free environment*

Highway environment - results after 7 years' exposure

The latest measurements of volume and ultrasonic pulse transmission time for the specimens at the highway exposure site were carried out after the 2002/2003 winter season, i.e. after seven winter seasons. Figures 11.14a and 11.14b show the volume change after seven winter seasons for concrete mixtures, with natural air and with entrained air respectively, exposed at the highway exposure site.

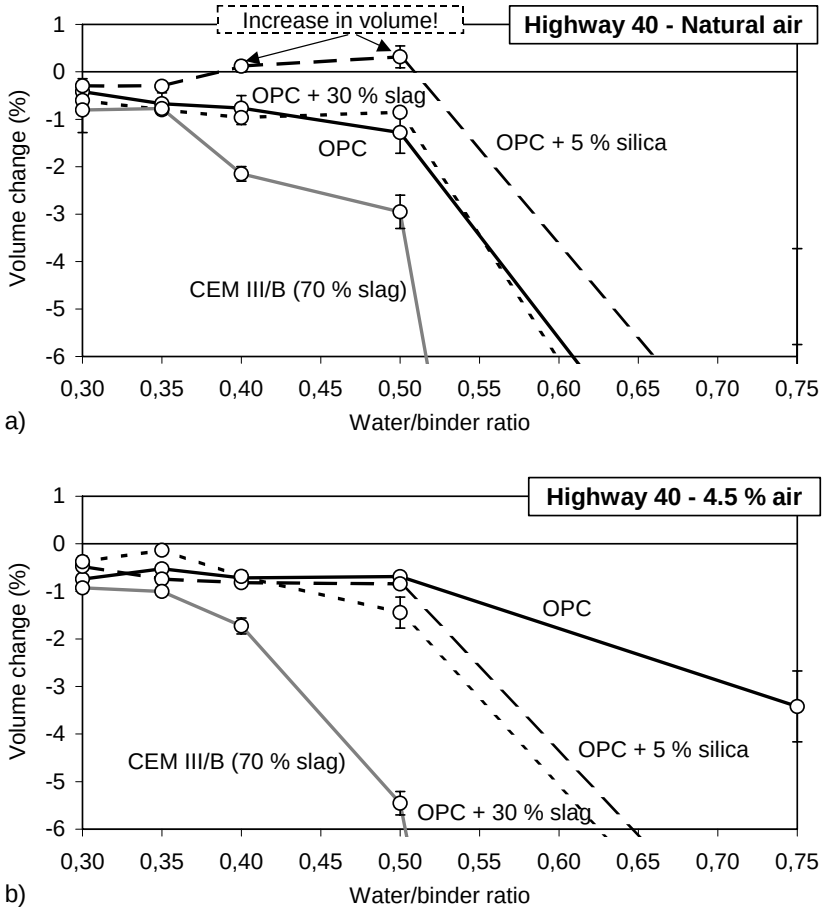

Figure 11.14 *Volume change after seven winter seasons at the highway exposure site. Concrete with different binder combinations and water/binder-ratios. a) Natural air, b) 4,5 % air*

As can be seen from Figure 11.14a, the amount of damage to concrete with natural air is somewhat greater, for the damaged concrete qualities after seven years than after five years, Figure 11.11a. However, the differences are small, except for the qualities with w/b-ratio of 0.75, which all show greater damage after seven years than after five years. The differences in damage depending on binder type are about the same after seven years as after five years of exposure.

In general, the effect of air entrainment is that the amount of damage to concrete with high water/binder ratios is reduced in comparison with the amount of damage to concrete without entrained air. However, this does not seem to be valid for concrete qualities with CEM III/B as binder. For these concrete qualities, with entrained air, the volume change is of the same order as - and sometimes even greater (w/b-ratios of 0.50 and 0.75) than - that for concrete without entrained air. For these qualities, entrained air does not seem to improve the scaling resistance. This behaviour is confirmed by the results from the freeze/thaw test carried out in the laboratory; see Table 11.6. In the laboratory test, the air-entrained concrete with CEM III/B as binder shows damage of the same order as for concrete without entrained air for all w/b-ratios.

Comparing the results for concrete with and without entrained air after seven years of exposure shows in general only small differences in volume change for concrete with w/b-ratios of 0.5 and below. However, the increases in volume for concrete qualities with OPC + 5 % silica that were observed in samples without entrained air cannot be observed when entrained air is used. This clearly shows the beneficial effect of air entrainment to prevent internal frost damage.

11.4.3 Internal frost damage

Internal frost damage in the form of micro-cracks in the paste leads to an increase in ultrasonic pulse transmission time (UPTT). This because the cracks prevent the ultrasonic pulse from taking the shortest path through the material; a longer path means an increase in transmission time.

The use of ultrasonic pulse transmission time measurements as an indication of internal damage is a simple, cheap and straightforward measurement technique. There are, however, some drawbacks to this method, making the results sometimes difficult to interpret. Some of these drawbacks are:

- Damage on the surface of the specimens makes it difficult or, if the damage is extensive, impossible to carry out transmission time measurements. The resistance to internal frost attack is thus difficult to investigate on material with poor scaling resistance.
- Changes in the surface zone such as cracks just beneath the surface, i.e. incipient external damage, and possibly also extensive carbonation, may change the transmission time, making it difficult to interpret the results.
- The results may vary with the operator carrying out the measurement. This effect can, however, be minimised by careful working instructions, but it can never be completely eliminated.

These drawbacks of the UPTT measuring technique makes it difficult to interpret small changes in the measured transmission time measurements. However, when there are marked changes in transmission time, and these changes persist from one year to the next,

the results are interpreted as indications of internal damage. As a complement, analysing thin sections or polished sections is a good way to confirm possible internal damage.

11.4.3.1 Internal frost damage - concrete without entrained air

Clear indications of internal damage were detected for some of the concrete qualities without entrained air used in this investigation. Figure 11.15 shows the relative transmission time after five years' exposure for different concrete qualities, all without entrained air. The relative transmission time is given in % and is calculated by dividing the measured transmission time after five years' exposure by the measured transmission time before exposure. A relative transmission time over 100 indicates possible internal damage. Values over about 110 are more certain indications of internal damage. A natural reduction of the transmission time with age can be seen for undamaged concrete with high w/b-ratios. For these qualities, a relative transmission time around 100 might be an indication of internal damage.

Highway environment

From Figure 11.15a, highway exposure, it can be seen that there is an increase in transmission time, indicating internal damage, for the concrete qualities with OPC and OPC + 5 % silica and a w/b-ratio 0.75. For concrete with OPC + 5 % silica as binder, the qualities with w/b- ratio 0.50 and to some extent also w/b-ratio 0.40 also show an increase in transmission time, indicating internal damage. The increase in transmission time together with the measured increase in volume, Figure 11.11a, indicate internal damage for these concrete qualities without air. To confirm the possible internal damage, polished sections from these qualities were investigated. Figure 11.16 shows photos of polished samples impregnated with epoxy resin and fluorescent dye for the three qualities without entrained air and with OPC + 5 % silica as binder.

From the photos in the figure, it can be seen that all three qualities show internal cracking, which causes the increase in volume and transmission time. It can also be seen that the cracking increases in severity with increasing w/b-ratio, which agrees with the increase in transmission time with increasing w/b-ratio and the more marked increase in volume for w/b 0.50 compared with w/b-ratio 0.40.

No polished sample was produced for the concrete quality with only OPC as binder and with a w/b-ratio of 0.75. Possible internal damage, as indicated by the increase in transmission time, can thus not be confirmed in this way. However, the marked increase in transmission time is regarded as a clear indication of internal damage.

For concrete with OPC + 30 % slag or CEM III/B as binder and with w/b-ratio 0.75, the surfaces of the specimens were so damaged that the ultrasonic pulse transmission time could not be measured, and so possible internal damage could not be detected. To detect possible internal damage, polished samples were made from both qualities, Figure 11.17.

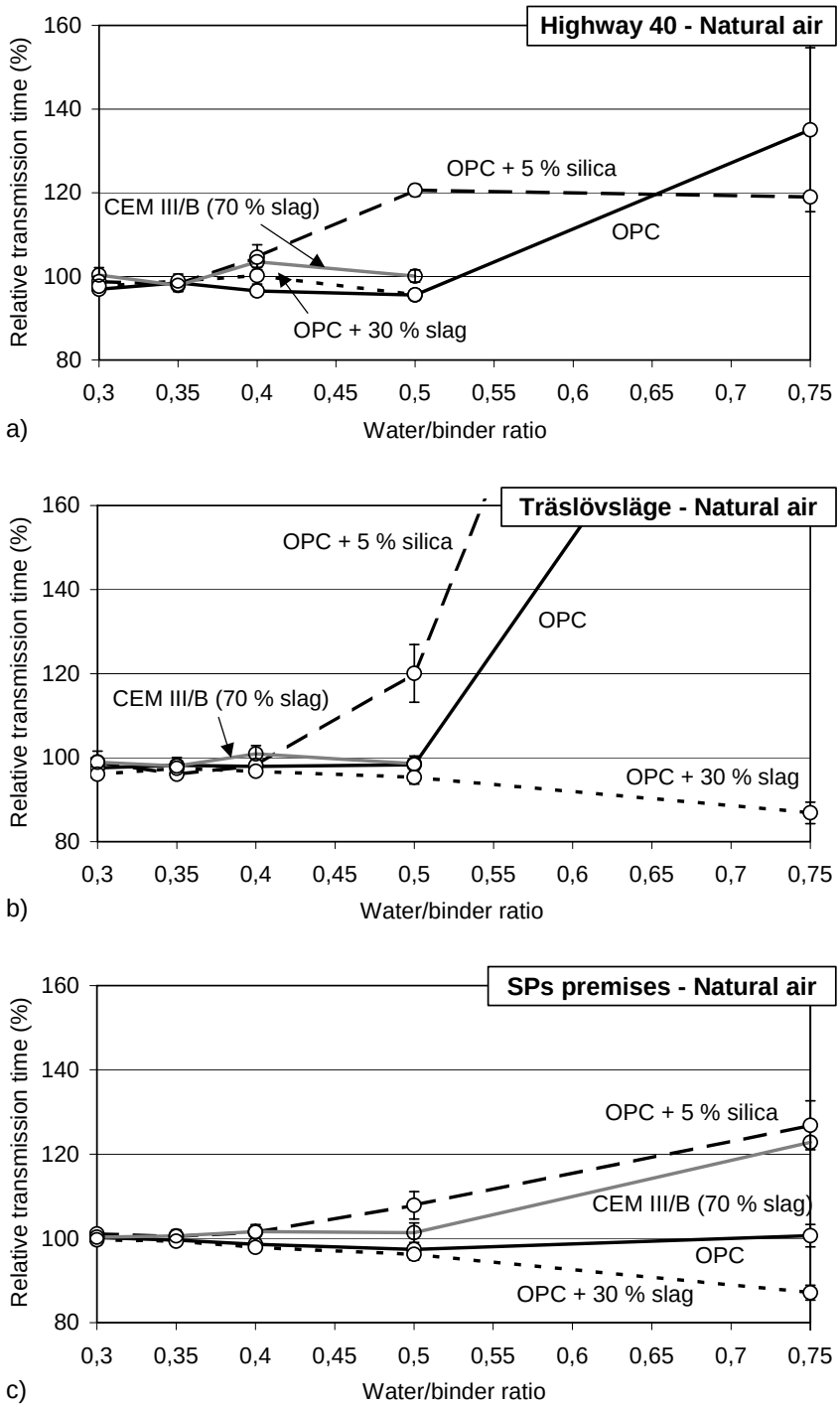

Figure 11.15 *Relative transmission time after five winter seasons. Concrete with different binder combinations and water/binder-ratios and without entrained air. a) Highway exposure, b) Marine exposure, c) Salt-free environment*

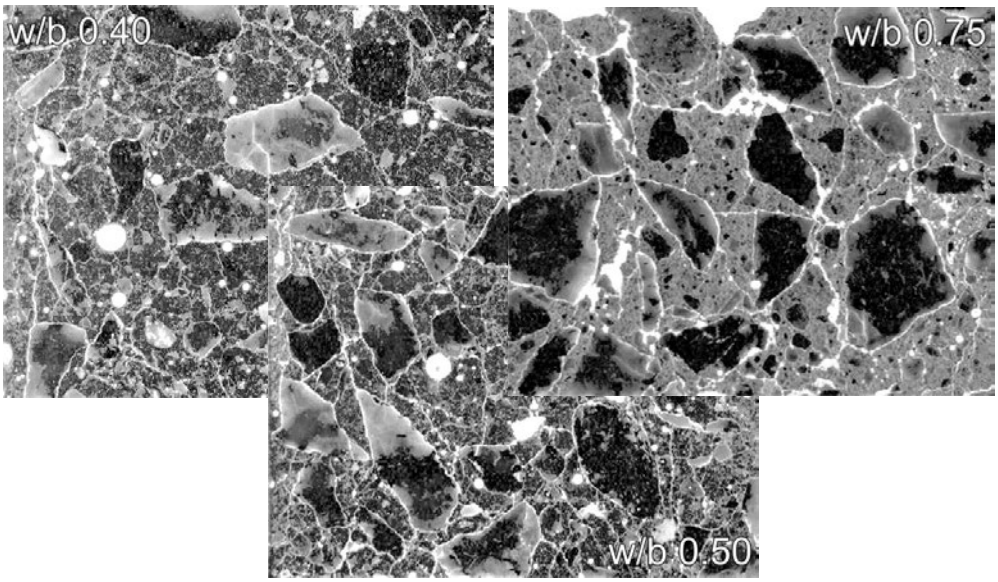

Figure 11.16 *Photos of polished samples impregnated with epoxy resin and fluorescent dye of three concrete qualities exposed for five years at the highway exposure site. All qualities have OPC + 5 % silica as binder and no entrained air. From left: w/b 0.40; w/b 0.50; w/b 0.75. Picture size: 60 ± 5 mm · 50 ± 5 mm.*

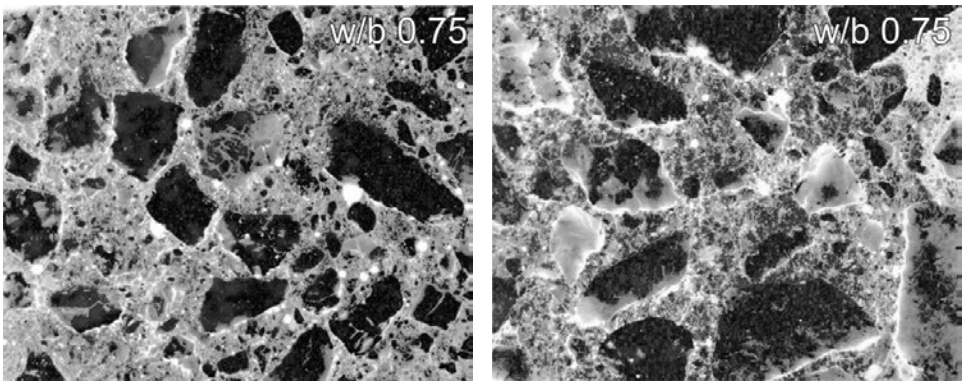

Figure 11.17 *Photos of polished samples impregnated with epoxy resin and fluorescent dye of two concrete qualities without entrained air exposed for five years at the highway exposure site. From left: OPC + 30 % slag with w/b 0.75; CEM III/B with w/b-ratio 0.75. Picture size: 60 ± 5 mm · 50 ± 5 mm.*

As can be seen from Figure 11.17, neither of the two materials with slag as part of the binder and with a w/b-ratio of 0.75 show any obvious signs of internal cracking.

Marine environment

Figure 11.15b shows the relative transmission time after five years' exposure at the marine exposure site for the different concrete qualities without entrained air.

The tendency at the marine exposure site is the same as at the highway exposure site, i.e. it is primarily the concrete qualities with high w/b-ratios that show increasing transmission times. It is the concrete qualities with OPC and OPC + 5 % silica as binder and with w/b-ratio 0.75 that show a marked increase in transmission time. For concrete with OPC + 5 % silica as binder, the w/b-ratio 0.50 quality also shows an increase in transmission time, indicating internal damage. This, together with the observed increase in volume for this quality seen in Figure 11.11b, is a further indication of internal damage. To confirm the possible internal damage, polished samples from these qualities were investigated. Figure 11.18 shows pictures of polished samples impregnated with epoxy resin and fluorescent dye for the two qualities without entrained air with OPC + 5 % silica as binder as well as the quality with only OPC as binder.

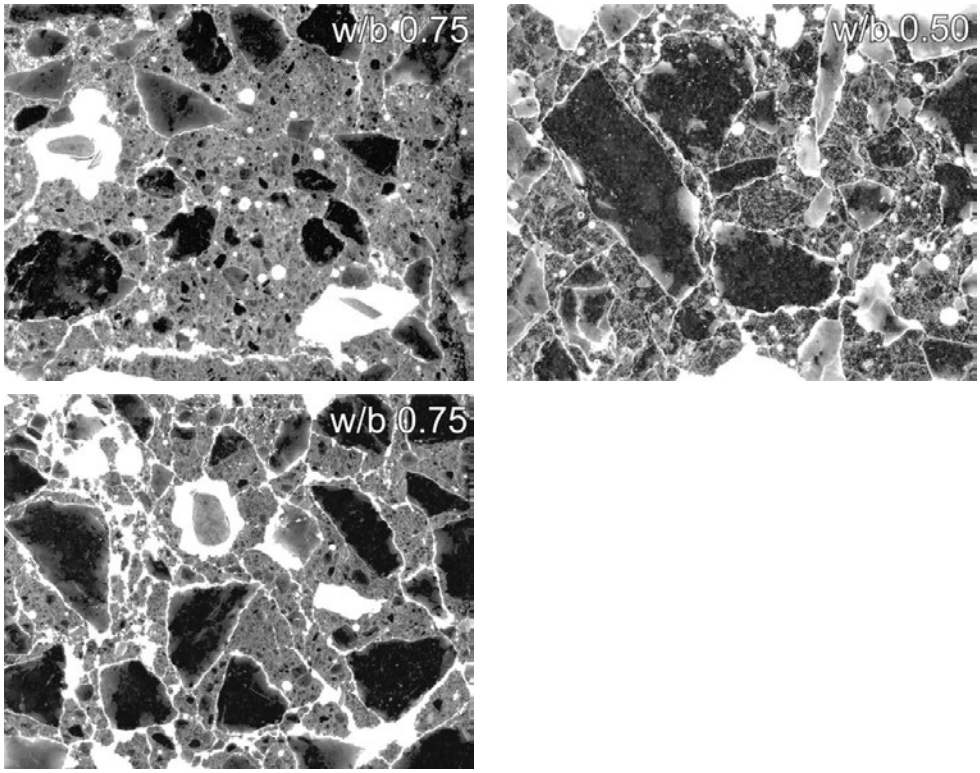

Figure 11.18 *Photos of polished samples impregnated with epoxy resin and fluorescent dye of three concrete qualities exposed for five years at the marine exposure site. From above left: OPC with w/b-ratio 0.75; OPC + 5 % silica with w/b-ratio 0.50; OPC + 5 % silica with w/b-ratio 0.75. Picture size: 60 ± 5 mm · 50 ± 5 mm.*

From the figure, it can be seen that qualities showing an increase in transmission time also show extensive internal cracking. The internal damage for the qualities with a w/b-ratio of 0.75 was so extensive that parts of the specimen fell apart during production of the polished samples. This can be seen in the photos as the marked light areas with irregular shapes.

For concrete with CEM III/B and a w/b-ratio of 0.75, the surfaces were severely damaged, which made it impossible to measure the ultrasonic pulse transmission time and thus to identify possible internal damage. However, to detect possible internal damage, a polished sample was produced and analysed; see Figure 11.19.

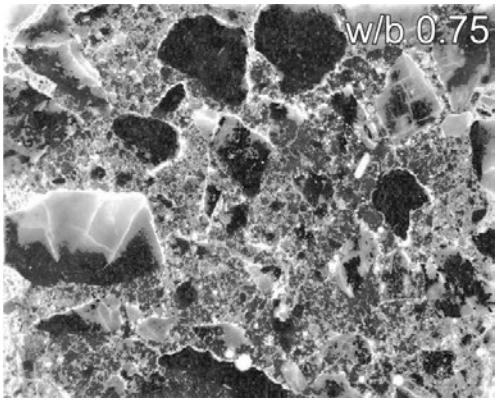

Figure 11.19 *Photo of a polished sample impregnated with epoxy resin and fluorescent dye of the concrete quality with CEM III/B as binder, w/b-ratio 0.75 and without entrained air. The concrete was exposed for five years at the marine exposure site. Picture size: 60 ± 5 mm · 50 ± 5 mm.*

As can be seen from the figure, there are no obvious signs of internal cracking. This is in agreement with the results for the same concrete quality exposed at the highway exposure site, Figure 11.17.

No indication of internal damage could be detected for concrete with OPC + 30 % slag as part of the binder, even at high w/b-ratios.

Environment without salt exposure

At the exposure site at SP's premises transmission time measurements could be made on all specimens, i.e. the external damage was limited, resulting in sufficiently sound surfaces for transmission time measurements to be carried out, even for qualities with high w/b-ratios. The results are shown in Figure 11.15c.

It can be seen in the figure that concrete qualities with OPC + 5 % silica and with CEM III/B as binder and with w/b-ratio 0.75 show significant increases in transmission

time, i.e. indicating internal damage. For concrete with only OPC as binder there is a slight increase in transmission time, although not enough to be interpreted as internal damage. Concrete with OPC and + 30 % slag show a marked reduction in transmission time, probably a result of continuing densification as a result of increasing hydration with age.

As can be seen, the concrete quality with CEM III/B as binder and with a w/b-ratio of 0.75 shows a marked increase in transmission time, indicating internal damage. However, since visual inspection of this material found extensive surface cracks after seven years of exposure (Figure 11.12), it is likely that the increase in transmission time is because of these cracks and not because of extensive internal cracking. This is confirmed by investigating a polished sample impregnated with epoxy resin and fluorescent dye.

For the concrete quality with OPC + 5 % silica as binder and with a w/b-ratio of 0.75, the increase in volume, however small (see Figure 11.11), together with the increase in transmission time, indicates internal damage. This is further confirmed by investigating a polished sample of this material, Figure 11.20. The figure also shows a picture of a polished sample from the concrete with OPC + 5 % silica as binder and with a w/b-ratio of 0.50. This quality also showed a small increase in transmission time, indicating internal damage.

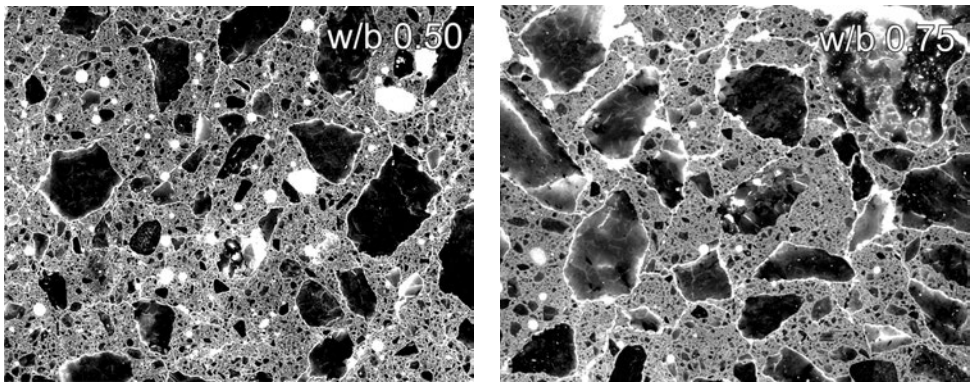

Figure 11.20 *Pictures of polished samples impregnated with epoxy resin and fluorescent dye of two concrete qualities exposed for five years at the exposure site at SP's premises. Both qualities had OPC + 5 % silica as binder and no entrained air. From the left: w/b 0.50; w/b 0.75.*

From the figure, it can be seen that for the concrete quality with a w/b-ratio of 0.75 there are signs of cracking, leading to the increase in transmission time. The signs of internal damage are not as apparent for the concrete with a w/b-ratio of 0.50, although there are indications of small cracks relatively close to the surface. These cracks probably cause the increase in transmission time.

11.4.3.2 Internal frost damage - concrete with entrained air

Figure 11.21 shows the relative transmission time for the concrete qualities with entrained air exposed at the three exposure sites. In general, the concrete qualities with entrained air show no clear indications of internal damage at any of the exposure sites. However, it can be seen from Figure 11.21a that the results after five years of exposure at the highway exposure site show a small indication of internal damage for the concrete quality with OPC as binder and with a w/b-ratio of 0.75.

Highway environment

Since all specimens with high w/b-ratio exposed at the highway exposure site showed considerable external damage, the increase in transmission for the quality with OPC as binder and with a w/b-ratio of 0.75 time was suspected to be due to damage close to the surface. To investigate the possible effect of damage at, or close to, the surface on the transmission time measurements, two corners were cut from one of the specimens with OPC as binder and a w/b-ratio of 0.75. This enabled transmission time measurements to be made on undamaged surfaces after six and seven years of exposure at the exposure site. The results from transmission time measurements on the cut surfaces after seven years' exposure is shown in Figure 11.22. From the figure, it can be seen that after seven years' exposure the concrete quality with OPC and with a w/b-ratio of 0.75 does not show any signs of increasing transmission time. The measured increase in transmission time after five years' exposure thus seems to be a result of damaged surfaces at the place of measurement. This can also explain the high scatter for the transmission time measurements for this concrete quality after five years' exposure.

It can thus be concluded that, for the concrete qualities with entrained air, no obvious indication of internal damage can be found after seven years' exposure at the highway exposure site.

Marine environment and environment without salt exposure

Figures 11.21b and 11.21c show the change in transmission time after five years' exposure at the marine test site and the test site at SP's premises respectively.

The specimens exposed at the marine exposure site and at SP's premises show about the same results. At these two exposure sites, the only quality that shows an increase in ultrasonic pulse transmission time is the concrete quality with CEM III/B as binder and with a w/b-ratio of 0.75. However, the increase is small and is probably due to a weakening of the concrete surface in the same way as was found for the same concrete quality but without entrained air, see Figure 11.12. No change in transmission time, indicating possible damage, is shown for the other concrete qualities.

It can thus be concluded that, for the qualities with entrained air, no quality showed any signs of internal damage, as indicated by a change in ultrasonic pulse transmission time, at any of the exposure sites, at least not after five or seven years' exposure.

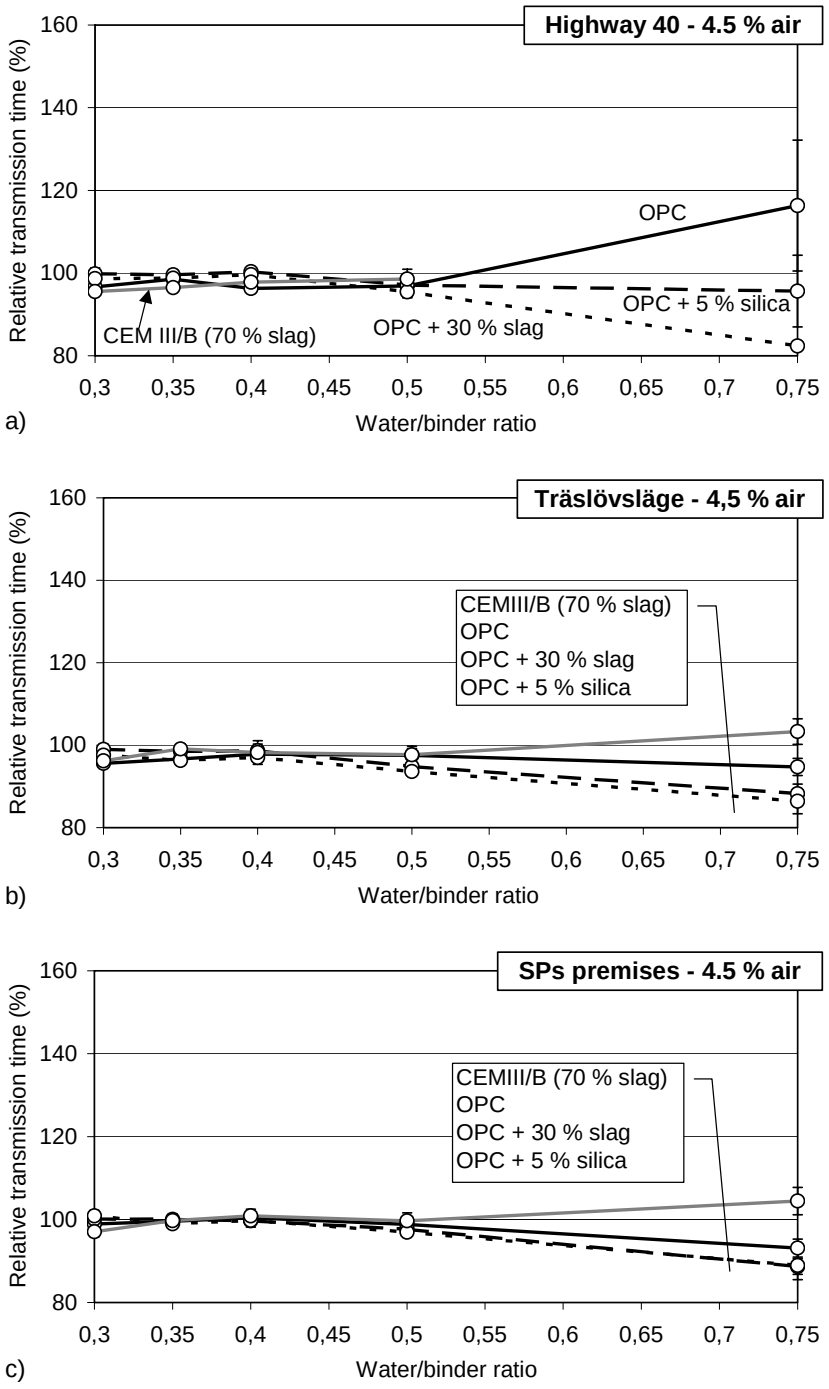

Figure 11.21 *Relative transmission time after five winter seasons. Concrete with different binder combinations and water/binder-ratios and with entrained air 4.5 %. a) Highway exposure, b) Marine exposure, c) Salt-free environment*

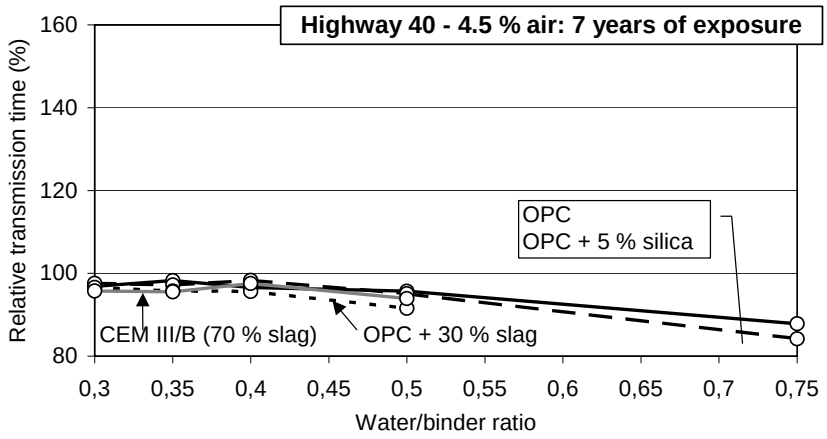

Figure 11.22 *Relative transmission time after seven winter seasons at the highway exposure site. Concrete with different binder combinations and water/binder-ratios and with entrained air (~4.5 %).*

11.4.4 Discussion - internal damage

The results from the transmission time measurements carried out on the specimens with and without entrained air exposed at the three field exposure sites have shown that there are only a few concrete qualities showing internal damage after five years' exposure. Table 11.7 shows a summary of the results.

Table 11.7 *Concrete qualities with potential internal damage indicated by a change in ultrasonic pulse transmission time at the three test sites.*

Concrete quality	**Highway**	**Marine**	**SP's premise**
OPC no air w/b 0.75	*Damaged*	*Damaged*	*Damaged*
OPC+5 % silica no air w/b 0.75	*Damaged*	*Damaged*	*Damaged*
OPC+5 % silica no air w/b 0.50	*Damaged*	*Damaged*	*Damaged*
OPC+5 % silica no air w/b 0.40	*Damaged*	No D. indication	No D. indication

As can be seen in the table, none of the concrete qualities showing internal damage included entrained air. It can also be seen that it is primarily concrete with high w/b-ratios that shows internal damage. Air entrainment and a w/b-ratio of 0.50 or below thus seems to result in concrete qualities with high enough internal frost resistance to withstand at least five winter seasons, probably more, at the exposure sites used in this investigation.

From Table 11.7 it can also be seen that internal damage occurs in specimens at all three test sites; that is, the development of internal damage seems to be independent of exposure climate, at least for the climates at the exposure sites used in this investigation. This is contrary to what was found for the development of external damage, for which the exposure climate appeared to have a clear influence on the amount of damage, which is

what could be expected. The risk of external damage increases with exposure to moisture and salt, whereas the risk of internal damage increases with exposure to moisture. At the three exposure sites, there is a marked difference in salt exposure but the exposure to moisture is about the same.

Concrete with 5 % silica as part of the binder

As can be seen in Table 11.7, it is only the concrete quality with OPC + 5 % silica as part of the binder and without entrained air that shows damage for qualities with w/b-ratios lower than 0.75. For concrete with this binder type, the quality with a w/b-ratio of 0.50 shows indications of damage at all three test sites, while of the quality with a w/b-ratio of 0.40 the specimens exposed at the highway exposure site show sign of damage. Damage is detected by an increase in transmission time, an increase in volume as well as in pictures from polished samples.

Homogeneity of the materials was investigated in order further to examine the reason for the observed internal damage for the concrete qualities without entrained air and with silica as part of the binder. This was done by visual investigations of thin sections from the three concrete qualities. The thin sections were produced from 150 mm spare cubes made from the same batches of concrete that the actual specimens exposed at the exposure sites were cast from. The spare cubes had been stored in the laboratory at 50 % RH and +20 °C since casting in 1996. Figure 11.23 shows pictures with the size of about 8 · 6 mm taken through the microscope from the thin sections

The pictures in Figure 11.23 are only small parts of the thin sections, which have a size of about 80 · 50 mm. However, from thorough examination of the thin sections, it can be concluded that the photos shown are representative of the thin sections. As can be seen from the figure, concrete with w/b-ratios of 0.50 and 0.75 seems homogeneous. For the concrete with a w/b-ratio of 0.40, however, the picture shows weaknesses between some large aggregates and the cement paste. These weaknesses are primarily seen on one side of the aggregates, which indicates that this could be a sign of bleeding for this concrete quality.

The bleeding seems primarily be around parts of the large aggregates. The paste and the smaller aggregates seem homogeneous, with no signs of bleeding. To what extent the observed bleeding around the larger aggregates could affect the internal frost resistance is not known. However, the existence of weak porous zones at the aggregate/paste interface is probably detrimental to the frost resistance. It can thus not be excluded that the observed internal damage for the concrete quality with a w/b-ratio of 0.40 exposed at the highway exposure site may be an effect of the observed bleeding. It can, however, be noted that the influence of the possible bleeding on the frost resistance is not so severe that internal damage is also seen at the marine exposure site and at the site at SP’s premises.

For the other concrete qualities, i.e. with w/b-ratio 0.50 and 0.75, the observed internal frost damage cannot be explained by any lack of homogeneity, such as bleeding.

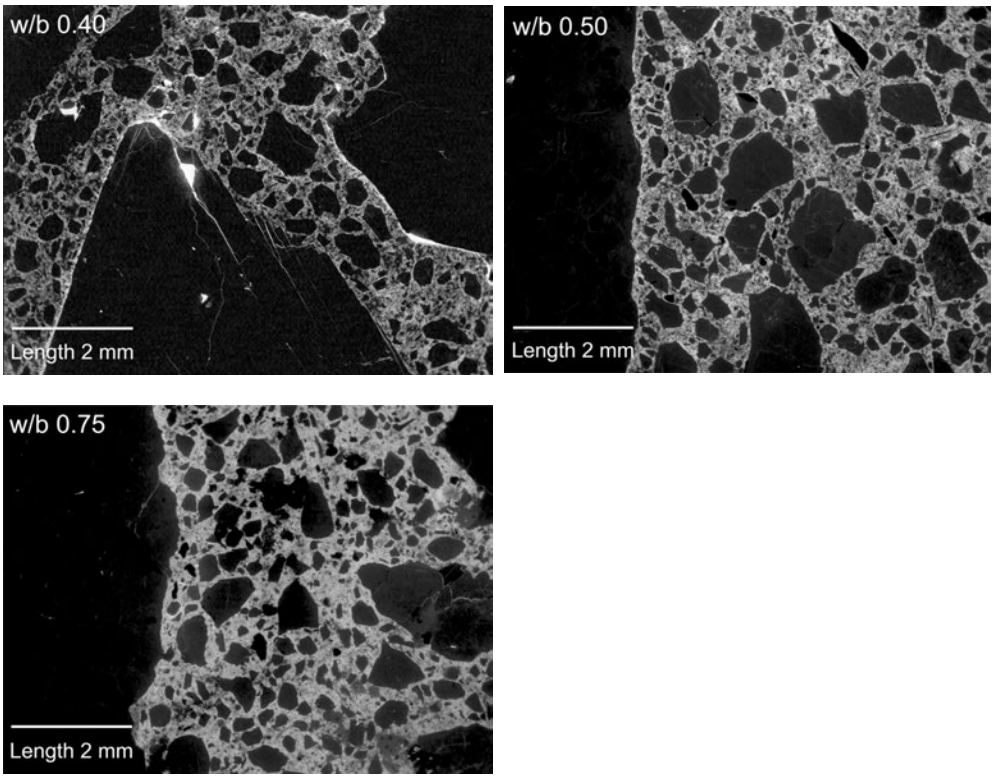

Figure 11.23 *Photos of parts of thin sections for concrete qualities with OPC + 5 % silica as binder and without entrained air.*
From above left: w/b 0.40; w/b 0.50; w/b 0.75.

Concrete with OPC alone as binder

To investigate if also concrete with only OPC as binder and with the same w/b-ratios showed signs of bleeding, thin section from qualities with w/b-ratios 0.40, 0.50 and 0.75 were produced. Figure 11.24 shows pictures taken through a microscope.

From the figure, it can be seen that for concrete with only OPC as the binder, and with w/b-ratios of 0.50 and 0.75, there are no signs of any inhomogeneity. However, for concrete with a w/b-ratio of 0.40, there are signs of weaknesses between some large aggregates and the cement paste, indicating bleeding. As for concrete with the same w/b-ratio but with 5 % silica as part of the binder (Figure 11.23), the weaknesses are primarily seen on one side of the aggregates, and around the large aggregates. The paste and the smaller aggregates seem homogeneous, with no signs of bleeding.

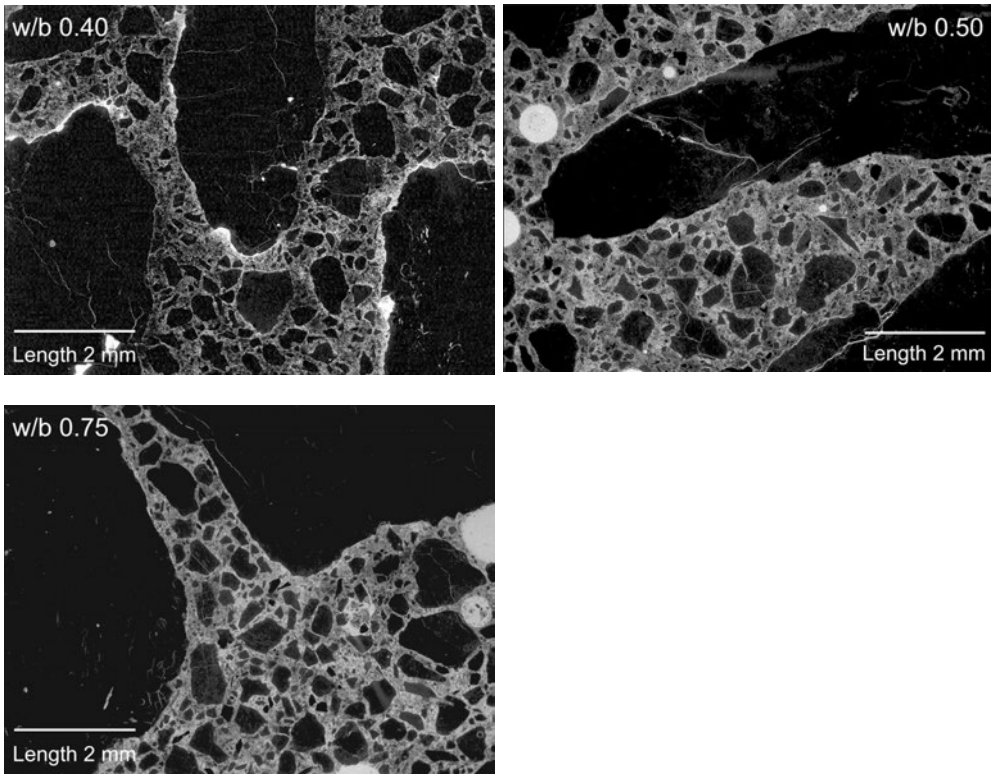

Figure 11.24 *Photos of parts of thin sections for concrete qualities with only OPC as binder and without entrained air.*
From above left: w/b 0.40; w/b 0.50; w/b 0.75.

Discussion

Comparing the appearance of possible bleeding by investigating the entire area of the thin sections shows that the signs of bleeding are at least as, and possibly even more, evident for the material with only OPC as binder than for the material with OPC and some silica as part of the binder. A possible explanation for the bleeding for these concrete qualities could be that a plasticiser was used for these qualities. No plasticiser was used for concrete with a w/b-ratio of 0.50 and above, and there are also no signs of any inhomogeneity.

Even if both concrete qualities with w/b-ratio 0.40 show signs of bleeding around the large aggregates, only the quality with 5 % silica as part of the binder shows signs of internal damage; at least, after seven years' exposure at the highway exposure site. There is thus no indication that the reason for the observed internal cracking should be because of the possible bleeding. If bleeding around the large aggregates had been the cause of the observed internal damage, then concrete with only OPC as binder should also be expected to show internal damage. The reason for the internal damage seems to be something else.

One possibility is that the natural air void system between the concrete qualities differs in a way that leads to internal frost damage for the concrete containing silica as part of the binder but not for the quality made with only OPC as binder. One possible reason for this could be due to a potential compatibility problem between the cement type, the silica and the plasticiser used.

The results from this investigation thus indicate that the concrete qualities with OPC + 5 % silica as binder and without entrained air seem more susceptible to internal frost damage than do the other concrete qualities, at least with the materials and compositions used in this investigation. It should be stressed that this negative effect of using silica as part of the binder has been observed only for concrete qualities without entrained air. If using a sufficient amount of, and properly distributed, entrained air, there are no signs of any negative effects on the frost resistance by using silica as part of the binder.

It must also be stressed that the observed damage to the concrete qualities with silica as part of the binder may be because of compatibility problems between the different concrete constituents and not solely because of the incorporation of silica. As was mentioned above there might, for example, be a compatibility problem between the cement type, the silica and the plasticiser used, resulting in a concrete with low resistance to internal frost damage. The observed possible bleeding around the large aggregates for concrete with a w/b-ratio of 0.40, both with and without silica as part of the binder, is an indication of this. However, the fact that only the concrete quality with silica as part of the binder shows signs of internal damage indicates that the incorporation of silica leads to other compatibility problems, e.g. to an inferior natural air-void system leading to poor frost resistance.

11.4.5 Comparison between freeze/thaw testing in the laboratory in accordance with SS 13 72 44 and results from the field investigations

For all concrete qualities in this investigation, the scaling resistance was tested in the laboratory at an age of 31 days according to SS 13 72 44, the ‘slab test’. (For a description of the ‘slab test’, see Chapter 2.) The results from testing in the laboratory can be compared with the results obtained at the field exposure sites. The laboratory test can in this way be ‘calibrated’ towards real conditions. When testing the durability according to standard methods in the laboratory, such as for example the scaling resistance, results are expected to be relevant for the actual durability in real exposure conditions. For the exposure climates in this investigation, it is the results from the marine and highway environment that are relevant for comparison with the laboratory results. This is because at these climates (exposure class XF 4 according to EN 206-1) concrete qualities’ proven scaling resistant in a salt-frost test are prescribed in Sweden. For the climate at the field exposure site at SP’s premises (no salt exposure), salt-frost testing is not prescribed, and so a comparison is not relevant. Since the climate at the highway has proven to be most aggressive with regard to external damage (scaling), the laboratory results are compared with results from this test site.

Figure 11.25 shows results from the 'slab test' carried out in the laboratory and the volume change after seven years of highway exposure. The diagram shows the scaling (kg/m²) after 56 freeze/thaw cycles as a function of the volume loss (%) after seven years' exposure at the highway exposure site. The acceptance criterion in the laboratory test is 1 kg/m^2 (illustrated by a horizontal line). For the specimens exposed at the field exposure sites, an acceptance criterion has to be assumed. Here, an acceptance criteria of 2 % volume loss after seven years' exposure, corresponding to somewhat less than 1 kg/m^2, is chosen as the acceptance criteria. The acceptance criteria of 2 % volume loss is shown by the vertical line in Figure 11.25. Filled symbols in the figure represent concrete without entrained air. Symbols with a white centre represent concrete with entrained air. Enlarged symbols represent qualities with internal damage detected by increase in volume and/or increase in ultrasonic pulse transmission time.

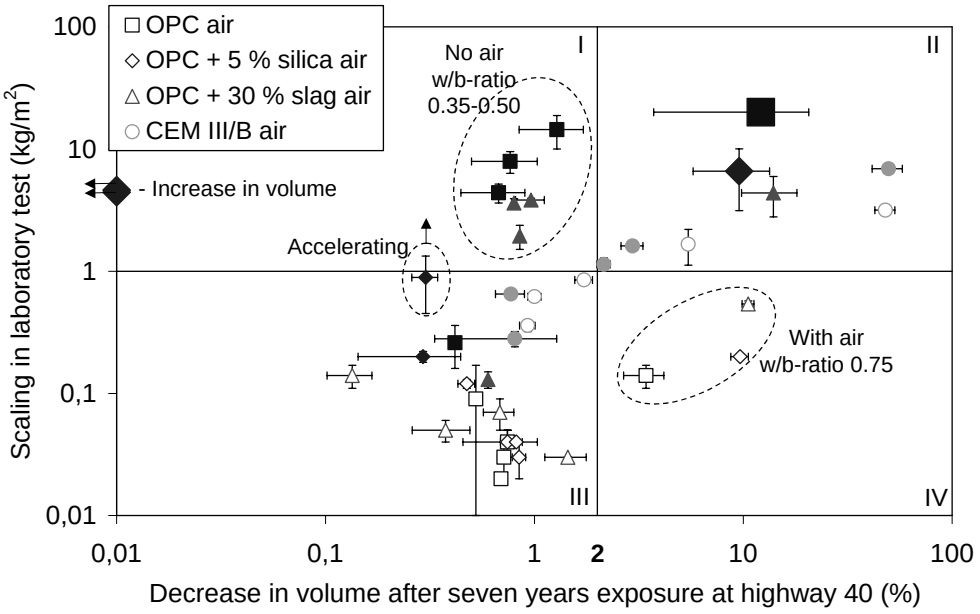

Figure 11.25 *Scaling according to the 'Slab test' (tested in the laboratory) as a function of the decrease in volume for specimens exposed at the highway exposure site for seven winter seasons. Filled symbols represent concrete without entrained air. Symbols with a white centre represent concrete with entrained air. Large symbols represent internal damage. Each point is a mean of four specimens for the laboratory test and two specimens for the exposure at the highway exposure site.*

From the results presented in Figure 11.25, it can be seen that only three qualities fall into the IV quadrant, which means that these three qualities are accepted by the laboratory test method, but fail in real conditions. This can be regarded as the worst case. These are all air-entrained qualities but with high water/binder ratios (0.75). The laboratory test method

is primarily intended to be used for normal bridge concrete, with entrained air and with a w/b-ratio below 0.5.

Most qualities fall into Quadrants II or III, which means that the test method and 'reality' agree. Some concrete qualities fall into Quadrant I, which means that the test method rejects them, but in real conditions only limited damage can be seen after seven years' exposure. However, as the concrete in Quadrant I shows only limited damage in the field, the test method results are on the safe side. None of these qualities has any entrained air, which makes them especially susceptible to frost damage. During the first seven years, the climate has not been aggressive enough significantly to damage these concrete qualities. However, one winter season with a more aggressive climate might cause internal damage as well as scaling on these qualities without entrained air, moving them into Quadrant II.

Two concrete qualities show an increase in volume and an increased transmission time when exposed in the field, indicating internal frost damage. These qualities also fail the acceptance criterion when tested in the laboratory.

One possible explanation for the limited scaling in the field for the concrete qualities in Quadrant I might be a positive effect of ageing. In a field investigation reported in Petersson (1995), it was found that concrete aged and exposed in a marine climate showed better scaling resistance when tested in the laboratory after ageing than did virgin concrete. This improvement of the scaling resistance was especially apparent for concrete without entrained air, as was also found in this investigation. This corresponds well with what is found in the laboratory, i.e. that carbonation considerably increases the scaling resistance for these concrete types with only OPC and OPC with a small amount of silica as part of the binder. The explanation to why the concrete qualities in Quadrant I failed the laboratory test but only shows small volume changes when exposed at the exposure site might be because:

- In the laboratory - the seven days of preconditioning specified in the test method is too short time for a concrete without air to reach a degree of carbonation that improves the scaling resistance to such a degree that the carbonated layer withstands the tough test procedure in the laboratory test.
- In real conditions - the specimens can continue to carbonate when exposed at the field exposure sites, resulting in a steadily improved scaling resistance with time.

On the whole, the results for concrete with w/b-ratio equal to or below 0.50, and with entrained air, shown in Figure 11.25, indicate that the slab test classifies these concrete qualities as could be expected. This is true for all binder types and combinations tested in this investigation.

Internal frost resistance

There are no requirements in the Swedish building regulations for testing internal frost resistance. The results from the present investigation, showing that some concrete qualities are susceptible to interior frost damage, raise a need for such requirements. It has, for

example, been shown that concrete qualities with relatively low w/b-ratios without air and also concrete containing air, but with high w/b-ratios, show indications of internal frost damage. The test method used today for testing the scaling resistance, SS 13 72 44, the 'slab test', is primarily intended for evaluating the scaling resistance, and not the resistance to internal frost damage. It cannot, however, be excluded that a concrete quality with relatively high scaling resistance could have a poor resistance to internal frost damage. For example, in this investigation, some concrete qualities without air and with OPC + 5 % silica as part of the binder have, in the field, shown only slight external damage but obvious internal damage. In the laboratory, these qualities failed the scaling test, and this shows the need for an appropriate test method evaluating also the internal frost resistance.

There is a need for requirements regarding concrete resistant to internal frost damage when exposed in environments corresponding to both exposure classes XF 3 and XF 4. Standards EN 206-1 and SS 13 70 03 prescribe that concrete intended for use in exposure class XF 3 must *either* have a minimum air content *or* have been proven salt-frost resistant. Exposure class XF 4 prescribes concrete proven to be salt-frost resistant but with no minimum air content. Since the effect of entrained air is at least as important, maybe even more important, for the resistance to internal frost damage as for scaling, it is highly desirable that there should be a complement to the existing salt-frost test that also clearly indicates possible internal frost damage. This is especially true when concrete qualities without air are intended to be used in environments corresponding to exposure classes XF 3 or XF 4. According to the current requirements, these concrete qualities are tested only with respect to resistance to scaling. On the basis of what has been found in this investigation, it is recommended that the resistance towards internal frost damage (using an appropriate test method) should be tested as well, at least for concrete qualities with no or low contents of entrained air.

A test method for evaluation of the susceptibility to internal frost damage has been developed in recent years at SP in Borås. The method is a further development of the method evaluating the scaling resistance, i.e. the 'slab test', and makes it possible simultaneously to evaluate the resistance to scaling and internal damage. The method has been evaluated using round robin tests in a couple of international projects; see Tang et al. (1997) and Tang et al. (2000). These studies have shown that the developed method can easily detect internal damage, and that the method shows both good reproducibility and good repeatability. The method has recently been recommended by RILEM for evaluation of internal deterioration, Tang & Petersson (2001). Further investigations about the correlation between results from the test method and real conditions are, however, needed to show the validity of the method.

11.4.6 Experience from other field investigations

There are few reports of extensive field investigations in which the freeze/thaw durability of different concrete qualities has been systematically studied. There is, however, one Canadian project, which includes a large number of field investigations of the freeze/thaw durability of concrete exposed in a marine climate. Some of the results from this study are presented below.

In 1978, the Canadian Centre for Mineral and Energy Technology (CANMET) started a long-term exposure testing program. Since then, a large number of specimens have been placed in the marine environment at the Treat Island exposure site in Cobscook Bay near Eastport in Maine on the east coast of USA. Up until 1994, 15 different research projects have been running, which have included the freeze/thaw durability of concrete with and without secondary cementitious materials. Results from these projects have been published in Bremner et al. (1989), Malhotra & Bremner (1996) and Bremner et al. (2003). The following is a presentation and discussion of the results from the two projects referred to as 'Phase 1' and 'Phase 5B' in the three publications. The 'Phase 1' project investigated the effect of incorporating slag, while the 'Phase 5B' project investigated the effect of incorporating silica as part of the binder.

Both investigations used specimens in the form of prisms (305 · 305 · 915 mm) mounted on racks and installed at mid-tide level, so that the specimens were exposed to a marine atmosphere and to immersion in sea water twice daily. The number of freeze/thaw cycles was registered by measuring the temperature at different levels below the concrete surface of a prism (152 · 152 · 508 mm). With the criteria used in Malhotra & Bremner (1996), i.e. the number of times the temperature drops below –2.2 °C in the centre of the prism, the number of freeze/thaw cycles was around 100 per year. Since the temperature was measured inside the specimens at Treat Island, while the present investigation has measured the air temperature at the marine exposure site at Träslövsläge harbour, it is difficult to compare the different climates with respect to temperature cycles. The immersion of the specimens in sea water twice daily at Treat Island makes the temperature comparison even more difficult. It seems, however, as if the number of passages at temperatures just below 0 °C are more frequent in the specimens at Treat Island than at Träslövsläge. However, this can probably partly be explained by the immersions in sea water twice daily. As far as the number of passages below low temperatures, e.g. –10 °C, are concerned, there seems to be a closer correlation between the climates at the two exposure sites. With –10 °C as the criterion for the temperature in the middle of the specimens, less than ten passages seems to be normal at Treat Island, see Malhotra & Bremner (1996) while, as can be seen in Table 11.3, the number of times during which the air temperature at Träslövsläge harbour falls below –10 °C is of about the same order or somewhat higher.

Since the specimens at Treat Island are immersed in sea water twice daily, the degree of saturation is probably considerably higher than for the specimens exposed only to natural precipitation and occasional splashing during storms at Träslövsläge harbour. However,

because of the high degree of saturation, the specimens at Treat Island ought to be less carbonated than at Träslövsläge harbour.

The prisms at the Treat Island exposure site are inspected annually. Inspection includes visual examination and rating, and ultrasonic pulse velocity testing. The visual rating is between '0' and '10', with '0' meaning no damage and '10' totally disintegrated; see Table 11.8.

Table 11.8 *Rating system used during visual inspections at Treat Island exposure site. From Bremner et al. (2003).*

Rating	Comment
0	Less than 15 aggregate particles are exposed
1	More than 15 aggregate particles are exposed
2	More than 50 % of the aggregate particles immediately below the surface are exposed on the top surface
3	More than 80 % of the top surface aggregate particles are exposed
4	Top surface aggregate particles are exposed over 20 % of their perimeter
5	More than 90 % of the top surface aggregate particles are completely exposed to one half of their perimeter
6	Less than 95 % of the volume of the specimen remaining or loss of five or more surface aggregate particles in a local area
7	Less than 80 % of the volume of the specimen remaining or loss of concrete in a local area of depth equal to more than twice the nominal aggregate size
8	Less than 50 % of the volume of the specimen remaining
9	Less than 20 % of the volume of the specimen remaining
10	Specimens gone

The following are results from a couple of investigations carried out at Treat Island up until 2003.

Concrete with slag as part of the binder

The 'Phase 1' project investigated a number of air-entrained concrete qualities containing different amounts of slag as part of the binder. Concrete qualities with different w/b-ratios, 0.40 - 0.60, and with slag contents of up to 65 % of the binder weight, were investigated. The cement type used was an ASTM Type I cement from a plant in New Brunswick, and the slag was a pelletized blast-furnace slag from a plant in Hamilton, Ontario. A sulphonated hydrocarbon air-entraining agent was used, resulting in an air content of the fresh

concrete of between 5.5 and 7.0 %. For complete concrete compositions and measured properties of the fresh concrete, as well as the compressive strength after 28 days, see Malhotra & Bremner (1996).

Figure 11.26 shows the visual rating for the air-entrained concrete with w/b-ratios of 0.40, 0.50 and 0.60 and with different amounts of slag (0, 25, 45 and 65 % by weight of the binder content), up until 25 years' exposure. Three specimens were used for the concrete with only OPC as the binder, and two specimens for the concretes containing slag. All ratings are mean values.

Concrete with entrained air and a w/b-ratio of 0.40

From Figure 11.26a, it can be seen that for concrete with entrained air (~6 %) and with a w/b-ratio of 0.40, the incorporation of slag as part of the binder does not noticeably affect the amount of frost damage during the first 17 years' exposure. After 17 years' exposure at Treat Island, no concrete showed a poorer visual rating than 2. However, the visual inspections after 20 and 25 years showed a somewhat increased amount of damage for the concrete qualities with 45 and 65 % slag as part of the binder than for the concrete qualities with lower or no slag content. It thus seems that for concrete with a w/b-ratio of 0.40, the incorporation of slag as part of the binder does not have a significant influence on the scaling resistance at young ages. However, after 20 to 25 years' exposure at the marine climate at Treat Island exposure site, there seems to be a somewhat negative effect on the scaling resistance by the incorporation of slag, at least for slag contents of 45 % or above.

Concrete with entrained air and a w/b-ratio of 0.50

From Figure 11.26b, it can be seen that for concrete with entrained air (~6 %) and with a w/b-ratio of 0.50, the incorporation of slag as part of the binder does considerably affect the amount of frost damage. One difference between concrete with and without slag as part of the binder is the development of damage after only a couple of years' exposure. After ten years' exposure, concrete with OPC alone as the binder shows only damage with a rating less than 1, whereas concrete with 65 % slag shows a rating of 3. During the first 17 years, it is primarily the concrete quality with 65 % slag as part of the binder that shows more damage than does concrete with 45 % slag, or less. However, at the inspection after 20 and 25 years' exposure, concrete containing a lower amount of slag shows a considerably greater amount of damage than does concrete without slag as part of the binder. As can be seen from the visual inspection after 25 years' exposure, the concrete without slag is rated as better than 2, whereas the damage for concrete with 45 % and 65 % slag as part of the binder is rated as 6. For concrete with 25 % slag as part of the binder, the amount of damage was in between. The results after 25 years' exposure at the marine exposure site at Treat Island exposure site thus show that there are seemingly small differences in observed amount of damage at young ages for concrete with 45 % slag, or below. However, after 25 years' exposure, it is clear that incorporation of a smaller amount of slag, i.e. 45 % and, to some extent, also 25 % leads to lower frost resistance than that of concrete with only OPC as binder.

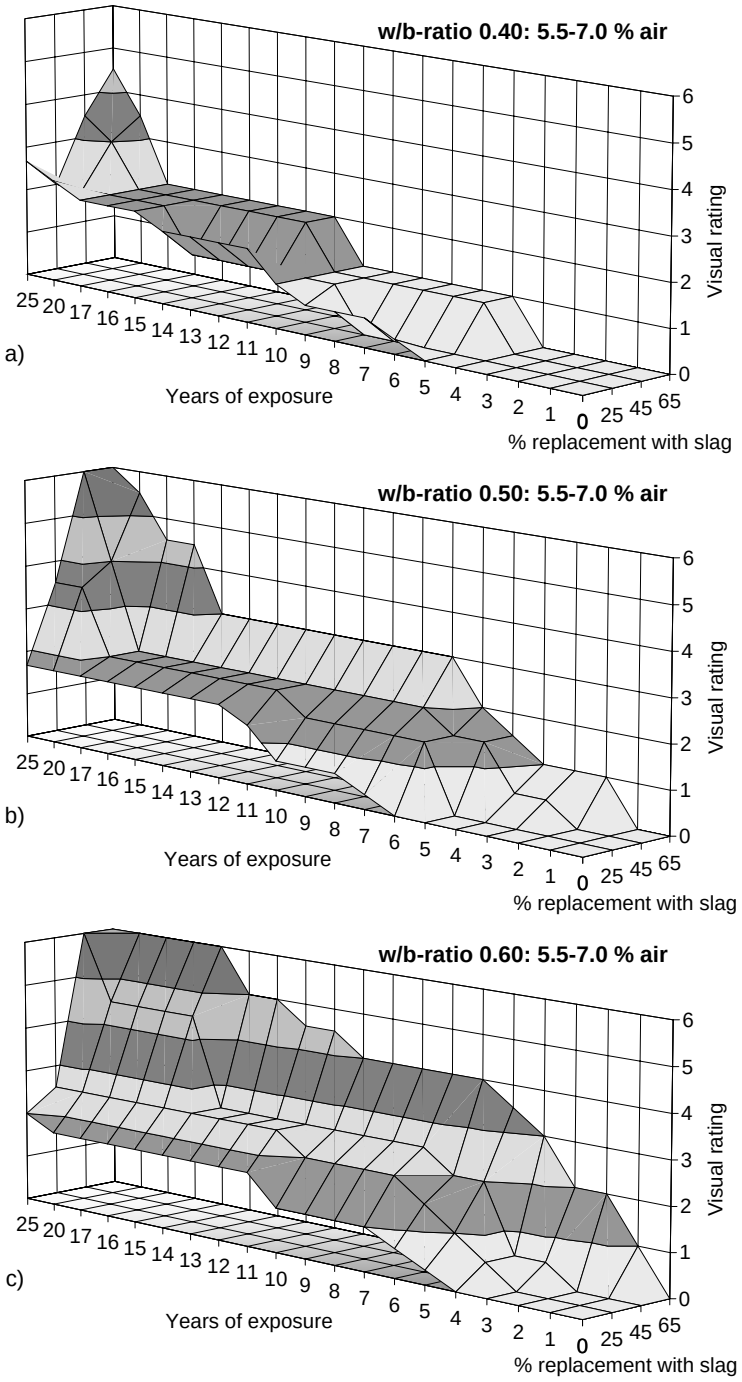

Figure 11.26 *Damage (visual rating 0-10) after up to 25 years' exposure at Treat Island exposure site. Air-entrained concrete containing different amounts of slag. Note the scale on axis 'Years' exposure'.*
a) w/b 0.40, b) w/b 0.50, c) w/b 0.60

Concrete with entrained air and a w/b-ratio of 0.60

From Figure 11.26c, it can be seen that for concrete with entrained air (~6 %) and with a w/b-ratio of 0.60, the incorporation of slag as part of the binder does considerably affect the amount of frost damage. Already during the first couple of years' exposure, concrete containing 65 % slag shows consiserable damage, whereas only slight damage can be observed for concrete with lower slag contents. After seven years' exposure, the concrete containing 65 % slag as part of the binder has reached a state where the amount of damage is rated as 4, i.e. where all the surface aggregates are exposed. After the same exposure time, concrete with 45 % slag shows a mean rating of 2.5, concrete with 25 % slag shows a rating of 2, and concrete with only OPC as binder shows a rating of 1. This pattern continues with increasing exposure time, i.e. the higher the slag content, the more extensive the surface damage. After 25 years' exposure, concretes with 45 % and 65 % slag as part of the binder show damage rated as 6, whereas concrete with only OPC as binder shows damage rated as 2. Concrete with 25 % slag as part of the binder shows only somewhat more damage than does concrete without slag, at least after 25 years' exposure.

The results after 25 years' exposure at the marine exposure site at Treat Island thus show that the tendency found at later ages for concrete with w/b-ratio 0.40 and 0.50 is valid also for concrete with a w/b-ratio of 0.60, i.e. the frost resistance decreases with increasing slag content. However, for concrete with a w/b-ratio of 0.60, there is already a marked difference in scaling resistance at young ages, depending on the amount of slag as part of the binder. This was not apparent for concrete with lower w/b-ratios until at later ages, i.e. after around 20 years' exposure. One explanation for this is the effect of carbonation.

Comparison with the present investigation

When comparing the results from the investigation at Treat Island with the results from the present investigation, it is primarily the results for the concrete qualities with entrained air at the marine exposure site that are of interest, Figure 11.13b. However, since the climate at Treat Island has been shown to be probably somewhat more aggressive than the marine climate in the present investigation, the results for the air-entrained concrete qualities at the highway exposure site should also be considered, Figure 11.13a. Even though in the present investigation the specimens have been exposed for only five years at the marine exposure site (seven years at the highway exposure site), the same tendencies can be seen, that is:

- **The effect of w/b-ratio on the scaling resistance.** For concrete containing large contents of slag as part of the binder, an increasing w/b-ratio leads to a reduction of salt/frost resistance. However, for concrete with only OPC as binder, the effect of w/b-ratio is less evident. At Treat Island, the specimens produced from concrete with only OPC as binder show about the same damage development within the w/b-ratio range 0.40 - 0.60. At the marine exposure site in the present investigation specimens produced of OPC concretes with entrained air and with a w/b-ratio range of 0.30 - 0.75 also show about the same amount of damage. At the highway exposure site, all concrete qualities with a w/b-ratio of 0.75 showed considerable damage. However, even at the highway exposure site, OPC concrete with w/b-

ratios in the 0.30 - 0.50 range showed no difference in damage depending on w/b-ratio, at least not after seven years' exposure.

- **The effect of slag content on the scaling resistance.** For concrete with high w/b-ratios (0.60 at Treat Island and 0.75 in the present investigation), there is a marked reduction in scaling resistance with increasing slag content. This is true also for concrete with lower slag contents, i.e. concrete with 45 % slag and, to some extent, also 25 % slag. For concrete with lower w/b-ratios (0.40 and 0.50), there are, during early years, at both marine exposure sites only small differences in scaling resistance between concrete qualities with up to about 45 % slag as part of the binder. However, for concrete that has been exposed for over 20 years at Treat Island exposure site, it is evident that the scaling resistance of concrete with lower w/b-ratios also decreases with increasing slag content, even at relatively low amounts of slag as part of the binder. This seems to be a slow ageing effect taking place first after some 20 years, and can therefore naturally not be seen at the marine exposure site in this investigation after only five years' exposure. However, at the highway exposure site in the present investigation, concrete with a w/b-ratio of 0.40 and CEM III/B (70 % slag) as binder also shows more damage than does concrete with only OPC as binder.

In both investigations, it is shown that concrete qualities with high slag contents (65 % and over) have a much lower frost resistance in marine environments (with salt exposure) than concrete without, or with only some, slag as part of the binder. These results show that the use of binder-combinations/types with high slag contents should be used with caution, if at all, in these types of climates. At later ages (after about 20 years), the investigation at Treat Island has shown that concrete with lower slag contents also shows less scaling resistance than does concrete without slag as part of the binder. This also shows that concrete with relatively small slag contents as part of the binder should also be used with caution, at least in the types of climates considered in these investigations.

The results from the Treat Island exposure site show that no definitive conclusions should be drawn after only a couple of years' exposure. The development of damage between 20 and 25 years is a proof of this. This should be borne in mind when evaluating the results from the present investigation. Several more years' exposure are needed before more definite conclusions can be drawn.

Concrete with silica as part of the binder

The 'Phase 5B' project investigated a number of concrete qualities containing different amounts of silica. Concrete qualities with a w/b-ratio of 0.60, with and without entrained air and with silica contents of up to 20 % of the binder weight, were investigated. The cement type used was an ASTM Type I cement from a plant in New Brunswick and the silica was of uncompacted form obtained from a silicon and ferrosilicon plant in Becancour, Quebec. A sulphonated hydrocarbon air-entraining agent was used for the air-entrained concrete qualities. The air content of the fresh concrete with entrained air was around 6 %, and that of the non air-entrained concrete was around 1 %. For complete

concrete compositions and measured properties of the fresh concrete, as well as the compressive strength after 28 and 90 days, see Malhotra & Bremner (1996).

Concrete with entrained air and a w/b-ratio of 0.60

Figure 11.27a shows the visual rating for air-entrained concrete and for concrete with natural air with a w/b-ratio of 0.60 and with different amounts of silica (0, 10, 15 and 20 % of the binder weight) up to 20 and 13 years' exposure respectively. One specimen was used for each concrete quality.

From the figure it can be seen that for air-entrained concrete with a w/b-ratio of 0.60 and with only OPC or OPC + 10 % silica as binder, the amount of damage during the first ten years is about the same. For concrete with higher contents of silica, however, there is already at young ages a markedly reduced scaling resistance with increasing silica content. At later ages, there is also a somewhat reduced scaling resistance for concrete with only 10 % silica as part of the binder in comparison with concrete with only OPC as binder.

Concrete with natural air and a w/b-ratio of 0.60

From Figure 11.27b, it can be seen that all concrete qualities without entrained air show considerable damage within a relatively short time of exposure, irrespective of silica content as part of the binder. However, there is a tendency for the damage to be visible at an earlier stage with increasing silica content as part of the binder. Even after two years' exposure, the specimens with 20 % silica as part of the binder show damage rated as 4. For concrete without silica as part of the binder, it takes seven years to reach a damage level exceeding a visual rating of 1. It can be seen that irrespective of silica content, the development of damage seems to be rather 'explosive' for concrete without entrained air; see, for example, the increase in damage between year 1 and 2 for concrete with 20 % silica as part of the binder (visual rating $0 \rightarrow 4$), and for concrete with only OPC as binder the increase in damage between year six and seven (visual rating $1 \rightarrow 7$). This rapid development of damage from a seemingly sound concrete surface to a totally deteriorated surface within only one winter season shows that concrete qualities without entrained air have to be used with great caution, if at all.

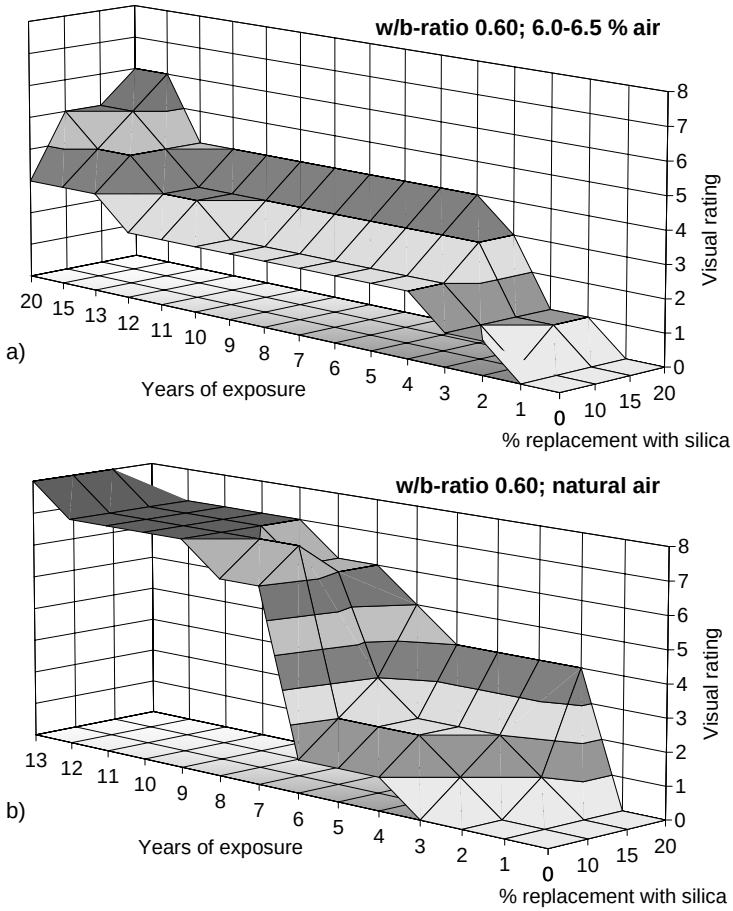

Figure 11.27 *Damage (visual rating 0-10) after up to 20 years' exposure at Treat Island exposure site. Concrete with a w/b-ratio of 0.60, containing different amounts of silica. a) air entrained, b) natural air*

Comparison with the present field investigation

The results from the investigation carried out at Treat Island are not directly comparable with the results found in the present investigation, because in the present investigation only 5 % silica was used, as against between 10 and 20 % in the Treat Island investigation. However, from the two investigations it can be concluded that:

- Concrete with low amounts of silica (up to about 10 %) results in about the same scaling resistance, at least during early years. However, at later ages, the investigation at the Treat Island exposure site has shown that the scaling resistance of concrete with entrained air and 10 % silica as part of the binder is somewhat reduced in comparison with that of concrete with only OPC as binder. For concrete with higher silica contents, the negative effect on the scaling resistance of incorporating silica as part of the binder is more evident, at least for the concrete qualities used in that investigation.

- For the concrete qualities without entrained air and with a w/b-ratio of 0.60 exposed for 13 years at Treat Island exposure site, all qualities showed considerable surface damage after 13 years, irrespective of the silica content. In the present investigation, the specimens with OPC or with OPC + 5 % silica as binder, and with no entrained air, exposed at the marine exposure site, show no noticeable signs of damage after five years' exposure, even for concrete qualities with a w/b-ratio of 0.75. These qualities, however, show signs of internal damage. Whether the specimens at Treat Island also exhibit internal damage is not known, because the ultrasonic pulse velocity measurements carried out on the specimens at Treat Island not have been accessible. For the same concrete qualities exposed at the highway exposure site, the specimens show substantial surface damage.
- A sudden, almost 'explosive', development of damage has been noted for concrete without entrained air, exposed in the climate at Treat Island. This indicates that concrete without entrained air and with seemingly limited damage may suddenly, within one winter season, show considerable damage, possibly caused by internal damage. This shows the importance of not drawing any firm conclusions about the salt-frost resistance of concrete qualities without entrained air after only a few winter seasons, even if they show seemingly little damage. As an example, see the concrete qualities in the present investigation without entrained air in Figure 11.25. After seven years' exposure, some of these qualities showed only limited surface damage but were rejected as concrete with 'poor scaling resistance' in the laboratory test. The sudden development of damage that occurred at Treat Island shows that only one winter season with an aggressive climate may lead to extensive damage for these concrete qualities too. In the present investigation, this rapid damage development for the concrete qualities without entrained air would move the qualities with limited scaling in Quadrant I (Figure 11.25) to the right into Quadrant II, where the scaling resistance is deemed as 'poor' both in the laboratory test and in reality.

11.4.7 Comparison between field investigations and laboratory tests

In many respects, the results from the laboratory investigation described in Chapter 3 into the effect of carbonation on the scaling resistance of concrete accords with the experience from the field investigations. Below some examples are given:

Concrete with OPC

In the laboratory, it was shown that for carbonated concrete with only OPC as binder, as opposed to uncarbonated concrete, there is a relatively small difference in the amount of damage depending on the w/b-ratio (0.35-0.55). Carbonation thus seems to result in a change of the material properties leading to a sufficiently high scaling resistance to withstand the actual climatic conditions irrespective of the w/b-ratio. In the field investigations, both those described here and those in the investigations at the Treat Island exposure site, these results are confirmed.

Concrete with slag

In the laboratory, it was shown that for carbonated concrete (w/b-ratio 0.45), incorporation of slag as part of the binder results in an increasing amount of damage with increasing slag content (20 - 65 % slag by weight of the binder). At low slag contents, up to some 35 %, the increase in damage is relatively small, but for concrete with 65 % slag the amount of damage was substantially increased in comparison with concrete with no, or only some, slag as part of the binder. These laboratory results were confirmed by experience from both the present field investigation and the investigation carried out at Treat Island.

Concrete with silica

The present field investigations have shown a tendency for concrete containing silica and without entrained air to be more susceptible to internal frost damage than concrete with only OPC as binder. This was not investigated in the laboratory investigations described in this thesis, and can therefore not be confirmed. However, there are other laboratory investigations reporting internal damage for concrete without entrained air and with silica as part of the binder. For example, in Feldrappe (2002), non air-entrained concrete with (8 %) and without silica, and with different w/b-ratios ranging from 0.25 to 0.45, was freeze/thaw tested using the German CDF/CIF test. From the measurements a marked decrease in dynamic E-modulus can be seen for concrete specimens containing silica with a w/b-ratio down to 0.35, indicating serious internal damage. For concrete without silica, only the quality with a w/b-ratio of 0.45 shows a slight decrease in dynamic E-modulus, indicating possible damage. This laboratory investigation confirms the findings from the field investigations presented above, i.e. concrete with silica as part of the binder and with no entrained air seems to be more susceptible to interior damage than do concrete with only OPC as binder. The reason for this does not need to be because of the silica, but may well be because of a compatibility problem with the plasticiser used. This could possibly destroy the natural air void structure leading to an increased susceptibility to internal damage.

It must be pointed out that the literature describes a large number of investigations reporting both positive and negative effects of silica as part of the binder with respect to the scaling resistance of concrete. This can, for example, be seen in the overviews in Marchand et al. (1994) and Pigeon & Pleau (1995). One reason for the discrepancy in results may be because of difficulties in obtaining good enough air void systems with respect to salt-frost scaling when silica is used, especially for concretes with low w/b-ratios. This because when silica is used, higher amounts of (and sometimes other types of) plasticisers or superplasticisers are used, compared to when producing concrete with only OPC as binder. An increase in the use of plasticiser may lead to an increased risk of obtaining an inferior air void system in respect of salt-frost resistance. However, with a well proportioned, air-entrained concrete containing sound materials, and where the compatibility between the cement type, secondary cementitious materials (e.g. silica), the air entraining agent and the plasticiser/superplasticiser is documented and tested, the incorporation of silica as part of the binder ought not to lead to a decrease in scaling resistance in comparison with that of concrete with only OPC as binder.

11.5 Conclusions

On the basis of five years' exposure of specimens at the field exposure sites in a marine, and a salt-free environment, and the seven years exposure of specimens in a highway environment the following conclusions can be drawn:

- There are substantial differences in external frost damage (scaling), depending on the exposure climate. The most extensive external frost damage is observed on concrete specimens exposed in the highway environment. Concrete exposed in the salt-free environment at SP's premises shows no noticeable external damage after five winter seasons.
- For all concrete qualities used in this investigation, scaling takes place only when exposed to an environment with salt. Internal damage, however, is observed on concrete qualities exposed at all three test sites, even when no salt is present.
- Concrete with OPC or OPC + 5 % silica as binder, with entrained air and a water/binder ratio of 0.50 or below, has good resistance to internal and external damage, at least after seven years' exposure. For concrete with 30 % slag as part of the binder, there are indications of damage for concrete with a w/b ratio of 0.50. But for qualities with a w/b ratio of 0.40 or below, there are no signs of either external or internal damage. Concrete with CEM III/B, however, shows substantial scaling, even with w/b-ratio as low as 0.40 and with entrained air.
- Internal damage is observed only for concrete qualities without entrained air and, in most cases, for concrete qualities with high water/binder ratios. However, for concrete qualities with OPC + 5 % silica as binder, internal damage is found at lower w/b-ratios, down to w/b-ratio 0.40.
- Comparing results from laboratory testing in accordance with SS 13 72 44 (the 'slab test'), with results after seven years' exposure at the highway exposure site, shows that the laboratory standard classifies most concrete qualities correctly. For some concrete qualities without entrained air, the laboratory test method results in a rejection, while in reality only limited damage can be seen. This improvement in scaling resistance with age has been reported in earlier field investigations and can be explained by a positive effect of ageing, i.e. carbonation.
- The temperature records at the highway and marine exposure sites show that cooling and heating rates of the same order as is used during freezing and thawing in the laboratory freeze/thaw test, SS 13 72 44, are not unusual in the field. Temperature cycles occurring in the field can even be in almost exact agreement with the part of the temperature cycle below 0 °C prescribed in the laboratory test. This shows that the prescribed temperature cycle in the freeze/thaw standard is not unnatural or too severe, at least not in comparison with the outdoor climate in south western Sweden.
- Experience of five years' exposure of different concrete qualities in the present field investigation correlates well with experience from the field investigations carried out by CANMET at the Treat Island marine exposure site on the North American east coast.

12 Concluding discussion and suggestions for future research

12.1 Introduction

The research described in this thesis consists of a number of investigations. For each investigation, the results are discussed and concluding remarks are given. The main conclusions from these investigations are summarised in this chapter, followed by a brief discussion of some selected results, divided into four parts:

- Proposed explanation for the effects of ageing on the salt-frost resistance of concrete.
- Comparison of the results from this investigation with the results presented in the literature.
- Comparison of the laboratory results with results from field exposure.
- Consequences of the effect of carbonation on the material properties of concrete

The results from this research have hopefully brought knowledge somewhat forward. There are, however, still a number of unsolved questions that need to be answered. Some of these are identified and presented at the end of this chapter.

12.2 Main conclusions

The following main conclusions can be drawn from the investigations presented in this thesis: They are valid for the materials and conditioning climates used; other materials and/or conditioning climates might lead to other results.

- Ageing effects such as hydration, drying and carbonation have a marked influence on the salt-frost resistance of concrete.
- Carbonation is the most dominant ageing effect with regard to salt-frost resistance. The influence of hydration and drying is in most cases small compared to the effect of carbonation.
- Carbonation has a positive influence on the salt-frost resistance for concrete with OPC alone as the binder and for concrete with OPC and silica (up to at least 10 %) or slag (up to some 30 %) as part of the binder.
- Carbonation has a negative influence on the salt-frost resistance for concrete with high contents of slag as part of the binder (over some 50 %)
- According to results from this investigation, the influence of carbonation on the salt-frost resistance can be explained by the physical changes of the pore structure taking place as a result of carbonation. Carbonation leads to a marked change in evaporable and freezable water content, as well as to changes in the behaviour during capillary suction and to a change in the critical degree of saturation.

12.3 Proposed explanation for the observed effects of ageing on the salt-frost resistance of concrete

The work described in Chapters 2 and 3 verifies the effect of ageing on the salt-frost resistance, and the main ageing processes of hydration, drying and carbonation were individually investigated. In these investigations, it was shown that at early ages (up to about 30 days) the effect of hydration and drying had a significant effect on the salt-frost resistance. However, the most dominant ageing effect on the salt-frost resistance was found to be the effect of carbonation. This was true at all ages. Although the effect of carbonation was different for materials with different binder types/combinations, it was found to be so strong that the other ageing effects were more or less insignificant in comparison, at least for older concrete (over 30 days of age).

The results from Chapter 3 show that for concrete with OPC alone, or OPC with small amounts of silica or slag, carbonation markedly increased the salt-frost resistance, although relatively more so for material with OPC alone as the binder. The effect of carbonation was the opposite for concrete with high contents of slag as part of the binder (65 %), i.e. carbonation led to a reduction of the salt-frost resistance. Figure 12.1 shows the amount of scaled off material after 14 freeze/thaw cycles for micro-concrete with different amounts of slag as part of the binder, all with a w/b-ratio of 0.45, conditioned in three different climates. The conditioning climates were: water-cured (never dried) until the start of testing, or dried in 65 % RH / +20 °C for seven days with (1 vol-%) and without carbon dioxide respectively. The age at test start was 31 days.

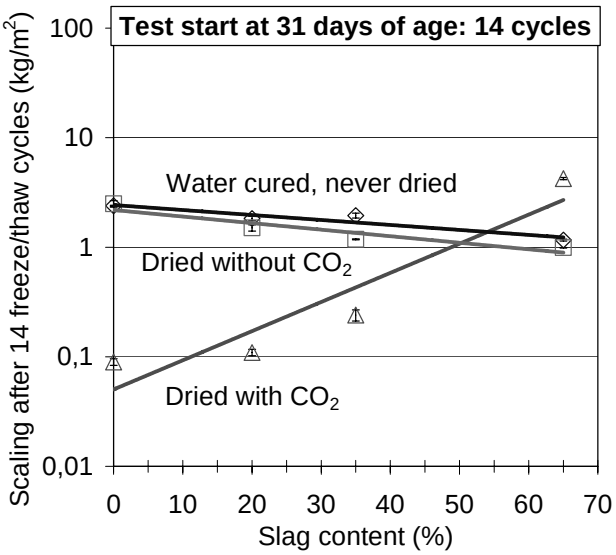

Figure 12.1 *Scaling after 14 freeze/thaw cycles as a function of slag content for specimens with a w/b-ratio of 0.45, conditioned in three different climates.*

The strong effect of carbonation on the amount of scaling, and the way that this differs depending on the slag content, can be seen in the figure. For concrete without slag, carbonated material (dried with CO_2) shows around 30 times *less* scaling than uncarbonated (dried without CO_2) material, whereas for concrete with 65 % slag as part of the binder carbonated material shows over five times *higher* scaling than does uncarbonated material. The marked effect of carbonation on the scaling resistance is thus completely different for materials with different slag contents. The figure also shows the relatively slight effect of drying compared to the effect of carbonation. The scaling for the water-cured specimens and the specimens dried in air without carbon dioxide is about the same, but the scaling for the specimens dried in air with carbon dioxide is markedly different. This shows that the effect of drying on the scaling resistance is more or less insignificant compared to the effect of carbonation.

In order to investigate and, if possible, explain the strong effect of carbonation on the salt-frost resistance, additional investigations were carried out. The physical changes of the pore structure for materials with different binder types/combinations caused as a result of carbonation were investigated by means of capillary suction and determination of the freezable water content. The effect of carbonation on the frost and salt-frost resistance was evaluated by estimating the time until a critical degree of saturation during capillary suction was reached, and also by a limited salt-frost test.

The results show that carbonation markedly changes the physical properties of the pore structure of all the investigated materials. Even though carbonation leads to a reduction of total porosity for all materials, the effect on the pore structure is markedly different, depending on the binder type of the material. Carbonation of mortar with OPC alone leads to a relatively finer pore system than for the uncarbonated material. For material with some silica as part of the binder, the reduction in porosity does not lead to any relative changes between the coarse and fine parts of the pore system. For mortar with high contents of slag as part of the binder, the pore structural changes leads to a marked coarsening of the pore system. The effect of carbonation on the pore structure is thus totally different for materials with different binder types/combinations.

The observed changes in pore structure markedly alter the amount of freezable and non-freezable water contents. For mortar with OPC alone or OPC and some silica as part of the binder, carbonation leads to a strong reduction of freezable water content, relatively more so for concrete with only OPC as the binder. The opposite applies for concrete with high contents of slag as part of the binder, i.e. carbonation leads to a marked increase in freezable water content.

Figure 12.2 shows an example of the freezable water content for carbonated and uncarbonated mortar with and without slag as part of the binder. The freezable water content was measured on capillary-saturated specimens during freezing, using low-temperature calorimetry.

From the figure, it can be seen that for mortar with only OPC as the binder, carbonation leads to a substantial reduction in freezable water content over the entire temperature range 0 to –55 °C. This reduction in freezable water content as a result of carbonation presumably leads to a higher frost and salt-frost resistance for this material having only OPC as the binder.

The effect of carbonation is the opposite for mortar with high contents of slag as part of the binder, i.e. carbonation leads to a marked increase in freezable water content, at least in the temperature range down to about –40 °C. The effect of carbonation thus leads to a markedly higher freezable water content and presumably therefore also to a lower frost and salt-frost resistance.

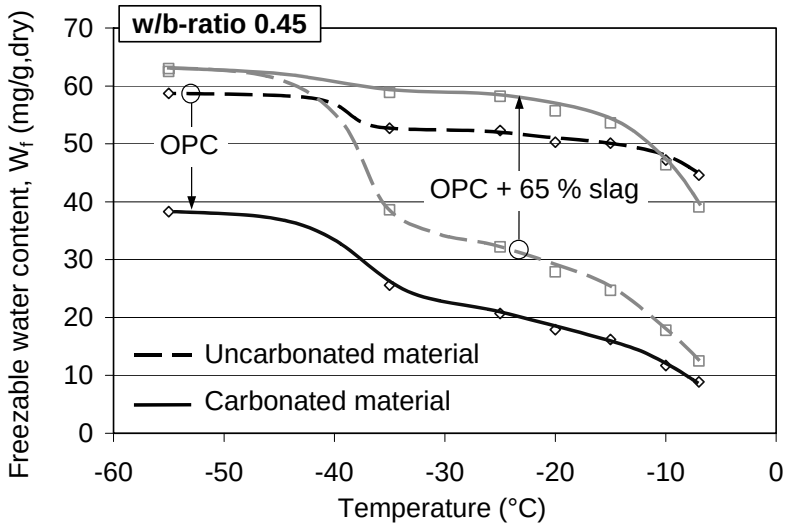

Figure 12.2 *Freezable water content during freezing for uncarbonated (dashed lines) and carbonated (full lines) material of mortar with OPC alone and with OPC + 65 % slag as part of the binder, both with a w/b-ratio of 0.45.*

The effect on the frost resistance of the change in freezable water content as a result of carbonation was confirmed by the evaluation of the critical degree of saturation and the long-time water absorption, at least for the material with OPC alone as the binder. For this material, uncarbonated mortar reached a critical degree of saturation within less than 24 hours of capillary suction, whereas for carbonated material a much longer time of capillary suction was needed before a critical degree of saturation was reached.

For materials with high slag contents, the effect of carbonation on the frost resistance evaluated by the S_{cr}-method was less apparent. The results indicated, however, that carbonated mortar reached the critical degree of saturation more rapidly than did the uncarbonated mortar.

When freeze/thaw tested in contact with a saline freezing medium, the effect of carbonation on the salt-frost resistance for mortar with slag as part of the binder is more apparent. The carbonated material was totally destroyed after only one freeze/thaw cycle, whereas the uncarbonated material showed to be significantly more resistant towards salt-frost damage.

For mortar with OPC alone as the binder, the carbonated material showed better salt-frost resistance than did the uncarbonated. Both materials were, however, relatively rapidly destroyed, which can be explained by the low natural air void content for this material, and the severity of the applied freeze/thaw method.

These results, i.e. that the carbonated mortar with high slag contents has very poor salt-frost resistance but seemingly higher frost resistance, correspond with the results presented in Stark & Ludwig (1997:1) for concrete containing high amounts of blast furnace slag. Stark & Ludwig explain this primarily by a chemical effect caused as a result of the formation of the 'metastable' carbonate phases vaterite and aragonite in the carbonated layer of slag concrete. However, this 'chemical' explanation for the negative effect of carbonation on the salt-frost resistance is not applicable to the materials and conditioning climates used in the present investigations. As was shown in Chapter 10, no significant amounts of the metastable carbonate phases could be found in carbonated paste with 65 % slag as part of the binder conditioned in an environment with elevated carbon dioxide content (1 vol-%). On the other hand, for carbonated material with OPC alone as the binder, small amounts of vaterite and aragonite could be detected. The chemical effect of carbonation on the salt-frost resistance proposed by Stark & Ludwig ought therefore, for the materials used in this investigation, be more dominant for the materials with OPC alone as the binder than for the material with high contents of slag. No such indications could be found in this investigation.

Since there is no support for a chemical explanation for the effect of carbonation on the salt-frost resistance, as proposed by Stark & Ludwig for the materials used in this investigation, *the effect of carbonation is explained here by the strong physical effect carbonation has on the pore struc*ture. Not only by the change in fine and coarse pores leading to a change in non-freezable and freezable water content, but also the effect on the structure of the pore system with regard to the existence of restrictions in the pore structure.

Even though the results from this investigation not could support or confirm the findings by Stark & Ludwig, a chemical influence on the salt-frost resistance cannot be excluded. The difference between the results from this study and the results presented by Stark & Ludwig shows that the processes of carbonation are complex and need a more comprehensive study to be fully understood.

12.4 Comparison of the results from this investigation with the results described in the literature

This investigation has looked at the effects of carbonation alone on the salt-frost resistance and on the properties of the pore structure. This was achieved by using materials conditioned in identical climates but with and without carbon dioxide, leading to carbonated and uncarbonated material exposed to the same drying conditions. By testing these materials at the same age, the effect of carbonation could be separated from other ageing effects.

In the literature review in Chapter 4, it was found that most research carried out in this area had investigated the combined influence of different ageing mechanisms, and not the influence of the individual effects. Other investigations that have studied the effect of carbonation on its own have used accelerated carbonation, achieved by means of higher concentrations of carbon dioxide than were used in this investigation. Carbonation using excessive carbon dioxide contents may lead to unnatural changes of the material properties. Elevated carbon dioxide content of up to 1 vol-% has been shown, in this investigation and in others, not to result in any adverse effects. Some investigations have studied carbonated material from the surface layer and uncarbonated material from the core, implying that the carbonated and uncarbonated materials had different material properties right from the start. In these investigations, the materials have also been dried in different ways. These differences between different investigations make it somewhat difficult to compare the results. Yet another uncertainty when comparing results is that different investigations use different test methods, both for evaluating the salt-frost resistance and for determining the material properties. In many investigations found in the literature, Mercury Intrusion Porosimetry was used, while here Low-Temperature Calorimetry was used.

Because of the discrepancies between this investigation and the investigations found in the literature, it may be difficult to compare the results. However, even though direct comparisons may be difficult, the tendencies found in this investigation may be compared with those found in the literature. Some results from the literature are compared below with the results from this investigation. For further discussion of the results found in the literature, see Chapter 4.

Effect of carbonation on the pore structure

Most investigations on the pore structural changes report a reduction in total porosity as a result of carbonation, both for materials with OPC alone and OPC with additions of slag as part of the binder; see e.g. Hilsdorf et al. (1984). This corresponds well with the findings from this investigation, where it was shown that the total porosity for all investigated materials was reduced as a result of carbonation.

The comprehensive investigations on the effect of carbonation carried out by researchers at the University of Karlsruhe, Germany, have further shown that carbonation of materials with high contents of slag as part of the binder leads to a coarsening of the pore structure, see e.g. Bier (1987). This has been confirmed by many others, e.g. Matala (1995), and was

also confirmed by this investigation. However, the results diverge for material with OPC alone as the binder. Most investigations report, in accordance with what was found here, that carbonation of material with OPC alone as the binder leads to a reduction of coarse porosity. However, in the investigation carried out by Matala, an increase in coarse porosity was reported, even for material with OPC alone as the binder. This discrepant result may be explained by the fact that the definition of coarse porosity can differ between different investigations, or that the evaluation of the pore structure was made using different test methods. The most probable explanation for the diverging results is, however, that the effect of carbonation was not separated in Matala's investigations. In fact, the materials investigated had different ages, different drying histories and different degrees of carbonation. The effect of 'carbonation' alone on the pore structure cannot therefore be evaluated from his investigations.

The findings that carbonation leads to a coarsening of the pore structure for material with slag as part of the binder, and a reduction of coarse pores for material with OPC alone as the binder, is further confirmed by field investigations presented in Litvan (1987).

Investigations into the effect of carbonation on materials with silica as part of the binder are rare. Matala (1988) and Matala (1998) report that carbonation of mortar with only OPC and with OPC and 5-20 % silica by weight leads to a coarsening of the pore structure, and particularly so for material with silica as part of the binder. This is contradictory to the results found in the present investigation, where it has been shown that carbonation of mortar with OPC alone as the binder leads to a strong reduction of coarse porosity, and that carbonation of mortar with OPC and some silica as part of the binder does not lead to any relative change between the fine and coarse porosity, but that carbonation leads to a considerable reduction of both. This discrepancy can be explained by, as was mentioned above, the fact that the materials tested in Matala's investigations differed in age, drying history and degree of carbonation. The results presented by Matala thus do not show the effect of carbonation on the pore structure, but the effect of the particular conditioning regimes used.

Effect of carbonation on the salt-frost resistance

The effect of carbonation on the salt-frost resistance was very clear in the present investigation. For material with OPC or with OPC and small amounts of silica or slag as part of the binder, carbonation resulted in a marked increase in salt-frost resistance. For materials with high contents of slag as part of the binder, the opposite applies, i.e. carbonation resulted in a marked decrease in salt-frost resistance. The results found here for material with high contents of slag as part of the binder correspond well with most of the results found in the literature, see e.g. Gunter et al. (1987) and Stark & Ludwig (1997:1).

For material with OPC alone as the binder, most investigations found in the literature report a positive effect of carbonation on the scaling resistance. However, diverging results exist. Matala (1995) reported, from a comprehensive study of the effect of carbonation on the salt-frost resistance, that carbonation of concrete with OPC resulted in

a decrease in the scaling resistance. However, as was mentioned above, it was not the effect of only carbonation but the effect of totally different conditioning regimes (age, drying history and degree of carbonation) that was investigated in Matala (1995). With this in mind, the results from that investigation can be disregarded as not being the effect of carbonation but more the effect of different drying histories.

Virtanen (1989) reports results from testing the salt-frost resistance of concrete with and without slag, aged in the field. According to the results, ageing leads to a relatively better salt-frost resistance for concrete with slag as part of the binder than without. These results are the opposite to what was found in this investigation and what has been reported in many of the investigations found in the literature. This can, however, be explained by the fact that it was the salt-frost resistance of primarily aged but uncarbonated surfaces that were tested; see the discussion in Chapter 4. The conclusion should thus be that for uncarbonated concrete the salt-frost resistance is better if slag is part of the binder than if only OPC is used. This result is confirmed by this investigation.

For material with OPC or with OPC and small amounts of silica as part of the binder, Matala (1998) reports that carbonation leads to a reduced scaling resistance. This is quite the opposite to what was found in this investigation. The discrepancy can, as mentioned above, be explained by the conditioning regimes used by Matala.

Jacobsen et al. (1997) investigated the effect of different drying regimes on the salt-frost resistance. As was shown in Chapter 4, the amount of scaling was markedly influenced by the conditioning climate, with the lowest scaling for concrete conditioned in 'mild' climates and much higher scaling for never-dried concrete and concrete dried at low relative humidities or high temperatures. Jacobsen et al. explain the influence of the drying regime on the amount of scaling by a change in the 'protective effect of the air-voids'.

From results found in the present investigation, the effect of drying may be explained by the effect of carbonation and not by a change in the 'protective effect of air-voids', at least for the 'virgin' concretes and those conditioned in climates with 'mild' drying. The scaling of the never-dried 'virgin' specimens was high. This was also the case in the present investigation, where never-dried specimens and specimens dried without carbon dioxide (see Chapter 3) showed about the same amount of scaling. However, the scaling was markedly lower for the specimens dried in a climate with carbon dioxide. The positive effect of mild drying is thus primarily an effect of carbonation and not due to a change in the protective effect of the air-voids.

The conditioning climates for very high evaporation rates in Jacobsen et al. (1997), were very tough. The climate with an evaporation rate of 200 $g/m^2 \cdot h$ was obtained by ventilating air with a relative humidity of 10 %, while that for 500 $g/m^2 \cdot h$ evaporation was obtained by ventilating air in an oven at +40 °C. Carbonation is slow at these low relative humidities and high temperatures, and may not result in the protective properties as was found at room temperature at intermediate relative humidities. This implies that in these tough drying regimes, carbonation may not result in an increase in salt-frost resistance.

Besides the absence of the positive effect of carbonation, the tough drying may also change the properties of the pore structure, as has previously been described by Sellevold & Bager (1985), thus leading to the low salt-frost resistance reported for materials conditioned in these tough climates.

In the investigations presented here, the effect of carbonation has been investigated only by conditioning in a temperature of +20 °C and a relative humidity of 65 %. Conditioning at higher temperatures and lower relative humidities may result in a different effect of carbonation on the salt-frost resistance. However, this is an unknown area, and needs to be further investigated.

Rönning (2001) investigated the effect of different curing conditions and the effect of ageing on the salt-frost resistance of concrete with and without silica as part of the binder. Rönning states:

> '*No clear systematic effects of curing conditions and ageing were found. The reasons for the observed, very mixed behaviour between different curing regimes and ageing remain to large extent unexplained.*'

This can be explained by the test procedure used by Rönning, where it was actually the effect of the boundary conditions for the cylinders during curing that was investigated, whereas the test surfaces for all specimens, which were cut from the cylinders, were conditioned identically, i.e. seven days in laboratory air at 65 % RH / +20 °C, followed by three days' resaturation. For more details, see Chapter 4.

Rönning also states that the effect of ageing was clearly negative for non-air-entrained concretes, whereas concrete with entrained air showed little difference in scaling as a result of ageing. This can possibly be explained by the fact that the test surfaces had different degrees of carbonation depending on at what age the seven days-long conditioning in laboratory air at 65 % RH / +20 °C was carried out. Conditioning specimens for the same time in the same climate, but at considerably different ages, probably results in different degrees of carbonation and thereby different protective properties of the test surface with regard to salt-frost resistance. The results reported in Rönning thus probably can be explained by the effect of carbonation on the protective properties of the surface layer with regard to the salt-frost resistance reported in this thesis.

Most investigations found in the literature explain the effect of carbonation on the salt-frost resistance as due to the pore structural changes caused by carbonation. The results presented here do also point towards a physical explanation for the effect of carbonation. However, as was mentioned earlier in this chapter, there are also reported chemical explanations for the effect of carbonation on the salt-frost resistance; see, for example, Stark & Ludwig (1997:1). The results from the present investigation do not support or confirm the chemical explanation, at least not for the materials and conditioning climates used here. However, using other materials and other conditioning climates may give other results.

Conclusion

From the comparison between the results from this investigation with the results found in the literature, it can be concluded that most results correspond. For those results that do not correspond, this can be explained by differences in the procedure of investigating the effect of carbonation. Here, the effect of carbonation has been separated from other ageing effects, whereas in many other investigations it is the sum of different ageing effects on the salt-frost resistance and the pore structural changes that has been investigated. Diverging results between this investigation and those where the effect of ageing as such has been investigated can therefore be expected.

12.5 Comparison of the laboratory results with results from field exposure

Chapter 11 of this thesis describes the experience from investigating the frost and salt-frost resistance of a large number of different concrete qualities exposed for up to seven years at three field exposure sites. The same concrete qualities as were exposed at field the exposure sites were also freeze/thaw tested in the laboratory using Swedish Standard SS 13 72 44, the 'Slab test'. Results after seven years' exposure of specimens exposed at the saline highway environment beside Highway 40 close to Borås shows that the results from evaluating the salt-frost resistance using the laboratory method correspond well with the results from field testing.

For some concrete qualities with OPC alone as the binder, or with small amounts of slag as part of the binder, and without entrained air, the laboratory standard rejects them as having poor scaling resistance. However, in the field, these concrete qualities show only slight damage, at least after seven years' exposure at the highway test site. This indicates that ageing for these concrete qualities leads to improved scaling resistance. Petersson (1996) reported similar results for concrete with only OPC or with OPC and some silica as part of the binder. This improvement in scaling resistance as a result of ageing for concrete with OPC as the binder, or with small additions of silica or slag as part of the binder, can be explained by the positive effect of the long carbonation period for the field exposure specimens on the scaling resistance.

From the field investigation presented in this thesis, and even more so from the field investigations carried out in a marine climate in a Canadian CANMET project and reported in (for example) Bremner et al. (2003), it was shown that the scaling resistance markedly decreases with increasing slag content as part of the binder. This was confirmed in this investigation by the laboratory studies presented in Chapter 3. The explanation for the adverse effect of slag as part of the binder on the scaling resistance is primarily the effect that carbonation has on the pore structure and thus on the freezable water content of the carbonated layer.

12.6 Consequences of the effect of carbonation of concrete

The results from the investigations about the effect of carbonation on the salt-frost resistance of concrete presented here have shown that carbonation leads to considerable changes in the material properties of the carbonated layer. It has also been shown that these changes in material properties are markedly different, depending on material composition, i.e. primarily depending on the binder type/combination used.

Consequences on other durability aspects

The observed changes in material properties have been shown to have major consequences for the salt-frost resistance of the investigated materials. This may serve as an example of the effect that carbonation may also have on other degradation mechanisms. The effect of carbonation should thus be considered for all damage mechanisms where the properties of the concrete surface play a role, i.e. not only the mechanisms leading to salt-frost damage. In fact, most degradation mechanisms are influenced in one way or another by the properties of the surface layer; consider, for example, the penetration of chlorides and the resulting risk of reinforcement corrosion. The risk of chemical breakdown may also be influenced by carbonation, both because of the somewhat different chemical composition of the carbonated layer and also because of the pore structural changes probably leading to changes in both gaseous and liquid permeability. Because of the probably important effect of carbonation on other degradation mechanisms, this ought to be further examined. This, however, was not an aim of this investigation, and so no such attempts have been made here.

It must be noted that since carbonation has such a significant effect on the physical properties, e.g. the constitution of the pore structure, the carbonated layer and the uncarbonated core material may be regarded as two different materials with different material properties. This is important, and must be regarded in research on cement-bound materials. In many investigations, both in the laboratory and in the field, the effect of carbonation is probably not taken into account, with the result that much research has been, and still is, carried out on partly carbonated materials. The results from research on partly carbonated material are valid only for the actual material with the specific degree of carbonation investigated. If, however, research is carried out on both carbonated and uncarbonated materials, more general knowledge is obtained, making it possible to evaluate the studied parameters for materials with different degrees of carbonation. The effect of carbonation should thus always be taken into account when research on cement-bound materials is undertaken. When researching uncarbonated material, systematic steps must be taken to avoid carbonation. It must, however, be noted that the methods for avoiding carbonation must not lead to other effects resulting in unnatural alterations of the material properties. Steps to avoid carbonation should therefore be carefully examined before being used in practice in the laboratory.

Consequences on freeze/thaw test methods

The observed strong effects of carbonation on the material properties of concrete have consequences when testing the salt-frost resistance in the laboratory. When testing in the laboratory, the same conditioning climate and the same conditioning time are used regardless of the concrete quality tested. This is, for example, true for both the Swedish Standard SS 13 72 44 and the German CDF-test, although with different conditioning times between the methods. According to SS 13 72 44, specimens are conditioned for seven days, whereas according to the CDF test specimens are conditioned for 21 days before freeze/thaw testing starts. Both methods use a climate with 65 % RH and +20 °C and with a specified evaporation rate.

However, since carbonation has been shown to have a strong but varying influence on the salt-frost resistance, depending on the binder type/combination of the material, this ought to be reflected in the freeze/thaw standards. With the same conditioning climates for materials which are differently affected by carbonation, there is a risk of an incorrect judgement, i.e. that results from laboratory testing do not correctly reflect the durability of aged material in the field.

Consider the following example: The salt-frost resistance of two different concrete qualities is to be evaluated: one with OPC alone as the binder, and one with high contents of slag as part of the binder. If conditioned for a too short a time, the positive effect of carbonation on the OPC concrete, and the negative effect of carbonation on the slag concrete, may not be noticeable. However, conditioning for a longer period may lead to other results. The conditioning time and conditioning climate is therefore of great importance in order to judge the salt-frost resistance correctly. This example serves just to show that, depending on the test procedure (in this case the length of conditioning climate), different results may be obtained. This is valid not only for concrete with only OPC or OPC with high amounts of slag as part of the binder, but also for all binder types and secondary cementitious materials as well as other constituents influencing the effect of carbonation on the salt-frost resistance. For example, high amounts of filler in different forms, e.g. lime stone filler, are used today in what is known as self-compacting concrete, and often in combination with new types of superplasticisers. How this will affect the salt-frost resistance, and the influence that carbonation has on the salt-frost resistance, is not known. More knowledge is needed in this field.

From what has been said above, it can be seen that a certain degree of carbonation before freeze/thaw testing starts is recommended. This would better reflect the marked effect of carbonation and lead to a more correct judgement of the salt-frost resistance. However, evaluating the salt-frost resistance is time-consuming, and there is no wish to prolong the time even further from concrete production until the test results are available. Because of this, the test methods need to be modified in a way that takes the effect of carbonation more into account, but does not considerably prolong the test time. As a suggestion, conditioning in a climate with somewhat increased carbon dioxide content should be evaluated. This, however, needs to be further investigated before applied in a standardised method.

Practical consequences

The marked effect of carbonation on the salt-frost resistance found in the laboratory and in the field investigations also has consequences in practice. From the results found, it can be recommended that:

- For concrete with OPC alone as the binder, or with OPC and some silica as part of the binder, it should be ensured that surfaces possibly exposed to a salt and moist environment and under frost attack should be able to reach a sufficient degree of carbonation before being exposed to frost attack. That is, structures or parts of structures possibly about to be exposed to a saline environment should preferably not be cast during the winter. If this is unavoidable, the parts should be protected so that carbonation can proceed without exposure to salt or frost for at least a couple of weeks.
- Concrete with high contents of slag as part of the binder must not be used in environments where a structure could be exposed to a saline climate under frost attack.
- Since ageing improves the salt-frost resistance of concrete with OPC or with OPC and some silica as part of the binder, it is likely that if a structure is not damaged during the first winter seasons the risk of later salt-frost damage is low. However, there is always a risk of attack if the environment changes towards more aggressive conditions with regard to salt-frost attack.
- As a quality control, concrete intended for structures exposed to saline and cold environments should be pre-tested using a laboratory test. The salt-frost resistance of an actual structure should also be confirmed by testing the salt-frost resistance of drilled-out cores from different parts of the structure in the laboratory. Swedish Standard 13 72 44 has proven suitable for evaluating the salt-frost resistance of concrete structures.

12.7 Suggestions for future research

Some unsolved questions and areas that need to be further investigated have been identified from the research carried out. The following are some suggestions for future research in order to increase knowledge of the effect of carbonation on salt-frost resistance, as well as of other damage mechanisms.

- **Investigate the chemical effect of carbonation further.** The physical effect of carbonation on the material properties has been shown to be very strong, both in this investigation and in investigations by others. However, the possible chemical effects of carbonation on the salt-frost resistance are less well documented. The differences in identified carbonate phases as a result of carbonation found here and in the literature show that the processes of carbonation are complex, and would need a more comprehensive study to be fully understood. Research on the carbonation process for materials with different binder types/combinations exposed to different climates would lead to increased knowledge about the carbonation

process and thus the possibility of a chemical explanation, as the one found in the literature, for the effect of carbonation on the salt-frost resistance.

- **Investigate the effect of carbonation on new types of materials used in concrete.** As has been shown here and in other investigations, carbonation leads to different effects on the material properties depending on material composition, primarily the binder type/combination. Since the mechanisms behind the effect of carbonation on (for example) pore structure is not fully understood, it is difficult to predict the effect of carbonation on new materials, materials of which we do not have any experience. When new types of materials used in concrete production are developed, the change in material properties as a result of carbonation for materials with these constituents ought to be thoroughly investigated. This is primarily applicable to new types of cement and secondary cementitious materials, although also to other materials that could possibly influence the effect of carbonation on the material properties, such as different filler types and admixtures such as plasticisers/superplasticisers.
- **Investigate if the influence of carbonation is sufficiently taken into account in the laboratory tests.** The strong effect of carbonation on the salt-frost resistance of concrete, which differs depending on binder type/composition, should be reflected in the standardised laboratory tests. Today, specimens are conditioned in normal air for a relatively short time, which means that the effect of carbonation may not be taken fully into account. The degree of carbonation obtained in the climates used during conditioning in accordance with the standardised methods needs to be investigated. The conditioning climates (relative humidity, temperature and evaporation rate) may vary somewhat within specified limits. Within these limits, there is a need to investigate if the effect of carbonation significantly varies. An evaluation of the degree of carbonation needed in order accurately to judge the salt-frost resistance with respect to the effect of carbonation should be carried out. If a higher degree of carbonation than obtained during conditioning in accordance with present standards is required for a correct judgement of the effect of carbonation, the possibility of using a somewhat increased carbon dioxide content during conditioning should be considered.
- **Investigate the effect of carbonation on other degradation mechanisms.** This investigation has considered the effect of carbonation only on the frost and salt-frost resistance. It has, however, been shown that carbonation markedly alters the material properties of the carbonated concrete surface. This implies that carbonation also ought to have major effects on other degradations mechanisms for which the pore structural properties are of importance. One example is the possible effect of carbonation on transportation of chlorides and other deleterious substances into concrete. Another example is the effect of carbonation on the process of leaching.
- **Continue investigating concrete in the field.** In the laboratory, investigations can be made under controlled conditions where the influence of different effects may be studied separately. However, laboratory results need to be confirmed by results from field investigations, not least when ageing effects are concerned. The

Canadian CANMET investigation, and the research carried out at three field exposure sites reported here, are examples of such field investigations. These kinds of investigations are important, not least when it comes to ‘calibrating’ models of degradation mechanisms and models predicting the service life of structures exposed to certain environments. However, investigating concrete in the field is a time-consuming process, where some results are found early and others not until several years or even decades later. Field test sites and investigations carried out there should therefore be regarded as a long-term investment, an investment we cannot afford to be without.

References

Ahlgren, L. (1972)
'Moisture fixation in porous building materials', Division of building technology, Lund institute of technology, Report 36, Lund, Sweden, 1972. (in Swedish)

Atlassi, E. H. (1993)
'A quantitative thermogravimetric study on the nonevaporable water in mature silica fume concrete', Thesis, Chalmers University of Technology, Department of Building Materials, Publication P-93:6, Gothenburg, Sweden, 1993.

Arnfelt, H. (1943)
'Damage on concrete pavements by wintertime salt treatment', Meddelande 66, Statens Väg-institut, Stockholm, Sweden, 1943. (in Swedish)

Auberg, R. (1998)
'Zuverlässige Prüfung des Frost- und Frost-Tausalz-Widerstands von Beton mit dem CDF- und CIF-Test', Universität GH Essen, Institut für Bauphysik und Materialwissenschaft, Band 6, pp. 46-61, Essen, Germany, 1998. (in German)

Bager, D. H., Sellevold E. J. (1986:1)
'Ice formation in hardened cement paste, Part I - Room temperature cured pastes with variable moisture contents', Cement and Concrete Research, Vol.16, pp. 709-720, 1986.

Bager, D. H., Sellevold E. J. (1986:2)
'Ice formation in hardened cement paste, Part II - Drying and resaturation on room temperature cured pastes', Cement and Concrete Research, Vol.16, pp. 835-844, 1986.

Bellander, U. (1973)
'Accelerated testing of compressive strength of concrete- Determination of degree of hydration', Swedish Cement and Concrete Institute, Report no. Fo7312/P5, Stockholm, Sweden, 1973. (in Swedish)

Bier, T. A. (1987)
'Influence of type of cement and curing on carbonation progress and pore structure of hydrated cement pastes', Proceedings of the Materials Research Society symposium - Microstructural Development During Hydration of Cement, Vol. 85, pp. 123-134, Boston, USA, 1987.

Bier, T. A. (1988)
'Karbonatisierung und Realkalisierung von Zementstein und Beton', Institut für Massivbau und Baustofftechnologie, University of Karlruhe, Dissertation, Heft 4, Germany, 1988. (in German)

Bonzel, J., Siebel, E. (1977)
'Neure Untersuchungen über den Frost-Tausaltz-Widerstand von Beton', Beton, Vol. 27: No. 4 (pp. 153-158), No. 5 (pp. 205-211) and No. 6 (pp. 237-244), 1977. (In German)

Brandes, C. (2002)
'The ageing influence within a durability test of concrete (performance concept) related to freeze/thaw and deicing salt resistance', 4th International PhD Symposium in Civil Engineering, Technische Universität München, Vol. 1, pp. 44-50, Munich, Germany, 2002.

Bremner, T.W. et.al. (1989)
'Role of supplementary cementing materials in concrete for the marine environment', in 'Durability of concrete - Aspects of admixtures and industrial by-products', Proceedings from the 2nd International Seminar on - Some aspects of admixtures and industrial by-products, (Swedish Council for Building Research, Gothenburg), pp. 23-32, 1989.

Bremner, T.W. et.al. (2003)
'Concrete incorporating cementitious materials for marine environment', International Seminar on Sustainable development in cement and concrete industries, Technical University of Polytechnic of Milan, Department Giulio Natta, Milan, Italy, 2003.

Byfors, J. (1980)
'Plain concrete at early ages', Swedish Cement and Concrete Institute, Report no. Fo 3:80, pp. 41, Stockholm, Sweden, 1980.

Cole, W. F., Kroone, B. (1960)
'Carbon dioxide in hydrated Portland cement', Journal of the American Concrete Institute, Vol. 31, No. 6, pp. 1275-1295, 1960.

Diamond, S. (2000)
'Mercury porosimetry - An inappropriate method for the measurement of pore size distributions in cement-based materials', Cement and Concrete Research, Vol.30, pp. 1517-1525, 2000.

Dunster, A. M. (1989)
'An investigation of the carbonation of cement paste using trimethylsilylation', Advances in Cement Research, Vol. 2, No. 7, pp. 99-106, 1989.

Everett, D. H. (1961)
'The thermodynamics of frost damage to porous solids', Trans. Faraday Soc., 57, 1961

Fagerlund, G. (1971)
'Degré critique de saturation - Un outil pour l'estimation de la résistance au gel des matériaux de construction', Matériaux et Construction, Vol. 4, No 23. pp. 271-285

Fagerlund, G. (1973)
'Critical degree of saturation when testing porous and brittle building materials', Lund Institute of Technology, Department of Building Technology, Report 34, Lund, Sweden, 1973. (in Swedish)

Fagerlund, G. (1974)
'Non-freezable water contents of porous building materials', Division of Building Technology, The Lund Institute of Technology, Report 42, Lund, Sweden, 1974.

Fagerlund G. (1977)
'The critical degree of saturation method of assessing the freeze/thaw resistance of concrete', Materials and Structures, Vol. 10. No. 58, 1977.

Fagerlund, G. (1979)
'Prediction of the service life of concrete exposed to frost action', Studies on concrete technology, Dedicated to Professor Sven G. Bergström on his 60th Anniversary, December 14, Swedish Cement and Concrete Research Institute, Stockholm, Sweden, 1979.

Fagerlund G. (1982)
'The influence of slag cement on the frost resistance of the hardened concrete', Swedish Cement and Concrete Research Institute, Research report 1:82, Stockholm, Sweden, 1982.

Fagerlund, G. (1988)
'Carbonation of concrete with fly ash cement', Nordic Research Symposium on Durable Concrete with Industrial By-products, Technical Research Centre of Finland, VTT Symposium 89, pp. 7-20, Espoo, Finland, 1988.

Fagerlund G. (1993)
'The long-time water absorption in the air-pore structure of concrete', Lund University, Division of Building Materials, Report TVBM-3051, Lund, Sweden, 1993.

Fagerlund, G. (2000)
'Compendium in Building materials', Course literature at the continuation course in Building Materials, Division of Building Materials, Lund Institute of Technology, Part 2, Chapter 21, Lund, 2000. (in Swedish)

Feldrappe, V. (2002)
'Frostwiderstand Hochfester Betone', contribution to the 41th Forschungskolloquium DAfStb, VDZ - Forschungsinstitut der Zementindustrie, Düsseldorf, Germany, 2002. (in German)

Gallé C. (2001)
'Effect of drying on cement-based materials pore structure as identified by mercury intrusion porosimetry. A comparative study between oven-, vacuum- and freeze-drying', Cement and Concrete Research 31, 2001.

Groves, G. W., et al. (1991)
'Progressive changes in the structure of hardened C_3S cement pastes due to carbonation', Journal of the American Ceramic Society, Vol. 74, No. 11, pp. 2891-2896, 1991.

Gunter, M., et al. (1987)
'Effect of curing and type of cement on the resistance of concrete to freezing in deicing salt solutions', Concrete Durability, American Concrete Institute, ACI SP-100, pp. 877 - 899, Detroit, USA, 1987.

Hall C. (1989)
'Water sorptivity of mortars and concretes: a review', Magazine of Concrete Research, Vol. 41, No. 147, 1989.

Hartmann, V. (1993)
'Optimierung und Kalibrierung der Frost-Tausalz-Prüfung von Beton - CDF-test', Fachbereich Bauwesen, Universität - GH - Essen, pp. 87-89, Germany, 1992. (in German)

Hasholt, M. (2002)
'Salt frost scaling - interaction of transport mechanisms and ice formation in concrete', Danish Technological Institute, Building Technology, Taastrup, Denmark, 2002.

Hilsdorf, H. K. et al. (1984)
'Carbonation, pore structure and durability', Proceedings of the RILEM seminar - Durability of Concrete Structures under Normal Outdoor Exposure, pp. 182-196, Hannover, Germany, 1984.

Houst, Y. F. (1993)
'Influence of moisture on carbonation shrinkage kinetics of hydrated cement paste', Proceedings of the 5^{th} International RILEM Symposium on Creep and Shrinkage of Concrete, Barcelona, Spain, EFN Spon, 1993.

Houst, Y. F. (1995)
'Microstructural changes of hydrated cement paste due to carbonation', Proceedings of the Materials Research Society's symposium - Mechanisms of Chemical Degradation of Cement-based Systems, Boston, 1995.

Hunt, C. M., Tomes, L. A. (1962)
'Reaction of hardened Portland cement paste with carbon dioxide', JOURNAL OF RESEARCH of the National Bureau of Standards - A. Physics and Chemistry, Vol. 66A, No. 6, pp. 473- 481, 1962.

Jacobsen, S. (1995)
'Scaling and cracking in unsealed freeze/thaw testing of Portland cement and silica fume concretes', Thesis, The Norwegian Institute of Technology, Division of Structural Engineering, Concrete section, No. 1995:101, Trondheim, Norway, 1995.

Jacobsen, S., et al. (1997)
'Frost deicer salt scaling testing of concrete: effect of drying and natural weathering', Cement, Concrete and Aggregates, CCAGDP, Vol. 19, No. 1, pp. 8-16, 1997.

Johannesson, B., Utgenannt, P. (2001)
'Microstructural changes caused by carbonation of cement mortar', Cement and Concrete Research, No. 31, 2001.

Kaufmann, J. (2000)
'Experimental identification of damage mechanisms in cementitious porous materials on phase transition of pore solution under frost deicing salt attack', Thesis, Department of Concrete/-Construction Chemistry at EMPA, EMPA Report No. 248, Dübendorf, Switzerland, 2000.

Knöfel D., Eβer G. (1992)
'Einfluβ unterschiedlicher Kohlendioxidkonzentrationen auf Zementmörtel', Internationalen Kolloquiums Werkstoffwissenschaften und Bausanierung, Teil 3, pp. 1408-1418, Esslingen, Germany, 1992. (in German)

Kropp, J. (1983)
'Karbonatisierung und transportvorgänge in Zementstein', Dissertation, Universität Karlsruhe, Germany, 1983. (in German)

Langham, E. J., Mason B. J. (1958)
'The heterogeneous and homogeneous nucleation of supercooled water', Proceedings from Royal Society, London, 1958.

le Sage de Fontenay, C., Sellevold, E. J. (1980)
'Ice formation in hardened cement paste - 1. Mature water saturated pastes', Durability of building materials and components, ASTM STP 691, P. J. Sereda and G. G. Litvan (editors), American society for testing and materials, 1980.

Lindmark, S. (1998)
'Mechanisms of salt-frost scaling of Portland cement-bound materials: Studies and hypothesis', Thesis, Report TVBM 1017, Lund University, Lund Institute of Technology, Division of Building Materials, Lund, Sweden, 1998.

Litvan, G.G. (1972)
'Phase transitions of adsorbates IV - Mechanism of frost action in hardened cement paste', Journal of the American Ceramic Society, 55, pp. 38-42, 1972.

Litvan, G. G. (1987)
'Carbonation of slag cements', Proceedings from the International Workshop on Granulated Blast Furnace Slag in Concrete, pp. 301-327, Toronto, Canada , 1987.

Malhotra, M., Bremner, T. (1996)
'Performance of concrete at Treat Island, U.S.A.: CANMET investigations', Concrete in Marine Environment, Proceedings from the third CANMET/ACI International Conference, SP-163, St. Andrews by-the-Sea, Canada, 1996.

Marchand, J., et al. (1994)
'The deicer salt scaling deterioration of concrete - An overview', Third international conference on Durability of concrete, ACI, SP-145, Nice, France, 1994.

Matala, S. (1988)
'The effect of carbonation on frost-salt resistance of condensed silica fume-, granulated blast furnace slag-, fly ash and OPC-concretes', Nordic Seminar on Carbonation of Concrete, Forskningsinstituttet for cement og betong (Research Institute for Cement and Concrete), SINTEF, Report STF65 A88095, Trondheim, Norway, 1988.

Matala S. (1995)
'Effects of carbonation on the pore structure of granulated blast furnace slag concrete', Helsinki University of Technology, Faculty of Civil Engineering and Surveying, Concrete Technology, Diss., Report 6, Espoo, Finland, 1995.

Matala, S. (1997)
'Pore structural changes of carbonated granulated blast furnace slag concrete and their effects on the frost-salt resistance', Proceedings of the 13th International Conference on Building Materials, Part 1, pp. 243 - 256, Weimar, Germany, 1997.

Matala, S. (1998)
'Effect of silica fume addition on the frost-salt scaling resistance of aged concrete', International Conference on Concrete under Severe Conditions, CONSEC ´98, pp. 1989-1998, Tromsö, Norway, 1998.

Matala, S. (2003)
Personal correspondence by e-mail, November, 2003.

Meyer, A. (1968)
'Investigations on the carbonation of concrete', Proceedings from the 5th International Symposium on the Chemistry of Cement, Vol. 3, pp. 394-401, Tokyo, Japan, 1968.

Neville, A. M. (1995)
'Properties of concrete', 4th Edition, Carbonation, pp. 497-506, Longman, Essex, England, 1995.

Oberholster R. E. (1987)
'Pore structure, permeability and diffusivity of hardened cement paste and concrete in relation to durability: status and prospect', 8th International Congress on the Chemistry of Cement, Rio, Brasil, 1987.

Parrott, L. J. (1987)
'A review of carbonation in reinforced concrete', British Cement Association, Crowthorne, Great Britain, 1987.

Parrott, L. J. (1991/92)
'Carbonation, moisture and empty pores', Advances in Cement Research, Vol. 4, No. 15, pp. 111-118, 1991/92.

Parrott, L. J. (1992)
'Variations of water absorption rate and porosity with depth from an exposed concrete surface: Effects of exposure conditions and cement type', Cement and Concrete Research, Vol. 22, No. 6, pp.1077-1088, 1992.

Parrott, L. J. (2003)
Personal correspondence by e-mail, December, 2003.

Persson, B. (1998)
'Quasi-instantaneous and long-term deformations of high-performance concrete - with some related properties', Lund University, Lund Institute of Technology, Division of Building Materials, Report TVBM-1016, Lund, Sweden, 1998.

Petersson, P.-E. (1995)
'Scaling resistance of concrete - Field exposure tests', Swedish National Testing and Research Institute, SP-report 1995:73, Borås, Sweden, 1995. (in Swedish).

Petersson, P.-E. (1996)
'Scaling resistance of concrete - Field exposure tests', Proceedings of a Nordic research seminar on Frost resistance of building materials, Lund Institute of Technology, Division of Building Materials, Report TVBM-3072, Lund, Sweden, 1996.

Petersson, P.-E. (1997)
'Reflections on scaling resistance testing of concrete', Selected research studies from Scandinavia, Dedicated to Professor Göran Fagerlund on his 60th anniversary, Division of Building Materials, Lund Institute of Technology. Report TVBM-3078, Lund, Sweden, 1997.

Pigeon, M., Pleau, R. (1995)
'Durability of concrete in cold climates', Modern concrete technology 4, E & FN Spon, London, England. 1995.

Pigeon, M. (1989)
'La durabilité au gel du béton', Materials and Structures, 22(127), pp. 3-14, 1989.

Pihlajavaara, S. E. (1968)
'Some results of the effect of carbonation on the porosity and pore size distribution of cement paste', Matériaux et constructions, Vol. 1, No. 6, pp. 521-526, 1968.

Powers, T. C., Brownyard, T. L. (1948)
'Studies of the physical properties of hardened Portland cement paste', Research Laboratories of the Portland Cement Association, Bull. 22, 1948.

Powers, T. C. (1949)
'The air requirement of frost-resistant concrete', Proceedings of the Highway Research Board, 29, pp. 184-211, 1949.

Powers, T.C., Helmuth, R.A. (1953)
'Theory of volume changes in hardened Portland cement paste during freezing', Proceedings of the Highway Research Board, 32, pp. 285-297, 1953

Powers, T. C. (1962)
'A hypothesis on carbonation shrinkage', Journal of the PCA Research and Development Laboratories, Vol. 4, No. 2, pp. 40-50, 1962.

Powers, T. C. (1965)
'The mechanisms of frost action in concrete', in Stanton Walker Lecture Series on the Material Science, Lecture No. 3, November, 1965.

Powers, T.C. (1975)
'Freezing effects in concrete', ACI Special publication SP-47, American Concrete Institute, Detroit, MI, pp. 1-11, 1975

Richardson, M. G. (1988)
'Carbonation of reinforced concrete - Its causes and management', Civil Engineering Department, Faculty of Engineering and Architecture, University College Dublin, Dublin, Ireland, 1988

Romberg Von H. (1978)
'Zementsteinporen und Betoneigenschaften', Beton-Informationen, 18, 1978. (in German)

Rönning, T. F. (2001)
'Freeze-thaw resistance of concrete effect of: curing conditions moisture exchange and materials', Thesis, The Norwegian Institute of Technology, Division of Structural Engineering, Concrete Section, Trondheim, Norway, 2001.

Scrivener K. L. & Gartner E. M. (1987)
'Microstructures gradients in cement paste around aggregate particles', Bonding in Cementitious Composites, Materials Research Society, Symposium proceedings Vol. 114, pp. 77-85, Pittsburgh, USA, 1987.

Sellevold, E. J., Bager D. H. (1980)
'Low temperature calorimetry as a pore structure probe', proceedings of the 7th International congress on the chemistry of cement, Vol. IV, Paris, 1980

Sellevold, E. J., Bager, D. H. (1985)
'Some implications of calorimetric ice formation results for frost resistance testing of cement products', Proceedings from a Workshop on "Beton & Frost" (Concrete & Frost) in Køge, Danish Concrete Association, Publication no. 22:85, pp. 47-77, Denmark, 1985.

Setzer M. J. (1976)
'New approach to describe frost action in hardened cement paste', in proceedings of the conference on hydraulic cement pastes: their structure and properties, Sheffield, pp. 312-325, 1976.

Setzer M. J. (1997)
'Basis of testing the freeze-thaw resistance: surface and internal deterioration', Proceedings of the International RILEM Workshop on Resistance of Concrete to Freezing and Thawing with or without De-icing Chemicals, University of Essen, RILEM proceedings 34, pp. 157-173, Essen, Germany, 1997.

Setzer, M. J. (2001)
'CIF test- Capillary suction, internal damage and freeze thaw test - Reference method and alternative methods A and B', Materials and Structures, Vol. 34, No. 243, pp. 515-525, 2001.

Shacklock B. W., Walker W. R. (1958)
'The specific surface of concrete aggregates and its relation to the workability of concrete', Cement and Concrete Association, Research Report No 4, London, 1958.

Slegers, P. A., Rouxhet, P. G. (1976)
'Carbonation of the hydration products of tricalcium silicate', Cement and Concrete Research, Vol. 6, pp. 381-388, 1976.

Smolszyk, H-G., Romberg, H. (1976)
'Der Einfluss der Nachbehandlung und der Lagerung auf die Nacherhärtung und Porenverteilung von Beton', Teil 1, Tonindustrie Zeitung, 100, Nr. 10, pp. 349-357, 1976.

Soers, E., Meyskens, M. (1991)
'Recent experience on microscopical quality control of concrete in relation to durability aspects', Proceedings of the Second International Symposium on Quality Control on Concrete Structures, State University of Ghent, pp. 269-276, Brussels, Belgium, 1991.

Stark, J., Wicht, B. (1995)
'Dauerhaftigkeit von Beton', Schriften der Hochschule für Architektur und Bauwesen Weimar, Fakultät Bauingenieurswesen, No. 100, pp. 31-32 and pp. 221-227, Weimar, Germany, 1995. (in German)

Stark, J. (1997)
'Frost resistance with and without deicing salt - a purely physical problem?', Proceedings of the International RILEM Workshop on Resistance of Concrete to Freezing and Thawing with or without De-icing Chemicals, University of Essen, RILEM Proceedings 34, pp. 83-99, Essen, Germany, 1997.

Stark, J., Ludwig, H.-M. (1997:1)
'Freeze-thaw and freeze-deicing salt resistance of concrete containing cement rich in granulated blast furnace slag', ACI Materials Journal, Vol. 94, No. 1, 1997.

Stark, J., Ludwig, H.-M. (1997:2).
'Freeze-deicing salt resistance of concretes containing cement rich in slag', Proceedings of the International RILEM Workshop on Resistance of Concrete to Freezing and Thawing with or without De-icing Chemicals, University of Essen, RILEM Proceedings 34, pp. 123-138, Essen, Germany, 1997.

Stark, J., Möser, B. (2002)
'Nano and microstructure of Portland cement paste', Proceedings of the International RILEM Workshop 'Frost resistance of concrete - From nano-structure of concrete and pore solution to macroscopic behaviour and testing', PRO 24, pp. 15-28, Essen, Germany, 2002.

Swenson, E. G., Sereda, P. J. (1968)
'Mechanism of the Carbonation Shrinkage of Lime and Hydrated Cement', Journal of Applied Chemistry, Vol. 18, No. 4, pp. 111-117, 1968.

Tang, L., et al. (1997)
'Evaluation of the ultrasonic method for detecting the freeze/thaw cracking in concrete', NORDTEST project No. 1321-97, SP Swedish National Testing and Research Institute, Building Technology, SP report 1997:37, Borås, Sweden, 1997.

Tang, L., et al. (2000)
'Evaluation of the modified slab test for resistance of concrete to internal frost damage', NORDTEST Project No. 1485-00, SP Swedish National Testing and Research Institute, Building Technology, SP report 2000:34, Borås, Sweden, 2000.

Tang, L., Utgenannt, P. (2000)
'Characterization of chloride environment along a highway', Proceedings from the fifth CANMET/ACI international conference on durability of concrete, Supplementary papers, Barcelona, Spain, 2000.

Tang, L., Petersson, P.-E. (2001)
'Slab test - Freeze/thaw resistance of concrete - Internal deterioration', Recommendations of RILEM TC 176-IDC: Test methods of frost resistance of concrete, Materials and Structures, Vol. 34, pp. 526-531, 2001.

Taylor, H. F. W. (1997)
'Cement chemistry', second edition, Thomas Telford Publishing, London, 1997.

Tuutti, K. (1982)
'Corrosion of steel in concrete', CBI Research, fo 4:82, Swedish Cement and Concrete Research Institute, Stockholm, Sweden, 1982.

Utgenannt, P. & Petersson, P.-E. (1997)
'Influence of preconditioning on scaling resistance for different types of test surfaces', Proceedings of the International RILEM workshop on Resistance of Concrete to Freezing and Thawing With or Without De-icing Chemicals, RILEM Proceedings 34, Essen, Germany, 1997.

Utgenannt, P. (1997)
'The effect of binder on the frost resistance of concrete - Test specimens produced in 1996 - Material and production data and results from durability testing in the laboratory', Swedish National Testing and Research Institute, BTB report no 1, 1997, (in Swedish).

Utgenannt, P. (1999)
'Influence of carbonation on the scaling resistance of OPC concrete', Proceedings of the International RILEM workshop on Frost Damage in Concrete, RILEM Proceedings 25, Minneapolis, USA, 1999.

Utgenannt, P., Petersson, P.-E. (2001)
'Frost resistance of concrete containing secondary cementitious materials - Experience from three field exposure sites', Proceedings from the NCR Workshop on Durability of exposed concrete containing secondary cementitious materials, The Nordic Concrete Federation, Hirtshals, Denmark, 2001.

Verbeck, G. J. & Klieger, P. (1957)
'Studies of 'salt' scaling of concrete', Highway Research Bulletine, Bull. 150, Washington D.C, USA, 1957

Verbeck, G. J. (1958)
'Carbonation of hydrated Portland cement', ASTM Special Publication, No. 205, pp. 17-36, 1958.

Vesikari, E. (1988)
'The effect of ageing on the durability of concrete including by-products', Proceedings from the Nordic research symposium - Durable Concrete with Industrial By-products, Technical Research Centre of Finland, pp. 104-112 Espoo, Finland, 1988.

Virtanen, J. (1989)
'Field study on the effects of additions on the salt-scaling resistance of concrete', Nordic Concrete Research, publication No.9, pp. 197-212, 1989.

Vourinen, J. (1969)
'On the freezable water in concrete', RILEM Symposium on the Durability of Concrete, Prague, September, 1969.

Warris, B. (1963)
'The influence of air-entrainment of the frost resistance of concrete, Part A, void distribution', Swedish Cement and Concrete Research Institute, Proc. No. 35, Stockholm, Sweden, 1963.

Wierig, H.-J. (1984)
'Longtime studies on the carbonation of concrete under normal outdoor exposure', Proceedings of the RILEM Seminar on the Durability of Concrete Structures under Normal Outdoor Exposure, Institut für Baustoffkunde und Materialprüfung, Universität Hannover, Germany, 1984.

Winslow D.N., Cohen M. D. et. al. (1994)
'Percolation and pore structure in mortars and concrete', Cement and Concrete Research, Vol. 24, pp. 25-37, 1994.

Wirje, A., Offrell, P. (1996)
'Environmental mapping - Chloride ingress at Highway 40', Lund University, Department of Building Materials, Report TVBM-7106, Lund, Sweden, 1996, (in Swedish).

Standards

ASTM C 457, 'Standard test method for microscopical determination of parameters of the air-void system in hardened concrete', 1998.

DS 423.36, 'Testing of concrete - hardened concrete - determination of the amount of silica fume in clumps', Edition 1, Danish Standard Association, 1995. (in Danish)

EN 206-1, 'Concrete - Part 1: Specification, performance, production and conformity', Edition 1, 2001.

EN 12350-7, 'Testing fresh concrete - Part 7: Air content - Pressure methods, Edition 1, 2000

NT-BUILD 381, 'Concrete, Hardened: Air void structure and air content', Approved 1991.

RILEM CDC 3, 'The critical degree of saturation method of assessing the freeze/thaw resistance of concrete', Compendium of RILEM Technical Recommendations, 1994 edition, Chapman & Hall, London, England, 1994.

RILEM TC 117-FDC, 'Test Methods for the Freeze/Thaw Resistance of Concrete. Slab Test and Cube Test', Materials and Structures, Vol. 28, No. 180, pp. 366-371, 1995.

SS 13 70 03, 'Concrete - Application of EN 206-1 in Sweden', Edition 1, Ratified 2001-05-23, Swedish Standards Institute, Stockholm, Sweden, 2001. (in Swedish)

SS 13 72 10, 'Concrete testing - Hardened concrete - Cube strength', Edition 1, Swedish Standards Institute, Stockholm, Sweden, 1978. (in Swedish)

SS 13 72 44, 'Concrete testing - Hardened concrete - Scaling at freezing', Edition 3, Swedish Standards Institute, Stockholm, Sweden, 1995. (in Swedish)

APPENDICES

APPENDIX 1

INFLUENCE OF PRECONDITIONING ON SCALING RESISTANCE FOR DIFFERENT TYPES OF TEST SURFACES

Published in the Proceedings of the International RILEM workshop on Resistance of Concrete to Freezing and Thawing With or Without De-icing Chemicals, in Essen, Germany, 1997 (RILEM Proceedings 34)

INFLUENCE OF PRECONDITIONING ON SCALING RESISTANCE FOR DIFFERENT TYPES OF TEST SURFACES

Preconditioning vs. scaling resistance of concrete

P. UTGENANNT and P-E. PETERSSON

Swedish National Testing and Research Institute, Borås, Sweden.

Abstract

When testing the salt scaling resistance of concrete, different test methods can be used. The difference in preconditioning climate, test surfaces used, the time the test specimens are subjected to the climate etc., give rise to difficulties when comparing results from different methods. In order to accurately be able to interpret and translate the results from these methods, it is necessary to learn more about the causes of the differences in results. In this investigation the influence of the preconditioning climate on the scaling resistance for various types of test surfaces is examined. The freeze/thaw test used is the Swedish standard SS 13 72 44, more commonly known as the ”slab test” or the ”Borås method”. Two concrete qualities, both with OPC as binder, were tested. Three types of test surfaces were investigated, surface cut 7 respectively 21 days after casting and cast surface. Two preconditioning climates were examined, 65% RH/20°C and 50% RH/20°C.

It was found that the scaling resistance is highly dependent on the preconditioning climate, irrespective of the test surface. For concrete with poor scaling resistance, the difference in scaling due to the preconditioning climate is initially large, but after 56 freeze/thaw cycles it is almost negligible. For concrete with good scaling resistance, however, the initial large difference remains throughout the test.

When the test surface was ground to a depth of about 0.6 mm just before resaturation and freeze/thaw testing, the scaling was almost independent of the preconditioning climate. These results indicate that a thin, frost resistant skin is produced on the surface of the test specimens, probably due to carbonation. The resistance of the skin seems to be strongly dependent on the preconditioning climate.

The results of this investigation are only valid for concrete produced with the type of cement used, i.e. OPC. Other cements, such as cement with blast furnace slag may show other results.

Keywords: preconditioning climate; test surface; freeze/thaw resistance; carbonation.

1 Introduction

When testing the freeze/thaw resistance of concrete according to the Swedish standard SS 13 72 44 [1, 3], ”the Borås method”, a cut concrete surface is tested, although other test surfaces can be used as well. In other test methods, such as the German CDF-test [2] and the German ”Cube Test” [3], cast surfaces are tested. In order to be able to evaluate results from different test methods, the differences in test procedure and preconditioning of test specimens have to be systematically studied. In this investigation the influence of the preconditioning climate and different test surfaces on the freeze/thaw resistance is examined.

To be able to improve the precision of the test methods, it is important to learn more about the mechanisms leading to freeze/thaw damage. As concluded in [4], carbonation seems to play an important role in the initial scaling. The carbonation of a concrete sur-face is strongly dependent on the conditioning climate and to some extent also on the structure of the surface. Consequently it is important to understand the influence of preconditioning and of the structure of the test surface on the freeze/thaw resistance.

2 Preconditioning climates and test surfaces

Two preconditioning climates and three types of test surfaces were investigated. The climates were 65% RH/20°C and 50% RH/20°C respectively, the wind velocity was below 0.1 m/s in both cases. In table 1 the types of test surfaces studied are presented.

Table 1. Test surfaces studied

Type of test surface
Surface cut 7 days after casting, subjected to the preconditioning climate for 21 days
Surface cut 21 days after casting, subjected to the preconditioning climate for 7 days
Surface cast against a plastic coated wooden board, subjected to the preconditioning climate for 21 days

To investigate if the influence of different climates on the frost resistance is dependent on the quality of a thin layer of the test surface, tests were carried out after grinding a layer approximately 0.6 mm thick from the test surface immediately before resaturation. These results were compared with results from unground specimens.

3 Materials

Two concrete mixes were used in the investigation, quality A with poor predicted freeze/thaw resistance and quality B with good predicted freeze/thaw resistance. The compositions are given in table 2. The aggregate used is natural gravel with particle

size 0-8 mm and crushed gneiss with particle size 8-16 mm. Both are classified as being frost resistant. The plasticizer, Melcrete, is naphthalene based and the air entraining agent, L 16, is a tall-oil derivative.

One single cement quality, Ordinary Portland Cement, Degerhamn std [5], was used for all mixes. Test results for concrete with other cement types such as, for example, blast furnace slag cement would probably lead to other results.

Table 2. Composition of the two concrete qualities used

Quality	Cement type[1)]	Cement (kg/m^3)	Aggregate (kg/m^3) 0-8	8-16	W/C	Plasticizer	Air entr. agent	Air (%)	Slump (mm)
A	OPC	420	927	890	0,40	yes	no	1,2	95
B	OPC	380	911	841	0,50	no	yes	2,9	80

[1)] OPC=Ordinary Portland Cement (Degerhamn std [5] is a low alkali, sulphur resistant cement)

4 Specimens and curing

For each concrete quality 8 cubes (150 mm) and 8 slabs (150·150·50 mm) were produced. The cubes were cast in metal moulds. The slabs were cast in cube moulds with a 50 mm thick separating layer dividing the mould into two parts, each 50 mm thick. The separating layer was plastic coated wooden board. The surfaces cast against the board were those to be tested.

Cubes and slabs were demoulded 24 hours after casting. They were then immediately placed in a water bath, at 20±2°C, where they remained until the concrete was 7 days old. After water curing, the cubes were placed in the two different climates, the same quantity of cubes in each climate. Half of the cubes were cut into specimens, (150·150·50 mm) 7 days after casting, i.e. immediately after water curing. The remaining cubes were cut into specimens 21 days after casting. In table 3, the different curing conditions and test surfaces are listed and numbered.

In this report, the numbers in table 3 will be found combined with concrete qualities ”A” and ”B” in table 2, e.g. ”A1” means specimens with concrete mixture ”A”, with a test surface cut 21 days after casting and stored in a climate room with 65% RH and 20°C. For each number in table 3, three specimens were tested for each concrete quality.

Table 3. Curing climates and test surfaces investigated

Number	Test surface	Climate
1	Cut 21 days after casting	65% RH/20°C
2	Cut 21 days after casting	50% RH/20°C
3	Cut 7 days after casting	65% RH/20°C
4	Cut 7 days after casting	50% RH/20°C
5	Cast surface	65% RH/20°C
6	Cast surface	50% RH/20°C

To determine the conditions in the climate rooms, the evaporation from a free water surface was measured. Table 4 presents an average value for the evaporation measured.

Table 4. Evaporation from a free water surface in the two climate rooms

Climate	Evaporation ($g/m^2 \cdot h$)
65% RH/20°C	33±2
50% RH/20°C	45±2

When the concrete was 26 days old, a rubber sheet was glued to all surfaces of the specimens except the test surface. The edge of the rubber sheet reached 20±1 mm above the test surface. Figure 1 shows the test setup. After the rubber was applied, the specimens were returned to the climate rooms.

After 28 days a layer of tap water (approx. 3 mm deep) was poured onto the surface of the three specimens in each series. They were then returned to the climate rooms and the resaturation continued for 72±2 hours. Three specimens from each series ”A1-A6” and ”B1-B6” were then freeze/thaw tested according to SS 13 72 44.

In order to study the influence of the concrete skin on frost resistance, complementary tests were performed. Four specimens were produced and cured identically for each test series. Directly before resaturation, an 0.6±0.2 mm thick layer was ground from the test surface on two of the four specimens. Then all four specimens were identically resaturated and tested. The results from ground and unground specimens were then compared.

These complementary tests were only carried out on quality B´, which is identical to quality B in table 2. Only the two types of test surfaces *cut 21 days after casting* and *cast surface* were included. For both types of test surfaces, the specimens were conditioned at 65% RH/20°C and 50% RH/20°C. This means that the combinations preconditioning/test surface 1, 2, 5 and 6 according to table 3 were studied.

5 Test procedure

The freeze/thaw test was performed in accordance with SS 13 72 44. After the resaturation period, i.e. when the concrete was 31 days old, all surfaces of the specimen except the test surface were thermally insulated with 20 mm thick polystyrene plastic as shown in figure 1. The tap water used for resaturation was removed and a 3% NaCl solution was poured onto the test surface. By applying a flat polyethylene sheet, as shown in figure 1, the solution was prevented from evaporating. The specimens were then placed in the freezers and subjected to repeated freezing and thawing in accordance with the freeze/thaw cycle shown in figure 2. The temperature in the NaCl solution was continuously measured during the test. The freezer is programmed so that the temperature falls within the limits in figure 2. A typical temperature cycle is also shown in the figure.

After 7, 14, 21 (not required by the standard), 28, 42 and 56 cycles the scaled material was collected and dried at 105°C until the material was completely dry, after which the weight of scaled material was measured. The results are given as the amount of scaled material per unit area.

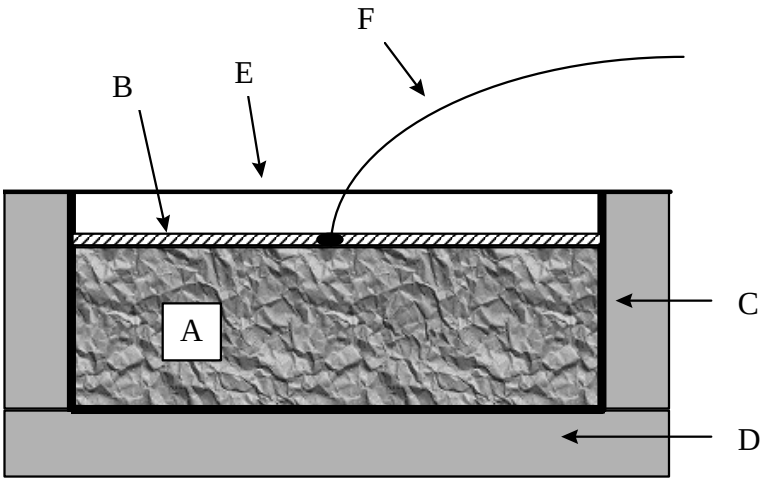

Figure 1. Test setup used for the freeze/thaw test. A- concrete specimen, B- 3% NaCl solution, C- rubber sheet, D- thermal insulation, E- polyethylene sheet, F- temperature measuring device.

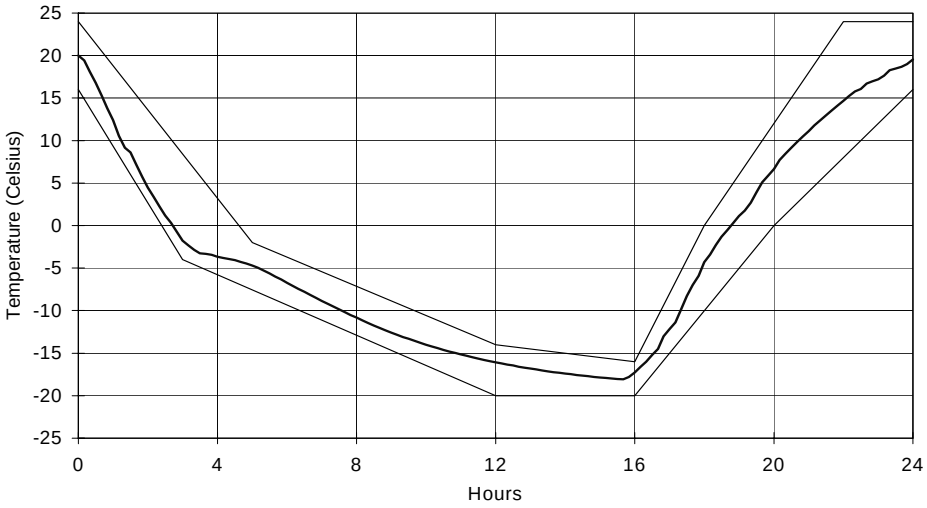

Figure 2. Temperature cycle used, in accordance with SS 13 72 44.

6 Results

The results from the freeze thaw tests are summarized in figures 3-7. The results are presented as the sum of scaled material in kg/m^2 as function of the number of freeze/thaw cycles.

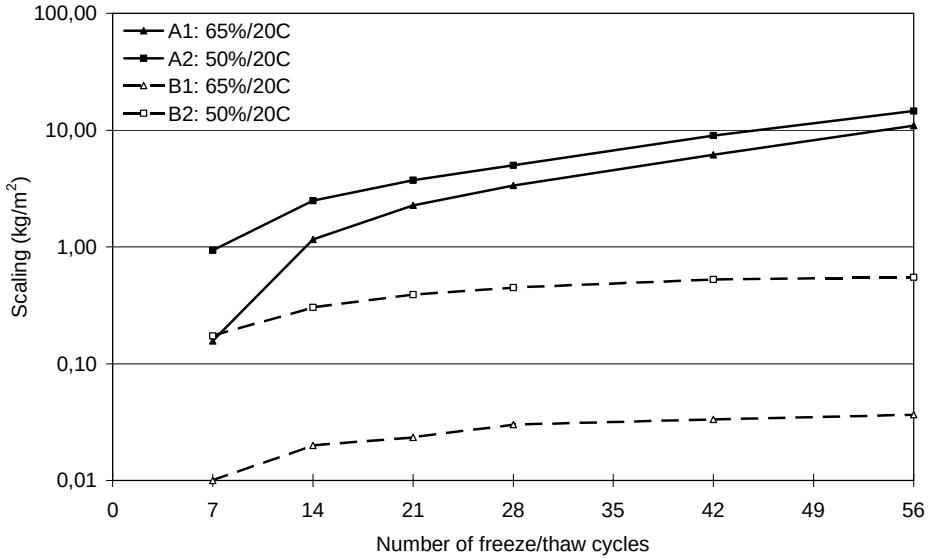

Figure 3. Scaling as function of the number of freeze/thaw cycles for specimens with the test surface cut 21 days after casting.

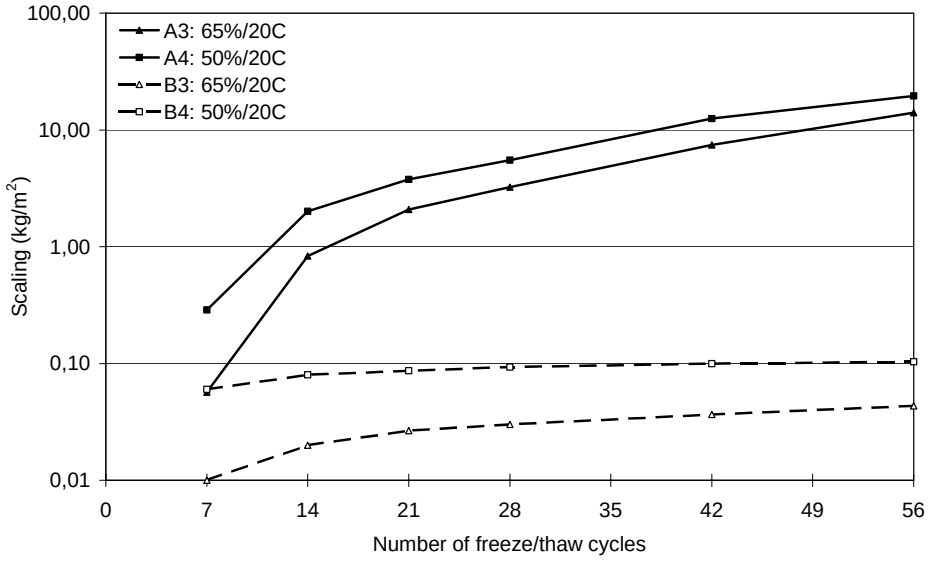

Figure 4. Scaling as function of the number of freeze/thaw cycles for specimens with the test surface cut 7 days after casting.

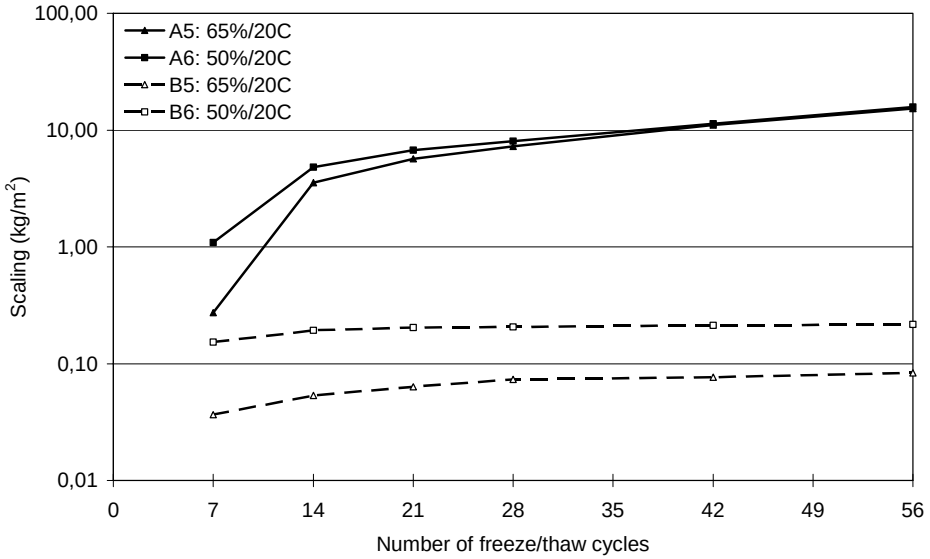

Figure 5. Scaling as function of the number of freeze/thaw cycles for specimens with cast test surface.

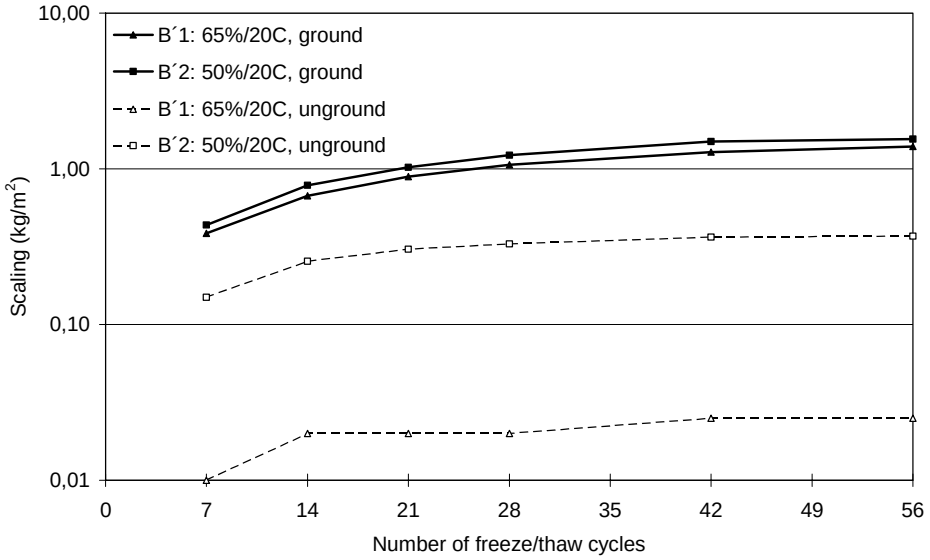

Figure 6. Scaling as function of the number of freeze/thaw cycles for specimens with the test surface cut 21 days after casting. Ground and unground test surfaces.

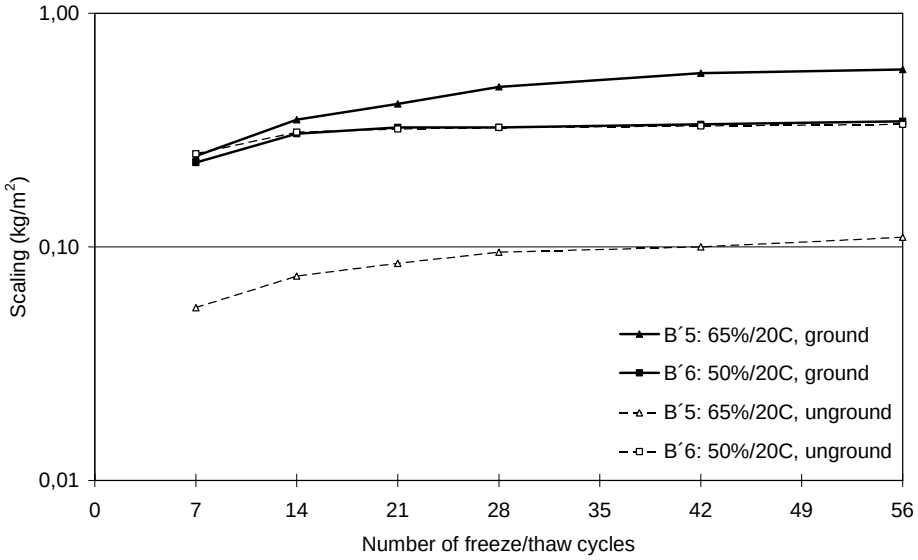

Figure 7. Scaling as function of the number of freeze/thaw cycles for specimens with cast test surface. Ground and unground test surfaces.

7 Discussion

Figure 3 shows the scaling for concrete cut 21 days after casting. From this figure it can be seen that for concrete with poor scaling resistance, the initial difference in scaling is strongly dependent on the preconditioning climate. Specimens conditioned at 50% RH, A2, have after 7 freeze/thaw cycles nearly six times greater scaling than specimens conditioned at 65% RH, A1. During the test, the difference in scaling gets gradually smaller, and after 56 cycles the difference is almost insignificant.

For concrete with good scaling resistance, the difference in scaling due to the different preconditioning climates after 7 cycles is much larger for specimens conditioned at 50% RH, B2, than for specimens conditioned at 65% RH, B1. This difference in scaling is, however, almost constant during the test, and still after 56 cycles, the scaling is much higher for B2 than for B1.

These observations show that specimens preconditioned at 65% RH have a better scaling resistance than specimens conditioned at 50% RH. For concrete with poor scaling resistance this difference can only be seen at the beginning of the test, at the end the scaling is approximately the same regardless of the preconditioning climate. This implies that a thin resistant skin is produced on the test surface and the resistance of this skin seems to be dependent on the climate in which the specimens have been stored. On specimens with poor scaling resistance, the resistance of the skin is too low to withstand scaling during the entire freeze/thaw test. After 7 cycles, the skin is still influencing the results but already after 14 cycles the skin seems to be entirely scaled off, which leads to the rate of scaling becoming less and less dependent on the preconditioning climate. On the other hand, on specimens with good scaling resistance, the resistance of the skin is high enough to influence the result throughout the test. The

skin is only broken locally and the initial difference in scaling for concrete conditioned in different climates is maintained during the test.

For specimens with other test surfaces, cut 7 days after casting, figure 4, and cast surface, figure 5, the tendency described above is exactly the same. For concrete with poor scaling resistance, the initial large difference resulting from the conditioning climate decreases while the test is running, and for concrete with good scaling resistance, the initial difference resulting from the conditioning climate remains almost constant during the test.

It can be observed that specimens with cast surfaces have approximately the same amount of scaling as specimens cut 21 days after casting. This is a bit surprising as the surface cast against mould mainly consists of cement paste while only about 30% of the cut surfaces consists of cement paste. Therefore, the scaling ought to be about three times higher for specimens with a cast test surface compared to a cut surface, at least if all other parameters are kept constant.

The explanation is that the duration of preconditioning is very important. The preconditioning period is 21 days for cast test surfaces while it is only 7 days for the cut surfaces. The effect of such a difference in curing conditions is illustrated in figure 8, where scaling results for different curing conditions, 7 or 21 days, for cut surfaces are presented. As can be seen, a longer preconditioning period leads to lower scaling in the interval 0.1-1.0 kg/m^2, when all other parameters are kept constant. Below 0.1 kg/m^2 the skin remains unbroken and the scaling will therefore be independent of the preconditioning time. Above about 1 kg/m^2 the skin is totally broken and the rate of scaling will thus be independent of the preconditioning time. The improved scaling resistance may be due to a higher degree of carbonation in the surface skin when the preconditioning period is prolonged.

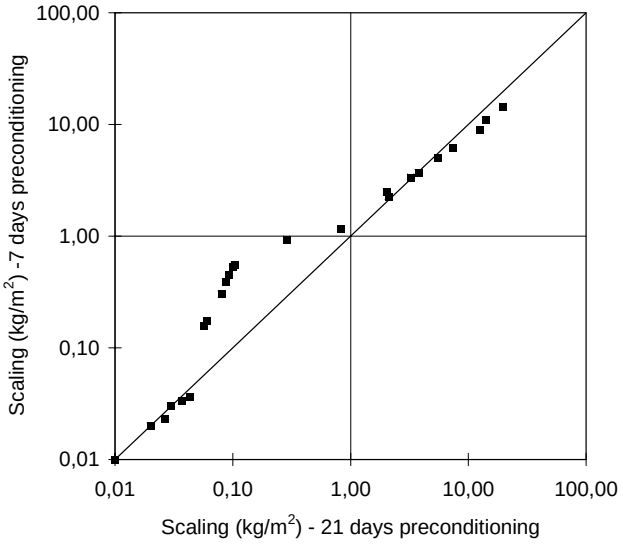

Figure 8. Scaling after the same number of freeze/thaw cycles for specimens cut 7 and 21 days after casting, i.e. preconditioned for 21 and 7 days respectively.

In order to study the importance of the concrete skin, additional tests were performed. A number of specimens were produced and treated according to the procedures described above. Directly before resaturation a layer of the test surface, approximately 0.6 mm thick, was removed by grinding some of the specimens. The other specimens were left unground. After this, all the specimens were identically treated and tested.

The results are presented in figures 6 and 7. The results show that there is a strong difference between the results for unground specimens, when preconditioned in different climates. This difference, however, more or less disappears when a thin layer of the test surface is removed. This investigation can not explain why the concrete skin is so important for the frost resistance. The carbonation of the skin, however, probably plays an important role.

These results are relevant for the type of concrete and binder used in this investigation. Other types of binder would probably lead to other results, see e.g. [6] and [7].

8 Conclusions

From this investigation, the following conclusions can be drawn:

1. The results from freeze/thaw tests are dependent on the preconditioning climate. Specimens conditioned at 50% RH/20°C have higher scaling, in freeze/thaw tests, than specimens conditioned at 65% RH/20°C.
2. For concrete with low freeze/thaw resistance the difference in scaling dependent on the preconditioning climate is large in the beginning of the freeze/thaw test, after 56 cycles the difference is insignificant. For concrete with good freeze/thaw resistance the initial difference in scaling is maintained during the test and is after 56 cycles almost as large as after 7 cycles.
3. The scaling resistance is increased with prolonged preconditioning time at least for concrete with OPC cement.
4. During preconditioning a thin carbonated skin is produced on the surface which strongly affects the scaling resistance. The properties of the skin seem to be highly dependent on the preconditioning climate.

9 References

1. Swedish Standard, SS 13 72 44, Edition 3 (1995), Concrete testing - Hardened concrete - Scaling at freezing.
2. RILEM Recommendation (1996), RILEM TC 117-FDC, Test method for the freeze-thaw resistance of concrete with sodium chloride solution (CDF), *Materials and Structures*, Vol. 29, No. 193. pp. 523-528.
3. RILEM TC 117-FDC (1995), Test method for the freeze-thaw resistance of concrete. Slab Test and Cube Test, *Materials and Structures*, Vol. 28, No. 180. pp. 366-371.
4. Setzer, M. J. (1997) Report, RILEM TC 117-FDC: Freeze-thaw and deicing resistance of concrete. *Materials and Structures*, Supplement March 1997.

5. Malmström, K. (1990) Cementsortens inverkan på betongs frostbeständighet, Rapport 1990:07, Swedish Testing and Research Institute.
6. Matala, S. (1995) Effects of carbonation on the pore structure of granulated blast furnace slag, Report 6, Helsinki University of Technology, Espoo.
7. Stark, J., Ludwig, H-M. (1997) Freeze-Thaw and Freeze-Deicing Salt Resistance of Concretes Containing Cement Rich in Granulated Blast Furnace Slag, *ACI Materials Journal*, Vol. 94, No. 1. pp. 47-55.

APPENDIX 2

INFLUENCE OF CARBONATION ON THE SCALING RESISTANCE OF OPC CONCRETE

Published in the Proceedings of the International RILEM workshop on Frost Damage in Concrete, in Minneapolis, USA, 1999 (RILEM Proceedings 25)

INFLUENCE OF CARBONATION ON THE SCALING RESISTANCE OF OPC CONCRETE

Peter Utgenannt
SP Swedish National Testing and Research Institute

Abstract
In this investigation the effect of carbonation on the salt scaling resistance for OPC concrete with various water/cement-ratio and two different air contents has been studied. Two preconditioning climates were examined, 65% RH/20°C without carbon dioxide and 65% RH/20°C with 1 vol-% of carbon dioxide. Preliminary results for concrete with a high blast furnace slag content are also presented. The results show that the scaling resistance is highly dependent on the preconditioning climate, irrespective of the water/cement ratio or air content. OPC concrete preconditioned in a climate with increased carbon dioxide content shows a much higher scaling resistance than concrete preconditioned in a climate free from carbon dioxide. The effect of carbonation is the opposite for concrete containing a high blast furnace slag content, i.e. carbonation of such concrete leads to a reduction of the scaling resistance.

1. Introduction

Different test methods can be used to test the salt scaling resistance of concrete. Differences in the preconditioning climate, test surfaces used, the time the specimens are subjected to the preconditioning climate etc. give rise to difficulties when comparing results from different methods. In order to accurately be able to interpret and translate the results of these methods, it is necessary to learn more about the causes of the differences in results.

In [1] the influence of the preconditioning climate on the scaling resistance for OPC concrete was investigated. Results from that investigation show that a thin, frost resistant skin was produced on the surface of the test specimens during curing. The resistance of the skin seemed to be strongly dependent on the preconditioning climate. It was proposed that the skin was produced due to carbonation.

In this investigation the effect of carbonation on the salt scaling resistance for concrete with various water/cement-ratios and two different air contents has been studied. The freeze/thaw test used is a cup method where specimens with cut test surfaces are subjected to freeze/thaw cycles which are similar to the cycle used in the Swedish standard SS 13 72 44, more commonly known as the 'slab test' or the 'Borås method' [2].

Six concrete qualities with OPC as binder were tested. Preliminary results for concrete with a high content of blast furnace slag are presented as well. Two preconditioning climates with different CO_2 concentrations were examined. In order to obtain the two climates with and without carbon dioxide two climate boxes were constructed, in which the relative humidity, the carbon dioxide content and the air flow could be varied.

The results from this investigation are valid only for concrete produced with the cement types used in this investigation. Other cements may show other results.

2. Preconditioning climates

The two preconditioning climates used were; 65% RH/20°C, free from carbon dioxide, and 65% RH/20°C with 1 vol-% of carbon dioxide. Two identical climate chambers were constructed in order to establish these climates [3]; see figure 1.

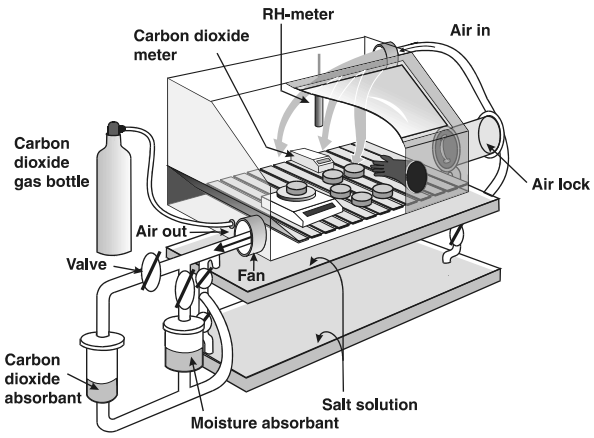

FIGURE 1. Climate chamber

The chambers enabled the relative humidity, the carbon dioxide content and the air flow to be varied. The climates in the chambers, i.e. relative humidity, air temperature, air flow speed and carbon dioxide content were continuously registered. The carbon dioxide content could be varied by using a carbon dioxide filter or by adding carbon dioxide from

a gas bottle. Relative humidity could be changed by varying the salt solution. Air flow could be varied by changing the speed of the fan that circulated the air out of the chamber, through the carbon dioxide filter, over the salt solution and into the chamber again.

3. Materials

Six 'micro' concrete qualities were used in this investigation: three water/cement-ratios, each with two different air contents. The compositions are given in table 1. The aggregate used was composed of fractions of a natural gravel with particle sizes of 0-0.5 mm, 0.5-1 mm, 1-2 mm, 2-4 mm and 4-8 mm. The grain size curve used was proportioned as a grain size curve normally used in concrete with 'normal' aggregate size, i.e. for aggregate up to 32 mm. The air entraining agent used, L 16, is a tall-oil derivative. No other admixtures were used.

TABLE 1. Concrete compositions.

Quality	**Cement type[1)]**	**W/C-ratio**	**Cement (kg/m^3)**	**Aggregate (kg/m^3)**					**Air entr. agent**
				0-0.5	**0.5-1**	**1-2**	**2-4**	**4-8**	
0.35 air	OPC	0.35	624	197	309	267	239	393	Yes
0.45 air	OPC	0.45	449	228	358	309	277	456	Yes
0.55 air	OPC	0.55	365	240	377	326	291	480	Yes
0.35	OPC	0.35	624	197	309	267	239	393	No
0.45	OPC	0.45	449	228	358	309	277	456	No
0.55	OPC	0.55	365	240	377	326	291	480	No

[1)] OPC= Ordinary Portland Cement (Degerhamn standard [4] is a low alkali, sulphur resistant cement)

The air content, spacing factor and specific surface were measured on face-ground samples of hardened concrete using microscopy. Results from microscopy measurements are presented in table 2. It can be noted that the spacing factors for concrete without entrained air is relatively low. This is explained by the high natural air content for this type of micro concrete.

TABLE 2. Results from measurements on face-ground samples of hardened concrete.

Quality	**Air: fresh (vol-%)**	**Air: hardened (vol-%)**		**Specific surface (mm^{-1})**	**Spacing factor (mm)**
		Total	**Voids<2mm**		
0.35 air	6.5	6.2	5.1	28	0.22
0.45 air	5.7	5.6	5.2	27	0.21
0.55 air	5.4	6.6	5.5	35	0.15
0.35	3.3	3.8	2.8	24	0.33
0.45	4.0	4.1	3.6	22	0.30
0.55	4.6	5.7	4.8	27	0.21

4. Specimens and curing

Two 100 mm × 105 mm (diameter × length) cylinders, and three 40 mm × 42 mm cylinders, were produced in each concrete quality. The cylinders were cast in plastic moulds. The specimens were demoulded 24 hours after casting. They were immediately placed in a water bath, at 20±2°C. The large cylinders remained in the water until the concrete was 21 days old. The small cylinders remained in the water for 28 days. At the age of 28 days the small cylinders were used to measure the compressive strength. The top and bottom surfaces of the cylinders were ground to approximately 1 mm depth before the compressive strength was measured. In table 3 the compressive strength is presented as the mean value of three cylinders.

TABLE 3. Compressive strength at the age of 28 days.

Quality	Compressive strength (MPa)	Standard deviation (MPa)
0.35 air	69.8	1.8
0.45 air	58.1	3.1
0.55 air	44.4	3.9
0.35	77.4	1.7
0.45	53.7	3.9
0.55	42.5	2.9

After water curing, the large cylinders were cut into two pieces, each 50 mm long. All sides of the specimens except the cut surface were insulated with 5 mm thick plastic. To prevent the cut surface from carbonation, the surface was kept wet and covered with a plastic film while the specimens were kept in normal air with carbon dioxide. As soon as all specimens were insulated, they were placed in the climate chambers. Two specimens of each concrete quality were placed in each of the two climate chambers, in which the climates were 65% RH/20°C without carbon dioxide, and 65% RH/20°C with 1 vol-% of carbon dioxide. The plastic film was removed from the cut test surface and the surface was wiped off with a moist cloth. The specimens were conditioned in the climate chambers for 7 days, after which they were resaturated by capillary suction for three days.

A complementary study of concrete containing a high blast furnace slag content was carried out as well. Specimens with the same composition as quality '0,45', but with 65% of the cement replaced by blast furnace slag, were produced and treated in the same way as described above. The chemical composition of the ground blast furnace slag is given in [5]. The concrete quality, hereinafter referred to as '65% slag', had an air content of 5,9%, of which 5,2% were voids<2 mm, a specific surface of 28 mm^{-1} and a spacing factor of 0,20 mm. The compressive strength at 28 days of age was 38,7 MPa (standard deviation 0,5 MPa).

5. Test procedure

The freeze/thaw test performed was a cup method with a freeze cycle which is similar to the freeze/thaw cycle used in the Swedish standard SS 13 72 44, i.e. a 24 hour cycle with temperatures between +24°C and -20°C, as shown in figure 3.

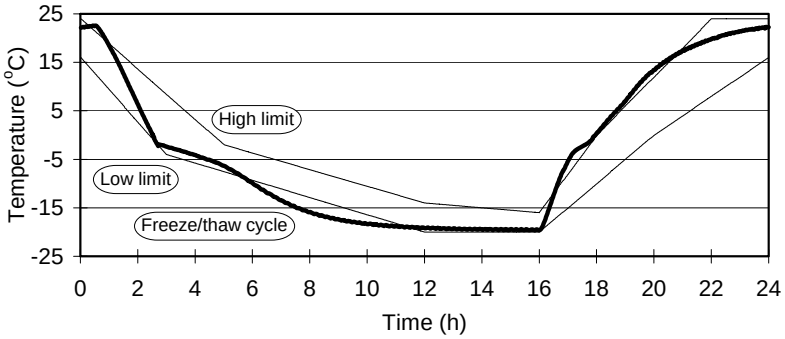

FIGURE 3. Freeze/thaw cycle used in this investigation and temperature limits according to SS 13 72 44.

After resaturation the specimens were placed with the test surface downwards in a cylindrical glass cup with diameter 135 mm. The cup was filled with 170 ml (12 mm) 3% NaCl solution. A plastic ring on the bottom of the dish maintained a 10 mm space between the test surface and the bottom of the dish. The temperature was measured in the salt solution under the test surface. The test set-up is shown in figure 4.

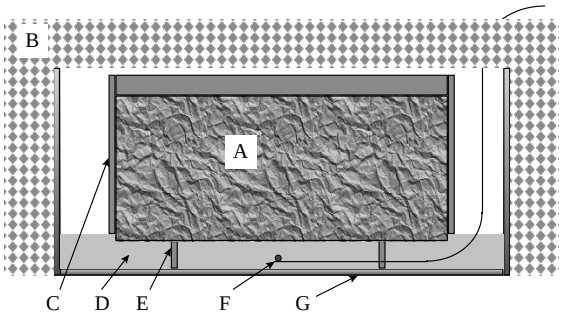

FIGURE 4. Set-up of the freeze/thaw test. A- Specimen, B- thermal insulation, C- plastic moisture insulation, D- 3% NaCl solution, E- spacer, F- temperature measuring device, G- glass cup

After 1, 4, 7, 14, 21, 28, 42 and 56 freeze/thaw cycles the scaled material was collected and dried at 105°C until the material was completely dry, after which the weight of the scaled material was measured. The results are given as the accumulated weight of the scaled material in kg/m^2 as function of the number of freeze/thaw cycles.

6. Results

The results from the freeze/thaw tests are given in table 4-6. Each result is a mean value of two specimens. In figure 5 results for OPC concrete with entrained air are presented and in figure 6 results for concrete containing 65% slag are presented.

TABLE 4. Results from freeze/thaw tests on OPC concrete *with entrained air*.

Environment	**Quality**	**Scaling (kg/m^2)**			
		7 cycles	**14 cycles**	**28 cycles**	**56 cycles**
1 vol-% CO_2	**0.35 air**	0.05	0.09	0.14	0.21
	0.45 air	0.05	0.08	0.13	0.16
	0.55 air	0.16	0.28	0.40	0.56
no CO_2	**0.35 air**	0.15	0.26	0.56	1.31
	0.45 air	0.78	1.49	2.65	4.52
	0.55 air	1.72	3.27	5.78	9.67

TABLE 5. Results from freeze/thaw tests on OPC concrete *without entrained air*.

Environment	**Quality**	**Scaling (kg/m^2)**			
		7 cycles	**14 cycles**	**28 cycles**	**56 cycles**
1 vol-% CO_2	**0.35**	0.07	0.11	0.17	0.36
	0.45	0.10	0.15	0.23	0.39
	0.55	0.50	0.67	0.87	1.41
no CO_2	**0.35**	0.73	1.39	2.58	4.64
	0.45	1.60	3.23	6.19	11.13
	0.55	1.42	3.02	5.93	12.16

TABLE 6. Results from freeze/thaw tests on concrete with 65% slag content *without entrained air*.

Environment	**Quality**	**Scaling (kg/m^2)**			
		7 cycles	**14 cycles**	**28 cycles**	**56 cycles**
1 vol-% CO_2	**65% slag**	2.48	4.23	5.71	7.29
no CO_2	**65% slag**	0.51	0.99	1.84	3.36

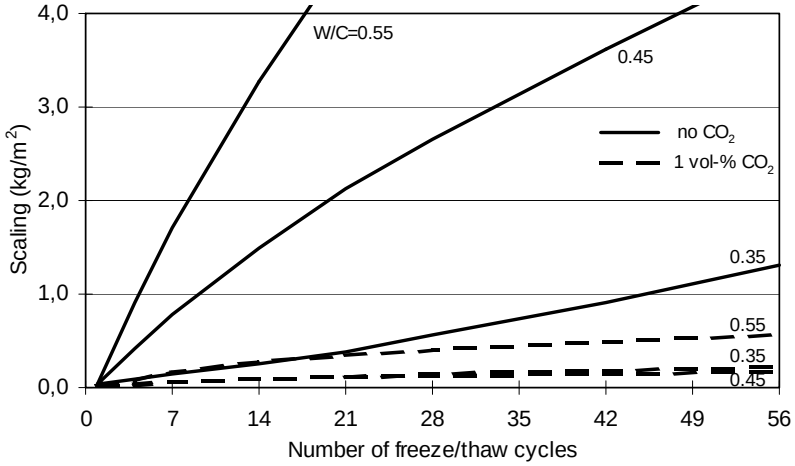

FIGURE 5. Scaling as a function of the number of freeze/thaw cycles for specimens *with entrained air*, conditioned in climate chambers with and without carbon dioxide.

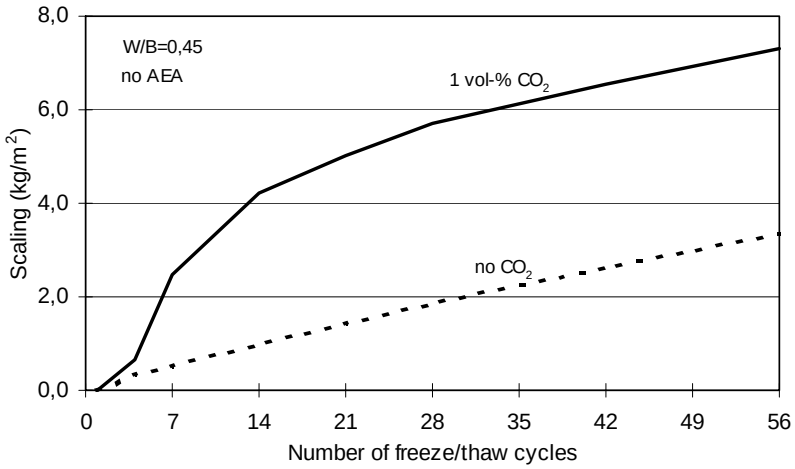

FIGURE 6. Scaling as a function of the number of freeze/thaw cycles for specimens with a *65% slag content and without entrained air*, conditioned in climates without carbon dioxide and with 1 vol-% of carbon dioxide.

7. Discussion

In figure 5 the scaling for concrete with entrained air is presented. From this figure it can bee seen that specimens preconditioned in an environment with increased carbon dioxide content, approx. 1 vol-%, show a much higher scaling resistance than do specimens conditioned in a environment free from carbon dioxide.

The results presented in table 5 show that for concrete without entrained air the tendency is the same as for concrete with entrained air, i.e. concrete with a carbonated test surface shows a much higher scaling resistance than does concrete with a test surface that is not carbonated. These results verifies the hypothesis in [1], i.e. the protective layer consists of a carbonated skin.

According to the test results presented in this investigation it is not possible to explain the effect of carbonation on the scaling resistance. One possible explanation, however, is the reduction of capillary porosity which takes place when OPC concrete carbonates [6, 7, 8, 9], and the positive effect this has on the scaling resistance. That is, the lower the capillary porosity the lower the amount of freezable water and the higher the scaling resistance.

In figure 6 the scaling for concrete without entrained air and with a content of 65% slag in the binder is presented. It can be seen that, as opposed to the results obtained with OPC concrete, the specimens conditioned in an environment with increased carbon dioxide content show a lower scaling resistance than concrete conditioned in an environment free from carbon dioxide. The appearance of the scaling ”curve” for the concrete conditioned in an environment with increased carbon dioxide content indicates that a layer, probably the carbonated skin, is scaled off during the first fourteenth freeze/thaw cycles, after which the scaling slows down and becomes comparable to the rate of scaling for uncarbonated concrete.

The observed reduced scaling resistance for carbonated concrete containing a large amount of slag can probably partially be explained by the coarsening of the pore structure that has been observed on carbonated concrete containing large contents of blast furnace slag [9, 10, 11, 12]. Another probable explanation of the effect of carbonation on the scaling resistance for concrete with a high slag content is the existence of metastable carbonates [13].

The accelerated curing that have been used in this investigation, was chosen in order to study the effect of a long time exposure in a short time. The used concentration, approx. 1 vol-% carbon dioxide, is about 30 times higher than the carbon dioxide content in 'normal' air. The use of high carbon dioxide concentrations has been reported to change the pore structure in a way that normal carbon dioxide concentrations would not do. In [14], however, it was found that curing in 1 vol-% result in approximately the same porosity and pore structure as curing in air with 0.03 vol-% carbon dioxide.

For OPC concrete the scaling resistance is substantially improved already after a short exposure to the carbon dioxide concentration existing in 'normal' air, i.e. approximately 0,03 vol-%. In table 7 results from an investigation carried out at SP are presented. The concrete was produced of the same OPC cement and with the same air entraining agent as were used in this investigation. The water/cement-ratio was 0.45 and the air content was 4.5%. The aggregate used was composed of fractions of a natural gravel with particle sizes of 0-8 mm, 4-8 mm and 8-16 mm. The freeze/thaw method used was SS 13 72 44 with the exception of that the concrete was 60 days old when conditioned for 7 days in two different climates, 65%RH/20°C in 'normal' air (approx. 0.03 vol-% CO_2) and in air without carbon dioxide.

TABLE 7. Results from freeze/thaw tests. Mean value of two specimens.

Environment	**Quality**	**Scaling (kg/m^2)**			
		7 cycles	**14 cycles**	**28 cycles**	**56 cycles**
0.03 vol-% CO_2	**0.45**	0.01	0.02	0.02	0.03
no CO_2	**0.45**	0.31	0.54	0.84	1.12

The results presented in this paper indicate the important influence of the carbonation on the scaling resistance. It can be seen that for some concrete qualities, such as OPC concrete, carbonation leads to an enhanced scaling resistance, while for other concrete qualities, such as concrete containing a high slag content, carbonation leads to a reduced scaling resistance. The influence of carbonation on the scaling resistance of concrete seems to vary widely depending on what kind of binder is used. These findings raise a question about the relevance of the existing test methods used for estimating the scaling resistance of concrete. In most existing test methods, there are no regulations about what kind of concrete that may be tested, and there are also no alternative procedures for different concrete qualities. The existing scaling test methods have generally been developed on the basis of experience of OPC concrete. When new types of concrete qualities, such as those with new types of binders, new admixtures, very low water/binder-ratios etc. are used, we often do not have the sufficient experience and knowledge of how they should be tested. To be able to test new types of concrete qualities, more knowledge is needed and the existing test methods probably need to be modified.

8. Conclusions

From this investigation, the following conclusions can be drawn:

1. Specimens of OPC concrete conditioned in an environment with increased carbon dioxide content, approx. 1 vol-%, show a much higher scaling resistance than do specimens of OPC concrete conditioned in a environment free from carbon dioxide. In other words, carbonation enhances the scaling resistance for OPC concrete.

2. For OPC concrete the scaling resistance is substantially improved already after a short exposure to the carbon dioxide concentration existing in 'normal' air, i.e. approximately 0,03 vol-%.
3. Specimens of concrete containing a high content of slag, 65% of the binder, conditioned in an environment with increased carbon dioxide content, approx. 1 vol-%, show a lower scaling resistance than do specimens conditioned in a environment free from carbon dioxide. In other words, carbonation reduces the scaling resistance for concrete containing a high slag content.
4. Carbonation of the concrete surface influences the scaling resistance in different ways depending on the concrete quality. Since all concrete exposed to an outdoor environment will be more or less carbonated, it is necessary to adjust the freeze/thaw standards, used to estimate the scaling resistance, to take the effect of carbonation into consideration. To be able to test new types of concrete qualities, more knowledge is needed and the existing test methods probably need to be modified.

9. Acknowledgements

The author is grateful to Dr. P-E. Petersson for all the helpful discussions and his encouragement and support. The author would also like to thank Prof. G. Fagerlund for his stimulating guidance and very valuable comments. This project is financially supported by the Swedish Council for Building Research and by the Development Fund of the Swedish Construction Industry.

10. References

1. Utgenannt P., Petersson P.-E., 'Influence of preconditioning on scaling resistance for different types of test surfaces', Proceedings of the International RILEM Workshop on Resistance of Concrete to Freezing and Thawing With or Without De-icing Chemicals, Essen, 1997.
2. Swedish Standard, SS 13 72 44, 'Concrete testing - Hardened concrete - Scaling at freezing', Edition 3 (1995).
3. Utgenannt P., 'Climate chamber for studies of the effect of carbonation', SP-rapport, (Swedish Testing and Research Institute, Borås, 1999).
4. Malmström, K., 'Cementsortens inverkan på betongs frostbeständighet', Rapport 1990:07, (Swedish Testing and Research Institute, Borås, 1990).
5. Utgenannt P., 'Provkroppar tillverkade 1996 - Material- och tillverkningsdata samt resultat från beständighetsprovning i laboratorium', BTB-rapport 1, (Swedish Testing and Research Institute, Borås, 1997).
6. Kropp J., 'Struktur und eigenschaften karbonatisierter betonrandzonen', *Bautenschutz Bausanierung*, Jahrgang 9, No. 2, 1986, 33-39.

7. Distler P., Kropp J., Hilsdorf H. K., 'Pore structure and transport parameters of concretes containing blended cements', 9th International Congress on the Chemistry of Cement, Volume 5, (National Council for Cement and Building Materials, New Delhi, 1992) 431-437.
8. Matsusato H., Ogawa K., Funato M., Sato T., 'Studies on the carbonation of hydrated cement and its effect on microstructure and strength', 9th International Congress on the Chemistry of Cement, Volume 5, (National Council for Cement and Building Materials, New Delhi, 1992) 363-369.
9. Parrott L. J., 'Variations of water absorption rate and porosity with depth from an exposed concrete surface: effects of exposure conditions and cement type', *Cement and Concrete Research*, Vol. 22, 1992, 1077-1088.
10. Matala S., 'Effects of carbonation on the pore structure of granulated blast furnace slag concrete', Helsinki University of Technology, Faculty of Civil Engineering and Surveying, Concrete Technology, Report 6, (Espoo, 1995).
11. Ngala V. T., Page C. L., 'Effects of carbonation on pore structure and diffusional properties of hydrated cement pastes', *Cement and Concrete Research*, Vol. 27, No. 7, 1997, 995-1007.
12. Soers E., Meyskens M., 'Recent experience on microscopical quality control of concrete in relation to durability aspects', in 'Quality control of concrete structures', Proceedings of the second international symposium, Brussels, June, 1991, (E & FN Spon, London, 1991) 269-276.
13. Stark J., Ludwig H.-M., 'Freeze-thaw and freeze-deicing salt resistance of concretes containing cement rich in granulated blast furnace slag', *ACI Materials Journal*, Vol. 94, No. 1, January-February, 1997, 47-55.
14. Knöfel D., Eβer G., 'Einfluβ unterschidlicher Kohlendioxidkonzentrationen auf Zementmörtel', Internationales Kolloquium Werkstoffwissenschaften und Bausanierung, Teil 3, Esslingen, 1992, (Ehningen, 1993) 1408-1418.

APPENDIX 3

FROST RESISTANCE OF CONCRETE CONTAINING SECONDARY CEMENTITIOUS MATERIALS – EXPERIENCE FROM THREE FIELD EXPOSURE SITES

Published in the Proceedings from The Nordic Concrete Federation Workshop on Durability of Exposed Concrete Containing Secondary Cementitious Materials, in Hirtshals, Denmark, 2001

Frost Resistance of Concrete Containing Secondary Cementitious Materials - Experience from Three Field Exposure Sites

Peter Utgenannt
Doctoral candidate
SP Swedish National Testing and Research Institute
Box 857, SE-501 15 Borås, Sweden
e-mail: peter.utgenannt@sp.se

Per-Erik Petersson
Professor, Head of the Department of Building Technology
SP Swedish National Testing and Research Institute
Box 857, SE-501 15 Borås, Sweden
e-mail: pererik.petersson@sp.se

ABSTRACT

Concrete samples made from different cement/binder types, including secondary cementitious materials, have been exposed at three different field test sites for five years. All the sites are situated in Sweden, one in a highway environment, one in a marine environment and one in an environment without salt exposure. The resistance to internal and external frost damage has been regularly evaluated by measurements of change in volume and ultrasonic pulse transmission time. The results after five years' exposure clearly indicate the highway environment as being the most aggressive with regard to external frost damage. The influence of the climate on the internal frost damage is less pronounced. Results show that concretes containing large amounts of slag in the binder have the severest scaling, whether with or without entrained air. For concrete without entrained air, qualities containing OPC + 5 % silica as binder seems to be more susceptible to internal damage than do the other qualities.

Key words: Freeze/thaw, Field test, Laboratory test, Secondary cementitious materials

1. INTRODUCTION

Frost resistance is one of the most important properties determining the durability of concrete in the Scandinavian countries, as well as in other European countries with cold climates. To be able to prove concrete qualities to be frost-resistant a number of test methods have been developed: for example, Swedish Standard SS 13 72 44 for scaling resistance [1], Finnish Standard SFS 5448 for dilation [2] and the measurement for critical degree of saturation [3].

These test methods have been developed primarily on the basis of experience of traditional concrete. When new types of concrete are introduced - for example, with new types of binders, filler materials, admixtures etc. - we do not know how to evaluate the test results or even if the freeze/thaw test methods used are relevant. More knowledge and experience of the salt/frost resistance of these new concrete qualities in the field is needed. One way to acquire this experience is to expose concrete specimens to representative outdoor environments. Such an investigation was started in Sweden in the mid-nineties. Three field exposure sites were established in the south-west of Sweden: one in a highway environment beside highway 40 (60 km east of Gothenburg), one in a marine environment at Träslövsläge harbour (80 km south of Gothenburg) and one in an environment without salt exposure on SP's premises in Borås (70 km east of Gothenburg). The air temperature and relative humidity ranges are the same at the highway exposure site and at SP's premises, with minimum temperatures between –15 °C and –20 °C, and with a precipitation of about 900 mm per year. The temperatures at the marine exposure site at Träslövsläge harbour are somewhat milder, and the precipitation is about 700 mm per year. The micro-climates surrounding the test specimens, however, vary significantly between the three sites, with the highway microclimate being the most moist and saline, and the climate at SP being the 'mildest', with no salt and only pure precipitation.

A large number of concrete mixtures of varying quality with different binder types/combinations, varying water/binder ratios and air contents were produced and placed at the field exposure sites. The frost damage has been regularly evaluated by measurements of the volume change of the specimens and the change in ultrasonic transmission time through each specimen. This paper presents results after five winter seasons for concrete qualities produced with four different binder combinations: one with Ordinary Portland Cement (OPC), one with a CEM III cement type and two with OPC and secondary cementitious materials.

2. MATERIALS AND SPECIMENS

The binder types/combinations studied in this investigation are shown in Table 1. For chemical composition, see [4].

Table 1 - Binder types/combinations investigated

	Binder type/combination	Comments
1	OPC[1)] (CEM I)	Low alkali, sulphur-resistant
2	OPC[1)] + 5 % silica by binder weight	Silica in the form of slurry
3	OPC[1)] + 30 % slag by binder weight	Ground blast furnace slag added in the mixer
4	CEM III/B	Dutch slag cement, ~70 % slag

[1)] OPC = Ordinary Portland Cement (Degerhamn standard [5] is a low-alkali, sulphur-resistant cement)

Ten different concrete qualities were produced for each of the binder types/combinations. Concrete qualities with five different water/binder (w/b) ratios (0.30, 0.35, 0.40, 0.50, 0.75), and with and without entrained air, were produced for all binder combinations. 0-8 mm natural and 8-16 mm crushed aggregate was used for all mixes. A naphthalene-based plasticizer, Melcrete, was used for mixtures with w/b-ratio of 0.40 and lower. The air-entraining agent used, L16, is a tall-oil derivative. A summary of concrete constituents and properties is presented in Table 2 below, for a complete presentation see [4].

Table 2 - Concrete qualities used in this investigation.

Binder type	w/b-ratio	Eqv. w/c-ratio[1]	Cement (kg/m^3)	SCM[2] (kg/m^3)	AEA[3]	Air content fresh (%)	Slump (mm)	Compressive strength (MPa) SS[4]	Recalc[5]	Scaling (kg/m^2)[6] 28	56
OPC	0.30	0.30	500	-	Yes	4.8	240	95	87	0.024	0.035
	0.35	0.35	450	-	Yes	4.8	190	95	87	0.054	0.085
	0.40	0.40	420	-	Yes	4.6	125	67	60	0.014	0.023
	0.50	0.50	370	-	Yes	4.6	90	49	44	0.017	0.022
	0.75	0.75	260	-	Yes	4.7	100	21	18	0.127	0.141
	0.30	0.30	500	-	No	1.1	120	102	93	0.156	0.256
	0.35	0.35	450	-	No	1.2	140	91	83	1.94	4.39
	0.40	0.40	420	-	No	0.8	130	87	79	3.11	7.92
	0.50	0.50	385	-	No	0.8	70	56	50	5.09	14.5
	0.75	0.75	265	-	No	0.9	60	31	27	4.34	>15
OPC+5% silica	0.30	0.29	475	25	Yes	4.6	100	103	94	0.041	0.119
	0.35	0.33	427.5	22.5	Yes	4.5	90	91	83	0.022	0.041
	0.40	0.38	399	21	Yes	4.8	105	72	65	0.023	0.035
	0.50	0.48	361	19	Yes	4.6	70	57	51	0.020	0.026
	0.75	0.71	237.5	12.5	Yes	4.3	70	25	22	0.19	0.20
	0.30	0.29	475	25	No	1.1	125	121	111	0.12	0.20
	0.35	0.33	427.5	22.5	No	1.1	90	105	96	0.36	0.89
	0.40	0.38	399	21	No	0.5	100	84	76	1.67	3.25
	0.50	0.48	370.5	19.5	No	1.2	60	67	60	1.86	4.61
	0.75	0.71	256.5	13.5	No	0.3	75	35	31	3.45	6.58
OPC+30% slag	0.30	0.34	350	150	Yes	4.8	230	90	82	0.031	0.045
	0.35	0.40	315	135	Yes	4.8	130	86	78	0.086	0.139
	0.40	0.45	294	126	Yes	4.4	110	65	58	0.041	0.067
	0.50	0.57	259	111	Yes	4.8	80	49	44	0.021	0.033
	0.75	0.85	175	75	Yes	4.4	100	20	17	0.490	0.538
	0.30	0.34	350	150	No	0.7	220	101	92	0.097	0.128
	0.35	0.40	315	135	No	1.1	140	91	83	1.78	3.61
	0.40	0.45	294	126	No	0.9	120	78	71	1.78	3.83
	0.50	0.57	273	117	No	1.3	80	52	46	0.864	1.94
	0.75	0.85	185.5	79.5	No	0.5	80	25	22	1.58	4.37
CEM III	0.30	0.30	520	-	Yes	4.8	200	78	71	0.245	0.356
(~70% slag)	0.35	0.35	460	-	Yes	4.7	200	74	67	0.434	0.615
	0.40	0.40	420	-	Yes	4.3	120	61	55	0.568	0.845
	0.50	0.50	380	-	Yes	4.5	70	46	41	0.993	1.66
	0.75	0.75	255	-	Yes	4.4	90	26	23	2.05	3.16
	0.30	0.30	520	-	No	0.8	200	99	90	0.221	0.281
	0.35	0.35	470	-	No	0.7	200	80	72	0.490	0.653
	0.40	0.40	420	-	No	0.9	125	68	61	0.837	1.14
	0.50	0.50	400	-	No	1.0	65	54	48	1.21	1.61
	0.75	0.75	265	-	No	0.1	100	31	27	3.94	6.89

[1] Eqv. w/c-ratio= water/(cement + 2∗silica + 0.6∗slag). Not applicable for CEM III cement.
[2] SCM – Secondary Cementitious Materials
[3] AEA – Air Entraining Agent
[4] Dry stored cubes tested according to SS 13 72 10 at the age of 28 days
[5] Recalculated to wet stored cubes according to $f_{wet,cube}=0.76*(f_{dry,cube})^{1.04}$
[6] According to the 'Slab test', SS 13 72 44, freeze/thaw started at the age of 31 days

All concrete batches were produced in the autumn of 1996, and a number of 150 mm cubes were cast from each batch. The cubes were demoulded 24 hours after casting, and stored in lime-saturated water for six days. They were then stored in a climate chamber (50 % RH / 20 °C) for a period of between one and a half and three months. Between eight and twelve days

before the specimens were placed at the field test sites, the cubes were cut, resulting in two specimens with the shape of a half 150 mm cube with one cut surface and the rest mould surfaces. After cutting, the specimens were stored in a climate chamber (50 % RH / 20 °C) until placed at the test site. During this second conditioning period, the volume of, and transmission time through, each specimen were measured. Two specimens of each mixture were then placed at each test site.

At the highway environment test site, the specimens were placed in steel frames close to the road, so that they were splashed by the passing traffic. At the marine test site, the specimens were mounted on top of a pontoon, thus exposing them to the saline marine environment but with no direct contact with the sea water, except when splashed over them by storms. The specimens at the test site without salt exposure were placed on top of loading pallets: here, they were exposed only to water from precipitation. At all sites, the specimens were exposed with the cut surface turned upwards.

3. TEST PROCEDURES

In order to be able to detect both internal and external frost damage, the change in volume and ultrasonic pulse transmission time was measured regularly. The first measurement was carried out before placing the specimens at the test sites. The specimens at the highway site have subsequently been measured once a year, and the specimens at the other two sites after two, four and five years.

The volumes of the specimens are calculated from results obtained from measuring the weight of the specimens in water and in air respectively. The ultrasonic pulse transmission time through the specimen is measured as a mean of three measurement positions, where possible, on each specimen.

The following laboratory tests were carried out on each concrete mix in order to determine the concrete characteristics:

Testing the fresh concrete:

- Air content
- Density
- Slump
- Remoulding test

Testing the hardened concrete:

- Compressive strength in accordance with Swedish standard (SS) 13 72 10.
- Salt/frost resistance in accordance with SS 13 72 44 ('the slab test').
- Microscopical determination of the air void system, in principal in accordance with ASTM C 457.

Results from these tests are given partly in Table 2 above, and fully in Reference 4.

4. RESULTS

Figures 1-4 present results from measurements of the volume change after five years of exposure at the three field exposure sites. The reference value is the initial volume before exposure. Figures 1-3 show the results for concrete produced without entrained air, exposed at the three exposure sites, while Figure 4 shows the results for concrete with entrained air (4-5 %) exposed at the test site in a highway environment. Each point is a mean value of measurements on two specimens.

Figures 5-7 show the relative transmission time after five years' of exposure at the three field exposure sites. The reference value is that of measurements before exposure. Each point is a mean value of up to three measurements on each two test specimens, i.e. a mean value of up to six measurements. For some qualities with w/b-ratio 0.75, no value is presented. This is because damage to the concrete surfaces was so severe that measurements were not possible.

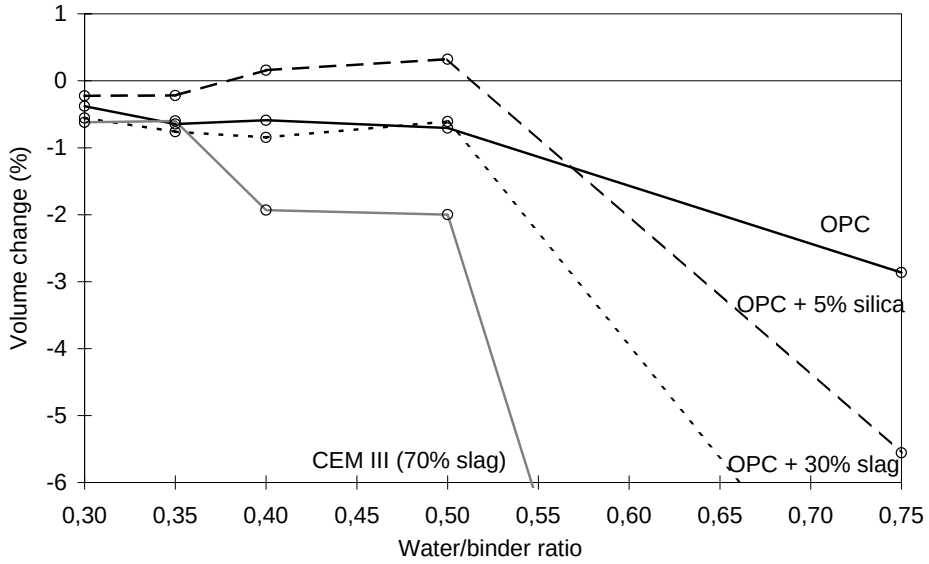

Figure 1 - Volume change after five winter seasons at the highway exposure site (Highway 40). Concrete with different binder combinations and water/binder ratios. No entrained air.

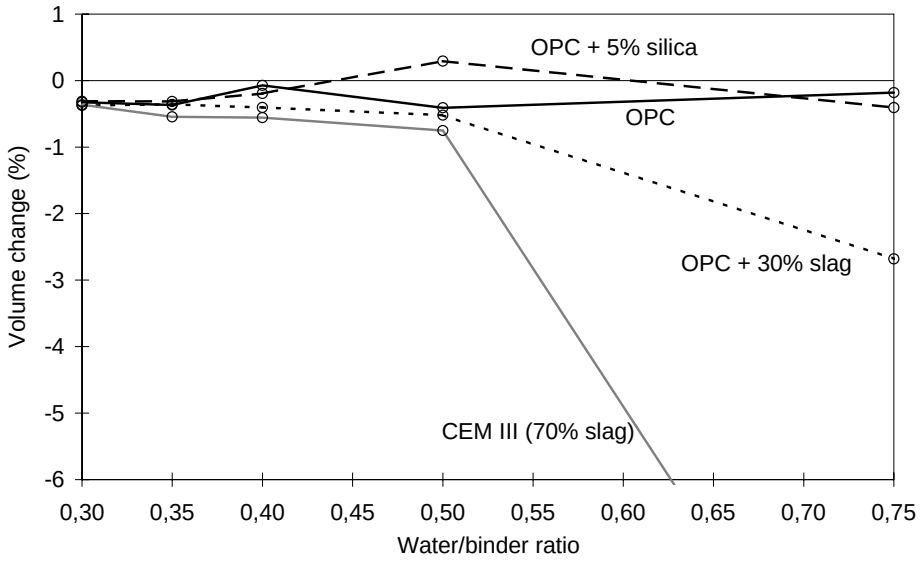

Figure 2 - Volume change after five winter seasons at the marine exposure site (Träslövsläge harbour). Concrete with different binder combinations and water/binder ratios. No entrained air.

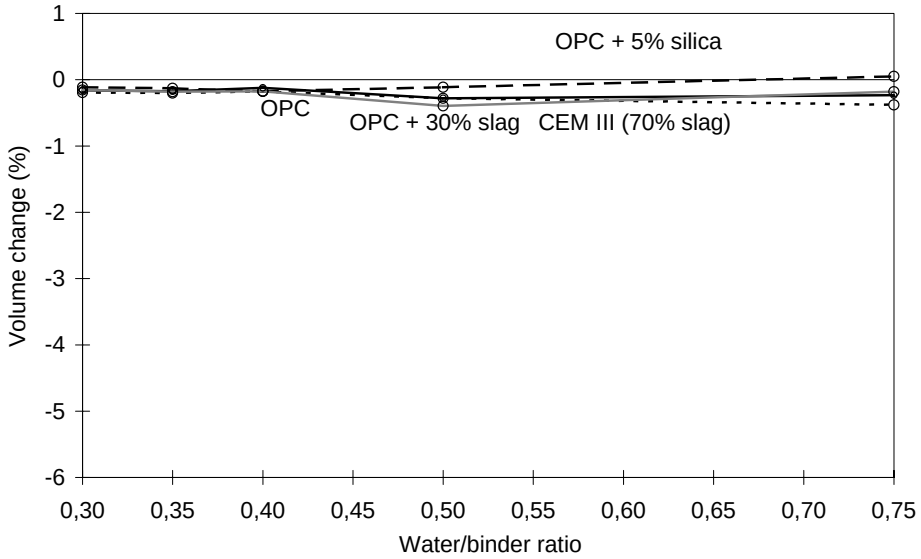

Figure 3 - Volume change after five winter seasons at the no-salt exposure site (SP in Borås). Concrete with different binder combinations and water/binder ratios. No entrained air.

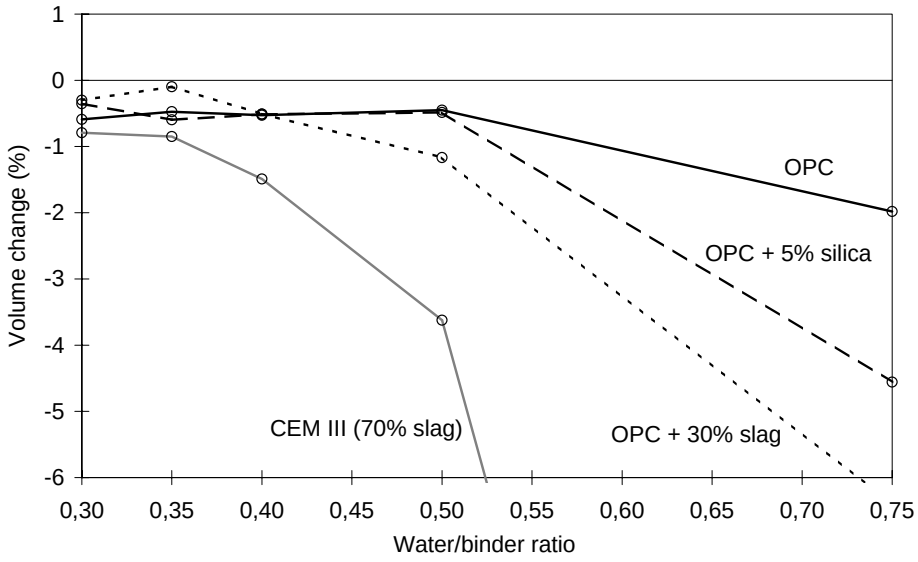

Figure 4 - Volume change after five winter seasons at the highway exposure site (Highway 40). Concrete with different binder combinations and water/binder ratios. With entrained air (4-5 %).

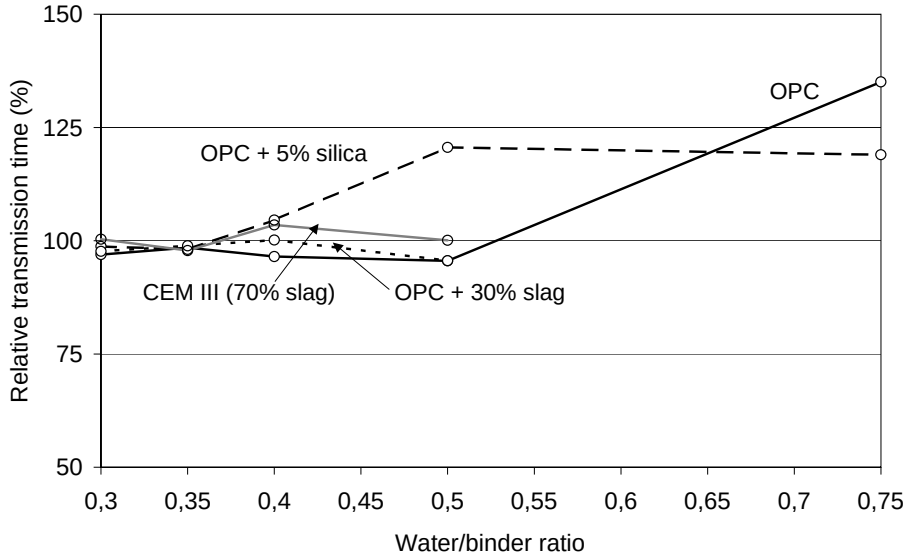

Figure 5 - Relative transmission time after five winter seasons at the highway exposure site (Highway 40). Concrete with different binder combinations and water/binder ratios. No entrained air.

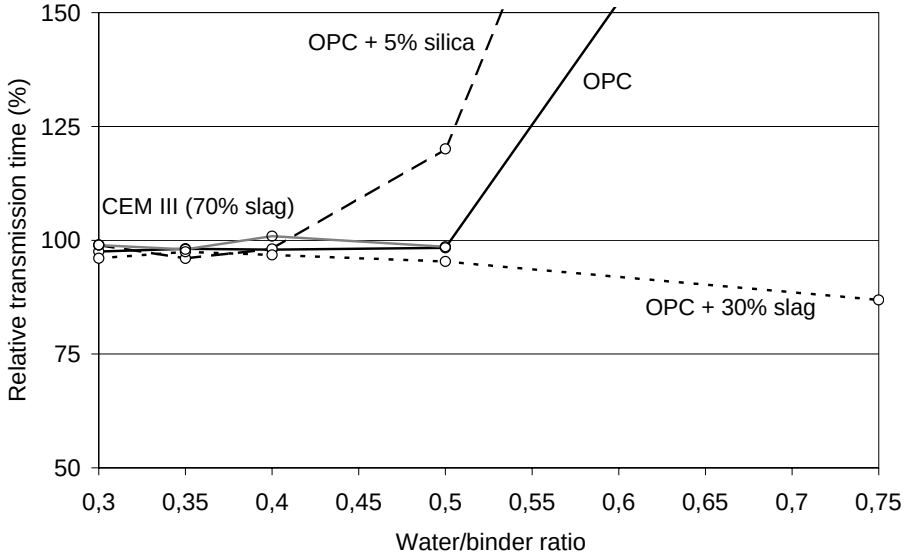

Figure 6 - Relative transmission time after five winter seasons at the marine exposure site (Träslövsläge harbour). Concrete with different binder combinations and water/binder ratios. No entrained air.

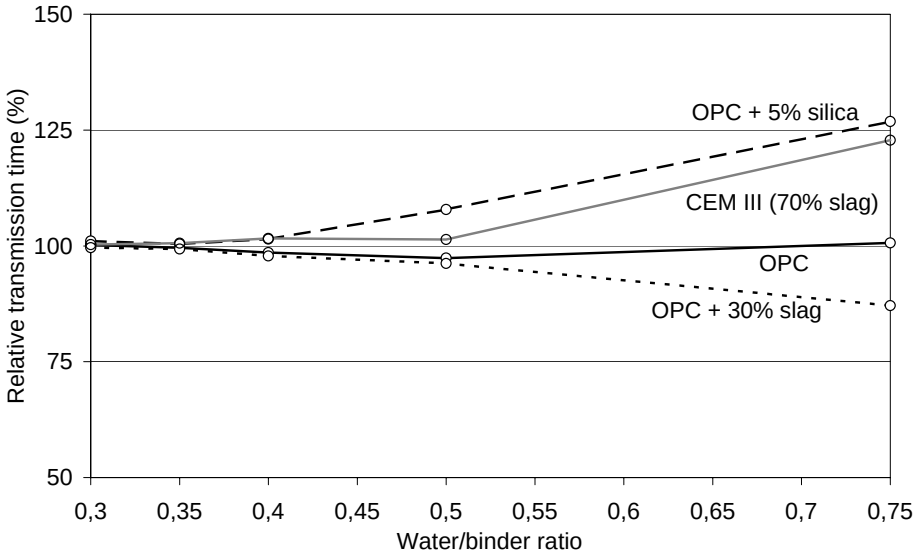

Figure 7 - Relative transmission time after five winter seasons at the no-salt exposure site (SP in Borås). Concrete with different binder combinations and water/binder ratios. No entrained air.

5. DISCUSSION

5.1 External frost damage

Figures 1, 2 and 3 show the external damage in the form of volume change after five winter seasons for different concrete qualities, all without entrained air, exposed in three different climates. Without comparing results from the different concrete qualities, it is clear that the climate has a large influence on the amount of external frost damage, i.e. surface scaling. Concrete exposed in a saline highway environment, Figure 1, shows much more extensive surface scaling than does concrete exposed in a salt-free environment. Concrete exposed in the marine environment shows external damage, but not as severe as concrete exposed in the highway environment, at least for qualities with w/b-ratios of 0.40 and over. These considerable differences in resistance to surface scaling can probably be explained by differences in:

- **Temperature**. The temperature in the marine environment is milder and fluctuates less than the temperature at the highway environment or the salt-free exposure site. However, the air temperature at these two latter sites is about the same.
- **Moisture conditions**. The moisture conditions at the different exposure sites vary significantly. During the winter months, the specimens at the highway site are subjected to a very moist environment, being constantly splashed by passing traffic. The specimens at the SP test site, however, are exposed only to natural precipitation.
- **Salt concentration**. The salt concentration in the water splashed over the samples at the highway site is, at least occasionally, much higher than the salt concentration in the marine environment. At the SP test site there is no exposure to salt.

Some significant differences with regard to surface scaling can be seen when comparing the different concrete qualities. For example, qualities with slag as part of the binder (CEM III and OPC + 30 % slag) show more severe external damage than mixtures with OPC and OPC + 5 % silica concrete, at least for qualities with w/b-ratio of 0.75. This is seen both at the highway and the marine exposure site. Concrete exposed at the salt-free test site, however, shows only small volume changes, irrespective of binder combination. Another significant difference is the increase in volume for some concrete qualities with OPC + 5 % silica as binder and with a w/b-ratio over 0.35. This increase is seen primarily at the highway and marine test sites. An increase in volume is probably caused by internal damage, i.e. micro-cracks: see further discussion below. A limitation of the volume measurements is that the measured volume is a net volume of both a negative and a positive element, in the respective forms of a volume loss due to surface scaling and a possible increase in volume due to internal cracking. Concrete qualities with an apparent volume loss might, therefore, also have a small increase in volume caused by internal cracking without this being observed. It is therefore important to complement volume measurements with other techniques in order to detect possible internal damage, e.g. ultrasonic pulse transmission time measurements.

Figure 4 shows the volume change after five winter seasons for concrete mixtures with entrained air exposed to the saline highway environment. In general, the volume changes for concrete with high water/binder ratios and entrained air are less than for concrete without entrained air (Figure 1). However, this is not valid for concrete qualities with CEM III as the binder. The volume change for qualities with CEM III as the binder and with entrained air is of the same order as (and sometimes even greater than) that for concrete without entrained air (w/b-ratios 0.50 and 0.75). For these qualities, entrained air does not seem to improve the

scaling resistance. This behaviour is confirmed by freeze/thaw testing in the laboratory, see Table 2. For concrete with CEM III as the binder, the air entrained qualities show damage of the same order as for concrete without air. For concrete with other binder types in this investigation, as expected, a significant improvement in scaling resistance is seen for qualities with entrained air compared to qualities without entrained air.

Comparing the results for concrete with and without entrained air after five years of exposure show in general only small differences in volume change for concrete with w/b-ratio 0.5 and below. However, the increases in volume for concrete qualities with OPC + 5 % silica that were observed in samples without entrained air are, as expected, not observed when entrained air is used.

5.2 Internal frost damage

Figures 5, 6 and 7 show the relative transmission time after five years of exposure for different concrete qualities, all without entrained air, exposed in three different climates. A relative transmission time over 100 indicates possible internal damage. Values over about 110 are more certain indications of internal damage. The results presented in Figures 5-7 show that a number of concrete qualities probably have internal damage and that there does not seem to be any significant difference between the different exposure climates. Table 3 shows the concrete qualities with possible internal damage at each test site.

Table 3 - Concrete qualities with potential internal damage at the three test sites. Detected by ultrasonic pulse transmission time.

Concrete quality	Highway	Marine	No salt exposure
OPC no air w/b 0.75	Damaged	Damaged	No D. indication
OPC+5 % silica no air w/b 0.75	Damaged	Damaged	Damaged
OPC+5 % silica no air w/b 0.50	Damaged	Damaged	Damaged
OPC+5 % silica no air w/b 0.40	Damaged	No D. indication	No D. indication
CEM III (70 % slag) no air w/b 0.75	Not measured	Not measured	Damaged

Combining the results from volume measurements with the transmission time measurements gives clear indications of internal damage for the concrete qualities with OPC + 5 % silica as binder shown in Table 3. Both an increase in volume and an increase in transmission time clearly indicate internal damage, probably micro-cracking. The surfaces of the qualities that show increased transmission time but no detectable increase in volume are too severely damaged to permit the detection of an increase in volume due to internal cracking. Microscopic techniques, such as analysis of polished sections or thin sections, could be used for finding further evidence of internal damage.

Polished sections were cut from each concrete quality listed in Table 3 to confirm and show possible internal cracking. The sections confirmed that the qualities judged as having internal damage when tested with ultrasonic pulse transmission time all showed internal cracking. Figure 8 show pictures of polished samples impregnated with epoxy resin and fluorescent dye for the three qualities with OPC + 5 % silica as binder listed in Table 3, exposed at the highway test site. The pictures show internal cracking in all three qualities, which increases in severity with increasing w/b-ratio.

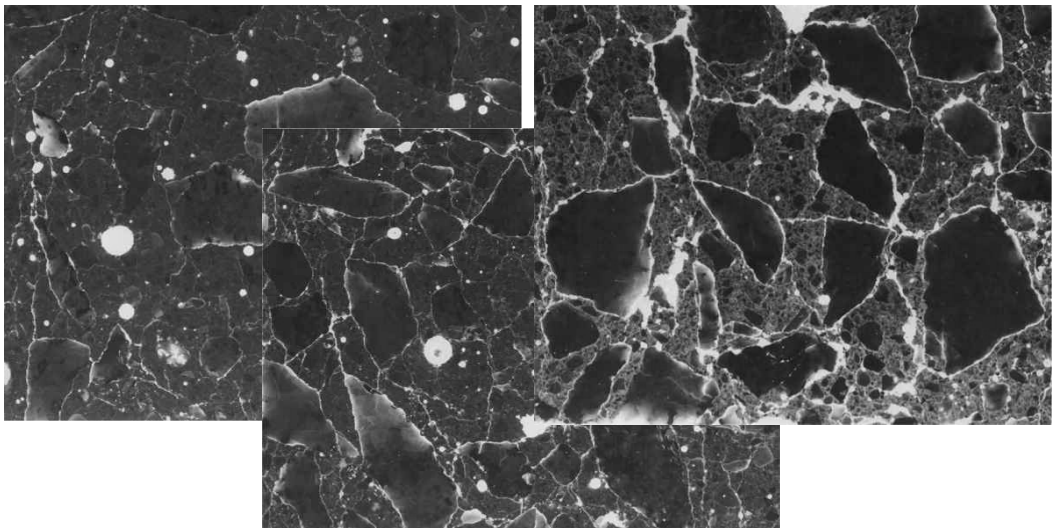

Figure 8 - Pictures of polished samples impregnated with epoxy resin and fluorescent dye of three concrete qualities exposed for five years at the highway exposure site. All with OPC + 5 % silica as binder and no air. From left: w/b 0.40; w/b 0.50; w/b 0.75.

The results from this investigation indicate that the concrete qualities with OPC + 5 % silica as binder and without entrained air seem more susceptible to internal frost damage than the other concrete qualities.

For the concrete quality with CEM III as binder in Table 3 it was not possible to measure the transmission time because of excessive surface damage. Microscopic analyses, however, show that the amount of internal damage, if any, is limited, see Figure 9. From the results discussed above, it seems as if the concrete qualities containing slag as part of the binder and without entrained air in this investigation are somewhat more resistant to internal damage than at least the concrete qualities with OPC + 5 % silica as binder. On the other hand, the concrete qualities with large amounts of slag as part of the binder seem to be more susceptible to scaling.

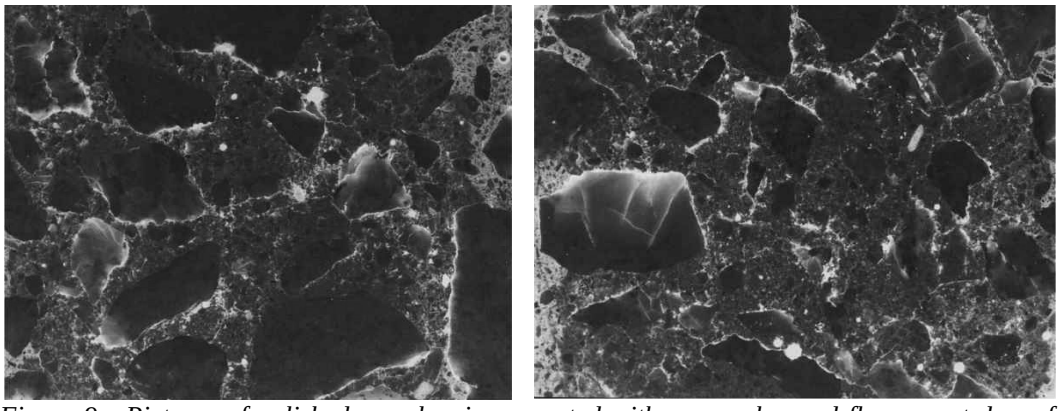

Figure 9 - Pictures of polished samples, impregnated with epoxy glue and fluorescent dye, of two concrete qualities exposed for five years at the highway and the marine exposure sites. From left: CEM III, no air and w/b 0.75, highway climate; CEM III, no air and w/b 0.75, marine climate.

A certain degree of 'healing' of specimens exposed at the highway site has been noted during the yearly measurements. Figure 10 shows results from yearly measurements of ultrasonic pulse transmission time on the three damaged concrete qualities with OPC + 5 % silica as binder.

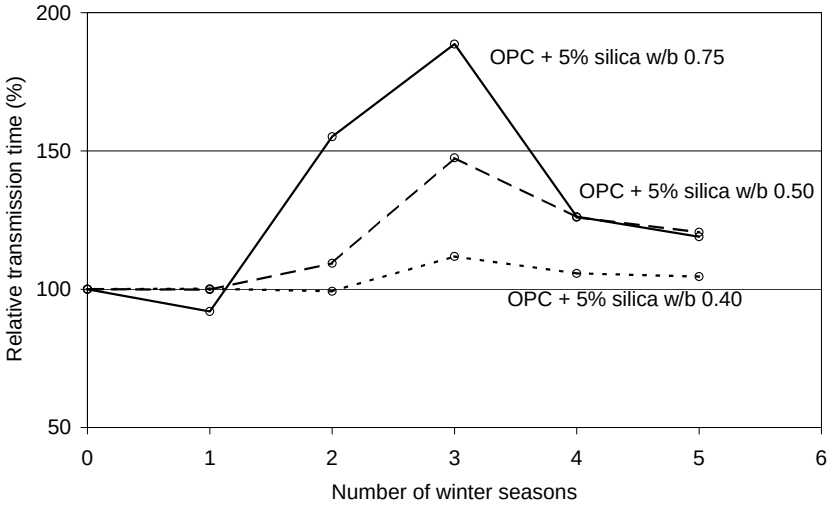

Figure 10 - Relative transmission time during five years of exposure at the highway exposure site.

The results in Figure 10 indicate a 'healing' effect after the third year, leading to reduced relative transmission time. Even though the reduction in relative transmission time or 'healing' seem substantial, the reduction can be caused by relatively limited healing. Only a few healing points are needed for an ultrasonic pulse to find a faster, shorter way through damaged material: see Figure 11. The healing can be explained by reaction between unhydrated cement and moisture transported in to the cracks, forming barriers of hydration products in the cracks and enabling the ultrasonic pulse to find a shorter way through the material.

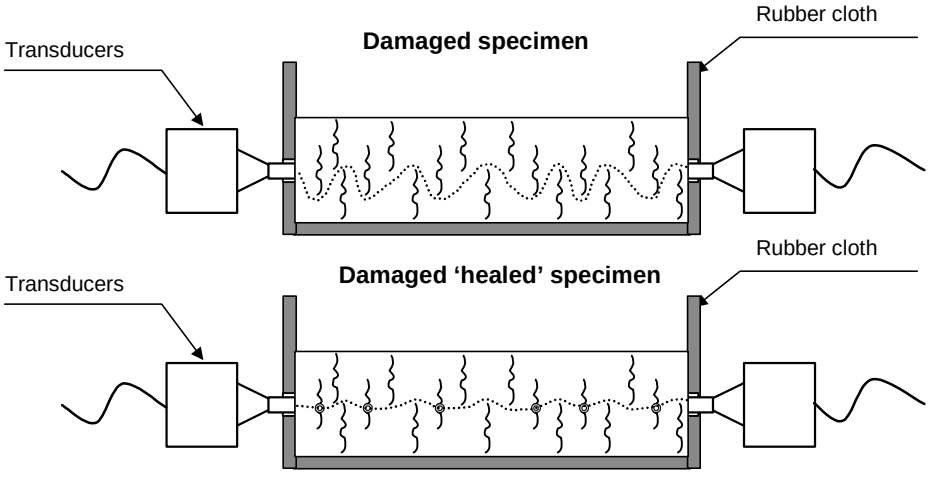

Figure 11 - Sketches of an ultrasonic pulse during transmission time measurements in a damaged specimen (top) and a specimen that has 'healed' (bottom).

This type of healing, where the hydration products form local barriers between cracks, gives no substantial healing in form of increased strength, durability or resistance to moisture or chlorides. Most of the network of micro cracks will probably still be open to an infiltration of moisture and chlorides, even though local healing creates a short cut for the ultrasonic pulse, resulting in a significantly shorter transmission time. This healing effect makes it hazardous to draw conclusions from single or even regular (if at long intervals) measurements of transmission time. A single measurement, after five year, on the concrete qualities shown in Figure 10 would lead to the conclusion that there might be some internal damage but not particularly severe. Evaluating results from yearly measurements and microscopic analysis (Figure 8) gives an indication of more severely damaged concrete. This is important knowledge when evaluating results not only from measurements in the laboratory but especially also when evaluating results from measurements in the field. From practical and economic points of view, it might be difficult to make measurements on building structures in the field on a more regular basis.

From the results described above, it can be noted that concrete with OPC or OPC + 5 % silica, with entrained air and a water/binder ratio of 0.50 or lower, seems to be salt/frost resistant in an aggressive highway environment, at least after five years' of exposure. Concrete qualities containing large amounts of slag as binder, however, seem to be less resistant to external salt/frost damage than concrete with OPC or OPC with some silica, at least when exposed to aggressive climates such as the highway or marine climate. These results are in agreement with results from an extensive field exposure investigation presented in [6]. In that investigation, a large number of concrete qualities with different amounts of slag and fly ash in the binder were exposed to the marine climate at the Treat Island exposure site, Canada. Results from that investigation clearly show that salt/frost resistance decreases with increasing amounts of slag as part of the binder; a result that is confirmed by the present investigation. As in the present investigation, the investigation at Treat Island also showed the positive effect of low water/binder ratio on the salt/frost resistance of concrete. The negative effects of high slag contents in the binder on the salt/frost resistance of concrete have been reported by several researchers, see [7, 8, 9, 10]. One probable explanation for this negative effect is the coarsening of the pore structure found in the carbonated skin of concrete containing slag [7, 9, 11]. Another probable explanation, presented in [9], is the existence of metastable carbonates in the carbonated zone of concrete rich in slag.

5.3 Correlation between laboratory and field tests

When testing the durability in the laboratory, e.g. salt/frost resistance, results are wanted that are relevant to durability in the actual field conditions. In the present investigation, each concrete quality was tested in the laboratory at the prescribed age of 28 days in accordance with the Swedish Standard for salt/frost resistance, SS 13 72 44 (the 'slab test'). Comparing the laboratory results with results from the field exposure site at SP's site (no salt exposure) is not relevant, since salt/frost resistant concrete are not prescribed in this climate. Concrete exposed at the marine and highway test sites is, however well suited for 'calibration' of the laboratory test method. Since the climate at the highway has proven to be most aggressive with regard to salt/frost resistance, the laboratory results are compared with results from this test site.

Figure 12 shows results from the laboratory tests and the volume change after five years of highway exposure. The diagram shows the scaling (kg/m²) after 56 freeze/thaw cycles as a function of the volume loss (%) after five years' highway exposure. The acceptance criterion in the laboratory test is 1 kg/m^2 (illustrated by a horizontal line). An acceptance criterion of 1.5 vol-

ume % (shown by the vertical line) after five years' exposure has been chosen for the field exposure specimens, corresponding to scaling of approximately 0.6 kg/m^2. Filled symbols represent concrete without entrained air. Symbols with a white centre represent concrete with entrained air. Enlarged symbols represent qualities with internal damage.

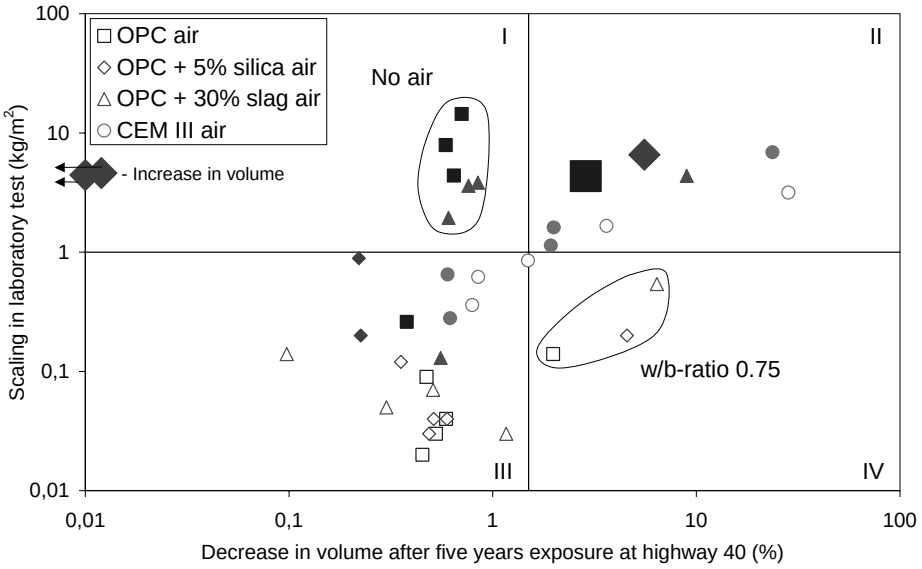

Figure 12 - Scaling resistance (tested in the laboratory) as a function of the decrease in volume for specimens exposed in the highway environment for five winter seasons. Filled symbols represent concrete without entrained air. Symbols with a white centre represent concrete with entrained air. Large symbols represent internal damage.

From the results presented in Figure 12, it can be seen that only three qualities fall into the IV quadrant, which is the worst case, and means that they are accepted by the test method, but fail in field exposure. These are air entrained qualities, however, with high water/binder ratios (0.75). The standard test method is primarily intended to be used for bridge concrete, with entrained air and with a w/b-ratio below 0.5.

Most qualities falls into quadrants II or III, which means that the test method and 'reality' correspond. Some concrete qualities fall into quadrant I, which means that the test method rejects them. However, as the concrete in quadrant I show only limited damage in the field, the test method results are on the safe side. None of these qualities has any entrained air, which makes them especially susceptible to frost damage. During the first five years, the climate has not been aggressive enough significantly to damage these qualities. However, one winter season with a more aggressive climate might cause internal damage as well as scaling on these qualities without entrained air, moving them into quadrant II. Two concrete qualities show an increase in volume and an increased transmission time, indicating internal frost damage. These qualities also fail the acceptance criterion when tested in the laboratory.

One explanation for the limited scaling in the field for the concrete qualities in quadrant I might be a positive effect of ageing. In a field investigation reported in [12], it was found that concrete aged and exposed in a marine climate showed better scaling resistance when tested in the labo-

ratory after aging than did virgin concrete. This increase in scaling resistance was especially apparent for concrete without entrained air, as was also found in this investigation. One effect of ageing that markedly improves the scaling resistance for OPC concrete is carbonation see [10].

On the whole, the results for concrete with w/b-ratio equal to or below 0.5 and with entrained air, shown in Figure 12, indicate that the slab test classifies these concrete qualities as could be expected. This is true for all binder combinations tested.

The results presented here are valid only for the materials, e.g. cement and binder types, used in this investigation. Other materials may lead to different results.

6. CONCLUSIONS

The following conclusions can be drawn after five years' exposure at the field exposure sites in a highway environment, a marine environment and a salt-free environment:

- There are substantial differences in external frost damage, depending on the environment. The most extensive external frost damage is observed on concrete specimens exposed in the highway environment. Concrete exposed in the salt-free environment shows only small changes in volume after five winter seasons.

- For all concrete qualities, scaling takes place only when exposed to salt. Internal damage, however, is observed on concrete qualities exposed at all three test sites, even when no salt is present.

- Concrete with OPC or OPC + 5 % silica as binder, with entrained air and a water/binder ratio of 0.5 or below, has good resistance to internal and external damage. Concrete with CEM III, however, suffers from severe scaling even with w/b-ratio below 0.5 and with entrained air.

- Internal damage is observed only for concrete qualities without entrained air and, furthermore, in most cases for concrete qualities with high water/binder ratios. However, for concrete qualities with OPC + 5 % silica as binder, internal damage is found at lower w/b-ratios, down to w/b 0.4.

- A 'healing' effect is observed on specimens with internal damage (cracking), making results from ultrasonic transmission time measurements hazardous to interpret. Interpreting results from single measurements can therefore lead to incorrect conclusions.

- Comparing results from laboratory testing in accordance with SS 13 72 44 (the 'slab test'), with results after five years of exposure at the field exposure sites, shows that the laboratory standard classifies most concrete qualities correctly.

7. ACKNOWLEDGEMENTS

This project is financially supported by FORMAS, the Development Fund of the Swedish Construction Industry and the cement producer Cementa AB.

8. REFERENCES

1. SS 13 72 44, 'Concrete testing- Hardened concrete- Frost resistance', Swedish Standards Institution (SIS, Stockholm), 3rd edition, 1995.
2. SFS 5448, 'Concrete, Durability, Freezing dilation', Finnish Standardisation Association (SFS), Helsinki, 1988.
3. Fagerlund, G., 'The critical degree of saturation method of assessing the freeze/thaw resistance of concrete', *Materials and Structures*, Vol.10, No.51, pp.217-229, 1977.
4. Utgenannt, P., 'The effect of binder on the frost resistance of concrete - Test specimens produced in 1996 - Material and production data and results from life testing in the laboratory', Swedish National Testing and Research Institute, BTB report no 1, 1997, (in Swedish).
5. Malmström, K., 'Cementsortens inverkan på betongs frostbeständighet' [The effect of cement type on the frost resistance of concrete], Swedish National Testing and Research Institute, Rapport 1990:07, 1990, (in Swedish).
6. Bremner, T.W. et.al., 'Role of supplementary cementing materials in concrete for the marine environment', in 'Durability of concrete – Aspects of admixtures and industrial by-products', Proceedings from the 2nd International seminar on - Some aspects of admixtures and industrial by-products, (Swedish council for building research, Gothenburg), 1989, pp. 23-32.
7. Gunter, M. et.al., 'Effect of curing and type of cement on the resistance of concrete to freezing in deicing salt solutions', ACI, SP 100, vol. 1, 1987, pp. 877-899.
8. Vesikari, E., 'The effect of ageing on the durability of concrete including by-products', in 'Durable concrete with industrial by-products', Proceedings from VTT Nordic research symposium 89, (Technical research center of Finland, Espoo), 1988, pp. 104-112.
9. Stark, J. et.al., 'Freeze-thaw and freeze-deicing salt resistance of concretes containing cement rich in granulated blast furnace slag', *ACI Materials Journal*, Vol. 94, No.1, 1997, pp. 47-55.
10. Utgenannt, P., 'Influence of carbonation on the scaling resistance of OPC concrete', Proceedings from the RILEM Workshop on Frost Damage in Concrete, Minneapolis, USA, 1999.
11. Matala, S., 'Effects of carbonation on the pore structure of granulated blast furnace slag concrete', Helsinki University of Technology, Faculty of Civil Engineering and Surveying, Concrete Technology, Report 6, Espoo, 1995.
12. Petersson, P.-E., 'Scaling resistance of concrete – Field exposure tests', Swedish National Testing and Research Institute, SP-report 1995:73, Borås, Sweden, 1995, (in Swedish).

APPENDIX 4

CHEMICAL ANALYSIS OF CEMENT AND SECONDARY CEMENTITIOUS MATERIALS

Chemical analysis and mechanical and physical properties of cement and secondary cementitious materials - Nominal values for materials used in investigations described in Chapters 2 to 10 of this thesis.

		OPC (Degerhamn std) Cementa AB	Silica slurry Tank in Aarhus Elkem A/S	Granulated Blast Furnace Slag Merox AB
		Spot sample 1999, week 46 [1]	Spot sample 1999 08 23 [2]	Spot sample 1999 12 01 [3]
CaO	**(%)**	64.6	0.61	31.2
SiO_2	**(%)**	22.2	93.3	32.7
SiC	**(%)**	-	0.97	-
C	**(%)**	-	1.68	-
Al_2O_3	**(%)**	3.21	0.72	12.8
Fe_2O_3	**(%)**	4.24	0.77	0.2 (FeO)
MgO	**(%)**	0.94	0.49	17.4
K_2O	**(%)**	0.63	0.81	0.57
Na_2O	**(%)**	0.07	0.20	0.58
Na_2O - ekv	**(%)**	0.48	0.73	0.96
SO_3	**(%)**	2.42	0.71	3.68
Cl^-	**(%)**	<0.01	0.05	0.02
Loss on ignition	**(%)**	0.67	2.17	1.4
Glass content	**(%)**	-	-	95.3
C_3S [4]		59.7	-	-
C_2S [4]		18.6	-	-
C_3A [4]		1.3	-	-
C_4AF [4]		12.9	-	-
Specific surface	**m^2/kg**	305	20400	506
Setting time	**min**	130	-	-
Dry material content	**(%)**	-	50.3	-
Compressive strength	**MPa**			
2 days		23.7	-	-
28 days		53.4	-	-

[1] Chemical analyses carried out at Scancem Research, and provided by the producer; measurements of mechanical and physical properties carried out at SP in Borås.

[2] Chemical analyses and measurements of mechanical and physical properties provided by the producer.

[3] Chemical analyses provided by the producer. Physical properties measured at SP in Borås.

[4] Calculated according to equations in ASTM C150:1998, pp. 141.

Chemical analysis and mechanical and physical properties of cement and secondary cementitious materials used for concrete at the field exposure sites, described in Chapter 11 of this thesis.

	OPC/CEM I (Degerhamn std) Cementa AB	Silica slurry Tank in Copenhagen Elkem A/S	Granulated Blast Furnace Slag Merox AB	CEM III/B Dutch slag cement (~75%) ENCI
	Spot sample 1996 07 25 [1)]	Spot sample 1996 05 28 [2)]	Spot sample 1996 08 13 [3)]	Spot sample Cy 11365[4)]
CaO (%)	65.1	0.02	35.5	42.1
SiO_2 (%)	22.6	93.3	36.0	30.3
SiC (%)	-	-	-	-
C (%)	-	-	-	-
Al_2O_3 (%)	3.41	-	10.3	13.6
Fe_2O_3 (%)	4.37	-	0.07	1.18
MgO (%)	0.75	0.42	14.9	8.5
K_2O (%)	0.58	0.84	0.60	0.66
Na_2O (%)	0.07	0.18	0.50	0.31
Na_2O - ekv (%)	0.45	0.73	0.89	0.74
SO_3 (%)	2.13	0.4	3.7	5.2
Cl^- (%)	0.01	0.06	<0.01	0.02
Loss on ignition (%)	0.52	1.9	1.0	0.5
Glass content (%)	-	-	~97	-
C_3S [5)]	58.0	-	-	-
C_2S [5)]	21.0	-	-	-
C_3A [5)]	1.6	-	-	-
C_4AF [5)]	13.3	-	-	-
Specific surface m^2/kg	305	22400	~500	-
Setting time min	145	-	-	-
Dry material content (%)	-	51	-	-
Compressive strength MPa				
1 day	10.0	-	-	-
2 days	18.4	-	-	-
7 days	33.8	-	-	-
28 days	52.3	-	-	-

[1)] Chemical analyses and measurements of mechanical and physical properties were carried out at Scancem Research, and provided by the producer.

[2)] Chemical analyses and measurements of physical properties were carried out at SP in Borås.

[3)] Chemical analyses and measurements of physical properties were provided by the producer.

[4)] Chemical analyses were carried out at SP in Borås.

[5)] Calculated according to equations in ASTM C150:1998, pp. 141.

APPENDIX 5

CALCULATION OF THE DEGREE OF HYDRATION

Calculation of the degree of hydration

The following discusses the procedure for calculating values for the degree of hydration at different ages for materials described in Chapter 3. It concludes with comments on an alternative equation used in investigations by others.

For concrete with OPC alone as the binder, the degree of hydration was calculated from measurements of the non-evaporable water content (heating to +1050 °C). The weight of the specimen, when in equilibrium at +105 °C and +1050 °C respectively, and the weight contributions of the different constituents, are shown in Figure 1.

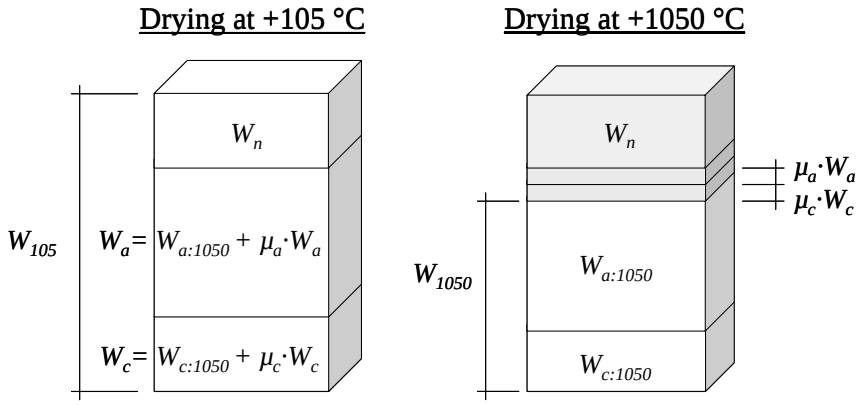

Figure 1. *Schematic diagram of the weight contribution from the different constituents; see explanation below.*

The symbols used in Figure 1 and in the following discussion represent:

W_a is the aggregate weight, calculated from the composition of the mix, Equation 1:

$$W_a = \frac{g}{1+g} \cdot (W_{105} - W_n) \qquad \text{[Eq. 1]}$$

W_c is the cement weight, calculated from the composition of the mix, Equation 2:

$$W_c = \frac{1}{1+g} \cdot (W_{105} - W_n) \qquad \text{[Eq. 2]}$$

W_n	is the non-evaporable water content	[kg]
W_{105}	is the weight after drying at +105 °C	[kg]
W_{1050}	is the weight after ignition at +1050 °C	[kg]
μ_c	is the ignition loss of the dry cement	[kg/kg]
μ_a	is the ignition loss of the aggregate	[kg/kg]
g	is the aggregate:cement ratio	[kg/kg]

The ignition loss of cement and aggregate is determined from separate samples of the aggregate and cement used.

The non-evaporable water content is calculated from:

$$W_n = W_{105} - W_{1050} - \mu_c \cdot W_c - \mu_a \cdot W_a$$

Inserting the expressions for W_c and W_a gives Equation 3:

$$W_n = W_{105} - W_{1050} - \mu_c \cdot \frac{1}{1+g} \cdot (W_{105} - W_n) - \mu_a \cdot \frac{g}{1+g} \cdot (W_{105} - W_n) \qquad \text{[Eq. 3]}$$

Deriving W_n from Equation 3 gives:

$$W_n = \frac{W_{105} - W_{1050} - \frac{\mu_c + g \cdot \mu_a}{1+g} \cdot W_{105}}{1 - \frac{\mu_c + g \cdot \mu_a}{1+g}}$$

which is the same as Equation 4:

$$W_n = W_{105} - \frac{W_{1050}}{\left(1 - \frac{\mu_c + \mu_a \cdot g}{1+g}\right)} \qquad \text{[Eq. 4]}$$

The cement content $W_{c:1050}$, or C, is given by:

$$C = W_c - \mu_c \cdot W_c = \frac{1}{1+g} \cdot (W_{105} - W_n) - \mu_c \cdot \frac{1}{1+g} \cdot (W_{105} - W_n)$$

which can be expressed as Equation 5:

$$C = \frac{1}{1+g}(1 - \mu_c) \cdot (W_{105} - W_n) \qquad \text{[Eq. 5]}$$

An alternative calculation can be made assuming:

$$W_{105} - W_n \approx W_{1050}$$

Which gives the more simplified expression for W_n / C , Equation 6:

$$\frac{W_n}{C} = \frac{W_{105} - W_{1050} - C \cdot \mu_c - A \cdot \mu_a}{C} \qquad \text{[Eq. 6]}$$

where the cement content can be calculated from Equation 7:

$$C = \frac{1}{1+g} \cdot W_{1050} \qquad \text{[Eq. 7]}$$

where:

C	is the cement content without ignition loss	[kg]
A	is the aggregate content without ignition loss	[kg]

Equations 6 and 7 give Equation 8:

$$\frac{W_n}{C} = \frac{W_{105} - W_{1050}}{\frac{1}{1+g} \cdot W_{1050}} - \mu_c - g \cdot \mu_a \qquad \text{[Eq. 8]}$$

A further simplification, ignoring the ignition losses from the cement (μ_c) and aggregate (μ_a), gives the following expression for W_n / C, Equation 9:

$$\frac{W_n}{C} = \frac{W_{105} - W_{1050}}{\frac{1}{1+g} \cdot W_{1050}} \qquad \text{[Eq. 9]}$$

When calculating the non-evaporable water content and the cement content from the equations above, it is assumed that:

- The composition of the specimen is representative, i.e. the composition of the specimen is the same as the composition of the mix.
- The weight loss from heating the material from +105 °C to +1050 °C comes solely from hydrated cement and ignition loss from cement and aggregate, i.e. weight loss from possible carbonation is disregarded.
- The aggregate:cement ratio after heating at +105 °C is equivalent to the ratio at mixing.

Example 1:

The following values were obtained for the 'OPC-45 air' mix at an age of 31 days:

W_{105}	= 0.08212 kg
W_{1050}	= 0.07932 kg
μ_c	= 0.005012 (kg/kg)
μ_a	= 0.005369 (kg/kg)
g	= 3.625 (kg/kg)

Dividing Equation 4 by Equation 5 gives:

$$\frac{W_n}{C} = 0.1386$$

Using Equation 8 gives:

$$\frac{W_n}{C} = 0.1388$$

Using Equation 9 gives:

$$\frac{W_n}{C} = 0.1633$$

Calculating W_n/C from Equations 4 and 5 or Equation 8 gives about the same results. The slight difference is explained by the fact that the assumption $W_{105} - W_n \approx W_{1050}$ is not fully correct, depending on the influence of the ignition loss from the cement and aggregate on W_{1050}. However, as long as the ignition losses from the cement and aggregate are small, the assumption is almost correct, which gives results of the same order as the more accurate Equations 4 and 5. The difference is far less than the error from sampling, drying, weighing and assuming no carbonation. However, using the simplified Equation 9 results in considerably higher values for W_n/C, showing that the ignition loss for cement and aggregate cannot totally be ignored.

In this investigation, Equations 4 and 5 have been used for calculation of W_n and C.

Studies by Powers and Brownyard (1948) showed that during hydration cement chemically binds about 25 % by weight of water. This leads to the following expression for the degree of hydration (α), Equation 10:

$$\alpha \approx 4 \cdot \frac{W_n}{C} \qquad \text{[Eq. 10]}$$

The degree of hydration for the materials of OPC at different ages, used in the investigation described in Chapter 3, is given in Table 3.7 (Chapter 3).

In other investigations, e.g. in Bellander (1973), Byfors (1980) and Persson (1998), Equation 11 has been used when calculating W_n/C:

$$\frac{W_n}{C} = \frac{W_{105} - W_{1050} - \mu_c \cdot \frac{1}{1+g} \cdot W_{105} - \mu_a \cdot \frac{g}{1+g} \cdot W_{105}}{W_{1050} - (1-\mu_a) \cdot \frac{g}{1+g} \cdot W_{105}} \qquad \textit{[Eq. 11]}$$

Using Equation 11 in example 1 above gives:

$$\frac{W_n}{C} = 0.1546$$

This results in a more than 10 % higher value for W_n/C than the values obtained when Equations 4 and 5 or Equation 8 are used. This can essentially be explained by the fact that, in Equation 11, the aggregate weight W_a and the cement weight W_c have been calculated from:

$$W_a = \frac{g}{1+g} \cdot W_{105}$$
$$W_c = \frac{1}{1+g} \cdot W_{105}$$

This seems erroneous; see Figure 1. This because it implies that the amount of aggregate and cement increases in a given sample when water is chemically bound to the cement, i.e. when W_n is increasing (the degree of hydration is increasing). Instead, when calculating the aggregate and cement weight from the dry specimen weight (+105 °C) the non-evaporable water content should be subtracted, i.e. as in Equations 1 and 2, above.

A simplification is to assume that W_{105}-$W_n \approx W_{1050}$. However, this presumes that the term in the denominator in Equation 11 adding the weight due to ignition loss from the aggregate has to be disregarded. This assumption would lead to the following equation:

$$\frac{W_n}{C} = \frac{W_{105} - W_{1050} - \mu_c \cdot \frac{1}{1+g} \cdot W_{1050} - \mu_a \cdot \frac{g}{1+g} \cdot W_{1050}}{\frac{1}{1+g} \cdot W_{1050}}$$

Which is the same as Equation (8).

The absolute values for W_n/C in investigations using Equation 11 are thus overestimated; in this example by about 10 %. The magnitude of the overestimation increases with increasing W_n in relation to the aggregate and cement content.

APPENDIX 6

RESULTS FROM SALT-FROST TESTING

Scaling in kg/m^2 for saturated (never-dried) specimens of 'micro' concrete with OPC and different w/b-ratios

Age at start of freeze/thaw test: 7 days

No. of freeze/thaw cycles	1	4	7	14	21	28
Specimen 1	0.04	0.68	1.30	2.09	2.73	3.29
Specimen 2	0.04	0.75	1.25	1.92	2.48	2.90
OPC-35 air: Mean (kg/m^2)	**0.04**	**0.71**	**1.28**	**2.00**	**2.60**	**3.09**
Standard deviation	0.00	0.05	0.04	0.12	0.18	0.27
Specimen 1	0.05	1.53	2.83	4.92	6.41	7.46
Specimen 2	0.04	1.14	2.05	3.43	4.40	5.29
OPC-45 air: Mean (kg/m^2)	**0.05**	**1.34**	**2.44**	**4.18**	**5.41**	**6.37**
Standard deviation	0.01	0.28	0.55	1.05	1.42	1.53
Specimen 1	0.06	1.62	2.74	4.79	6.28	7.67
Specimen 2	0.10	1.53	2.64	4.72	6.28	7.40
OPC-55 air: Mean (kg/m^2)	**0.08**	**1.58**	**2.69**	**4.76**	**6.28**	**7.53**
Standard deviation	0.03	0.06	0.07	0.05	0.00	0.19

Age at start of freeze/thaw test: 17 days

No. of freeze/thaw cycles	1	4	7	14	21	28	42	56
Specimen 1	0.03	0.20	0.42	1.01	1.54	1.95	2.89	3.83
Specimen 2	0.02	0.21	0.43	0.99	1.50	1.96	2.84	3.64
OPC-35 air: Mean (kg/m^2)	**0.03**	**0.20**	**0.42**	**1.00**	**1.52**	**1.96**	**2.86**	**3.74**
Standard deviation	0.01	0.00	0.01	0.02	0.03	0.01	0.04	0.13
Specimen 1	0.04	1.06	1.91	3.44	4.88	6.11	8.59	10.7
Specimen 2	0.03	0.99	1.72	3.10	4.31	5.31	7.10	8.61
OPC-45 air: Mean (kg/m^2)	**0.03**	**1.03**	**1.81**	**3.27**	**4.60**	**5.71**	**7.85**	**9.63**
Standard deviation	0.00	0.05	0.14	0.24	0.40	0.56	1.05	1.44
Specimen 1	0.04	1.78	3.31	6.51	8.63	10.8	14.2	17.3
Specimen 2	0.07	1.89	3.30	5.98	8.24	10.2	13.4	16.4
OPC-55 air: Mean (kg/m^2)	**0.06**	**1.84**	**3.30**	**6.25**	**8.44**	**10.5**	**13.8**	**16.8**
Standard deviation	0.02	0.08	0.00	0.37	0.27	0.40	0.61	0.67

Age at start of freeze/thaw test: 24 days

No. of freeze/thaw cycles	1	4	7	14	21	28	42	56
Specimen 1	0.02	0.14	0.31	0.78	1.22	1.69	2.45	3.41
Specimen 2	0.03	0.13	0.30	0.69	1.10	1.53	2.21	3.04
OPC-35 air: Mean (kg/m^2)	**0.02**	**0.13**	**0.31**	**0.74**	**1.16**	**1.61**	**2.33**	**3.23**
Standard deviation	0.00	0.01	0.01	0.06	0.09	0.11	0.18	0.26
Specimen 1	0.03	0.79	1.45	2.89	4.22	5.47	7.84	10.3
Specimen 2	0.05	0.79	1.42	2.77	3.98	5.16	6.99	9.02
OPC-45 air: Mean (kg/m^2)	**0.04**	**0.79**	**1.44**	**2.83**	**4.10**	**5.32**	**7.42**	**9.63**
Standard deviation	0.01	0.01	0.03	0.08	0.17	0.22	0.60	0.86
Specimen 1	0.03	1.74	3.20	6.50	9.13	11.6	15.4	18.6
Specimen 2	0.05	1.53	3.02	5.59	7.76	10.1	14.3	18.1
OPC-55 air: Mean (kg/m^2)	**0.04**	**1.64**	**3.11**	**6.05**	**8.45**	**10.8**	**14.8**	**18.3**
Standard deviation	0.01	0.15	0.13	0.64	0.97	1.01	0.77	0.36

Scaling in kg/m^2 for saturated (never-dried) specimens of 'micro' concrete with OPC and different w/b-ratios

Age at start of freeze/thaw test: 31 days

No. of freeze/thaw cycles	1	4	7	14	21	28	42	56
Specimen 1	0.03	0.14	0.30	0.77	1.19	1.65	2.47	3.35
Specimen 2	0.03	0.13	0.26	0.63	0.99	1.31	2.00	2.69
OPC-35 air: Mean (kg/m^2)	**0.03**	**0.13**	**0.28**	**0.70**	**1.09**	**1.48**	**2.23**	**3.02**
Standard deviation	0.00	0.01	0.03	0.10	0.14	0.24	0.33	0.47
Specimen 1	0.03	0.57	1.09	2.37	3.56	4.85	7.27	9.40
Specimen 2	0.02	0.54	1.12	2.40	3.49	4.55	6.51	8.42
OPC-45 air: Mean (kg/m^2)	**0.03**	**0.55**	**1.10**	**2.39**	**3.53**	**4.70**	**6.89**	**8.91**
Standard deviation	0.01	0.02	0.03	0.02	0.05	0.22	0.54	0.70
Specimen 1	0.04	1.52	2.84	5.76	8.31	10.8	15.6	19.8
Specimen 2	0.04	1.45	2.82	5.95	8.58	11.2	15.5	19.6
OPC-55 air: Mean (kg/m^2)	**0.04**	**1.48**	**2.83**	**5.85**	**8.45**	**11.0**	**15.6**	**19.7**
Standard deviation	0.00	0.05	0.01	0.13	0.19	0.34	0.09	0.19

Age at start of freeze/thaw test: 38 days

No. of freeze/thaw cycles	1	4	7	14	21	28	42	56
Specimen 1	0.04	0.16	0.42	0.93	1.43	1.96	2.85	3.82
Specimen 2	0.02	0.12	0.37	0.80	1.25	1.68	2.61	3.60
OPC-35 air: Mean (kg/m^2)	**0.03**	**0.14**	**0.39**	**0.86**	**1.34**	**1.82**	**2.73**	**3.71**
Standard deviation	0.02	0.02	0.04	0.09	0.13	0.19	0.17	0.15
Specimen 1	0.03	0.53	1.10	2.39	3.72	4.98	7.57	10.11
Specimen 2	0.03	0.56	1.26	2.63	3.88	4.98	7.20	9.43
OPC-45 air: Mean (kg/m^2)	**0.03**	**0.55**	**1.18**	**2.51**	**3.80**	**4.98**	**7.39**	**9.77**
Standard deviation	0.00	0.02	0.11	0.17	0.11	0.00	0.26	0.48
Specimen 1	0.04	1.44	3.17	6.68	10.0	12.9	18.2	24.0
Specimen 2	0.03	1.69	3.35	6.88	9.83	12.8	17.6	23.8
OPC-55 air: Mean (kg/m^2)	**0.03**	**1.57**	**3.26**	**6.78**	**9.91**	**12.9**	**17.9**	**23.9**
Standard deviation	0.01	0.17	0.13	0.14	0.12	0.14	0.42	0.13

Age at start of freeze/thaw test: 66 days

No. of freeze/thaw cycles	1	4	7	14	21	28	42	56
Specimen 1	0.02	0.11	0.27	0.66	0.98	1.27	2.09	2.96
Specimen 2	0.02	0.11	0.26	0.61	0.89	1.16	1.82	2.53
OPC-35 air: Mean (kg/m^2)	**0.02**	**0.11**	**0.26**	**0.63**	**0.93**	**1.22**	**1.95**	**2.74**
Standard deviation	0.00	0.01	0.01	0.04	0.07	0.08	0.19	0.30
Specimen 1	0.03	0.44	0.92	2.03	3.21	4.40	7.07	10.2
Specimen 2	0.05	0.51	1.01	2.09	3.21	4.29	6.74	9.24
OPC-45 air: Mean (kg/m^2)	**0.04**	**0.48**	**0.97**	**2.06**	**3.21**	**4.35**	**6.90**	**9.74**
Standard deviation	0.01	0.05	0.06	0.04	0.01	0.08	0.23	0.71
Specimen 1	0.06	1.13	2.29	5.34	8.41	11.5	18.6	25.0
Specimen 2	0.06	1.09	2.23	4.82	7.44	10.2	15.6	21.6
OPC-55 air: Mean (kg/m^2)	**0.06**	**1.11**	**2.26**	**5.08**	**7.93**	**10.9**	**17.1**	**23.3**
Standard deviation	0.01	0.03	0.04	0.37	0.68	0.90	2.12	2.43

Scaling in kg/m^2 for saturated (never-dried) specimens of 'micro' concrete with OPC and different w/b-ratios

Age at start of freeze/thaw test: 122 days

No. of freeze/thaw cycles	**1**	**4**	**7**	**14**	**21**	**28**	**42**	**56**
Specimen 1	0.02	0.10	0.29	0.73	1.09	1.55	2.36	3.29
Specimen 2	0.02	0.11	0.30	0.67	1.01	1.39	2.15	2.88
OPC-35 air: Mean (kg/m^2)	**0.02**	**0.11**	**0.29**	**0.70**	**1.05**	**1.47**	**2.25**	**3.08**
Standard deviation	0.00	0.00	0.01	0.05	0.05	0.11	0.15	0.29
Specimen 1	0.04	0.57	1.19	2.57	3.89	5.30	7.89	10.6
Specimen 2	0.03	0.50	1.16	2.23	3.42	4.61	7.04	9.79
OPC-45 air: Mean (kg/m^2)	**0.04**	**0.54**	**1.18**	**2.40**	**3.65**	**4.95**	**7.47**	**10.2**
Standard deviation	0.01	0.05	0.02	0.24	0.33	0.49	0.60	0.60
Specimen 1	0.05	1.41	2.74	5.86	9.21	12.5	18.6	25.1
Specimen 2	0.07	1.28	2.56	5.39	8.00	11.3	17.7	23.8
OPC-55 air: Mean (kg/m^2)	**0.06**	**1.34**	**2.65**	**5.63**	**8.60**	**11.9**	**18.2**	**24.4**
Standard deviation	0.01	0.09	0.13	0.33	0.86	0.81	0.62	0.90

Age at start of freeze/thaw test: 276 days

No. of freeze/thaw cycles	**1**	**4**	**7**	**14**	**21**	**28**	**42**	**56**
Specimen 1	0.04	0.16	0.36	0.83	1.24	1.62	2.44	3.30
Specimen 2	0.04	0.15	0.36	0.79	1.14	1.52	2.27	2.93
OPC-35 air: Mean (kg/m^2)	**0.04**	**0.16**	**0.36**	**0.81**	**1.19**	**1.57**	**2.35**	**3.11**
Standard deviation	0.00	0.01	0.00	0.03	0.07	0.07	0.12	0.26
Specimen 1	0.05	0.59	1.16	2.38	3.63	4.93	7.51	10.1
Specimen 2	0.04	0.56	1.16	2.25	3.19	4.33	6.79	9.11
OPC-45 air: Mean (kg/m^2)	**0.05**	**0.58**	**1.16**	**2.32**	**3.41**	**4.63**	**7.15**	**9.62**
Standard deviation	0.01	0.02	0.00	0.09	0.31	0.43	0.51	0.73
Specimen 1	0.05	1.41	2.67	5.50	8.18	10.9	16.9	22.7
Specimen 2	0.04	1.23	2.39	5.17	7.77	11.00	17.1	23.5
OPC-55 air: Mean (kg/m^2)	**0.05**	**1.32**	**2.53**	**5.33**	**7.97**	**10.9**	**17.0**	**23.1**
Standard deviation	0.01	0.13	0.20	0.23	0.29	0.08	0.14	0.61

Scaling in kg/m^2 for dried (without carbon dioxide) specimens of 'micro' concrete with OPC and different w/b-ratios

Age at start of freeze/thaw test: 17 days

No. of freeze/thaw cycles	1	4	7	14	21	28	42	56
Specimen 1	0.02	0.37	0.53	0.85	1.05	1.27	1.57	1.80
Specimen 2	0.02	0.31	0.47	0.77	0.96	1.14	1.44	1.68
OPC-35 air: Mean (kg/m^2)	**0.02**	**0.34**	**0.50**	**0.81**	**1.01**	**1.21**	**1.51**	**1.74**
Standard deviation	0.00	0.04	0.04	0.06	0.06	0.09	0.09	0.09
Specimen 1	0.02	0.57	1.01	1.95	2.53	3.05	3.83	4.46
Specimen 2	0.02	0.56	1.07	1.87	2.39	2.87	3.70	4.36
OPC-45 air: Mean (kg/m^2)	**0.02**	**0.57**	**1.04**	**1.91**	**2.46**	**2.96**	**3.76**	**4.41**
Standard deviation	0.00	0.01	0.04	0.06	0.10	0.13	0.09	0.07
Specimen 1	0.02	0.50	0.96	2.01	2.77	3.45	4.60	6.15
Specimen 2	0.02	0.55	1.01	1.82	2.50	3.09	4.12	5.02
OPC-55 air: Mean (kg/m^2)	**0.02**	**0.53**	**0.99**	**1.91**	**2.64**	**3.27**	**4.36**	**5.59**
Standard deviation	0.00	0.03	0.04	0.14	0.19	0.25	0.34	0.80

Age at start of freeze/thaw test: 24 days

No. of freeze/thaw cycles	1	4	7	14	21	28	42	56
Specimen 1	0.01	0.19	0.32	0.56	0.81	1.05	1.50	1.90
Specimen 2	0.02	0.18	0.30	0.54	0.77	1.04	1.46	1.80
OPC-35 air: Mean (kg/m^2)	**0.02**	**0.18**	**0.31**	**0.55**	**0.79**	**1.05**	**1.48**	**1.85**
Standard deviation	0.00	0.01	0.01	0.01	0.03	0.01	0.03	0.07
Specimen 1	0.02	0.63	1.26	2.30	3.02	3.54	4.48	5.31
Specimen 2	0.02	0.61	1.30	2.45	3.17	3.70	4.39	5.01
OPC-45 air: Mean (kg/m^2)	**0.02**	**0.62**	**1.28**	**2.37**	**3.09**	**3.62**	**4.44**	**5.16**
Standard deviation	0.00	0.01	0.03	0.10	0.11	0.11	0.07	0.21
Specimen 1	0.03	0.88	1.63	3.26	4.43	5.41	6.94	8.34
Specimen 2	0.02	0.76	1.63	3.06	4.12	5.04	6.56	8.11
OPC-55 air: Mean (kg/m^2)	**0.02**	**0.82**	**1.63**	**3.16**	**4.28**	**5.22**	**6.75**	**8.22**
Standard deviation	0.00	0.08	0.00	0.14	0.22	0.26	0.27	0.16

Age at start of freeze/thaw test: 31 days

No. of freeze/thaw cycles	1	4	7	14	21	28	42	56
Specimen 1	0.01	0.20	0.33	0.59	0.81	1.09	1.62	2.21
Specimen 2	0.02	0.14	0.26	0.51	0.72	0.95	1.40	1.90
OPC-35 air: Mean (kg/m^2)	**0.01**	**0.17**	**0.29**	**0.55**	**0.77**	**1.02**	**1.51**	**2.05**
Standard deviation	0.01	0.04	0.05	0.06	0.06	0.10	0.15	0.22
Specimen 1	0.02	0.75	1.31	2.37	3.24	4.04	5.53	7.07
Specimen 2	0.03	0.86	1.43	2.61	3.51	4.20	5.40	6.60
OPC-45 air: Mean (kg/m^2)	**0.02**	**0.80**	**1.37**	**2.49**	**3.37**	**4.12**	**5.46**	**6.83**
Standard deviation	0.01	0.07	0.09	0.17	0.19	0.11	0.09	0.33
Specimen 1	0.04	1.31	2.34	4.44	6.42	8.07	10.7	12.9
Specimen 2	0.03	1.35	2.51	4.74	6.62	8.39	11.2	13.8
OPC-55 air: Mean (kg/m^2)	**0.04**	**1.33**	**2.43**	**4.59**	**6.52**	**8.23**	**11.0**	**13.4**
Standard deviation	0.00	0.03	0.12	0.21	0.14	0.23	0.37	0.63

Scaling in kg/m^2 for dried (without carbon dioxide) specimens of 'micro' concrete with OPC and different w/b-ratios

Age at start of freeze/thaw test: 38 days

No. of freeze/thaw cycles	1	4	7	14	21	28	42	56
Specimen 1	0.01	0.12	0.22	0.46	0.71	1.02	1.56	2.20
Specimen 2	0.02	0.17	0.29	0.54	0.79	1.09	1.68	2.25
OPC-35 air: Mean (kg/m^2)	**0.02**	**0.14**	**0.26**	**0.50**	**0.75**	**1.05**	**1.62**	**2.22**
Standard deviation	0.00	0.03	0.05	0.06	0.06	0.05	0.08	0.03
Specimen 1	0.02	0.73	1.35	2.58	3.57	4.62	6.59	8.27
Specimen 2	0.04	0.73	1.22	2.35	3.37	4.20	5.64	6.95
OPC-45 air: Mean (kg/m^2)	**0.03**	**0.73**	**1.28**	**2.47**	**3.47**	**4.41**	**6.12**	**7.61**
Standard deviation	0.01	0.00	0.10	0.16	0.14	0.30	0.67	0.93
Specimen 1	0.02	1.34	2.36	4.61	6.39	7.96	11.0	13.9
Specimen 2	0.04	1.46	2.50	4.83	6.63	7.96	10.7	13.3
OPC-55 air: Mean (kg/m^2)	**0.03**	**1.40**	**2.43**	**4.72**	**6.51**	**7.96**	**10.8**	**13.6**
Standard deviation	0.01	0.09	0.10	0.15	0.17	0.00	0.19	0.47

Age at start of freeze/thaw test: 66 days

No. of freeze/thaw cycles	1	4	7	14	21	28	42	56
Specimen 1	0.00	0.08	0.17	0.37	0.63	0.96	1.64	2.32
Specimen 2	0.01	0.09	0.18	0.38	0.64	0.92	1.46	2.08
OPC-35 air: Mean (kg/m^2)	**0.01**	**0.08**	**0.18**	**0.38**	**0.63**	**0.94**	**1.55**	**2.20**
Standard deviation	0.01	0.00	0.01	0.01	0.00	0.03	0.12	0.17
Specimen 1	0.02	0.69	1.36	2.77	4.01	5.21	7.65	10.0
Specimen 2	0.02	0.73	1.38	2.72	3.91	5.10	7.08	8.96
OPC-45 air: Mean (kg/m^2)	**0.02**	**0.71**	**1.37**	**2.75**	**3.96**	**5.15**	**7.36**	**9.49**
Standard deviation	0.00	0.03	0.02	0.04	0.07	0.08	0.41	0.76
Specimen 1	0.02	1.67	3.27	6.32	9.19	11.6	15.9	20.5
Specimen 2	0.03	1.68	3.15	6.11	8.61	10.9	15.0	18.5
OPC-55 air: Mean (kg/m^2)	**0.02**	**1.68**	**3.21**	**6.22**	**8.90**	**11.2**	**15.4**	**19.5**
Standard deviation	0.01	0.01	0.09	0.15	0.41	0.51	0.68	1.37

Age at start of freeze/thaw test: 122 days

No. of freeze/thaw cycles	1	4	7	14	21	28	42	56
Specimen 1	0.01	0.13	0.26	0.52	0.85	1.25	2.12	2.99
Specimen 2	0.01	0.14	0.26	0.50	0.78	1.12	1.83	2.44
OPC-35 air: Mean (kg/m^2)	**0.01**	**0.14**	**0.26**	**0.51**	**0.82**	**1.19**	**1.98**	**2.71**
Standard deviation	0.00	0.01	0.00	0.02	0.05	0.09	0.21	0.39
Specimen 1	0.03	0.79	1.44	2.81	4.21	5.54	8.20	10.6
Specimen 2	0.03	0.75	1.48	2.82	4.04	5.13	7.51	9.96
OPC-45 air: Mean (kg/m^2)	**0.03**	**0.77**	**1.46**	**2.82**	**4.12**	**5.34**	**7.85**	**10.3**
Standard deviation	0.00	0.03	0.03	0.00	0.11	0.29	0.49	0.45
Specimen 1	0.05	2.25	4.16	7.45	10.6	13.6	19.0	24.1
Specimen 2	0.05	1.97	3.73	7.14	9.85	12.1	17.5	22.3
OPC-55 air: Mean (kg/m^2)	**0.05**	**2.11**	**3.95**	**7.29**	**10.2**	**12.8**	**18.2**	**23.2**
Standard deviation	0.00	0.20	0.31	0.22	0.56	1.09	1.05	1.33

Scaling in kg/m^2 for dried (without carbon dioxide) specimens of 'micro' concrete with OPC and different w/b-ratios

Age at start of freeze/thaw test: 276 days

No. of freeze/thaw cycles	**1**	**4**	**7**	**14**	**21**	**28**	**42**	**56**
Specimen 1	0.03	0.11	0.25	0.41	0.62	0.92	1.60	2.45
Specimen 2	0.03	0.09	0.18	0.32	0.47	0.70	1.30	1.96
OPC-35 air: Mean (kg/m^2)	**0.03**	**0.10**	**0.21**	**0.36**	**0.54**	**0.81**	**1.45**	**2.20**
Standard deviation	0.00	0.01	0.05	0.06	0.10	0.16	0.22	0.34
Specimen 1	0.05	0.72	1.47	2.91	4.22	5.85	8.54	11.3
Specimen 2	0.06	0.82	1.61	3.28	4.86	6.31	8.95	11.4
OPC-45 air: Mean (kg/m^2)	**0.06**	**0.77**	**1.54**	**3.10**	**4.54**	**6.08**	**8.74**	**11.3**
Standard deviation	0.00	0.07	0.10	0.26	0.45	0.32	0.28	0.09
Specimen 1	0.05	1.62	3.37	6.61	9.11	11.8	17.0	21.8
Specimen 2	0.05	1.60	3.09	6.62	9.29	12.1	17.7	23.7
OPC-55 air: Mean (kg/m^2)	**0.05**	**1.61**	**3.23**	**6.61**	**9.20**	**11.9**	**17.4**	**22.7**
Standard deviation	0.01	0.02	0.20	0.01	0.13	0.22	0.47	1.35

Scaling in kg/m^2 for dried (with carbon dioxide) specimens of 'micro' concrete with OPC and different w/b-ratios

Age at start of freeze/thaw test: 17 days

No. of freeze/thaw cycles	1	4	7	14	21	28	42	56
Specimen 1	0.01	0.05	0.07	0.09	0.11	0.13	0.18	0.24
Specimen 2	0.02	0.06	0.07	0.10	0.12	0.15	0.19	0.25
OPC-35 air: Mean (kg/m^2)	**0.02**	**0.05**	**0.07**	**0.09**	**0.11**	**0.14**	**0.19**	**0.24**
Standard deviation	0.01	0.00	0.00	0.01	0.01	0.01	0.01	0.01
Specimen 1	0.02	0.05	0.08	0.14	0.18	0.21	0.25	0.28
Specimen 2	0.02	0.05	0.08	0.12	0.15	0.18	0.21	0.23
OPC-45 air: Mean (kg/m^2)	**0.02**	**0.05**	**0.08**	**0.13**	**0.16**	**0.19**	**0.23**	**0.26**
Standard deviation	0.00	0.00	0.01	0.02	0.02	0.02	0.03	0.03
Specimen 1	0.01	0.05	0.15	0.43	0.56	0.67	0.83	1.00
Specimen 2	0.02	0.10	0.25	0.60	0.84	1.05	1.34	1.50
OPC-55 air: Mean (kg/m^2)	**0.02**	**0.08**	**0.20**	**0.51**	**0.70**	**0.86**	**1.08**	**1.25**
Standard deviation	0.01	0.03	0.07	0.12	0.20	0.27	0.36	0.35

Age at start of freeze/thaw test: 24 days

No. of freeze/thaw cycles	1	4	7	14	21	28	42	56
Specimen 1	0.02	0.04	0.06	0.10	0.12	0.15	0.19	0.25
Specimen 2	0.02	0.03	0.08	0.11	0.15	0.17	0.19	0.26
OPC-35 air: Mean (kg/m^2)	**0.02**	**0.03**	**0.07**	**0.10**	**0.13**	**0.16**	**0.19**	**0.25**
Standard deviation	0.00	0.00	0.01	0.01	0.02	0.01	0.01	0.01
Specimen 1	0.01	0.03	0.05	0.08	0.11	0.12	0.14	0.15
Specimen 2	0.02	0.03	0.08	0.11	0.13	0.15	0.18	0.19
OPC-45 air: Mean (kg/m^2)	**0.01**	**0.03**	**0.07**	**0.09**	**0.12**	**0.14**	**0.16**	**0.17**
Standard deviation	0.00	0.00	0.02	0.02	0.02	0.02	0.03	0.03
Specimen 1	0.02	0.04	0.12	0.23	0.30	0.34	0.41	0.44
Specimen 2	0.01	0.04	0.12	0.26	0.35	0.41	0.48	0.52
OPC-55 air: Mean (kg/m^2)	**0.02**	**0.04**	**0.12**	**0.25**	**0.32**	**0.38**	**0.44**	**0.48**
Standard deviation	0.00	0.00	0.01	0.02	0.04	0.05	0.05	0.06

Age at start of freeze/thaw test: 31 days

No. of freeze/thaw cycles	1	4	7	14	21	28	42	56
Specimen 1	0.00	0.02	0.04	0.07	0.08	0.10	0.12	0.16
Specimen 2	0.01	0.03	0.06	0.08	0.11	0.12	0.15	0.19
OPC-35 air: Mean (kg/m^2)	**0.00**	**0.03**	**0.05**	**0.07**	**0.09**	**0.11**	**0.13**	**0.18**
Standard deviation	0.00	0.01	0.01	0.01	0.02	0.01	0.02	0.02
Specimen 1	0.01	0.04	0.06	0.09	0.12	0.14	0.16	0.19
Specimen 2	0.01	0.03	0.06	0.09	0.11	0.13	0.16	0.22
OPC-45 air: Mean (kg/m^2)	**0.01**	**0.03**	**0.06**	**0.09**	**0.12**	**0.14**	**0.16**	**0.21**
Standard deviation	0.00	0.01	0.00	0.01	0.00	0.00	0.00	0.02
Specimen 1	0.01	0.05	0.10	0.23	0.29	0.34	0.41	0.50
Specimen 2	0.01	0.04	0.10	0.18	0.26	0.34	0.42	0.54
OPC-55 air: Mean (kg/m^2)	**0.01**	**0.04**	**0.10**	**0.20**	**0.28**	**0.34**	**0.41**	**0.52**
Standard deviation	0.00	0.00	0.00	0.04	0.03	0.00	0.00	0.03

Scaling in kg/m^2 for dried (with carbon dioxide) specimens of 'micro' concrete with OPC and different w/b-ratios

Age at start of freeze/thaw test: 38 days

No. of freeze/thaw cycles	**1**	**4**	**7**	**14**	**21**	**28**	**42**	**56**
Specimen 1	0.02	0.05	0.07	0.09	0.10	0.12	0.18	0.28
Specimen 2	0.02	0.05	0.07	0.10	0.12	0.14	0.19	0.28
OPC-35 air: Mean (kg/m^2)	**0.02**	**0.05**	**0.07**	**0.09**	**0.11**	**0.13**	**0.19**	**0.28**
Standard deviation	0.00	0.00	0.00	0.01	0.01	0.01	0.01	0.00
Specimen 1	0.01	0.04	0.08	0.10	0.12	0.13	0.16	0.20
Specimen 2	0.02	0.05	0.08	0.12	0.15	0.17	0.22	0.26
OPC-45 air: Mean (kg/m^2)	**0.02**	**0.05**	**0.08**	**0.11**	**0.13**	**0.15**	**0.19**	**0.23**
Standard deviation	0.01	0.00	0.01	0.02	0.02	0.03	0.04	0.04
Specimen 1	0.02	0.05	0.11	0.19	0.24	0.28	0.36	0.50
Specimen 2	0.03	0.07	0.13	0.22	0.30	0.37	0.48	0.61
OPC-55 air: Mean (kg/m^2)	**0.02**	**0.06**	**0.12**	**0.20**	**0.27**	**0.33**	**0.42**	**0.56**
Standard deviation	0.01	0.01	0.01	0.02	0.04	0.06	0.09	0.08

Age at start of freeze/thaw test: 66 days

No. of freeze/thaw cycles	**1**	**4**	**7**	**14**	**21**	**28**	**42**	**56**
Specimen 1	0.01	0.02	0.03	0.06	0.10	0.15	0.31	0.61
Specimen 2	0.01	0.03	0.04	0.08	0.12	0.20	0.36	0.56
OPC-35 air: Mean (kg/m^2)	**0.01**	**0.02**	**0.04**	**0.07**	**0.11**	**0.17**	**0.33**	**0.59**
Standard deviation	0.00	0.01	0.01	0.02	0.02	0.03	0.04	0.03
Specimen 1	0.01	0.02	0.03	0.06	0.08	0.09	0.15	0.24
Specimen 2	0.01	0.03	0.04	0.08	0.10	0.13	0.22	0.36
OPC-45 air: Mean (kg/m^2)	**0.01**	**0.03**	**0.04**	**0.07**	**0.09**	**0.11**	**0.18**	**0.30**
Standard deviation	0.00	0.00	0.01	0.01	0.02	0.03	0.05	0.08
Specimen 1	0.01	0.08	0.17	0.27	0.35	0.42	0.55	0.67
Specimen 2	0.01	0.10	0.20	0.34	0.41	0.46	0.58	0.69
OPC-55 air: Mean (kg/m^2)	**0.01**	**0.09**	**0.18**	**0.30**	**0.38**	**0.44**	**0.57**	**0.68**
Standard deviation	0.00	0.02	0.02	0.05	0.04	0.03	0.02	0.02

Age at start of freeze/thaw test: 122 days

No. of freeze/thaw cycles	**1**	**4**	**7**	**14**	**21**	**28**	**42**	**56**
Specimen 1	0.01	0.02	0.03	0.05	0.07	0.09	0.16	0.25
Specimen 2	0.01	0.03	0.04	0.05	0.08	0.10	0.17	0.27
OPC-35 air: Mean (kg/m^2)	**0.01**	**0.02**	**0.04**	**0.05**	**0.08**	**0.10**	**0.16**	**0.26**
Standard deviation	0.00	0.00	0.00	0.00	0.01	0.01	0.01	0.02
Specimen 1	0.01	0.03	0.05	0.07	0.09	0.10	0.14	0.16
Specimen 2	0.01	0.03	0.06	0.08	0.09	0.10	0.13	0.16
OPC-45 air: Mean (kg/m^2)	**0.01**	**0.03**	**0.05**	**0.08**	**0.09**	**0.10**	**0.13**	**0.16**
Standard deviation	0.00	0.00	0.01	0.00	0.00	0.00	0.01	0.00
Specimen 1	0.01	0.06	0.15	0.28	0.36	0.42	0.52	0.59
Specimen 2	0.01	0.07	0.17	0.32	0.40	0.46	0.58	0.70
OPC-55 air: Mean (kg/m^2)	**0.01**	**0.06**	**0.16**	**0.30**	**0.38**	**0.44**	**0.55**	**0.64**
Standard deviation	0.00	0.01	0.01	0.03	0.02	0.03	0.04	0.08

Scaling in kg/m^2 for dried (with carbon dioxide) specimens of 'micro' concrete with OPC and different w/b-ratios

Age at start of freeze/thaw test: 276 days

No. of freeze/thaw cycles	**1**	**4**	**7**	**14**	**21**	**28**	**42**	**56**
Specimen 1	0.05	0.12	0.15	0.22	0.25	0.33	0.50	0.85
Specimen 2	0.05	0.10	0.14	0.19	0.23	0.28	0.43	0.71
OPC-35 air: Mean (kg/m^2)	**0.05**	**0.11**	**0.15**	**0.20**	**0.24**	**0.31**	**0.47**	**0.78**
Standard deviation	0.00	0.01	0.01	0.02	0.02	0.03	0.05	0.09
Specimen 1	0.05	0.11	0.17	0.23	0.27	0.35	0.42	0.50
Specimen 2	0.04	0.09	0.14	0.19	0.23	0.30	0.37	0.42
OPC-45 air: Mean (kg/m^2)	**0.04**	**0.10**	**0.16**	**0.21**	**0.25**	**0.33**	**0.39**	**0.46**
Standard deviation	0.01	0.02	0.02	0.03	0.03	0.04	0.04	0.06
Specimen 1	0.03	0.11	0.22	0.34	0.45	0.55	0.64	0.75
Specimen 2	0.03	0.07	0.12	0.18	0.23	0.29	0.38	0.46
OPC-55 air: Mean (kg/m^2)	**0.03**	**0.09**	**0.17**	**0.26**	**0.34**	**0.42**	**0.51**	**0.61**
Standard deviation	0.00	0.02	0.07	0.12	0.16	0.18	0.18	0.20

Scaling in kg/m^2 for saturated (never-dried) specimens of 'micro' concrete with OPC and different amounts of slag as part of the binder

Age at start of freeze/thaw test: 17 days

No. of freeze/thaw cycles	1	4	7	14	21	28	42	56
Specimen 1	0.03	1.16	2.04	3.64	4.79	5.83	7.48	9.24
Specimen 2	0.02	1.10	1.89	3.28	4.40	5.26	6.62	7.78
20%slag-45: Mean (kg/m^2)	**0.03**	**1.13**	**1.97**	**3.46**	**4.60**	**5.54**	**7.05**	**8.51**
Standard deviation	0.00	0.04	0.10	0.25	0.28	0.40	0.61	1.03
Specimen 1	0.02	1.37	2.28	3.82	4.89	5.76	7.18	8.31
Specimen 2	0.04	1.62	2.76	4.33	5.50	6.39	7.89	9.35
35%slag-45: Mean (kg/m^2)	**0.03**	**1.49**	**2.52**	**4.08**	**5.19**	**6.07**	**7.53**	**8.83**
Standard deviation	0.01	0.18	0.33	0.36	0.43	0.44	0.50	0.73
Specimen 1	0.06	0.98	1.50	2.36	2.98	3.38	4.31	5.06
Specimen 2	0.04	1.01	1.54	2.31	2.82	3.22	4.12	4.84
65%slag-45: Mean (kg/m^2)	**0.05**	**0.99**	**1.52**	**2.33**	**2.90**	**3.30**	**4.21**	**4.95**
Standard deviation	0.02	0.02	0.03	0.03	0.11	0.12	0.13	0.16

Age at start of freeze/thaw test: 31 days

No. of freeze/thaw cycles	1	4	7	14	21	28	42	56
Specimen 1	0.02	0.48	0.98	1.89	2.77	3.60	5.33	6.87
Specimen 2	0.03	0.49	0.95	1.77	2.45	3.12	4.42	5.78
20%slag-45: Mean (kg/m^2)	**0.03**	**0.49**	**0.96**	**1.83**	**2.61**	**3.36**	**4.87**	**6.33**
Standard deviation	0.01	0.01	0.02	0.08	0.23	0.34	0.65	0.77
Specimen 1	0.02	0.48	0.88	1.88	2.69	3.55	5.01	6.19
Specimen 2	0.03	0.59	1.08	2.02	2.88	3.59	4.99	6.31
35%slag-45: Mean (kg/m^2)	**0.03**	**0.53**	**0.98**	**1.95**	**2.78**	**3.57**	**5.00**	**6.25**
Standard deviation	0.01	0.08	0.14	0.10	0.13	0.03	0.01	0.08
Specimen 1	0.05	0.41	0.66	1.18	1.61	2.08	2.87	3.69
Specimen 2	0.04	0.38	0.62	1.15	1.60	2.03	2.83	3.56
65%slag-45: Mean (kg/m^2)	**0.04**	**0.39**	**0.64**	**1.16**	**1.60**	**2.06**	**2.85**	**3.62**
Standard deviation	0.00	0.02	0.03	0.02	0.01	0.04	0.03	0.10

Age at start of freeze/thaw test: 73 days

No. of freeze/thaw cycles	1	4	7	14	21	28	42	56
Specimen 1	0.02	0.35	0.76	1.48	2.15	2.90	4.36	5.76
Specimen 2	0.03	0.37	0.80	1.49	2.15	2.86	4.11	5.49
20%slag-45: Mean (kg/m^2)	**0.02**	**0.36**	**0.78**	**1.49**	**2.15**	**2.88**	**4.24**	**5.62**
Standard deviation	0.00	0.02	0.03	0.01	0.01	0.03	0.18	0.19
Specimen 1	0.03	0.41	0.79	1.44	2.02	2.60	3.73	4.75
Specimen 2	0.02	0.34	0.71	1.36	1.94	2.46	3.55	4.50
35%slag-45: Mean (kg/m^2)	**0.03**	**0.37**	**0.75**	**1.40**	**1.98**	**2.53**	**3.64**	**4.62**
Standard deviation	0.01	0.05	0.06	0.06	0.06	0.10	0.13	0.17
Specimen 1	0.04	0.34	0.48	0.77	1.05	1.34	1.94	2.58
Specimen 2	0.03	0.32	0.49	0.77	1.05	1.32	1.92	2.50
65%slag-45: Mean (kg/m^2)	**0.04**	**0.33**	**0.49**	**0.77**	**1.05**	**1.33**	**1.93**	**2.54**
Standard deviation	0.01	0.01	0.00	0.00	0.00	0.01	0.01	0.06

Scaling in kg/m^2 for saturated (never-dried) specimens of 'micro' concrete with OPC and different amounts of slag as part of the binder

Age at start of freeze/thaw test: 122 days

No. of freeze/thaw cycles	**1**	**4**	**7**	**14**	**21**	**28**	**42**	**56**
Specimen 1	0.02	0.41	0.78	1.52	2.26	3.02	4.49	6.10
Specimen 2	0.03	0.35	0.77	1.47	2.14	2.86	4.20	5.59
20%slag-45: Mean (kg/m^2)	**0.02**	**0.38**	**0.78**	**1.50**	**2.20**	**2.94**	**4.34**	**5.84**
Standard deviation	0.00	0.04	0.01	0.04	0.08	0.11	0.20	0.36
Specimen 1	0.02	0.23	0.55	1.06	1.52	1.91	2.87	3.88
Specimen 2	0.02	0.28	0.61	1.16	1.65	2.09	3.02	3.89
35%slag-45: Mean (kg/m^2)	**0.02**	**0.25**	**0.58**	**1.11**	**1.58**	**2.00**	**2.94**	**3.88**
Standard deviation	0.00	0.03	0.04	0.07	0.09	0.13	0.11	0.01
Specimen 1	0.02	0.19	0.30	0.52	0.75	1.00	1.48	2.04
Specimen 2	0.04	0.32	0.46	0.73	0.98	1.26	1.85	2.53
65%slag-45: Mean (kg/m^2)	**0.03**	**0.25**	**0.38**	**0.63**	**0.87**	**1.13**	**1.67**	**2.28**
Standard deviation	0.02	0.09	0.11	0.14	0.16	0.18	0.26	0.34

Scaling in kg/m^2 for dried (without carbon dioxide) specimens of 'micro' concrete with OPC and different amounts of slag as part of the binder

Age at start of freeze/thaw test: 17 days

No. of freeze/thaw cycles	1	4	7	14	21	28	42	56
Specimen 1	0.00	0.53	0.95	1.80	2.25	2.69	3.37	4.04
Specimen 2	0.01	0.48	0.96	1.75	2.22	2.59	3.14	3.66
20%slag-45: Mean (kg/m^2)	**0.00**	**0.51**	**0.96**	**1.78**	**2.24**	**2.64**	**3.26**	**3.85**
Standard deviation	0.00	0.03	0.00	0.03	0.03	0.07	0.16	0.27
Specimen 1	0.01	0.41	0.74	1.18	1.38	1.52	1.73	2.01
Specimen 2	0.01	0.47	0.89	1.39	1.66	1.83	2.10	2.36
35%slag-45: Mean (kg/m^2)	**0.01**	**0.44**	**0.81**	**1.29**	**1.52**	**1.67**	**1.91**	**2.18**
Standard deviation	0.00	0.05	0.11	0.15	0.20	0.22	0.26	0.25
Specimen 1	0.01	0.16	0.30	0.41	0.47	0.55	0.76	0.98
Specimen 2	0.01	0.17	0.33	0.46	0.51	0.57	0.77	1.02
65%slag-45: Mean (kg/m^2)	**0.01**	**0.16**	**0.31**	**0.43**	**0.49**	**0.56**	**0.77**	**1.00**
Standard deviation	0.00	0.01	0.02	0.04	0.03	0.02	0.01	0.03

Age at start of freeze/thaw test: 31 days

No. of freeze/thaw cycles	1	4	7	14	21	28	42	56
Specimen 1	0.01	0.41	0.77	1.43	1.95	2.48	3.56	4.61
Specimen 2	0.01	0.45	0.88	1.57	2.16	2.64	3.54	4.45
20%slag-45: Mean (kg/m^2)	**0.01**	**0.43**	**0.83**	**1.50**	**2.06**	**2.56**	**3.55**	**4.53**
Standard deviation	0.00	0.03	0.08	0.10	0.15	0.11	0.01	0.11
Specimen 1	0.01	0.36	0.58	1.17	1.76	2.33	3.44	4.36
Specimen 2	0.01	0.39	0.64	1.19	1.70	2.19	3.08	3.98
35%slag-45: Mean (kg/m^2)	**0.01**	**0.37**	**0.61**	**1.18**	**1.73**	**2.26**	**3.26**	**4.17**
Standard deviation	0.00	0.02	0.04	0.01	0.04	0.09	0.25	0.26
Specimen 1	0.01	0.27	0.46	0.99	1.42	1.87	2.67	3.44
Specimen 2	0.01	0.38	0.56	0.99	1.38	1.81	2.55	3.28
65%slag-45: Mean (kg/m^2)	**0.01**	**0.32**	**0.51**	**0.99**	**1.40**	**1.84**	**2.61**	**3.36**
Standard deviation	0.00	0.08	0.07	0.00	0.03	0.05	0.09	0.12

Age at start of freeze/thaw test: 73 days

No. of freeze/thaw cycles	1	4	7	14	21	28	42	56
Specimen 1	0.01	0.30	0.56	1.11	1.66	2.20	3.44	4.82
Specimen 2	0.02	0.34	0.60	1.09	1.58	2.05	3.12	4.14
20%slag-45: Mean (kg/m^2)	**0.01**	**0.32**	**0.58**	**1.10**	**1.62**	**2.13**	**3.28**	**4.48**
Standard deviation	0.00	0.02	0.03	0.01	0.05	0.10	0.23	0.49
Specimen 1	0.01	0.22	0.38	0.72	1.09	1.53	2.45	3.41
Specimen 2	0.01	0.16	0.32	0.65	0.97	1.36	2.21	2.96
35%slag-45: Mean (kg/m^2)	**0.01**	**0.19**	**0.35**	**0.68**	**1.03**	**1.44**	**2.33**	**3.19**
Standard deviation	0.00	0.04	0.04	0.05	0.08	0.12	0.17	0.32
Specimen 1	0.01	0.17	0.29	0.59	0.88	1.22	1.78	2.47
Specimen 2	0.01	0.14	0.26	0.55	0.82	1.11	1.72	2.32
65%slag-45: Mean (kg/m^2)	**0.01**	**0.15**	**0.27**	**0.57**	**0.85**	**1.17**	**1.75**	**2.39**
Standard deviation	0.00	0.03	0.02	0.02	0.05	0.08	0.04	0.10

Scaling in kg/m^2 for dried (without carbon dioxide) specimens of 'micro' concrete with OPC and different amounts of slag as part of the binder

Age at start of freeze/thaw test: 122 days

No. of freeze/thaw cycles	**1**	**4**	**7**	**14**	**21**	**28**	**42**	**56**
Specimen 1	0.02	0.23	0.45	0.88	1.29	1.83	2.92	4.29
Specimen 2	0.02	0.13	0.29	0.61	0.97	1.40	2.44	3.53
20%slag-45: Mean (kg/m^2)	**0.02**	**0.18**	**0.37**	**0.74**	**1.13**	**1.62**	**2.68**	**3.91**
Standard deviation	0.00	0.07	0.11	0.20	0.22	0.30	0.34	0.53
Specimen 1	0.01	0.08	0.17	0.44	0.72	1.10	1.83	2.63
Specimen 2	0.01	0.07	0.18	0.42	0.68	0.97	1.68	2.44
35%slag-45: Mean (kg/m^2)	**0.01**	**0.07**	**0.17**	**0.43**	**0.70**	**1.04**	**1.75**	**2.54**
Standard deviation	0.00	0.00	0.00	0.01	0.04	0.09	0.10	0.13
Specimen 1	0.01	0.08	0.16	0.43	0.66	0.92	1.47	2.12
Specimen 2	0.01	0.07	0.15	0.39	0.60	0.82	1.31	1.86
65%slag-45: Mean (kg/m^2)	**0.01**	**0.07**	**0.15**	**0.41**	**0.63**	**0.87**	**1.39**	**1.99**
Standard deviation	0.00	0.00	0.01	0.03	0.04	0.07	0.11	0.18

Scaling in kg/m^2 for dried (with carbon dioxide) specimens of 'micro' concrete with OPC and different amounts of slag as part of the binder

Age at start of freeze/thaw test: 17 days

No. of freeze/thaw cycles	1	4	7	14	21	28	42	56
Specimen 1	0.01	0.03	0.07	0.15	0.22	0.29	0.43	0.61
Specimen 2	0.00	0.02	0.07	0.15	0.21	0.31	0.45	0.65
20%slag-45: Mean (kg/m^2)	**0.01**	**0.03**	**0.07**	**0.15**	**0.22**	**0.30**	**0.44**	**0.63**
Standard deviation	0.00	0.00	0.00	0.00	0.00	0.01	0.01	0.03
Specimen 1	0.01	0.09	0.35	0.66	0.86	1.04	1.34	1.68
Specimen 2	0.01	0.12	0.54	1.04	1.23	1.44	1.72	2.04
35%slag-45: Mean (kg/m^2)	**0.01**	**0.11**	**0.45**	**0.85**	**1.04**	**1.24**	**1.53**	**1.86**
Standard deviation	0.00	0.02	0.14	0.27	0.26	0.29	0.27	0.25
Specimen 1	0.01	0.25	2.77	5.01	5.74	6.17	6.58	6.81
Specimen 2	0.01	0.16	2.73	4.77	5.63	6.13	6.62	6.90
65%slag-45: Mean (kg/m^2)	**0.01**	**0.21**	**2.75**	**4.89**	**5.68**	**6.15**	**6.60**	**6.85**
Standard deviation	0.00	0.06	0.02	0.17	0.08	0.03	0.03	0.06

Age at start of freeze/thaw test: 31 days

No. of freeze/thaw cycles	1	4	7	14	21	28	42	56
Specimen 1	0.01	0.03	0.07	0.10	0.14	0.18	0.26	0.33
Specimen 2	0.01	0.03	0.05	0.11	0.16	0.22	0.35	0.46
20%slag-45: Mean (kg/m^2)	**0.01**	**0.03**	**0.06**	**0.11**	**0.15**	**0.20**	**0.30**	**0.40**
Standard deviation	0.00	0.00	0.01	0.01	0.02	0.03	0.06	0.09
Specimen 1	0.01	0.10	0.14	0.26	0.39	0.54	0.99	1.34
Specimen 2	0.01	0.05	0.09	0.22	0.35	0.48	1.03	1.34
35%slag-45: Mean (kg/m^2)	**0.01**	**0.07**	**0.12**	**0.24**	**0.37**	**0.51**	**1.01**	**1.34**
Standard deviation	0.00	0.03	0.04	0.03	0.03	0.05	0.03	0.00
Specimen 1	0.01	0.80	2.55	4.30	5.18	5.74	6.55	7.36
Specimen 2	0.01	0.49	2.41	4.17	4.90	5.68	6.57	7.23
65%slag-45: Mean (kg/m^2)	**0.01**	**0.64**	**2.48**	**4.23**	**5.04**	**5.71**	**6.56**	**7.29**
Standard deviation	0.00	0.22	0.10	0.09	0.20	0.04	0.02	0.09

Age at start of freeze/thaw test: 73 days

No. of freeze/thaw cycles	1	4	7	14	21	28	42	56
Specimen 1	0.01	0.04	0.07	0.12	0.15	0.19	0.32	0.51
Specimen 2	0.01	0.02	0.06	0.11	0.17	0.22	0.30	0.46
20%slag-45: Mean (kg/m^2)	**0.01**	**0.03**	**0.06**	**0.11**	**0.16**	**0.21**	**0.31**	**0.49**
Standard deviation	0.00	0.01	0.01	0.01	0.01	0.02	0.02	0.04
Specimen 1	0.01	0.08	0.16	0.29	0.41	0.58	0.98	1.48
Specimen 2	0.01	0.06	0.14	0.27	0.43	0.64	1.09	1.65
35%slag-45: Mean (kg/m^2)	**0.01**	**0.07**	**0.15**	**0.28**	**0.42**	**0.61**	**1.04**	**1.57**
Standard deviation	0.00	0.01	0.02	0.01	0.01	0.04	0.08	0.12
Specimen 1	0.01	0.36	1.24	1.94	2.52	2.98	3.83	4.54
Specimen 2	0.01	0.26	1.39	2.33	2.85	3.31	4.06	4.68
65%slag-45: Mean (kg/m^2)	**0.01**	**0.31**	**1.31**	**2.13**	**2.68**	**3.15**	**3.94**	**4.61**
Standard deviation	0.00	0.07	0.11	0.28	0.24	0.24	0.16	0.10

Scaling in kg/m^2 for dried (with carbon dioxide) specimens of 'micro' concrete with OPC and different amounts of slag as part of the binder

Age at start of freeze/thaw test: 122 days

No. of freeze/thaw cycles	**1**	**4**	**7**	**14**	**21**	**28**	**42**	**56**
Specimen 1	0.01	0.03	0.07	0.14	0.17	0.20	0.30	0.54
Specimen 2	0.00	0.02	0.04	0.10	0.13	0.16	0.32	0.64
20%slag-45: Mean (kg/m^2)	**0.01**	**0.03**	**0.05**	**0.12**	**0.15**	**0.18**	**0.31**	**0.59**
Standard deviation	0.00	0.01	0.02	0.03	0.03	0.03	0.01	0.07
Specimen 1	0.00	0.02	0.06	0.15	0.21	0.29	0.56	0.96
Specimen 2	0.00	0.04	0.09	0.22	0.32	0.45	0.85	1.34
35%slag-45: Mean (kg/m^2)	**0.00**	**0.03**	**0.08**	**0.19**	**0.27**	**0.37**	**0.71**	**1.15**
Standard deviation	0.00	0.02	0.02	0.05	0.08	0.11	0.20	0.27
Specimen 1	0.01	0.17	0.78	1.34	1.74	2.14	2.83	3.45
Specimen 2	0.01	0.10	0.78	1.47	1.91	2.32	2.97	3.56
65%slag-45: Mean (kg/m^2)	**0.01**	**0.14**	**0.78**	**1.40**	**1.83**	**2.23**	**2.90**	**3.51**
Standard deviation	0.00	0.05	0.00	0.09	0.12	0.13	0.10	0.07

Scaling in kg/m^2 for saturated (never-dried) specimens of 'micro' concrete with OPC and different amounts of silica as part of the binder

Age at start of freeze/thaw test: 17 days

No. of freeze/thaw cycles	1	4	7	14	21	28	42	56
Specimen 1	0.01	0.66	1.51	3.19	4.19	5.25	6.99	8.64
Specimen 2	0.02	0.82	1.63	2.99	4.51	5.63	7.42	9.04
OPC2-45 air: Mean (kg/m^2)	**0.01**	**0.74**	**1.57**	**3.09**	**4.35**	**5.44**	**7.21**	**8.84**
Standard deviation	0.01	0.11	0.09	0.14	0.22	0.27	0.31	0.28
Specimen 1	0.01	0.77	1.67	3.13	4.31	5.33	7.00	8.50
Specimen 2	0.02	1.03	1.93	3.56	4.72	5.64	7.30	8.97
5%sil-45 air: Mean (kg/m^2)	**0.01**	**0.90**	**1.80**	**3.35**	**4.51**	**5.49**	**7.15**	**8.74**
Standard deviation	0.00	0.18	0.18	0.30	0.29	0.22	0.21	0.33
Specimen 1	0.01	0.47	1.03	2.30	3.39	4.41	5.94	7.31
Specimen 2	0.02	0.61	1.22	2.40	3.48	4.45	6.06	7.38
10%sil-45 air: Mean (kg/m^2)	**0.01**	**0.54**	**1.13**	**2.35**	**3.44**	**4.43**	**6.00**	**7.35**
Standard deviation	0.01	0.09	0.13	0.07	0.06	0.03	0.08	0.05

Age at start of freeze/thaw test: 31 days

No. of freeze/thaw cycles	1	4	7	14	21	28	42	56
Specimen 1	0.03	0.79	1.46	2.94	4.29	5.48	8.19	11.0
Specimen 2	0.03	0.74	1.42	2.69	3.96	5.01	7.05	9.31
OPC2-45 air: Mean (kg/m^2)	**0.03**	**0.76**	**1.44**	**2.82**	**4.13**	**5.24**	**7.62**	**10.2**
Standard deviation	0.00	0.04	0.03	0.18	0.23	0.34	0.81	1.22
Specimen 1	0.03	0.39	0.84	1.77	2.58	3.38	4.70	5.85
Specimen 2	0.02	0.47	0.90	1.92	2.77	3.52	4.73	5.92
5%sil-45 air: Mean (kg/m^2)	**0.03**	**0.43**	**0.87**	**1.85**	**2.68**	**3.45**	**4.72**	**5.88**
Standard deviation	0.00	0.05	0.04	0.11	0.13	0.10	0.02	0.05
Specimen 1	0.03	0.43	0.77	1.51	2.17	2.73	3.75	4.61
Specimen 2	0.02	0.42	0.76	1.56	2.22	2.81	3.73	4.48
10%sil-45 air: Mean (kg/m^2)	**0.03**	**0.42**	**0.77**	**1.53**	**2.20**	**2.77**	**3.74**	**4.54**
Standard deviation	0.00	0.01	0.01	0.04	0.04	0.06	0.01	0.09

Age at start of freeze/thaw test: 66 days

No. of freeze/thaw cycles	1	4	7	14	21	28	42	56
Specimen 1	0.04	0.45	0.90	1.93	3.24	4.46	6.83	9.48
Specimen 2	0.03	0.52	0.97	2.01	3.20	4.24	6.93	9.33
OPC2-45 air: Mean (kg/m^2)	**0.03**	**0.49**	**0.94**	**1.97**	**3.22**	**4.35**	**6.88**	**9.41**
Standard deviation	0.00	0.05	0.05	0.06	0.02	0.16	0.07	0.10
Specimen 1	0.03	0.25	0.53	1.03	1.59	2.06	2.94	3.89
Specimen 2	0.02	0.25	0.52	1.01	1.60	2.13	3.04	4.05
5%sil-45 air: Mean (kg/m^2)	**0.02**	**0.25**	**0.52**	**1.02**	**1.60**	**2.10**	**2.99**	**3.97**
Standard deviation	0.01	0.00	0.01	0.01	0.01	0.05	0.07	0.11
Specimen 1	0.03	0.21	0.38	0.68	1.01	1.27	1.77	2.30
Specimen 2	0.02	0.21	0.40	0.77	1.10	1.36	1.91	2.49
10%sil-45 air: Mean (kg/m^2)	**0.02**	**0.21**	**0.39**	**0.73**	**1.05**	**1.32**	**1.84**	**2.40**
Standard deviation	0.01	0.00	0.01	0.07	0.06	0.07	0.10	0.13

Scaling in kg/m^2 for saturated (never-dried) specimens of 'micro' concrete with OPC and different amounts of silica as part of the binder

Age at start of freeze/thaw test: 136 days

No. of freeze/thaw cycles	1	4	7	14	21	28	42	56
Specimen 1	0.02	0.54	1.08	2.22	3.27	4.38	6.85	9.35
Specimen 2	0.02	0.65	1.37	2.75	3.75	4.85	6.62	8.59
OPC2-45 air: Mean (kg/m^2)	**0.02**	**0.60**	**1.23**	**2.49**	**3.51**	**4.62**	**6.73**	**8.97**
Standard deviation	0.00	0.08	0.20	0.37	0.34	0.33	0.16	0.54
Specimen 1	0.01	0.12	0.32	0.70	1.13	1.53	2.38	3.22
Specimen 2	0.01	0.12	0.31	0.72	1.12	1.52	2.27	3.00
5%sil-45 air: Mean (kg/m^2)	**0.01**	**0.12**	**0.31**	**0.71**	**1.13**	**1.52**	**2.33**	**3.11**
Standard deviation	0.00	0.00	0.01	0.02	0.00	0.01	0.08	0.15
Specimen 1	0.01	0.07	0.18	0.41	0.59	0.75	1.10	1.42
Specimen 2	0.01	0.07	0.16	0.37	0.56	0.73	1.08	1.44
10%sil-45 air: Mean (kg/m^2)	**0.01**	**0.07**	**0.17**	**0.39**	**0.57**	**0.74**	**1.09**	**1.43**
Standard deviation	0.00	0.00	0.01	0.03	0.02	0.01	0.01	0.02

Scaling in kg/m^2 for dried (without carbon dioxide) specimens of 'micro' concrete with OPC and different amounts of silica as part of the binder

Age at start of freeze/thaw test: 17 days

No. of freeze/thaw cycles	1	4	7	14	21	28	42	56
Specimen 1	0.01	0.39	0.81	1.58	2.21	2.70	3.36	3.94
Specimen 2	0.00	0.30	0.69	1.45	2.11	2.60	3.36	3.98
OPC2-45 air: Mean (kg/m^2)	**0.01**	**0.34**	**0.75**	**1.51**	**2.16**	**2.65**	**3.36**	**3.96**
Standard deviation	0.01	0.07	0.09	0.09	0.08	0.07	0.01	0.03
Specimen 1	0.01	0.40	0.79	1.50	2.13	2.67	3.64	4.61
Specimen 2	0.01	0.30	0.59	1.22	1.80	2.26	3.15	3.99
5%sil-45 air: Mean (kg/m^2)	**0.01**	**0.35**	**0.69**	**1.36**	**1.96**	**2.47**	**3.40**	**4.30**
Standard deviation	0.00	0.07	0.14	0.20	0.23	0.29	0.35	0.43
Specimen 1	0.01	0.17	0.35	0.94	1.48	1.98	2.89	3.81
Specimen 2	0.02	0.21	0.41	0.98	1.51	2.05	2.93	3.72
10%sil-45 air: Mean (kg/m^2)	**0.01**	**0.19**	**0.38**	**0.96**	**1.50**	**2.02**	**2.91**	**3.77**
Standard deviation	0.00	0.03	0.04	0.03	0.02	0.05	0.03	0.07

Age at start of freeze/thaw test: 31 days

No. of freeze/thaw cycles	1	4	7	14	21	28	42	56
Specimen 1	0.01	0.57	1.10	1.97	2.69	3.50	5.05	6.69
Specimen 2	0.01	0.21	1.04	1.85	2.49	3.07	4.14	5.17
OPC2-45 air: Mean (kg/m^2)	**0.01**	**0.39**	**1.07**	**1.91**	**2.59**	**3.28**	**4.60**	**5.93**
Standard deviation	0.00	0.25	0.04	0.08	0.14	0.30	0.65	1.08
Specimen 1	0.01	0.31	0.60	1.35	2.13	2.79	4.02	5.20
Specimen 2	0.01	0.21	0.58	1.27	1.89	2.42	3.47	4.48
5%sil-45 air: Mean (kg/m^2)	**0.01**	**0.26**	**0.59**	**1.31**	**2.01**	**2.60**	**3.75**	**4.84**
Standard deviation	0.00	0.07	0.02	0.06	0.17	0.26	0.39	0.51
Specimen 1	0.02	0.26	0.57	1.33	2.09	2.73	3.93	4.87
Specimen 2	0.01	0.25	0.51	1.12	1.78	2.33	3.34	4.20
10%sil-45 air: Mean (kg/m^2)	**0.01**	**0.26**	**0.54**	**1.23**	**1.94**	**2.53**	**3.64**	**4.53**
Standard deviation	0.00	0.01	0.04	0.15	0.22	0.28	0.42	0.47

Age at start of freeze/thaw test: 66 days

No. of freeze/thaw cycles	1	4	7	14	21	28	42	56
Specimen 1	0.01	0.62	1.11	2.35	3.54	4.55	6.54	8.85
Specimen 2	0.02	0.61	1.13	2.16	3.30	4.27	6.25	8.35
OPC2-45 air: Mean (kg/m^2)	**0.02**	**0.61**	**1.12**	**2.25**	**3.42**	**4.41**	**6.40**	**8.60**
Standard deviation	0.00	0.00	0.01	0.13	0.17	0.19	0.20	0.35
Specimen 1	0.01	0.24	0.47	1.05	1.65	2.15	3.23	4.12
Specimen 2	0.01	0.27	0.52	1.08	1.67	2.13	3.09	4.00
5%sil-45 air: Mean (kg/m^2)	**0.01**	**0.26**	**0.50**	**1.07**	**1.66**	**2.14**	**3.16**	**4.06**
Standard deviation	0.00	0.02	0.04	0.02	0.01	0.02	0.10	0.09
Specimen 1	0.02	0.21	0.41	0.81	1.22	1.53	2.13	2.66
Specimen 2	0.01	0.19	0.39	0.79	1.22	1.52	2.16	2.68
10%sil-45 air: Mean (kg/m^2)	**0.02**	**0.20**	**0.40**	**0.80**	**1.22**	**1.52**	**2.15**	**2.67**
Standard deviation	0.00	0.01	0.01	0.01	0.00	0.00	0.02	0.01

Scaling in kg/m^2 for dried (without carbon dioxide) specimens of 'micro' concrete with OPC and different amounts of silica as part of the binder

Age at start of freeze/thaw test: 136 days

No. of freeze/thaw cycles	1	4	7	14	21	28	42	56
Specimen 1	0.02	0.31	0.91	1.99	3.15	4.36	6.92	9.77
Specimen 2	0.03	0.36	0.97	1.92	2.88	3.88	5.87	8.26
OPC2-45 air: Mean (kg/m^2)	**0.02**	**0.34**	**0.94**	**1.96**	**3.01**	**4.12**	**6.39**	**9.01**
Standard deviation	0.00	0.03	0.04	0.05	0.19	0.34	0.75	1.06
Specimen 1	0.01	0.14	0.38	0.79	1.19	1.54	2.29	2.99
Specimen 2	0.02	0.13	0.38	0.79	1.22	1.61	2.35	3.16
5%sil-45 air: Mean (kg/m^2)	**0.01**	**0.13**	**0.38**	**0.79**	**1.21**	**1.57**	**2.32**	**3.08**
Standard deviation	0.00	0.01	0.00	0.00	0.02	0.05	0.04	0.12
Specimen 1	0.01	0.10	0.25	0.51	0.53	0.82	1.09	1.48
Specimen 2	0.01	0.07	0.22	0.44	0.59	0.72	1.07	1.40
10%sil-45 air: Mean (kg/m^2)	**0.01**	**0.09**	**0.24**	**0.47**	**0.56**	**0.77**	**1.08**	**1.44**
Standard deviation	0.00	0.02	0.03	0.05	0.04	0.07	0.02	0.06

Scaling in kg/m^2 for dried (with carbon dioxide) specimens of 'micro' concrete with OPC and different amounts of silica as part of the binder

Age at start of freeze/thaw test: 17 days

No. of freeze/thaw cycles	1	4	7	14	21	28	42	56
Specimen 1	0.00	0.02	0.06	0.11	0.16	0.17	0.21	0.25
Specimen 2	0.00	0.01	0.04	0.11	0.16	0.18	0.21	0.23
OPC2-45 air: Mean (kg/m^2)	**0.00**	**0.01**	**0.05**	**0.11**	**0.16**	**0.18**	**0.21**	**0.24**
Standard deviation	0.00	0.00	0.01	0.00	0.00	0.01	0.00	0.02
Specimen 1	0.00	0.03	0.08	0.18	0.27	0.31	0.41	0.53
Specimen 2	0.01	0.02	0.07	0.17	0.23	0.29	0.37	0.47
5%sil-45 air: Mean (kg/m^2)	**0.00**	**0.02**	**0.07**	**0.17**	**0.25**	**0.30**	**0.39**	**0.50**
Standard deviation	0.00	0.01	0.01	0.01	0.03	0.02	0.03	0.04
Specimen 1	0.01	0.04	0.15	0.43	0.58	0.72	0.98	1.23
Specimen 2	0.00	0.03	0.19	0.47	0.64	0.79	1.05	1.34
10%sil-45 air: Mean (kg/m^2)	**0.01**	**0.04**	**0.17**	**0.45**	**0.61**	**0.76**	**1.01**	**1.29**
Standard deviation	0.00	0.00	0.03	0.03	0.04	0.05	0.05	0.08

Age at start of freeze/thaw test: 31 days

No. of freeze/thaw cycles	1	4	7	14	21	28	42	56
Specimen 1	0.01	0.06	0.07	0.12	0.18	0.19	0.22	0.26
Specimen 2	0.01	0.04	0.06	0.10	0.15	0.18	0.20	0.23
OPC2-45 air: Mean (kg/m^2)	**0.01**	**0.05**	**0.07**	**0.11**	**0.17**	**0.18**	**0.21**	**0.24**
Standard deviation	0.00	0.01	0.01	0.02	0.02	0.01	0.02	0.02
Specimen 1	0.01	0.06	0.10	0.17	0.22	0.28	0.40	0.57
Specimen 2	0.01	0.04	0.07	0.13	0.18	0.22	0.35	0.53
5%sil-45 air: Mean (kg/m^2)	**0.01**	**0.05**	**0.09**	**0.15**	**0.20**	**0.25**	**0.38**	**0.55**
Standard deviation	0.00	0.01	0.02	0.03	0.03	0.04	0.04	0.03
Specimen 1	0.01	0.09	0.22	0.48	0.70	0.93	1.44	1.98
Specimen 2	0.01	0.08	0.18	0.39	0.59	0.77	1.28	1.78
10%sil-45 air: Mean (kg/m^2)	**0.01**	**0.09**	**0.20**	**0.44**	**0.64**	**0.85**	**1.36**	**1.88**
Standard deviation	0.00	0.00	0.03	0.06	0.08	0.11	0.11	0.14

Age at start of freeze/thaw test: 66 days

No. of freeze/thaw cycles	1	4	7	14	21	28	42	56
Specimen 1	0.01	0.02	0.04	0.06	0.10	0.12	0.18	0.29
Specimen 2	0.01	0.03	0.06	0.08	0.16	0.17	0.22	0.29
OPC2-45 air: Mean (kg/m^2)	**0.01**	**0.03**	**0.05**	**0.07**	**0.13**	**0.15**	**0.20**	**0.29**
Standard deviation	0.00	0.00	0.01	0.01	0.05	0.04	0.03	0.00
Specimen 1	0.01	0.04	0.08	0.17	0.29	0.38	0.59	0.82
Specimen 2	0.01	0.04	0.08	0.17	0.32	0.46	0.80	1.18
5%sil-45 air: Mean (kg/m^2)	**0.01**	**0.04**	**0.08**	**0.17**	**0.30**	**0.42**	**0.69**	**1.00**
Standard deviation	0.00	0.00	0.00	0.00	0.02	0.06	0.15	0.26
Specimen 1	0.01	0.06	0.16	0.42	0.69	0.90	1.36	1.81
Specimen 2	0.01	0.07	0.17	0.40	0.60	0.78	1.21	1.62
10%sil-45 air: Mean (kg/m^2)	**0.01**	**0.06**	**0.17**	**0.41**	**0.64**	**0.84**	**1.28**	**1.71**
Standard deviation	0.00	0.01	0.00	0.02	0.06	0.09	0.11	0.13

Scaling in kg/m^2 for dried (with carbon dioxide) specimens of 'micro' concrete with OPC and different amounts of silica as part of the binder

Age at start of freeze/thaw test: 136 days

No. of freeze/thaw cycles	1	4	7	14	21	28	42	56
Specimen 1	0.00	0.01	0.03	0.05	0.07	0.09	0.12	0.16
Specimen 2	0.01	0.02	0.03	0.05	0.09	0.13	0.23	0.34
OPC2-45 air: Mean (kg/m^2)	**0.01**	**0.02**	**0.03**	**0.05**	**0.08**	**0.11**	**0.18**	**0.25**
Standard deviation	0.00	0.00	0.00	0.00	0.01	0.03	0.08	0.12
Specimen 1	0.01	0.03	0.06	0.13	0.20	0.25	0.38	0.54
Specimen 2	0.00	0.02	0.05	0.10	0.15	0.22	0.36	0.54
5%sil-45 air: Mean (kg/m^2)	**0.00**	**0.02**	**0.05**	**0.12**	**0.17**	**0.23**	**0.37**	**0.54**
Standard deviation	0.00	0.01	0.01	0.02	0.04	0.02	0.01	0.00
Specimen 1	0.00	0.04	0.10	0.25	0.38	0.50	0.79	1.12
Specimen 2	0.01	0.04	0.09	0.22	0.34	0.46	0.70	0.99
10%sil-45 air: Mean (kg/m^2)	**0.01**	**0.04**	**0.10**	**0.24**	**0.36**	**0.48**	**0.75**	**1.05**
Standard deviation	0.00	0.00	0.01	0.02	0.03	0.03	0.06	0.09

APPENDIX 7

CALCULATION OF THE AGGREGATE SURFACE AREA TO BINDER PASTE VOLUME RATIO - EXAMPLE

Example of calculation of the aggregate surface area to binder-paste volume ratio for mortar, micro-concrete and concrete with w/b-ratio 0.45.

Table 1 shows the composition of the mortar used the investigations described in Chapter 5 to 9, as well as the composition of the 'micro-concrete' used in the investigation described in Chapter 3 and that of a representative 'normal' concrete, all with a w/b-ratio of 0.45. The table also shows approximate values of the specific surface area for different aggregate fractions (based on measurements presented by Shacklock & Walker (1958)).

Table 1 Mix compositions for mortar, micro-concrete and a 'normal' concrete, all with a w/b-ratio of 0.45. A mean specific surface has been assumed for each aggregate fraction, based on results in Shacklock & Walker (1958).

		Mortar	***Micro-concrete***	***Concrete***
Cement (kg/m^3)		*699.9*	*448*	*400*
Water (kg/m^3)		*315.0*	*201.6*	*180*
Aggregate content (kg/m^3)		*1240*	*1624*	*1800*
Aggregate	***Specific surface (mm^{-1})***	***Particle size distributions of the gradings used, content in %***		
0.125 / 0.25 mm	*30*	*33*	*14*	*9*
0.25 / 0.50 mm	*15*	*33*	*14*	*11*
0.50 / 1.0 mm	*10*	*33*	*17*	*11*
1.0 / 2.0 mm	*6*	-	*19*	*11*
2.0 / 4.0 mm	*2*	-	*22*	*10*
4.0 / 8.0 mm	*1*	-	*14*	*12*
8.0 /16.0 mm	*0.5*	-	-	*36*

The surface area (A_{agg}) of the aggregate and the binder-paste volume (V_{paste}) per m^3 mix is calculated (assuming an aggregate density of 2700 kg/m^3, a cement density of 3100 kg/m^3 and a water density of 1000 kg/m^3):

Mortar:

$$A_{agg} = (30 \cdot 0.33 + 15 \cdot 0.33 + 10 \cdot 0.33) \cdot \frac{1240}{2700 \cdot 10^{-9}} = 8.3 \cdot 10^9 \, mm^2$$

$$V_{paste} = \left(\frac{699.9}{3100} + \frac{315}{1000} \right) \cdot 10^9 = 0.54 \cdot 10^9 \, mm^3$$

Micro-concrete:

$$A_{agg} = (30 \cdot 0.14 + 15 \cdot 0.14 + 10 \cdot 0.17 + 6 \cdot 0.19 + 2 \cdot 0.22 + 1 \cdot 0.14) \cdot \frac{1624}{2700 \cdot 10^{-9}} = 5.9 \cdot 10^9 \, mm^2$$

$$V_{paste} = \left(\frac{448}{3100} + \frac{201.6}{1000} \right) \cdot 10^9 = 0.35 \cdot 10^9 \, mm^3$$

Concrete:

$$A_{agg} = (30 \cdot 0.09 + 15 \cdot 0.11 + 10 \cdot 0.11 + 6 \cdot 0.11 + 2 \cdot 0.10 + 1 \cdot 0.12 + 0.5 \cdot 0.36) \cdot \frac{1800}{2700 \cdot 10^{-9}}$$

$$A_{agg} = 4.4 \cdot 10^{9}\, mm^{2}$$

$$V_{paste} = \left(\frac{400}{3100} + \frac{180}{1000} \right) \cdot 10^{9} = 0.31 \cdot 10^{9}\, mm^{3}$$

Dividing the surface area of the aggregate by the paste volume results in the following values; Mortar: 15.4, Micro-concrete: 16.9 and Concrete: 14.2 mm^2/mm^3

APPENDIX 8

WATER ABSORPTION DURING
CAPILLARY SUCTION

Water absorption during capillary suction in kg/m^2 related to the dry weight (+105 °C). Specimen thickness 5.0 mm. At time zero, specimens were in equilibrium with 65 % RH at +20 °C.

OPC w/b-ratio 0.35 Carbonated material

Time (days)	0	0.00	0.01	0.01	0.02	0.03	0.06	0.08	0.12	0.16	0.20	0.25	0.33	0.79	1.87
Time (root(s))	0	15	23	31	39	54	70	85	101	116	132	147	168	262	402
1103	0.56	0.61	0.63	0.64	0.66	0.70	0.73	0.76	0.79	0.81	0.83	0.84	0.86	0.92	0.93
1109	0.56	0.62	0.64	0.67	0.70	0.75	0.80	0.84	0.88	0.90	0.91	0.91	0.91	0.92	0.93
1111	0.57	0.63	0.65	0.67	0.70	0.76	0.80	0.84	0.87	0.90	0.91	0.92	0.93	0.94	0.95
Mean (kg/m^2)	0.57	0.62	0.64	0.66	0.69	0.74	0.78	0.82	0.85	0.87	0.88	0.89	0.90	0.93	0.94
Standard dev.	0.01	0.01	0.01	0.02	0.02	0.03	0.04	0.05	0.05	0.05	0.05	0.04	0.04	0.01	0.01

Time (days)	2.82	3.92	8.01	11.0	17.0	25.2	31.0	48.9	63.1	93.0	148	253	331	Vacuum
Time (root(s))	494	582	832	975	1211	1474	1636	2055	2334	2835	3577	4676	5348	saturation
1103	0.94	0.95	0.96	0.96	0.96	0.97	0.97	0.97	0.98	0.98	0.99	0.99	1.00	0.99
1109	0.94	0.95	0.96	0.96	0.97	0.97	0.97	0.98	0.98	0.99	0.99	1.00	1.01	1.03
1111	0.96	0.97	0.98	0.98	0.98	0.99	0.99	0.99	1.00	1.00	1.01	1.02	1.02	1.03
Mean (kg/m^2)	0.95	0.95	0.96	0.97	0.97	0.98	0.98	0.98	0.99	0.99	1.00	1.00	1.01	1.02
Standard dev.	0.01	0.01	0.01	0.01	0.01	0.01	0.01	0.01	0.01	0.01	0.01	0.01	0.01	0.03

OPC w/b-ratio 0.35 Uncarbonated material

Time (days)	0	0.00	0.01	0.01	0.02	0.03	0.08	0.16	0.33	0.93	1.93	3.03	7.16	10.1	16.1
Time (root(s))	0	15	23	31	39	54	85	116	168	283	409	512	786	935	1179
0106	0.54	0.83	0.95	1.05	1.09	1.09	1.09	1.10	1.10	1.11	1.11	1.11	1.12	1.12	1.13
0110	0.52	0.83	0.94	1.04	1.08	1.08	1.08	1.09	1.09	1.09	1.10	1.10	1.11	1.12	1.12
0116	0.52	0.82	0.92	1.02	1.05	1.06	1.07	1.07	1.07	1.08	1.09	1.09	1.10	1.10	1.10
Mean (kg/m^2)	0.53	0.83	0.94	1.04	1.07	1.08	1.08	1.08	1.09	1.09	1.10	1.10	1.11	1.11	1.12
Standard dev.	0.01	0.01	0.01	0.02	0.02	0.02	0.01	0.01	0.01	0.01	0.01	0.01	0.01	0.01	0.01

Time (days)	24.2	30.1	48.1	62.2	92.1	147	252	330	Vacuum
Time (root(s))	1445	1613	2038	2318	2821	3566	4668	5341	saturation
0106	1.13	1.13	1.13	1.14	1.15	1.15	1.17	1.18	1.20
0110	1.12	1.13	1.13	1.14	1.15	1.15	1.17	1.17	1.20
0116	1.11	1.11	1.11	1.12	1.13	1.14	1.15	1.16	1.17
Mean (kg/m^2)	1.12	1.12	1.13	1.13	1.14	1.15	1.16	1.17	1.19
Standard dev.	0.01	0.01	0.01	0.01	0.01	0.01	0.01	0.01	0.02

Water absorption during capillary suction in kg/m^2 related to the dry weight (+105 °C). Specimen thickness 5.0 mm. At time zero, specimens were in equilibrium with 65 % RH at +20 °C.

OPC w/b-ratio 0.45 Carbonated material

Time (days)	0	0.00	0.01	0.01	0.02	0.03	0.06	0.08	0.12	0.16	0.20	0.31	0.35	1.01	2.34
Time (root(s))	0	15	23	31	39	54	70	85	101	116	132	162	173	296	450
1205	0.40	0.49	0.52	0.55	0.57	0.62	0.66	0.69	0.73	0.75	0.78	0.81	0.81	0.83	0.84
1208	0.40	0.49	0.52	0.55	0.58	0.63	0.68	0.72	0.76	0.79	0.81	0.82	0.82	0.83	0.84
1215	0.40	0.48	0.51	0.54	0.57	0.62	0.66	0.71	0.74	0.77	0.80	0.82	0.82	0.83	0.84
Mean (kg/m^2)	0.40	0.49	0.52	0.55	0.58	0.62	0.67	0.71	0.74	0.77	0.80	0.82	0.82	0.83	0.84
Standard dev.	0.00	0.00	0.00	0.00	0.01	0.01	0.01	0.02	0.02	0.02	0.02	0.01	0.00	0.00	0.00

Time (days)	5.44	9.11	15.1	22.3	33.0	47.1	77.2	132	231	288	Vacuum
Time (root(s))	685	887	1141	1388	1689	2018	2583	3380	4470	4990	saturation
1205	0.86	0.86	0.87	0.88	0.89	0.89	0.90	0.91	0.92	0.93	0.96
1208	0.86	0.86	0.88	0.88	0.89	0.90	0.91	0.92	0.93	0.93	0.96
1215	0.86	0.86	0.87	0.88	0.89	0.89	0.90	0.91	0.92	0.93	0.96
Mean (kg/m^2)	0.86	0.86	0.87	0.88	0.89	0.90	0.90	0.91	0.92	0.93	0.96
Standard dev.	0.00	0.00	0.00	0.00	0.00	0.00	0.00	0.00	0.00	0.00	0.00

OPC w/b-ratio 0.45 Uncarbonated material

Time (days)	0	0.00	0.01	0.01	0.02	0.03	0.06	0.08	0.12	0.16	0.25	0.96	2.27	5.38	9.04
Time (root(s))	0	15	23	31	39	54	70	85	101	116	147	288	443	682	884
0203	0.38	0.85	1.00	1.04	1.05	1.05	1.05	1.05	1.06	1.06	1.06	1.07	1.09	1.10	1.11
0206	0.38	0.86	1.00	1.05	1.05	1.06	1.06	1.06	1.07	1.07	1.07	1.09	1.10	1.12	1.13
0214	0.38	0.83	1.00	1.04	1.04	1.05	1.05	1.05	1.06	1.06	1.06	1.07	1.09	1.10	1.11
Mean (kg/m^2)	0.38	0.85	1.00	1.04	1.05	1.05	1.05	1.06	1.06	1.06	1.06	1.08	1.09	1.11	1.11
Standard dev.	0.00	0.01	0.00	0.01	0.00	0.00	0.01	0.01	0.01	0.01	0.01	0.01	0.01	0.01	0.01

Time (days)	15.0	22.2	33.0	47.1	77.0	132	231	288	Vacuum
Time (root(s))	1139	1386	1688	2017	2580	3379	4469	4989	saturation
0203	1.11	1.11	1.11	1.12	1.12	1.13	1.14	1.15	1.18
0206	1.13	1.14	1.14	1.14	1.15	1.15	1.16	1.17	1.21
0214	1.12	1.12	1.12	1.13	1.13	1.14	1.15	1.15	1.19
Mean (kg/m^2)	1.12	1.12	1.13	1.13	1.13	1.14	1.15	1.16	1.19
Standard dev.	0.01	0.01	0.01	0.01	0.01	0.01	0.01	0.01	0.02

Water absorption during capillary suction in kg/m^2 related to the dry weight (+105 °C). Specimen thickness 5.0 mm. At time zero, specimens were in equilibrium with 65 % RH at +20 °C.

OPC w/b-ratio 0.55 Carbonated material

Time (days)	0	0.00	0.01	0.01	0.02	0.03	0.06	0.08	0.12	0.16	0.20	0.25	0.33	0.79	1.87
Time (root(s))	0	15	23	31	39	54	70	85	101	116	132	147	168	262	402
1303	0.25	0.40	0.46	0.53	0.59	0.69	0.72	0.72	0.73	0.73	0.73	0.73	0.73	0.74	0.75
1307	0.25	0.44	0.50	0.56	0.61	0.70	0.74	0.75	0.75	0.75	0.75	0.75	0.76	0.77	0.78
1315	0.24	0.35	0.40	0.45	0.50	0.59	0.64	0.66	0.66	0.66	0.66	0.66	0.67	0.67	0.69
Mean (kg/m^2)	0.25	0.42	0.48	0.54	0.60	0.69	0.73	0.74	0.74	0.74	0.74	0.74	0.75	0.75	0.77
Standard dev.	0.00	0.04	0.05	0.06	0.06	0.06	0.05	0.04	0.05	0.05	0.05	0.05	0.05	0.05	0.05

Time (days)	2.82	3.92	8.01	11.0	17.0	25.2	31.0	48.9	63.1	93.0	148	253	331	Vacuum
Time (root(s))	494	582	832	975	1211	1474	1636	2055	2334	2835	3577	4676	5348	saturation
1303	0.76	0.77	0.79	0.81	0.81	0.82	0.82	0.82	0.82	0.82	0.83	0.83	0.83	0.83
1307	0.79	0.80	0.83	0.84	0.84	0.85	0.85	0.85	0.85	0.85	0.85	0.86	0.86	0.86
1315	0.69	0.70	0.72	0.73	0.73	0.74	0.74	0.74	0.75	0.75	0.75	0.76	0.76	0.83
Mean (kg/m^2)	0.78	0.79	0.81	0.82	0.83	0.83	0.83	0.83	0.84	0.84	0.84	0.84	0.85	0.84
Standard dev.	0.05	0.05	0.06	0.06	0.06	0.05	0.05	0.05	0.05	0.05	0.05	0.05	0.05	0.02

OPC w/b-ratio 0.55 Uncarbonated material

Time (days)	0	0.00	0.01	0.01	0.02	0.03	0.08	0.16	0.33	0.93	1.93	3.03	7.16	10.1	16.1
Time (root(s))	0	15	23	31	39	54	85	116	168	283	409	512	786	935	1179
0304	0.29	0.90	1.04	1.04	1.05	1.05	1.06	1.06	1.07	1.09	1.10	1.12	1.14	1.15	1.15
0310	0.27	0.87	1.02	1.02	1.03	1.03	1.04	1.04	1.05	1.07	1.09	1.10	1.12	1.13	1.13
0316	0.28	0.89	1.04	1.05	1.05	1.06	1.06	1.07	1.08	1.10	1.12	1.13	1.15	1.16	1.16
Mean (kg/m^2)	0.28	0.89	1.03	1.04	1.04	1.05	1.05	1.06	1.06	1.08	1.10	1.12	1.14	1.14	1.15
Standard dev.	0.01	0.01	0.01	0.01	0.01	0.01	0.01	0.01	0.01	0.01	0.01	0.01	0.02	0.01	0.01

Time (days)	24.2	30.1	48.1	62.2	92.1	147	252	330	Vacuum
Time (root(s))	1445	1613	2038	2318	2821	3566	4668	5341	saturation
0304	1.15	1.15	1.15	1.15	1.16	1.16	1.17	1.17	1.21
0310	1.14	1.14	1.14	1.14	1.14	1.15	1.16	1.16	1.19
0316	1.16	1.16	1.16	1.16	1.16	1.17	1.18	1.18	1.20
Mean (kg/m^2)	1.15	1.15	1.15	1.15	1.16	1.16	1.17	1.17	1.20
Standard dev.	0.01	0.01	0.01	0.01	0.01	0.01	0.01	0.01	0.01

Water absorption during capillary suction in kg/m^2 related to the dry weight (+105 °C). Specimen thickness 5.0 mm. At time zero, specimens were in equilibrium with 65 % RH at +20 °C.

OPC + 35 % slag w/b-ratio 0.45 Carbonated material

Time (days)	0	0.00	0.01	0.01	0.02	0.03	0.06	0.08	0.12	0.16	0.20	0.25	0.48	1.00	2.01
Time (root(s))	0	15	23	31	39	54	70	85	101	116	132	147	204	293	417
1404	0.34	0.45	0.49	0.54	0.57	0.64	0.69	0.72	0.74	0.76	0.77	0.77	0.78	0.79	0.80
1407	0.33	0.45	0.49	0.52	0.55	0.61	0.65	0.69	0.72	0.74	0.75	0.75	0.76	0.77	0.78
1415	0.32	0.44	0.48	0.52	0.55	0.61	0.66	0.69	0.72	0.73	0.74	0.74	0.75	0.75	0.76
Mean (kg/m^2)	0.33	0.45	0.49	0.53	0.56	0.62	0.67	0.70	0.73	0.74	0.75	0.75	0.76	0.77	0.78
Standard dev.	0.01	0.01	0.01	0.01	0.01	0.02	0.02	0.02	0.02	0.02	0.02	0.02	0.02	0.02	0.02

Time (days)	3.09	7.17	10.2	16.2	24.3	30.2	48.1	62.3	92.3	147	246	330	Vacuum
Time (root(s))	517	787	939	1182	1450	1615	2039	2320	2823	3567	4613	5342	saturation
1404	0.81	0.83	0.84	0.85	0.86	0.86	0.87	0.88	0.88	0.89	0.90	0.91	0.96
1407	0.79	0.81	0.82	0.83	0.84	0.84	0.85	0.85	0.86	0.86	0.88	0.88	0.93
1415	0.77	0.79	0.80	0.81	0.81	0.82	0.83	0.83	0.84	0.84	0.86	0.86	0.89
Mean (kg/m^2)	0.79	0.81	0.82	0.83	0.84	0.84	0.85	0.85	0.86	0.87	0.88	0.88	0.92
Standard dev.	0.02	0.02	0.02	0.02	0.02	0.02	0.02	0.02	0.02	0.02	0.02	0.02	0.03

OPC + 35 % slag w/b-ratio 0.45 Uncarbonated material

Time (days)	0	0.00	0.01	0.01	0.02	0.03	0.06	0.08	0.12	0.16	0.20	0.25	0.33	0.89	1.22
Time (root(s))	0	15	23	31	39	54	70	85	101	116	132	147	170	277	325
0403	0.46	0.79	0.89	0.97	1.00	1.01	1.02	1.02	1.02	1.03	1.03	1.03	1.03	1.05	1.05
0406	0.46	0.77	0.87	0.95	1.00	1.01	1.02	1.02	1.03	1.03	1.03	1.03	1.04	1.05	1.05
0416	0.46	0.77	0.87	0.94	0.98	1.00	1.00	1.00	1.01	1.01	1.01	1.01	1.02	1.02	1.03
Mean (kg/m^2)	0.46	0.78	0.88	0.95	0.99	1.01	1.01	1.02	1.02	1.02	1.02	1.03	1.03	1.04	1.04
Standard dev.	0.00	0.01	0.01	0.02	0.01	0.01	0.01	0.01	0.01	0.01	0.01	0.01	0.01	0.01	0.01

Time (days)	1.99	6.06	9.10	15.1	23.2	29.1	47.0	61.2	91.1	146	251	329	Vacuum
Time (root(s))	414	724	887	1140	1417	1585	2015	2299	2806	3554	4659	5333	saturation
0403	1.06	1.08	1.09	1.09	1.09	1.09	1.10	1.10	1.12	1.13	1.14	1.14	1.25
0406	1.07	1.08	1.09	1.09	1.10	1.10	1.11	1.11	1.12	1.13	1.14	1.15	1.24
0416	1.04	1.06	1.07	1.07	1.07	1.08	1.08	1.09	1.10	1.11	1.12	1.13	1.24
Mean (kg/m^2)	1.06	1.07	1.08	1.09	1.09	1.09	1.10	1.10	1.11	1.12	1.13	1.14	1.24
Standard dev.	0.01	0.01	0.01	0.01	0.01	0.01	0.01	0.01	0.01	0.01	0.01	0.01	0.00

Water absorption during capillary suction in kg/m^2 related to the dry weight (+105 °C). Specimen thickness 5.0 mm. At time zero, specimens were in equilibrium with 65 % RH at +20 °C.

OPC + 65 % slag w/b-ratio 0.35 Carbonated material

Time (days)	0	0.00	0.01	0.01	0.02	0.03	0.06	0.08	0.12	0.16	0.20	0.25	0.48	1.00	2.01
Time (root(s))	0	15	23	31	39	54	70	85	101	116	132	147	204	293	417
1505	0.44	0.62	0.66	0.71	0.74	0.78	0.82	0.84	0.86	0.87	0.87	0.88	0.89	0.90	0.90
1510	0.43	0.54	0.59	0.64	0.69	0.77	0.82	0.84	0.84	0.85	0.85	0.85	0.85	0.86	0.86
1514	0.43	0.53	0.58	0.62	0.67	0.75	0.81	0.84	0.85	0.86	0.86	0.86	0.87	0.87	0.88
Mean (kg/m^2)	0.43	0.56	0.61	0.66	0.70	0.77	0.81	0.84	0.85	0.86	0.86	0.86	0.87	0.88	0.88
Standard dev.	0.01	0.05	0.05	0.04	0.04	0.01	0.00	0.00	0.01	0.01	0.01	0.01	0.02	0.02	0.02

Time (days)	3.09	7.17	10.2	16.2	24.3	30.2	48.1	62.3	92.3	147	246	330	Vacuum
Time (root(s))	517	787	939	1182	1450	1615	2039	2320	2823	3567	4613	5342	saturation
1505	0.92	0.92	0.93	0.94	0.95	0.95	0.95	0.96	0.96	0.97	0.99	0.99	1.05
1510	0.87	0.89	0.89	0.90	0.91	0.91	0.92	0.92	0.93	0.94	0.95	0.95	1.02
1514	0.89	0.90	0.91	0.91	0.92	0.92	0.93	0.94	0.95	0.96	0.97	0.98	1.03
Mean (kg/m^2)	0.89	0.91	0.91	0.92	0.93	0.93	0.93	0.94	0.95	0.96	0.97	0.97	1.03
Standard dev.	0.02	0.02	0.02	0.02	0.02	0.02	0.02	0.02	0.02	0.02	0.02	0.02	0.02

OPC + 65 % slag w/b-ratio 0.35 Uncarbonated material

Time (days)	0	0.00	0.01	0.01	0.02	0.03	0.06	0.08	0.12	0.16	0.20	0.25	0.33	0.40	0.89
Time (root(s))	0	15	23	31	39	54	70	85	101	116	132	147	170	185	277
0505	0.66	0.80	0.85	0.90	0.94	1.00	1.04	1.05	1.06	1.06	1.07	1.07	1.07	1.07	1.08
0508	0.68	0.82	0.85	0.88	0.91	0.95	0.98	1.01	1.02	1.04	1.05	1.06	1.07	1.07	1.08
0511	0.67	0.77	0.80	0.83	0.86	0.90	0.93	0.96	0.98	1.00	1.02	1.03	1.04	1.04	1.06
Mean (kg/m^2)	0.67	0.80	0.84	0.87	0.90	0.95	0.98	1.01	1.02	1.04	1.04	1.05	1.06	1.06	1.07
Standard dev.	0.01	0.02	0.03	0.03	0.04	0.05	0.05	0.05	0.04	0.03	0.03	0.02	0.02	0.02	0.01

Time (days)	1.22	1.99	6.06	9.10	15.1	23.2	29.1	47.0	61.2	91.1	146	251	329	Vacuum
Time (root(s))	325	414	724	887	1140	1417	1585	2015	2299	2806	3554	4659	5333	saturation
0505	1.08	1.09	1.10	1.10	1.11	1.11	1.12	1.13	1.14	1.16	1.17	1.18	1.19	1.34
0508	1.09	1.10	1.11	1.12	1.12	1.13	1.14	1.15	1.16	1.18	1.20	1.21	1.21	1.36
0511	1.06	1.07	1.08	1.09	1.10	1.10	1.11	1.12	1.13	1.14	1.16	1.17	1.17	1.34
Mean (kg/m^2)	1.08	1.09	1.10	1.10	1.11	1.12	1.12	1.13	1.14	1.16	1.17	1.18	1.19	1.35
Standard dev.	0.01	0.01	0.01	0.01	0.01	0.01	0.01	0.02	0.02	0.02	0.02	0.02	0.02	0.01

Water absorption during capillary suction in kg/m^2 related to the dry weight (+105 °C). Specimen thickness 5.0 mm. At time zero, specimens were in equilibrium with 65 % RH at +20 °C.

OPC + 65 % slag w/b-ratio 0.45 Carbonated material

Time (days)	0	0.00	0.01	0.01	0.02	0.03	0.06	0.08	0.12	0.16	0.20	0.31	0.35	1.01	2.34
Time (root(s))	0	15	23	31	39	54	70	85	101	116	132	162	173	296	450
1604	0.34	0.53	0.62	0.71	0.79	0.90	0.91	0.92	0.92	0.93	0.93	0.93	0.93	0.94	0.96
1616	0.34	0.61	0.72	0.81	0.88	0.93	0.93	0.94	0.94	0.94	0.94	0.95	0.95	0.96	0.98
1617	0.35	0.55	0.63	0.71	0.78	0.90	0.92	0.93	0.93	0.93	0.93	0.94	0.94	0.95	0.97
Mean (kg/m^2)	0.34	0.57	0.66	0.74	0.81	0.91	0.92	0.93	0.93	0.93	0.94	0.94	0.94	0.95	0.97
Standard dev.	0.00	0.04	0.05	0.06	0.05	0.01	0.01	0.01	0.01	0.01	0.01	0.01	0.01	0.01	0.01

Time (days)	5.44	9.11	15.1	22.3	33.0	47.1	77.2	132	231	288	Vacuum
Time (root(s))	685	887	1141	1388	1689	2018	2583	3380	4470	4990	saturation
1604	0.97	0.98	1.00	1.01	1.01	1.03	1.05	1.06	1.07	1.07	1.11
1616	1.00	1.01	1.03	1.04	1.04	1.05	1.08	1.09	1.09	1.09	1.13
1617	0.99	1.00	1.01	1.01	1.02	1.03	1.05	1.06	1.07	1.07	1.12
Mean (kg/m^2)	0.99	1.00	1.01	1.02	1.02	1.04	1.06	1.07	1.08	1.08	1.12
Standard dev.	0.01	0.02	0.02	0.01	0.02	0.01	0.02	0.02	0.01	0.01	0.01

OPC + 65 % slag w/b-ratio 0.45 Uncarbonated material

Time (days)	0	0.00	0.01	0.01	0.02	0.03	0.06	0.08	0.12	0.16	0.25	0.96	2.27	5.38	9.04
Time (root(s))	0	15	23	31	39	54	70	85	101	116	147	288	443	682	884
0605	0.54	0.75	0.82	0.88	0.94	1.01	1.02	1.03	1.03	1.03	1.04	1.05	1.06	1.07	1.08
0609	0.55	0.77	0.84	0.91	0.96	1.03	1.04	1.05	1.05	1.05	1.05	1.07	1.08	1.09	1.10
0614	0.52	0.79	0.87	0.93	0.98	1.01	1.02	1.03	1.03	1.03	1.03	1.05	1.06	1.08	1.08
Mean (kg/m^2)	0.54	0.77	0.84	0.91	0.96	1.02	1.03	1.03	1.04	1.04	1.04	1.05	1.07	1.08	1.09
Standard dev.	0.01	0.02	0.03	0.03	0.02	0.01	0.01	0.01	0.01	0.01	0.01	0.01	0.01	0.01	0.01

Time (days)	15.0	22.2	33.0	47.1	77.0	132	231	288	Vacuum
Time (root(s))	1139	1386	1688	2017	2580	3379	4469	4990	saturation
0605	1.08	1.09	1.09	1.10	1.12	1.14	1.15	1.16	1.30
0609	1.11	1.11	1.11	1.12	1.14	1.16	1.17	1.18	1.33
0614	1.09	1.09	1.10	1.11	1.13	1.15	1.16	1.17	1.31
Mean (kg/m^2)	1.09	1.10	1.10	1.11	1.13	1.15	1.16	1.17	1.31
Standard dev.	0.01	0.01	0.01	0.01	0.01	0.01	0.01	0.01	0.02

Water absorption during capillary suction in kg/m^2 related to the dry weight (+105 °C). Specimen thickness 5.0 mm. At time zero, specimens were in equilibrium with 65 % RH at +20 °C.

OPC + 65 % slag w/b-ratio 0.55 Carbonated material

Time (days)	0	0.00	0.01	0.01	0.02	0.03	0.06	0.08	0.12	0.16	0.20	0.25	0.31	0.40	0.96
Time (root(s))	0	15	23	31	39	54	70	85	101	116	132	147	163	185	288
1708	0.27	0.65	0.79	0.89	0.93	0.94	0.95	0.95	0.96	0.96	0.96	0.96	0.96	0.97	0.99
1712	0.27	0.60	0.72	0.84	0.90	0.92	0.93	0.93	0.93	0.94	0.94	0.94	0.94	0.95	0.96
1716	0.27	0.61	0.76	0.89	0.94	0.95	0.96	0.96	0.97	0.97	0.97	0.97	0.98	0.98	1.00
Mean (kg/m^2)	0.27	0.62	0.76	0.87	0.93	0.94	0.94	0.95	0.95	0.95	0.96	0.96	0.96	0.97	0.98
Standard dev.	0.00	0.03	0.03	0.03	0.02	0.02	0.02	0.02	0.02	0.02	0.02	0.02	0.02	0.02	0.02

Time (days)	1.28	2.05	6.13	9.17	15.1	23.3	29.1	47.1	61.3	91.2	146	251	329	Vacuum
Time (root(s))	332	421	728	890	1143	1419	1586	2018	2301	2808	3555	4659	5334	saturation
1708	0.99	1.01	1.05	1.06	1.07	1.07	1.07	1.08	1.08	1.08	1.09	1.09	1.09	1.14
1712	0.97	0.98	1.02	1.03	1.04	1.04	1.04	1.04	1.04	1.04	1.05	1.05	1.05	1.15
1716	1.00	1.02	1.06	1.07	1.07	1.08	1.08	1.08	1.08	1.08	1.08	1.09	1.09	1.15
Mean (kg/m^2)	0.99	1.00	1.04	1.05	1.06	1.06	1.06	1.07	1.07	1.07	1.07	1.08	1.08	1.15
Standard dev.	0.02	0.02	0.02	0.02	0.02	0.02	0.02	0.02	0.02	0.02	0.02	0.02	0.02	0.01

OPC + 65 % slag w/b-ratio 0.55 Uncarbonated material

Time (days)	0	0.00	0.01	0.01	0.02	0.03	0.06	0.08	0.12	0.16	0.90	2.27	2.97	6.11	9.03
Time (root(s))	0	15	23	31	39	54	70	85	101	116	278	443	507	727	883
0703	0.39	0.74	0.85	0.94	0.98	0.99	0.99	0.99	1.00	1.00	1.02	1.04	1.04	1.06	1.06
0711	0.38	0.77	0.90	0.97	0.98	0.99	0.99	1.00	1.00	1.00	1.02	1.05	1.06	1.07	1.08
0714	0.38	0.75	0.86	0.95	0.97	0.98	0.98	0.98	0.99	0.99	1.01	1.04	1.04	1.05	1.06
Mean (kg/m^2)	0.38	0.75	0.87	0.95	0.97	0.98	0.99	0.99	0.99	1.00	1.02	1.04	1.05	1.06	1.07
Standard dev.	0.01	0.02	0.03	0.02	0.01	0.00	0.01	0.01	0.01	0.01	0.00	0.01	0.01	0.01	0.01

Time (days)	17.1	23.1	40.9	55.1	85.0	140	239	323	Vacuum
Time (root(s))	1217	1411	1881	2181	2710	3479	4545	5284	saturation
0703	1.07	1.07	1.08	1.09	1.10	1.12	1.15	1.17	1.29
0711	1.09	1.09	1.10	1.10	1.11	1.13	1.17	1.19	1.30
0714	1.07	1.07	1.08	1.08	1.10	1.12	1.15	1.17	1.29
Mean (kg/m^2)	1.08	1.08	1.08	1.09	1.10	1.12	1.16	1.18	1.29
Standard dev.	0.01	0.01	0.01	0.01	0.01	0.01	0.01	0.01	0.00

Water absorption during capillary suction in kg/m^2 related to the dry weight (+105 °C). Specimen thickness 5.0 mm. At time zero, specimens were in equilibrium with 65 % RH at +20 °C.

OPC + 5 % silica w/b-ratio 0.35 Carbonated material

Time (days)	0	0.00	0.01	0.01	0.02	0.03	0.06	0.08	0.12	0.16	0.20	0.25	0.31	0.40	0.46
Time (root(s))	0	15	23	31	39	54	70	85	101	116	132	147	163	185	199
1802	0.75	0.80	0.82	0.84	0.86	0.91	0.94	0.97	1.00	1.02	1.04	1.06	1.07	1.08	1.08
1813	0.75	0.80	0.81	0.83	0.84	0.88	0.91	0.94	0.97	1.00	1.02	1.04	1.06	1.07	1.08
1815	0.75	0.81	0.84	0.86	0.89	0.94	0.99	1.02	1.04	1.06	1.07	1.08	1.09	1.09	1.10
Mean (kg/m^2)	0.75	0.80	0.82	0.84	0.86	0.91	0.95	0.98	1.00	1.03	1.05	1.06	1.07	1.08	1.09
Standard dev.	0.00	0.01	0.01	0.02	0.02	0.03	0.04	0.04	0.04	0.03	0.03	0.02	0.02	0.01	0.01

Time (days)	0.96	1.28	2.05	6.13	9.17	15.1	23.3	29.1	47.1	61.3	91.2	146	251	329	Vac.
Time (root(s))	288	332	421	728	890	1143	1419	1586	2018	2301	2808	3555	4659	5334	sat.
1802	1.09	1.10	1.10	1.12	1.12	1.13	1.13	1.14	1.14	1.15	1.15	1.16	1.17	1.18	1.24
1813	1.09	1.10	1.10	1.11	1.12	1.12	1.13	1.13	1.14	1.14	1.14	1.15	1.17	1.17	1.23
1815	1.10	1.10	1.11	1.12	1.12	1.13	1.14	1.14	1.14	1.15	1.15	1.16	1.17	1.18	1.24
Mean (kg/m^2)	1.09	1.10	1.10	1.12	1.12	1.13	1.13	1.13	1.14	1.14	1.15	1.16	1.17	1.18	1.23
Standard dev.	0.00	0.00	0.00	0.00	0.00	0.00	0.00	0.00	0.00	0.00	0.00	0.00	0.00	0.00	0.01

OPC + 5 % silica w/b-ratio 0.35 Uncarbonated material

Time (days)	0	0.00	0.01	0.01	0.02	0.03	0.06	0.08	0.12	0.16	0.90	2.27	2.97	6.11	9.03
Time (root(s))	0	15	23	31	39	54	70	85	101	116	278	443	507	727	883
0804	0.73	0.88	0.95	1.00	1.06	1.14	1.16	1.16	1.16	1.16	1.17	1.17	1.17	1.18	1.19
0810	0.74	0.92	0.99	1.05	1.11	1.17	1.18	1.18	1.18	1.19	1.19	1.20	1.20	1.21	1.22
0814	0.74	0.90	0.96	1.00	1.06	1.14	1.17	1.17	1.17	1.17	1.19	1.19	1.19	1.20	1.20
Mean (kg/m^2)	0.74	0.90	0.97	1.02	1.07	1.15	1.17	1.17	1.17	1.17	1.18	1.19	1.19	1.20	1.20
Standard dev.	0.01	0.02	0.03	0.03	0.03	0.02	0.01	0.01	0.01	0.01	0.01	0.01	0.01	0.02	0.01

Time (days)	17.1	23.1	40.9	55.1	85.0	140	239	323	Vacuum
Time (root(s))	1217	1411	1881	2181	2710	3479	4545	5284	saturation
0804	1.19	1.19	1.20	1.21	1.22	1.24	1.25	1.26	1.32
0810	1.22	1.22	1.23	1.24	1.25	1.27	1.28	1.29	1.34
0814	1.21	1.22	1.22	1.23	1.24	1.25	1.27	1.28	1.35
Mean (kg/m^2)	1.21	1.21	1.22	1.23	1.24	1.25	1.27	1.27	1.34
Standard dev.	0.02	0.02	0.02	0.02	0.01	0.01	0.02	0.02	0.01

Water absorption during capillary suction in kg/m^2 related to the dry weight (+105 °C). Specimen thickness 5.0 mm. At time zero, specimens were in equilibrium with 65 % RH at +20 °C.

OPC + 5 % silica w/b-ratio 0.45 Carbonated material

Time (days)	0	0.00	0.01	0.01	0.02	0.03	0.06	0.08	0.12	0.16	0.20	0.31	0.35	1.01	2.34
Time (root(s))	0	15	23	31	39	54	70	85	101	116	132	162	173	296	450
1906	0.40	0.46	0.49	0.51	0.53	0.58	0.61	0.65	0.68	0.71	0.72	0.74	0.74	0.75	0.76
1917	0.40	0.49	0.53	0.57	0.60	0.67	0.72	0.74	0.75	0.75	0.75	0.76	0.76	0.76	0.78
1919	0.40	0.47	0.50	0.53	0.55	0.60	0.64	0.68	0.72	0.75	0.76	0.76	0.76	0.77	0.78
Mean (kg/m^2)	0.40	0.48	0.50	0.53	0.56	0.61	0.66	0.69	0.71	0.73	0.75	0.75	0.75	0.76	0.77
Standard dev.	0.00	0.02	0.02	0.03	0.04	0.05	0.05	0.05	0.03	0.03	0.02	0.01	0.01	0.01	0.01

Time (days)	5.44	9.11	15.1	22.3	33.0	47.1	77.2	132	231	288	Vacuum
Time (root(s))	685	887	1141	1388	1689	2018	2583	3380	4470	4990	saturation
1906	0.77	0.78	0.79	0.80	0.81	0.82	0.83	0.84	0.85	0.85	0.89
1917	0.79	0.80	0.82	0.82	0.84	0.85	0.85	0.86	0.87	0.87	0.92
1919	0.79	0.80	0.81	0.82	0.83	0.84	0.85	0.86	0.87	0.87	0.92
Mean (kg/m^2)	0.78	0.79	0.80	0.81	0.82	0.83	0.85	0.85	0.86	0.86	0.91
Standard dev.	0.01	0.01	0.01	0.01	0.02	0.01	0.01	0.01	0.01	0.01	0.02

OPC + 5 % silica w/b-ratio 0.45 Uncarbonated material

Time (days)	0	0.00	0.01	0.01	0.02	0.03	0.06	0.08	0.12	0.16	0.25	0.96	2.27	5.38	9.04
Time (root(s))	0	15	23	31	39	54	70	85	101	116	147	288	443	682	884
0907	0.55	0.85	0.95	1.04	1.07	1.07	1.08	1.08	1.08	1.08	1.08	1.10	1.11	1.11	1.12
0911	0.58	0.85	0.94	1.03	1.08	1.09	1.10	1.10	1.10	1.10	1.11	1.12	1.12	1.14	1.14
0917	0.57	0.82	0.92	1.01	1.06	1.07	1.07	1.07	1.08	1.08	1.08	1.09	1.10	1.11	1.11
Mean (kg/m^2)	0.57	0.84	0.94	1.03	1.07	1.08	1.08	1.08	1.09	1.09	1.09	1.10	1.11	1.12	1.12
Standard dev.	0.01	0.01	0.01	0.02	0.01	0.01	0.01	0.01	0.01	0.01	0.01	0.01	0.01	0.01	0.01

Time (days)	15.0	22.2	33.0	47.1	77.0	132	231	288	Vacuum
Time (root(s))	1139	1386	1688	2017	2580	3379	4469	4990	saturation
0907	1.13	1.13	1.13	1.13	1.14	1.15	1.17	1.17	1.26
0911	1.15	1.15	1.15	1.15	1.16	1.18	1.19	1.19	1.28
0917	1.12	1.12	1.12	1.13	1.14	1.15	1.16	1.17	1.26
Mean (kg/m^2)	1.13	1.13	1.13	1.14	1.15	1.16	1.17	1.18	1.27
Standard dev.	0.02	0.01	0.01	0.01	0.01	0.02	0.01	0.01	0.01

Water absorption during capillary suction in kg/m^2 related to the dry weight (+105 °C). Specimen thickness 5.0 mm. At time zero, specimens were in equilibrium with 65 % RH at +20 °C.

OPC + 5 % silica w/b-ratio 0.55 Carbonated material

Time (days)	0	0.00	0.01	0.01	0.02	0.03	0.06	0.08	0.12	0.16	0.20	0.25	0.95	2.33	3.05
Time (root(s))	0	15	23	31	39	54	70	85	101	116	132	147	286	449	513
11005	0.28	0.46	0.54	0.60	0.67	0.74	0.75	0.75	0.75	0.75	0.75	0.75	0.76	0.78	0.78
11011	0.28	0.46	0.54	0.62	0.69	0.76	0.77	0.77	0.78	0.78	0.78	0.78	0.79	0.81	0.81
11019	0.28	0.45	0.53	0.60	0.66	0.74	0.75	0.75	0.75	0.75	0.75	0.75	0.77	0.78	0.79
Mean (kg/m^2)	0.28	0.46	0.54	0.61	0.67	0.75	0.75	0.76	0.76	0.76	0.76	0.76	0.77	0.79	0.79
Standard dev.	0.00	0.00	0.01	0.01	0.01	0.01	0.01	0.01	0.01	0.01	0.01	0.01	0.01	0.01	0.01

Time (days)	6.18	9.08	17.2	23.1	41.0	55.2	85.1	140	239	323	Vacuum
Time (root(s))	731	886	1219	1413	1882	2184	2712	3481	4546	5285	saturation
11005	0.80	0.82	0.83	0.83	0.84	0.84	0.85	0.84	0.85	0.85	0.90
11011	0.83	0.85	0.86	0.86	0.87	0.87	0.87	0.87	0.87	0.88	0.93
11019	0.80	0.82	0.83	0.84	0.84	0.84	0.85	0.85	0.85	0.86	0.92
Mean (kg/m^2)	0.81	0.83	0.84	0.84	0.85	0.85	0.85	0.85	0.86	0.86	0.92
Standard dev.	0.01	0.02	0.01	0.02	0.02	0.01	0.01	0.02	0.02	0.02	0.01

OPC + 5 % silica w/b-ratio 0.55 Uncarbonated material

Time (days)	0	0.00	0.01	0.01	0.02	0.03	0.06	0.08	0.22	0.91	2.02	4.08	6.94	15.0	21.0
Time (root(s))	0	15	23	31	39	54	70	85	136	281	417	594	774	1139	1347
01005	0.46	0.89	1.03	1.11	1.12	1.12	1.12	1.12	1.13	1.15	1.16	1.17	1.18	1.18	1.18
01010	0.47	0.89	1.04	1.11	1.11	1.12	1.12	1.12	1.13	1.15	1.16	1.17	1.18	1.19	1.19
01015	0.46	0.87	1.02	1.10	1.11	1.11	1.11	1.12	1.12	1.14	1.16	1.17	1.18	1.19	1.19
Mean (kg/m^2)	0.46	0.88	1.03	1.11	1.11	1.12	1.12	1.12	1.13	1.15	1.16	1.17	1.18	1.19	1.19
Standard dev.	0.00	0.01	0.01	0.01	0.00	0.01	0.01	0.00	0.00	0.00	0.00	0.00	0.00	0.00	0.00

Time (days)	38.9	53.1	83.0	138	237	321	Vacuum
Time (root(s))	1834	2142	2678	3454	4526	5267	saturation
01005	1.18	1.18	1.19	1.20	1.21	1.22	1.31
01010	1.19	1.19	1.20	1.21	1.22	1.22	1.33
01015	1.19	1.20	1.20	1.21	1.22	1.23	1.31
Mean (kg/m^2)	1.19	1.19	1.20	1.20	1.21	1.22	1.32
Standard dev.	0.00	0.01	0.01	0.01	0.01	0.01	0.01

Water absorption during capillary suction in kg/m^2 related to the dry weight (+105 °C). Specimen thickness 5.0 mm. At time zero, specimens were in equilibrium with 65 % RH at +20 °C.

OPC + 10 % silica w/b-ratio 0.45 Carbonated material

Time (days)	0	0.00	0.01	0.01	0.02	0.03	0.06	0.08	0.12	0.16	0.20	0.25	0.38	0.95
Time (root(s))	0	15	23	31	39	54	70	85	101	116	132	147	180	286
11104	0.51	0.57	0.59	0.62	0.64	0.67	0.71	0.74	0.77	0.79	0.82	0.83	0.86	0.87
11117	0.51	0.59	0.62	0.64	0.67	0.72	0.75	0.79	0.81	0.83	0.84	0.85	0.86	0.87
11118	0.51	0.58	0.60	0.62	0.64	0.69	0.73	0.76	0.79	0.81	0.83	0.85	0.87	0.88
Mean (kg/m^2)	0.51	0.58	0.60	0.63	0.65	0.69	0.73	0.76	0.79	0.81	0.83	0.84	0.86	0.87
Standard dev.	0.00	0.01	0.01	0.01	0.02	0.02	0.02	0.02	0.02	0.02	0.01	0.01	0.01	0.01

Time (days)	2.33	3.05	6.18	9.08	17.2	23.1	41.0	55.2	85.1	140	239	323	Vacuum
Time (root(s))	449	513	731	886	1219	1413	1882	2184	2712	3481	4546	5285	saturation
11104	0.88	0.88	0.89	0.89	0.90	0.91	0.92	0.93	0.94	0.95	0.96	0.97	1.05
11117	0.88	0.88	0.89	0.90	0.91	0.92	0.93	0.94	0.95	0.95	0.96	0.97	1.06
11118	0.89	0.89	0.90	0.90	0.92	0.92	0.93	0.94	0.95	0.96	0.97	0.98	1.07
Mean (kg/m^2)	0.88	0.88	0.89	0.90	0.91	0.91	0.93	0.94	0.95	0.95	0.96	0.97	1.06
Standard dev.	0.00	0.01	0.01	0.00	0.01	0.01	0.00	0.01	0.00	0.00	0.00	0.01	0.01

OPC + 10 % silica w/b-ratio 0.45 Uncarbonated material

Time (days)	0	0.00	0.01	0.01	0.02	0.03	0.06	0.08	0.22	0.91	2.02	4.08	6.94	15.0
Time (root(s))	0	15	23	31	39	54	70	85	136	281	417	594	774	1139
01102	0.63	0.90	0.99	1.07	1.11	1.11	1.12	1.12	1.12	1.13	1.13	1.14	1.14	1.14
01111	0.64	0.89	0.98	1.07	1.11	1.12	1.12	1.12	1.13	1.13	1.14	1.14	1.15	1.15
01118	0.64	0.87	0.96	1.04	1.10	1.12	1.12	1.12	1.13	1.14	1.14	1.14	1.15	1.15
Mean (kg/m^2)	0.64	0.89	0.98	1.06	1.11	1.12	1.12	1.12	1.13	1.13	1.14	1.14	1.15	1.15
Standard dev.	0.01	0.01	0.02	0.02	0.01	0.00	0.00	0.00	0.00	0.00	0.00	0.00	0.00	0.00

Time (days)	21.0	38.9	53.1	83.0	138	237	321	Vacuum
Time (root(s))	1347	1834	2142	2678	3454	4526	5267	saturation
01102	1.15	1.15	1.16	1.17	1.18	1.19	1.20	1.35
01111	1.15	1.16	1.17	1.17	1.19	1.20	1.21	1.37
01118	1.16	1.17	1.17	1.18	1.19	1.21	1.21	1.37
Mean (kg/m^2)	1.15	1.16	1.17	1.18	1.19	1.20	1.21	1.36
Standard dev.	0.00	0.01	0.01	0.01	0.01	0.01	0.01	0.01

APPENDIX 9

CALCULATION OF THE CORRECTED DEGREES OF SATURATION

Calculation of the corrected degrees of saturation

The following discusses the procedure for calculating corrected values for the degree of saturation presented in Chapter 7.

The results presented in Figure 7.3 (Chapter 7) were calculated strictly in accordance with the procedure in RILEM CDC 3. This involves measuring the fully saturated weight of specimens dried at +105 °C and then vacuum-saturated. It was found, as described in Chapter 6, that this procedure to determine the vacuum-saturated weight did not give the highest value for the saturated weight. Instead, it was shown that the highest value for the saturated weight was given by vacuum drying rather than by drying at +105 °C before vacuum saturation. Given this, the values for the saturated weights using vacuum drying were used when evaluating the results from the capillary suction test. Since different procedures to determine the saturated weights have been used when determining the critical degree of saturation, both here and in the capillary suction test, the results cannot be compared without a correction. To be able to use the calculated degree of saturation from the long-time water absorption in the capillary suction test in Chapter 6 for estimating the time until a critical degree of saturation is reached, the values for the saturated weights for the specimens used here in the S_{cr}-test therefore have to be corrected.

From the capillary suction test in Chapter 6, the difference between the vacuum-saturated weights using vacuum drying and the weights after drying at +105 °C have been calculated; see Table 6.1 in Chapter 6. On the basis of these measurements, the weights for the vacuum-saturated specimens in the S_{cr}-test have been corrected using Equation 1:

$$Q_{Scr:sat:vacuum} = Q_{Scr:sat:105} \cdot (1 + k) \qquad \text{[Eq. 1]}$$

where

$Q_{Scr:sat:vacuum}$ is the calculated vacuum-saturated weight after vacuum drying for a specimen in the S_{cr}-test [kg]

$Q_{Scr:sat:105}$ is the measured vacuum-saturated weight after drying at +105 °C for a specimen in the S_{cr}-test [kg]

k is the correction factor calculated on the basis of measurements of the vacuum-saturated weight using two different drying techniques (Chapter 6): vacuum drying and drying at +105 °C. k is material-dependent, i.e. each carbonated and uncarbonated mortar has its own correction factor. k is calculated as a mean of three specimens. For each specimen, the correction factor was calculated from:

$$k = \left(\frac{Q_{w.abs:sat:vacuum} - Q_{w.abs:sat:105}}{Q_{w.abs:sat:105}} \right)$$

where

$Q_{w.abs:sat:vacuum}$ is the measured vacuum-saturated weight after vacuum drying for a specimen in the capillary suction test, Chapter 6. [kg]

$Q_{w.abs:sat:105}$ is the measured vacuum-saturated weight after drying at +105 °C for a specimen in the capillary suction test, Chapter 6. [kg]

After correction of the vacuum-saturated weights, calculations of 'corrected' degrees of saturation have been carried out.

From the corrected results, it should be possible to compare the degree of saturation for specimens from the S_{cr}-test with the degree of saturation from the specimens used in the capillary suction test (Chapter 6). However, when comparing the calculated degree of saturation reached after (for example) 24 hours of capillary suction for the specimens in the S_{cr}-test with the degree of saturation after the same time of capillary suction for the specimens used in the capillary suction test (Chapter 6), it was found that these values did not always correlate; see Table 1 (All specimens in the S_{cr}-test were, during the first saturation, subjected to the same capillary suction procedure as the specimens in the capillary suction test). Since, in both cases, the same type of specimens and the same test procedure were used, it was expected that water absorption over the same period of time would result in the same degree of saturation.

Table 1 *Degree of saturation after 24 hours of water absorption. All values are means of measurements on three specimens.*

Mortar quality		**S_{cr} specimens**		**Capillary suction specimens[2)]**
		Drying at +105 °C	**Vacuum drying[1)]**	
OPC-45	**Uncarbo.**	0.893	0.859	0.904
	Carbo.	0.909	0.836	0.870
OPC + 65 % sl-45	**Uncarbo.**	0.859	0.803	0.804
	Carbo.	0.848	0.833	0.847
OPC + 5 % si-45	**Uncarbo.**	0.899	0.861	0.865
	Carbo.	0.893	0.803	0.837

[1)] Calculated after correction of the vacuum-saturated weights in the S_{cr}-test. Vacuum saturation after vacuum drying instead of drying at +105 °C. Correction were made on the basis of experience from the capillary suction test in Chapter 6.

[2)] The degree of saturation after 24 hours of capillary suction calculated from the equations describing the water absorption after the nick point; see Chapter 6.

The fact that the degree of saturation after the same time of capillary suction differs to the extent shown in Table 1 is unsatisfactory. With these differences, the time until the critical degree of saturation cannot be estimated with any credibility. To be able to calculate when a critical degree of saturation is reached from the long-time water absorption test in Chapter 6, it is essential that the water absorption 'behaviour' is the same for all specimens used in the S_{cr} test and in the capillary suction test. We need to find the reason for

the differences and, if possible, correct for it, in order to be able to compare the long-time absorption and the critical degree of saturation.

Since, when calculating the degree of saturation, only three weights for each specimen have to be known (except for the weights needed for volume calculations) - the dry weight $Q_{dry:105}$, the vacuum-saturated weight $Q_{sat:a}$ and the actual weight after capillary suction during time t, Q_t - there seems to be only two main reasons for the differences in degree of saturations mentioned above:

1. Difference in water absorption due to differences in the materials and/or test procedures influencing Q_t as well as $Q_{sat:a}$ and $Q_{dry:105}$
2. Changes in the specimen weights during the S_{cr}-test due to the S_{cr}-test procedure influencing primarily $Q_{dry:105}$ and $Q_{sat:a}$.

These probable explanations are discussed below.

1. Differences in material and/or test procedure used for capillary suction

The same materials, and the same type of specimens, have been used in the capillary suction test, described in Chapter 6, and in the S_{cr}-test described here (see Chapter 5). The only difference is that the specimens used in the capillary suction test were 14 months old at the start of the test, and 19 months old in the S_{cr}-test, i.e. a difference of about five months. Theoretically, there could be a small difference in the degree of hydration depending on the age difference at the start of the tests, resulting in different porosities and pore structures but, as the specimens in both tests were quite old, this probably has only a minor effect on the capillary suction behaviour.

The applied capillary suction test procedure, described in Chapter 6, was identical during both tests, except for at what times the specimen weights was measured. During the capillary suction test, the specimen weights were measured after 4, 9, 16, 25, 49, 81, etc. minutes, whereas during the S_{cr}-test the weights were measured less frequently at first, i.e. after 9, 25, 49, 81, etc. minutes. This may have had a slight effect on the water uptake during the first hour of capillary suction, but probably not after 24 hours, which is of interest here.

In order to investigate the existence of differences in the water uptake behaviour during capillary suction, the results from capillary suction for the S_{cr}-specimens and the specimens used in the capillary suction test were compared. Figure 1 shows the percentage weight increase during capillary suction in relation to the weight at the start of the test, for specimens in the S_{cr}-test and for specimens in the capillary suction test. At the start of capillary suction, the specimens were in equilibrium with 65 % RH. In the figure all points are means of three specimens.

From Figure 1 it can be seen that the appearance of the capillary suction curves are almost identical, indicating no important difference in material properties or test procedure.

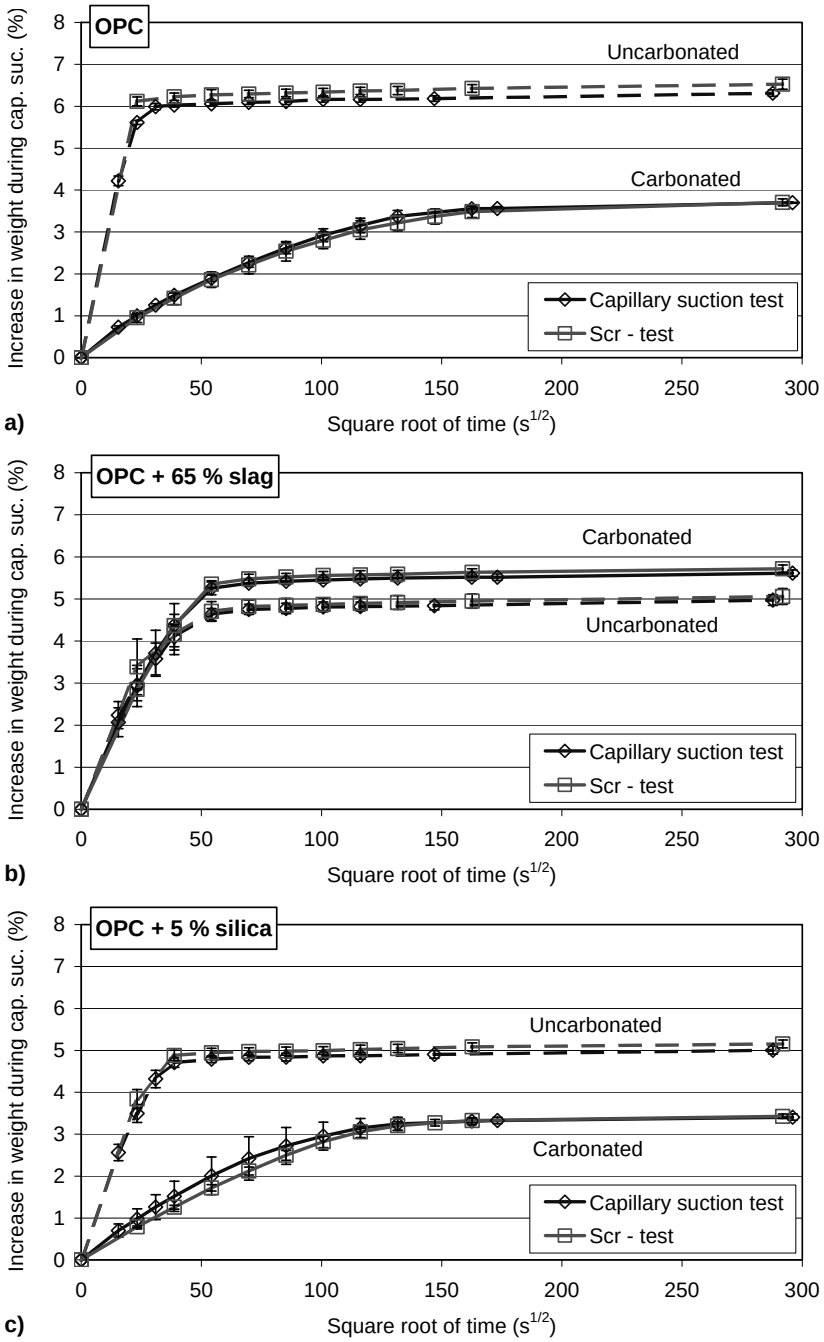

Figure 1 *Increase in weight in relation to the initial weight at test start during capillary suction as a function of the square root of time for carbonated and uncarbonated mortars of different qualities. Results from two individual measurements; S_{cr}-test and capillary suction test (Chapter 6).*
a) OPC, b) OPC + 65 % slag, c) OPC + 5 % silica.

Table 2 shows the water uptake after 24 hours of capillary suction for the specimens in the two individual capillary suction tests.

Table 2 *Water uptake as increase in weight (%) after 24 hours of capillary suction. All values are means of measurements on three specimens.*

Mortar quality		Water uptake, increase in weight (%)			
		S_{cr} specimens		Capillary suction spec.	
		Mean	Std.dev.	Mean	Std.dev.
OPC-45	**Uncarbo.**	6.53	0.12	6.31	0.08
	Carbo.	3.71	0.08	3.70	0.01
OPC + 65 % sl-45	**Uncarbo.**	5.06	0.19	4.98	0.12
	Carbo.	5.72	0.09	5.61	0.08
OPC + 5 % si-45	**Uncarbo.**	5.15	0.09	5.01	0.09
	Carbo.	3.43	0.05	3.41	0.07

Comparing the water uptake results from the two individual capillary suction tests (Figure 1 and Table 2) shows only small differences, which are probably within the uncertainty of measurement. It must be noted that the specimens used in the S_{cr}-test were conditioned for five more months in the climate chambers before the capillary suction test was started than was the case for the specimens used in the capillary suction test. This means that the specimens used in the S_{cr}-test had longer to respond to the climate in the chambers, e.g. the uncarbonated specimens could dry for five months longer than the specimens used in the capillary suction test. This longer period of drying can be one explanation for the fact that all S_{cr}-specimens of uncarbonated mortar qualities show higher water uptake after 24 hours of capillary suction than the specimens used in the capillary suction test. That is, during the longer preconditioning period in the climate chambers, the S_{cr}-specimens had reached a dryer state and thereby absorbed more water (related to the initial weight) when subjected to capillary suction. Given this, the difference in water uptake between the uncarbonated specimens does not need to be an indication of differences in material properties, but can be explained by differences in water content at the start of the capillary suction test caused by the different conditioning times.

In addition, the longer preconditioning time for the carbonated specimens could affect the water uptake. However, for the carbonated specimens, a longer preconditioning time could result in both a weight increase due to increased carbonation and a weight loss due to further drying. The weight could also change in either way because of changes in the sorption isotherm. The relative effects of these possible causes of weight change are impossible to estimate. It can, however, be seen that the water uptake is almost identical for the carbonated specimens irrespective of preconditioning time, which indicates that the five months longer preconditioning has no important effect on the capillary suction behaviour of these carbonated materials.

Assuming a maximum difference in water uptake of about 2 %, for example, for the carbonated OPC + 65 % slag mortar, the S_{cr}-specimens show about 2 % higher water absorp-

tion than the specimens used in the capillary suction test. A difference of 2 % in water uptake results in a maximum difference of less than 0.02 in the degree of saturation. This indicates that differences in material homogeneity and differences in the capillary suction test procedure cannot be the main reason for some of the substantial differences in degrees of saturations shown in Table 1 above. To explain these differences there must be other reasons, probably in the S_{cr}-test procedure.

2. Changes in weight due to the S_{cr}-test procedure

The S_{cr}-test procedure involved drying at +50 °C for one week, followed by vacuum saturation and drying at +50 °C to the desired degree of saturation, followed by subjection to six freeze/thaw cycles. If the specimens were not damaged during freezing and thawing, they were reused by drying and resaturating the material to the desired degree of saturation before being subjected to the next round of freeze/thaw cycles. This procedure was repeated five times, and may have led to undesired effects on the specimen weights, for example:

- During handling in the room climate (which was kept to a minimum), or during drying at +50 °C, uncarbonated samples might increase in weight due to carbonation, markedly changing the dry weight $Q_{dry:105}$ at the end of the test. A correct dry weight is very important in order to be able to calculate the degree of saturation correctly; see Equation 7.1 (Chapter 7). Carbonation also leads to undesired changes in the porosity and pore structure, affecting the degree of saturation.
- During vacuum saturation in water, leaching from the specimens might lead to weight loss and a change in porosity and pore structure.

All specimens in this investigation have been subjected to five drying (+50 °C)/vacuum saturation and freeze/thaw cycles, i.e. the drying and freezing continued after some of the specimens were regarded as damaged. The specimen weights were measured after each period of drying at +50 °C; from these dry weights, the relative weight change after each drying at +50 °C compared to the weight after the first drying at +50 °C could be calculated. This relative weight change during the course of the S_{cr}-test is shown in Figure 2. Since there is most probably a weight change during the first drying as well (although this is not known), a corrected 'dry weight' before the first drying could be calculated. This was done by assuming that the weight change during the first drying was equal to the weight change during the second drying. The dry weight before the first drying was calculated from Equation 2:

$$Q_{dry:50:before} = Q_{dry:50:1} - \left(Q_{dry:50:1} - Q_{dry:50:2}\right) \qquad \text{[Eq. 2]}$$

where

$Q_{dry:50:before}$	is the calculated dry specimen weight before the first drying at +50 °C	[kg]
$Q_{dry:50:1}$	is the measured specimen weight after the first drying at +50 °C	[kg]
$Q_{dry:50:2}$	is the measured specimen weight after the second drying at +50 °C	[kg]

This corrected weight was used when calculating the relative weight change between the measured dry weights after each drying period and the dry weight before the first drying. The relative percentage weight change in Figure 2 was calculated from Equation 3:

$$\frac{Q_{dry:50:n} - Q_{dry:50:before}}{Q_{dry:50:before}} \cdot 100 \qquad \text{[Eq. 3]}$$

where

$Q_{dry:50:before}$ is the calculated dry specimen weight before the first drying at +50 °C [kg]
$Q_{dry:50:n}$ is the dry specimen weight after the n:th drying procedure at +50 °C [kg]

As can be seen from Figure 2, the drying/resaturation cycle results in a substantial weight change, although this differs for different materials. All the uncarbonated materials showed a marked increase in weight, which can be a result of gradual carbonation. For the carbonated materials, there are in general only small weight changes, although the decrease in weight of carbonated mortar with OPC and 65 % slag as part of the binder is considerable, especially after the second drying.

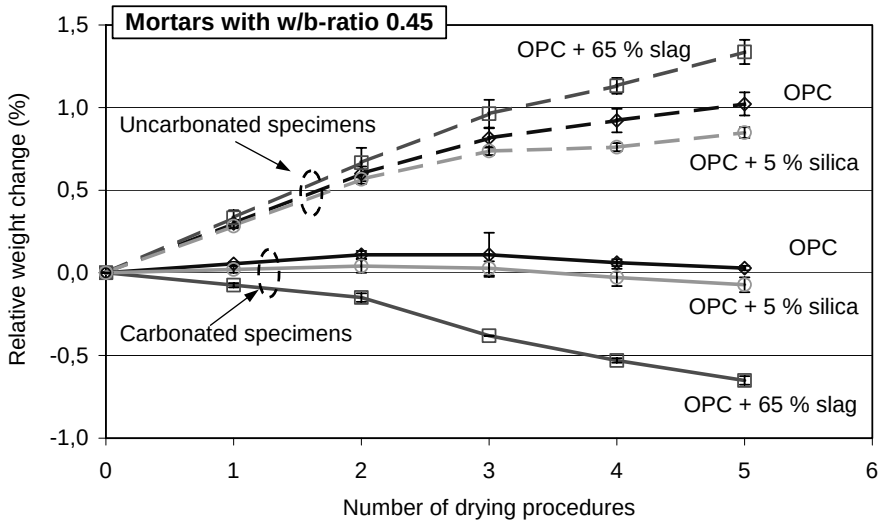

Figure 2 *Relative weight change as a function of the number of drying procedures related to the dry weight before the first drying at +50 °C. Values are means of measurements on three specimens.*

A slight variation in weight can probably be explained by small differences in the oven temperature between the drying periods. The oven used is calibrated to be within ±5 °C from the set temperature, although in reality the temperature spread is probably lower. The large decrease in weight for the carbonated mortar with OPC and 65 % slag as binder could be due to leaching during vacuum saturation. Leaching could also occur for the uncarbonated specimens during vacuum saturation. However, the loss of weight due to

leaching for uncarbonated specimens is much lower than the weight increase due to possible carbonation. From these measurements, it is not possible to predict the relative amount of carbonation and leaching.

The probable carbonation during drying and resaturation of the uncarbonated specimens leads to uncertainties about whether the material properties are affected. In order to estimate the extent of the undesired carbonation, the weight increase during the S_{cr}-test is compared to the weight difference between uncarbonated and carbonated specimens from the capillary suction test (Chapter 6). An approximate increase in weight due to carbonation can be calculated from the weights of the specimens used in the capillary suction test. The relative weight difference between the dry weight (+105 °C), $Q_{dry:105}$, for carbonated specimens and the dry weight (+105 °C) for uncarbonated specimens was calculated from the specimens used in the capillary suction test. Table 3 shows the percentage increase in weight due to carbonation relative to the dry weight of the uncarbonated specimens. Corrections are made for differences in specimen weight before the conditioning started.

Table 3 *Increase in dry weight (+105 °C) due to carbonation for specimens in the capillary suction test, Chapter 6. Values are means of three specimens.*

Mortar quality	Weight increase due to carbonation (%)
OPC - 45	6.6
OPC + 65 % slag - 45	4.1
OPC + 5 % silica - 45	7.2

The effect of carbonation and leaching during the test procedure can influence the results in two ways:

1. Carbonation and leaching may lead to changes in the properties of the materials, e.g. the porosity and pore structure, which alters the critical degree of saturation.
2. Carbonation and leaching gradually change the weight of the specimens, leading to an error when determining the dry weight (+105 °C) and the vacuum-saturated weight at the end of the test.

The first effect is applicable to the qualities with large weight changes and where the specimens are deemed as damaged at a late stage, i.e. after four to five drying/resaturation and freeze/thaw cycles. Table 4 shows the number of drying/resaturation and freeze/thaw cycles needed before the specimens were regarded as damaged.

From Table 4 and Figure 2, it can be seen that it is primarily uncarbonated mortar with OPC + 5 % silica and OPC + 65 % slag that shows a relatively high weight increase during the repeated drying/resaturation cycles and at the same time is regarded as damaged after a high number of freeze/thaw cycles. For the uncarbonated OPC-45 mortar, the specimens (as can be seen in Table 4) were already damaged before the first drying cycle, i.e. during the first freeze/thaw cycle.

Table 4 *Number of drying/resaturation and freeze/thaw cycles before the specimens were deemed as damaged.*

Mortar quality		Number of drying/resaturation and freeze/thaw cycles
OPC-45	**Uncarbo.**	0[1)]
	Carbo.	4-5
OPC + 65 % sl-45	**Uncarbo.**	2-5
	Carbo.	3
OPC + 5 % si-45	**Uncarbo.**	5
	Carbo.	5

[1)] Uncarbonated OPC-45 mortar was damaged already during the first freeze/thaw cycle, which is prior to the first drying procedure.

If comparing the weight increase during the drying/resaturation processes in Figure 2 with the weight increase after full carbonation in Table 3, it can be seen that the weight increase of mortar with OPC + 5 % silica is about 0.8 % after five drying/resaturation and freeze/thaw cycles, compared to 7.2 % at full carbonation. This indicates that a little more than 10 % of the possible carbonation has occurred (this assumes that carbonation during the drying/resaturation process leads to formation of the same type of carbonation products as during carbonation during conditioning in the climate chamber). The effect of this rather limited carbonation on the pore structure and thereby on the critical degree of saturation is difficult to predict. However, as has been shown in other investigations presented in this thesis, limited amounts of carbonation might also lead to substantial changes in durability. For example, it was shown in Chapter 3 that a small amount of carbonation has a considerable effect on the salt-frost resistance. If the fairly small amount of carbonation found here influences the frost resistance in the same way as carbonation has been shown to influence the salt-frost resistance, i.e. in a positive way for mortar with OPC + 5 % silica, this could be one explanation for the relatively high frost resistance found for uncarbonated material of this mortar quality in the S_{cr}-test. Both carbonated and uncarbonated mortars with OPC + 5 % silica have namely in this test been shown to be difficult to saturate to a critical degree. The gradual carbonation during the test procedure may be the reason for this.

For the uncarbonated mortar with OPC + 65 % slag, there is an increase in weight of between 0.7 and 1.3 % depending on the number of drying/resaturation and freeze/thaw cycles that occurred before the critical degree was reached, Figure 2. Compared to full carbonation, about 4.1 %, this weight increase represents about 15-30 % carbonation (as was described above, this assumes that carbonation during the drying/resaturation process leads to formation of the same type of carbonation products as during carbonation during conditioning in the climate chamber). It was shown in Chapter 3 that the effect of carbonation on mortar with high slag contents in the binder was negative with respect to salt-frost resistance. Here, the fairly extensive undesired carbonation ought also to have had an effect on the frost resistance. The great spread in the results for the uncarbonated mortars with 65 % slag as part of the binder, which makes it difficult to point out a critical

degree of saturation, may be explained by the effect of carbonation of the partly carbonated (uncarbonated)- specimens.

For the carbonated mortars, it is only mortar with OPC + 65 % slag that shows a marked weight change during the S_{cr}-test procedure. However, the weight change for this mortar quality is not due to an increase but, on the contrary, to a decrease in weight as a result of the drying/resaturation processes. After three drying/resaturation and freeze/thaw cycles, the weight loss is about 0.4 %. This weight loss can probably be explained by leaching and/or a chemical breakdown of carbonate products during heating and resaturation. The effect on the critical degree of saturation is difficult to predict. For mortars with OPC or with OPC + 5 % silica, there is no weight change during the S_{cr}-test, implying that the saturation values for these qualities are less inaccurate than for the other qualities.

The effect of the weight change during the repeated drying and resaturation cycles on the calculated degree of saturation is that the weight change causes errors in the determination of the dry (+105 °C) and the vacuum-saturated weights. These weights are determined at the end of the S_{cr}-test, i.e. after all five drying/resaturation and freeze/thaw cycles have been carried out. The uncertainties in the weights for the dry and vacuum-saturated specimens leads to large uncertainties when calculating the degree of saturation.

The effect of the weight change during the course of the S_{cr}-test as a result of the repeated drying/resaturation cycles on the degree of saturation may be illustrated by calculating the degree of saturation for the uncarbonated ‘OPC - 45’ mortar. Calculating the mean degree of saturation for the specimens of this mortar quality at the time of damage, i.e. after the first freeze/thaw cycle, using the dry and saturated weights measured after the additional five drying and/resaturation and freeze/thaw cycles were carried out, gives a critical degree of saturation of 0.893. However, if we correct the dry and vacuum-saturated weights based on the measured weight increase during the course of the test, the calculated degree of saturation is 0.984. This means a difference of over 0.09 in the degree of saturation for this material as a result of the weight change taking place during the course of the S_{cr}-test.

In this example, it is assumed that the relative increase in weight which is measured at +50 °C is the same at +105 °C and at vacuum saturation. This assumption is necessary, but is a rough simplification. However, even if the relative weight change for the dry (+105 °C) and vacuum-saturated weight may differ somewhat from that measured at +50 °C, it is shown that the weight change during the course of the test might be an important source of uncertainty.

Compared to the effect of differences in water uptake during capillary suction on the degree of saturation after 24 hours of capillary suction (Table 2), the possible effect of weight change during the S_{cr}-test seems to predominate.

As has been shown above, the weight changes during the S_{cr}-test influence the calculated degrees of saturation to a great extent. Because of this, corrections have to be made in

order to obtain somewhat more reliable results. Since the measured dry and vacuum-saturated weights at the end of the S_{cr}-test are the most affected and uncertain values, they cannot be used for calculation of the degree of saturation.

There are a couple of alternative ways of calculating the degree of saturation without the dry and vacuum-saturated weights, although all include using the results from the capillary suction test in Chapter 6. All alternatives give about the same results. Here, an alternative is used where it is assumed that the total open porosity is the same for all specimens of the same mortar quality. It is also assumed that the degree of saturation during capillary suction is the same for all specimens of the same mortar quality after the same time of capillary suction. These assumptions are based on the indication that the homogeneity and material properties for specimens of the same mortar quality seem to be even. This is illustrated by the low scatter and the fact that the weight changes during conditioning in the climate chambers are almost exactly the same (see Figures 5.1 and 5.2 in Chapter 5), as well as during capillary suction (see Figure 1).

A further indication of homogeneous materials for the specimens used in the two different tests is the density evaluation shown in Table 5. In no case does the coefficient of variation exceed 0.5 %, which is probably within the uncertainty of measurement. The calculated densities are based on the specimen weights in equilibrium with 65 % RH (after conditioning for 330 days in the climate chamber) and the specimen volume measured after the capillary suction tests were concluded.

Table 5 *Densities (specimens in equilibrium with 65 % RH) calculated from the specimen weights after 330 days preconditioning in the climate chambers divided by the volume measured after conclusion of the capillary suction test. Values are means of three specimens.*

		OPC-45		**OPC + 65 % sl-45**		**OPC + 5 % si-45**	
		Uncarbo.	**Carbo.**	**Uncarbo.**	**Carbo.**	**Uncarbo.**	**Carbo.**
Capillary suction specimens							
Mean	(kg/m^3)	2141	2284	2087	2146	2140	2263
Standard deviation	(kg/m^3)	6	2	9	6	3	7
Coefficient of var.	(%)	0.27	0.08	0.42	0.28	0.14	0.32
S_{cr}- specimens							
Mean	(kg/m^3)	2139	2284	2096	2147	2144	2265
Standard deviation	(kg/m^3)	7	10	9	10	3	7
Coefficient of var.	(%)	0.32	0.45	0.41	0.46	0.12	0.29
Cap. suc. + S_{cr}-specimens							
Mean (6 specimens)	(kg/m^3)	2140	2284	2091	2147	2142	2264
Standard deviation	(kg/m^3)	6	7	9	7	3	6
Coefficient of var.	(%)	0.27	0.29	0.44	0.34	0.16	0.28

Homogenous mortar qualities are essential if the assumptions of equal total open porosity and equal degree of saturation after the same capillary suction time for all specimens of

the same quality are to be reliable. Based on these assumptions, the degree of saturation can be calculated without the dry and vacuum-saturated weights having to be known, as described below:

Consider Equation 7.1 (Chapter 7) for calculation of the degree of saturation. The denominator is an expression of the open pore volume measured after the last freeze/thaw cycle, compensated for possible volume changes during the course of the test. Since the weights $Q_{(sat:a)n}$ and $Q_{dry:105}$ have been shown to be impractical to use because of the gradual weight change during the course of the S_{cr}-test, these weights are not relevant and Equation 7.1 cannot be used as such. However, based on the assumption of equal total open porosity for all specimens of the same quality, the denominator in Equation 7.1 can be changed to $V_{p:open}$, where $V_{p:open}$ is the volume of open pores before the freeze/thaw test starts. The volume of open pores is calculated for each specimen from Equation 4:

$$V_{p:open} = \frac{P_{tot}}{100} \cdot \frac{(Q_{sat:a} - Q_{sat:w})}{\rho_w} \qquad \text{[Eq. 4]}$$

where:

P_{tot}	is the total open porosity in %. From Table 6.2 in Chapter 6.	[%]
$Q_{sat:a}$	is the weight in air of a vacuum-saturated specimen before the start of the freeze/thaw test.	[kg]
$Q_{sat:w}$	is the weight in water of a vacuum-saturated specimen before the start of the freeze/thaw test.	[kg]
ρ_w	is the density of water (1000 kg/m^3).	[kg/m^3]

The term $(Q_{sat:a}\text{-}Q_{sat:w})/\rho_w$ is the volume of each individual specimen at the start of the freeze/thaw test.

Assuming that all specimens of the same concrete quality have reached the same degree of saturation after the same time of capillary suction makes it possible to calculate the dry weight ($Q_{dry:105}$) of each specimen used in the S_{cr}-test from Equation 5:

$$Q_{dry:105} = Q_t - S_t \cdot V_{p:open} \cdot \rho_w \qquad \text{[Eq. 5]}$$

where:

Q_t	is the weight of a specimen used in the S_{cr}-test at time t during capillary suction	[kg]
S_t	is the mean degree of saturation at time t for specimens of the same quality as the specimen with weight Q_t, but from the specimens used in the capillary suction test in Chapter 6.	[-]

The degree of saturation after a specified time during capillary suction has to be known if we are to be able to calculate the dry weight. Here, the degree of saturation after 24 hours of capillary suction is used. The degree of saturation after 24 hours is used because this is far beyond the nick-point for all materials, which is desirable, and because the specimens

used in the S_{cr}-test were subjected to capillary suction for 24 hours. The mean degree of saturation after 24 hours of the specimens used in the capillary suction test in Chapter 6 is calculated and shown in Table 1.

The following is an example of calculation of the volume of open pores and the dry weight of a specimen used in the S_{cr}-test.

Example for an uncarbonated specimen (no. 0905) of mortar quality 'OPC + 5 % silica - 45':
The specimen weight after 24 hours of capillary suction was 48.76 gram. The volume of the specimen ($Q_{sat:a}$-$Q_{sat:w}$)/ρ_w was 21.66 cm^3, and the total open porosity for this uncarbonated material was 25.4 % (Table 6.2). The mean degree of saturation after 24 hours for specimens in the capillary suction test in Chapter 6 was 0.865 (Table 1).

The open pore volume for this individual specimen is calculated from:

$$V_{p:open} = \frac{25.4}{100} \cdot 21.66 = 5.50\ cm^3$$

The dry weight ($Q_{dry:105}$) is calculated from:

$$Q_{dry:105} = 48.76 - 0.865 \cdot 5.50 \cdot 1 = 44.0\ gram$$

For this individual specimen, these values for the dry weight and the open pore volume are used when calculating the degree of saturation during the course of the S_{cr}-test.

After the dry weight and the open pore volume have been calculated for each specimen, the degree of saturation after each freeze/thaw procedure can be calculated. However, to be able to calculate the degree of saturation, it is necessary to compensate the open pore volume for possible volume changes of the specimens during the course of the S_{cr}-test. This is done by adding a possible volume difference between the specimen volume before the n:th freeze/thaw cycle and before the first freeze/thaw cycle to the volume of open pores before the freeze/thaw test, as shown in Equation 6:

$$S_n = \frac{Q_n - Q_{dry:105}}{V_{p:open} + (V_n - V_0)} \cdot \frac{1}{\rho_w} \qquad \text{[Eq. 6]}$$

where:

S_n	is the degree of saturation during the n:th freeze/thaw cycle	[-]
Q_n	is the weight of a specimen before the n:th freeze/thaw cycle	[kg]
$Q_{dry:105}$	is the calculated dry specimen weight (+105 °C), based on results from Chapter 6	[kg]
$V_{p:open}$	is the calculated volume of open pores before the test start, i.e. before first freeze/thaw cycle, based on results from Chapter 6	[m^3]
V_n	is the volume of a specimen before the n:th freeze/thaw cycle	[m^3]
V_0	is the volume of a specimen before the test start, i.e. before first freeze/thaw cycle	[m^3]
ρ_w	is the density of water (1000 kg/m^3)	[kg/m^3]

As was discussed above and shown in Figure 2, the weights of some of the specimens used in the S_{cr}-test were markedly changed by such mechanisms as possible carbonation and leaching during the course of the S_{cr}-test (repeated drying/resaturation and freeze/thaw cycles). It was also shown that these weight changes could lead to errors when calculating the degrees of saturation. In order to minimise these errors, the measured weights during the course of the S_{cr}-test were also corrected with respect to the measured weight change during the repeated dryings at +50 °C. This correction was carried out as follows:

- As was discussed above, the weight change of the specimens during the first drying at +50 °C is not known. It is therefore assumed that the weight change during the first drying is the same as during the second drying. A 'dry weight' before the first drying at +50 °C is therefore calculated as described above, from Equation 2
- The difference between the weight after the subsequent dryings at +50 °C and the 'dry weight' before the first drying was calculated for all specimens. This calculated weight change is used when calculating corrected values of the specimen weights according to Equation 7.

$$Q_{n:corrected} = Q_n - (Q_{dry:50:n} - Q_{dry:50:before}) \qquad \text{[Eq. 7]}$$

where

$Q_{n:corrected}$	is the corrected specimen weight after the n:th drying/resaturation cycle	[kg]
Q_n	is the specimen weight after the n:th drying/resaturation cycle	[kg]
$Q_{dry:50:n}$	is the dry specimen weight (+50 °C) after the n:th drying/resaturation cycle	[kg]
$Q_{dry:50:before}$	is the calculated 'dry' specimen weight (+50 °C) before the first drying/resaturation cycle. Calculated from Equation 2.	[kg]

This correction of the specimen weights is carried out after each drying/resaturation procedure for all specimens that have not reached the critical degree of saturation before the first drying/resaturation procedure; see Table 4.

With the assumptions concerning equal total open porosities and equal degree of saturation after the same time of capillary suction for all specimens of the same mortar quality, as well as correcting the specimen weights for changes in weight during the course of the S_{cr}-test, corrected values for the degree of saturation have been calculated; see Appendix 10 and Figure 7.4 in Chapter 7.

APPENDIX 10

CALCULATED DEGREES OF SATURATION

Calculated degrees of saturation as determined in accordance with the procedure in RILEM CDC 3. Results discussed in Chapter 7.

OPC - 45	First		Second		Third		Fourth		Fifth		Sixth	
Uncarbonated	S_{cap1}	E_1/E_0	S_{cap2}	E_2/E_0	S_3	E_3/E_0	S_4	E_4/E_0	S_5	E_5/E_0	S_6	E_6/E_0
0202	0.904	0.90	-	-	-	-	-	-	-	-	-	-
0213	0.887	0.84	-	-	-	-	-	-	-	-	-	-
0216	0.889	0.83	-	-	-	-	-	-	-	-	-	-
Carbonated												
1206	0.917	1.01	0.905	1.01	0.916	1.02	0.957	1.01	0.977	0.88	-	-
1212	0.916	1.01	0.903	1.01	0.934	1.01	0.945	1.01	0.983	0.93	0.988	0.75
1218	0.894	1.02	0.883	1.01	0.909	1.01	0.929	1.01	0.963	0.93	0.989	0.72

OPC + 65 % slag - 45	First		Second		Third		Fourth		Fifth		Sixth	
Uncarbonated	S_{cap1}	E_1/E_0	S_{cap2}	E_2/E_0	S_3	E_3/E_0	S_4	E_4/E_0	S_5	E_5/E_0	S_6	E_6/E_0
0603	0.852	1.01	0.838	0.958	0.862	0.85	-	-	-	-	-	-
0607	0.866	1.02	0.848	0.988	0.868	0.95	0.879	0.93	0.902	0.91	0.935	0.91
0615	0.860	1.02	0.846	0.988	0.858	0.86	-	-	-	-	-	-
Carbonated												
1607	0.839	1.00	0.832	0.975	0.871	0.90	0.912	0.77	-	-	-	-
1611	0.849	1.01	0.840	0.981	0.882	0.93	0.908	0.86	-	-	-	-
1612	0.857	1.00	0.847	0.975	0.867	0.91	0.896	0.84	-	-	-	-

OPC + 5 % silica - 45	First		Second		Third		Fourth		Fifth		Sixth	
Uncarbonated	S_{cap1}	E_1/E_0	S_{cap2}	E_2/E_0	S_3	E_3/E_0	S_4	E_4/E_0	S_5	E_5/E_0	S_6	E_6/E_0
0902	0.898	1.02	0.890	1.01	0.915	1.00	0.927	1.01	0.940	0.97	0.958	0.96
0905	0.893	1.02	0.878	1.01	0.897	0.99	0.921	1.01	0.940	0.99	0.965	0.93
0918	0.905	1.01	0.895	1.01	0.914	1.02	0.930	1.02	0.963	0.99	0.968	0.94
Carbonated												
1902	0.902	1.01	0.889	1.00	0.923	1.00	0.942	0.99	0.995	0.97	0.994	0.94
1910	0.887	1.01	0.878	0.99	0.920	0.98	0.954	0.99	0.993	0.91	0.999	0.88
1914	0.890	1.01	0.884	0.98	0.921	0.98	0.951	0.96	0.980	0.93	0.995	0.88

Calculated corrected degrees of saturation, assuming all specimens of the same mortar quality have the same open porosity and the same degree of saturation after the same time of capillary suction. Results are discussed in Chapter 7.

OPC - 45	First		Second		Third		Fourth		Fifth		Sixth	
Uncarbonated	S_{cap1}	E_1/E_0	S_{cap2}	E_2/E_0	S_3	E_3/E_0	S_4	E_4/E_0	S_5	E_5/E_0	S_6	E_6/E_0
0202	0.906	0.90	-	-	-	-	-	-	-	-	-	-
0213	0.906	0.84	-	-	-	-	-	-	-	-	-	-
0216	0.906	0.83	-	-	-	-	-	-	-	-	-	-
Carbonated												
1206	0.869	1.01	0.853	1.01	0.858	1.02	0.900	1.01	0.920	0.88	-	-
1212	0.869	1.01	0.849	1.01	0.871	1.01	0.873	1.01	0.909	0.93	0.930	0.75
1218	0.869	1.02	0.851	1.01	0.868	1.01	0.890	1.01	0.922	0.93	0.956	0.72

OPC + 65 % slag - 45	First		Second		Third		Fourth		Fifth		Sixth	
Uncarbonated	S_{cap1}	E_1/E_0	S_{cap2}	E_2/E_0	S_3	E_3/E_0	S_4	E_4/E_0	S_5	E_5/E_0	S_6	E_6/E_0
0603	0.802	1.01	0.766	0.958	0.766	0.85	-	-	-	-	-	-
0607	0.802	1.02	0.761	0.988	0.755	0.95	0.745	0.93	0.752	0.91	0.767	0.91
0615	0.802	1.02	0.760	0.988	0.743	0.86	-	-	-	-	-	-
Carbonated												
1607	0.848	1.00	0.848	0.975	0.893	0.90	0.957	0.77	-	-	-	-
1611	0.848	1.01	0.848	0.981	0.896	0.93	0.941	0.86	-	-	-	-
1612	0.848	1.00	0.846	0.975	0.871	0.91	0.922	0.84	-	-	-	-

OPC + 5 % silica - 45	First		Second		Third		Fourth		Fifth		Sixth	
Uncarbonated	S_{cap1}	E_1/E_0	S_{cap2}	E_2/E_0	S_3	E_3/E_0	S_4	E_4/E_0	S_5	E_5/E_0	S_6	E_6/E_0
0902	0.868	1.02	0.838	1.01	0.840	1.00	0.837	1.01	0.848	0.97	0.858	0.96
0905	0.868	1.02	0.830	1.01	0.825	0.99	0.833	1.01	0.850	0.99	0.866	0.93
0918	0.868	1.01	0.835	1.01	0.828	1.02	0.831	1.02	0.860	0.99	0.858	0.94
Carbonated												
1902	0.834	1.01	0.823	1.00	0.852	1.00	0.871	0.99	0.902	0.97	0.929	0.94
1910	0.834	1.01	0.823	0.99	0.858	0.98	0.889	0.99	0.919	0.91	0.941	0.88
1914	0.834	1.01	0.823	0.98	0.851	0.98	0.880	0.96	0.897	0.93	0.931	0.88

APPENDIX 11

CLIMATE AT THE EXPOSURE SITES
DURING WINTER SEASONS 1996 - 2003

Climate at the highway exposure site during winter season 1996 - 1997

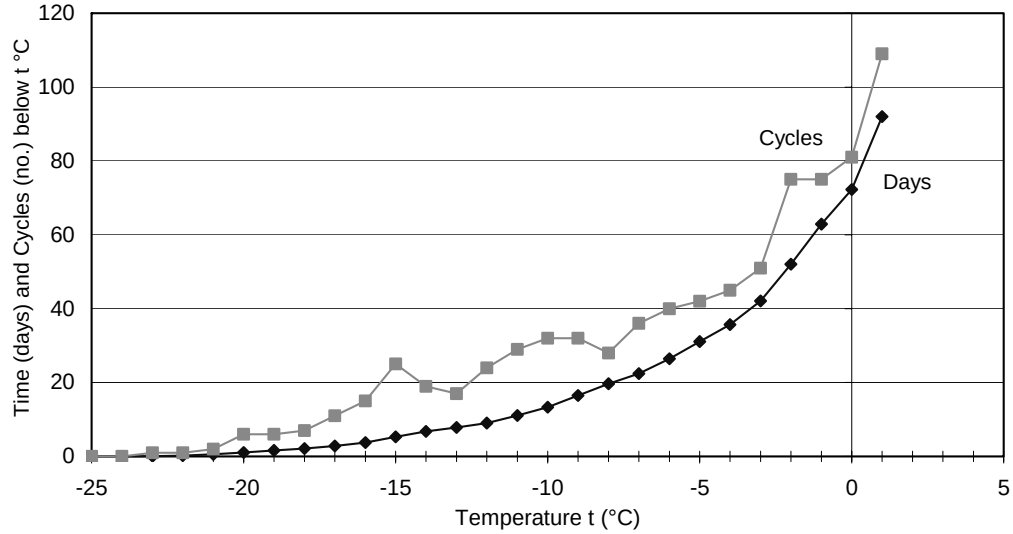

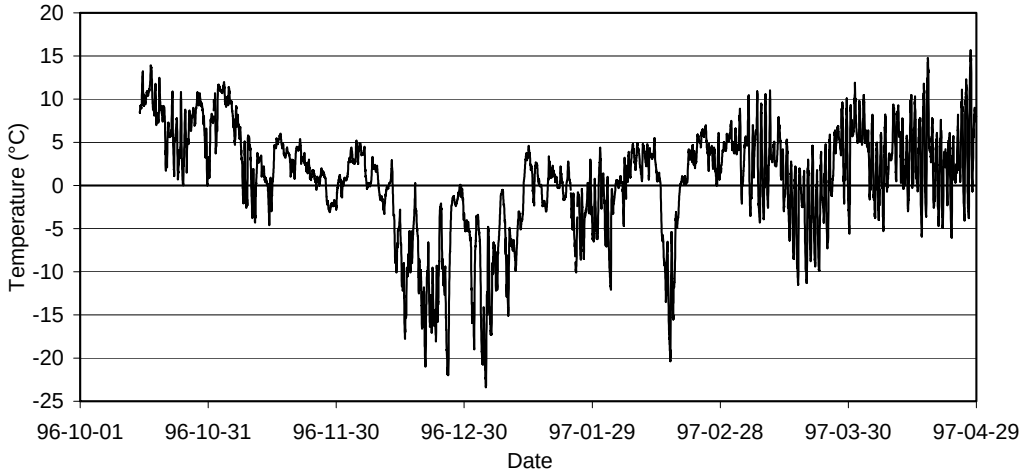

Temperature	Oct.[1]	Nov.	Dec.	Jan.	Feb.	Mar.	Apr.
Mean (°C)	7.4	3.2	-4.6	-3.9	0.2	1.7	3.7
Max (°C)	13.9	12.0	5.2	4.6	7.0	11.9	15.7
Min (°C)	0.0	-4.6	-22.0	-23.4	-20.4	-11.5	-6.1

Relative humidity	Oct.[1]	Nov.	Dec.	Jan.	Feb.	Mar.	Apr.
Mean (%)	91.2	92.7	93.5	93.3	86.6	72.4	64.2
Standard dev. (%)	9.4	7.5	4.5	9.4	12.0	24.0	29.7

Precipitation[2]	Oct.	Nov.	Dec.	Jan.	Feb.	Mar.	Apr.
Rain (mm fluid)	94.7	146.9	58.5	18.7	139.1	48.1	41.5
Precipitation as fluid	94.7	146.9	58.5	18.7	139.1	48.1	41.5

[1] Measured from the 15th of October

[2] Precipitation from a climate station owned by the Swedish Meteorological and Hydrological Institute (SMHI). No division into different precipitation types.

Climate at the highway exposure site during winter season 1997 - 1998

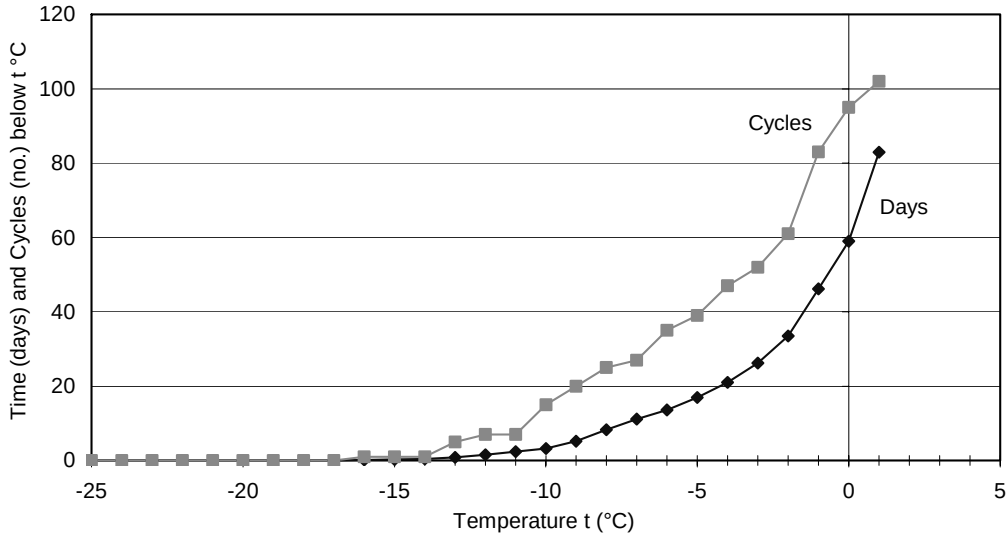

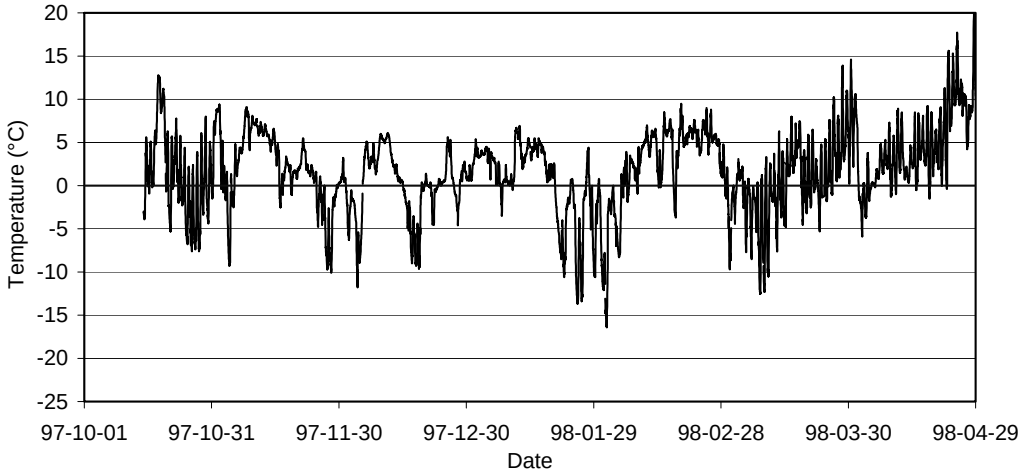

Temperature	Oct.(1	Nov.	Dec.	Jan.	Feb.	Mar.	Apr.
Mean (°C)	1.5	2.1	0.0	-0.1	3.1	0.8	5.2
Max (°C)	12.8	9.4	6.1	6.9	9.5	14.6	23.3
Min (°C)	-7.6	-10.1	-11.8	-15.8	-16.4	-12.5	-5.9

Relative humidity	Oct.(1	Nov.	Dec.	Jan.	Feb.	Mar.	Apr.
Mean (%)	83.8	88.0	91.1	85.8	90.4	73.3	74.2
Standard dev. (%)	15.5	9.4	5.9	14.9	12.9	25.8	24.0

Precipitation	Oct.(2	Nov.	Dec.	Jan.	Feb.	Mar.	Apr.
Rain (mm fluid)	0.7	25.9	57.9	34.9	38.8	3.9	31.0
Snow (mm as snow)	0	88.0	130.8	105.6	174.9	223.3	286.0
Snow/rain mixed	0	3.7	4.9	3.5	2.7	5.5	18.1
Precipitation as fluid	0.7	35.4	72.0	46.2	56.8	27.3	63.2

(1 Measured from the 15th of October, (2 Measured from the 22nd of October

Climate at the highway exposure site during winter season 1998 - 1999

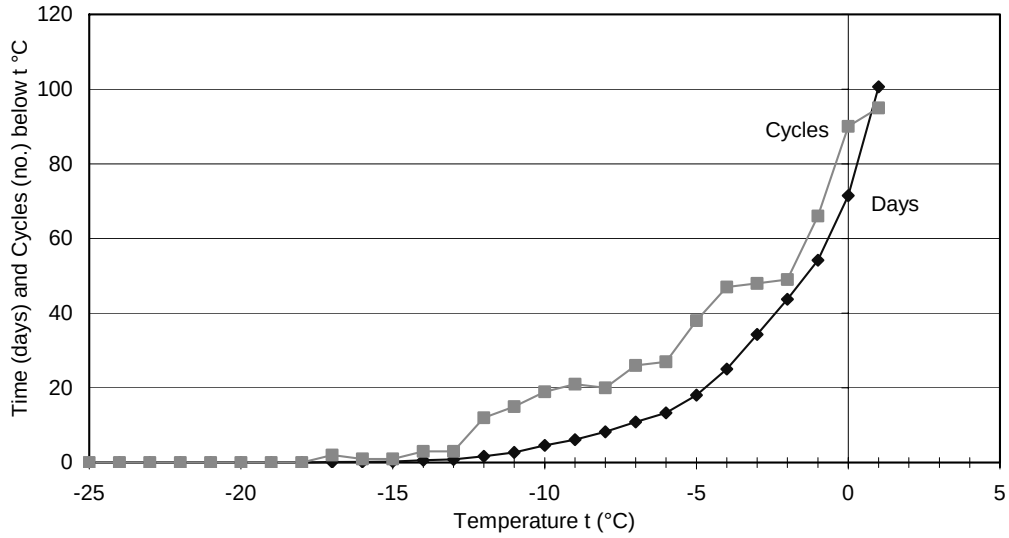

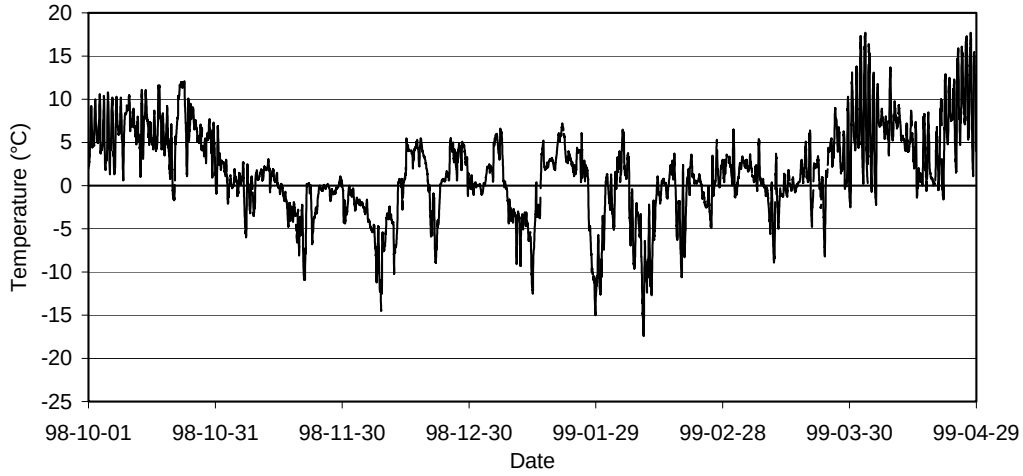

Temperature	Oct.	Nov.	Dec.	Jan.	Feb.	Mar.	Apr.
Mean (°C)	6.3	-0.8	-0.9	-0.6	-1.6	1.5	6.7
Max (°C)	12.1	3.8	5.5	7.2	6.5	13.8	17.7
Min (°C)	-1.7	-10.9	-14.5	-15.0	-17.4	-8.9	-2.2

Relative humidity	Oct.	Nov.	Dec.	Jan.	Feb.	Mar.	Apr.
Mean (%)	84.3	87.7	92.0	89.4	88.0	86.4	71.2
Standard dev. (%)	15.3	9.0	5.7	6.1	12.0	15.4	27.3

Precipitation	Oct.	Nov.	Dec.	Jan.	Feb.	Mar.	Apr.
Rain (mm fluid)	116.0	3.5	32.3	82.3	24.7	25.9	42.0
Snow (mm as snow)	0.1	247.4	424.3	123.9	193.6	215.0	216.0
Snow/rain mixed	9.3	23.1	33.8	26.6	9.3	42.4	39.5
Precipitation as fluid	117.9	32.9	81.5	100.0	45.9	55.9	71.5

Climate at the highway exposure site during winter season 1999 - 2000

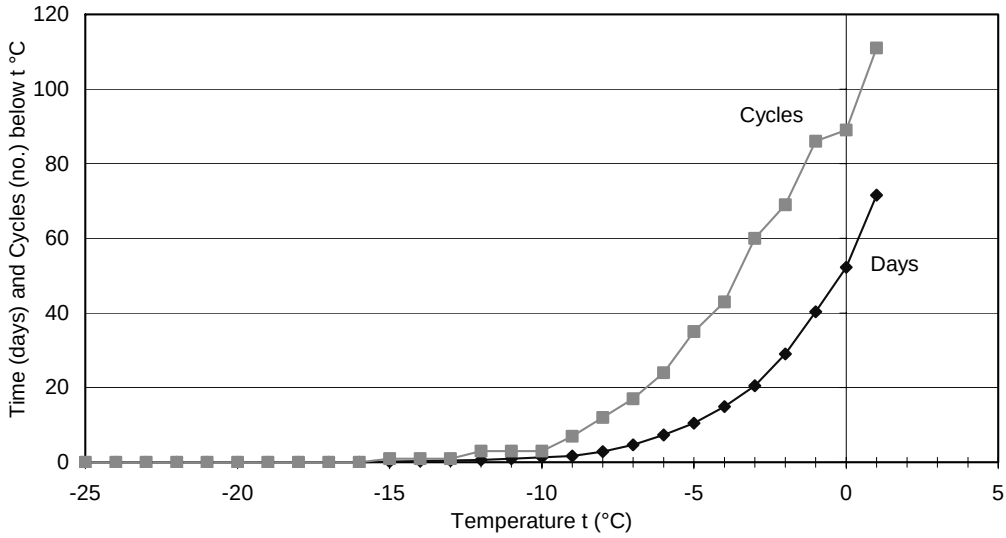

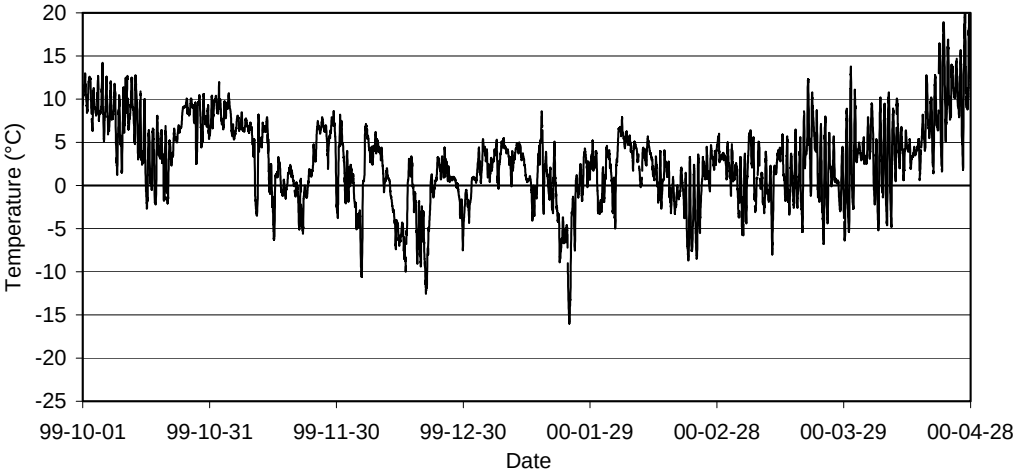

Temperature	Oct.	Nov.	Dec.	Jan.	Feb.	Mar.	Apr.
Mean (°C)	7.0	4.0	-0.7	0.7	1.4	1.5	7.6
Max (°C)	14.2	12.0	7.5	8.6	7.9	13.8	27.4
Min (°C)	-2.7	-6.3	-12.5	-16.0	-8.7	-8.0	-5.2

Relative humidity	Oct.	Nov.	Dec.	Jan.	Feb.	Mar.	Apr.
Mean (%)	85.0	88.4	90.1	86.7	89.2	72.7	73.1
Standard dev. (%)	14.4	9.1	9.0	15.4	10.7	23.2	26.5

Precipitation	Oct.	Nov.	Dec.	Jan.	Feb.	Mar.	Apr.
Rain (mm fluid)	59.2	36.7	78.1	60.7	75.6	18.2	61.1
Snow (mm as snow)	0	16.9	398.8	109.8	57.8	184.2	0.2
Snow/rain mixed	0	11.3	92.9	14.7	43.1	31.6	5.3
Precipitation as fluid	59.2	40.7	136.6	74.6	90.0	42.9	62.2

Climate at the highway exposure site during winter season 2000 - 2001

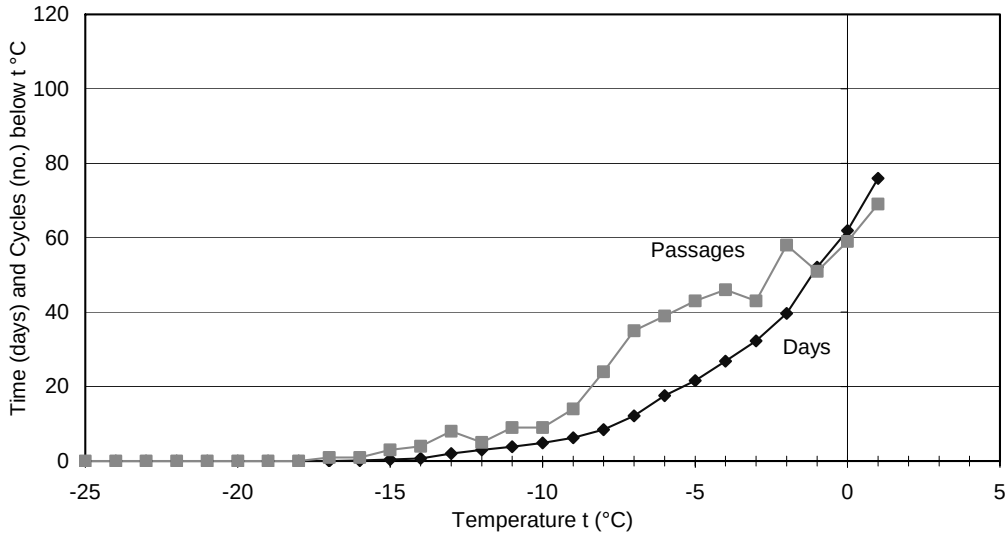

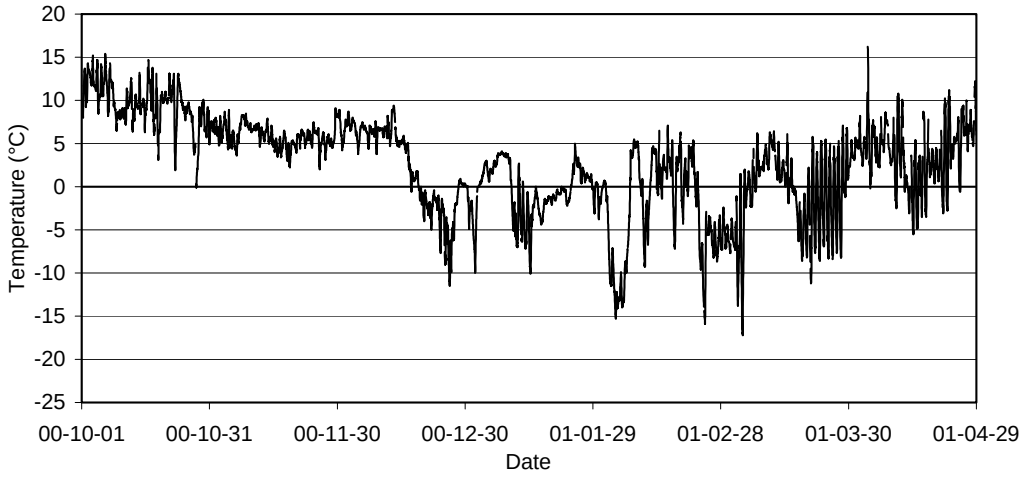

Temperature	Oct.	Nov.	Dec.	Jan.	Feb.	Mar.	Apr.
Mean (°C)	9.5	5.9	2.2	-0.4	-2.7	-0.8	4.1
Max (°C)	15.4	9.1	9.4	5.0	7.1	7.1	16.6
Min (°C)	-0.1	2.0	-11.5	-10.1	-15.9	-17.2	-5.5

Relative humidity	Oct.	Nov.	Dec.	Jan.	Feb.	Mar.	Apr.
Mean (%)	89.8	91.9	92.1	91.5	82.7	77.8	81.0
standard dev. (%)	6.8	3.8	2.9	4.5	13.6	20.3	18.8

Precipitation	Oct.	Nov.	Dec.	Jan.	Feb.	Mar.	Apr.
Rain (mm fluid)	144.9	94.2	89.2	18.5	30.9	25.1	64.4
Snow (mm as snow)	0	0.3	215.3	120.6	204.1	46.5	48.0
Snow/rain mixed	0	5.1	18.5	22.4	6.1	10.2	20.5
Precipitation as fluid	144.9	95.3	114.4	35.0	52.5	31.8	73.3

Climate at the highway exposure site during winter season 2001 - 2002

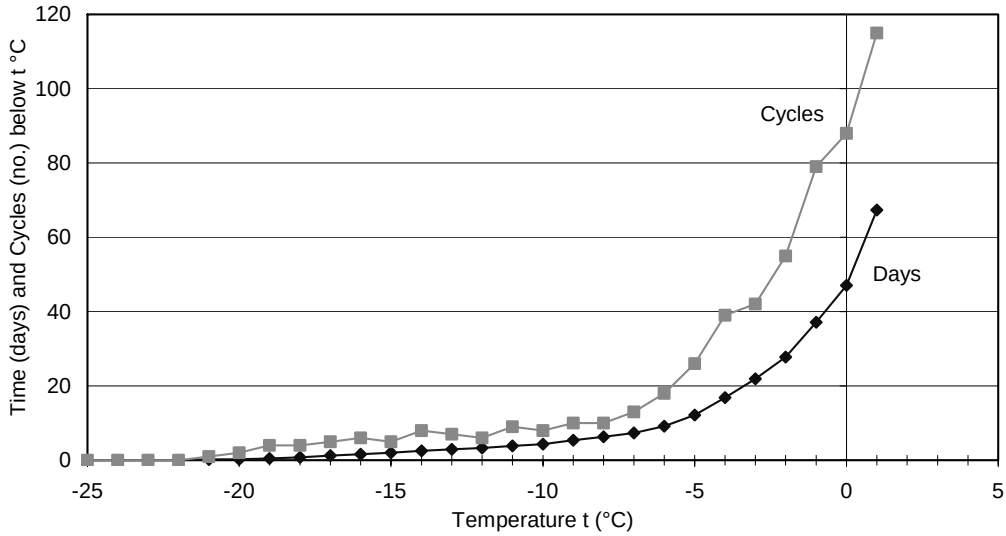

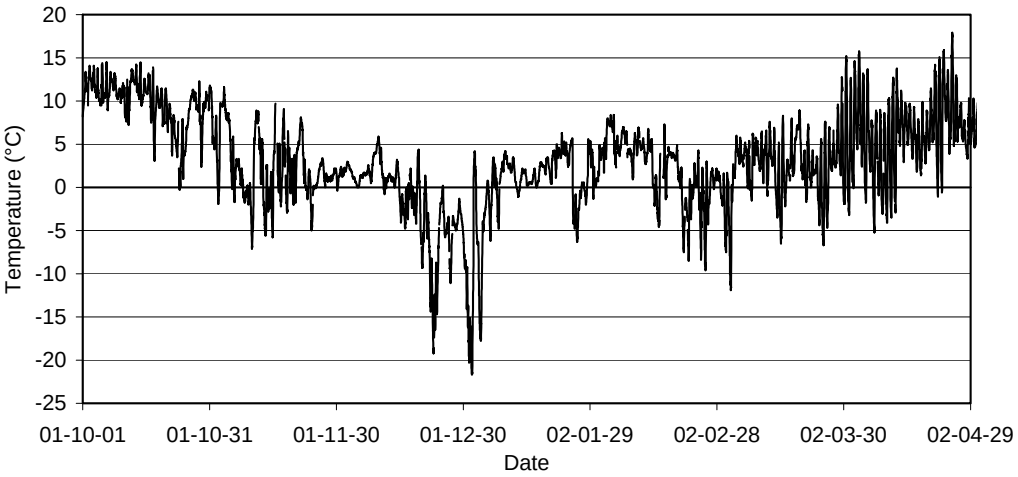

Temperature	Oct.	Nov.	Dec.	Jan.	Feb.	Mar.	Apr.
Mean (°C)	9.8	2.1	-2.2	0.5	2.2	2.4	6.4
Max (°C)	14.5	11.6	5.9	6.3	8.4	15.2	17.9
Min (°C)	-0.3	-7.1	-21.1	-21.7	-9.6	-11.9	-5.2

Relative humidity	Oct.	Nov.	Dec.	Jan.	Feb.	Mar.	Apr.
Mean (%)	86.4	83.0	90.2	91.6	85.0	78.0	72.1
Standard dev. (%)	9.5	15.8	8.5	8.6	13.9	19.1	21.1

Precipitation	Oct.	Nov.	Dec.	Jan.	Feb.	Mar.	Apr.
Rain (mm fluid)	98.1	22.4	6.1	49.2	84.6	48.9	23.8
Snow (mm as snow)	0	52.8	403.6	178.7	237.0	67.7	0.1
Snow/rain mixed	0	15.3	29.2	27.3	50.9	37.2	0
Precipitation as fluid	98.1	30.7	52.3	72.5	118.5	63.1	23.8

Climate at the highway exposure site during winter season 2002 - 2003

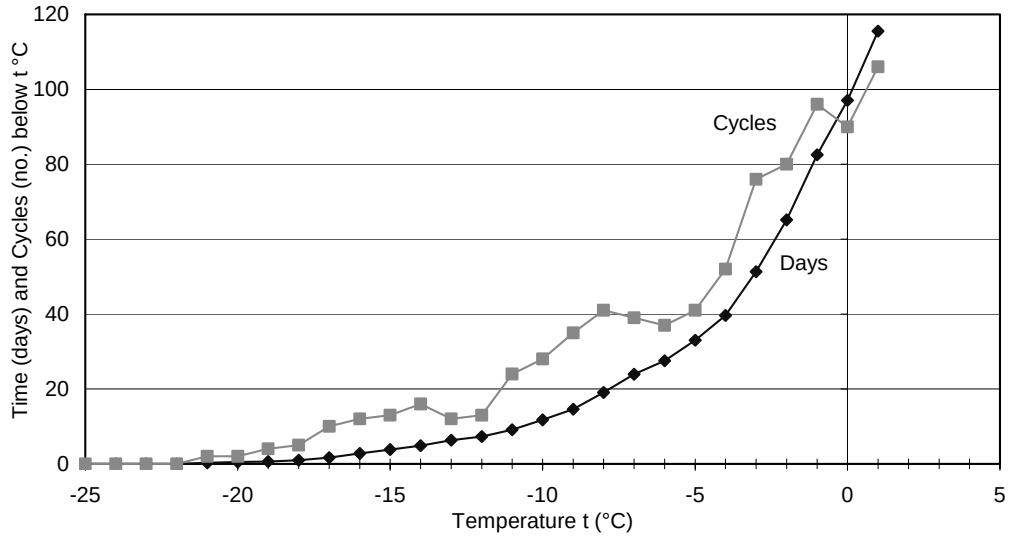

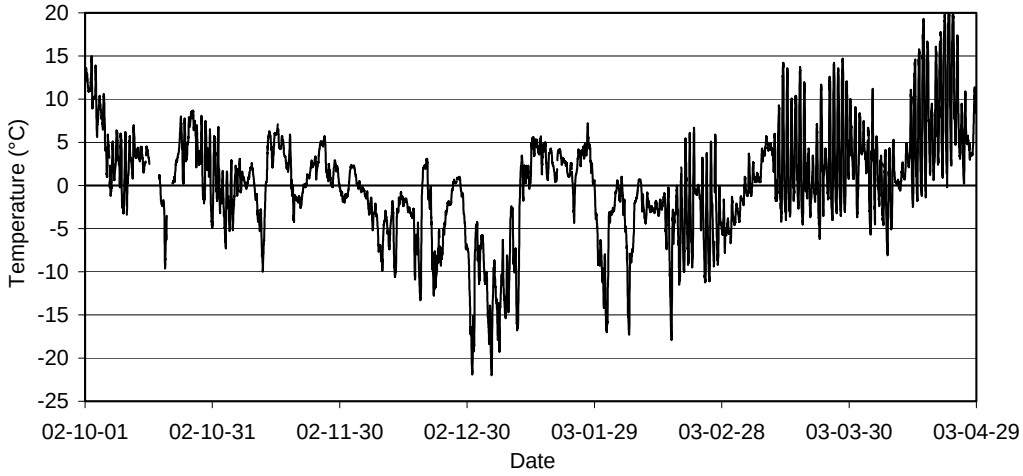

Temperature	Oct.	Nov.	Dec.	Jan.	Feb.	Mar.	Apr.
Mean (°C)	4.1	0.9	-3.8	-3.0	-3.8	1.9	5.4
Max (°C)	15.0	7.1	3.1	7.2	6.7	14.7	21.7
Min (°C)	-9.6	-10.0	-21.9	-22.0	-17.9	-6.7	-8.1

Relative humidity	Oct.	Nov.	Dec.	Jan.	Feb.	Mar.	Apr.
Mean (%)	85.2	87.9	87.0	88.9	87.9	75.4	68.0
Standard dev. (%)	11.8	8.3	7.7	7.7	10.2	22.5	25.5

Precipitation	Oct.	Nov.	Dec.	Jan.	Feb.	Mar.	Apr.
Rain (mm fluid)	42.9	35.4	5.1	30.0	0.6	12.1	55.7
Snow (mm as snow)	198.4	69.7	154.5	138.2	194.0	20.7	23.6
Snow/rain mixed	6.6	31.4	8.7	21.9	19.0	11.8	21.9
Precipitation as fluid	64.1	48.7	22.3	48.2	23.8	16.5	62.4

Climate at the marine exposure site during winter season 1996 - 1997

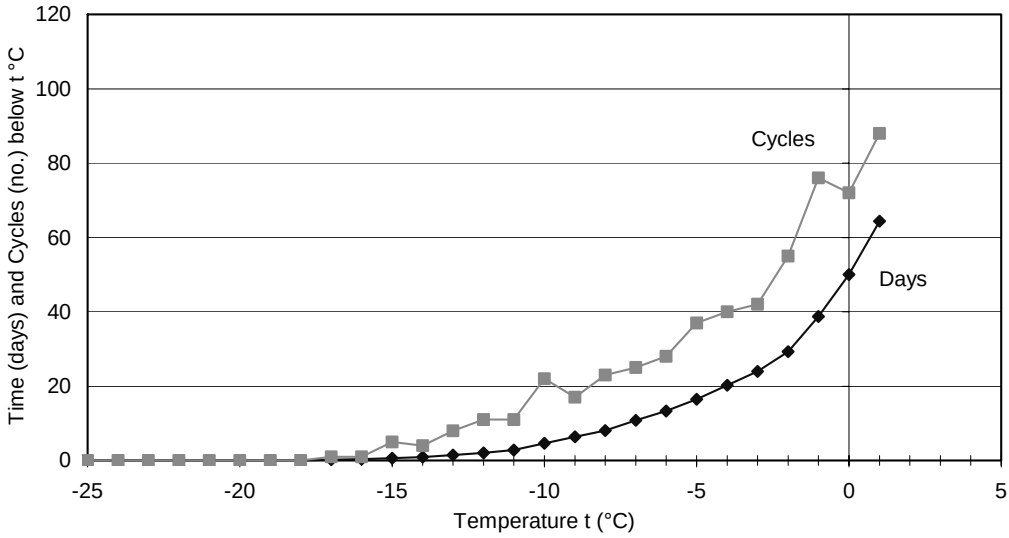

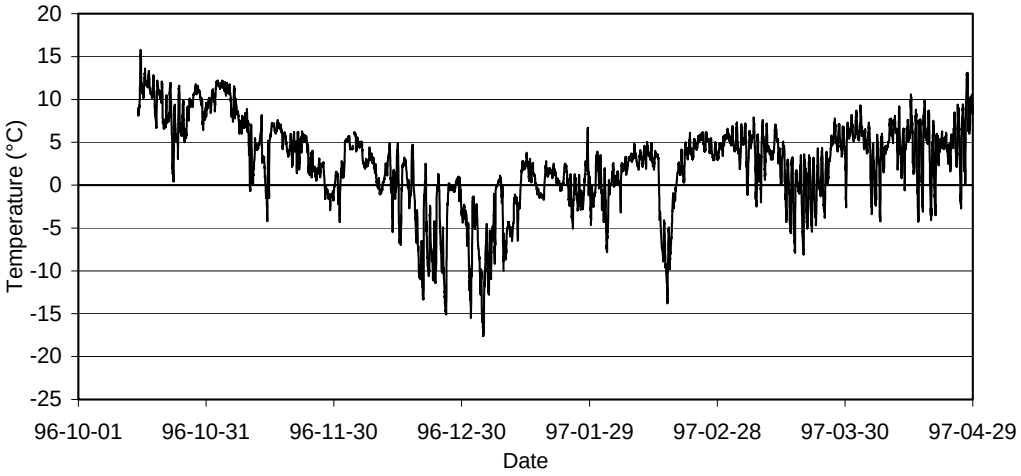

Temperature	Oct.(1	Nov.	Dec.	Jan.	Feb.	Mar.	Apr.
Mean (°C)	9.2	5.2	-1.1	-1.9	1.5	2.8	4.9
Max (°C)	15.8	12.2	6.2	6.7	6.2	8.2	13.1
Min (°C)	0.4	-4.2	-15.1	-17.6	-13.8	-8.1	-4.3

Relative humidity	Oct.(1	Nov.	Dec.	Jan.	Feb.	Mar.	Apr.
Mean (%)	84.7	83.0	84.4	89.7	86.1	79.5	72.5
Standard dev. (%)	13.4	12.8	13.7	10.4	11.0	18.0	21.8

Precipitation	Oct.(1	Nov.	Dec.	Jan.	Feb.	Mar.	Apr.
Rain (mm fluid)	111.8	108.8	93.2	6.7	58.6	31.9	45.4
Snow (mm as snow)	0	5.9	126.1	66.3	174.8	1.6	3.9
Snow/rain mixed	0	13.1	6.6	0.8	189.6	0.8	2.7
Precipitation as fluid	111.8	112.0	107.1	13.5	114	32.2	46.3

(1 Measured from the 15th of October

Climate at the marine exposure site during winter season 1997 - 1998

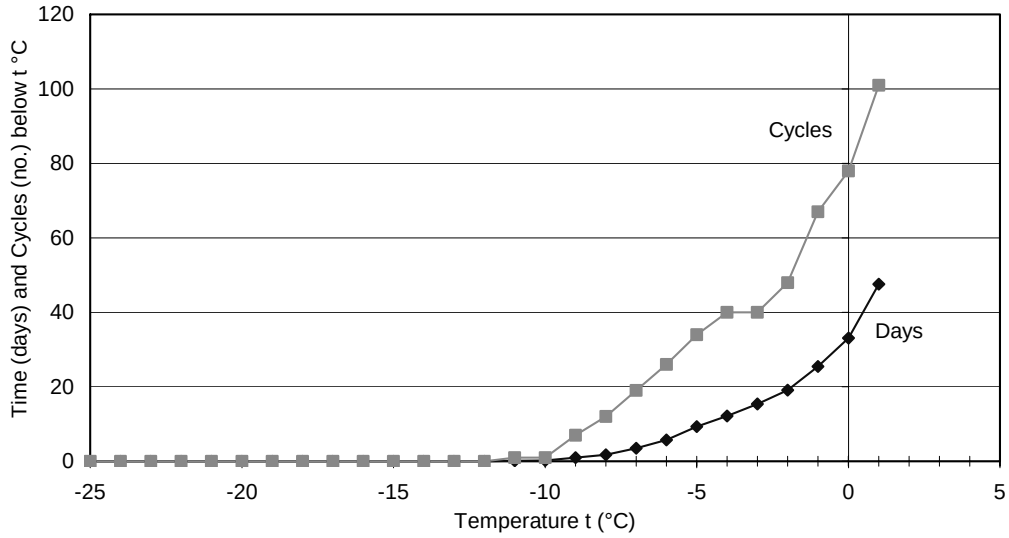

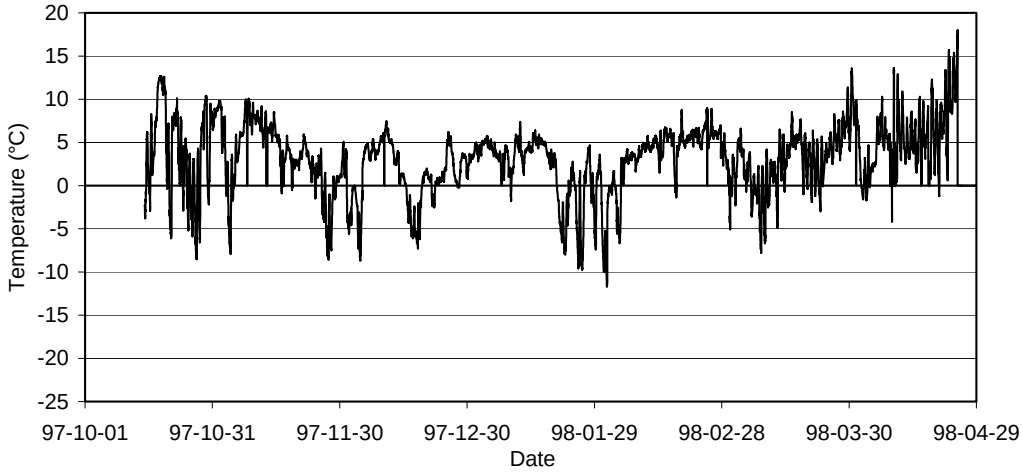

Temperature	Oct.(1	Nov.	Dec.	Jan.	Feb.	Mar.	Apr.
Mean (°C)	4.1	3.4	1.2	1.5	4.0	3.0	6.0
Max (°C)	12.7	10.1	7.5	7.4	9.0	13.6	20.9
Min (°C)	-8.5	-8.6	-8.7	-11.7	-11.3	-7.8	-4.2

Relative humidity	Oct.(1	Nov.	Dec.	Jan.	Feb.	Mar.	Apr.
Mean (%)	78.4	84.9	88.8	83.9	88.3	74.6	77.8
Standard dev. (%)	15.7	10.1	5.5	13.4	9.1	16.6	16.3

Precipitation	Oct.(1	Nov.	Dec.	Jan.	Feb.	Mar.	Apr.
Rain (mm fluid)	11.3	15.2	68.4	85.8	41.2	88.6	47.1
Snow (mm as snow)	0.2	24.5	44.4	77.8	64.6	306.6	17.1
Snow/rain mixed	1.3	3.2	1.5	25.5	45.2	76.0	71.8
Precipitation as fluid	11.6	18.3	73.1	98.7	56.7	134.5	63.2

(1 Measured from the 15th of October

Climate at the marine exposure site during winter season 1998 - 1999

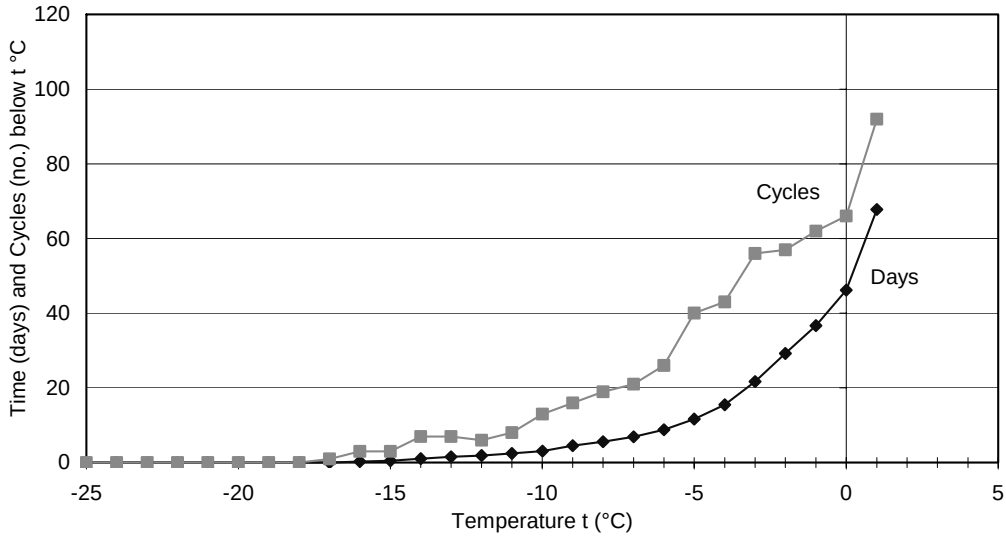

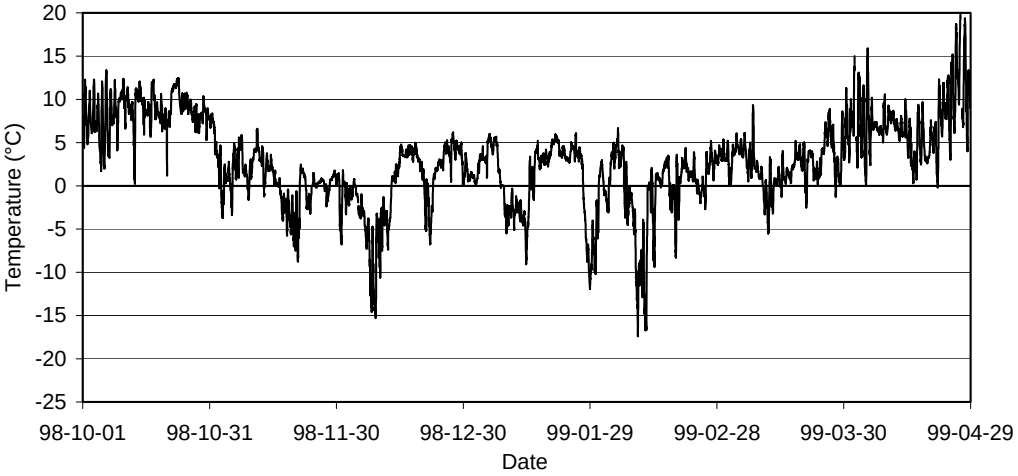

Temperature	Oct.	Nov.	Dec.	Jan.	Feb.	Mar.	Apr.
Mean (°C)	8.8	0.6	-0.2	0.7	-0.4	2.8	7.5
Max (°C)	13.4	7.1	6.2	6.1	6.7	11.3	20.4
Min (°C)	0.2	-8.8	-15.3	-11.9	-17.4	-5.5	-0.2

Relative humidity	Oct.	Nov.	Dec.	Jan.	Feb.	Mar.	Apr.
Mean (%)	84.1	91.2	89.0	87.5	83.2	82.1	80.8
Standard dev. (%)	11.9	7.7	10.8	9.6	15.6	13.2	15.4

Precipitation	Oct.	Nov.	Dec.	Jan.	Feb.	Mar.	Apr.
Rain (mm fluid)	263.4	17.8	72.6	128.7	28.0	28.7	184.7
Snow (mm as snow)	0	115.6	97.4	76.5	157.8	99.6	25.5
Snow/rain mixed	0	24	66.7	16.4	63.3	109.5	88.4
Precipitation as fluid	263.4	34.2	95.7	139.6	56.4	60.6	204.9

Climate at the marine exposure site during winter season 1999 - 2000

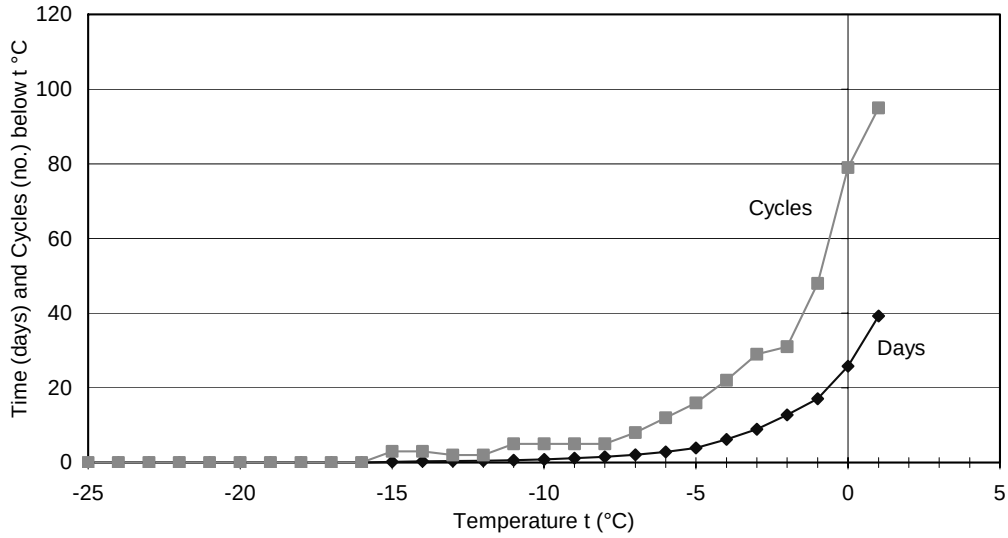

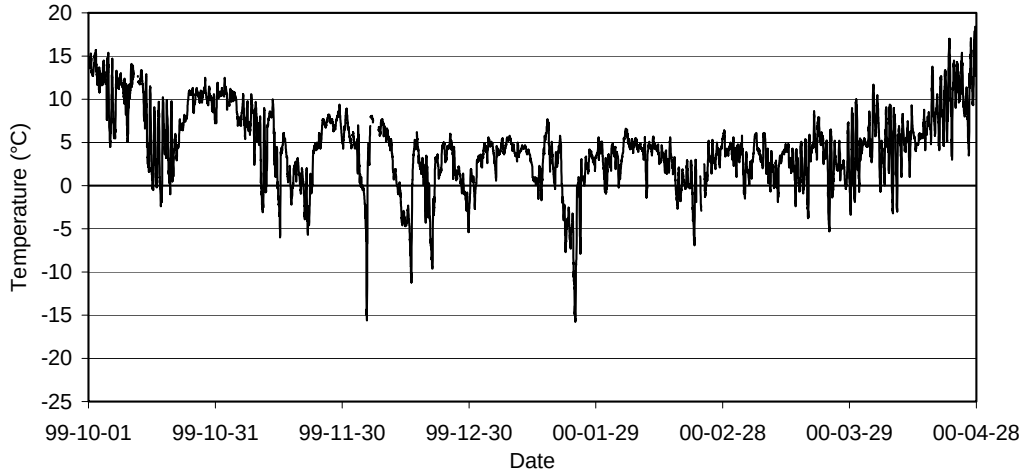

Temperature	Oct.	Nov.	Dec.	Jan.	Feb.	Mar.	Apr.
Mean (°C)	9.1	5.3	1.8	2.1	3.0	2.9	8.5
Max (°C)	15.7	12.5	8.9	7.7	6.6	10.0	27.5
Min (°C)	-2.4	-6.0	-15.6	-15.8	-6.9	-5.3	-3.2

Relative humidity	Oct.	Nov.	Dec.	Jan.	Feb.	Mar.	Apr.
Mean (%)	82.7	85.5	84.8	83.2	85.7	76.4	78.2
Standard dev. (%)	14.2	11.3	12.0	15.1	10.5	18.6	17.5

Precipitation	Oct.	Nov.	Dec.	Jan.	Feb.	Mar.	Apr.
Rain (mm fluid)	0[(1]	0[(1]	187.5	45.9	140.0	37.5	55.5
Snow (mm as snow)	0	0	26.8	113.7	7.8	96.0	99.9
Snow/rain mixed	0	0	88.9	79.4	3.8	64.1	56.5
Precipitation as fluid	0[(1]	0[(1]	208.0	73.2	141.5	59.9	76.8

[(1] Dubious value

Climate at the marine exposure site during winter season 2000 - 2001

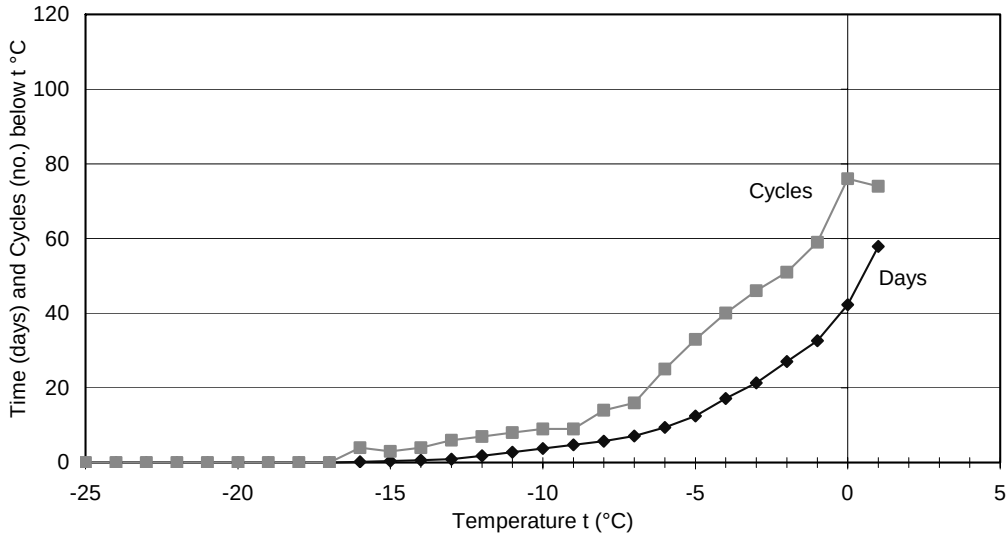

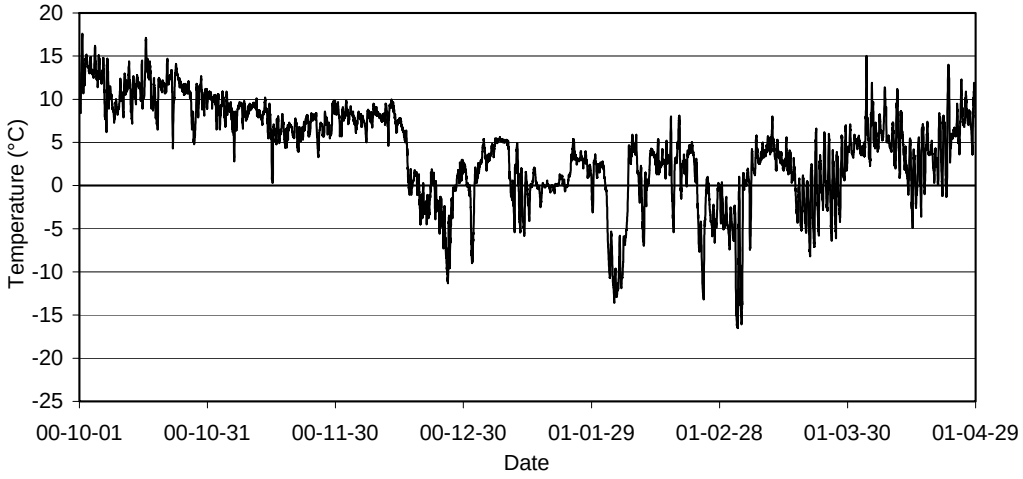

Temperature	Oct.	Nov.	Dec.	Jan.	Feb.	Mar.	Apr.
Mean (°C)	11.2	7.6	3.3	1.4	-1.0	0.2	5.4
Max (°C)	17.6	10.9	10.0	5.6	8.1	8.0	17.7
Min (°C)	4.3	0.3	-11.3	-9.0	-13.6	-16.5	-4.9

Relative humidity	Oct.	Nov.	Dec.	Jan.	Feb.	Mar.	Apr.
Mean (%)	86.9	88.3	89.7	88.2	81.7	77.7	80.8
Standard dev. (%)	7.7	5.6	5.3	6.7	12.9	16.4	15.5

Precipitation	Oct.	Nov.	Dec.	Jan.	Feb.	Mar.	Apr.
Rain (mm fluid)	214.5	99.6	64.3	18.9	29.3	13.7	127.1
Snow (mm as snow)	0	0	46.6	87.5	177.3	25.0	19.5
Snow/rain mixed	0	0	18.0	78.1	96.9	3.3	2.5
Precipitation as fluid	214.5	99.6	72.6	43.3	66.4	16.9	129.6

Climate at the marine exposure site during winter season 2001 - 2002

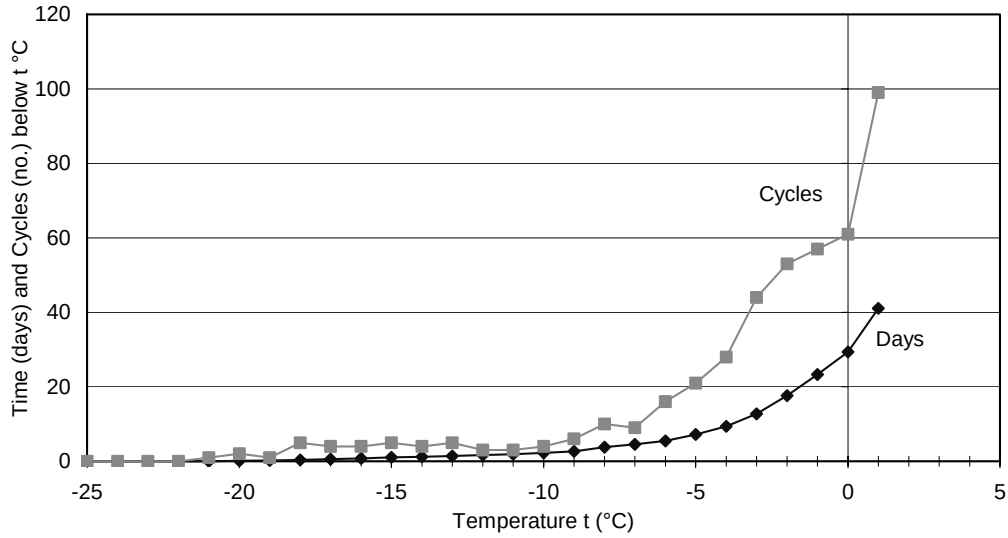

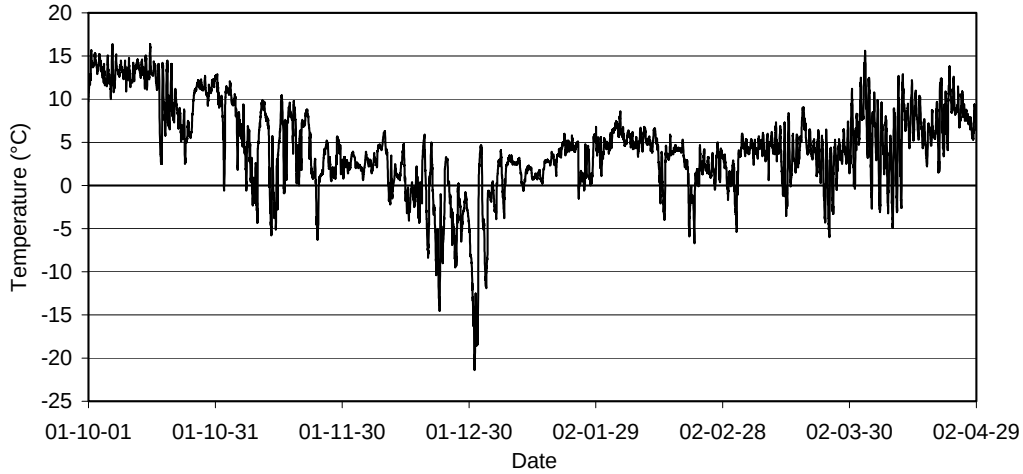

Temperature	Oct.	Nov.	Dec.	Jan.	Feb.	Mar.	Apr.
Mean (°C)	11.5	4.6	-0.9	1.8	3.5	3.5	6.9
Max (°C)	16.4	12.1	6.3	6.8	8.6	11.2	15.6
Min (°C)	2.5	-6.3	-21.4	-18.4	-6.7	-6.0	-4.9

Relative humidity	Oct.	Nov.	Dec.	Jan.	Feb.	Mar.	Apr.
Mean (%)	87.4	79.4	87.4	89.6	83.4	79.8	77.2
Standard dev. (%)	10.0	16.8	11.2	11.1	13.7	16.1	17.4

Precipitation	Oct.	Nov.	Dec.	Jan.	Feb.	Mar.	Apr.
Rain (mm fluid)	70.3	89.4	16.2	55.5	303[(1]	30.9	14.6
Snow (mm as snow)	0	3.7	216.8	70.5	103.3	7.2	0.1
Snow/rain mixed	0	4.4	61.8	133.6	107.5	45.6	0
Precipitation as fluid	70.3	90.7	50.2	89.3	334.8[(1]	40.7	14.6

[(1] Dubious value

Climate at the marine exposure site during winter season 2002 - 2003

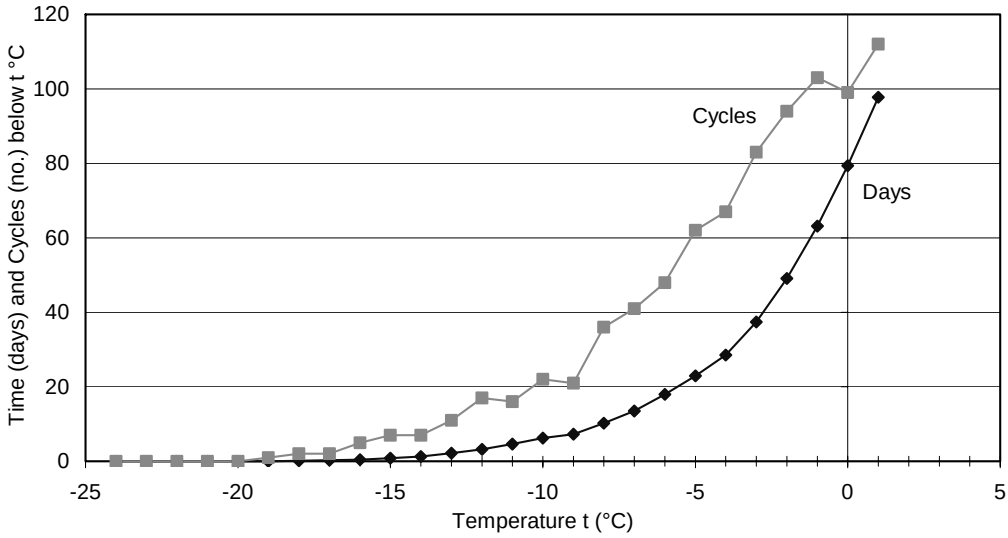

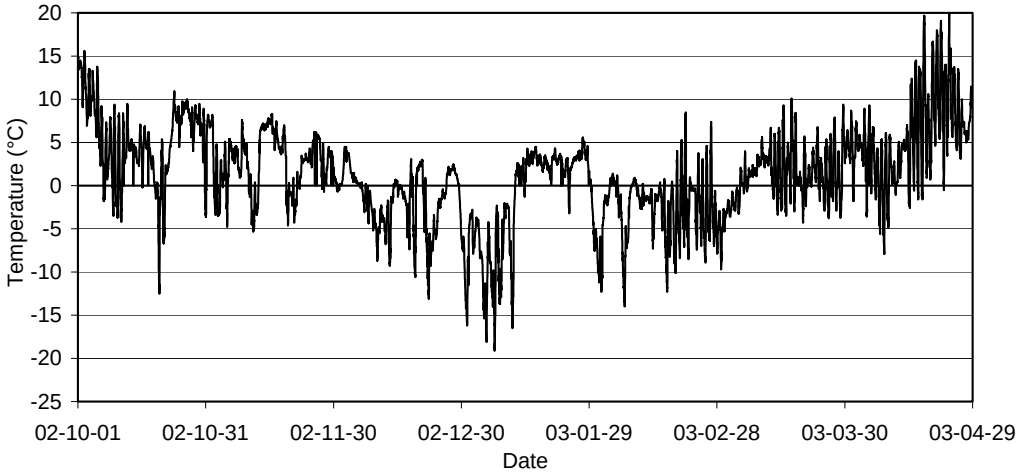

Temperature	Oct.	Nov.	Dec.	Jan.	Feb.	Mar.	Apr.
Mean (°C)	5.3	2.7	-2.0	-1.8	-2.5	1.3	6.1
Max (°C)	15.6	8.3	4.5	5.6	8.5	10.1	20.5
Min (°C)	-12.5	-5.3	-16.2	-19.1	-14.0	-8.7	-7.9

Relative humidity	Oct.	Nov.	Dec.	Jan.	Feb.	Mar.	Apr.
Mean (%)	78.2	80.7	76.4	83.4	79.9	75.3	59.6
Standard dev. (%)	13.5	11.3	12.5	9.9	12.8	17.9	24.5

Precipitation	Oct.	Nov.	Dec.	Jan.	Feb.	Mar.	Apr.
Rain (mm fluid)	86.7	65.2	43.3	43.8	24.0	4.5	75.9
Snow (mm as snow)	0	6.8	15.0	61.1	41.9	3.4	42.8
Snow/rain mixed	0	26.1	17.9	17.6	73.3	11.3	20.1
Precipitation as fluid	86.7	71.1	48.4	53.4	42.9	7.1	84.2